Thalamo-cortical mechanisms of sleep spindles and spike-wave discharges in WAG/Rij rats

Disclosing information hidden in the electroencephalogram

een wetenschappelijke proeve op het gebied van de Sociale Wetenschappen

Proefschrift

ter verkrijging van de graad van doctor
aan de Radboud Universiteit Nijmegen
op gezag van de Rector Magnificus prof. dr. S.C.J.J. Kortmann,
volgens besluit van het College van Decanen
in het openbaar te verdedigen op dinsdag 23 December 2008,
om 10.30 uur precies
door

Evgenia Sitnikova

geboren op 27 juli 1974

te Volgograd (Rusland)

Promoters:

Prof. Dr. A.M.L. Coenen

Dr. E.L.J.M. van Luijtelaar

Manuscriptcommissie:

Prof. Dr. J. van Opstal (Dept. of Biophysics, Radboud University Nijmegen, The Netherlands, chairman)

Prof. Dr. G.K. Kostopoulos (Dept. of Neurophysiology, University of Patras, Greece)

Prof. Dr. V.V.Raevsky (Institute of Higher Nervous Activity RAS, Moscow, Russia)

The major part of this thesis was prepared at the Nijmegen Institute for Cognition and Information (NICI), Department of Biological Psychology (Head: Prof. Dr. A.M.L. Coenen), Radboud University Nijmegen. Experimental results described in this thesis were obtained at the NICI-Biological Psychology.
Results presented in Chapter 4.3 were obtained in collaboration with the Department of Non-linear processes (Saratov State University, Saratov, Russia) and results in Chapter 5.2 were part of collaboration with the Department of Nano- and Biomedical Technologies (Saratov State University). Some parts of this thesis were prepared at the Institute of Higher Nervous Activity and Neurophysiology, Moscow, Russia.

The research was financially supported by grant 01-08 from the National Epilepsy Foundation (NEF) to Dr. E.L.J.M. van Luijtelaar.
Donders Institute for Brain, Cognition and Behaviour Centre for Cognition (former NICI) financed publication of this thesis

Thalamo-cortical mechanisms of sleep spindles and spike-wave discharges in WAG/Rij rats. Disclosing information hidden in the electroencephalogram Evgenia Sitnikova/NICI: Nijmegen Institute for Cognition and Information / PhD Thesis
Radboud University Nijmegen, Nijmegen, The Netherlands, 2008

ISBN:

Printed by Printpartners Ipskamp Nijmegen The Netherlands

List of abbreviations

SWD – spike-wave discharges

The rat strains used as models of absence epilepsy
WAG/Rij rats –Wistar Albino Glaxo from Rijswijk
GAERS - Genetic Absence Epilepsy Rats from Strasbourg

Non-epileptic rat strain:
ACI - August Copenhagen Irish, black agouti rats

Epileptiform components of SWD (according to Weir, 1965):
Sp1 – Spike 1
Sp2 – Spike 2
PT – positive transient

SmI – primary somatosensory cortex
VPM – the ventroposteromedial thalamic nucleus
RTN – the reticular thalamic nucleus

Contents

Chapter 1
General Introduction[1]

CONTENTS

Electroencephalography (EEG). A historical overview

EEG is an acronym for **e**lectro**e**ncephalo**g**ram ("electro" = electrical signals, "encephalo" = the brain, "graph" = a recording).

> *Electroencephalogram.* Record of electrical activity of the brain taken by means of electrodes placed on the surface of the head, unless otherwise specified [INSECN, 1974].
>
> *Electroencephalogram.* Electrical potentials recorded from the brain, directly or through overlying tissues [Lopes da Silva, 2002].

Electroneurophysiology has a history of more than hundred years [cited by Goldensohn et al., 1997; Coenen et al., 1998]. In 1875, a Liverpool physician and medical school lecturer Richard Caton first demonstrated that electrical signals could be measured directly from the surface of animal brain. The father of clinical electroencephalography, the German psychiatrist Hans Berger, recorded electrical activity from human brain and introduced the term ‘electroencephalogram’. The first published EEG data from humans appeared in 1929, when Hans Berger published a paper in which he presented 73 recordings.

Between Caton and Berger, Adolph Beck in 1890 found that sensory stimuli (flashes or sounds) induced slow changes of electrical brain activity (slow wave response, evoked potentials). Fleischl von Marxow (1890) made a similar observation. A Russian scientist, Vasili Yakovlevich Danilevsky in his doctoral thesis (1877) described electrical brain activity in dogs. Another Russian physiologist, Nikolai Evgenjevich Wedensky, recorded electrical activity from peripheral (nerves) and central neural system using a telephone (the results were published in his master's thesis in 1884). In 1913, Vladimir V. Pravdich-Neminsky published photographic recordings of electrical brain activity in dogs and introduced the term ‘electrocerebrogram’.

From that time, electroencephalographic investigations have led to major advances in studying sleep and epilepsy. Electroencephalography is the most popular method for the analysis of spontaneous brain oscillations and evoked (event-related) potentials, changes of electrical brain activity during anaesthesia and sleep, during sensory perception and voluntary activity, etc. Nowadays, EEG investigation is necessary in clinical practice for the diagnosis and prognosis of various neural disorders, especially, in epileptic patients.

Several spontaneous rhythms can be encountered in EEG of animals and humans during different behavioral states, whereas peculiar (paroxysmal) patterns appear in EEG during epileptic seizures. Mechanisms that underlie spontaneous rhythmic activity in a brain were studied by V.V. Danilevski (1875) and A. Beck (1890), who described EEG desynchronization in animals; by I.M. Sechenov, who found spontaneous rhythms in medulla oblongata in the frog and by H. Berger, who described *alpha* and *beta* rhythms in human EEG.

---

[1] Separate parts of this Chapter are published in:
van Luijtelaar G and Sitnikova E. Global and focal aspects of absence epilepsy: the contribution of genetic model. Neurosci. Biobehav. Rev., 2006; 30: 983-1003.

Application of EEG in epilepsy

Even before H. Berger's landmark report (1929), where he described spontaneous brain electrical activity in human brain, N. Cybulski and S. Jelenska-Macieszyna (1914) at the University of Cracow in Poland published the first photographs of paroxysmal activity during experimental focal seizures in dogs [cited by Goldensohn et al., 1997]. In 1931, H. Berger demonstrated the first recordings of spike-and-wave activity obtained in epileptic patients (Fig. 1.1). Two years later, in 1933, he published an EEG record during a brief episode of "*simple automatic activity with no other movement*" [cited by Goldensohn et al., 1997]. It is worthwhile remembering that H. Berger first suggested using EEG investigations in clinical practice [cited by Bronzino, 1995].

In 1935, Frederick Gibbs, Hallowell Davis, and William G. Lennox at Boston City Hospital demonstrated spike-and-wave complexes during clinical absence seizures. Since that time, clinical application of the EEG rapidly increased and EEG recording technique has been profoundly improved. Over the years, the EEG helps in making short- and long-term prognoses of different neurological and psychiatric disorders. EEG investigation is necessary for the diagnosis of epilepsy (especially in patients with atypical epileptic syndromes); it also offers important prognostic information.

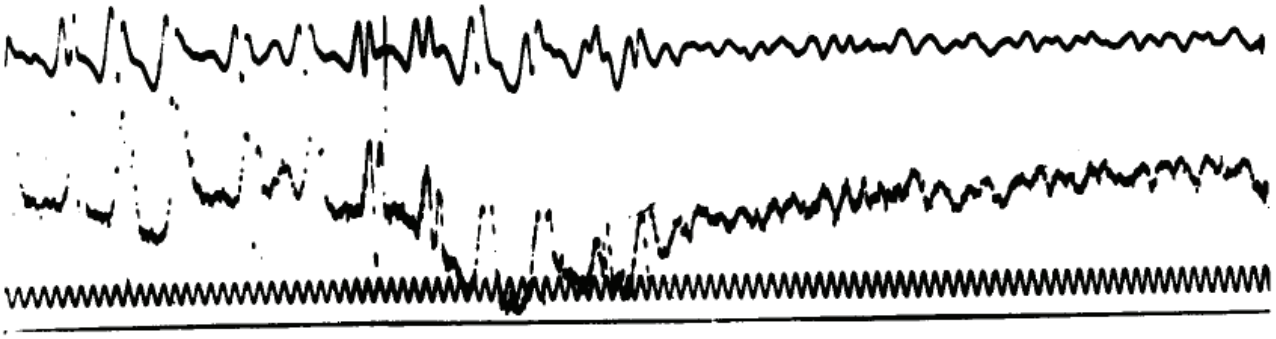

Figure 1.1. EEG record made by H.Berger in 18-year-old girl during a seizure. High voltage spike-and-wave complexes appear with frequency of about 3 per second [from Goldensohn et al., 1997].

Frontiers of EEG research

Since Berger's time, EEG data acquisition systems have progressively improved. High capacity digital storage devises and state-of-art engineering technologies are helpful in processing of large amount of information and analysis of EEG data. A technological progress in a field of EEG encourages interdisciplinary research including experimental/theoretical neuroscience, psychophysiology, cognitive neuroscience, biophysics, psychology, computational neuroscience, neuronal modeling and others [Lopes da Silva, 2002]. More and more sophisticated methods of EEG analysis are aimed in unraveling global brain processes of sleep and wakefulness, perception, sensori-motor integration and higher cognitive functions. EEG data are ultimately important source of clinically-related information and new methods of EEG data analysis are developed in order to better understand mechanisms underlying normal and abnormal brain functions [Lopes da Silva, 2002].

Neuronal processes that underlie EEG have been elaborated in several biophysical theories [Freeman, 1975; Coenen, 1995; Nunez, 2000; Lopes da Silva, 2002]. Apparently, EEG sums up extra-cellular field potentials produced by tens of millions neurons [Nunez, 2000]. These large groups of neurons are integrated into "*neural masses*" throughout the widespread mutual interactions (a concept of Freeman [1975]). Synchronous activation of neuronal populations resulted in high-voltage fluctuations of local field potentials and yielded a variety of oscillatory EEG patterns [Coenen, 1995].

The present thesis aims to investigate thalamo-cortical network mechanisms of self-sustained oscillations, such as natural sleep spindles and generalized spike-wave discharges (absence seizures). We first perform time-frequency EEG analysis using traditional methods (Fourier transform, analysis of auto-spectra, cross-spectra and cross-correlations) and relatively new continuous wavelet transform. Second, we characterize disturbances in the thalamo-cortical neuronal network mechanism of generalized spike-wave discharges, using traditional coherence analysis and novel Granger causality estimations.

Spike-wave discharges (SWD) in animal models of absence epilepsy

Absence epilepsy is a non-convulsive generalized type of epilepsy which is characterized by a brief impairment of consciousness (absence) with minimal myoclonic jerks of eyes and peri-oral automatisms [Panayiotopoulos, 2001]. Absence seizures are first described by Poupart in 1705. In 1770, Tissot called them '*petits accés*' (petit mal) and distinguished from the '*grands accés*' (grand mal). The name 'absence seizures' is introduced by Calmeil in 1824 [cited by Temkin, 1971]. In contrast to the other generalized epilepsies, absence epilepsy is never accompanied by aura or convulsions. Also, the pharmacological profile of absence seizures

differs from that of other primary generalized seizures, moreover, some of the well-known anti-convulsant drugs (i.e., carbamazepine, phenytoin, and tiagabine) aggravate absence seizures [Genton et al., 2001] and some drugs (i.e. ethosuximide) are only effective in absence epilepsy.

The onset of typical absence seizures cannot be predicted based on clinical signs. In EEG, absences appear abruptly as generalized synchronous bilateral 2.5-5 Hz spike-and-wave complexes. The Committee on Terminology of the International Federation of Societies for Electroencephalography and Clinical Neurophysiology (IFSECN) defines spike-and-slow-wave complex as '*a pattern consisting of a spike followed by a slow wave'* (1974).

Spike-and-wave complexes may be brief (2–5 sec) or long (15–30 sec) [Panayiotopoulos, 2005], they may be recorded in different forms of idiopathic generalized epileptic syndromes, such as childhood absence epilepsy, juvenile absence epilepsy, juvenile myoclonic epilepsy, myoclonic absence epilepsy and eyelid myoclonia with absences [Gibbs et al., 1935; Panayiotopoulos, 1999 and 2005]. EEG morphology of the spike-and-wave complexes is different in different forms of epilepsy. For instance, multiple spikes in spike-and-slow-wave complexes ('multiple spike-and-slow-wave complexes') are common for absences during sleep and for absence epilepsy with older age of onset [Chatrian, 1974; Panayiotopoulos, 1999 and 2005]. The presence of more than 3 spikes per wave may indicate a bad prognosis [Panayiotopoulos, 2005]. Polyspiking in spike-and-wave complexes (polyspike-wave complexes) often associates with impairment of intrinsic cortical mechanisms [Timofeev et al., 1998]. Spatial distribution of spike-and-wave complexes varies from patient to patient [Weir, 1965; Blume, 2002]. Altogether it is suggested that EEG pattern of absence seizures is intricate and it is determined by local neuronal processes, by neuronal network activity and by neuronal synchronization. The m orphology of spike-wave complexes and underlying neuronal mechanisms have not been studied in details.

Animal models of absence epilepsy

In some rodent strains, such as GAERS (Genetic Absence Epilepsy Rats from Strasbourg) and WAG/Rij (Wistar Albino Glaxo from Rijswijk), spike-wave seizures appear spontaneously in the EEG [Danober et al., 1998, Coenen and van Luijtelaar, 2003; Depaulis and van Luijtelaar, 2006]. Behavioral expression of spike-wave seizures in rodents is similar to the clinical manifestation of absence seizures in humans, e.g. immobility, minimal facial myoclonic jerks and twitches [van Luijtelaar and Coenen, 1986; Marescaux et al., 1992]. Absence seizures in rats and in humans have a genetic origin, although the genes are not yet identified [Vadász et al., 1995; Depaulis and van Luijtelaar, 2006][2]. Both GAERS and WAG/Rij rat strains are considered as valid models of human absence epilepsy [Danober et al., 1998; Coenen and van Luijtelaar, 2003].

In the current thesis, all experimental data are collected in adult WAG/Rij rats. Absence seizures in our animals were discovered twenty years ago and their EEG manifestation was called 'spike-wave discharges' or SWD [van Luijtelaar and Coenen, 1986]. It is accepted that electroencephalographic pattern of SWD resembles 'spike-and-wave complexes' in human absence epilepsy. The waveform and frequency of EEG seizures is varied in different species (rats, humans, cats). In order to make a parallel between EEG profile of spike-wave seizures in WAG/Rij rats and in human patients (**Chapter 3.1)**, EEG pattern of SWD is delineated in accordance to the guidelines of clinical electroencephalography [INSECN, 1974; Weir, 1965].

Cellular and network mechanisms of SWD

Studies in GAERS [Marescaux et al., 1992; Avanzini et al., 2000] and WAG/Rij rats [Inoue et al., 1993] showed that although SWD are recorded in the cortex, they have a thalamic origin. Large electrolytic lesions of the lateral thalamus [Vergnes and Marescaux, 1992] and also chemical lesions of the RTN suppressed SWD in GAERS [Avanzini et al., 1992; Avanzini et al. 1993].

Some theories assume that spike-wave activity is triggered by pacemaker cells located in the reticular thalamic nucleus (RTN), in other words, it originates from the thalamus [Blumenfeld 2002; Avanzini et al., 2003]. Others emphasize that SWD are initiated in the somatosensory cortex (SmI) and that the thalamus is only secondarily involved [Meeren et al., 2002; 2005]. The latter theory is that absence seizures have a focal onset. This point of view is supported by clinical neurophysiologists, who noted that spike-and-wave seizures are not fully generalized [Holmes et al., 2004; Craiu et al., 2006].

In the last few decades, experimental and computational studies led to tremendous progress towards identifying basic cellular and network mechanisms underlying spike-wave activity [refs in Destexhe and Sejnowski, 2001; Blumenfeld, 2002; Steriade, 2003]. Some point to a critical role for the thalamus in generation of absence seizure, but others stress an important role of the neocortex (Table 1.1).

Experimental studies in animal models of absence epilepsy demonstrated that cortical and thalamic neurons produce prolonged firing bursts during the 'spike' component of local field potential and that neurons are silent

[2] In humans some familial forms of absences have been identified, while an overall genetic predisposition indicates that this is a multifactorial disorder (George Kostopoulos, personal communication).

during the 'wave' component [e.g., Steriade, 1974; Avoli et al., 1983; Buzsaki et al., 1988; Inoue et al., 1993; Seidenbecher et al., 1998]. In particular, it is shown that the spike in the SWD is associated with synchronous neuronal bursts while the wave reflects the inhibitory phase mediated by fast $GABA_A$ and slow $GABA_B$ postsynaptic potentials [Inoue et al., 1993; Seidenbecher et al., 1998]. In HVSs ('high voltage spike-and-wave patterns', equivalent to SWD), the spike component in local field potential as recorded at cortical surface is characterized by neuronal bursts in almost all layers (bottom plot in Fig. 1.2, component *a1*=spike) [Kandel and Buzsaki, 1997].

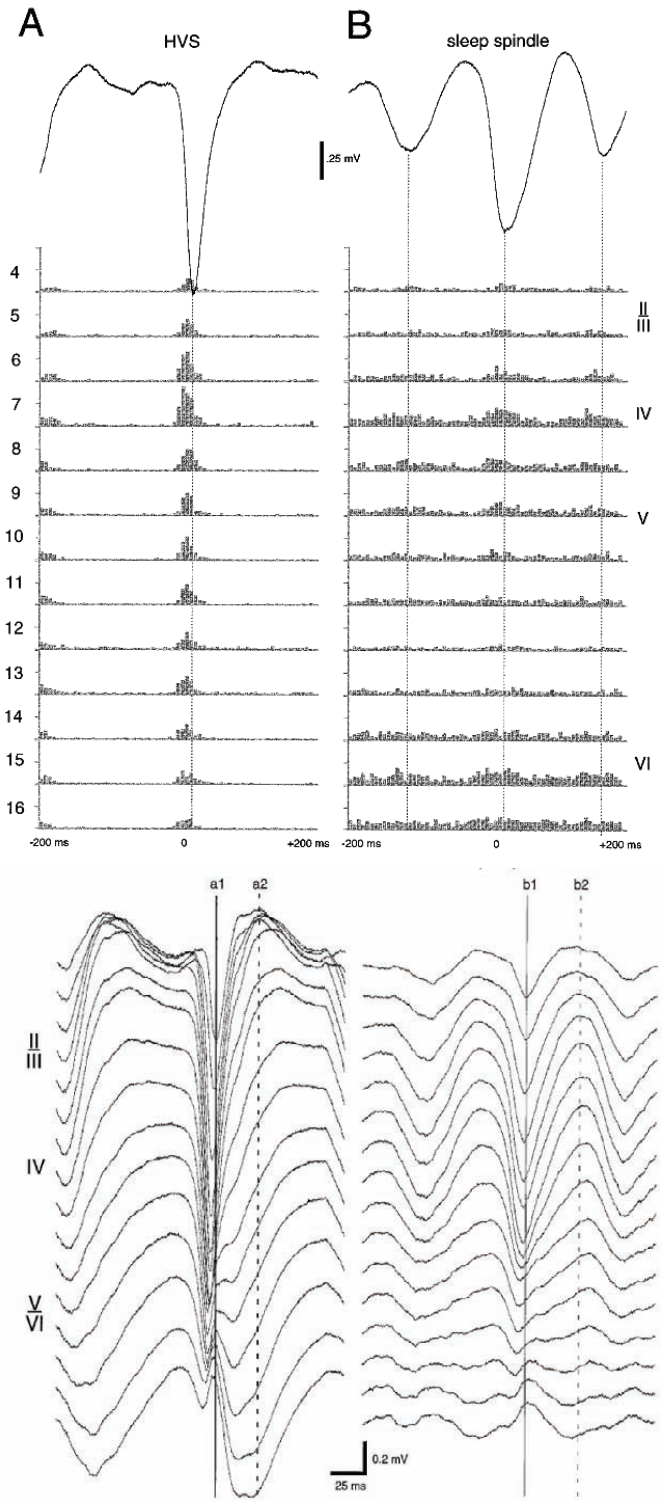

Figure 1.2. Depth profiles of 'high voltage spike-and-wave patterns' (HVSs, equivalent to SWD, A) and sleep spindles (B). The upper plot shows the distribution of single unit activity in different layers of the neocortex and neuronal field potential recorded simultaneously from layer IV. Note the stronger recruitment of neurons during HVSs compared to sleep spindles. Unit discharges during the Wave component of HVSs are completely suppressed. The bottom plot shows components of HVSs: a1 - Spike and a2 - Wave; b1 - surface-negative and b2 - surface-positive components of sleep spindle [from Kandel and Buzsáki, 1997].

It is remarkable that some physiological and anatomical features in rodent brain are crucially different from that in the feline brain (earlier theories were grounded on neurophysiological data from cats). The frequency of SWD in rats is 7–11 Hz [van Luijtelaar and Coenen, 1986; Coenen and van Luijtelaar, 2003], but in cats, it is 3-4.5 Hz that is about the same to 2.5-4 Hz in humans. In cats, GABA-ergic inhibitory interneurons are present throughout the thalamus, including relay nuclei, but in rats, inhibitory interneurons are absent in thalamus, except the lateral geniculate nucleus and reticular thalamic nucleus [Jones, 1985, Ohara et al., 1983]. In rats, in contrast to cats and humans, the vast majority of thalamic nuclei receive only external inhibitory inputs from the RTN, while intrinsic inhibition is absent in the largest part of the thalamus.

Table 1.1. The role of the thalamus versus the cortex in generation of absence seizures

Thalamus	References	Cortex	References
Spike-and-wave seizures are depressed after thalamic lesions or pharmacological inactivation of the thalamus.	Pellegrini et al., 1979; Avoli and Gloor, 1982; Vergnes and Marescaux, 1992	A form of spike-and-wave activity can still be present in the cortex after thalamic inactivation or thalamectomy.	Marcus and Watson, 1966; Pellegrini et al., 1979; Steriade and Contreras, 1998
Cortical and thalamic cells exhibit prolonged firing in phase with the 'spike' component and silent during the 'wave'.	Pollen, 1964; Steriade, 1974; Avoli et al., 1983; Buzsaki et al., 1988; Inoue et al., 1993; Seidenbecher et al., 1998.	During spike-and-wave occuring in the siezures cortex, majority of thalamic neurons are steadily hyperpolarized and completely silent.	Steriade and Contreras, 1995; Pinault et al., 1998
Spindle oscillations, which are generated by thalamic circuits, can be gradually transformed into spike-and-wave discharges. Manipulations that promote or antagonize spindles also affect spike-and-wave seizures.	Steriade et al. 1994; Avoli and Gloor, 1982; Kostopoulos, 2000; van Luijtelaar, 1997; refs in Destexhe and Sejnowski 2001.	The threshold for epileptogenesis was much lower in the cortex compared to the thalamus.	Steriade and Contreras, 1998
Knock-out mice lacking the gene for the T-type calcium current in thalamic relay cells display a resistance to absence seizures. This suggests that bursting activity in thalamic cells mediated by T-type current is responsible for spike-wave seizures.	Kim et al., 2001.	Injections of high doses of $GABA_A$ antagonists (penicillin or bicuculline) into the cortex resulted in spike-and-wave seizures.	Gloor et al., 1979; Steriade and Contreras, 1998

Sleep spindles

Sleep spindles are among the most numerous spontaneous EEG events. Sleep spindles can be recorded in EEG of humans and in mammals during non-REM sleep [reviewed in De Gennaro and Ferrara, 2003; De Gennaro et al., 2005]. The name "spindle" refers to its characteristic the waxing and waning envelope. Sleep spindles were first described by Loomis et al. (1935). The first commonly accepted definition given by Rechtschaffen and Kales (1968): waxing and waning oscillations of 12–14 Hz and of at least 0.5 seconds duration. Steriade (1993) defines sleep spindles as "waxing-and-waning field potentials of 7 to 14 Hz, grouped in sequences that last for 1 to 3 s and recurrence every 3 to 10 s". The International Federation of Societies for Electroencephalography and Clinical Neurophysiology gives the following definition: "sleep spindle is a group of rhythmic waves characterized by progressively increasing then decreasing amplitude" [IFSECN, 1974].

Sleep spindles have met great interest of neurobiologists and clinicians, because they are linked to synaptic plasticity in neuronal networks and memory processes and play likely a role in the consolidation of declarative memory and 'offline memory processing' [Buzsáki, 1998].

Spindles are known to be produced by the reciprocal interactions between inhibitory neurons in the reticular thalamic nucleus and excitatory neurons in relay thalamic nuclei [Steriade, 1993, 2003, 2005; Steriade and Llinas, 1988]. *In vitro,* it is shown that thalamic neurons are capable to generate endogenous rhythmic activity (neuronal bursting in the thalamus). At hyperpolarized membrane potentials, thalamic neurons stay in so-called "burst mode" and produce high-frequency bursts (300 Hz) of action potentials [Steriade et al., 1993; Coenen et al., 1995; Avanzini et al., 2000]. Slow-wave sleep is a favourable state for sleep spindles to emerge [De Gennaro and Ferrara, 2003; De Gennaro et al., 2005]. During this state the reticular thalamic nucleus (RTN) strongly inhibits the major part of the thalamus [Steriade, 2005], and triggers highly synchronized burst activity in a large population of thalamo-cortical neurons. These neuronal bursts are distributed over the thalamo-cortical system and correspond to

spindle sequences in the EEG (Fig. 1.2). The crucial role of the thalamus in sleep spindles has been demonstrated in *in vivo* experiments. It is shown that spindles are present in the thalamus after complete removal of the cerebral cortex. In addition, sleep spindles are completely absent in the isolated cortex and in athalamic animals [Steriade and Llinas, 1988].

Generic relationship between sleep oscillations and spike-wave discharges

Sleep oscillations and spike-wave discharges can be distinguished by different amplitude, by having different temporal and spatial profiles [Drinkenburg et al., 1991; Kostopoulos, 2000; Destexhe and Sejnowski, 2001]. SWD can be recorded throughout the entire neocortex (they are generalized) and typically occur synchronously in the two hemispheres (bilaterally synchronized) [Panayiotopoulos, 1999, 2005; Marescaux et al., 1992; Coenen and van Luijtelaar, 2003; Steriade, 2003]. In contrast, sleep spindles are more local oscillations [De Gennaro and Ferrara, 2003; Kandel and Buzsáki, 1997]. The waveform of SWD and sleep spindles is markedly different. SWD have an asymmetric pattern with distinctive spike and wave components. In contrast, sleep spindles are consisted of waves which are more sinusoidal in shape, although the surface-negative portion is often sharper [Kandel and Buzsáki, 1997]. The spike component is absent in sleep spindles. Figure 1.2 (upper plot) shows that HVSs(=SWD) and sleep spindles were characterized by different depth profile of unit activities. Sleep spindles neuronal bursts were absent in deep layers (in layer VI and at the bottom of layer V; channels 11-13), but during HVSs firing activity was detected in all cortical layers. Electrical potential of HVSs and sleep spindles as recorded at cortical surface are generated by several neuronal dipoles. In HVSs, the earliest spike-associated changes of field potential corresponds to surface-positive component with a source in layers II–III and a sink in layers V–VI. The major spike corresponds to a major sink in layer IV. A delayed surface-negative potential was associated with a sink in layers II–III and this potential is reversed in deeper layers.

It has long been proposed that sleep spindles and SWD are triggered by the thalamus. Early investigators showed that spindle waves and SWD could be evoked by repetitive stimulation of intralaminar thalamic nuclei and thus they both represent 'recruiting' responses [Demsey and Morison, 1942; Morison and Demsey, 1942; Jasper and Drooglever-Fortuyn, 1946]. Latter on, it was found that spindle waves are more similar to the 'augmenting' response evoked by repetitive simulation of sensorimotor thalamic nuclei [Spencer and Brookhart, 1961; Morin and Steriade, 1981]. More accurately, spindles type I (monophasic negative) were associated to recruiting responses and spindles type II (biphasic sharper, associated to more firing) to augmenting.

In 1968, Pierre Gloor introduced a *cortico-reticular* theory of primary generalized absence by showing that sleep spindles could be transformed into SWD when neocortex becomes hyperexcitable. In a feline penicillin model, it was shown that SWD develop in the same circuits, which normally generate sleep spindles, by an initially cortical transformation of one every two or more spindle waves to a spike component of SWD, while the next one or more spindle waves are eliminated and replaced by a slow negative wave [cited by Kostopoulos, 2000].

A variety of experimental and theoretical studies have further supported the notion that sleep spindles are related to SWD [Steriade et al. 1994; Avoli and Gloor, 1982; van Luijtelaar, 1997; Kostopoulos, 2000; refs in Destexhe and Sejnowski 2001]. Sleep spindles typically appear during slow-wave sleep and they are typically more numerous at sleep onset. SWD also appear during drowsiness and during the initial stages of sleep (stages I-II) and later during transitions between REM and slow-wave sleep [van Luijtelaar and Coenen, 1988; Drinkenburg et al., 1991]. Both sleep spindles and SWD are produced in the same thalamo-cortical circuit (Figure 1.3) [Gloor et al., 1990; Avanzini et al., 1992, 1993; Kandel and Buzsáki, 1997; Destexhe and Sejnowski, 2001; Steriade et al., 1993; Steriade 2001, 2003, 2005].

A common neurophysiologic mechanism is known to underlay both sleep spindles and SWD in two rodent models of absence epilepsy, in GAERS [Avanzini, 2000] and WAG/Rij rats [Kandel and Buzsáki, 1997; van Luijtelaar, 1997]. Also pharmaco-EEG investigations in WAG/Rij rats reveal a functional relationship between sleep spindles and SWD [van Luijtelaar, 1997]. The dramatic reduction in forebrain responsiveness during sleep and the common thalamo-cortical mechanisms suggest a generic relationship between sleep oscillations and SWD. However, the genuine relationship between sleep spindles and SWD is now a matter of a hot debate [Steriade, 2003; Pinault, 2006; van Luijtelaar and Bikbaev, 2007]. We will address this problem in **Chapters 4.1** and **4.2**.

It seems unlikely that sleep spindles themselves prompt SWD [Pinault, 2006]. This point of view is confirmed by investigating thalamic and cortical cellular mechanisms of spontaneous SWD in GEARS [Pinault et al., 2001; Pinault 2003; 2006]. It was found that SWD are derived from medium-voltage 5–9 Hz oscillations, which clearly differ from spindle oscillations (7-15 Hz). **Chapter 3.3** examines amplitude-frequency characteristics of EEG immediately prior to the onset of SWD in WAG/Rij rats (SWD-precursors).

The 'cortico-reticular' theory [Gloor, 1968; 1969; 1978] assumes that hyperexcitability of cortical neurons plays a crucial role in transformation of normal oscillations into seizure activity. This theory considers the cortex 'as a whole', but different cortical regions seems to differ in respect to the epileptogenesis. A global role of the

cortex in absence epilepsy is demonstrated in GAERS by the spreading depression technique [Vergnes and Marescaux, 1992]. In these experiments the cortex of a single hemisphere is completely deactivated by unilateral application of KCl onto the cortical surface. This causes an immediate abolishment of SWD in the injected cortex, but SWD remain in the untreated hemisphere both in cortex and thalamus. The same effect is found in cats with penicillin-induced SWD in which KCl-induced spreading depression prevents the transformation of sleep spindles into epileptic bursts; therefore, SWD are abolished [Gloor et al., 1979]. SWD can also be reduced with surgical removal of the cortex [Avoli and Gloor, 1982; refs in Kostopoulos, 2000]. All these data suggest that SWD can be produced in a well-interconnected thalamo-cortical network in which an intact cortex should interact with an intact thalamus.

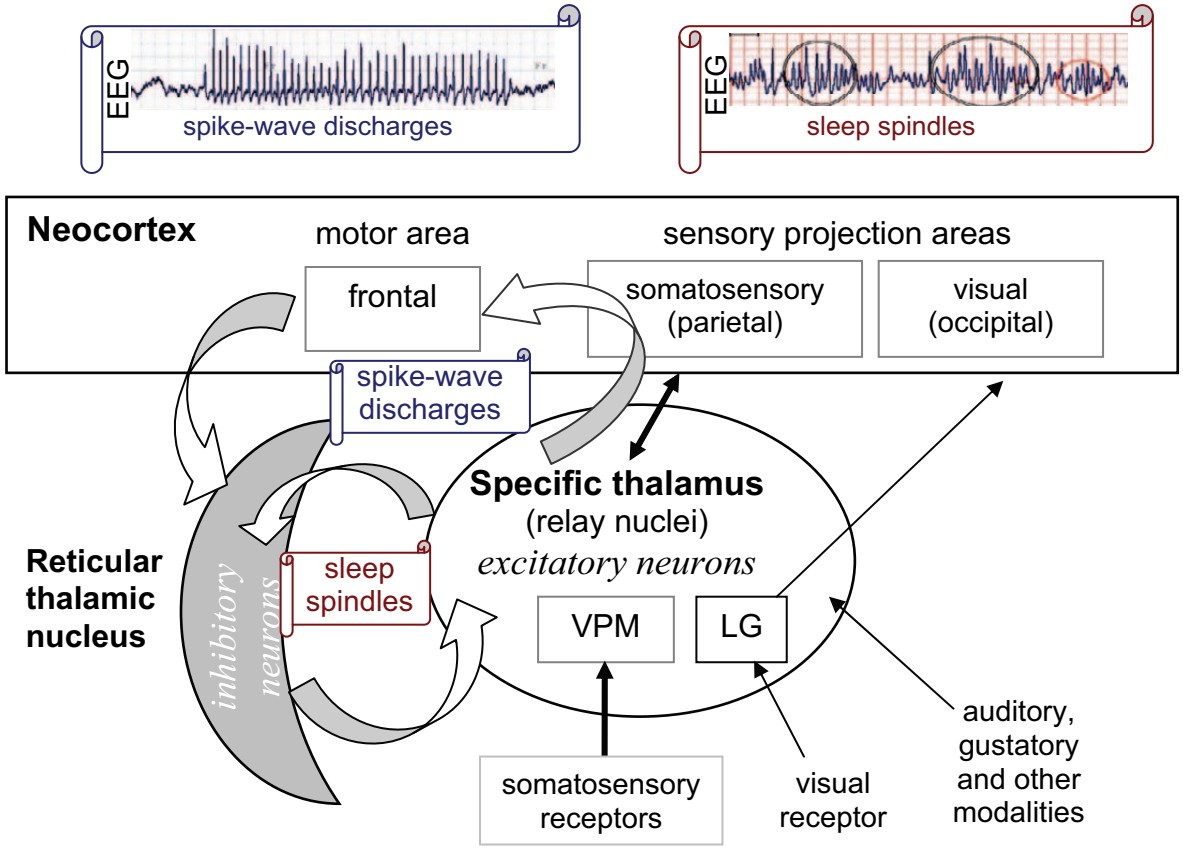

Figure 1.3. Spike-wave discharges and sleep spindles are both generated in a thalamo-cortical network. This network includes neurons in the reticular thalamic nucleus, specific thalamus and neocortex. Sleep spindle sequences are triggered by GABA-ergic cells of the *reticular thalamic nucleus* (RTN); mutual synaptic interactions between the RTN and the specific thalamus are required for the progress of sleep spindle events [Steriade and Deschênes, 1984; Steriade and Llinás, 1988]. The specific part of the thalamus consists of many nuclei that distribute sensory information of various sensory modalities to the corresponding primary sensory areas in the neocortex. In their turn, cortical cells send feedback projections to the thalamus. The *ventroposteromedial nucleus* (VPM) is the major relay somatosensory nucleus in the thalamus. It is known to have anatomic and functional relations with the epileptic zone in the parietal cortex [Meeren et al., 2002]. The lateral geniculate nucleus (LG) projects to the visual cortex and it might play a role in EEG oscillations in the posterior cortex (i.e., spindle activity and SWD type II).

It seems likely that thalamocortical processes can account for both spindles and spike-and-wave rhythms. In addition to that, intracortical circuits play a major role in spike-and-wave rhythms, but their role in sleep spindles is low. In our animal subjects, primary epileptogenic processes are likely to take place in the SmI. More precisely, SWD are initiated in the area of facial projections [Meeren et al., 2002].

It is likely that the occurrence of this type of SWD is under control of both local (intracortical) and global (thalamocortical network) mechanisms. An adequate way to investigate local and global mechanisms that underlie SWD, is to investigate whether they are identically influenced by the same manipulations. We used this approach and changed pharmacologically first the neuronal excitability, locally in the epileptic zone in the neocortex (local reversible deactivation of this zone with lidocaine) and, secondly, in the whole thalamo-cortical network (by means of depletion of noradrenergic neurotransmission with clonidine).

Oscillatory activity in the perioral area of the primary somatosensory cortex (SmI) in rodents as a source of SWD

In 2002, Meeren and co-workers demonstrated that SWD initially appear in the restricted area in the SmI; their cortical focus theory was subsequently placed in a historical theoretical perspective [Meeren et al., 2005]. Before that, Seidenbecher and co-workers (1998) have already mentioned that the SmI plays an important role in SWD in GAERS. These authors found that before the paroxysm is evident on the gross EEG, precursor activity ("embryonic" SW seizures) can typically be recorded in cortical units and in the thalamus. Generation of SWD is associated with spike-concurrent, rhythmic burst-like activity in (mono-)synaptically connected regions of the specific (somatosensory) thalamic regions, the SmI (layers IV/V) and the reticular thalamic nucleus. SWD-correlated activity in layers IV/V of the SmI starts significantly earlier than the related burst firing in the reticular and ventrobasal thalamic neurons [Seidenbecher et al., 1998].

Rhythmic activity in the neocortex occurs due to synchronous firing of the excitatory 'intrinsically bursting' pyramidal cells and inhibitory interneurons [Fellous et al., 2001; Silva et al., 1991; Steriade, 2001]. Intrinsically bursting pyramidal neurons are located in deep cortical layers and produce rhythmic recurrent spike bursts of 5–10 Hz [Connors and Gutnick, 1990; Flint and Connors, 1996]. Network interactions with local inhibitory interneurons govern synchronization of burst activity in a population of bursting neurons [Fellous et al., 2001]. When a large number of neurons starts firing in synchrony, a sharp 5–10 Hz rhythm can be recorded as a field potential.

The firing of cortical neurons significantly influences thalamic activity, since descending cortico-thalamic afferents (Fig. 1.2B) are several times more dense than thalamo-cortical ascending ones [Rouiller and Welker, 2000]. The pyramidal neurons of the deep cortical layers (V and VI) send dense descending projections to various subcortical structures; therefore, cortical oscillations could easily be transferred to the thalamus and other subcortical structures [Deschênes et al., 1998].

The area of the snout and vibrissae in the SmI is capable to initiate SWD [Meeren et al., 2002], because this cortical region in rodents is specific in respect to functional and anatomic features. The largest region of the SmI in the rodents is occupied by perioral sensory projections, including the vibrissae (Fig. 1.4A). The area of perioral projections in the SmI is a central part of the vibrissal trigeminal system (Fig. 1.4B). In rats and some other rodents, vibrissae are the instrument of 'active sensation' that is involved in exploratory behavior ('whisking') and this has a large functional significance. Whisking is characterized by rhythmic movements of vibrissae with a frequency of 10 Hz ('whisker twitching', Ahissar et al., 1997). Those movements are triggered by neuronal bursts that first appear in the vibrissal area in the SmI as a cortical rhythm 7–12 Hz [Nicolelis et al., 1995] and than spread throughout the subcortical centers of the trigeminal system (Fig. 1.2B, thalamus, brainstem) [Nicolelis et al., 1995; Nicolelis and Fanselow, 2002]. This rhythm is blocked by cortical lesions and by local injections of muscimol ($GABA_A$ agonist) into the vibrissal region of the SmI [Nicolelis and Fanselow, 2002].

In rodents, somatosensory rhythm, sleep spindles and SWD appear with the same frequencies (7-12 Hz). We share the opinion of the group of Nicolelis that '*7-12 Hz oscillations alone cannot lead to seizure activity. Instead, genetic manipulations (like those resulting from successive inbreeding) are required to make epileptic activity to emerge*' [Wiest and Nicolelis, 2003, p. 914]. Due to a genetic predisposition to absence epilepsy, WAG/Rij rats show serious disturbances in protein and enzyme synthesis, in properties of ion channels and membrane, as well in neurotransmission and neuromodulation [Coenen and van Luijtelaar, 2003]. Therefore, cortical excitability in WAG/Rij rats is altered, albeit this excitability seems to be more local than it was assumed by Gloor and co-workers, and it is accompanied by impairment of inhibitory mechanisms. Moreover, 7-12 Hz somatosensory rhythm in WAG/Rij rats may be transformed into SWD. Microanatomy of the neocortex in WAG/Rij rats is somewhat abnormal. A quantitative morphometric study of Golgi-stained slices of the frontal and parietal (somatosensory) cortex shows that the geometry of pyramidal cells in the superficial cortical layers (I-III) is changed or even impaired [Karpova et al. 2005]. Apical dendrites of these cells are often split in two branches, decline and run in non-perpendicular directions and an abnormal pattern of dendritic arborization is found in the SmI in WAG/Rij rats. Disturbances in dendritic trees, a receptive part of pyramidal neurons, may cause an impairment of communications between individual neurons. As known, pyramidal cells of superficial layers send long-range projections to remote cortical regions, thus they may synchronize intrinsic cortical oscillations [Gray and McCormick, 1996]. Therefore, associations between the prime epileptic zone in the perioral area in the SmI and other cortical areas may be changed in a way that facilitates synchronization, propagation and generalization of SWD.

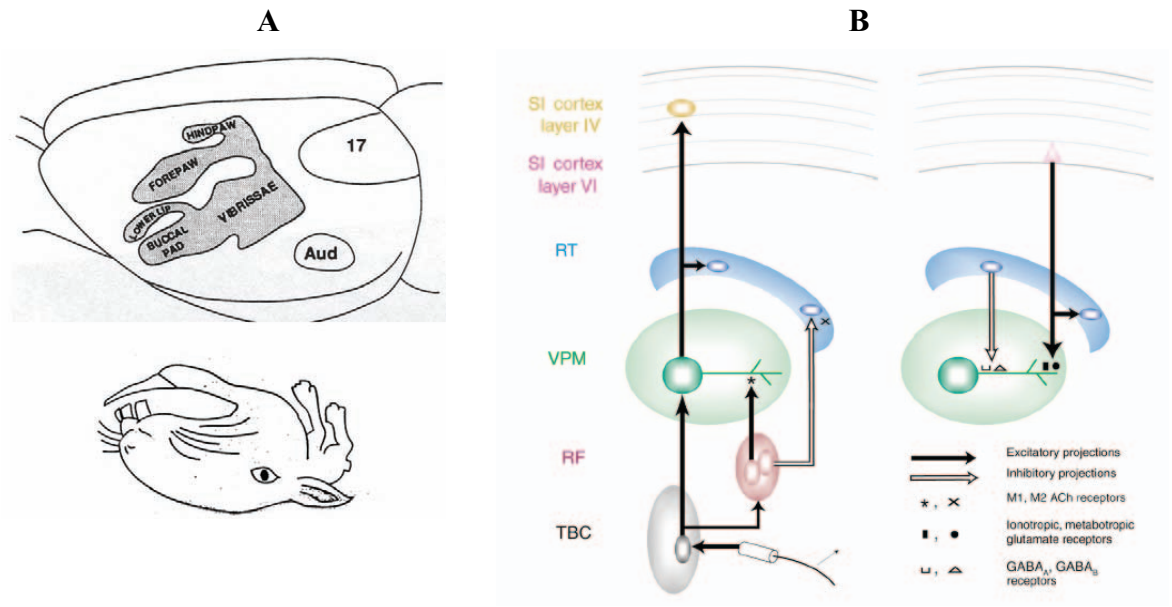

Figure 1.4. Functional representation of whiskers in rat brain **A**. Somatotopic organization of sensory representations area in the cortex. A large area of facial projections in the somatosensory cortex occupied by projections from vibrissae. **B**. Ascending (afferent, left plot) and descending (efferent, right plot) pathways in the trigeminal somatosensory system in rats. Information from whiskers (afferent pathway, left plot) is delivered to the trigeminal brainstem complex (TBC) and to the brainstem reticular formation (RF). Then it is directly sent to the ventroposteromedial thalamic nucleus (VPM) and, indirectly, to the reticular thalamic RT [adopted from Nicolelis and Fanselow, 2002].

Rats are nocturnal animals and use their vibrissae instead of vision more readily. As known, the genetic predisposition to absence epilepsy is higher in albino than in other rat strain such as hooded, brown and agouti rats [Inoue et al., 1990]. The presence of the albino gene in albino rats worsens the visual abilities and poor vision could be compensated by other sensory systems. Probably, in albino rats with predisposition to epilepsy, the functional demands of the vibrissae system are too high and the system is overloaded. As a result, the normal somatosensory 10 Hz rhythm may be transformed into abnormal hypersynchronous high-voltage 10 Hz SWD. **Chapter 6.1** shows that SWD in the primary epileptic zone are endowed with specific elements (fast EEG components and polyspiking), which may be associated with the processes of initiation of SWD I. The role of the focal epileptogenic area in the incidence of SWD is examined by local deactivation of this zone with unilateral microinjections of lidocaine (**Chapter 6.2**).

Aims and outline of the thesis

The present thesis is based on the results of electroencephalographic examination of normal and paroxysmal electrical brain activity recorded in cortex and thalamus in a genetic model of absence epilepsy (WAG/Rij rats). All individuals of this strain exhibit spontaneous spike-wave discharges (SWD), which are the prominent EEG hallmarks of absence epilepsy. According to the widely accepted *cortico-reticular* theory [Gloor, 1969; Kostopoulos, 2000; Meeren et al., 2005], SWD are derived from spindle oscillations. In this thesis we provide some cons and pros to this theory, we describe and compare basic EEG properties of spindle oscillations and SWD, we also examine thalamo-cortical mechanisms and probable generic relationship between spindle oscillations and SWD. Spindles are classified into anterior and posterior types based on their EEG features and topographic distribution (**Chapter 2.1**). Thalamo-cortical mechanisms underlying anterior and posterior sleep spindles are presented in **Chapter 2.2**. Particular attention is given to the role of the thalamus in the two spindle types, because thalamic circuits are thought to be primarily involved in sleep spindles [Spencer and Brookhart, 1961; Morin and Steriade, 1981; Steriade, 1993, 2003, 2005; Steriade and Llinas, 1988].

As known, WAG/Rij rats exhibit two types of spike-wave paroxysms - generalized SWD type I and local occipital SWD type II [van Luijtelaar and Coenen, 1986]. The two types of SWD differ in frequency and amplitude and also have a different pharmacological profile [Midzianovskaia et al., 2001]. SWD I are the true absence epileptic discharges, whereas SWD II do not seem to have clinical correlates. Neuronal mechanisms of SWD II and their relation to the generalized absence seizures remain unknown. **Chapter 3** examines and compares electrographic features of SWD I and SWD II in spatially and functionally segregated parts of the cortico-thalamic system. **Chapter 3.1** describes EEG profiles of SWD I and SWD II (e.g. the EEG waveforms of the two types of

spike-wave paroxysms) as recorded in cortex and thalamus. **Chapter 3.2** illustrates that SWD I and II can be distinguished by adrenergic controlling mechanism.

It has been suggested that anterior sleep spindles are transformed into a generalized type I SWD and posterior sleep spindles - into a local occipital type II SWD [van Luijtelaar, 1997]. A generic relationship between sleep spindles and SWD has been suggested based on outcomes in the feline penicillin model [Gloor, 1969; Steriade et al. 1994; Kostopoulos, 2000], but there are some doubts about the pro-epileptogenic nature of spindle oscillations [Pinault, 2006]. Besides sleep spindles, the rat's somatosensory system produces another spontaneously occurring 5-9 Hz rhythm which significantly differs from spindle oscillations [Pinault et al, 2005]. These medium-voltage 5-9 Hz oscillations precede SWD in GAERS (precursors of SWD, Pinault et al, 2001; 2005]. **Chapter 3.3** examines precursor activity of SWD I in WAG/Rij rats, elaborates their electrographic features and thalamo-cortical network mechanisms. **Chapter 4** tests the validity of Gloor's theory (1969, 1978) on the functional relation between SWD and sleep spindles. Recent investigations in animal models support an alternative to Gloor's point of view, namely, that SWD and sleep spindles are independent phenomena. Indeed, the thalamus (thalamic neuronal circuits) plays a primary role in triggering sleep spindles, while processes in the neocortex (e.g., large-scale synchronization and hyperaxatability of cortical neurons) are crucial in initiating and sustaining SWD [Steriade and Deschênes, 1984; Steriade and Llinás, 1988; Steriade et al. 1994; Steriade, 2001; refs in Destexhe and Sejnowski 2001]. In the rat model, a focus of SWD was detected in the somatosensory cortical area [Meeren et al., 2002; Meeren et al., 2005] confirmed by Manning et al. (2003; 2004) and Richards et al. (2003). Altogether this suggests that the thalamo-cortical network mechanisms of SWD and sleep spindles are different. In order to disclose these differences (**Chapter 4.1**), first, EEG properties of SWD (type I and II) and sleep spindles (anterior and posterior) are compared with the aid of EEG power spectrum analysis. Second, thalamo-cortical network mechanisms underlying anterior sleep spindles and SWD I are described using power spectrum and cross-correlation analyses. **Chapter 4.2** presents a neuronal model, which simulates the waveform of local field potentials of sleep spindle and SWD. This model is used to examine neuronal mechanisms in the cortex, such as spatiotemporal summation of trans-membrane currents and neuronal synchronization, which are responsible for the occurrence of sleep spindles and SWD and also for the probable transformation 'spindles → SWD'. A relationship between anterior sleep spindles and SWD I is further examined in **Chapter 4.3** using continuous wavelet transform. In all, **Chapter 4** aims to disclose what processes in the thalamo-cortical network

Several modern computational techniques and advanced methods of EEG analysis are used to extract 'hidden' information from the EEG in order to localize the source of SWD and to anticipate the onset of 'absences' as early as possible (in rats, Meeren et al., 2002; Refs for human data in Mormann et al., 2007). In order to characterize functional coupling in cortico-thalamo-cortical circuitry at the onset of SWD in **Chapter 5.1**, we employ EEG coherence as a traditional frequency domain measure of linear correlations between two EEG channels. Furthermore, in **Chapter 5.2** we use linear Granger causality in order to identify the coupling strength and directionality of information transport between frontal cortex and thalamus at the onset and at the end of SWD.

The two abovementioned theories, e.g. the Gloor's theory [Gloor, 1969; Kostopoulos, 2000] and Meeren's theory [Meeren et al., 2002; Meeren et al., 2005] stress the crucial role of the cortex in absence epilepsy. Gloor's theory suggests that a diffuse increase of neuronal excitability in the cortex causes the gradual transformation of thalamically generated spindle activity into SWD. Meeren's theory suggests that a local cortical zone triggers SWD and does not consider sleep spindles as to putative precursors of SWD. Recent studies in GAERS provided strong evidences that SWD are preceded by the medium-voltage 5–9 Hz oscillations [Pinault et al., 2001] produced by the somatosensory part of thalamo-cortical system and launched by the frontoparietal cortex [Pinault, 2003; Pinault et al., 2006]. The current thesis concentrates on the local cortical mechanisms of SWD type I (**Chapter 6**). **Chapter 6.1** demonstrates that the fast EEG components are present in the local frontal and parietal cortical regions at the onset of SWD (type I), thus indicating enhanced processes of epileptogenesis in these cortical areas. **Chapter 6.2** shows that deactivation of the local area in the SmI affects the occurrence of SWD I. General Discussion (**Chapter 7**) describes the local and global important role cortical SWD I, thalamo-cortical network mechanisms of SWD I and SWD II and sleep spindles. Table 1.2 sums up topic problems addressed in the current thesis.

Table 1.2. Thesis outlines and references to the published materials

	Topic problems (numbered issues are addressed in Chapter 7 "General discussion")	Thesis	Published form
Sleep spindles			
1	EEG analysis of sleep spindles in WAG/Rij rats. Similarities and distinctions between anterior and posterior sleep spindles.	Chapter 2.1	(1) Sitnikova E, van Luijtelaar G. *Sleep-Wake in the Netherlands,* 2003, 14, 76-79
2	Thalamo-cortical network mechanisms of anterior and posterior sleep spindles (analyses of cross-spectrum and cross-correlations).	Chapter 2.2	(2) Sitnikova E, van Luijtelaar G. *Sleep-Wake in the Netherlands*, 2005, 16, 133-136 and 137-140
SWD			
3	SWD in WAG/Rij rats (average EEG waveform analysis). (1) The electroencephalographic profiles of SWD type I and type II in WAG/Rij rats. (2) Correspondence between SWD in WAG/Rij rats and spike-and-wave complexes in humans.	Chapter 3.1	(3) Sitnikova E, van Luijtelaar G. Epilepsia, 2007; 48(12): 2296–2311.
4	Noradrenergic control of SWD I and SWD II. The influence of depletion of noradrenergic neurotransmission (i.p. clonidine injections) on the incidence and properties of SWDs.	Chapter 3.2	(4) Sitnikova E, van Luijtelaar G. *Brain Res Bull.* 2005; 64(6): 533-540
5	The role of the thalamus in SWD I and SWD II.	Chapters 3.1, 3.2	(3) and (4)
6	Precursor activity of SWD I (EEG power spectrum and coherence analyses): amplitude-frequency characteristics and thalamo-cortical network mechanisms of seizure-precursors and subsequent SWD I.	Chapter 3.3	(5) Sitnikova E, van Luijtelaar G. *Epilepsy Res., 2008* (submitted)
Sleep spindles and SWD			
7	Distinctions between SWD and sleep spindles disclosed with time-frequency EEG analysis	Chapters 4.1, 4.3	(6) Sitnikova E, van Luijtelaar G, *Epilepsia*. 2003. 44(Suppl. 8) P147. 72 (Abstract)
8	Neuronal network mechanisms of sleep spindles and SWD. Intracortical neuronal processes underlying occurrence of sleep spindles and SWD (computational network modeling).	Chapter 4.2	(8) Sargsyan A, Sitnikova E, Melkonyan A, Mkrtchian H, van Luijtelaar G. *J Neurosci. Methods*. 2007; 164(1): 161-176
9	Relationship between SWD I and anterior sleep spindles: their EEG structure disclosed with continuous wavelet transform and further implication	Chapter 4.3	(7) Sitnikova E, Hramov A, Koronovsky A, van Luijtelaar G, *J Neurosci. Methods* 2008 (submitted)
Cortical and thalamic network mechanisms of SWD (type I)			
10	Cortico-cortical and cortico-thalamic network synchronization at the onset of SWD (analysis of EEG coherence)	Chapter 5.1	(9) Sitnikova E. van Luijtelaar G., *Epilepsy Res.* 2006; 71(2-3): 159-180
11	The local and global role of the somatosensory cortex in the initiation of SWD I	Chapters 6.1, 6.2	(3) (10) van Luijtelaar G, Sitnikova E. *Neurosci Biobehav Rev.* 2006; 30(7): 983-1003. (Review paper) (11) Sitnikova, van Luijtelaar. *Brain Res.* 2004; 1012(1-2): 127-137
12	Interactions between thalamus and cortex during SWD (type I) examined with traditional methods (cross-correlation, grand average EEG, coherence) and novel approach (Granger causality for causal relations)	Chapter 5.2 (Chapters 4.1, 3.1, 5.1)	(12) Sitnikova E, Dikanev T, Smirnov D, Bezruchko B, van Luijtelaar G. *J Neurosci. Methods* 2008; 170(2): 245-254;
13	Methodological considerations and technical questions	Chapter 7	

Chapter 2
Electroencephalographic characterization of sleep spindles in WAG/Rij rats*

CONTENTS

ABSTRACT

The present Chapter describes the time-frequency characteristics of anterior and posterior sleep spindles as recorded during non-REM sleep in WAG/Rij rats. Anterior sleep spindles (frequency about 11 Hz) were expressed in the frontal EEG and posterior sleep spindles (frequency about 10 Hz) in the occipital EEG. In the cortex, the amplitude of anterior spindles was higher than those in posterior spindles. The same amplitude difference was found in the thalamus, i.e., in the ventroposteromedial nucleus (VPM) and, to a lesser extent, in the reticular thalamic nucleus (RTN). The power spectrum of thalamic sleep spindle activity revealed a relatively high contribution of *theta*. As compared to pre-spindle background EEG, anterior sleep spindles showed more power in *delta-theta-alpha* bands in the cortex and more *alpha* activity in the thalamus; posterior sleep spindles had more *alpha* activity in the occipital cortex and less *delta* activity in the thalamus.

Analysis of thalamo-cortical associations was performed in the frequency domain (cross-spectrum) and in the time domain (cross-correlation). A strong functional coupling between the frontal cortex, the VPM and the RTN was found during anterior sleep spindles. A cross spectrum analysis demonstrated strong intracortical and intrathalamic associations in the frequencies of 2-3 Hz, 8-10 Hz and 11-12 Hz, but thalamo-cortical associations were restricted to 11 Hz. During posterior spindles, limited associations were found in intracortical and intrathalamic EEG pairs (centered at 9-10 Hz), whereas the RTN and the occipital cortex were associated in the non-spindle frequency of 7-8 Hz. The following conclusions were drawn: (1) in comparison to the pre-spindle EEG, both spindle types displayed higher *alpha* activity in the characteristic cortical areas; (2) the quantitative and qualitative power spectrum parameters of anterior and posterior sleep spindles differ in the cortex and also in the thalamus;(3) the source of distinction between the two spindle types might lie in the RTN.

In general, it is found that anterior and posterior sleep spindles differ in respect to thalamo-cortical interactions, suggesting that the two spindle types are generated in different oscillatory networks and distributed over different cortical areas. Altogether this results in a characteristic topography of sleep spindles.

---

* Adapted after:

Sitnikova E., van Luijtelaar G. Anterior and posterior sleep spindles in rats: a spectral analytical approach. Sleep-Wake research in the Netherlands, 2003; 14: 76-79.

Sitnikova E., van Luijtelaar G. Thalamic and cortical correlates of sleep spindles in rats. Sleep-Wake research in the Netherlands, 2005; 16: 137-140.

Sitnikova E, van Luijtelaar G. Evolution of anterior and posterior sleep spindles in rats. Sleep-Wake research in the Netherlands, 2005; 16, 133-136.

Sitnikova E., van Luijtelaar G. Thalamo-cortical mechanisms of various types of sleep spindles in rats. Int. J. Psychophysiol.; 2004, 54(1-2): 169 (Abstracts of the 12-th Word Congress of Psychophysiology, Porto Carras, Greece, September 18-23, 2004).

INTRODUCTION

Sleep spindles are a heterogeneous group of EEG oscillations, which show remarkable differences in frequency, in time-evolution, in reaction to drugs and in occurrence in the circadian phase. Gibbs and Gibbs (1950) were the first who mentioned a specific spatial distribution of sleep spindles over the cortex. More recently, McCormick et al. (1997) elaborated the topography of visually scored sleep spindles in healthy humans and demonstrated a maximal spindle amplitude in central EEG leads. A power density of the non-REM sleep EEG in the frequencies of sleep spindles showed two distinct peaks at 12.0 and 14.0 Hz [Jobert et al., 1992] or at 11.5 and 13.0 Hz [Werth et al., 1997]. The first peak (~ 12 Hz) was localized in the frontal area and the second peak (~14 Hz) in the central and occipital regions [Jankel and Niedermeyer, 1985; Jobert et al., 1992; Werth et al., 1997; Zygierewicz et al., 1999; Anderer et al., 2001]. Based on this information, sleep spindles were divided in two types, i.e., frontal and centro-parietal sleep spindles. In animals, the topographical distribution of sleep spindles has not been studied in such details as in humans, because of the limited number of EEG channels available in animals and of the insufficiency of EEG mapping techniques. The topography of sleep spindles in rats has only been studied by the group of Gottesmann [Terrier and Gottesmann, 1978; Gandolfo et al., 1985] as well as in cats by Destexhe and Sejnowski (2001) and by Steriade (2003). It seems likely that basic mechanisms of sleep spindles in humans and animals are principally the same, but a comparison based on topographical distributions of sleep spindles in animals is lacking. Indeed, in Wistar rats anterior sleep spindles are most intensive in the primary motor cortex (Krieg's area 4, 6, 10), while posterior sleep spindles predominantly occur in the associative (visual) area 18a [Terrier and Gottesmann, 1978; Gandolfo et al., 1985]. Anterior and posterior sleep spindles were described in outbred Wistar and in WAG/Rij rats [Gandolfo et al., 1985; van Luijtelaar, 1997]. Kandel and Buzsaki (1997) also mentioned that *'sleep spindles are more restricted spatially and can occur in isolation in various cortical areas'* (p. 6789). However, these authors did not perform a systematic analysis of EEG topography of spindle activity.

One of the most widespread and trusted method of EEG analysis in the frequency domain is power spectrum estimation using a standard Fast Fourier Transform (FFT). Power spectrum analysis has been used in clinical EEG research, for instance, for the study of topographic differences of sleep spindles in the frequency domain of the human EEG [e.g., Jobert et al., 1992; Werth et al., 1997]. In **Chapter 2.1** an FFT was used in order to examine the EEG properties of the two types of (anterior and posterior) spindles in WAG/Rij rats. In the present analysis, sleep spindles were identified visually, because the EEG morphology of spindles is best perceived by visual analysis. Visual detection of sleep spindles is widely used in practice. Furthermore, in **Chapter 4.2,** the recognition of sleep spindle is computerized with the aid of the continuous wavelet transform.

Sleep spindles are generated by a thalamo-cortical network that involve neurons in the reticular thalamic nucleus, thalamo-cortical cells in the relay thalamic nuclei and cortical cells (see **Chapter 1.2**, Fig. 1.2). GABA-ergic neurons of the RTN are known to be primarily involved in the generation of spindle sequences acting as a pacemaker cells [Steriade et al., 1993; Steriade and Llinas, 1988; refs in Destexhe and Sejnowski, 2001; Steriade, 2003]. The question arises weather the RTN plays the same role in anterior and posterior sleep spindles. Here, the electrical activity in the cortex and in the specific thalamus (the ventroposteromedial nucleus of thalamus, VPM) and the RTN was examined and compared during the two spindle types.

Investigators of sleep spindles in animals and in humans use different approaches and their results cannot be easily compared. Animal studies are directed towards neuronal mechanisms of sleep spindles (such as membrane and channel properties, electrical current in neuronal networks), while studies in humans often use brain imaging techniques, such as scalp EEG recordings and MEG, and localize electrical sources of spindle activity. However, they tend to disregard subcortical neuronal sources of sleep spindles [Anderer et al., 2001; Ishii et al., 2003; Shih et al., 2000]. There is only one unique source localization study in human EEG in which two discrete sources in the thalamus were found to be responsible for two spindle types [Ueda et al., 2000]. However, no further investigations were performed in order to confirm and disprove these results. It is still questioned whether two local spindle types have a common source (most likely in the thalamus), or whether they have separate sources.

As known, there are only sparse anatomic and functional connections between anterior and posterior areas of the cortex. Probably, each cortical area sustains a specific type of sleep spindles, so that EEG properties of local spindles of differential locations may be slightly different. The present Chapter examines EEG properties of anterior and posterior sleep spindles at the cortical and thalamic level (VPM and RTN), whereas **Chapter 2.2** examines the relationship between cortical and thalamic counterparts during anterior and posterior sleep spindles with a cross-spectrum analysis.

It is known that different parts of the specific thalamus send terminals to different cortical areas, which implies the existence of functionally independent thalamo-cortical circuits. These circuits may produce local sleep spindles with different features. For instance, in Wistar rats, anterior sleep spindles are localized in the

somatosensory and motor cortex [Terrier and Gottesmann, 1978], and these areas are known to receive dense projections form the ventrobasal complex of the thalamus [Kolb, 1990], while posterior sleep spindles are present in the occipital visual cortex [Terrier and Gottesmann, 1978], which is related to *the lateral geniculate nucleus*. In the current thesis attention is paid to the VPM, since this nucleus densely innervates frontal and parietal areas of the neocortex and might be particularly involved in the generation of anterior sleep spindles. The VPM does not have direct projections to the occipital cortex, therefore, it is not expected that the VPM will be involved in posterior sleep spindles. In this Chapter the role of the RTN and VPM in both spindle types is investigated, firstly, by measuring the amplitude of electrical activity; secondly, by means of power spectrum analysis of the thalamic and cortical activity; and, thirdly, by the analysis of cross-correlations between cortex, VPM and RTN. It is also hypothesized that the occurrence of each spindle types is associated with specific frequency modulation of the background EEG. In **Chapter 2.1** changes in EEG power over *delta*, *theta* and *alpha* bands that accompany the transition towards either anterior or posterior sleep spindles, are defined.

METHODS

Animals

Experiments were performed on nine male 11-12 months old WAG/Rij rats (body weigh 320-360 g). Animals were born and raised in the laboratory of the Department of Biological Psychology of the Radboud University Nijmegen. Rats were kept in pairs in standard cages with food and water available *ad libitum* and maintained on a 12-12h light-dark cycle (white light on at 18:00). After surgery, housing conditions were the same except that rats were housed individually. Distress and suffering of animals were minimal. The experiments were conducted in accordance with the regulation of animal experimentation in the Netherlands and were approved by the Ethical Committee on Animal Experimentation of the Radboud University Nijmegen (RU-DEC).

Surgery procedure and histological control

Rats were chronically implanted with six still stainless electrodes for monopolar recordings (two sets of tripolar electrodes Plastic One Inc. Roanoke, VI, USA: MS 333/2A, diameter 0.125 mm). Two epidural electrodes were located over the frontal (AP 2; L 2.5) and occipital (AP -7; L 6) cortical areas (Krieg's areas 6 and 18A in which anterior and posterior spindle occur with the highest probability [Terrier and Gottesmann, 1978]). Two depth electrodes were implanted in the ventroposteromedial nucleus of thalamus (VPM, AP –3.5; L 2.5; H 7.2) and in the rostral pole of the reticular thalamic nucleus (RTN, AP –1.5; L 2.2; H 7.2). The remaining two electrodes were placed symmetrically over both sides of the cerebellum and used as ground and reference electrodes. All coordinates are given in mm relative to bregma [Paxinos and Watson, 1986].

Surgery was performed under isoflurane anesthesia, while body temperature was monitored and maintained at 37°C with a heating pad. For post-surgery analgesia rats received a 0.1 mg/kg i.m. injection of 0.324 mg/ml buprenorfinehydrochloride (Temgesic®, Reckitt & Colman Products Ltd., Kingston-Upon Hull, UK). After that, animals were allowed to recover for at least 10 days.

Post mortem histological control was performed to verify the positioning of depth electrodes. Rats were deeply anesthetized with an overdose of sodium pentobarbital (Nembutal, 60 mg/kg i.p.) and small electrolytic lesions were made through the recording electrodes (DC current 10 μA, 10 sec). Next, animals were intracardially perfused with 0,9% NaCl followed by 4% paraformaldehyde (pH=7.3). Then, brains were removed, kept in the same fixative for 24 hours and transferred into 30% buffered sucrose. Serial coronal sections 60 μm were cut in a cryostat at – 20° C and stained with 0.1% cresyl violet. Location of electrodes was established referring to Paxinos and Watson atlas of the rat brain (1986).

EEG recording

The EEG was recorded in freely moving rats in a noise-isolated Faraday cage during 5-7 hours in the dark period of the light-dark cycle. Rats were habituated to the recording procedure and to Plexiglas recording cages (25 cm X 30 cm width, 35 cm high) for two hours. Recording session started the next day. Animals returned to the same cages and recordings of the EEG were made simultaneously with behavioral observations.

EEG signals were fed into a multi-channel differential amplifier via a swivel contact, band-pass filtered between 1-500 Hz, digitized with 1024 samples/second/per channel (Data Acquisition Hardware and Software, DATAQ Instruments, Inc., Akron, OH) and stored on hard disk.

EEG pattern identification

Sleep spindles were selected in the EEG during slow-wave sleep (intermediate stage of sleep was not included). Sleep spindles were identified visually during non-REM sleep using formal criteria [IFSECN, 1974;

Steriade et al., 1993]. To put more accuracy in spindle detection, raw cortical EEGs were additionally 5-15 Hz band-pass filtered, which was recommended by Schimicek et al. (1980). Sleep spindles were recognized as having a regularly shaped sinusoidal form with a spindle-like envelope and a minimal duration of 500 msec. The amplitude of sleep spindles exceeded the background of more than two times (Fig. 2.1). We evaded generalized sleep spindles, i.e., those that appeared simultaneously in the frontal and occipital EEG, and only focused on local sleep spindles. Anterior sleep spindles were present on the frontal EEG, but not in the occipital EEG. Oppositely, posterior sleep spindles were only present only in the occipital EEG. All local sleep spindles were marked in the full-length EEG and 30-70 representatives of each spindle type in each animal were used for statistical analysis.

EEG analysis

Data analysis was performed on 700 ms epochs with anterior sleep spindles, and on 500 ms epochs with posterior spindles. The chosen epoch lengths correspond to the mean duration of each spindle type (Table 1). 700-ms epochs that precede spindle activity (pre-spindle EEG) starting on 1.4 sec before spindle onset were selected as the (non-oscillatory) background EEG (40 samples per animal).

Hanning windowed Fast Fourier Transform (FFT) with 0.25 Hz resolution was used to compare the EEG frequency profile of anterior sleep spindles, posterior sleep spindles and the pre-spindle EEG. Power spectra were averaged per channel, per spindle type and per animal. The power spectra were computed for all recording sites using the *full* spectrum, $P_{full}(\omega)$. A power spectrum was defined as the square modulus of FFT with a complex conjunction between the real and imaginary parts of FFT function [Challis and Kitney, 1991].

$P_{full}(\omega) = F(\omega) * F(\omega) = |F(\omega)|^2$ where $F(\omega)$ is the Fourier transform; ω - discrete frequencies and * - complex conjunction.

The following quantitative parameters were measured in the power spectrum of sleep spindles: (i) peak frequency, i.e., mean frequency of each spindle type at its proper cortical area, (ii) total EEG power in the cortex and in the thalamus, (iii) EEG power in the frontal and occipital cortex in the selected frequency bands: 1-4.5 Hz (*delta*), 7.5-9 Hz (*theta*), 9-12 Hz (*alpha* was also divided in two sub-bands 9-10.5 Hz $alpha_{low}$ and 10.75-12 Hz – $alpha_{high}$).

The waveforms of the power spectra in different EEG channels were compared after eliminating amplitude differences between frontal, occipital and thalamic channels. EEG power was normalized by the maximum amplitude value at each spectrum.

In order to assess the linear synchronization between two EEG channels in the frequency domain, we computed a cross-spectrum (a normalized version of cross-spectrum is the ordinary coherence). A cross-spectrum measures a correspondence between power densities in the selected EEG channels [Bronzino, 1984; Lopes da Silva et al., 1986],

$CS_{ch1,ch2}(\omega) = \Sigma\, P_{compl\ ch1,i}(\omega) \times P_{compl\ ch2,i}(\omega)$ where $CS_{ch1,ch2}(\omega)$ is the cross-spectrum between selected channels (ch1 and ch2); $P_{compl\ ch1,i}(\omega)$ and $P_{compl\ ch2,i}$ are the complex power spectra of selected channels; *i* is the number of individual sleep spindle; ω are discrete frequencies.

The cross-spectra (μV^2) were computed in six electrode pairs: fronto-occipital (intracortical), VPM-RTN (intrathalamic) and in four possible cortico-thalamic pairs. Cross-spectrograms were further analyzed for the presence of peaks in the frequency domain. Also the absolute amplitudes of cross-spectral densities were analyzed. These numerical data were used to describe frequency-specific strength of coupling between the chosen EEG channels.

A cross-correlation function was used to measure the linear correlation between two signals as a function of their time delay [e.g., Quian Quiroga et al., 2000; Pereda et al., 2005]. This function ranges from -1 (complete linear inverse correlation) to +1 (complete linear direct correlation). If *x(t)* and *y(t)* are normalized signals with zero mean and unit variance, their cross-correlation function is:

$C_{x,y}(\tau) = \frac{1}{N-\tau}\sum x(k+\tau)y(k)$ where N is the total number of data points (the size of time window) and τ is the time lag between the signals. We examined cross-correlations in fronto-occipital (intracortical), VPM-RTN (intrathalamic) and in four cortico-thalamic pairs. Examples of the cross-correlation functions are shown in Fig. 2.9A. We will come back to cross-correlation analysis in **Chapter 4.1**, in which in particular Fig. 4.5 presents an average cross-correlation function for anterior spindles and for the waking EEG.

EEG analysis was performed with Brain Vision Analyser, © BrainProducts GmbH.

Statistical analysis

The results are expressed as mean ± SD. Analysis of variance (ANOVA) was used to analyze the distribution of EEG power density (= spectral power) with two factors: 'spindle-types' and 'frequency band'. Fisher LSD test was used for *post-hoc* analysis. General parameters of sleep spindles (e.g., duration, mean frequency, total amplitude) were compared using paired t-tests. In all cases, the level of significance was $p < 0.05$.

RESULTS

Local amplitude-frequency parameters of anterior and posterior sleep spindles: frequency domain (Fourier) analysis

General EEG characteristics of sleep spindles

Anterior sleep spindles were identified in the frontal EEG, but only when concomitant spindle activity was absent in the occipital EEG. Similarly, posterior sleep spindles were identified in the occipital EEG (Fig. 2.1) in cases when anterior spindling was absent.

Histological examination showed that in five out of nine rats one depth electrode was placed in the RTN, while in eight out of nine rats the second electrode was positioned in the VPM. EEG data from animals with misplaced electrodes were excluded. Cortical spindle activity (both anterior and posterior spindles) was rarely accompanied by spindle-like counterparts in the thalamus (Fig. 2.1). Both spindle types were preceded by virtually the same pre-spindle activity. No differences in EEG power spectrum were found immediately prior to anterior and posterior spindles. Therefore, we combined pre-spindle epochs of both spindle types and used them as a common 'background' activity for forthcoming spindles.

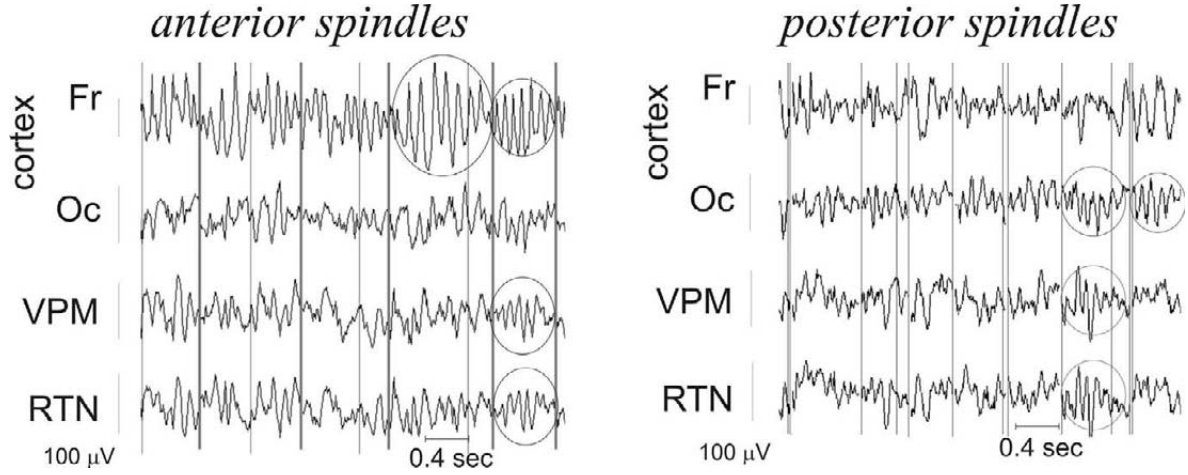

Figure 2.1. Two types of sleep spindles as recorded in WAG/Rij rat (male, six months old). Anterior and posterior spindles are indicated by circles. Anterior spindles are present in the frontal EEG channel (Fr) and posterior spindles in the occipital channel (Oc). Spindle oscillations are either present or absent in the thalamus (VPM – ventroposteromedial thalamic nucleus; RTN – reticular thalamic nucleus).

Anterior sleep spindles are distinguished from posterior spindles by a lower frequency and a longer duration (Table 2.1). Besides, anterior sleep spindles appeared more frequently than posterior spindles.

Table 2.1. Basic quantitative parameters of sleep spindles (mean ± S.D., n=9 rats)

	Total number of events	**Duration**, sec	**Frequency**, Hz	**Total EEG power**, μV^2	
				frontal cortex	occipital cortex
anterior spindles	445	0.68 ± 0.08	11.14 ± 1.02	11.3 ± 1.7	4.2 ± 0.6
posterior spindles	313	0.59 ± 0.07 *	10.16 ± 0.88 *	7.3 ± 1.6 *	8.6 ± 2.1 *

* significant differences between anterior and posterior sleep spindles, paired t-test, $p<0.05$.

Qualitative EEG power spectrum analysis

The power spectrum of anterior sleep spindles as recorded in the frontal cortex displayed an elevation between 9 - 13 Hz (peak ~ 11 Hz, Fig. 2.2A). Power spectra of posterior spindles and pre-spindle EEG of the frontal EEG were very congruent; both of them were flat and showed a gradual downward slope. In the occipital cortex, posterior sleep spindles showed an elevation in the *alpha* frequencies (8-12 Hz) and a protruded peak in ~ 10 Hz (Fig. 2.2B), but power spectra of anterior spindles and pre-spindle EEG were virtually identical.

In contrast to what was found in the cortex (Fig. 2.2A,B), the power spectrum of sleep spindles in the thalamus (Fig. 2.3C) revealed moderate power in the *alpha* range, whereas the power in *delta* band was high., Power spectra of sleep spindles (both anterior and posterior) in the VPM was similar to that in the RTN.

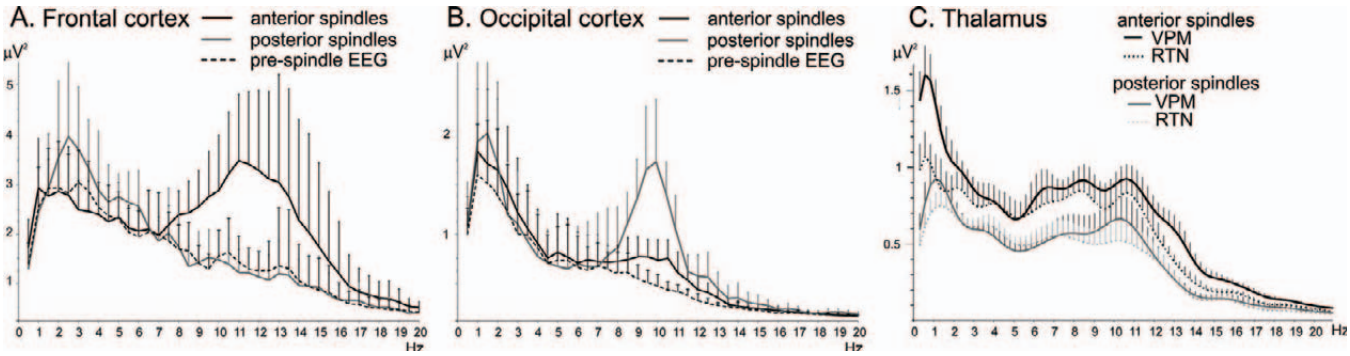

Figure 2.2. Power spectra of sleep spindles and background EEG immediately prior to spindles (pre-spindle EEG) as measured in the cortex (**A**-**B**, mean ± S.D.) and in the thalamus (**C**, mean ± S.E.).

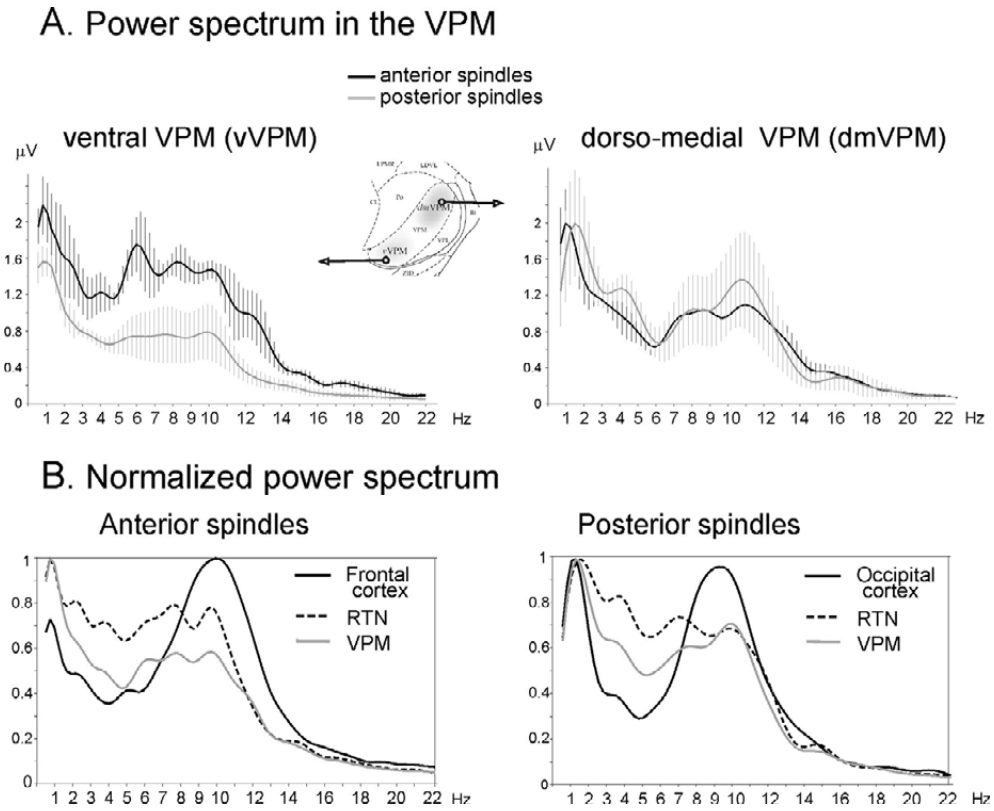

Figure 2.3. Power spectrum of anterior and posterior sleep spindles as measured in the specific areas of the neocortex and in the thalamus. The VPM – the ventroposteromedial thalamic nucleus, (dmVPM, n=3 rats; vVPM n=4 rats and RTN – the reticular thalamic nucleus, n=5 rats). Posterior sleep spindles in the thalamus had a spectral peak ~ 11 Hz, in the occipital cortex it was ~ 10 Hz. Both spindle types showed high *theta* activity in the thalamus.

More accurate revision of electrode positions in the VPM revealed a fine difference across subjects. In five out of eight rats, this electrode was implanted in the ventral part of the VPM (vVPM), and three others in the dorsomedial part (dmVPM). Two spindle types were distinguished by slightly different power spectra in the dmVPM and vVPM (Fig 2.3A). The ~ 11 Hz spectral peak typical for posterior sleep spindles, was present in the vVPM, but was less clear in the dmVPM. Both spindles types had relatively high *theta* activity in the thalamus as compared to the cortex (Fig 2.2 and 2.3).

Quantitative analysis of EEG power spectrum

The total EEG power of the anterior spindles in the frontal EEG was significantly higher compared to the power of the posterior spindles and, *vice versa*, in the occipital EEG, posterior spindles displayed higher total power than anterior spindles (details of ANOVA and *post-hoc* tests are indicated in Fig. 2.4). It is interesting that the total power of sleep spindles as measured in the non-specific cortical areas, i.e., the frontal cortex for posterior spindles and the occipital cortex for anterior spindles, was the same and it did not differ from the power measured during pre-spindle periods. No significant differences were found between the total power of sleep spindles (both types) and pre-spindle epochs in the thalamus, yet these spindle oscillations showed a strong tendency for having a higher power (especially in the VPM).

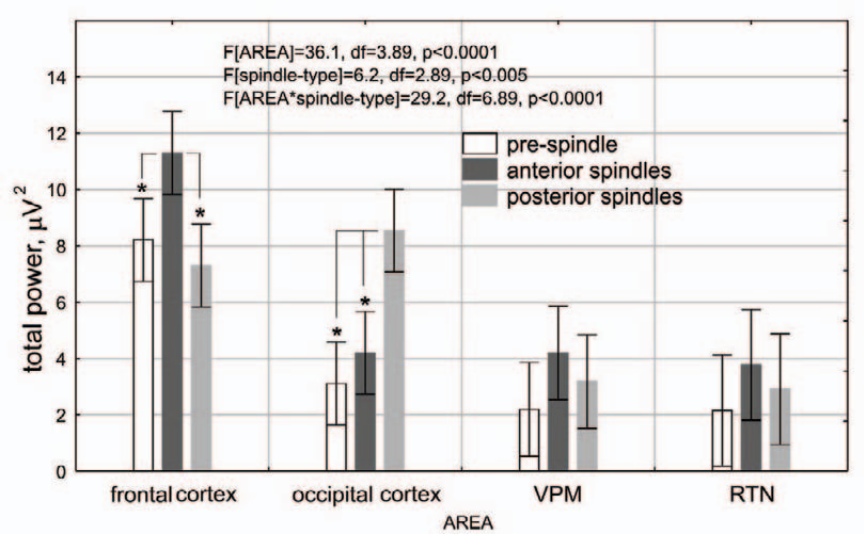

Figure 2.4. Total EEG power of sleep spindles and pre-spindle background EEG (mean ± SD), as measured in the thalamus (VPM – the ventroposteromedial thalamic nucleus; the RTN – the reticular thalamic nucleus) and the cortex.
ANOVA, * - significant differences, *post-hoc* Fisher test.

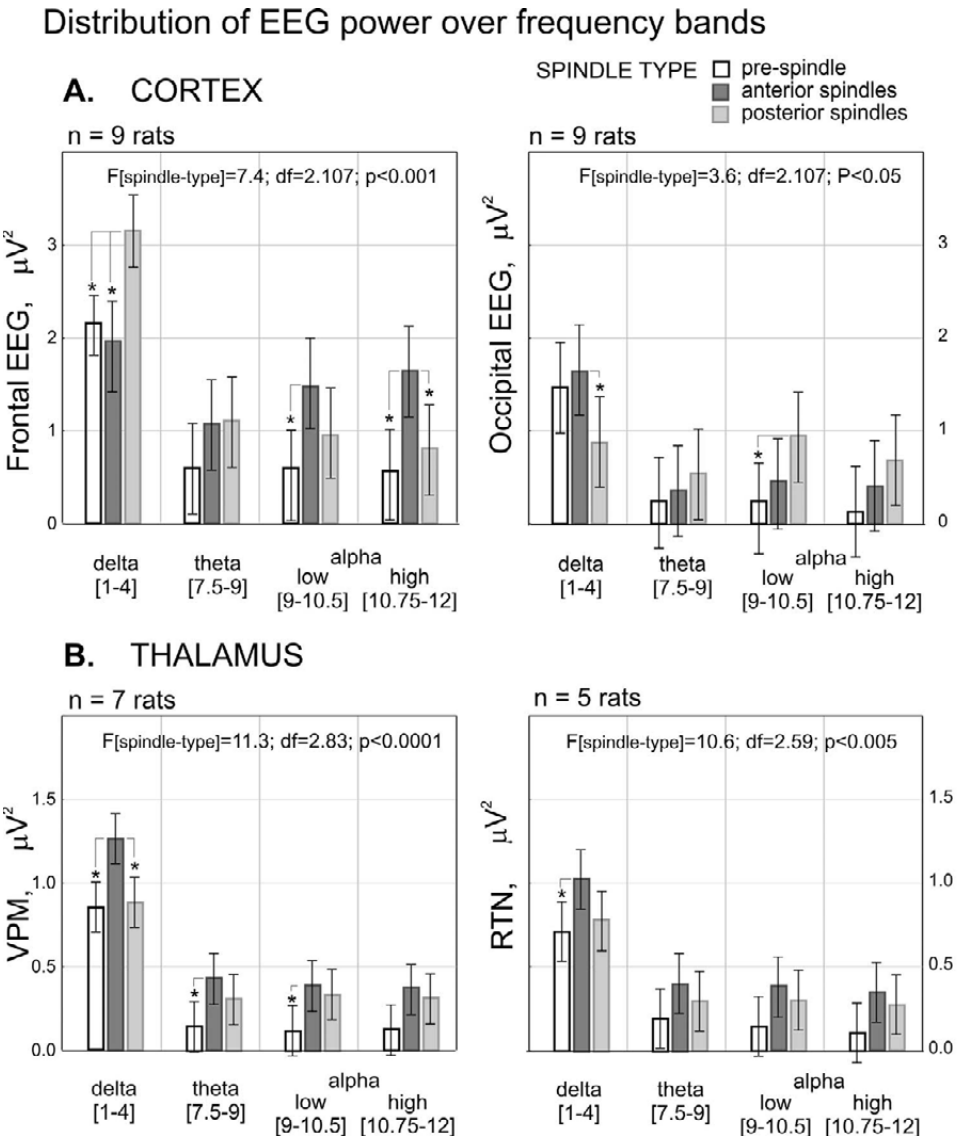

Figure 2.5. Power density in the specific frequency bands in two spindle types and in pre-spindle EEG, as measured in the cortex and the thalamus (mean ± SD). Abbreviations are similar to Fig. 2.4.

In order to examine changes in EEG power that accompany the occurrence of sleep spindles, the power density in the selected frequency bands in pre-spindle epochs and both spindle types was measured and compared (Fig. 2.5). The outcomes of the ANOVA showed that, in each EEG location, two spindle types and pre-spindle epochs showed different distributions of EEG power in the following bands: *delta*, *theta*, $alpha_{low}$ (9-10.5 Hz) and $alpha_{high}$ (10.75-12 Hz). The most significant differences were found in the thalamus (VPM) and in the frontal cortex, but were moderate in the occipital cortex.

Anterior sleep spindles in the frontal cortex (Fig. 2.5A, left graph) showed significantly higher power in $alpha_{low}$ and $alpha_{high}$ sub-bands as compared to posterior sleep spindles and to pre-spindles epochs. No differences were found between posterior spindles and pre-spindles epochs. The power in *theta* band in all investigated phenomena was the same, but the power in *delta* band in the posterior sleep spindles was higher than in the anterior spindles and in the pre-spindles epochs. In the occipital cortex, no significant differences were found between anterior spindles and pre-spindle EEG.

Posterior sleep spindles in the occipital cortex (Fig. 2.5A, right graph) were distinguished from anterior spindles and pre-spindle epochs by having higher power in the $alpha_{low}$ (9-10.5 Hz) and lower power in the *delta* frequencies.

In the thalamus as recorded in the VPM, the power spectra of anterior sleep spindles (but not posterior spindles) were significantly distinguished from pre-spindle epochs. The occurrence of anterior sleep spindles in the VPM was accompanied by an increase of power in *delta*, *theta* and $alpha_{low}$ bands, and the same tendencies were found in the RTN. The power density of posterior spindles in both thalamic nuclei (VPM and RTN) could not be distinguished from pre-spindle EEG.

In Fig. 2.6 we consider the pre-spindle EEG as a common background from which the two spindle types are to emerge. According to our analysis, changes in power band content in transition from pre-spindle to anterior spindle activity were different in frontal cortex and the thalamus; both thalamic nuclei (VPM and RTN) displayed an increase of *delta*, but the frontal cortex expressed higher power in spindle-specific *alpha* band ($alpha_{low}$+$alpha_{high}$). Both frontal cortex and the VPM showed an elevation in $alpha_{low}$ (9-10.5 Hz). Posterior sleep spindles were not accompanied by quantitative changes in the thalamus, being localized in the occipital cortex, these spindles showed a decrease in *delta* and increase in $alpha_{low}$ (9-10.5 Hz).

Altogether this suggests that WAG/Rij rats have two types of local 'area-specific' sleep spindles: anterior spindles with a frequency of 11.1 Hz in the frontal, and posterior spindles in the occipital cortical areas with a frequency of 10.1 Hz. Although both types of sleep spindles showed higher power in *alpha* band as compared to pre-spindle epochs, anterior spindles were accompanied by a broader increase in power densities in the VPM (*delta*+*theta*+$alpha_{low}$), in the RTN (*delta*) and in the frontal cortex ($alpha_{low}$+$alpha_{high}$), but posterior spindles were characterized by an increase in $alpha_{low}$ in the occipital cortex with a limited thalamic contribution. During both spindle types, thalamic counterparts show substantial *delta* and *theta* components. The dorsomedial part of the VPM shows more *theta*, especially during anterior sleep spindles, while the ventral part (vVPM) shows more *alpha*, especially at the presence of posterior sleep spindles.

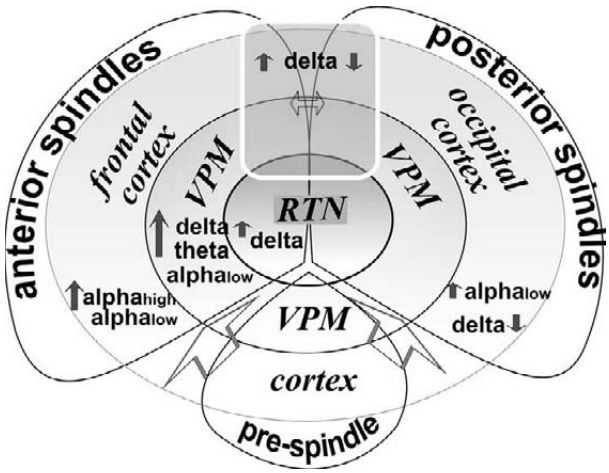

Figure 2.6. Summary of data from Fig 2.5 illustrating the dynamic changes in specific frequency bands: *delta* (1-4 Hz), *theta* (7.5-9 Hz), $alpha_{low}$ (9-10.5 Hz) and $alpha_{high}$ (10.75-12 Hz). Pre-spindle EEG (a common background for both spindle types) is shown in the bottom. A large empty arrow pointing to the left upper corner indicates transformation pre-spindle -> anterior spindles. The symmetric arrow towards the right upper corner indicates the transformation pre-spindle -> posterior spindles. The upper part of the graph (the white rectangular) highlights differences between spindle types.

Thalamo-cortical mechanisms of anterior and posterior sleep spindles

Analysis of cross-spectrum

A cross-spectrum function was computed in order to characterize the strength of synchronization between different parts of the thalamo-cortical circuitry during anterior and posterior sleep spindles. The cross-spectrum is a measure of similarity between power densities of two signals, while the normalized version of cross-spectrum represents the ordinary coherence.

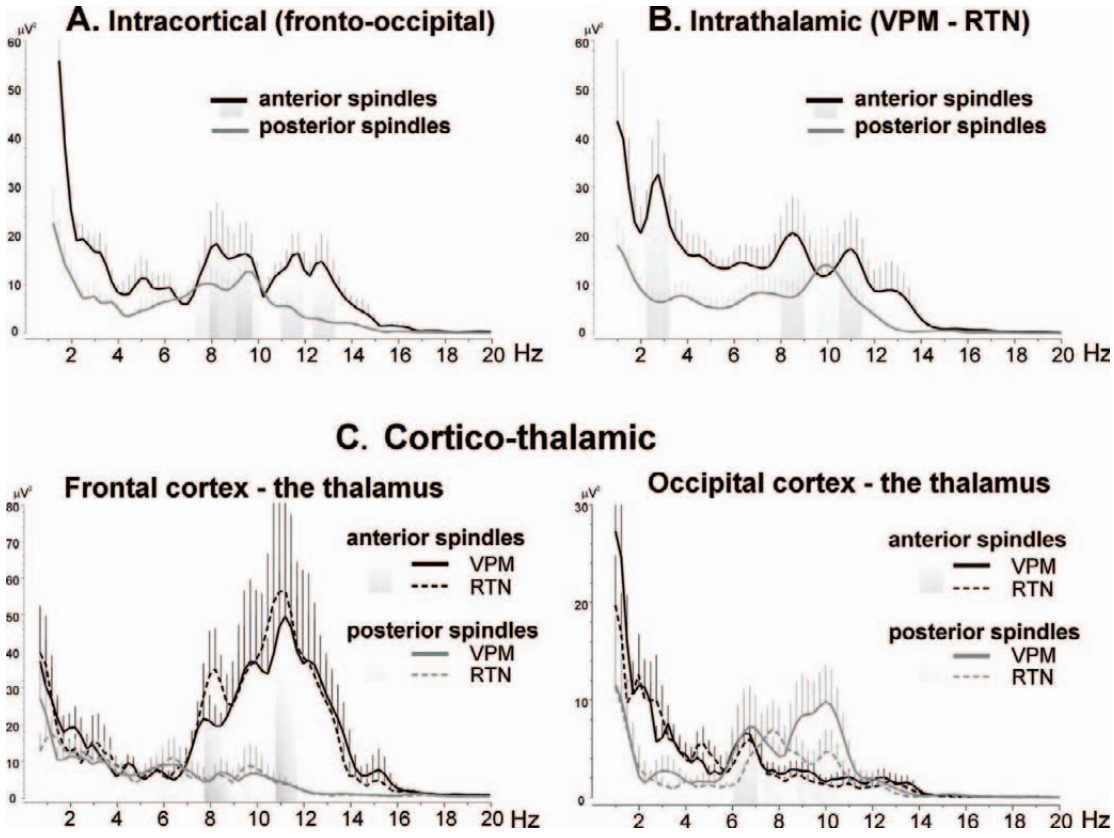

Figure 2.7. Cross power spectra between cortical (frontal and occipital) and thalamic (the VPM – the ventroposteromedial thalamic nucleus and the RTN - the reticular thalamic nucleus) electrodes, mean ± S.E.M.

The averaged cross-spectra were computed in six electrode pairs: fronto-occipital (intracortical), VPM-RTN (intrathalamic) and in the four possible cortico-thalamic pairs (Fig. 2.7). Cross-spectra of anterior spindles between two cortical and two thalamic pairs (black lines in Fig. 2.7A,B) showed a double peak in *alpha* frequencies (8-9 Hz and 11-12 Hz) and high *delta* activity. Cross-spectra of the fronto-thalamic pairs showed a relatively small 8 Hz peak and a high-amplitude 11-12 Hz peak, in contrast to the cross-spectra of the occipito-thalamic pairs, which showed a 6-7 Hz peak (black lines in Fig. 2.7C).

The cross spectra between two cortical and two thalamic pairs during posterior sleep spindles (gray lines in Fig. 2.7A, B) showed an *alpha* peak around 9-10 Hz. Among different cortico-thalamic pairs, the cross-spectrum of 'occipital cortex - VPM' was somewhat peculiar: it revealed two relatively large peaks with a frequency of 7 and 10 Hz. The cross-spectrum characterizing the associations between occipital cortex and RTN, had a prominent 8 Hz peak. Cross spectra in fronto-thalamic pairs were smooth and low-amplitude (gray lines in Fig. 2.7C), which suggested a low association strength between these channels and which also suggested that fronto-thalamic associations did not play a role in posterior spindles.

Figure 2.8 summaries the results of cross-spectral analysis. It shows that anterior sleep spindles are characterized by strong associations in 8.2-8.5 Hz and 11-12 Hz between the frontal cortex, the VPM and the RTN. The presence of 11-12 Hz peaks in cross-spectra 'VPM-RTN' suggests that the generation of spindle rhythm requires strong coupling between these structures. It is intriguing that anterior spindles showed additional peak associations in the thalamus in the 2-3 Hz. Posterior sleep spindles had narrow-band associations restricted to the mean frequency of the posterior sleep spindles (~10 Hz). Power of cross-spectrum in the pair 'occipital cortex - RTN' was low with a peak centered in non-spindle frequency, e.g., 7.8 Hz. Although the RTN is integrated into the thalamo-cortical loop for the production of posterior sleep spindles, its integration is relatively weak and rather peculiar (the occurrence of 7.8 Hz peak in 'occipital-RTN' cross-spectrum).

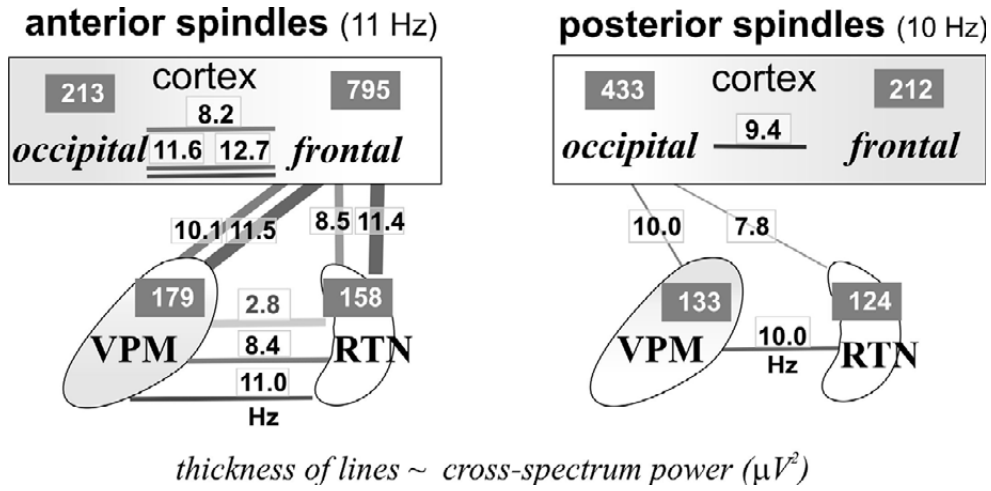

Figure 2.8. Frequency-specific characteristics of functional coupling in the thalamo-cortical circuit during anterior and posterior sleep spindles as defined with cross-spectrum analysis. Black numbers at the connecting lines are the central frequencies of associations (peak frequencies in corresponding cross-spectra, Hz), while the line thickness is proportional to peak power density, μV^2. Total EEG power in each area is shown in gray squares, μV^2.

To generalize, anterior and posterior sleep spindles showed different association patterns between frontal and occipital cortical areas and the thalamus. The thalamo-cortical oscillatory network comprises several (local) circuits and each circuit could produce characteristic type of sleep spindles, which are projected to different cortical areas, resulting in topographical differences of sleep spindles as measured in the cortex. Anterior sleep spindles could be produced in a strongly coupled neuronal network comprising the [RTN] - [VPM] - [frontal cortex]. However, in posterior sleep spindles, functional coupling between the (occipital) cortex and the thalamus (VPM and RTN) is relatively weak. Although the RTN associates with the VPM, it has only weak associations with the occipital cortex in non-spindle frequencies. Therefore a role of the RTN in posterior sleep spindles remains obscure.

Analysis of cross-correlations

Analysis of cross-correlations was performed on the same data set as used for cross-spectral analysis. Anterior and posterior sleep spindles were compared with each other and with the EEG episodes during passive wakefulness.

During passive wakefulness, coefficients of cortico-thalamic cross-correlation, $C_{x,y}$, were high and positive, suggesting a strong in-phase synchronization between the frontal cortex and the thalamus, e.g a direct information flow from the thalamus to the cortex. Frontal cortex constantly lagged both thalamic nuclei with time delay (τ) 1-3 msec and occipital cortex - with τ = 15-25 msec.

The overall pattern of cross-correlation in sleep spindles remarkably differed from that of the waking EEG Cortico-thalamic cross-correlations in both spindle types were complex and comprised three phases, positive-. negative-positive. The negative cross-correlations, which appeared with minimal time delay (τ = 3-5 msec), were weak, suggesting out-of-phase (inverse) associations, while two positive peaks ($\tau \sim$ -28 and +32 msec) were relatively strong (Fig.2.9B), suggesting a strong backward information flow from the cortex to the thalamus (probably, cortico-thalamic feedback).

Cross-correlations between the cortex and two parts of the VPM (vVPM and dmVPM) were distinguished, especially during posterior spindles: (1) no significant cross-correlations were found between the cortex (both frontal and occipital) and the vVPM, (2) cross-correlations 'frontal cortex – dmVPM' were characterized by significantly different τ (53 msec) as compared to that in anterior spindles (43 msec). Altogether this suggests a different functional contribution vVPM and dmVPM in the two spindle types: both the vVPM and dmVPM are involved in the anterior spindles, but only the dmVPM in posterior spindles.

This all means that straightforward relationships thalamus→cortex, which are predominant during wakefulness, seems to be reversed during sleep spindles (Fig.2.9C). In both spindle types, the cortex intensively communicates with the thalamus (cortico-thalamic feedback associations). Cortico-thalamic associations during anterior spindles involve both ventral and dorsomedial parts of the VPM as well as the RTN; they are more

widespread as compared to the more narrow cortico-thalamic associations during posterior spindles (those are centered in the dorsomedial VPM and the RTN).

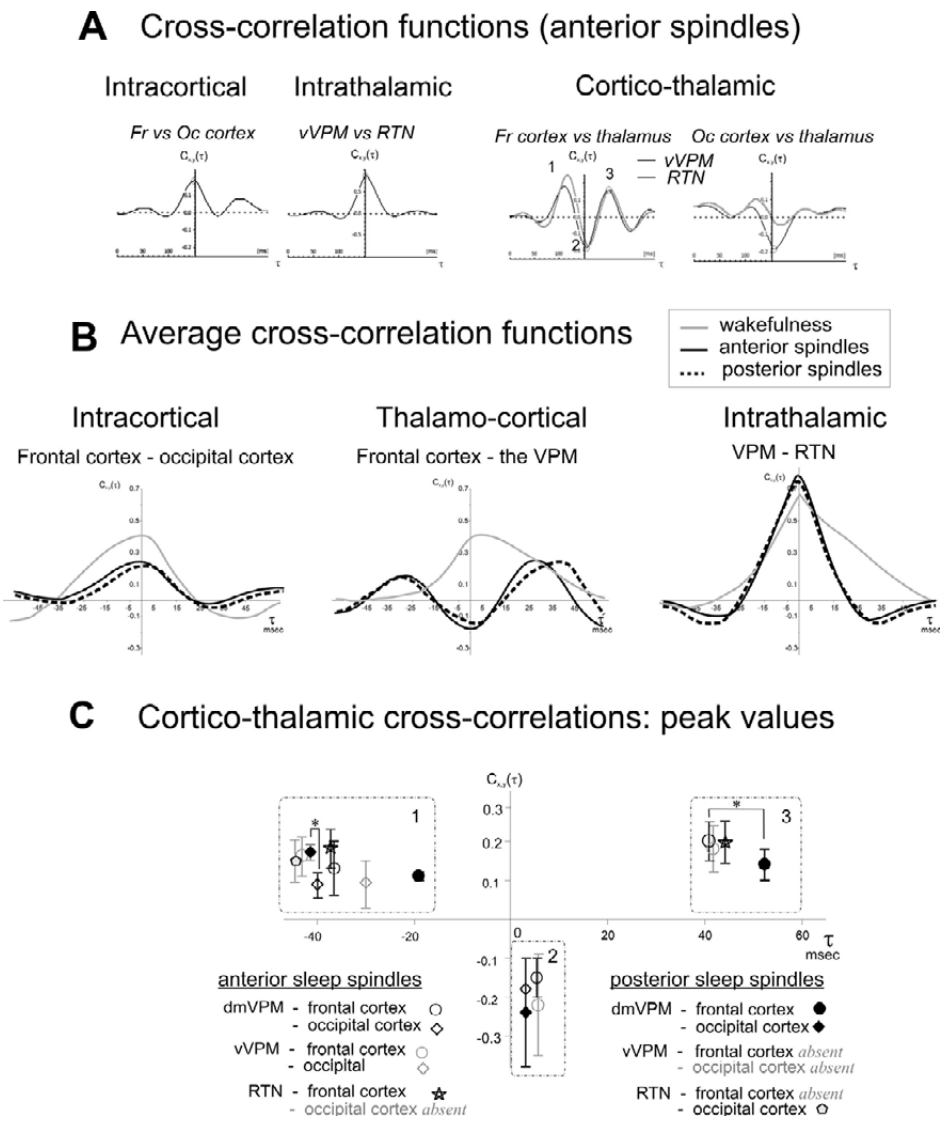

Figure 2.9. Application of cross-correlation analysis for examining cortico-thalamic associations during two types of sleep spindles in WAG/Rij rats. **A**. Examples of cross-correlation functions. **B.** Averaged cross-correlation functions. Note that in waking state cross-correlations are direct ($C_{x,y}>0$), but in both spindle types, intracortical and intrathalamic cross-correlations are direct ($C_{x,y}>0$), but cortico-thalamic cross-correlations are inversed ($C_{x,y}<0$). **C.** Average peak values of cortico-thalamic cross-correlations during anterior and posterior spindles. The most substantial differences between two spindle types are found between frontal cortex and thalamus (in anterior spindles $C_{x,y}<0$, but in posterior spindles $C_{x,y}>0$).

In Fig. 2.10 it is summarized that cross-correlations during anterior sleep spindles are detected between RTN–(vVPM+dmVPM)–frontal cortex, and during posterior spindles between the RTN–dmVPM–(occipital+frontal cortices). Noteworthy is that during anterior spindles, both the dmVPM and vVPM associates with the frontal cortex, while during posterior spindles only the dorsomedial part of the VPM associates with the occipital cortex. It seems that anterior and posterior sleep spindles are not equally propagated over the VPM: anterior spindles may occupy both the dorsomedial and ventral poles of the VPM, whereas the posterior sleep spindles more readily appear in the dorsomedial pole. Also in posterior sleep spindles, the spectral peak in the dmVPM is higher than in the vVPM. These two observations suggest that the dmVPM is preferably involved in the propagation of both type sleep spindles, while vVPM is only involved in anterior sleep spindles.

The RTN demonstrates strong associations with the cortex during anterior and posterior sleep spindles. Although the frequency profile of associations 'occipital cortex – RTN' is peculiar (cross-spectrum analysis revealed a peak in non-spindle frequency, 7.5-8 Hz, Figs. 2.7 and 2.8), the RTN might still be involved in the sustaining and propagating of posterior sleep spindles. Altogether, (1) the overall pattern of associations between the cortex and the RTN differs in two spindle types; (2) functional coupling in thalamo-cortical system during anterior sleep spindles is stronger than during posterior spindles.

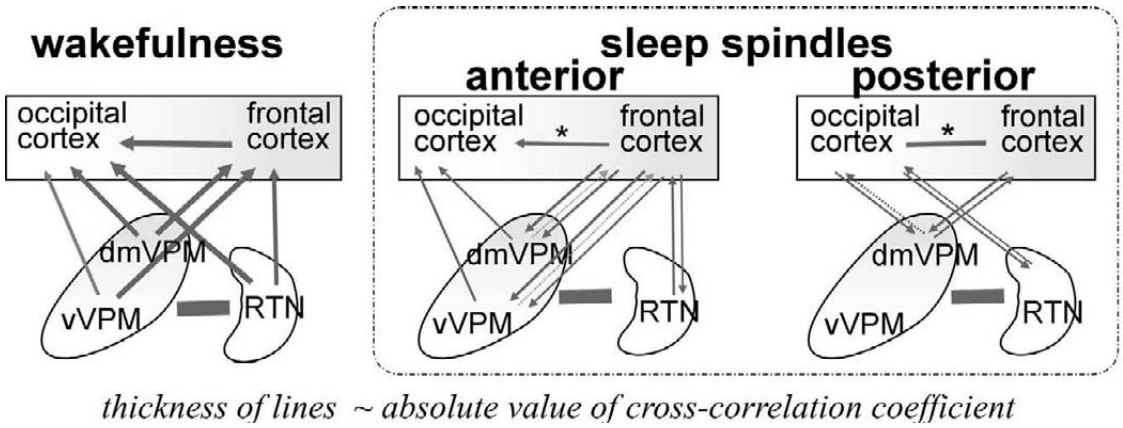

Figure 2.10. Summary of cross-correlation analysis illustrating thalamo-cortical network associations during two types of sleep spindles. Arrows interconnect those structures in which $|C_{x,y}|>0.05$ and arrow's tip is directed towards the lagging structure ($\tau>0$)

In summary, local cortical sleep oscillations, anterior and posterior sleep spindles, are characterized by different associations across the thalamo-cortical neuronal network. In anterior sleep spindles, the frontal cortex associates with the relay thalamic nucleus (VPM) and with the RTN with peak frequencies in 2-3 Hz, 8-10 Hz and 11-12 Hz. In posterior spindles, network associations are relatively weak: occipital cortex associates with the VPM (dorsomedial part) in frequencies of 9-10 Hz. The RTN strongly associates with the VPM, but weakly with the occipital cortex (in frequencies of 7-8 Hz). A role of the RTN in posterior sleep spindles seems obscure. We found that associations between the RTN with the cortex differ in two spindle types. Therefore, the RTN may control propagation of spindle sequences over the cortex and underlie topographic distinctions between anterior and posterior spindles in the cortex. A key role of the RTN in initiation of sleep spindle activity is well known, and our study adds that the RTN may, probably indirectly, also control propagation of sleep spindles and their distribution over the cortex.

DISCUSSION

The present study confirms that WAG/Rij rats have two types of local spindle oscillations, anterior and posterior sleep spindles. Anterior sleep spindles are present in the frontal cortex with a mean frequency of 11 Hz, whereas posterior spindles are restricted to the occipital cortex and are slower (10 Hz). Besides that, posterior spindles have lower amplitude than anterior ones. In the cortical site, where each spindle type has been specified (specific area), the power EEG spectrum shows high-amplitude *alpha* activity and a sharp peak around the mean frequency, whereas simultaneous activity at other cortical sites (nonspecific area) displays a flat power spectrum with a very low activity in the *alpha* range for both spindle types. Altogether this suggests that the chosen identification criteria of sleep spindles are relevant.

Alpha band was divided in two sub-bands and each of them was centered around the mean frequency of two spindle types: $alpha_{low}$ (9-10.5 Hz) includes peak frequency of posterior spindles (10 Hz) and $alpha_{high}$ (10.75-12 Hz) includes peak frequency of anterior spindles (~11 Hz). As compared to pre-spindle EEG, posterior spindles showed higher power in $alpha_{low}$ only in the occipital cortex, but not in the thalamus. In contrary, anterior spindles showed higher power in $alpha_{high}$ and $alpha_{low}$ in the frontal cortex, while the thalamus (only VPM, but not RTN) showed more power in $alpha_{low}$ It is important that both spindle types showed an elevation of $alpha_{low}$ in the specific cortical area (as compared to pre-spindle EEG), but elevation of $alpha_{high}$ is only found in the anterior spindles and in the frontal cortex, but not in the thalamus. This suggests that the 1 Hz gap between the mean frequency of the anterior and posterior sleep spindles may have a cortical (but not thalamic) origin and could not be explained by frequency drifts in individual spindles.

Analysis of dynamics of EEG power in the selected frequency bands during transition from pre-spindle activity to sleep spindles showed that the occurrence of spindles in the cortex is associated with an increase of total power, but the thalamus showed just a tendency to increase the total EEG power.

Involvement of the thalamus in generation of two spindle types

Oscillatory patterns of thalamically recorded sleep spindles were irregular (in power spectrum, several sub-dominant frequencies, blurred spectral peaks; this is in accordance with the visual observation that sleep spindles in the thalamus did not reveal such a regular shape as their well-shaped counterparts in the cortex). The power spectrum of cortically recorded sleep spindles shows a clear spectral peak in 10 or in 11 Hz (mean frequency of

sleep spindles). In thalamic spectra, those peaks are less pronounced and non-spindle frequencies had relatively high power. This could be accounted for by the cyto-architecture of neuronal tissue around recording electrodes. As known, 80% of cortical neurons are pyramidal cells in which apical dendrites are oriented in the same (parallel) direction, therefore the neocortex is filled up by dipoles with large dipole moments and is capable of generating high-amplitude electrical field potentials [Lopes da Silva and van Rotterdam, 1982; Lopes da Silva et al., 1986]. In the thalamus, neurons are distributed in a more chaotic way and their dipole moments may sometimes damp each other. Subsequently, oscillatory spindle activity in the thalamus could be less regular than that in the cortex.

It is reported here that, in the thalamus, the amplitude difference between anterior and posterior sleep spindles is less significant than in the cortex. In fact, amplitude differences between two spindle types are more pronounced in the VPM rather than in the RTN. In the VPM, anterior sleep spindles show a strong tendency for having higher total power (due to more power in *delta*, *theta* and $alpha_{low}$ bands), as compared to posterior spindles; whereas in the RTN amplitude differences between two spindle types were found in the *delta* band only. To summarize, anterior and posterior sleep spindles in the cortex displayed different power per frequency bands; the same but smaller distinctions are present in the VPM, while in the RTN distinctions are minor.

In the power spectrum analysis, we focused on the most representative frequency bands (*delta*, *theta* and *alpha*), because it is known that a neuronal mechanism accounts for a balance between *delta* and *alpha* EEG components during sleep. As is known, thalamo-cortical neurons generate spindle sequences when their membrane potential is between -55 and -65 mV, and produce *delta* waves when the membrane potential is below -70 mV [Nunez et al., 1992]. This may explain the occurrence of sleep spindles with different frequencies, e.g., the frequency of sleep spindles depends on the duration of the hyperpolarization-rebound sequences in thalamo-cortical neurons: the longer the period of hyperpolarization, the slower the spindle sequences [Steriade, 2003]. In a population of thalamic neurons, membrane potentials of single cells may fluctuate. Some neurons may generate spindle sequences and others may be hyperpolarized enough to produce *delta* oscillations. On the level of field potentials this will result in a coincidence of spindle and *delta* waves (this is often seen in the EEG during non-REM sleep). The fact that periods of hyperpolarization last longer with increasing sleep depth has two consequences: firstly, *delta* activity increases at the expense of higher frequencies [Uchida et al., 1991]; secondly, more hyperpolarized neurons produce slower spindle sequences. As a result, the frequency of sleep spindles becomes lower as sleep deepens (in transition towards *delta*-wave sleep).

The thalamo-cortical network seems to have a mechanism which keeps a proper balance between *delta*, *theta* and *alpha* that is necessary to maintain either anterior or posterior spindle activity. The waveform of the power spectrum of anterior and posterior sleep spindles as measured at the specific cortical areas, was similar, suggesting that both spindle types represent the same oscillatory activity. The 10 and 11 Hz peaks in power spectra are considered as resonance frequencies occurring in the thalamo-cortical circuit during posterior and anterior sleep spindles. This idea is supported by the presence of peaks in the thalamo-cortical cross-spectra with the same frequency.

In the thalamus, anterior sleep spindles have more power in *delta*, *theta* and $alpha_{low}$ bands as compared to pre-spindle EEG. Posterior spindles are characterized by the same tendencies. These data are obtained at the level of local field potential (on macroscopic level) and we tend to interpret these results in terms of neuronal network processes. In order to produce steady and regular oscillations with a certain frequency, a large number of neurons must synchronize their firing activity in a specific frequency mode. In case of anterior sleep spindles, the VPM and frontal cortex display high power in frequencies 9-10.5 Hz ($alpha_{low}$), suggesting that these two structures sustain oscillations in the same frequency mode of $alpha_{low}$ and their firing activity is synchronized in this sub-band. In agreement to this hypothesis are the results of cross-spectrum analysis: 10.1 Hz peak characterizes ‘frontal cortex - VPM’ pair.

As far as the distribution of EEG power is concerned, anterior and posterior sleep spindles show differences in the thalamus. In the ventroposteromedial thalamic nucleus, the dorsomedial part (dmVPM) reveals more *theta* during anterior sleep spindles, while the ventral part (vVPM) shows more *alpha* during posterior sleep spindles. Perhaps, different functional properties of these two parts of the VPM and different anatomic connections with the cortex could underlie their different involvement in two types of spindles. As known, the VPM is a principal sensory nucleus of the trigeminal system. Its dorsal part, the dmVPM, specifically interconnects the facial region in the sensorimotor cortex [Haidarliu and Ahissar, 2001], while the ventral part of the VPM is innervated by other thalamic nuclei and by brainstem structures [Carvell and Simons, 1990; Brecht et al., 1997]. Hence, an intensive interconnection between the dmVPM and the sensorimotor cortex may by crucial for generating and sustaining thalamo-cortical rhythmic activity (e.g. anterior and at some extent, posterior sleep spindles), while through the vVPM spindle activity may be delivered to other subcortical structures.

Here we found that the thalamus (VPM and RTN) sustains a relatively high power in *theta* band during both spindle types (peaks in 8-9 Hz), but in the cortex *theta* is relatively low. The role of the thalamic *theta*-band activity in sleep spindle types remains obscure. This problem might perhaps be solved with single-unit or

intracellular recordings of thalamic activity. In sleep spindles, thalamo-cortical functional coupling (analysis of cross-spectrum) shows two maxima in 10-11 Hz and in 7-8 Hz. To date, 7-8 Hz peaks are well pronounced in the cross-spectra between occipital cortex and the thalamus.

The role of the RTN in the posterior spindles is less obvious than in the anterior spindles. According to cross-spectrum analysis, the RTN associates with the VPM during posterior spindles in frequency of 10 Hz (Fig. 2.6B), suggesting that RTN-VPM network sustains and, probably, generates 10 Hz rhythm. We show that the VPM associates with the occipital cortex in the 10 Hz frequency, but there are no direct connections between these areas (only indirect connections throughout the somatosensory cortex). On the other hand, the RTN displays weak ~ 8 Hz associations with the occipital cortex, suggesting that the occipital cortex does not associate with the RTN in a way as it does in anterior sleep spindles. Altogether, this suggests a different involvement of the RTN in local spindle activity. Namely, throughout other thalamic nuclei, the RTN may be linked to the frontal (sensorimotor) cortex, but it may have sparse connections with occipital (visual) cortical area. Therefore, the RTN could be more strongly incorporated in thalamo-cortical network during anterior spindles than during posterior spindles.

Particularities of sleep spindles WAG/Rij rats

WAG/Rij rats are an inbred strain that originates from Wistar Albino rats. The WAG/Rij rat has been used as a genetic model of absence epilepsy for almost two decades [van Luijtelaar and Coenen 1986; reviewed in Coenen and van Luijtelaar, 2003]. In general, characteristics of sleep spindles in WAG/Rij rats are similar to Wistar rats [Terrier and Gottesmann, 1978; Gandolfo et al., 1985]. The only dissimilarity concerns the frequency of posterior sleep spindles. The present study reports on ~10 Hz posterior sleep spindles, but in Wistar rats the frequency of posterior sleep spindles is higher, 12.4 Hz [Terrier and Gottesmann, 1978]. Sleep spindles in WAG/Rij rats might have low frequency because of a genetic predisposition to epilepsy.

Until now, it is unclear how epilepsy affects the EEG features of sleep spindles. On one hand, in children with primary generalized epilepsy, the mean frequency and length of the spindles are normal, suggesting that the thalamo-cortical circuits can still make normal spindles [Myatchin and Lagae, 2007]. On the other hand, patients with generalized epilepsy may have slower sleep spindles, but it could be a side-effect of medication [Drake et al., 1991; Angeleri et al., 1993]. Recently, Myatchin and Lagae (2007) have found that the frequency of the slow (<12 Hz) sleep spindles, occurring at the beginning of sleep stage 2 in the untreated children with primary generalized epilepsy, is higher than in healthy control (12.9 vs 12.2 Hz), but did not differ from that in the treated group (12.6 Hz). In contrast, in the untreated group, the percentage of spindles in stage 2 is significantly lower (as compared to healthy control). After medication, the number of sleep spindles is restored (the treated primary generalized group did not differ significantly from the control group, as did the untreated primary generalized group). Our animals are drug-free and a low frequency of sleep spindles may therefore be caused by absence epilepsy *per se*. The EEG in WAG/Rij rats looks pretty normal, except for periods with absence attacks, when the thalamo-cortical circuit produces high-voltage 8-10 Hz spike-wave discharges [van Luijtelaar and Coenen, 1986; Kandel and Buzsaki 1997; Coenen and van Luijtelaar, 2003]. In patients with primary generalized epilepsy the macro-organization of sleep is disrupted: patients more rapidly enter into sleep stage 2, but this stage 2 is characterized by fewer sleep spindles. WAG/Rij rats also show disturbances of sleep structure: they have longer periods of intermediate stage of sleep as compared to non-epileptic Wistar rats [Gandolfo et al., 1990]. The sleep cycle and the non-REM sleep duration are shortened in WAG/Rij rats as compared to non-epileptic ACI rats (August Copenhagen Irish, black agouti rats) by the presence of SWD, but only during periods when light sleep dominates, not during deep non-REM sleep [van Luijtelaar and Bikbaev, 2006]. Although spindles and spike-wave discharges share the same thalamo-cortical circuitry, their age-dependent dynamic and distribution across the sleep cycle is not the same. This suggests that a functioning thalamo-cortical circuit in WAG/Rij and in ACI rats might be under control of different mechanisms.

The present study shows the results of EEG power spectrum analysis of sleep spindles in the thalamus. We found that the thalamus is more involved in anterior spindles than in posterior spindles. In the thalamus, sleep spindles are accompanied by a relatively high *theta* activity, whereas in the cortex *theta* activity is low. A strong functional coupling occurs within the thalamo-cortical network in the range of mean frequency of sleep spindles and with a frequency ~ 8 Hz. The most strong associations during anterior sleep spindles are found between the frontal cortex, the VPM and the RTN, suggesting that these parts of the circuit are involved in the propagation of anterior sleep spindles. In posterior sleep spindles, the RTN, in dialogue with the VPM, has less specific associations with the occipital cortex. To date, the cortical expression of sleep spindles in rats is not simply a fingerprint of thalamic activity.

Chapter 3
Spike-wave discharges type I and II

CONTENTS

Spike-and-wave complexes are stereotypic electroencephalographic patterns that accompany different forms of idiopathic generalized epileptic syndromes, such as childhood absence epilepsy, juvenile absence epilepsy, juvenile myoclonic epilepsy, myoclonic absence epilepsy, and eyelid myoclonia with absences [Gibbs et al., 1935; Panayiotopoulos, 1999, 2005]. In some rodent strains, such as Genetic Absence Epilepsy Rats from Strasbourg (GAERS) and Wistar Albino Glaxo from Rijswijk (WAG/Rij), spike-and-wave discharges (SWD) spontaneously appear in the electroencephalogram (EEG) [Danober et al., 1998; Coenen and van Luijtelaar, 2003; Depaulis and van Luijtelaar, 2006].

In addition to the generalized SWD type I, a local occipital paroxysm, e.g., SWD type II, is found in about 50% of WAG/Rij rats at the age more than 6 months [van Luijtelaar and Coenen 1986; Midzianovskaia et al., 2001; Schridde and van Luijtelaar, 2005]. The two types of SWD differ not only in frequency and amplitude, they also have different pharmacological [Midzianovskaia et al., 2001], genetic [Gauguier et al., 2004] and ontogenetic profiles [Schridde and van Luijtelaar, 2005]. Moreover, SWD type II lacks a clinical correlate. The origin of SWD type II and their relation to the generalized absence seizures are still unknown.

A subcortical origin of absence epilepsy in humans was first proposed Jasper and Kershman (1941). Their idea was supported by Morison and Dempsey (1942), who found experimental support that a subcortical pacemaker of absence seizures might be located in the thalamus. The thalamus distributes seizure activity throughout the cortex in both hemispheres via bilateral projections. It is difficult to confirm the presence of the source of absence epilepsy in humans (similar to animals) in the thalamus, because patients with typical absence epilepsy rarely undergo invasive monitoring with depth electrodes and it is extremely rare cases when electrical activity can be recorded directly from the thalamus. Animal models help to solve this problem by offering the possibility to combine surface and subcortical recordings. Our investigations are performed in WAG/Rij rat model of human absence epilepsy [Coenen and van Luijtelaar, 2003]. A series of EEG studies in WAG/Rij rats [reviews Coenen and van Luijtelaar, 2003; van Luijtelaar and Sintikova, 2006] confirm that a functionally intact thalamocortical network is required for the generation of SWD. **Chapter 3.1** is focused onto electrographic structure of SWD I and SWD II as recorded in spatially and functionally segregated parts of the thalamo-cortical system. In **Chapter 3.2** distinctions between SWD I and SWD II are further evaluated by studying noradrenergic mechanisms which may control the incidence of SWD.

Pro-epileptogenic 5–9 Hz oscillations in EEG are known to occur immediately before episodes with spontaneous absence epilepsy in GAERS [Pinault et al., 2001; 2006]. The medium-voltage 5–9 Hz forerunners of seizure activity are referred to as the precursors of SWD in GAERS. Since SWD in GAERS are equal to SWD type I in WAG/Rij rats, it is assumed that that the same 5–9 Hz oscillations can act as precursor activity for SWD I in WAG/Rij rats; if these oscillations are not present in WAG/Rij rats, then they are specific for GAERS and they can be considered as epiphenomena of absence epilepsy in the GAERS model. **Chapter 3.3** describes amplitude-frequency characteristics of seizure precursor activity (preSWD episodes) in WAG/Rij rats. Short EEG epochs immediately prior to SWD I are examined in order to disclose early EEG changes that may anticipate the onset of SWD I. The role of the cortex and the thalamus in SWD-precursors is assessed with the aid of spectral and coherence analysis. This Chapter also aims to define a probable relationship between electrographic properties of SWD-precursors and subsequent SWD I.

3.1 EEG structure of SWD type I and II *

ABSTRACT

Purpose: The waveform of spontaneous spike-wave discharges (SWD) in the electroencephalogram (EEG) was delineated in the WAG/Rij rat model of absence epilepsy according to the definitions of clinical electroencephalography. We defined four elements in SWD based on the schema of Weir (1965): 'Spike 1' and 2, Positive Transient (PT), and Wave. The EEG patterns of generalized type I and local type II SWD in cortical and thalamic areas were analyzed.
Methods: EEGs were recorded in freely moving rats epidurally from different cortical regions and with deep electrodes from the specific and reticular thalamic nuclei. Grand average SWD waveforms were computed to assess spatiotemporal patterns of seizures.
Results: SWD I in the frontal cortex comprised of a large Spike 2 + Wave, and in the thalamus PT + Wave. Small transient spikes were associated with SWD I in the anterior-middle part of the cortex. SWD II were found in the occipital cortex as a sequence of (occasional) Spike 1 + PT + Wave.
Conclusions: The EEG structure of SWD in WAG/Rij rats was comparable with that of epileptic patients, suggesting face validity of the WAG/Rij model. Fast transients spikes are an integrative part of SWD I. Time-amplitude linkage between cortical and thalamic counterparts of SWD I suggests a complex spatiotemporal organization of SWD I. The thalamus sustained SWD I, but not SWD II.

INTRODUCTION

In humans, spike-and-wave complexes are regular and symmetrical generalized discharges of 2.5–4 Hz. The Committee on Terminology of the International Federation of Societies for Electroencephalography and Clinical Neurophysiology (IFSECN) defines *spike-and-slow-wave complex* as "*a pattern consisting of a spike followed by a slow wave"* (3). However, more than 40 years ago, Weir (1965) defined four epileptiform elements in spike-and-wave complexes based on electroencephalograms (EEGs) from nearly 200 patients with petit mal epilepsy. In particular, he wrote: *"a small, short duration negative spike, followed by a prominent positive transient from which the second, larger amplitude spike takes origin. The last element is the negative wave component; it is not a complete dome but approximates the first three-quarters of one"* (4, p. 285).

Clinical concomitants of absence seizures in humans and genetic rodent models are similar, e.g., behavior immobility and minimal facial myoclonic facial jerks [van Luijtelaar and Coenen, 1986; Marescaux et al., 1992; Willoughby and Mackenzie, 1992]. Absence seizures in rats and in humans have a genetic origin, although the genes are not identified as yet [Vadász et al., 1995; Depaulis and van Luijtelaar, 2006]. Both GAERS and WAG/Rij rat strains are considered as valid models of human absence epilepsy [Danober et al., 1998; Coenen and van Luijtelaar, 2003]. Also the electroencephalographic pattern of SWD resembles those in humans with absence seizures; however no attempts were made to compare them in detail. In this Chapter we investigate whether and how Weir's classification of the epileptiform elements in the spike-and-wave complex can be applied to SWD in WAG/Rij rats.

A vast body of data obtained in vitro and in vivo experiments showed that SWD are produced in the cortico-thalamo-cortical neuronal circuits [e.g. Steriade 2003; Avanzini et al., 2003; Danober et al., 1998]. These circuits are formed by mutually interconnected neurons located in the neocortex, specific thalamic nuclei and the reticular thalamic nucleus (RTN). While some theories assume that spike-wave activity originates from the thalamus and it is triggered by pacemaker cells located in the RTN [e.g., Blumenfeld 2002; Avanzini et al., 2003], others emphasize that SWD are initiated in the somatosensory cortex and that the thalamus is only secondary involved [Meeren et al., 2002; 2005; van Luijtelaar and Sitnikova, 2006]. Meeren and co-workers (2002) found that the activity in the cortical epileptic focus leads thalamic activity only during the first few cycles of SWD. After this initial period (five hundred milliseconds from the onset), cortical and thalamic areas lead and lagged each other unpredictably. This suggests that the full expression of SWD takes some transitory period during which the waveform of seizures may change. In the present Chapter we evaluate dynamic changes by comparing the waveform of SWD immediately after the onset and in subsequent seizure cycles.

A few early reports in humans provided ambiguous depth profiles of SWD (reviewed in Blumenfeld, 2002), though spike-wave activity seemed to be present in the mesencephalon and diencephalon [Angeleri et al., 1964;

* Published in:
Sitnikova E, van Luijtelaar G. Electroencephalographic characterization of Spike-Wave Discharges in cortex and thalamus in WAG/Rij rats. Epilepsia, 2007, 48 (12), 2296–2311

Jasper et al., 1947], including the thalamus [Williams, 1953]. Detailed mapping of the subcortical spread of SWD in rodent models showed that high-voltage rhythmic activity was present in the thalamus, but not in limbic structures, including the hippocampus [Vergnes et al., 1987; Inoue et al., 1993; Kandel and Buzsaki, 1997]. It was noted that thalamic and cortical counterparts of SWD were dissimilar in WAG/Rij rats: the former had a 'spindle-like' waveform with an 'arched appearance' [Meeren et al., 2002]. However, previous comparative studies were not quantitative and no clear differences were described for the difference between surface and depth EEG recordings of SWD. In the present study we compare temporal structure of cortical and thalamic SWD in WAG/Rij rats.

Midzianovskaia et al. (2001) presented cortical maps for the spike and the wave components of SWD (both types I and II) in WAG/Rij rats and showed that the spike had its maximum in the frontal area and the wave – in the occipital area. In the present study we employ a statistical method (grand average of the spike-wave discharge) to evaluate the waveform of SWD in the most characteristic cortical zones, e.g. frontal and occipital areas, in which either the spike or the wave displayed their amplitude maximum.

METHODS

Animals

Experiments were performed in nine male WAG/Rij rats (11-12 month old, body weight 370-410 g) which were born and raised in the laboratory of the Department of Biological Psychology of Radboud University Nijmegen. The experiments were conducted in accordance with the regulation of animal experimentation in the Netherlands and were approved by the Ethical Committee on Animal Experimentation of Radboud University Nijmegen. Before surgery rats were kept in pairs in standard cages with food and water available *ad libitum* and a 12-12h light-dark cycle (white light on at 18:00). After surgery animals were individually housed and allowed to recover for at least 10 days. Distress and suffering of animals were minimal.

Surgery procedure and histological control

Stereotactic surgery was performed under isofluorane anesthesia while body temperature was monitored and maintained at 37°C with a heating pad. Electrodes were implanted in small separate circular opening in the skull (diameter = 1-2 mm). Electrode sets were mounted on the skull with a crown of dental cement and fixed with embedded mounting screws. Rats received a 0.1 mg/kg i.m. injection of 0.324 mg/ml buprenorfinehydrochloride (Temgesic®, Reckitt & Colman Products Ltd., Kingston-Upon Hull, UK) for post-surgery analgesia immediately after completion of surgery,

Upon completion of the EEG recording sessions, rats were deeply anesthetized with an overdose of sodium pentobarbital (200 mg/kg i.p.); their brains were stained with Nissl for the histological verification of depth electrodes positions. To facilitate the recognition of electrode tips on brain slices, small electrolytic lesions were made by passing DC current (10 μA, 10 sec) via the depth electrodes. Rats were then perfused with 4% formaldehyde in neutral 0.1 M phosphate buffer via the ascending aorta. The brains were removed and post-fixed in the same fixative solution plus 20% sucrose. Serial coronal sections 60 μm thick were made with a cryostat. Slices were then mounted on gelatin-coated glasses and stained with 0.1% cresyl violet. Electrode positioning was verified using the same atlas of the rat brain [Paxinos and Watson, 1986]. Rats, in which depth electrodes appeared to be misplaced, were excluded.

Electrode setup

Rats received two sets of tripolar stainless steel electrodes (0.25 mm diameter) with non-insulated tips (Plastic One Inc. Roanoke, VI, USA: MS 333/2A). Two electrodes were placed epidurally on the right side over the frontal [AP 2; L 2.5] and occipital cortex [AP -7; L 6]. Other two electrodes were implanted in the ventroposteromedial thalamic nucleus VPM [AP –3.5; L 2.5; H 7.2] and in the rostral part of the reticular thalamic nucleus, RTN [AP –1.5; L 2.2; H 7.2]. The remaining two electrodes were placed symmetrically over two hemispheres of the cerebellum and used as ground and reference. All coordinates are given in mm relative to bregma according to the rat brain atlas of Paxinos and Watson (1986).

EEG recording

EEGs were recorded in freely moving rats during the dark period of the day-night cycle (because spontaneous absence seizures are more frequent during the dark phase [van Luijtelaar and Coenen, 1988]). Recordings were performed in a noise-isolated experimental chamber continuously during 5-7 hours. Animals were placed in Plexiglas recording cages (25 x 30 cm and 35 cm high) a day before EEG recording session and were habituated to EEG recording system and to connecting leads. EEG signals were fed into a multi-channel

differential amplifier via a swivel contact, filtered between 1 and 500 Hz, digitized with 1024 samples/second/per channel (CODAS software) and stored on hard disk.

EEG analysis

SWD I and SWD II were detected using criteria described in the earlier reports [van Luijtelaar and Coenen 1986; Midzianovskaia et al., 2001]. SWD I were recognized in the frontal EEG as a train of surface negative 7-10 Hz spikes with amplitude at least three times higher than the background. Duration of SWD I was more than 1 sec. SWD I were detected automatically based on the threshold value of the EEG slope in the frontal channel with efficiency 97-100% in the artifact-free EEG (the algorithm and original software were developed by P.L.C. van den Broek, NICI, University of Nijmegen, the Netherlands). SWD II consisted of sharp repetitive positive 6-7 Hz waves and lasted longer than 0.5 sec (more than three waves in a sequence) and were identified visually in the occipital EEG in the absence or just little concurrent rhythmic activity in the anterior cortex. The numbers of SWD I and SWD II were scored per hour and compared using t-test for related samples.

Details of seizure morphology were examined in the EEG as recorded from various cortical, hippocampal and thalamic regions in both groups of animals. In order to access area-specific elements in SWD, episodes with SWD were visually inspected for the presence of a consistent trend in the spatiotemporal distribution of electroencphalographic seizure activity.

Statistical analysis of the waveform of SWD was performed in the second group of animals. Twenty episodes with SWD I and ten episodes with SWD II per subject were randomly selected. Each SWD I was labeled with two markers. The first marker indicating the initial cycle, was placed on the apex of the first negative spike in the frontal EEG. The second marker indicating fully grown SWD I, was put on the apex of a periodic spike occurring around 2 sec after the seizure onset (after the first marker). SWD II were selected and labeled in the occipital EEG by putting a marker at the apex of the first sharp positive deflection. Marker positioning was applied to all investigated channels. Time interval 0.5 sec before the onset of SWD was used for baseline correction. Averaged EEG amplitude was computed in 1 sec period including 0.5 sec before and 0.5 sec after the marker. Data were averaged per channel and per rat using the commercially available software package Brain Vision Analyzer (BrainProducts GmbH). The grand EEG average was constructed for all subjects for each electrode position. This EEG average was considered as typical seizure waveform for that specific brain region.

Components of SWD were identified according to the original description of Weir (1965, for more details see Table 3.1, part II). The amplitude and timing of epileptiform components were measured and than statistically compared using t-tests for related samples. To characterize polarity relations between the negative and the positive phases in SWD, the ‘indices of polarity’ (k, the ratio between maximum negativity and maximum positivity) was computed. Progressive changes in EEG seizure polarity were accessed by comparing the ‘indices of polarity’ in the initial cycle and in the (subsequent) middle part of SWD I using Chi^2 test.

RESULTS

Descriptive characteristics of SWD. Phenotypes of SWD type I and type II

SWD were detected in all (eighteen) subjects: SWD I occurred in 100% of the animals, 10-45 seizures per hour (27 ± 11, mean ± SD), SWD II occurred in 72 %, 1-8 per hour, 2.9 ± 1.8. SWD II were less numerous than SWD I ($p<0.001$).

The basic configuration and topographic distribution of electrical seizure activity was assessed in both groups of animals. Figure 3.1A illustrates the cortical distribution of SWD I and II and their absence in the dorsal hippocampus. The bottom plates show the cortical and thalamic equivalents of SWD I and II.

SWD I invaded practically all investigated areas. In that respect they were generalized (Fig. 3.A), although their expression at the occipital cortex was minimal, in agreement with earlier reports [Midzianovskaia et al., 2001; Vergnes et al., 1987]. SWD I in the frontal cortex consisted of repetitive high-voltage negative spikes and low-voltage negative waves (Fig. 3.1A). SWD I spread throughout the cortex with a very consistent spatial gradient: the amplitude of the spike component was maximal in the frontal cortex and declined in the posterior direction. The amplitude of the spike in the epileptic zone of SWD I (the perioral region of the somatosensory cortex [Meeren et al., 2002]) was lower than in the frontal cortex. The amplitude of the wave in the fronto-parietal cortex was lower than in the occipital cortex.

SWD I in both thalamic channels were recognized as a complex of positive sharp waves and slow dome-shaped negative waves. The positive polarity of thalamic SWD I was opposite to that observed in the fronto-parietal cortex. The morphology of SWD I in cortex and thalamus was constant across animals.

Table 3.1. Characteristic elements in EEG spike-and-wave complexes in epileptic patients and in WAG/Rij rats.

Part I. Some specific EEG terms and definitions given by the International Federation of Societies for Electroencephalography and Clinical Neurophysiology (IFSECN) [1974] [1]

Spike	A transient clearly distinguished from background activity, with pointed peak at conventional paper speeds and duration from 20 to under 70 msec. Main component is generally negative relative to other areas.
Wave	Any change of the potential difference between pair of electrodes in EEG recording.
Spike-and-slow-wave complex	A pattern consisting of a spike followed by a slow wave. Comment: hyphenation facilitates use of term in plural form: spike-and-slow wave complexes or spike-and-slow-waves.
Multiple spike-and-slow-wave complex	A sequence of two or more spikes associated with one or more slow waves. Preferred to synonym: polyspike-and-slow-wave complex.
Multiple spike complex	A sequence of two or more spikes. Preferred to synonym: polyspike complex.
Sharp wave	A transient clearly distinguished from background activity, with pointed peak at the paper speeds; duration 70 – 200 msec.
Complex	A sequence of two or more waves having a characteristic form or recurring with a fairly consisting form, distinguished from background activity
Epileptiform patterns	include spikes and sharp waves, alone or accompanied by slow waves, occurring singly or in bursts lasting at most a few seconds"

Part II. General description of epileptiform elements in spike-wave complexes

	In patients [2]	**In WAG/Rij rats [3]**	
		SWD I	**SWD II**
Spike 1 (Sp1)	The small negative triphasic spike - appears in 44% of all records. Duration ~ 10 msec.	The small negative spike - appears in the occipital cortex and in the specific (ventroposterior) thalamic nucleus. Duration ~ 25 msec in the occipital cortex and ~ 15 msec in the thalamus.	- appears sporadically in the occipital cortex
Positive transient (PT)	A positive portion of a complex. The sharp positive deflection interrupted by the negative spike. - amplitude varied from being approximately equal to double of the negative wave; Duration ~ 100-150 msec.	Diversified positive component - appears in the cortex and in the thalamus (in the frontal cortex, due to the overlap with the 'spike 2', has two phases, an early and late; is sharp and uniform in the posterior cortex and the thalamus); Duration ~ 40 msec in the occipital cortex and ~ 20 msec in the thalamus	Sharp positive deflection; - maximum in the occipital cortex; Duration 40-60 msec.
Spike 2 (Sp2)	The "classical" negative spike that interrupts the positive transient and is followed by the slow negative wave; - maximum in frontal areas; The amplitude of 'Sp2' is several times higher than the amplitude of 'Sp1' ; Duration ~ 30-90 msec.	The large negative spike - appears in the frontal cortex and absent in other sites; The amplitude is more than ten times higher than the amplitude of 'Sp1'. Duration 25-35 msec	Absent
Wave	The least clearly abnormal potential. Surface negative wave, which joins with the positive transient; Duration ~ 150-200 msec (200-500 msec if measured together with the positive transient).	Slow negative wave - appears with variable amplitude in cortex and thalamus (usually low in frontal cortex and high in thalamus); Duration 40-60 msec (the same in different regions).	- maximum in occipital cortex; Duration 80-100 msec.

[1] Cited by: Chatrian GE (Chairman), Bergamini L, Dondey M, Klass DW, Lennox-Buchthal M, Petersen I (1974) A glossary of terms most commonly used by clinical electroencephalographers. Electroencephalogr Clin Neurophysiol 37: 538-548.
[2] Data from Weir B (1965)
[3] Our own data

Amplitude and frequency of SWD I progressively changed during a seizure. In the first few (two-four) cycles, the amplitude of the spike increased and did not change significantly during a seizure (Fig. 3.1, Table 3.2). The amplitude of the last few spikes decreased abruptly and was several times lower than the amplitude of the

spikes at the beginning. The amplitude of the waves tended to increase during a seizure at all cortical sites. The frequency of SWD reduced from 10-12 Hz to 4-6 Hz at the end (Fig. 3.1A). This seizure dynamics was in close agreement with previous reports [Drinkenburg et al., 1993; Midzianovskaia et al., 2001]. The contribution of the present study was to highlight temporal evolution of SWD I in the thalamus. The amplitude of the thalamic SWD progressively increased during a seizure (see Table 3.2 for quantitative data – the major seizure component, positive transient, PT, increased in amplitude from 85 to 124 μV in the RTN and from 78 to 108 μV in the VPM).

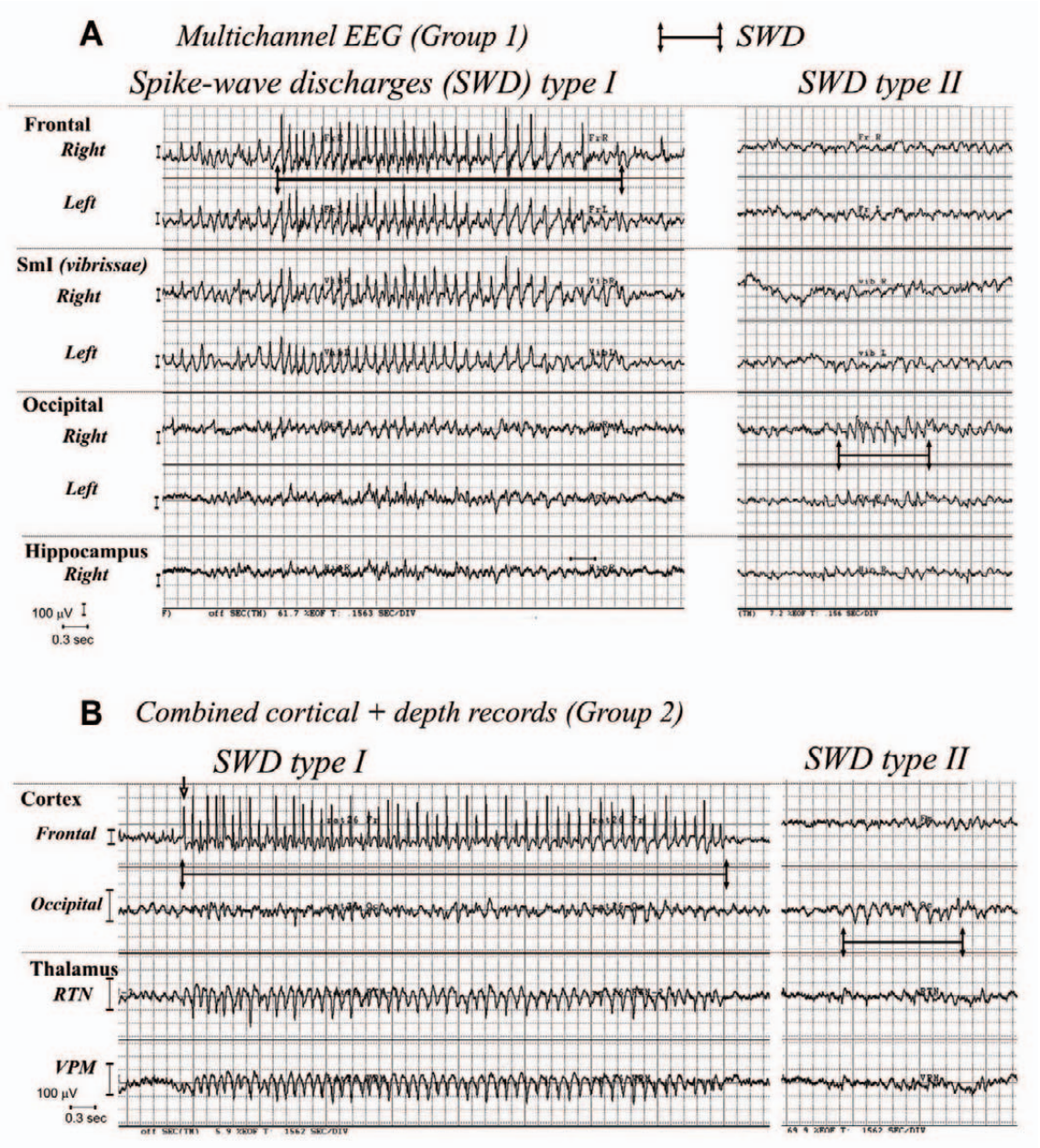

Figure 3.1. Electroencephalographic expression of spike-wave discharges (SWD) in cortex and thalamus in WAG/Rij rats. (**A**) Distribution of generalized SWD type I and local SWD II across the cortex and dorsal hippocampus. Amplitude of SWD I decreased in the anterior-posterior direction. The high amplitude negative spikes are present in the fronto-parietal areas, but they are less recognizable in the occipital EEG. SWD II are present in the occipital cortex but poorly expressed in the anterior and middle cortical regions and in the dorsal hippocampus. (**B**) SWD I and SWD II recorded simultaneously in the cortex and in the thalamus. In SWD I, the negative spike predominates in the frontal cortex and the sharp positive wave predominates in the thalamus. SWD II are hardly visible in the thalamic nuclei. Negativity is presented upward. *Abbreviations*: RTN - reticular thalamic nucleus; VPM – ventroposteromedial thalamic nucleus (specific somatosensory nucleus of the ventrobasal complex). Black small arrows indicate the onset of SWD.

The presence of SWD II was restricted to the occipital cortex and did not spread to anterior cortical areas and the dorsal hippocampus (Fig. 3.1B). Interestingly, the waveform of the local occipital SWD II resembled the waveform of SWD I in the same occipital EEG site.

SWD in WAG/Rij rats in terms of clinical electroencephalography

The EEG pattern of SWD in WAG/Rij rats fitted the descriptions given by the international guidelines for clinical electroencephalographers (IFSECN, ref. Chatrian et al., 1974). Table 3.1, part I, gives the definitions for the terms used in the present paper. It was found that SWD in the rats consisted of several elements which were analogues to the elements in spike-and-wave complexes in the human EEG (Table 3.1, part II). Although special the distribution and duration of spike-and-wave complexes in humans and in rats were distinctive, the similarity between them is striking (see 'Discussion').

SWD type I appeared in the fronto-parietal cortex as three-phasic potentials consisting of the early positive transient (PT_{early}), the high-voltage negative 'Spike 2' and the late positive component PT_{late} (Fig. 3.2a, Table 3.1). PT_{early} was an inconsistent element in which the shape and magnitude varied across seizures, across channels and across animals.

In the occipital cortex and thalamus, SWD I consisted of high amplitude sharp PT and dome-shaped negative Wave. An additional small and sharp negative spike that often appeared at the transition between PT and Wave (Sp1 in Fig. 3.2Bb) fitted Weir's definition of 'Spike 1' (4): 'a small, short duration negative spike, followed by a prominent positive transient' (p.285, Weir, 1965).

SWD type II was present in the occipital cortex as two-phasic negative-positive deflections; they were hardly visible in the fronto-parietal cortical area, dorsal hippocampus and thalamus. SWD II comprised the high amplitude sharp PT and the dome-shaped negative Wave (Fig. 3.2C, 3.2Cc). The small negative 'Spike 1' sometimes appeared on the positive slope prior to PT.

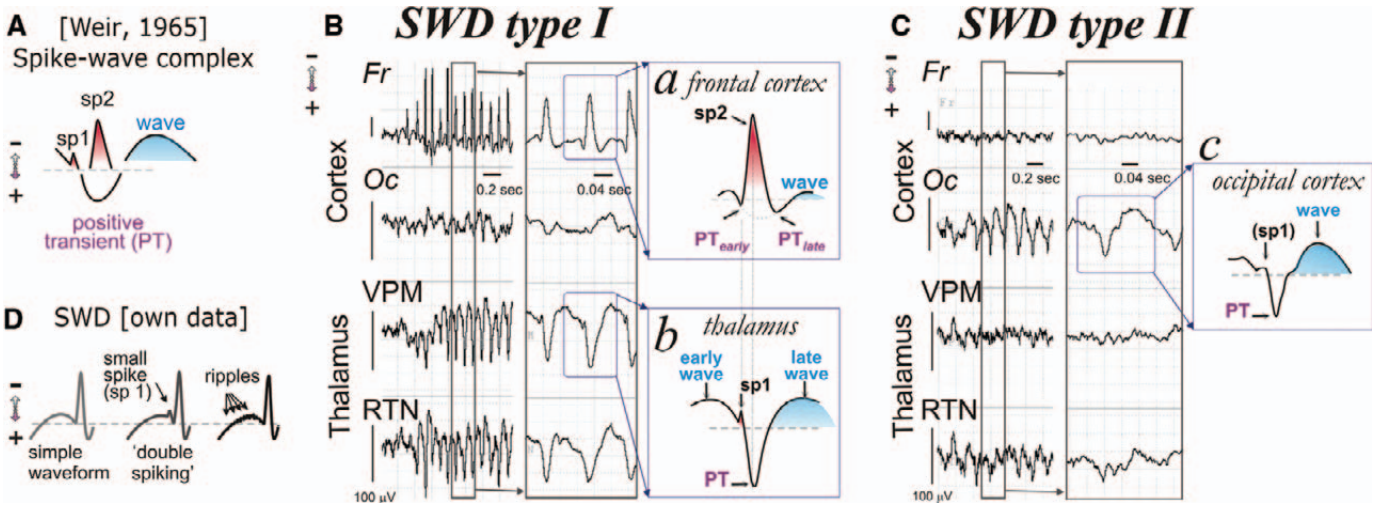

Figure 3.2. Schema illustrating EEG pattern of SWD in epileptic patients and in WAG/Rij rats. **(A)** Replica from the original paper of Weir (1965). The author defined the following epileptiform elements: Sp1 – early negative spike 1, PT – positive transient, Sp2 – late negative spike 2 and negative wave. **(B-C)** Application of Weir's classification to SWD in WAG/Rij rats. Both SWD type I and II show epileptiform elements comparable to Weir's Sp1, Sp2, PT, and Wave. Insertions ***a-c*** show electrical seizure activity: ***a***, in the frontal cortex, SWD I appeared as a sequence of PT_{early} – Sp2 – PT_{late} – wave; ***b***, in the thalamus, (Sp1) – PT – wave and ***c***, SWD II in the occipital cortex (Sp1) – PT – Wave. *Abbreviations:* Fr - frontal cortex; Oc – occipital cortex; VPM – ventroposteromedial nucleus of the thalamus; RTN - reticular thalamic nucleus.

Statistical analysis of SWD

Grand average waveforms of SWD I and SWD II were constructed in the second group of rats (n=9). These animals had epidural electrodes in the frontal and occipital areas and depth electrodes in the VPM and RTN. Cortical SWD I were studied in all nine rats. Thalamic EEG data were derived from five rats in which depth electrodes were located in the VPM and RTN (as verified by histological examination). SWD II were found in six rats and among them five rats had thalamic electrodes in VPM and RTN. EEGs from those five rats were used to analyze SWD II.

The grand average waveforms of SWD I and SWD II were smooth and had relatively high signal-to-noise ratios (aperiodic low-amplitude components and noise were attenuated, Fig. 3.3). Fig. 3.4 summarizes grand averages SWD I and shows typical spike-wave patterns (so-called local seizure 'archetypes').

General pattern description of SWD type I

Spike 2 appeared in the frontal cortex with excessively high amplitude and interfered the positive phase, therefore, PT seemed fragmented in two discontinuous elements with 'Spike 2' as a boundary. 'Spike 2' lasted 25-

35 msec, which is comparable with the duration of 'Spike 2' detected in humans (30-90 msec, [Weir, 1965]), considering the lower interspike frequency in man.

Spike 1 was present in the VPM and in the occipital cortex (arrow in Fig. 3.3A), but absent in the frontal cortex and in the RTN. In spite of its small amplitude, 'Spike 1' was not eliminated by the averaging process, suggesting that this element was constantly present across seizures and across animals. The duration of the 'Spike 1' was around 15-25 msec (Table 3.1, part 2), that is two times longer than in humans (10 msec, Weir, 1965).

Wave was a negative slow component, it could be recognized in all EEG channels in both SWD I and SWD II. Wave had a stereotypic configuration but varied in amplitude. It was clearly less pronounced in the frontal cortex, in contrast to the occipital cortex and the thalamus, in which the 'Wave' appeared as a high amplitude deflection (between 34 and 65 μV, Fig. 5A and Table 3.2).

PT was found in all investigated EEG sites; despite its widespread distribution, configuration and amplitude PT was distinct in different recording sites. PT was shorter (20 msec) in rats than in humans (100-150 msec, Weir, 1965). The amplitude of PT in the cortex was usually lower than the amplitude of the negative 'Spike 2'. In the frontal EEG, PT was split into PT_{early} and PT_{late}. These fragments were heterogeneous with diversified profiles and amplitudes. PT appeared in the occipital cortex only when seizures were fully developed. Also, PT cortex was shorter and sharper in the occipital than (both PT_{early} and PT_{late}) in the frontal cortex. PT appeared in the thalamus as sharp and with high amplitude, resembling 'sharp wave'.

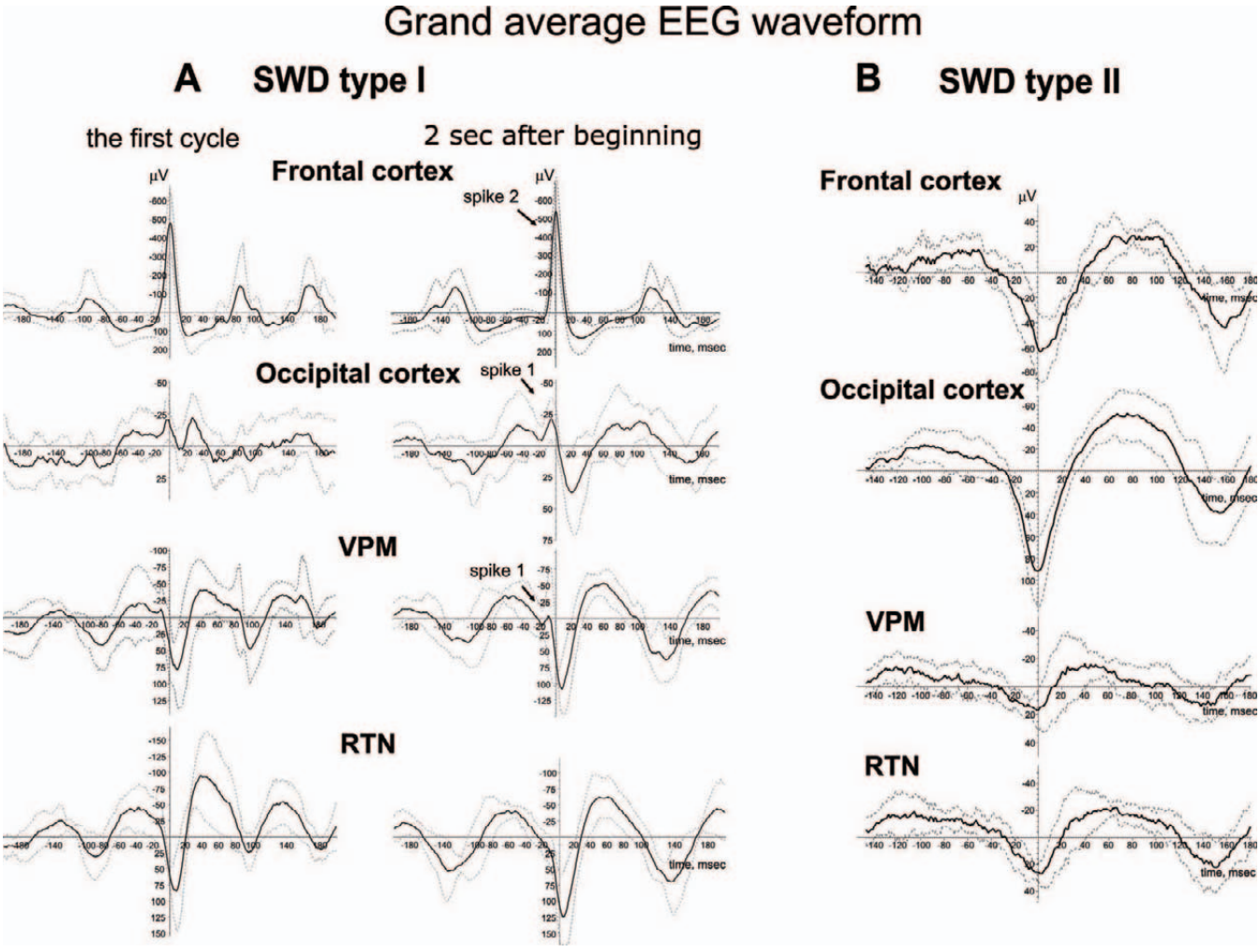

Figure 3.3. Grand average waveforms of SWD type I and type II in the cortex and the thalamus (RTN - reticular thalamic nucleus; VPM – ventroposteromedial thalamic nucleus; μV ± S.D., n = 5 rats, 20 epochs per animal for SWD I, 10 epochs for SWD II per animal). Note the peculiar dynamic behavior of 'Spike 1'. It was seen in fully grown SWD I in the occipital cortex and it correlates with modifications of this component in the VPM, where 'Spike 1' became sharper than during initial seizure cycle.

Table 3.2. The amplitude (mean ± SD, μV) and timing (msec, between brackets) of epileptiform elements in SWD I

	initial cycle				middle part			
Weir's elements	**Frontal cortex**	**Occipital cortex**	**Reticular thalamic nucleus, RTN**	**Ventroposteromedial nucleus, VPM**	**Frontal cortex**	**Occipital cortex**	**Reticular thalamic nucleus, RTN**	**Ventropostero eromedial nucleus, VPM**
Wave (preceding)			-43 ± 27 (-48)	-21 ± 57 (-39)			-41 ± 14 (-62)	-34 ± 11 (-61)
Spike 1		-20 ± 16 * (-5)		-12 ± 36 (-12)		-21 ± 17 (-6)		-3 ± 67 (-10)
Spike 2	-478 ± 162				-554 ± 175			
Positive transient (late)	128 ± 91 (22)		85 ± 62 (7)	78 ± 57 (9)	138 ± 62 (30)	37 ± 32 (20)	124 ± 70 (6)	108 ± 49 (7)
Wave (subsequent)		-21 ± 20 * (25)	-95 ± 58 (36)	-41 ± 40 (40)		-18 ± 30 (74)	-62 ± 33 (58)	-53 ± 21 (59)

Time relations were accessed in relation to the gross frontal 'Spike 2' (time zero). N = 5 rats. VPM - ventroposteromedial nucleus
* – these elements in the immature occipital SWD I did not meet the classification of Weir.

Temporal relations between epileptiform components of SWD I in cortex and thalamus

The very large-amplitude *Spike 2* was the most prominent component in the rat's EEG seizure complex, therefore it was used as a benchmark to access timing in a sequence of epileptiform elements. When the apex of 'Spike 2' in the frontal EEG coincided with time zero, it was found that 'Spike 1' occurred with a negative time lag and Wave with a positive time lag (for the numerical data we refer to Table 3.2, time lags are given between brackets). Time difference between frontal 'Spike 2' and 'Spike 1' in the VPM was -12 msec; between frontal 'Spike 2' and occipital 'Spike 1' it was -5(-6) msec. PT_{early} (20 msec) appeared before 'Spike 2' and was followed by PT_{late} (22 msec). PT appeared simultaneously in the thalamus and occipital cortex and both PT's were followed by the frontal 'Spike 2' with a time delay ranging from 6 to 9 msec.

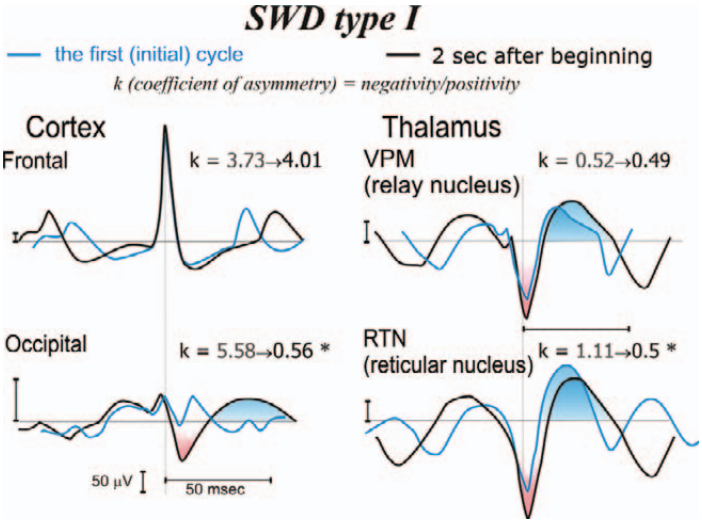

Figure 3.4. Typical waveforms of cortical and thalamic SWD I immediately at the onset (black line) and two seconds after the onset (grey line) as recorded in cortex and in thalamus. Cortical and thalamic seizures did not perfectly coincide with each other neither in phase nor in time. There was no straight pair-wise correspondence between certain elements of cortical and thalamic SWD I. The presence of large positive transient (PT) in both thalamic loci creates the illusion that thalamic SWD I are inverted compared to SWD I in the frontal cortex.
The most obvious dynamic changes in EEG morphology were found in the occipital cortex, where the initial cycle of SWD I characterized by very small positive component and two subsequent negative spikes. Later on, the positive transient in occipital SWD I seemed to grow and replaced the second negative spike. It is interesting that the waveform of fully grown occipital SWD I resembled thalamic seizures. To quantify dynamic changes in the polarity of SWD I we computed index k as a ratio between the maximum of negativity and the maximum of positivity.

To summarize, there were no congruency between the waveform of cortical and thalamic counterparts of spike-wave seizures. Cortical and thalamic seizures consisted of different components which followed each other with a consistent time shift. The latter suggests a strong temporal coupling of the electrical activity in the cortico-thalamic system during SWD I.

Dynamic changes of the waveform of SWD I

At the onset, SWD I display already a well formed EEG profile. The waveform of SWD I did not substantially change over time in frontal cortex and thalamus, except in the occipital EEG (Fig. 3.3A, B and 3.4). Moderate changes were noticed concerning the shape of the wave component. In the frontal EEG, the wave became more pronounced and more isolated as seizure progresses. In the thalamus, the distance between the two subsequent negative waves in the middle of SWD I became larger than it was in the initial cycle, indicating a decrease of the intrinsic frequency of SWD I.

The EEG pattern of SWD I in the occipital cortex changed substantially with time (Fig. 3.4). The positive phase was poorly pronounced at seizure onset and PT was not recognized. Instead, two negative components were present (somewhat primordial seizure components): the first was a sharp 'Spike 1', the second was an unspecified component which appeared 30 msec later.

Symmetry and polarity in SWD I

The *polarity* of the EEG paroxysm was established according to the IFSECN recommendations (3). Here, we characterized symmetry/asymmetry in spike-wave pattern as a ratio between the two extreme negative and the positive amplitude values (k, 'index of polarity' see Methods section and Fig. 3.4).

In the frontal cortex, SWD I were asymmetric (k=3.7) due to the disproportionately high negative phase (Spike 2) as compared to the positive transient. SWD I became even more asymmetric as seizure progresses and k was equal to 4.0 in the fully grown SWD I.

In the thalamus, SWD I were much more symmetrical compared to their cortical counterparts. During the initial cycle, SWD I in the VPM were positively oriented (k=0.52, PT was higher than Wave, Fig.3.4), also in the fully developed SWD I, the positive deflection was two times larger in amplitude than the negative deflection (k=0.49, Fig. 3.4). In the RTN, the initial cycle of SWD I was symmetrical (k=1.1, Wave was slightly higher than PT) and the positive phase increased in the fully developed SWD I and their pattern became more asymmetric (k=0.5, Fig. 3.4, Table 3.2). In the occipital cortex, SWD I showed a polarity shift as seizure developed. Initially, the positive component in the occipital SWD I was very weak and SWD I was oriented negatively. The occurrence of the well-shaped PT in mature SWD I was associated with a phase shift in the positive direction.

Therefore, symmetry in SWD changed as seizure progresses, and in different recording areas these changes were different. One common feature, an increase of the absolute values of the positive phases, was obtained during the evolution of SWD I in both thalamic sites and in the occipital cortex.

Table 3.3. The amplitude of comparable elements in SWD type I and II (μV mean ± SD; n = 5 rats).

`	Frontal cortex		Occipital cortex		Reticular thalamic nucleus, RTN		Ventroposteromedial nucleus, VPM	
	SWD I	SWD II	SWD I	SWD II	SWD I	SWD II	SWD I	SWD II
Positive transient	138 ± 62	63± 29	37 ± 32	92± 30 ^{S*}	124 ± 70	26 ± 9 ^{S}	108 ± 49	17 ± 13 ^{S}
Wave (subsequent)	-	-28 ± 6	-18 ± 30	-49± 24 *	-62 ± 33	-21 ± 5 ^{S}	-53 ± 21	-18 ± 17 ^{S}

^{S} – elements of SWD I and SWD II had significantly different amplitude, $p<0.05$, paired t-test.
* - elements of SWD II in the occipital channel had significantly higher amplitude than in the frontal channel, $p<0.05$, paired t-test.

SWD type I as compared to SWD type II

The largest difference between SWD I at the frontal cortex and SWD II at the occipital cortex was the presence of the large Sp 2 in the SWD I in the frontal cortex. SWD I and SWD II revealed the same components (PT and Wave) in the occipital cortex, however SWD I displayed 'Spike 1', while SWD II did not. PT was significantly higher in SWD II than in SWD I in the occipital cortex. All components of SWD II in the occipital cortex were significantly higher in amplitude than in the frontal cortex and in the thalamus (all p's<0.05, Table 3.3), suggesting that SWD II had an occipital distribution. This is in agreement with earlier reports [Midzianovskaia et al., 2001]. In the thalamus, amplitude of PT in SWD I was significantly higher than amplitude PT in SWD II (Table 3.3) and it seemed that the two types of SWD were clearly different at the level of the thalamus. Only rudimentary SWD II activity was present in the thalamus and frontal cortex, it mirrored and perhaps passively followed the occipital activity. This is in contrast to the classical SWD I; its phenotype showed large topographic differences in waveform architecture dependent on the recording area.

DISCUSSION

The present study provides statistical descriptions of SWD occurring in cortex and thalamus in a genetic model of absence epilepsy, the WAG/Rij strain of rats. Based on principles of clinical electroencephalography and the classification of Weir, we found similarities in EEG patterning of spike-wave seizures in our rats and in patients with absence epilepsy. The SWD in rats appeared as a unique constellation of epileptiform events that were described using Weir's classification of elements into 'Spike 1', 'Spike 2', PT and Wave [Weir, 1965].

The classical SWD type I and the local SWD type II are both multi-phasic negative-positive-negative potentials, however they consist of different epileptiform elements. SWD I in the frontal cortex appeared as sequence PT_{early}– Sp2 – PT_{late} and in the thalamus as (Sp1) – PT_{late} – Wave. SWD II was recognized in the occipital cortex as a short train of (Sp1) – PT – Wave.

General remarks on the waveform of SWD

The EEG pattern of SWD in WAG/Rij is not identical to that in humans, however, the human pattern is mimicked by the rats. In the present study we used intracortical electrodes for both deep and surface (epidural) EEG recordings. The electrodes are implanted in close vicinity of the sources of electrical activity and the problem of inequality of EEG signals recorded from thalamic and cortical sources might be less. Anyway, we found well pronounced SWD I in the thalamus; this means that thalamic structures are capable to reproduce stereotypic epileptic activity on the level of local field potentials. Depth EEG recordings done in the past cast some doubt on the role of the thalamus in absence seizures in humans. As known, subcortical SWD appear to be less regular and pronounced than SWD recorded simultaneously in the cortex [Angeleri et al., 1964]. Electrical activity derived from deep brain structures is not comparable with activity originating from the scull surface considering differences in spatial organization of neuronal current sources and resulting electric fields and dipoles. Depth EEG electrodes are surrounded by radial distributed sources of electrical activity. Therefore the resulting currents damp each other and produce dispersion of electrical fields [Lopes da Silva and van Rotterdam, 1982]. Distinctions in morphology between SWD in rats and humans can be explained by differences in scalp versus intracranial recording, needle vs disk electrodes, configuration of electrical fields, choice of the location and type of reference [Rodin, 1989], the absence of convolutions in the cerebral cortex of rodents, the smaller size of the brain, and interspecies difference in the frequency of SWD.

We found that the waveform of SWD I in VPM and RTN have a similar appearance as previously described: "the thalamic discharges were characterized by slow negative waves combined with a positive sharp wave or positive spike. The positive spike was preceded by a highly sharp (small) negative spike appearing on the decreasing slope of the negative wave at certain thalamic recording sites," (Meeren et al, 2002, p. 1488). In this description, 'the positive sharp wave' precisely matches the definition of PT and the 'highly sharp (small) negative spike' – to 'Spike 1'. Our data strongly agree with Meeren's et al's observation that a sharp negative spike (Spike 1) was present in SWD I in the VPM, but absent in the RTN. Besides that, elements of SWD I appeared in the RTN and in the VPM virtually without a time delay and they were tightly time locked, suggesting that epileptogenic processes in these two nuclei are closely interconnected.

On the temporal evolution of SWD I

The temporal evolution of SWD I is characterized by a decrease in frequency. This follows from the period between two subsequent waves in the thalamus: at the beginning it was ~80 msec, in the middle part it was ~120 msec respectively. Therefore, the initial seizure frequency was ~12.5 Hz and reduced with time to ~8.3 Hz, in agreement with other data [Drinkenburg et al., 1993; Midzianovskaia et al., 2001]. Similar dynamics were recently described with a modified wavelet analyses, albeit with higher frequencies at the beginning of the SWD [Bosnyakova et al., 2006]. We also found progressive changes in seizure polarity: the shift in negativity/positivity asymmetry was associated with an increase of the positive phase. Noteworthy is that the temporal evolution of SWD I in the frontal cortex did not follow this scenario.

The initial cycle of SWD I in the occipital cortex comprised atypical elements that were absent in mature seizures. Probably, occipital neurons are not perfectly integrated in the oscillatory machinery that start producing SWD I. In that sense, SWD I are not completely generalized during the initial stage. Several cycles should pass until SWD I become fully developed and the spike-wave pattern in the remote cortical areas (such as occipital one) acquire a mature waveform. Tiny transient changes of the waveform characterize the time evolution of SWD I in the thalamus. The absence of significant dynamic modifications in the waveform of SWD I in the frontal cortex and in the thalamus confirms that the spike-wave rhythm is highly constant and stabile.

Differences between SWD type I and SWD type II

The differences between SWD I and II were as follows: SWD II had lower amplitude, lower frequency (6-7 Hz), opposite EEG polarity, shorter duration (~ 1 second). These characteristics, including the fronto-parietal distribution of SWD I and occipital predominance of SWD II, are in agreement with previous reports [van Luijtelaar and Coenen 1986; Midzianovskaia et al., 2001]. Comparative studies of SWD I and SWD II have shown that these seizure types have a different pharmacology, genetics and ontogeny, yet very little is known about neurophysiological mechanisms of SWD II. Virtually nothing is known about the source of type II SWD; therefore it is important to note that SWD II are nearly absent in the thalamus and in the dorsal hippocampus. The present analysis further underlines differences in the averaged waveform of cortical SWD I and SWD II. In particular, the phenotype of the fronto-parietal SWD I was characterized by a high voltage negative 'Spike 2' in the frontal EEG derivation, a small 'Spike 1' in the occipital SWD I, that appeared 5-6 msec prior to the frontal 'Spike 2' and a low amplitude Wave. In contrast, local occipital SWD II were characterized by an occasional 'Spike 1' and high-amplitude Wave.

We found that SWD II were nearly absent in the thalamus and dorsal hippocampus, but the waveform of local occipital SWD II resembled the waveform of SWD I in the same occipital EEG site. We assume that SWD II might appear in the EEG when the thalamus (at least its somatosensory part) is not integrated into the epileptogenic network, thus preventing generalization of primordial SWD I. This results in 'residual' SWD II in the occipital cortex. In contrast, SWD II may have a cortical occipital origin. They may appear in the occipital cortex as 'underdeveloped' (non-generalized) spike-wave activities, furthermore, the thalamus and the anterior cortex might merely be passive followers of this occipital rhythm.

Cortical expression of SWD and their thalamic equivalents

The EEG profile of SWD I differed in the cortex and in the thalamus. First, SWD I had small waves in the cortex, in the thalamus the wave component was relatively large. Second, the negative 'Spike 2' was extremely high in the frontal cortex, but it was absent in the thalamus. Instead, 'Spike 1' was more stable in the thalamus than in the cortex.

SWD I occur simultaneously in the cortex and thalamus, but they were not congruent to each other. First, SWD I in the anterior-middle cortex and in the thalamus had an opposite polarity. As known, signals recorded simultaneously from the surface and the depth of the brain with a common reference electrode, show polarity reversal [Freeman, 1978; Coenen, 1995]. The same polarity reversal was found in petit mal patients [Hayne et al., 1949] and likely to reflect an opposite orientation of electrical currents formed by the superficial and deep neural mass [Lopes da Silva and van Rotterdam, 1982]. Second, the largest component of thalamic SWD I was the sharp positive transient (PT) that appeared in both thalamic loci 7-9 msec after the frontal 'Spike 2'. This time lag can be accounted for by the synaptic delay. It seems likely that synchronous bursting of cortical cells during 'Spike 2' could enter the thalamus via dense descending projections [Deschênes et al., 1998] resulting to a sharp positive deflection (PT) in both thalamic leads. This creates the illusion that thalamic SWD I are inverted compared to frontal cortical SWD I.

The frontal cortex can augment the spike element because of dense mutual (ascending and descending) associations between pyramidal neurons in deep cortical layers and numerous thalamic nuclei (including somatosensory thalamic nucleus, the VPM). Besides that, the frontal cortex sends and receives long distance intracortical projections [Kolb, 1990; Rouiller and Welker, 2000]. Therefore, it is also engaged in the generalization and propagation of SWD I. In all, the frontal cortex plays a key role in the distribution of spike-wave activity throughout the horizontal and vertical pathways of the thalamo-cortical circuitry.

Opposite to the frontal (and parietal) cortical regions, the occipital cortex seems to be passively involved in SWD I. The waveforms of SWD I in the thalamus and in the occipital cortex were very congruent (Fig. 3.3-3.4), suggesting that the occipital cortex may simply mirror epileptiform activity derived from the thalamus and is just passively involved in the propagation of spike-wave activity.

CONCLUSIONS

(1) Both types of SWD in WAG/Rij rats represent a sequence of elements, which are relevant for elements in spike-wave complexes as has been described in patients with absence seizures (Weir, 1960). In that sense SWD in our subjects resemble spike-and-slow wave activity in humans.

(2) Elements of SWD I in the frontal cortex are PT_{early} – Sp2 – PT_{late}; in the occipital cortex they are (Sp1) – PT – Wave, and in the thalamus (Sp1) – PT – Wave. The elements of SWD I are area-specific and show different patterns in distinct EEG channels due to neuronal properties and cytoarchitecture.

(3) The largest component of SWD I, 'Spike 2', is most pronounced in the frontal cortex, smaller in the parietal cortex and absent the occipital cortex, suggesting that 'Spike 2' may by augmented by local processes within the anterior cortex.

(4) Wave is present in the neocortex and in the thalamus. More generalized Wave (as compared to Spikes) may relate to the processes of neuronal generalization.

(5) Complexity of spatiotemporal pattern of SWD I can be accounted for the specific contribution of reciprocally interconnected neuronal populations in cortex and thalamus.

(6) The occipital cortex is unable to generate any *de novo* elements. The waveform of SWD I in the occipital cortex resembles the waveform in the thalamus, therefore occipital SWD I may be just a fingerprint of thalamic activity.

(7) 'Spike 2' in frontal SWD I relates to a delayed (6-9 msec) positive deflection on thalamic records, suggesting a descending propagation of paroxysmal activity from frontal cortex to thalamus.

(8) SWD type II is characterized in the occipital cortex as: PT – negative Wave. Simultaneous activity in the frontal cortex, VPM and RTN was low, suggesting that SWD II only passively spread over the investigated thalamo-cortical loci.

3.2 Adrenergic control of SWD type I and II †

ABSTRACT

The alpha-2 adrenoreceptor agonist clonidine in low dose inhibits the release of noradrenaline and aggravates absence seizures. The present study examines properties of two types of spike-wave discharges (SWD) in a genetic model of absence epilepsy, the WAG/Rij rats. After reduction of noradrenergic neurotransmission with clonidine (0.00625 mg/kg, i.p.), the electrical activity was recorded in the neocortex, the ventroposteromedial nucleus (VPM) and the reticular thalamic nucleus (RTN).

Clonidine temporally reduced percentage of wakefulness but did not affect sleep. Clonidine decreased the spectral power of sleep EEG (mostly in the delta band), this effect was found in the cortex and in the VPM. Clonidine increased the incidence of SWD type I (generalized); the spectral power of SWD I was lower in the frontal cortex (mostly in 1–9 and 30–100 Hz) and in the VPM (1–5 Hz), but higher in the RTN (9–14 Hz). Local occipital SWD (type II) had a tendency to be less numerous after clonidine, they had a lower power in the 5–9 Hz band in the occipital cortex, in the VPM and in the RTN. It can be concluded that strengthening of 9–14 Hz activity in the RTN may underlie clonidine-induced aggravation of SWD I.

INTRODUCTION

In **Chapter 3.1** we reported on a difference in EEG morphology between two types of SWD. We also mentioned that they differ in respect topographic distribution [Midzianovskaia et al., 2001] and **Chapter 4.1** reports on spectral properties between two types of SWD. This section describes noradrenergic mechanisms that control the incidence of SWD I and SWD II. Systemic injections of alpha-2 agonist clonidine are known to aggravate generalized SWD type I, but do not influence local occipital SWD type II [van Luijtelaar, 1997]. Probably, noradrenergic neuromodullatory supply is necessary for the occurrence of SWD I, but not SWD II. It seems likely that noradrenergic system modulates thalamo-cortical activity thus promoting SWD I, but SWD II remain unaffected.

An importance of noradrenergic modulation of epilepsy (in particular, absence epilepsy and SWD) has been confirmed by extensive literature. The central noradrenergic system is among intrinsic anti-epileptic mechanisms can normally protect the brain against paroxysmal activity. On the synaptic level noradrenaline (NA) adjusts a balance between excitation and inhibition, this impedes neurons to enter a hyperexcitatory state, therefore the probability of absence seizures diminishes for review on anti-epileptic activity of NA (see Refs. [Weinshenker and Szot, 2002; and Giorgi et al., 2004]). Activation of alpha-2 AR on dendrites and soma of noradrenergic neurons of the *locus coeruleus* (autoreceptors) reduces firing of noradrenergic neurons that inhibit NA release [Langer, 1974; Svensson et al., 1975; Gobert et al., 1998].

Historically, clonidine is used as a selective agonist of alpha-2 AR [Ruffolo and Hieble, 1994; Bylund et al., 1994]. Alpha-2 AR is also present on terminals of other neuromodulatory neurons (heteroreceptors) such as dopaminergic and serotoninergic neurons [Svensson et al., 1975; Gobert et al., 1998, Scheibner et al., 2001]. These receptors are 10 times less sensitive to clonidine than autoreceptors [Maura et al., 1985]. Since almost all brain structures receive NA-containing terminals from the *locus coeruleus* [Aston-Jones et al., 1984; Jones, 1985; Jones and Moore, 1985], peripheral administration of clonidine reduces noradrenergic neurotransmission throughout the entire brain. In particular, weakening of the ascending adrenergic innervation may facilitate bursting activity of the thalamo-cortical neurons [Steriade and Deschenes, 1984; McCormick, 1989; McCormick, 1991] and reinforce oscillatory activity in the thalamocortical loop (relay nuclei in the thalamus, the reticular thalamic nucleus (RTN) and the neocortex [Steriade 2003; Avanzini et al., 2000]). In such an indirect way clonidine may promote generalized SWD I. However, clonidine is unable to provoke *de novo* SWD in non-epileptic animals [Marescaux et al., 1992]. As known, some rat strains with absence epilepsy have a congenital deficit of aminergic system [Vantini et. al., 1984; Buzsáki et al., 1990] this gives a room for clonidine to have a specific pro-absence effect. Mechanism by which clonidine can intensify absence seizures is still unknow. Buzsaki et al. [1991] showed that clonidine promote SWD via both pre-synaptic and post-synaptic alpha-2 AR. Here we examine the hypothesis that the more synchronous thalamic activity after clonidine injections results to the increase of SWD I.

Clonidine aggravates absence epilepsy in a dose-dependent manner [Micheletti et al., 1987; Buzsáki et al 1991]. The administration of clonidine in a low dose results in electroencephalographic and behavioural sedation

† Published in:
Sitnikova E, van Luijtelaar G. Reduction of adrenergic neurotransmission with clonidine aggravates spike-wave seizures and alters activity in the cortex and the thalamus in WAG/Rij rats. Brain Research Bulletin. 2005; 64(6): 533-540.
Sitnikova E, van Luijtelaar G. Alpha-2 adrenergic mechanisms of spike-wave activity and sleep EEG in rats. Sleep-Wake in the Netherlands, 2004; 15: 67-70.

[Drew et al., 1979; Hayashi et al., 1993; Seidel et al., 1995; Bischoff et al., 1998], apparently associated with the reduction of noradrenergic neurotransmission. Low-vigilance and transitory states are favourable for the occurrence of SWD [Lannes et al., 1988; Drinkenburg et al., 1991]; therefore clonidine-induced sedation may indirectly influence SWD. High doses of the drug (higher than 0.1 mg/kg) can also intensify some side effects (decrease of temperature, heart and respiratory rates, salivation etc. [Pickworth et al., 1982]) and result to dissociation between EEG and behavioural activities. Here we use clonidine in minimal dosage 0.00625 mg/kg: it is enough to inhibit NA release via pre-synatic mechanisms [Langer, 1974; Svensson et al., 1975] and to enhance SWD I in WAG/Rij rats [van Luijtelaar, 1997], yet it is insufficient to influence other neuromodulatory systems via heteroreceptors [Cervo and Samanin, 1991] or to destroy the usual pattern of EEG and behaviour [Drew et al., 1979; Pastel and Fernstrom, 1984; Fontana and Schefke, 1989; Frankhuyzen and Mulder, 1982].

In the present chapter we examine how depletion of noradrenergic innervation (systemic injections of clonidine) changes the number and the properties of SWD I and SWD II. We also examine changes of electrical activity in the cortex and the thalamus during SWD I, SWD II and normal sleep.

METHODS

Experiments were performed in nine male WAG/Rij rats (11-12 month old, body weight 370-410 g). '*Surgery procedure and histological control*', '*Electrode setup*' and '*EEG recording*' are the same to that described in **Chapter 3.1** 'Methods'.

Clonidine (Catapresan®, 0.15 mg/ml clonidinehydrochloride, Boehringer Ingelheim bv, Alkmaar, the Netherlands) was intraperitoneally injected in a dose of 0.00625 mg/kg. The EEG was recorded in freely moving rats in a noise-isolated Faraday cage during 4 h immediately after the cessation of injection. Animals were allowed to habituate to a Plexiglas recording cage (25 cm×30 cm width, 35 cm high) for an hour before each recording session, 6 h base-line EEG was recorded prior to the pharmacological experiment and used as control. All recording sessions were performed during the dark period, when the incidence of SWD I is known to be higher [van Luijtelaar and Coenen, 1988]. The EEG signals were fed into a multi-channel differential amplifier via a swivel contact, band-pass filtered between 1 and 500 Hz, digitized with 1024 samples/s and stored onto hard disk (Data Acquisition Hardware and Software, DATAQ Instruments Inc., Akron, OH).

Two types of SWD were detected on the frontal and occipital cortical derivations (Fig. 3.1 in **Chapter 3.1**) using criteria described by van Luijtelaar and Coenen (1986) and by Midzianovskaia et al. (2001). SWD I were detected automatically based on the threshold value of the EEG slope (software developed by P.L.C. van den Broek (NICI, University of Nijmegen, The Netherlands). The number of SWD I and II after injections of clonidine was scored on the full-length EEG records, i.e. during 4 h after each injection. Number and duration of SWD were calculated and averaged in 30 min blocks. Periods of sleep and waking were counted and presented in percentages in time-blocks of 30 min. The cumulative time of SWD I (total time of seizures) was also examined in 30 min intervals. General linear model (GLM) of ANOVA was used for the two-factor analysis: the effect of clonidine (factor 'Drug') was estimated over time (factor 'Time').

EEG analysis

A Hanning windowed Fast Fourier Transform (FFT) was performed in the whole EEG segments with SWD activity (0.1 Hz resolution). The spectrum of SWD I in control was compared with the spectrum of SWD during the first, second and third hours after injection of clonidine. Coherence (non-normalized) was measured in intracortical EEG pairs (between the frontal and occipital EEG) and cortico-thalamic pairs (between the frontal cortex and VPM) as a square of the cross-spectrum of the two channels with 0.1 Hz (Brain Vision Analyser Software © BrainProducts GmbH). The maximal value of coherence was computed and averaged. Paired t-test was used for statistical analysis.

In addition to that, 1-sec (1024 samples) EEG epochs during non-REM sleep (n=20 per animal), SWD I (n=20 per animal) and SWD II (5–20 per animal) were selected for the statistical analysis of EEG power. Episodes with SWD I begun 500 ms after the first spike in a train of SWD; episodes with SWD II started immediately from the first spike. In clonidine conditions the EEG samples were taken in a period 30–90 min after injection. Total EEG power and power of the specific frequency bands: 1-5 Hz, 5-9 Hz, 9-14 Hz, 14-30 Hz, 30-60 and 60-100 Hz were calculated and statistically compared with t-tests for related samples ($p<0.05$).

RESULTS

Effect of clonidine on vigilance

After injections of clonidine animals were sluggish and drowsy. Accelerated breathing, twitching of vibrissae and eyes, facial myoclonic jerks were often observed during periods of immobility, all these behavioral manifestations were accompanied by steady SWD I.

Percentage of wakefulness after injections of clonidine significantly decreased compared to control ($F(1,6)=5.09$, $p<0.05$). This effect was significant at the beginning of the post-injection period and disappeared at the end of the second hour after injection (post-hoc paired t-test, $p<0.05$, Fig. 3.5B). Decrease of wakefulness is likely to occur at the expense of the prolonged seizures. Clonidine significantly increased total time of seizures ($F(1,6)=35.7$, $p<0.002$), but did not affect amount of sleep (Fig. 3.5B). In total, pro-absence effect of clonidine lasted around 90 minutes; this corresponds well to half-life of the drug [Castro and Eisenach, 1989].

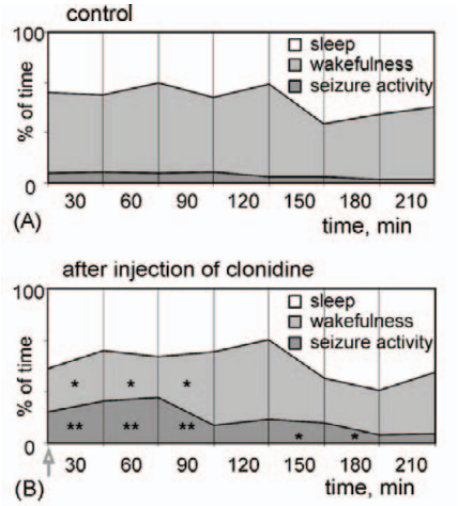

Figure 3.5. Transient changes of behavioral states after i.p. injection of clonidine (0.00625 mg/kg, n=8 rats). Asterisked are significant changes, post-hoc analysis, paired t-test - * $0.005<p<0.05$; ** - $p<0.005$.

EEG pattern of SWD I and SWD II

All experimental animals had spontaneous SWD. EEG at the frontal cortical contained clear high-voltage SWD I, which lasted 5.8 ± 1.4 sec (± SD). SWD II were present on the occipital cortical EEG lead and were recognized as sharp 6-7 Hz waves (Fig. 3.1). SWD I were abundantly present in all subjects (25 – 45 seizures per hour), six out of eight rats had SWD II (2 - 5 per hour).

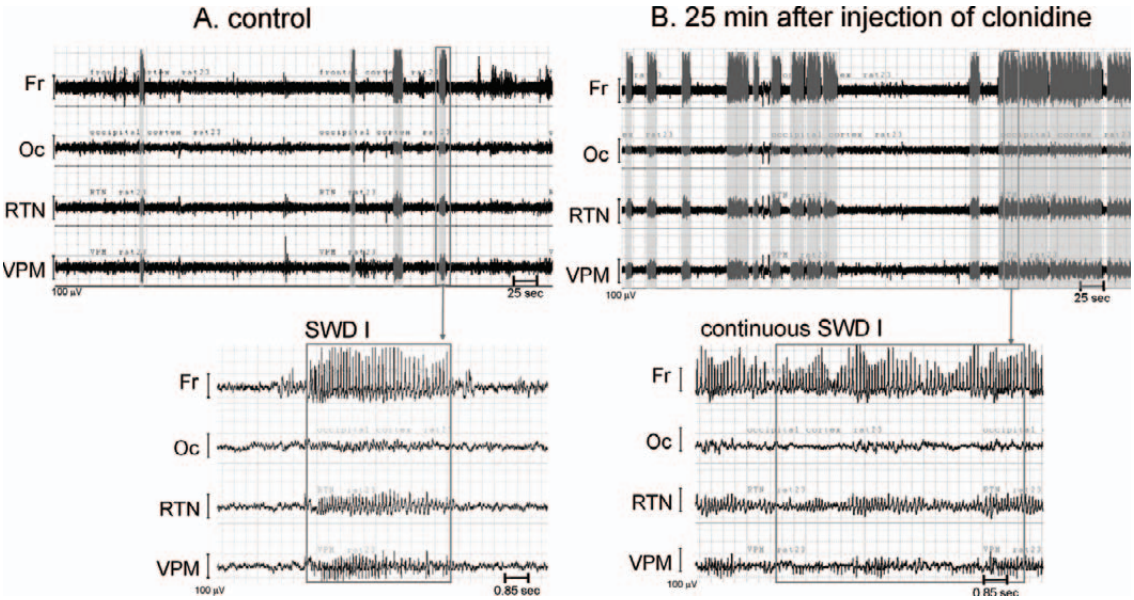

Figure 3.6. Records of electrical activity in the cortex (Fr - frontal, Oc - occipital), in the ventroposteromedial thalamic nucleus (VPM) and in the reticular thalamic nucleus (RTN) in control (A) and after injection of clonidine (0.00625 mg/kg, B). Periods with SWD I are shaded, typical examples of SWD I are shown below in larger time resolution.

Effect of clonidine on the dynamic and duration of SWD

The EEG pattern of SWD I after injection of clonidine was less regular than the pattern of control SWD I: amplitude and frequency of the spikes fluctuated (Fig. 3.6B). Compared to control, after injection of clonidine SWD I lasted longer (from 5 to 30 sec, mean = 13.3 ± 3.6 sec, ± SD), this effect was significant ($F(1,6)=17.8$, $p<0.01$) and a significant 'Drug–Time' interaction - $F(1,6)=14.9$, $p<0.01$) and temporal effect of 'Time' - $F(1,6)=27.3$, $p<0.001$) was also found.

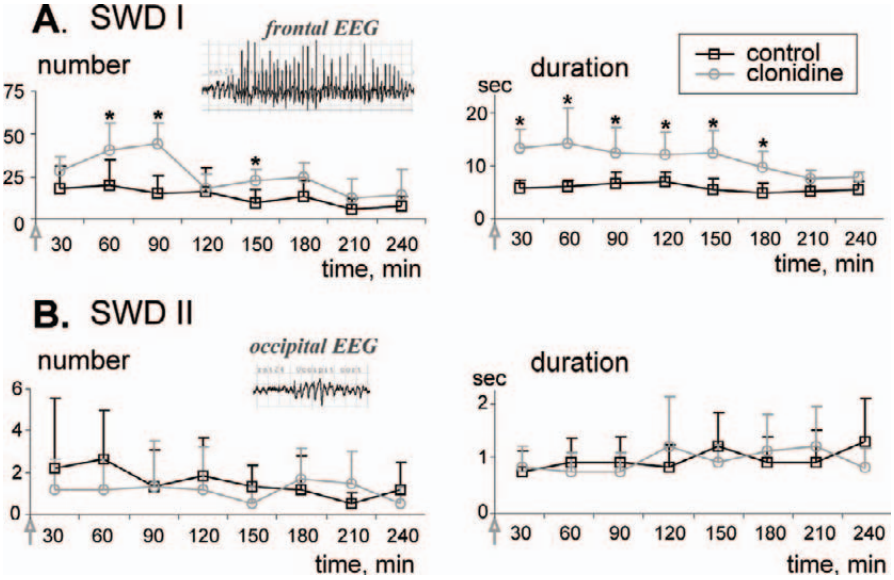

Figure 3.7. Time course of incidence and duration of SWD after clonidine injection (0.00625 mg/kg). SWD I (A) were aggravated and lasted longer till the end of the third hour (n=8 rats, mean ± SD). * - significant changes, post-hoc analysis, paired t-test, $p<0.05$.Clonidine did not significantly affect SWD II (B, n=6 rats, mean ± SD).

Number of SWD I increased nearly twice during the first hour after clonidine injection as compared to control (38 ± 23 versus 69 ± 20 seizures per hour). This effect of clonidine was significant $F(1,6)=21.6$, $p<0.005$). The incidence of SWD I changed over time (factor 'Time' - $F(1,6)=80.9$, $p<0.005$), interaction factors 'Drug' and 'Time' was also significant ($F(1,6)=25.8$, $p<0.01$). Clonidine was most effective 30-90 minutes after injection (post-hoc analysis, paired t-test, $p<0.05$, Fig. 3.7A).

SWD II after injection of clonidine tended to be reduced in number (4.8 ± 4.3 versus 2.3 ± 2.2 per hour, ± SD, Fig. 3.7B). Appearance of SWD II highly varied from subject to subject, therefore the effect of clonidine on SWD II is less clear than that on SWD I.

Effect of clonidine on the spectral features of SWD

The lower regularity of the spike-components of SWD I, which were seen on EEG after injection of clonidine, might have been one of the reasons why the shape of power spectrum of SWD I including the peak frequency (Fig. 3.8B) was not changed. The pattern of EEG spectrum of SWD I was nearly the same after clonidine than after control (Fig. 3.8A).

Intracortical coherence significantly decreased during the first hour after clonidine injection ($p<0.05$, paired t-test), cortico-thalamic coherence was not changed (Fig. 3.8C). Noteworthy was that in both conditions, the strength of coherence between the frontal and occipital cortices was lower than between the frontal cortex and the VPM.

Effect of clonidine on the amplitude characteristics of SWD and sleep EEG

Visual inspection of sleep EEG revealed that EEG amplitude after injection of clonidine was lower than in control; sleep spindles and delta waves appeared less frequently. Clonidine injections resulted in a decrease of the EEG power during sleep, SWD I and SWD II. Compared to control, EEG spectral power during sleep significantly decreased in the frontal and occipital cortical cortices and in the VPM mainly due to a decrease of low (1-4 Hz) frequencies (Fig. 3.9A).

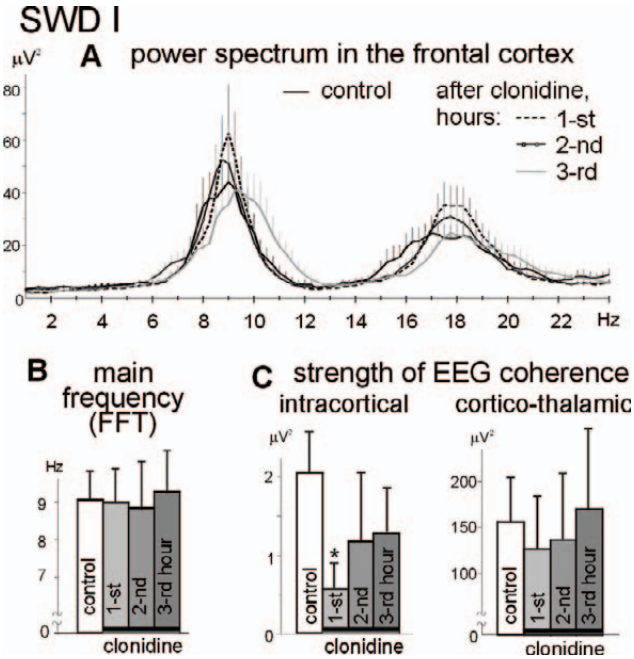

Figure 3.8. Amplitude characteristics of SWD I after administration of clonidine (0.00625 mg/kgm, (n=8 rats, mean ± SD, * - $p<0.05$, significant changes, paired t-test). Clonidine did not change the shape of EEG power spectrum (A), nor mean frequency (B), but it temporally diminished fronto-occipital (intracortical) coherence (C).

Total power of SWD I was significantly lower in the frontal cortex after clonidine administration compared to control, the decrease in power was found in the 1-5 Hz, 9-14 Hz and 30 - 100 Hz frequency bands. In contrast, the electrical activity in the RTN increased with clonidine, the power of 9-14 Hz was significantly higher than in the control condition (Fig. 3.9B).

Total power of SWD II in the occipital cortex and in the VPM decreased after clonidine injections, this was mainly due to the reduction in 5-9 Hz, also the electrical activity in the RTN had a low power in the 5-9 Hz band (Fig. 3.9C).

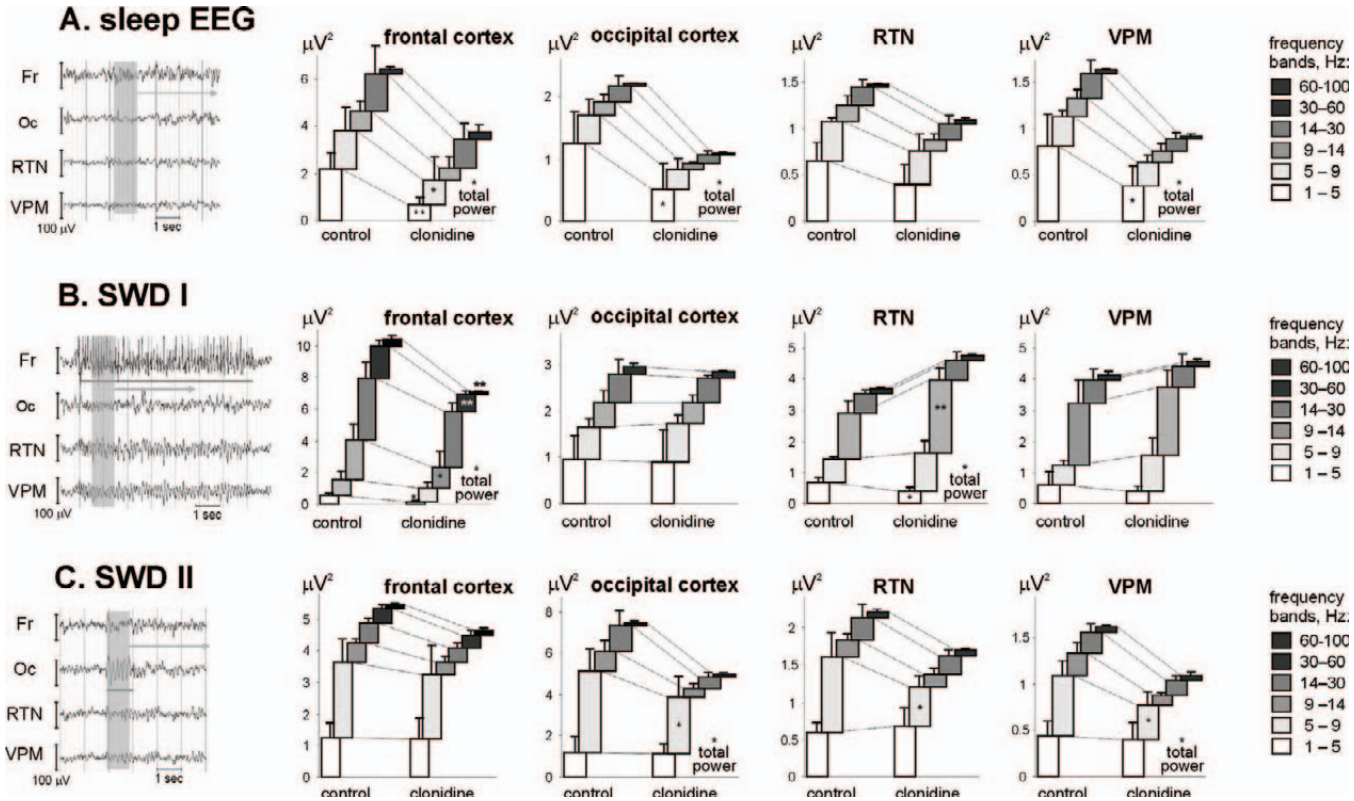

Figure 3.9 Changes in power of electrical activity during sleep (A), SWD I (B) and SWD II (C) 30-90 min after injection of clonidine. Noteworthy that clonidine increased 9-14 Hz activity in the RTN only during SWD I; SWD II contained less power in the band with the peak frequency, 5-9 Hz. * - significant changes, paired t-test, $p<0.05$.

DISCUSSION

The present study shows that pharmacological reduction of noradrenergic neurotransmission with low-dose of alpha-2 agonist clonidine had the following effects: (1) increased time spent by animals in waking state; (2) increased the incidence and duration of SWD I; (3) reduced fronto-occipital coherence during SWD I (for one hour); (4) decreased of EEG power during sleep and during SWD I and SWD II; (5) affected activity in the RTN: increased total EEG power and alpha activity during SWD I, and decrease theta activity during SWD II.

Effect of clonidine in vigilance and sleep EEG

In our experiment i.p. injection of clondine decreased vigilance for approximately 1.5 hour. A sedative effect of clonidine is known for a long time [Drew et al., 1979; Hayashi et al., 1993; Seidel et al., 1995]. This effect might be a consequence of the inhibition of noradrenergic modulation, in addition to that, clonidine may directly affect 'sleep-active neurons' in the preoptic hypothalamic area (these neurons have mostly alpha 2-receptors), that would also facilitate low vigilance states and promote sleep [Osaka and Matsumura, 1995]. Altogether, this explains well why wakefulness in our subjects decreased after clonidine. Here we did not find a sleep-promoting effect of the drug. Probably, the dosage of clonidine was too low (0.00625 mg/kg) to make our subjects fully asleep, yet a soporific effect of clonidine was found in higher (0.02-0.04 mg/kg) dose [Seidel et al., 1995]). In the present dose, clonidine induced drowsiness, e.g. a state, which is favorable for SWD to appear [Lannes et al., 1988; Drinkenburg et al., 1991]. *Per se*, this low vigilance state cannot cause such an enormous amount of long-lasting SWD, as we found here.

The amount of sleep did not change with clonidine, but the properties of sleep EEG have altered: delta activity decreased in the cortex and in the VPM. Clonidine is known to suppress delta activity in non-epileptic rats [Pastel and Fernstrom, 1984] but, in opposite, it enhances delta EEG activity in humans [Bischoff et al., 1998]. Clonidine seems to oppositely affect oscillatory activity in thalamo-cortical and hippocampal circuits, namely, it suppress hippocampal theta activity and enhance alpha (thalamo-cortical) activity [Emilien, 1989; Kitchigina et al., 2003]. SWD are known to originate from thalamo-cortical circuit and comprise a strong alpha band component. Here we did not found drastic changes of alpha frequencies after injections of clonidine, in contrast to a considerable decrease of delta and theta EEG components. A genetic predisposition to absence seizures and SWD in our subjects may be underlain by impairment of thalamo-cortical neuronal system [Avanzini et al., 2000; Buzsaki et al., 1990; Coenen and van Luijtelaar, 2003]. As known, delta oscillations and SWD share same thalamo-cortical mechanisms [reviewed in Steriade 2003] and at the same time, delta and alpha activity cannot be produced at the same time [Nuñez at al., 1992]. By decreasing delta activity, clonidine might create a favourable state for thalamo-cortical circuit to generate SWD.

Effect of clonidine in thalamo-cortical activity during SWD

Clonidine is known to promote absence seizures in various rodent models: in WAG/Rij rats [van Luijtelaar, 1997], in GAERS [Micheletti et al., 1987], in Fisher 344 [Buzsaki, 1991], and also in old Charles River rats [Kleinlogel, 1985]. To explain the absence-seizure promoting effect of clonidine, Buzsáki and co-workers [1991] assumed that clonidine may interact not only with presynaptic alpha-2 AR, but also with a specific type of postsynaptic alpha-2 AR in the thalamus. It is not possible to make a difference between presynaptic and postsynaptic effects of drugs affecting alpha-2 AR (e.g. AR on the terminals of the *locus coeruleus* and target cells). According to our data, clonidine injection resulted in a decrease of EEG power all over the cortex and the thalamus, except the RTN, where an increase in power was found only during SWD I and mainly in 9-14 Hz. This could mean that the RTN, rather than the VPM, may control occurrence of SWD I by putative modulatory alpha2-adrenergic mechanisms. In the RTN, an enlargement of electrical activity in 9-14 Hz (mean frequency of SWD I) may imply high neuronal synchronization therefore the RTN might be responsible for SWD-promoting effect of clonidine. Moreover, the RTN seems to be more sensitive to noradrenergic modulation as compared to the rest parts of the thalamus. As known, the RTN receives the most dense innervation from noradrenergic terminals, the latter are extended throughout the thalamus but concentrated within the thalamic reticular nucleus [Swanson and Hartman, 1978].

Another indication of changes in the thalamo-cortical system is a reduction of fronto-occipital coherence during the first hour after injections of clonidine. This weakening of intracortical associations is intriguing: the number of generalized SWD type I is increased in clonidine-injected subjects, but frontal and occipital areas are not synchronized. This means that clonidine-induced seizures appeared less generalized as compared to SWD I in drug-free animals. It is important that fronto-occipital dissociation was found only during the first hour after injection and returned the initial level as soon as the number of SWD I is restored. This assumes that fronto-occipital dissociation may be involved in preventing the further propagation of paroxysmal activity.

We indicated that clonidine altered EEG power in the cortex and in the thalamus. After clonidine injections, sleep EEG revealed less delta activity in the cortex and the thalamus. A decrease was found in theta band in all locations during SWD II. A decrease was also found in alpha band during SWD I, but only in the frontal cortex, whereas alpha activity in the RTN, in opposite, increased. In general, clonidine affected power around the main frequency of SWD (type I and type II).

It is known that density of alpha-2 AR in the cortex and thalamus is low [Happe et al., 2004] and it seems unlikely that functional changes are mediated directly by postsynaptic alpha-2 AR. Clonidine inhibits adrenergic neurotransmission via presynaptic alpha-2 AR resulting to a general decrease of NA this diminishes activation of postsynaptic alpha-1 AR and probably beta AR. The density of alpha-1 AR in the frontal cortex and in the thalamus is known to be higher than in the occipital cortex [Jones et al., 1985], therefore, clonidine induced different changes in local EEG.

As known, the density of alpha-2 AR in the hippocampus, amygdala and septum [Happe et al., 2004] is very high, suggesting that clonidine may directly affect the activity of these structures. Clonidine in low doses is known to suppress hippocampal theta activity [Kitchigina et al., 2003]. In our experiments, clonidine reduced theta activity during SWD II. This effect was observed in the occipital cortex and in the thalamus, and probably reflects the reduction of the hippocampal activity. Thalamo-cortical oscillations, e.g. sleep spindles and SWD I, are modulated by another noradrenergic mechanism, which is probably mediated by more complex interaction between presynaptic alpha-2 and postsynaptic alpha-1 and beta AR. Due to this complex NA modulation, thalamic relays neurons may easily switch from tonic to bursting firing mode [McCormick, 1989; McCormick, 1991] and start producing hypersynchronous thalamo-cortical oscillations which are recorded in our subjects as SWD I.

Mechanism of alpha-adrenergic modulation of absence epilepsy

Clonidine may have a pro-absence effect because of combination of several factors. First is a reduction of efficacy of noradrenergic supply. NA adjusts a balance between excitation and inhibition therefore it is regarded as an intrinsic anti-epilectic agent. NA is known to modulate the efficacy of inputs, rather than directly activates postsynaptic targets [Armstrong-James and Fox, 1983, McCormick, 1991]. Clonidine activates presynaptic alpha-2 adrenoreceptors (autoreceptors) on the neurons of locus coeruleus (LC), providing a negative feed-back of NA-release [Svensson et al., 1975; Langer, 1980]. Low level of NA results to a hyperpolarization of neurons and thalamo-cortical cells easily turn into 'busting mode' and start producing regular oscillations [McCormick, 1989, McCormick et al., 1991], i.e. SWD. This effect is mediated by postsynaptic (alpha and beta) AR.

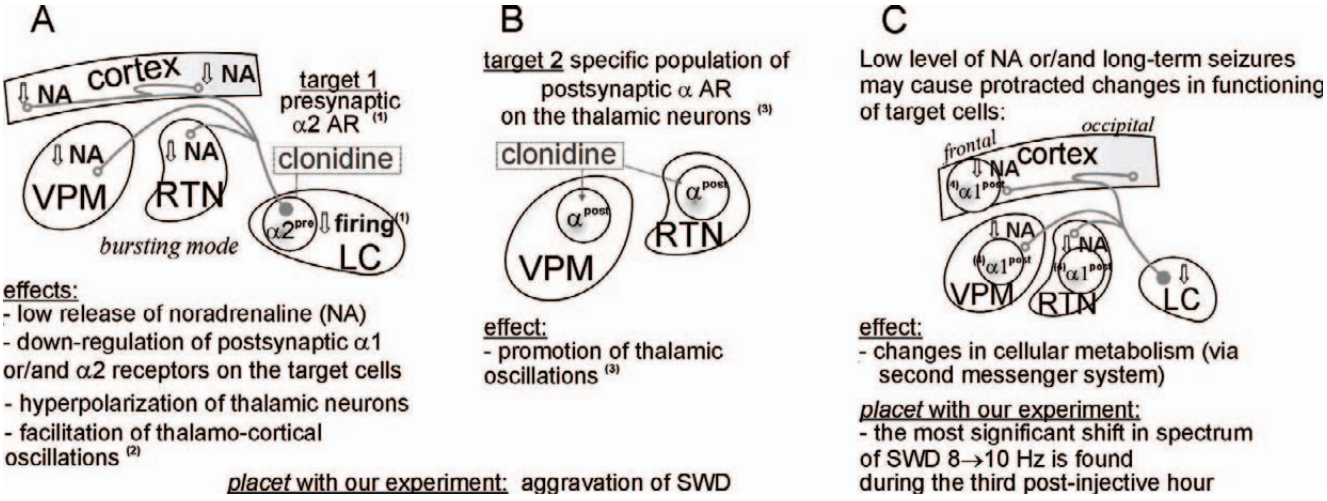

Figure 3.10. Alpha-adrenergic mechanism by which alpha-2 agonist clonidine may modulate spike-wave activity. (**A**) The drug may aggravate seizures affecting noradrenergic neurotransmission. Clonidine reduces NA release by acting via the presynaptic alpha-2 AR ($a2^{pre}$) in the locus coeruleus (LC) [[1] Svensson et al., 1975; Langer, 1980]. This causes hyperpolarisation and promotes bursting activity of thalamo-cortical neurons [[2] McCormick, 1989, McCormick et al., 1991] that facilitates genesis of SWD. (**B**) A specific pool of postsynaptic alpha AR (α^{post}) in the thalamus might be primarily involved in seizure-aggravated effect of clonidine [[3] Buzsáki et al., 1991]. (**C**) Retarded changes in the spectrum of SWD, which were observed in the third post-injective hour, may be explained by secondary alterations on postsynaptic membranes and changes in neuronal metabolism.

Figure 3.10A illustrates abovementioned effect of clonidine. It is important that a decrease of alpha-noradrenergic neurotransmission either 9with alpha-1 antagonists or alpha-2 agonists) never induces *de novo* SWD in non-epileptic animals [Marescaux et al., 1992b], therefore, clonidine do not act as a primary pro-absence agent.

Density of alpha AR in subcortical structures of Fisher 344 rats (which have spontaneous absence seizures [Buzsaki et al., 1991]) is three times lower than in non-epileptic Buffalo rats [Vantini et. al., 1984, Buzsaki et al., 1990]. To date, in addition to NA release, clonidine may also inhibit release of other monoaminergic neuromodulators such as dophamine and serotonine [Langer, 1980; Gobert et al., 1998]. Altogether may provide a cumulative action and result to strengthening of SWD.

Second, a sedative effect of clonidine [Drew et al. 1979; Makela et al., 1986; for reference on humans in Bischoff et al., 2004], which is explained by lowering of noradrenergic modulatory effect on the thalamic and cortical neurons have. This effect is mediated by postsynaptic AR (alpha1 and beta) which are known to be dense in the cortex and the thalamus [Jones et al., 1985, Diop et al., 1987]. The decrease of vigilance occurs in the present study during the first hour after clonidine injection. Clonidine is known to have clear soporific effect in dose 0.02-0.04 mg/kg [Seidel et al., 1995]. We used the drug in a very low dose (0.00625 mg/kg), so that rats did not fall into sleep, but stayed in transition between sleep and wakefulness, were drowsy. I.e. clonidine promotes transitory state of vigilance which is favourable for SWD to appear [Lannes et al., 1988; Drinkenburg et al., 1991]. Clonidine may also affect the "sleep-active neurons" in the preoptic area (these neurons have mostly alpha 2-receptors) resulting to a decrease of vigilance and promotion of sleep [Osaka and Matsumura, 1995]. However, sedative effect of clonidine could not be a prime reason of such a large amount of long-lasting SWD and *status epilepticus* as it is found here.

Third, clonidine may impair interactions between electrical activity over the brain [Bischoff et al., 1998, Emilien, 1989; Hayashi and Maze, 1993], it induces disballance between EEG and behaviour [Pastel and Fernstrom, 1984] and provokes non-classical states of vigilance [Pickworth et al., 1982]. Conclusively, clonidine may alter normal pattern of interactions within a brain and promote abnormal states such as absence seizures. Fourth, clonidine is a well-known centrally acting antihypertensive agent [Myers, 1977; Hayashi and Maze, 1993; Szabo, 2002]. Systemic injections of clonidine decreased blood pressure on the periphery, but increased blood flow in the cerebral cortex [Klupp et al., 1970]. Clonidine also interferes with endocrine system: it affects glucose homeostasis, thyroid and parathyroid hormones, adrenal steroid metabolism. All these factors might have a cumulative effect on the neurohumoral homeostasis and facilitate seizure-aggravated effect of the drug.

Spectral analysis of SWD I does not give us an insight to a mechanism by which clonidine has so clear pro-absence effect. Power spectrum of SWD I in the cortex and the thalamus during the first and the second hours after injections was the same to that in control. Slight but significant decrease in power of 7.5-8.5 Hz is found in the VPM during the first hour after injection. This fact may contribute to a hypothesis of Buzsáki et al. (1991) that clonidine promotes SWD due to activation of a specific postsynaptic AR in the thalamus (Fig. 3.10B).

CONCLUSIONS

The pharmacological reduction of noradrenergic neurotransmission with systemic injections of clonidine increased the number and duration of SWD I, but did not affect the number of SWD II.

Several factors may contribute to the increase of SWD I after clonidine injections. First, direct or indirect activation of pacemaker cells in the RTN. Second, impairment of interactions within the cortex, i.e., a decrease in EEG power in the cortex and weakening of intracortical coherence may facilitate occurrence of SWD I.

The noradrenergic system might selectively control SWD I, but not SWD II, at the level of the RTN.

3.3 EEG precursor activity of SWD type I [‡]

ABSTRACT

We examined periods in the electroencephalograms (EEG) that immediately preceded spontaneously occurring spike-wave discharges (SWD), i.e., epochs with seizure precursor activity (preSWD), in the WAG/Rij rat model of absence epilepsy. PreSWD epochs in the frontal EEG were divided in four classes based on the EEG power in *delta-theta-alpha* frequency bands. It was found that 95% of these epochs show high power in the delta band (1-4 Hz) and 73% contained powerful theta (4.5-8 Hz). By having large theta component, preSWD epochs in our subjects resemble the 5-9 Hz medium-voltage oscillations that were previously described before the onset of SWD in GAERS, yet in our subjects, preSWD epochs did not show the well-shaped (presumably theta) rhythm in EEG. It is concluded that a coalescence of delta and theta in the cortical EEG is most favorable for the occurrence of SWD. The thalamocortical coherence increased at the onset of SWD, however, no features of EEG coherence could be considered as unique for any of the subtype of preSWD epochs. Coherence between frontal cortex and thalamus was higher then intracortical coherence. Reticular and ventroposteromedial thalamic nuclei were strongly mutually coupled even before the onset of SWD.

INTRODUCTION

Absence seizures in humans and in animal models of absence epilepsy begin abruptly and unpredictably. There are no obvious clinical or electroencephalographic signs that can be used in order to anticipate the occurrence of absence seizures. Only some less specific disturbances can be found by close visual inspection in the background EEG immediately before the onset of SWD. Seizure precursor activity in humans has been referred to as 'poorly developed epileptiform discharges' [Inouye et al., 1990]. It has been shown that in Genetic Absence Epilepsy Rats from Strasbourg (GAERS) that SWD are preceded by medium-voltage 5–9 Hz oscillations [Pinault et al., 2001]. The presence of these pro-epileptic 5–9 Hz medium-voltage oscillations [Pinault et al., 2001] has not been confirmed in another animal models of absence epilepsy (e.g. in the WAG/Rij[§] strain of rats that resembles GAERS in many respects [Danober et al., 1998; Depaulis and van Luijtelaar, 2006]). Therefore, the possibility cannot be excluded that 5–9 Hz oscillatory precursors of absence seizures (SWD) are merely an epiphenomenon characterizing the GAERS strain. In the present study we examine EEG activity in WAG/Rij rats in order to figure out weather WAG/Rij rats exhibit the same 5–9 Hz oscillations (or similar oscillatory patterns) as GAERS in the EEG just prior to SWD.

The 5-9 Hz oscillatory activity preferably appears in the EEG during a specific behavioral state, in which animals are awake, but less alert (they sit in a safe environment and not do not anticipate any imminent stimulus) [Pinault et al., 2001; Pinault, 2003]. Interestingly, these oscillations were detected in epileptic (GAERS) as well as in non-epileptic rat strains. Therefore, 5–9 Hz oscillations in rodents may be considered as 'normal' (i.e., physiological) and they are not necessarily associated with absence epilepsy. It is still obscure why 5–9 Hz rhythmic activity precedes SWD in epileptic rats, but it does not encourage absence seizures in non-epileptic animals.

The cellular mechanisms of the medium-voltage 5–9 Hz oscillations have been investigated in drug-free GAERS by Pinault and co-workers (2003; 2006). These authors found that, firstly, absence-related 5–9 Hz oscillations were generated by interconnected neurons in the somatosensory part of the thalamo-cortical system. Secondly, neurons in layer IV of the somatosensory cortex began to fire at 5–9 Hz a few milliseconds earlier than neurons in the corresponding specific and reticular thalamic nuclei. Thirdly, cortical neurons were capable to modulate membrane potentials of thalamic neurons throughout dense cortico-thalamic synaptic interactions. Altogether these findings suggest that cortical neurons in layer IV largely affect neuronal activity in the functionally related thalamic nuclei. In such a way, the cortex initiates a pro-epileptic state, in which the cortico-thalamo-cortical network produces 5–9 Hz seizure-precursor rhythm followed by SWD. It is hypothesized that ~~an~~ impairment in the cortico-thalamo-cortical system in epileptic animals results in seizure-precursor (5–9 Hz) rhythm that is subsequently transformed in absence seizures. Our study is directed towards epileptic processes that may underlie the transformation of seizure-precursor activity (preSWD, a presumable 5-9 Hz activity) into SWD. In order to describe the dynamic changes of neuronal network synchronization, EEG coherence in the cortico-thalamo-cortical network, including frontal and occipital cortical areas and ventroposteromedial nucleus (VPM,

[‡] Submitted paper:
Sitnikova E, van Luijtelaar G. Precursors of spontaneous spike-wave seizures in the electroencephalogram in WAG/Rij rats: power spectrum and coherence analyses. Epilepsy Research, 2008.

[§] WAG/Rij rat strain is a valid and widely used genetic animal model of absence epilepsy [van Luijtelaar and Coenen, 1986; Coenen and van Luijtelaar, 2003].

somatosensory relay thalamic nucleus) and reticular thalamic nucleus (RTN) before, and after the onset of absence seizures will be measured.

The results are divided in three parts: (1) amplitude-frequency EEG parameters of preSWD epochs as measured in the cortex, in the VPM and RTN; (2) relationship between electroencephalographic properties of preSWD and subsequent seizure activity; (3) cortico-thalamo-cortical network associations as measured during preSWD and subsequent SWD (EEG coherence).

METHODS

Animals

The EEG was recorded in five male WAG/Rij rats of one year old (body weigh 320-360 g). Animals were born and raised at the laboratory of Biological Psychology, Donders Institute for Brain, Cognition and Behavior of Radboud University Nijmegen (The Netherlands). They were kept in pairs in standard cages with food and water available *ad libitum* and 12-12h light-dark cycle, with white lights on at 18:00. After surgery, housing conditions were the same except that rats were housed individually. Distress and suffering of animals was kept to a minimum. The experiments were conducted in accordance with the legislations and regulations for animal care and were approved by the Ethical Committee on Animal Experimentation of the Radboud University Nijmegen.

EEG recording design and equipment

All animals were equipped with six stainless steel electrodes (Plastic One Inc. Roanoke, VI, USA: MS 333/2A). Two EEG electrodes were placed epidurally over the cortex in the frontal (AP 2; L 2.5) and occipital (AP -7; L 6) areas, skull flat. Another two EEG electrodes were implanted in the ventroposteromedial nucleus of the thalamus (VPM, AP –3.5; L 2.5; H 7.2) and in the reticular thalamic nucleus (RTN, AP –1.5; L 2.2; H 7.2). All coordinates are given in mm relative to bregma. Ground and reference electrodes were placed symmetrically over both sides of the cerebellum. Electrodes were permanently attached to the rat's skull with dental cement.

Stereotactic surgery was performed under isofluorane anesthesia. For post-surgery analgesia rats were i.m. injected with buprenorfinehydrochloride (Temgesic®, Reckitt & Colman Products Ltd., Kingston-Upon Hull, UK) in a dose of 0.1 mg/kg. Animals were allowed to recover from surgery for at least 10 days.

The location of depth electrodes was verified *post mortem*. Rats were deeply anesthetized with overdose of Nembutal, their brains were removed, sectioned (serial coronal 60 μm sections) and stained for Nissl (0.1% cresyl violet). Electrode positioning was determined in accordance to the stereotaxic atlas of the rat's brain [Paxinos and Watson, 1986].

The EEG was recorded in freely moving rats while staying in a Plexiglas recording cages (25 cm x 30 cm surface, 35 cm high) that was placed in a noise-isolated Faraday cage. The recording session lasted 5-7 hours and took place in the dark period of the light-dark cycle, the rats were simultaneously observed. One day before the EEG recording session, the rats were allowed to habituate to the recording procedure.

The EEG signals were fed into a multi-channel differential amplifier via a swivel contact, band-pass filtered between 1-500 Hz, digitized with 1024 samples/second/per channel (Data Acquisition Hardware and Software, DATAQ Instruments, Inc., Akron, OH) and stored on hard disk.

EEG analysis

All SWD in full-length EEG were marked and 1 sec epochs immediately before and 1 sec after the onset of SWD were analyzed. Power spectrum analysis was performed in the selected EEG epochs using the traditional Fast Fourier transform.

EEG event recognition. SWD (type I) were detected in the frontal EEG using criteria of van Luijtelaar and Coenen (1986). Briefly, SWD appeared as a train of asymmetric 8-11 Hz sharp spikes interfered by waves. SWD lasted longer than 2 sec and their amplitude was at least three times higher than the background amplitude (usually it exceeded the background more than five times). The first sharp (often biphasic) spike was marked as the onset of SWD.

Power spectrum analysis. A Hanning windowed Fast Fourier Transform (FFT) of EEG signals was performed with 0.5 Hz resolution (Brain Vision Analyser, ©BrainProducts GmbH). The resultant power spectrum was averaged per event and per animal. EEG power in frequency bands of delta, 1-4 Hz; theta, 4.5-8 Hz and alpha, 8.5-12 Hz was calculated. Statistical analysis was performed with the aid of an ANOVA and *post-hoc* LSD test.

EEG coherence was measured in order to access linear synchronization between cortical and thalamic signals. The coherence measures a degree of similarity between two signals in the frequency domain [Challis and Kitney, 1991]. It is a normalized function of cross-power spectrum:

$Coh_{1,2}(\omega) = |G_{1,2}(\omega)|^2 / |G_{1,1}(\omega) \times G_{2,2}(\omega)|$; $Coh_{1,2}(\omega)$ - coherence between channels 1 and 2; ω - discrete frequencies (here we assigned ω with bin = 0.5 Hz); $G_{1,2}(\omega)$ - cross-power spectrum of the Channel 1 and 2; $G_{1,1}(\omega)$ and $G_{2,2}(\omega)$ – two individual spectra (autospectra) of Channel 1 and 2.

Coherence was computed in six EEG channel pairs: (1) *intracortical* (between frontal and occipital channels); (2) *intrathalamic* (between VPM and RTN) and (3-6) *thalamo-cortical* in four pairs (frontal-VPM, frontal-RTN, occipital-VPM, occipital-RTN). Measurements were made in two subsequent epochs: 1 sec preSWD and the first sec of SWD. Coherence spectra were computed with 0.5 Hz frequency resolution from 0.5 to 31.5 Hz, averaged per 1.5 Hz bins. Differences between coherence in preSWD epochs and during SWD epochs were statistically evaluated with paired t-tests.

RESULTS

Power spectrum analysis of SWD-precursors

In total, 477 SWD-precursor epochs (preSWD, from 47 to 153 per animal) were analyzed.

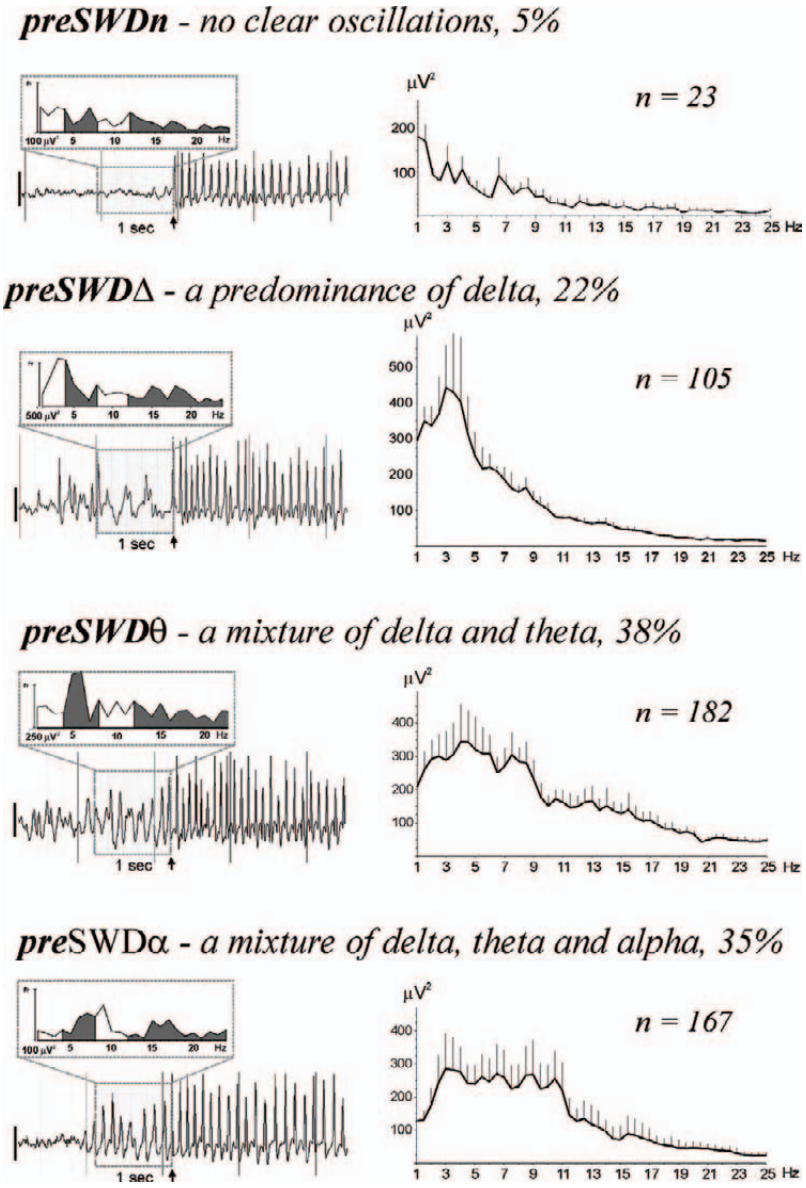

Figure 3.11. Power spectrum of SWD-precursors (preSWD) in WAG/Rij rats as measured in the frontal EEG. Four classes of preSWD epochs are distinguished based on the waveform of the power spectrum and on the distribution of EEG power over the frequency bands. A representative example of preSWD activity and its power spectrum are shown on the left side; the right graphs depict the averaged power spectra (per rat and per class, mean ± SE, bin=0.5 Hz). Noteworthy is that all classes of preSWD epochs, except preSWDn, show relatively high power in the delta frequency range.

In the frontal cortex, the epochs with preSWD activity were heterogeneous with respect to the waveform of EEG activity and their power spectra varied considerably. The epochs with preSWD were subdivided in four classes based on the value of EEG power in *delta* (1-4 Hz), *theta* (4.5-8 Hz) and *alpha* (8.5-12 Hz) frequency bands (Fig. 3.11 and Table 3.4). Almost all (95%) of preSWD epochs showed a peak in *delta* frequencies (1-4 Hz). Among them, 22% of preSWD epochs, in which power in the *delta* band exceeded the EEG power in the other bands, were classified as preSWDΔ. 38% of the preSWD epochs showed predominant *theta* activity (4.5-8 Hz), they were named preSWDθ, while 35% of the preSWD epochs contained a maximum power in the *alpha* band, they were named preSWDα. Interestingly, preSWDα showed in addition relatively high power in the *delta* and *theta* bands. 5% of the preSWD epochs, preSWDn, were characterized by low-amplitude desynchronized EEG and showed a flat power spectrum. PreSWDn were rather atypical (see below).

Distribution of EEG power over delta-theta-alpha frequency bands

It was tested whether the distribution of the various frequency bands was different for the four classes of precursor epochs activity in the frontal and occipital cortex and VPM with a two way ANOVA ('preSWD class' and 'Band' as factors. The data used in this analysis are presented in Fig. 3.12).

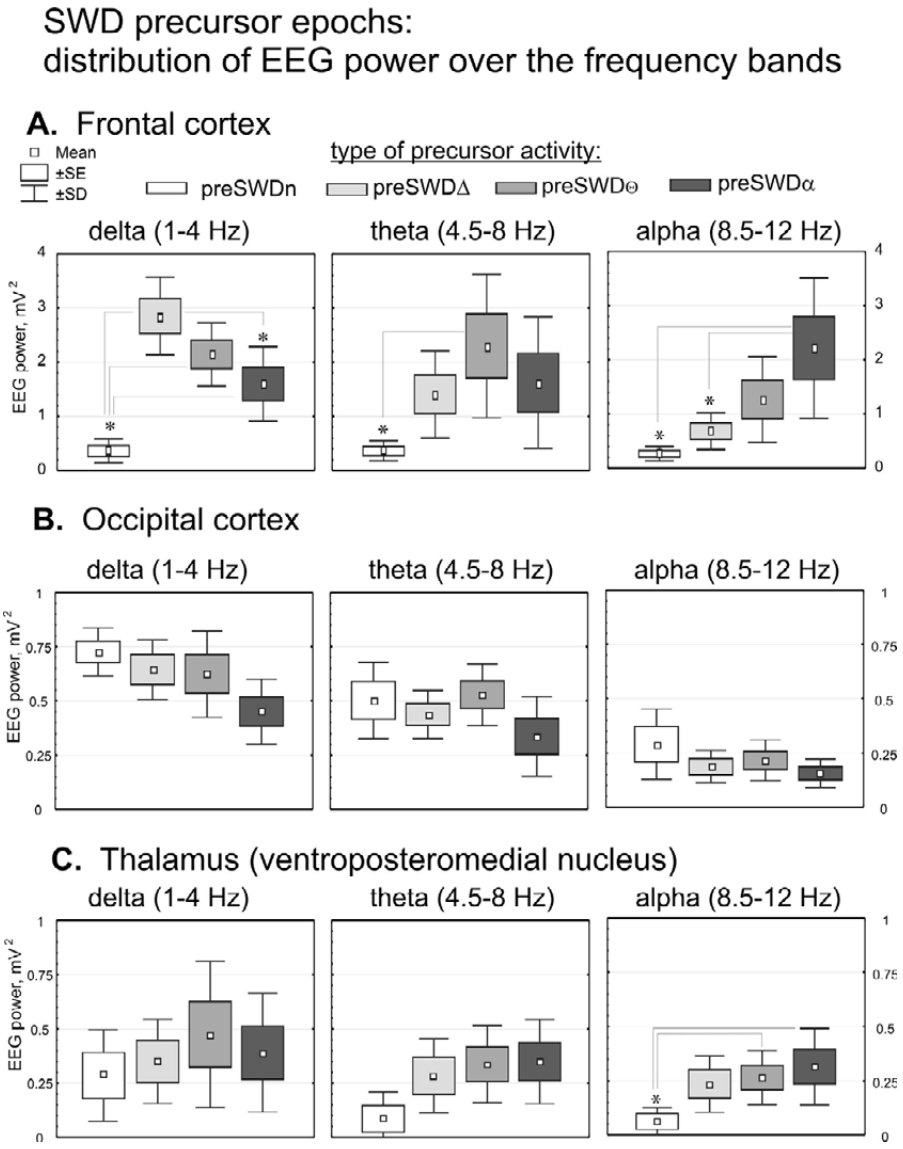

Figure 3.12 Statistical analysis of EEG power density in the four classes of SWD-precursors (GLM, two-factors ANOVA). **A**. In the frontal EEG, factors 'PreSWD class' and 'Band' are significant, as well as the interaction 'PreSWD class'*'Band' (all p's<0.05). **B**. In the occipital EEG, factors 'PreSWD class' and 'Band' are significant (p's<0.05), but the interaction is not. **C**. In the thalamus, factors 'PreSWD class' and 'Band' are significant (p's<0.05), but no interactions between these factors.
* - significant differences as determined with LSD *post-hoc* test (p<0.05). Note that preSWDn epochs are exceptional in respect to significantly lower power in the frontal cortex and in the thalamus as compared to the other classes of preSWD epochs.

Frontal cortex (Fig. 3.12A). Significant differences were found for the different preSWD epochs (factor 'PreSWD class' $F(3.41)=15.4$, $p<0.0001$), but the factor 'Band' was not significant ($F(2.41)=2.6$, $p>0.05$); however, the interaction between 'PreSWD class' and 'Band' was significant ($F(6.41)=2.8$, $p<0.05$). The subsequent one-way ANOVA indicated significant differences between different classes of preSWD epochs ($F(3,50)=10.2$, $p<0.0005$). Post-hoc tests (LSD) showed that all epochs contained more power (all p's<0.05) compared to preSWDn epochs. Also the interaction was further analyzed: differences between different classes of preSWD epochs were significant in the *delta* band ($F(3,14)=13.3$, $p<0.005$), in the *theta* band ($F(3,14)=3.3$, $p=0.05$) and in the *alpha* band ($F(3,14)=5.06$, $p<0.005$). More specifically, preSWDΔ epochs had more *delta* power than preSWDn and preSWDθ epochs (p's<0.05; asterisked in Fig. 3.12A); preSWDθ epochs had higher *theta* power than preSWDn epochs ($p<0.05$); preSWDα had higher *alpha* power than preSWDn and preSWDΔ epochs (p's<0.05).

Altogether this confirms, first, that our criteria for dividing preSWD epochs in four classes were statistically reliable. Second, that in the frontal EEG, amplitude-frequency EEG parameters in seizure-precursors epochs were quite variable. It was not possible to assess a single common pattern of seizure-precursor activity (likewise 5-9 Hz oscillations in GAERS [Pinault, 2001]), instead, we propose an empirical classification of preSWD based on (significant) difference of EEG power as measured in traditional frequency bands.

Occipital EEG. Two-way ANOVA revealed some differences between different classes of preSWD epochs (factor 'PreSWD class' $F(3,41)=4.6$, $p<0.014$; factor 'Band' $F(2,41)=37.4$, $p<0.0001$) and no interaction between these factors, Fig. 3.12B. Differences in power between different preSWD epochs (*post-hoc* test for the factor 'Band') were not found neither in *delta* band ($F(3,14)=1.6$, $p>0.05$), nor in *theta* band ($F(3,14)=1.4$, $p>0.05$), nor in *alpha* band ($F(3,14)=1.5$, $p>0.05$).

The one-way ANOVA for the factor 'Band' showed significant differences in power ($F(2,50)=32.6$, $P<0.00001$). Post-hoc tests showed that the power was largest in the *delta* band, followed by *theta* and *alpha* (all p's<0.05).

Thalamus (ventroposteromedial nucleus). Power in the investigated frequency bands also differed for the different preSWD epochs (Fig. 3.12C): factor 'PreSWD epoch' $F(3.41)=6.9$, $p<0.005$; factor 'Band' $F(2.41)=4.4$, $p<0.01$, but no interaction between these factors. The one-way ANOVA showed that the factor 'PreSWD epoch' was significant ($F(3,50)=4.1$, $p<0.05$) with preSWDn epochs contained less power than the other classes of preSWD epochs (all p's<0.05).

According to one-way ANOVA for the factor 'Band', differences in power only approached the level of significance ($F(2,51)=3.1$, $p=0.055$).

Table 3.4. Peak frequencies of SWD-precursors and subsequent SWD

	% from the total amount of seizures	SWD-precursors			SWD		
		Frontal EEG	Specific thalamus (VPM)	Reticular thalamic nucleus	Frontal EEG	Specific thalamus (VPM)	Reticular thalamic nucleus
preSWDn	5	no peaks - desynchronized EEG			9-10.5	8.5; 10.0; 11.5	9.5
preSWDΔ	22	3.0	2.0; 7.0	2.0; 7.5	10.0	9.5	9.5
preSWDθ	38	4.0-4.5; 7.5	1.0; 7.0	1.0; 7.5	10.0	9.5-10.0	8.5; 10.0
preSWDα	35	3.0; 6.5; 9.0; 10.5	1.0; 6.5-7.0; 9.0	1.0; 6.5	10.0-10.5	8.5-9.5	9.0

We found dissimilarities in the shape of the power spectra between the frontal cortex and the thalamus (Fig. 3.13). In all classes of seizure precursor epochs (except preSWDn), power spectra in the thalamus revealed peaks in *delta* (1-2 Hz) and in *theta* frequencies (6.5-7.0 Hz, Table 3.4). *Delta* peaks in the cortex were found in frequencies 3-4 Hz. It is remarkable that, in the thalamus, all classes of preSWD epochs (except preSWDn) were characterized by a substantial *theta* component (note spectral peaks in *theta* frequencies indicated by arrows in Fig. 3.13), white *theta* peaks were less pronounced in the frontal cortex and were missing in the preSWDΔ epochs (22% of all preSWD).

Power spectrum analysis of preSWD epochs as recorded in the frontal and occipital cortex and in the thalamus leads to the following conclusions:

1) In the frontal EEG recordings, different classes of preSWD epochs showed the most sharp and significant differences in power spectrum and the same tendencies were observed in the thalamus, while differences were absent in the occipital cortex.

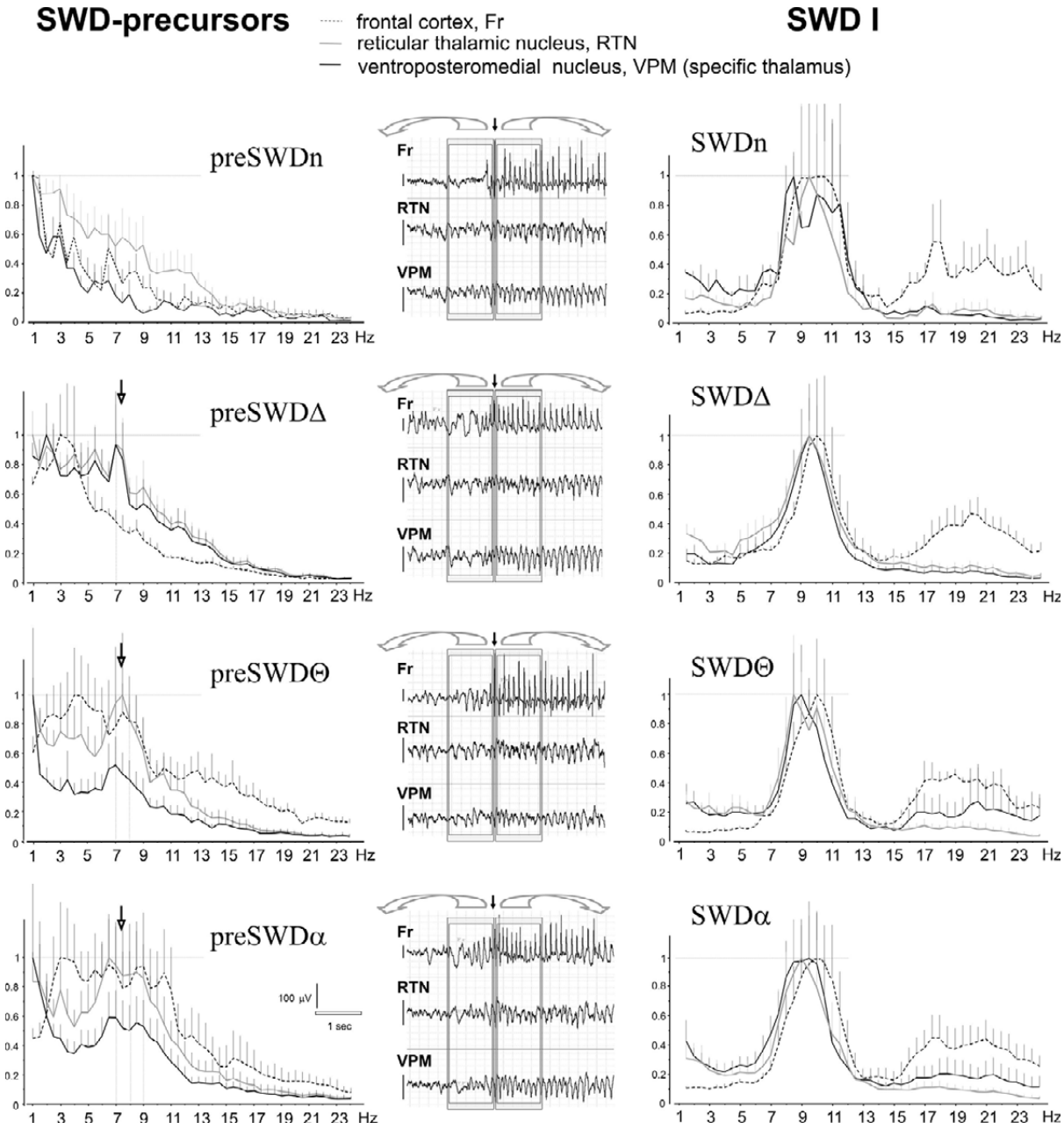

Figure 3.13 Normalized power spectra of preSWD epochs and subsequent SWD. The EEG power spectra profile of preSWD epochs in the frontal cortex is distinguished from that in the thalamus. The most remarkable distinction is that all classes of preSWD (except preSWDn) show peaks in theta frequencies (~ 7 Hz as indicated by arrows). In preSWDΔ epoch, *theta*-band component is nearly absent in the frontal cortex, but it is present in the thalamus. During SWD (type I), power spectra in the frontal cortex and the thalamus closely coincide with each other, however, peak frequencies of SWD in the frontal cortex and in the thalamus showed a consistent shift (~10 Hz versus ~9 Hz with approximately 0.5-1.5 Hz difference).

2) In the frontal EEG recordings, almost all preSWD epochs showed 3-4 Hz peaks in their power spectrum and 95% of preSWD epochs contained a powerful *delta* component. *Delta* power was maximum in preSWDΔ (22% of all investigated epochs) as compared to other classes of preSWD epochs.

3) The peak frequency of *delta* differed in the thalamus and in the cortex (1-2 Hz versus 3-4 Hz); this might suggest that SWD-promoting *delta* components have independent (putative) sources in the cortex and in the thalamus.

4) The power in *delta* band in the frontal EEG appeared to be maximum in preSWDΔ epochs, where preSWDθ ≈ preSWDΔ > preSWDα > preSWDn. In the occipital cortex and in the thalamus, all classes of preSWD epochs showed the same power in *delta* band.

5) An exceptional preSWDn epochs (that prerequisite 5% of all SWD) in the frontal cortex displayed extremely low EEG power in all frequency bands; in the thalamus, delta and theta power showed a tendency to be lower, and power in alpha band was significantly lower.

6) The power in *theta* band in the frontal EEG was highest in preSWDθ epochs that was significantly higher than in preSWDn and showed a tendency to be low than in preSWDα and preSWDΔ epochs. In the occipital cortex and in the thalamus, power in *theta* band did not differ in different classes of preSWD epochs.

7) The power in *alpha* band in the frontal EEG differed significantly in different subtypes of preSWD epochs, i.e., preSWDθ ≈ preSWDα > preSWDΔ > preSWDn, and the same tendencies were observed in the thalamus. The power in *alpha* band as recorded in the occipital EEG was the same in all classes of preSWD epochs.

Correspondence between SWD-precursors and subsequent SWD I

The differences between cortical and thalamic power spectra that we notified between the four classes of preSWD epochs were no longer present during subsequent seizure activity. During SWD, the waveform of cortical and thalamic power spectra was similar (Fig. 3.13). A sharp ~ 10 Hz peak was found in the frontal cortex in all SWD subtypes, and, in the thalamus, this peak was detected in frequencies between 8.5 and 9.5 Hz. It seems striking that the peak frequency of frontal EEG during SWD was constantly above the corresponding values obtained in the thalamus (difference in peak frequency was 0.5-1.5 Hz, Table 3.4).

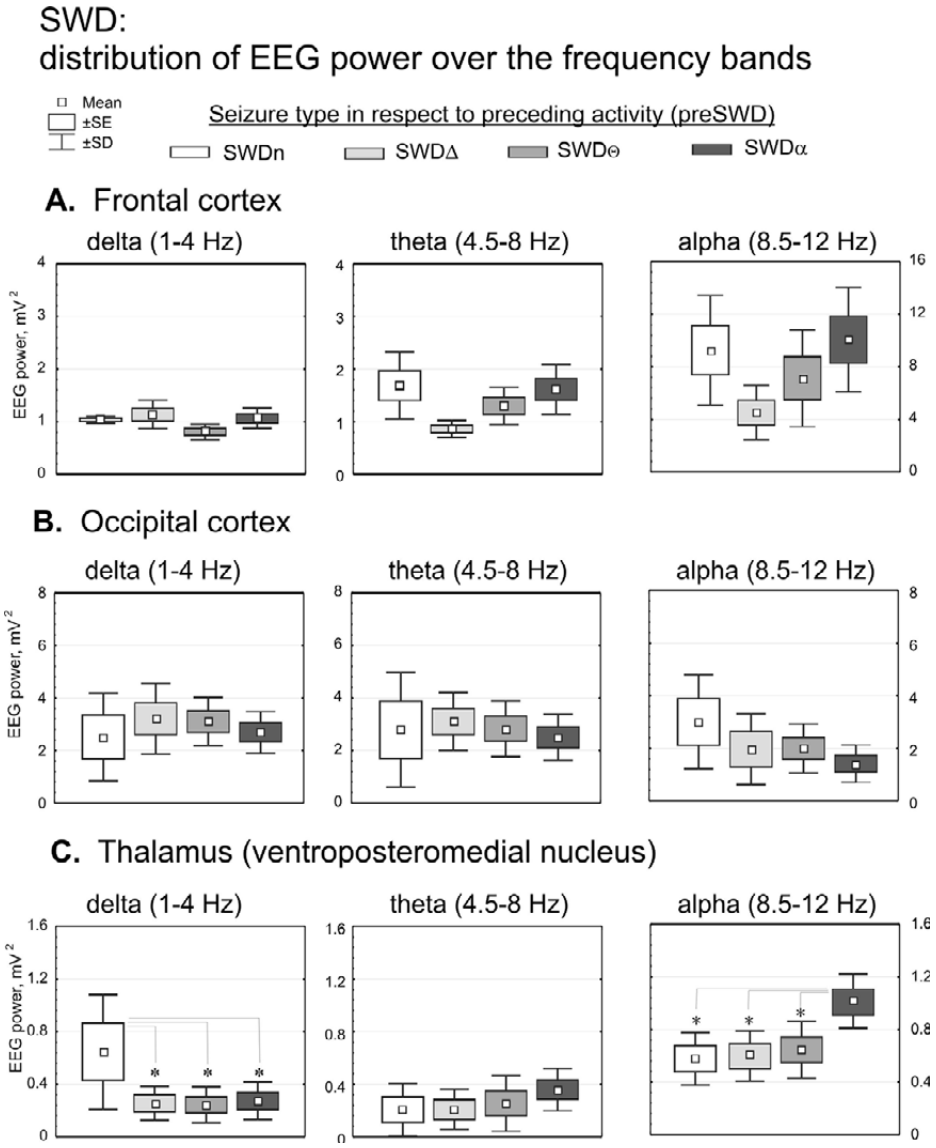

Figure 3.14 Statistical estimations of EEG power during SWD epochs which are preceded by different preSWD (GLM two-way ANOVA, the design of data analysis is similar to that in Fig. 3.12). **A**. In the frontal EEG, power in alpha band is several times higher than in other bands (note four-hold difference in scale). The factor 'Band' is significant ($p<0.0001$), but the factor 'PreSWD class' is not significant. **B**. In the occipital EEG, the investigated factors are not significant. **C**. In the thalamus, the factor 'Band' is significant ($p<0.0001$), the factor 'PreSWD class' is not significant. Interactions 'PreSWD class'*'Band' are significant ($p<0.05$).

* - significant differences as determined by LSD post-hoc test.

In order to elucidate a putative relationship between the class of the preceding EEG activity and the subsequent SWD, the electroencephalographic properties (i.e., frequency profile) of SWD were related to the differences in precursor epochs. The power distribution over the *delta*, *theta* and *alpha* frequency bands was statistically analyzed using a GLM ANOVA procedure with factors 'PreSWD class' (4 levels) and 'Band' (3 levels).

In the frontal EEG (Fig. 3.14A), the factor 'Band' was highly significant ($F(2.42)=40.1$, $p<0.0001$). *Post hoc* tests for the factor 'Band' showed more *alpha* as compared to *delta* and *theta* power (all p's<0.05). In fact, the alpha power was more than four times higher than the power in the *delta* and *theta* bands (note scale difference in Fig.3.14A). The factor 'PreSWD class' and interaction were not significant.

In the occipital EEG (Fig. 3.14B), neither the factor 'Band', nor 'PreSWD class', nor the interaction was significant. This suggests that the frequency profile of SWD in the occipital cortex was rather flat and similar for different preSWD epochs.

In the thalamus (VPM, Fig. 3.14C), the factor 'Band' was significant $F(2.42)=25.3$, $p<0.0001$, but the factor 'PreSWD class' was not. Results of *post-hoc* tests for the 'Band' were similar to that in the frontal EEG: preSWD epochs had more power in the *alpha* band than in *theta* and in *delta* bands (p's<0.05). The interaction 'Band'*'PreSWD class' was significant $F(2.42)=3.0$, $p<0.05$. As compared to the other classes of preSWD epochs, thalamic counterpart of preSWDn epochs showed significantly higher *delta* and preSWDα - more *alpha* (p's<0.05, LSD *post-hoc* test, asterisked in 3.14C).

Altogether, there was a simple relationship between EEG power content (a distribution of EEG power over *delta-theta-alpha* bands) in SWD and the type of SWD-precursor activity in the frontal and occipital EEG recordings: no clear effects could be ascribed to the type of seizure-precursor activity as determined in the frontal cortex. The significant 'Band' effect indicates that the frequency spectra of SWD in the frontal cortex and in the thalamus contained quite some *alpha* frequencies. In the thalamus, the frequency distribution of EEG power in SWD was predetermined by the type of seizure-precursor activity (significant interaction 'Band'*'PreSWD class'). 5% of SWD, which were preceded by a desynchronized frontal EEG (preSWDn epochs), displayed an enlarged *delta* in the thalamus; seizures, whose precursor epochs had exaggerated *alpha* activity in the frontal EEG (preSWDα), were characterized by high *alpha* activity in the thalamus (but no longer in the cortex).

Thalamo-cortical network associations during SWD-precursors and subsequent SWD I: EEG coherence study

It is well accepted that SWD are caused by large-scale neuronal synchronization in the thalamo-cortical network. In this oscillatory network, the cortex is thought to be recruited by the thalamus [Destexhe and Sejnowski, 2002] primarily through the RTN [Buzsáki, 1991; Avanzini et al., 1992; 2000; Blumenfeld and McCormick, 2000 etc]. Recently, several studies in animal models of absence epilepsy cast doubts about the primary role of the RTN in absence epilepsy, suggesting that the neocortex, rather than the thalamus, plays the major role in initiating spike-wave seizures [Sitnikova and van Luijtelaar, 2004; Timofeev and Steriade, 2004; Meeren et al., 2002; 2005; Pinault, 2003; Pinault et al., 2001, 2006; Polack et al., 2007]. In the present Chapter we access dynamic changes of network synchronization between the cortex (frontal and occipital areas) and the thalamus (ventroposteromedial and reticular nuclei) during the pre-ictal stage of absence seizures by measuring the ordinary coherence. EEG coherence analysis was performed in continuous EEG data, including preSWD and subsequent SWD. In theory, the value of coherence may vary from 0 to 1 and a value close to zero indicates no correlation between two EEG channels and a value close to 1 - high correlations. In the current study, the coherence was analyzed in frequencies from 0.5 to 31.5 Hz and coefficients of coherence were averaged per 1.5 Hz bin for the statistical analysis (Fig.3.15).

Intrathalamic coherence (Fig. 3.15B). The highest values of coherence (peak values above 0.8) were detected between RTN and VPM irrespective of the subtypes of preSWD epochs, suggesting that these nuclei are highly coupled even before the onset of seizure. Intrathalamic coherence just slightly changed with the onset of SWD. Significant changes in intrathalamic coherence were found in transitions from preSWDn to SWDn and from preSWDΔ to SWDΔ, while coherence remained unchanged in transitions from preSWDθ to SWDθ and from preSWDα to SWDα. In SWDn, coherence increased in the narrow frequency band, i.e. 8-9.5 Hz, as compared to preSWDn. Transition from preSWDΔ to SWDΔ were characterized by a broader increase of coherence, i.e., from 9.5 to 17 Hz. Only SWDΔ showed a decrease of coherence in 3.5-5 Hz and in 26-31.5 Hz (preSWDΔ versus SWDΔ, Fig. 3.15B), while all other seizure subtypes showed only a tendency of *theta* coherence (4-9.5 Hz) to be reduced as compared to subsequent SWD.

Intracortical fronto-occipital coherence (Fig. 3.15A) was higher (maximum 0.1-0.25) in preSWDn than in other preSWD epochs (maximum 0.05-0.1); also in SWDn, peak values of coherence were higher (0.4) than in the

other SWD (maximum 0.2). The frequency profile of intracortical coherence showed significant changes in transition from preSWD to SWD and the most significant increase of coherence was found between 17.5-21.5 Hz. More specifically, SWDn showed an increase of coherence in 11-12.5 Hz and SWDΔ - in 11-14 Hz.

Usually (in 75% of seizures), coherence in *alpha* band increased with seizure onset, except transition preSWDα→SWDα, when *alpha* coherence did not change. In all investigated transitions we found an increase of coherence in harmonic (*beta*) frequencies, 17-23 Hz. In preSWDΔ to SWDΔ and in preSWDθ to SWDθ, the increase of coherence in *beta* frequencies was particularly strong and widespread (i.e., two-three fold increase in 21.5-31.5 Hz and in 17-27.5 Hz correspondingly).

Thalamo-cortical coherence (Fig. 3.15C) was two times higher than intracortical coherence as measured during SWD (maximum values of thalamo-cortical coherence were between 0.4-0.6, whereas the maximum of intracortical coherence - 0.2-0.4). The onset of all seizure subtypes correlated with an increase of coherence between frontal cortex and the VPM. The most robust increase was detected in *alpha* frequencies (8-14 Hz) and a moderate increase was found in *beta* frequencies (> 14 Hz). SWDn epochs were again exceptional: they showed the most narrow-band increase of coherence, i.e. in 9-12.5 Hz, and did not demonstrate an increase in beta coherence, as did the remaining subtypes of SWD. A particularly strong increase in *beta* coherence was found at the transition from preSWDθ to SWDθ and at preSWDα to SWDα . In the latter case, the increase of thalamo-cortical coherence was particularly widespread, i.e., 11-31.5 Hz.

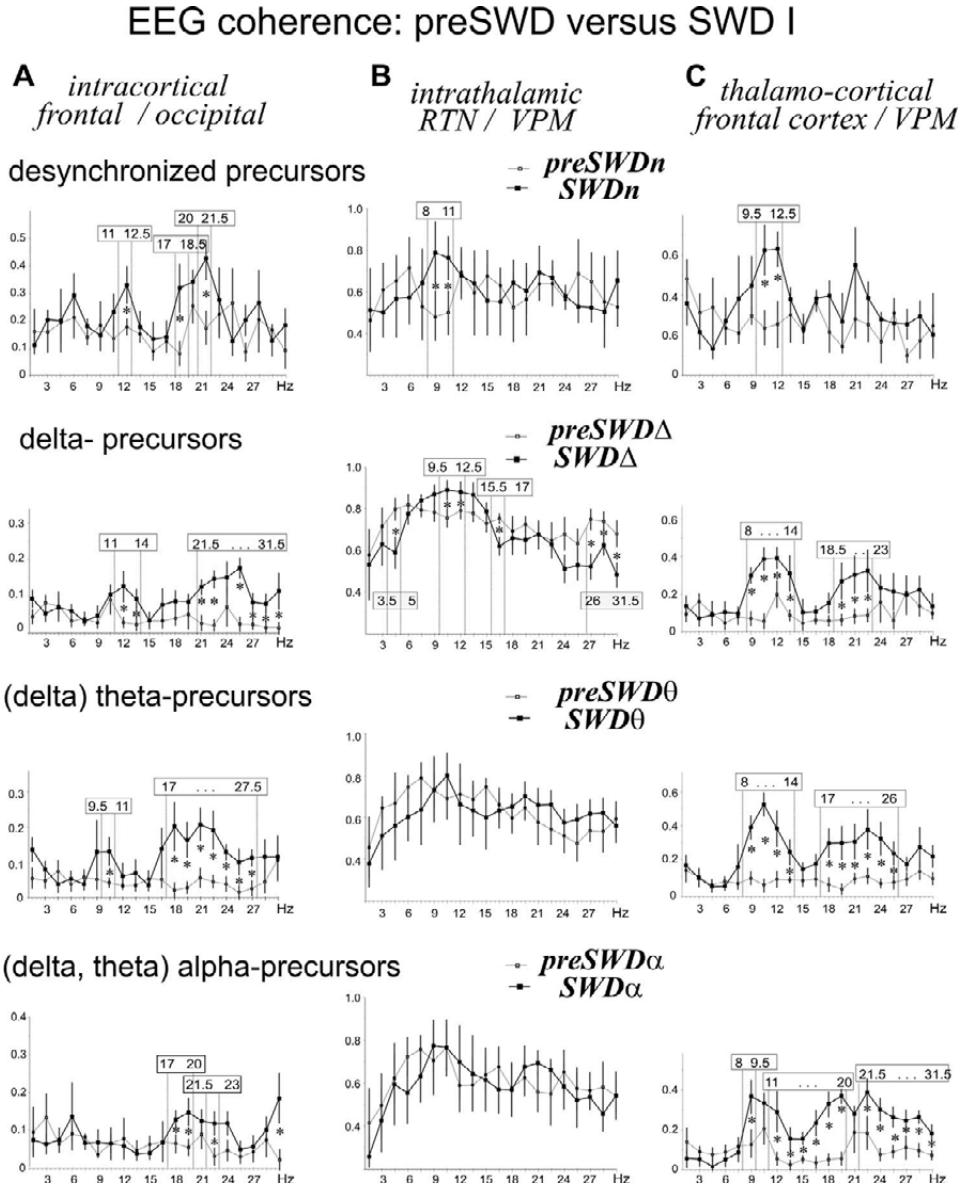

Figure 3.15. EEG coherence characterizing different subtypes of preSWD and subsequent SWD (averaged per rat and per 1.5 Hz bin, mean ±S.E., asterisked are significant differences paired t-test, $p<0.05$).

DISCUSSION

In the present Chapter we examined EEG activity immediately prior to SWD (preSWD epochs) by means of Fourier analyses and also elaborated thalamo-cortical network mechanisms of preSWD by measuring EEG coherence. In our subjects, WAG/Rij rats, preSWD epochs were characterized by a remarkable diversity in the waveform and time-frequency characteristics, therefore, we were could not identify a common EEG pattern seizure-precursor activity, as has been reported by Pinault et al (2001) in GAERS (these authors convincingly demonstrate that SWD in GAERS derive from medium voltage 5–9 Hz). In agreement to that, we found that 73% of preSWD in our rats contain powerful activity in the *theta* range, suggesting that in WAG/Rij rats, similar to GAERS, absence seizures are preceded by essential 5–9 Hz (*theta*) in EEG. An even larger percentage of SWD was also preceded by *delta* activity, suggesting that at least in WAG/Rij rats *delta* is the predominant characteristic component in frontal EEG preceding SWD.

Conformity of our data with similar studies in GAERS and in human patients

PreSWD epochs are classified in four types based on the properties of their power spectrum as measured in the frontal EEG. The classification was based on statistical tests, more precisely, by the assessment and comparison of the EEG power in the *delta*, *theta* and *alpha* frequency bands with the aid of analyses of variance. Its outcomes showed that the classification of preSWD is justified considering that the four types of preSWD epochs as measured in the frontal EEG, are statistically different: preSWDΔ, preSWDθ, and preSWDα show significantly more power in, respectively, *delta*, *theta* and *alpha* frequency bands than in most of the other bands. More precise, preSWDΔ epochs were characterized by the highest power *delta* band, preSWDθ - the highest power in *theta* band, preSWDα - the highest power in *alpha* band and preSWDn showed the least power in all investigated frequency bands.

Our data are comparable in some extent with the recent observations of Aarabi and co-workers (2007), who investigated spike-wave seizures in human EEG. These authors compared the waveform of EEG recorded in a few seconds before the onset of spike-wave seizures with the background EEG and also distinguished four types of seizure-precursors. They reported that in about 14% of cases, seizure-precursor activity was characterized by synchronized EEG with high-amplitude slow activity. This may correspond to preSWDΔ in our animals (22% of all preSWD epochs) that showed an amplitude maximum in the *delta* band. Aarabi and co-workers (2007) also found that less than 10% seizures were preceded by some transient events in EEG, such as spikes and spike and wave activity, and about 6 % of seizure-precursors could not be differentiated from the background EEG. The least subtype may correspond to preSWDn in our rats (5% of all preSWD epochs) that have a flat EEG spectrum and a somewhat desynchronized EEG. According to Aarabi and co-workers (2007), the vast majority (71%) of the seizure-precursors in humans, are characterized by the disappearance of *alpha* or *theta* activity. In contrast, we found a substantial *theta* component in preSWDθ, and preSWDα epochs these classes of seizure-precursors comprised 73% (35 + 38%) of all seizures (Fig. 3.11).

The only, albeit serious, discrepancy between seizure-precursors in humans and in epileptic rats (GAERS and our WAG/Rij rats) concerns *theta*(*alpha*) activity: it is reduced in humans, but aggravated in rats. 5–9 Hz medium-voltage oscillations that prerequisite SWD in GAERS [Pinault, 2001] are known to primary involve somatosensory thalamus and fronto-parietal (somatosensory and motor) cortex [Pinault et al., 2006]. Considering the differences in the frequency of spike-wave discharges between humans and the rodent models, as well as species differences in architecture of thalamo-cortical somatosensory system and essential anatomical differences between the rodent and human brain, it is not surprising that some pro-epileptogenic EEG activity, in this case 5–9 Hz, is absent in humans. It seems crucial that, despite high variability of preictal EEG waveforms, Aarabi et al. (2007) are able to define a specific signature in cortical EEG that is reproducible in each patient, but did not appear in other patients. In our subjects, SWD-precursors also varied from animal to animal, but we did not perform individual analysis. In the future, it is worth paying more attention to the individual properties of SWD-precursor activity.

Involvement of the thalamus and occipital cortex in EEG seizure-precursor activity

The distribution of EEG power over *delta-theta-alpha* frequency bands in the occipital cortex in various subtypes of preSWD epochs sharply differs from that observed in the frontal EEG. The amount of *delta* and *theta* was equal in 75% of preSWD epochs (not in preSWDα epochs, where the power in both bands is lower than in the alpha band. It seems that the frontal and occipital cortical regions are different in the way of sustaining SWD-precursor activity. Characteristic *theta*- and *alpha*-components in preSWDθ and preSWDα epochs (38% and 35% of the total amount of SWD respectively) may locally be produced by neuronal networks that involve the frontal cortex, but not the occipital cortex.

We found that in the thalamus power in *theta* and *alpha* bands was the same in 95% of preSWD epochs (except preSWDn epochs). The power of thalamic *delta* was the same in all preSWD epochs (100%, including preSWDn), but in the frontal cortex the power of *delta* was high in preSWDθ and in preSWDΔ epochs, moderate in preSWDα and minimal in preSWDn epochs.

Pinault and co-workers (2003; 2006) found that 5-9 Hz oscillations are coherently present in cortex and thalamus. They also showed that SWD-precursor oscillations originate in the cortex and enter the thalamus with a few milliseconds time delay [Pinault et al., 2006]. This assumes strong thalamo-cortical coupling during preSWD activity. We found that thalamo-cortical correlation is relatively weak during preSWD, peak values of thalamo-cortical coherence reach values of 0.1 (0.25 in preSWDn). The inconsistency between Pinault and co-workers and our results can be explained by differences in recording procedure. First, Pinault et al. (2001, 2003) recorded in the somatosensory cortex and related thalamic sites, we recorded from the frontal cortex and the VPM (these areas are known to lack direct ascending connections); second, experiments of Pinault et al. (2001, 2003) were mostly performed under neuroleptic analgesia, we used freely moving animals. Third, Pinault et al. used multi-unit and single-unit recordings, but we recorded and analyzed local field potential. It is known that field potentials are generated by different neuronal elements in the cortex (i.e., mostly straight-trunked pyramidal cells with longitudinal orientation and large dipole polarity) and in the thalamus (i.e., neurons with radial dendrites forming dipoles with a specific orientation and little polarity) [Lopes da Silva and van Rotterdam, 1982], therefore, results of EEG coherence studies might not fully correspond to results of coherence studies based on unit activity.

Our power spectral analysis shows that in the frontal cortex, preSWD epochs have peaks in the *delta* range (around 3-4 Hz, Fig. 3.11 and Table 3.4). Fig. 3.13 in the frontal cortex, preSWDΔ showed only one peak in *delta* band, but in the thalamus – one peak in *delta* and another one in *theta* band. Based on our data, we stress the role of cortical and thalamic *delta* activity in the initiation and further development of SWD (see the next few paragraphs).

Power spectrum of 95% preSWD epochs (except preSWDn) as measured in the frontal cortex and in the thalamus, reveal prominent peaks in *delta* frequencies (besides peaks in preSWD-specific frequencies), albeit thalamic *delta* is centered at the lowest edge of the frequency scale (i.e., 1-2 Hz), but in the cortex, the peak frequency of *delta* is found in 3-4 Hz (Table 3.4). In other words, the *delta* component of preSWD epochs in the cortex and the thalamus has 2 Hz difference in peak frequency. Probably, there are two independent sources of *delta* during preSWD epochs – one is located in the cortex and another one – in the thalamus. This agrees with recent findings of Steriade and his group who distinguished two types of delta generated in the thalamus and in the cortex [Steriade, 2002][**]. Cortical delta oscillations survive thalamectomy, but little is known about their cellular mechanisms. One of the hypotheses suggests that cortical delta could be driven by the firing activity of intrinsically bursting neurons [Amzica and Steriade, 1998]. Thalamic delta (1-4 Hz) is generated intrinsically by thalamic relay neurons as a result of the interplay between two intrinsic currents (low-threshold Ca^{2+} current, I_T, and hyperpolarization activated cation current, I_h).

From seizure-precursor towards a seizure

Different classes of preSWD activity showed remarkable differences in the waveform of cortical and thalamic power spectra. However, within a single second after the onset of SWD, cortical and thalamic power spectra closely resemble each other (Fig. 3.13). It seems that the similarities between electroencephalographic features of cortical and thalamic signals increase with seizure onset. The occurrence of SWD was associated with a sharp ~10 Hz peak in the frontal cortex and in the thalamus. However, the average peak frequency in the thalamus (8.5-9.5 Hz) was lower than the mean frequency in the frontal cortex (10 Hz, Table 3.4).

A 0.5-1.5 Hz gap between the mean frequency of thalamic and cortical absence seizures may appear because neurons in these two structures may fire in different frequencies during SWD. It was found that the thalamus is readily sustains a 6.5-7.0 Hz rhythm during the pre-epileptic state [Pinault, 2006] and, when SWD start, the thalamus might transform the original cortical epileptic ~10 Hz seizure rhythm to a slightly lower frequency. At the beginning, SWD have a frequency of ~10-11 Hz or even higher [Bosnyakova et al., 2007] and the cortex is leading the thalamus [Meeren et al., 2002], initially the cortical oscillations force the thalamus to follow this rhythm, however after 500 msec the cortex is no longer leading the thalamus and consequently, the influence of the thalamus on the cortex becomes bigger. As a consequence, the preferred thalamic frequency might become more dominant and the frequency drops further to 7-8 Hz in the cortex and to 6.5-7.0 Hz in the thalamus.

In the present Chapter we have found that that the transition from preSWD to a fully blown SWD is characterized by abrupt and robust changes in the EEG. First, the shape of power spectra is changed. Large differences are found between various preSWD epochs in EEG power spectra as measured in the frontal and

[**] see also M. Bazhenov, I. Timofeev 'Thalamocortical oscillations' Scholarpedia, 2006; 1(6):1319. http://www.scholarpedia.org/article/Thalamocortical_oscillations

occipital cortex and in the thalamus, however, the differences in cortical power spectra quickly disappeared within the first second of a SWD and the effects of the preceding epoch quickly vanished and could not be detected. In the thalamus, there is a correspondence between frequency profile of SWD and their precursor epochs: seizures, whose precursor epochs in the frontal EEG are desynchronized (preSWDn epochs), have an enlarged *delta*, and seizure-precursors with exaggerated *alpha* activity in the frontal EEG (preSWDα) are followed by seizures with high *alpha* activity in the thalamus (while the enlarged *alpha* component in the frontal cortex has disappeared).

Second, the power in the investigated frequency bands is quickly changed. The predominant presence of *delta* and *theta* characterizing almost all preSWD epochs is replaced by a predominant activity in the *alpha* band during SWD (Figs. 3.12 and 3.14); this general picture was found in cortex and thalamus.

Third, intracortical, intrathalamic and thalamo-cortical coherence is largely changed. The occurrence of SWD is accompanied by an increase of intracortical and thalamo-cortical coherence in 9.5-14 Hz and in the frequency band of the first harmonic, i.e. *beta* (Fig. 3.15).

It is assumed that amplitude-frequency properties in preSWD epochs may depend on coordination and consolidation of thalamic and cortical parts within the entire network. The variability of seizure-precursor activity may be caused by dynamic changes of synchronization between specific parts throughout the cortico-thalamo-cortical network. Probably some local factors may predetermine the characteristics of the preSWD epochs. Unfortunately, we cannot figure out a single mechanism that may govern the variability of amplitude-frequency characteristics of precursor epochs in the frontal EEG, but we found a correspondence between some features of preSWD and subsequent SWD. For instance, the high power of *alpha* in preSWDα is the most probable reason why transition preSWDα to SWDα is not accompanied by an increase in the *alpha* coherence in the thalamo-cortical pair, as it does in the rest subtypes of SWD. In all cases, the transition from preSWD to SWD corresponds to an increased *beta* coherence. Perhaps this finding is related to the theory that fast activity may trigger seizures and that synchronization in a network might be responsible for the spreading of seizure activity.

Chapter 4
Relationship between sleep spindles and SWD

CONTENTS

It is well accepted that a common thalamo-cortical mechanism underlie the occurrence of sleep spindle oscillations and absence seizures [Steriade and Deschênes, 1984; Kostopoulos, 2000; reviewed in Steriade, 2003 and in Meeren et al., 2005]. Animal models of human primary (idiopathic) absence epilepsy are beneficial for investigating various aspects of absence epilepsy, including neuronal, genetic and cellular mechanisms, as well as treatment and diagnosis [Danober et al., 1998; Marescaux et al., 1992; Vadász et al., 1995; Coenen and van Luijtelaar, 2003; Depaulis and van Luijtelaar, 2005]. One of the first experimental animal models was the 'feline penicillin model of generalized epilepsy', in which generalized bilaterally synchronous spike-wave discharges were induced by systemic injections of penicillin [Prince and Farell, 1969]. In high concentration, penicillin disturbs GABA-ergic neurotransmission and acts as a GABAa-antagonist, resulting in hyper-excitatory responses of cortical neurons to the activation of thalamocortical afferents [Avoli and Gloor, 1982; Gloor and Fariello 1988; Kostopoulos, 2000]. This neurophysiological mechanism is thought to underlie a transformation of sleep spindles into SWD [Gloor, 1969, 1978]: *'SWD develops in the same circuit, which normally generate sleep spindles, by an initially cortical transformation of one every two or more spindle waves to a 'spike' component of SWD, while the next spindle wave or waves are eliminated and replaced by a slow negative wave'* (cited by Kostopoulos, 2000).

Animal models of epilepsy have been used to discover cellular, subcellular and neuronal network mechanisms which are known to be responsible for the functional relationship between sleep spindles and SWD [Avanzini et al., 1993; Avanzini et al., 1992; 2000; Avoli and Gloor, 1982; Blumenfeld, 2002]. EEG studies in genetic rodent models also reveal that time-frequency EEG properties of sleep spindles and SWD are similar [Drinkenburg et al., 1993; Kandel and Buzsaki, 1997]. It is also known that sleep spindles and SWD more often occur during low vigilance states such as drowsiness, light slow-wave sleep, passive wakefulness [Drinkenburg et al., 1991] and that they are controlled by the same neuromodulatory systems [Buzsáki et al., 1991; van Luijtelaar, 1997]. The principle results of the above mentioned studies could be summed up in the following statements:

In the feline penicillin model of generalized epilepsy, it is shown that hyperexcitability of cortical neurons underlies the transformation of normal spindle activity into SWD, suggesting that epileptogenic processes take place in the cortex [Prince and Farell, 1969].

In rat models of absence epilepsy, sleep spindles and high voltage spindles (HVS = spike-wave discharges) are characterized by the same distribution of extracellular currents throughout the cortical depth [Kandel and Buzsaki, 1997]. As known, a depth profile of cortical field potentials depends on the activity of thalamo-cortical afferents, and the thalamus provides the same excitatory input to the cortex during sleep spindles and during absence seizures.

Several computational models prove that strong hyperexcitation and hypersynchronization in the neocortex are crucial for the occurrence of spike-wave discharges [Destexhe and Sejnowski, 2000; Sargsyan et al., 2007]. All this implies that thalamic neurons are acting in the same 'oscillatory mode' during normal spindle activity and during absence seizures. In particular, spindle-like sequences are delivered to a hyperexcitable neocortex where (in the cortex) they are transformed into hypersynchronous SWD. In other words, the cortex is the prime source for the transformation of sleep spindles into SWD; the thalamus, which plays an active role in providing the basis oscillatory spindle pattern, has a passive role in sustaining and distributing epileptic discharges.

SWD more often appear during quiet wakefulness, in drowsiness and transitions towards slow-wave sleep. Sleep spindles are also abundant during these states [Drinkenburg et al., 1991]. The circadian dynamics of SWD positively correlate with the dynamics of light slow-wave sleep [van Luijtelaar and Coenen, 1988], therefore, the same arousal systems of the brain may control the occurrence of both sleep spindles and SWD [Buzsáki et al., 1988; 1991]. The spectral characteristics of normal sleep spindles in WAG/Rij rats are similar to those in SWD [Drinkenburg et al., 1993].

The present chapter aims (1) to compare EEG features of sleep spindles and SWD in WAG/Rij rats, (2) to find out similarities and distinctions between SWD, sleep spindles and seizure-precursor activity (preSWD) and, finally (3) to disclose thalamo-cortical network mechanisms, which are responsible for the occurrence of normal spindling and paroxysmal spike-wave activity. To achieve these aims, we use several approaches, such as analysis of power spectrum and cross-correlations (**Chapter 4.1**), simulation tool (a neuronal model which simulates cortical field potential of SWD and sleep spindles, **Chapter 4.2**) and continuous wavelet transform (**Chapter 4.3**). Wavelet analysis in **Chapter 4.3** provides us with a clue for the selective identification of sleep spindles and SWD.

4.1 Correspondence between local cortical rhythmic activity:
anterior sleep spindles versus SWD I and posterior sleep spindles versus SWD II*

INTRODUCTION

Two types of spontaneous SWD have been distinguished in the EEG of WAG/Rij rats. The first type, SWD I, is more or less generalized and it is predominant in the fronto-parietal cortex. The second type, SWD II, is localized in the occipital region [van Luijtelaar and Coenen, 1986; Midzianovskaia et al., 2001]. Sleep spindles are divided in two classes, i.e., anterior and posterior sleep spindles, as indicated in Wistar rats [Terrier and Gottesmann, 1978; Gandolfo et al., 1985], in WAG/Rij rats [van Luijtelaar, 1997; see also **Chapter 2**] and also in humans [Jobert et al., 1993]. Considering the same anterior-posterior topographic distribution of sleep spindles and SWD, it is hypothesized that anterior sleep spindles are functionally linked to SWD I and posterior spindles – to SWD II. In order to examine this hypothesis, we compare EEG power spectrum of corresponding types of sleep spindles and SWD: anterior spindles versus SWD I and posterior spindles versus SWD II.

Besides this topographic difference, SWD I differ from SWD II in many other aspects. In comparison to SWD I, SWD II are shorter, have lower frequency 5-7 Hz (vs 9-11 Hz in SWD I) and have a different pharmacological profile [van Luijtelaar and Coenen, 1986; van Luijtelaar, 1997; Midzianovskaia et al., 2001; Sitnikova and van Luijtelaar, 2005]. All WAG/Rij rats older than 6 months have SWD I, but only ~ 50% of these rats have SWD II [Schridde and van Luijtelaar, 2005]. The origin and phenomenology of SWD II is uncertain and the EEG pattern of SWD II is poorly investigated. Although two types of SWD differ in terms of their electrographic structure [van Luijtelaar and Coenen, 1986; Midzianovskaia et al., 2001] and neuromodulatory (noradrenergic and dophaminergic) supply [Midzianovskaia et al., 2001; Sitnikova and van Luijtelaar, 2005; **Chapter 3.2**], both SWD types comprise the same epileptiform (Weir's) elements [Sitnikova and van Luijtelaar, 2007; see also **Chapter 3.1**]. This implies that both SWD types could be considered as genuine epileptic phenomena. However, behavioral observations contradict this point of view: no clinical manifestations of absence seizures are seen during SWD II.

It is known that the waveform of SWD I is gradually changing from the beginning towards the end: the amplitude of spikes gradually diminishes towards the end of SWD I, whereas the amplitude of the waves are elevated [Midzianovskaia et al., 2001] and the frequency of SWD I monotonously decreases from 10 to 7 Hz [Drinkenburg et al., 1993]. Altogether, the waveform of SWD I at the end closely resembles the waveform of SWD II. We hypothesize that SWD II a 'residual' local form of spike-wave seizures which appear in the occipital cortex when SWD I in the fronto-parietal cortex are no longer present. Here we test this hypothesis by examining the amplitude-frequency characteristics of SWD I (at the beginning and at end of a seizure) and by comparing these characteristics in SWD I and SWD II. Measurements were made in fontal and occipital EEG.

Thalamic and cortical activity during anterior spindles and SWD I are investigated in more details. The results help to understand thalamo-cortical neuronal network mechanisms underlying a putative functional relationship between spindle and SWD.

METHODS

Animals and EEG recording design

Nine male 11-12 months old WAG/Rij rats (body weigh 320-360 g), which were born and raised in the laboratory of the Department of Biological Psychology of the Radboud University Nijmegen, were chronically implanted with six still stainless electrodes (Plastic One Inc. Roanoke, VI, USA: MS 333/2A) for monopolar EEG recordings. Two electrodes were implanted epidurally over the frontal (AP 2; L 2.5) and occipital (AP -7; L 6) cortical areas. Two depth electrodes were implanted in the ventroposteromedial nucleus of thalamus (VPM, AP –3.5; L 2.5; H 7.2) and in the rostral pole of the reticular thalamic nucleus (RTN, AP –1.5; L 2.2; H 7.2). All coordinates are given in mm relative to bregma [Paxinos and Watson, 1986]. Ground and reference electrodes were placed symmetrically over both sides of the cerebellum. Post mortem histological control (standard Nissl staining of brain slices) was performed to verify the positioning of deep (thalamic) electrodes.

Description of EEG patterns

SWD and sleep spindles were identified in the frontal and occipital EEG channels during 5-7 hours. EEG pattern of SWD type I and II in rodents fulfill the criteria given by the International Federation of Societies for

* Published in:
Sitnikova E.Yu.; G. van Luijtelaar The relation between two types of spike-wave discharges and sleep spindles: a spectral analytical approach. Epilepsia. 2003, 44, Suppl. 8, 72, P147 (Abstracts of the 25-th International Epilepsy Congress. Lisbon, Portugal October 2003)

Electroencephalography and Clinical Neurophysiology, IFSECN [Sitnikova and van Luijtelaar, 2007]. SWD I and SWD II were detected using criteria described in van Luijtelaar and Coenen (1986) and Midzianovskaia et al. (2001). SWD I were recognized in the frontal EEG as a train of surface negative 7-10 Hz spikes with amplitude at least three times higher than the background. Duration of SWD I was more than 1 sec. SWD I were detected automatically based on the threshold value of the EEG slope in the frontal channel with efficiency 97-100% in the artifact-free EEG (the algorithm and original software were developed by P.L.C. van den Broek, NICI, University of Nijmegen, the Netherlands).

SWD II consisted of sharp repetitive positive 6-7 Hz waves and lasted longer than 0.5 sec (more than three waves in a sequence), and were identified visually in the occipital EEG in the absence or with just little concurrent rhythmic activity in the frontal EEG.

Sleep spindles were detected visually in EEG during non-REM sleep (see Method section in **Chapter 2** for details). Briefly, sleep spindles were recognized as regular sinus oscillations shaped in spindle-like envelope; they lasted longer than 500 ms and their maximal amplitude was more than twice higher than background (Fig. 2.1A in **Chapter 2**). Anterior sleep spindles were present on the frontal EEG, but not in the occipital EEG. Oppositely, posterior sleep spindles were only present only in the occipital EEG. 30-70 representatives of each spindle type were collected in each animal.

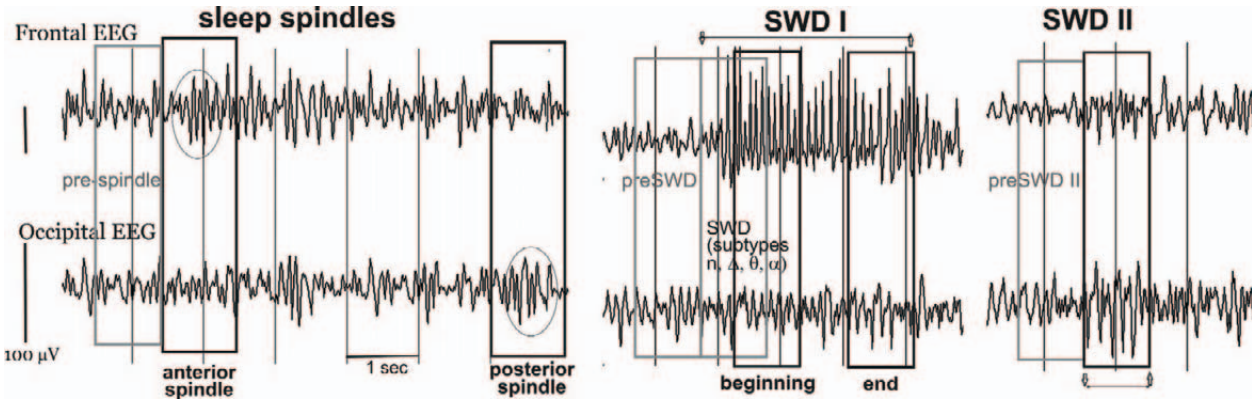

Figure 4.1. Sleep spindles and SWD were recorded in the frontal and occipital EEG. Type I phenomena (anterior sleep spindles and SWD I) were detected in the frontal EEG. Type II phenomena (posterior sleep spindles and SWD II) – in the occipital EEG. 1 sec EEG epochs were selected for time-frequency analysis (shown by rectangles). The onset of SWD I and II was determined by the first spike and the end – by the last spike in spike-wave sequence in the frontal EEG (SWD I) and in the occipital EEG (SWD II).

EEG sample length was 1 sec for all investigated phenomena. In spindles shorter than 1 sec, the initial point was shifted in order to get the entire spindle in the middle of the time-window. Figure 4.1 gives examples of the investigated phenomena in EEG, i.e., anterior and posterior sleep spindles, SWD I and SWD II. Two datasets were used to describe SWD I: first (black rectangles in Fig. 4.1) included 1 sec epochs at the beginning (0.5 sec after the first spike) and 1 sec epochs at the end (immediately before the last spike); the second dataset (grey rectangles in Fig. 4.1) included precursors of SWD I (preSWDn, preSWDα, preSWDθ, preSWDΔ, see **Chapter 3.3**) and subsequent seizure activity corresponding to a subtype of precursor.

Power spectrum EEG analysis

Hanning windowed Fast Fourier transform (FFT) with 0.5 Hz resolution was used to compare EEG features of the selected epochs in the frequency domain. Power spectra were averaged per channel, per EEG event type and per animal. The following quantitative parameters were determined and compared: (i) duration and (ii) mean frequency in the appropriate cortical areas, (iii) EEG power in the frontal and occipital cortex summed over the following frequency bands: 1-4.5 Hz (delta), 5-8.5 Hz (theta), 9-13.5 Hz (alpha), 14-31.5 Hz (beta), 32-59.5 Hz (gamma1) and 60-100 Hz (gamma2). ANOVA was used for the statistical analysis.

In order to eliminate amplitude differences between channels, power density of every frequency band of both spindle types in cortex and thalamus, every band was normalized to the total EEG power.

Cross-correlation EEG analysis

Cross-correlation function was used to measure the linear correlation between two signals as a function of their time delay [e.g., Quian Quiroga et al., 2000; Pereda et al., 2005]. This function ranges from -1 (complete linear inverse correlation) to +1 (complete linear direct correlation). Cross-correlation function of two signals (time series) $x(t)$ and $y(t)$:

$$C_{x,y}(\tau) = \frac{1}{N-\tau}\sum x(k+\tau)y(k)$$

where N is the total number of data points (the size of time window) and τ is the time lag between the signals (an example of cross-correlation functions is shown in Fig. 2.9A) We examined cross-correlations in intracortical (fronto-occipital), intrathalamic (VPM-RTN) and cortico-thalamic pairs (frontal-VPM; frontal-RTN) and included episodes of anterior sleep spindles, SWD I and 1 sec periods of EEG during passive wakefulness (n = 50 per rat).

Power spectrum and cross-correlation analyses were performed using Brain Vision Analyser software, © BrainProducts GmbH.

RESULTS

Sleep spindles and SWD in the frontal and occipital cortical areas

Table 4.1 describes some general features of anterior sleep spindles and SWD I (type I phenomena that were predominant in the frontal EEG) and posterior spindles and SWD II (type II phenomena that were expressed in the occipital EEG).

Table 4.1 Descriptive statistic of the investigated EEG phenomena (epoch length = 1 sec).

	Number of EEG samples	Mean duration (sec) ± S.D.	Mean frequency (Hz) ± S.D.	Total power (μV) ± S.D. [2]
type I				
anterior sleep spindles	445	0.68 ± 0.08	11.14 ± 1.02	11.3 ± 1.7
SWD I (0.5 after seizure onset) [1]	297	6.71 ± 0.58 *	9.14 ± 0.47 [1]	24.8±6.5 *
type II				
posterior sleep spindles	299	0.59 ± 0.07	10.16 ± 0.88	8.6 ± 2.1
SWD II	194	0.89 ± 0.29	6.58 ± 0.70 *	11.8±2.7 *

* - significant differences between sleep spindles and SWD (t-test, $p<0.05$);
[1]– as measured during 1 sec period from 0.5 to 1.5 sec after the onset of SWD (average across SWDn, SWDα, SWDθ, SWDΔ)
[2]– total power of type I phenomena was measured in the frontal EEG and type II phenomena – in the occipital EEG.

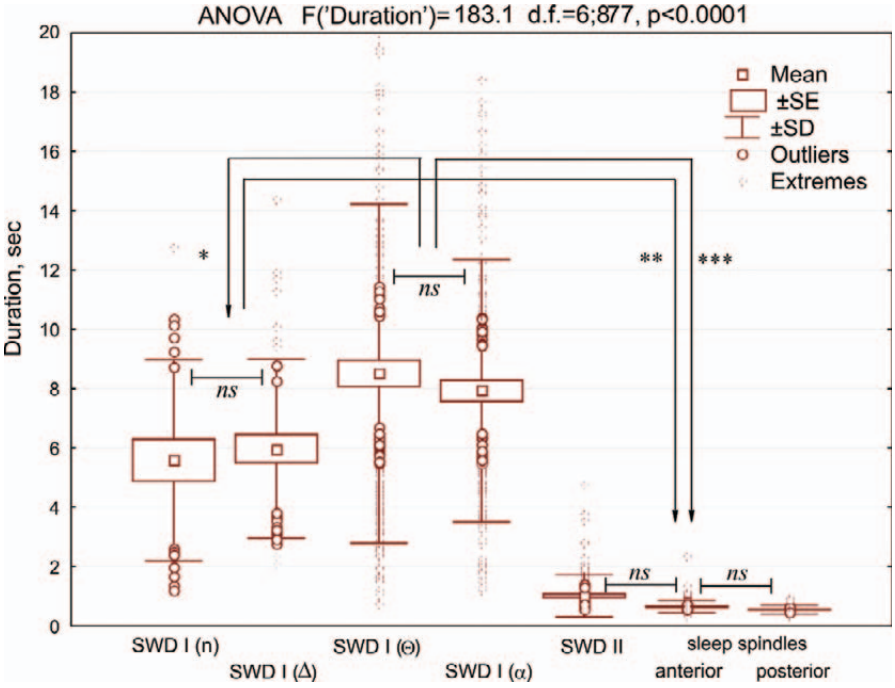

Figure 4.2. Results of the one-way ANOVA on the duration of SWD and sleep spindles. SWD I lasted significantly longer as compared to sleep spindles (anterior and posterior) and SWD II. Duration of SWD I seems to be predetermined by SWD-precursor activity (preSWDn, preSWDΔ , preSWDα and preSWDθ, see description in the text).

Type I phenomena. As compared to anterior spindles, SWD I lasted ten times longer, their amplitude was nearly two times higher, and their mean frequency was (~ 2 Hz) significantly lower (note that these data described SWD I periods from 0.5 to 1.5 sec after the onset).

Type II phenomena. Posterior spindles and SWD II had the same duration, but the frequency of SWD II was ~ 3.5 Hz lower than frequency of posterior sleep spindles.

Duration of the spindles and SWD (separately for each subtype SWDn, SWDα, SWDθ, SWDΔ) was further analyzed using a one-way ANOVA (Fig. 4.2). Duration of anterior spindles, posterior spindles and SWD II did not differ significantly, but it was significantly lower than found for all subtypes of SWD I (LSD-test, all p's<0.001; see also Table 4.1). SWD I, which followed by preSWDα and preSWDθ, lasted significantly longer as compared to seizures preceded by preSWDn and preSWDΔ (LSD-test, all p's<0.05). Therefore, SWD-precursor activity (preSWDn, preSWDΔ , preSWDα and preSWDθ) affects the length of subsequent SWD I.

In the average power spectra (Fig. 4.3), the frequency of the major peak ('mean frequency') varied from 6 Hz in SWD II up to 10-11 Hz in sleep spindles (Table 4.1). SWD II were distinguished from all other EEG phenomena by having a low frequency and high power in the theta band (Fig. 4.3).

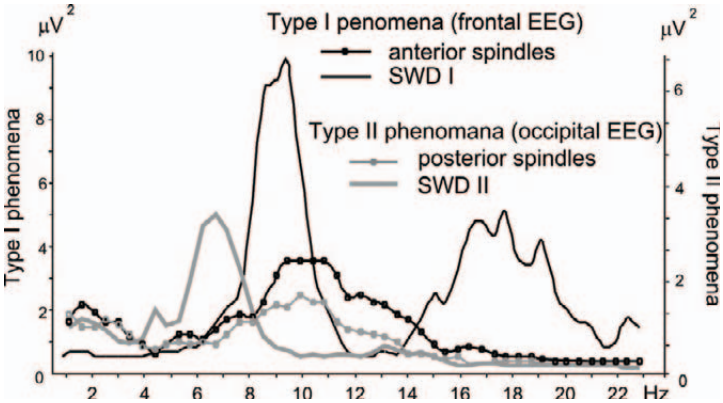

Figure 4.3. Mean spectrograms of the four investigated EEG events (n=9 rats) as measured in their characteristic areas. SWD I were distinguished by high power around 10 Hz and in the harmonic beta frequencies.

Power spectra of both sleep spindles and SWD I displayed high power in alpha frequencies (9-12 Hz), suggesting that these EEG phenomena were characterized by the same rhythmic component in the alpha frequency band. Besides that, the following principal differences in the power spectrum of sleep spindles and SWD should be noted.

(1) In SWD I, ~ 9 Hz spectral peak was several times higher as compared to the ~ 10-11 Hz peak in sleep spindles. Occurrence of this sharp and high ~ 9 Hz peak in the power spectrum of SWD I may be brought about by high-voltage periodic spike component. A smooth spectral peak in both spindle types may suggest a considerable variability of intra-spindle frequencies.
(2) Mean frequencies of SWD were lower than in sleep spindles (difference between SWD I and anterior spindles was ~ 2 Hz and between SWD II and posterior spindles ~3.5 Hz).
(3) Power spectrum of sleep spindles (and SWD II) displayed relatively high power in delta frequencies (1-4 Hz, Fig. 4.3), while in SWD I low frequencies were suppressed.
(4) Power spectrum of SWD I displayed additional peaks in harmonic frequencies (i.e., 16-20 Hz that doubles fundamental seizure frequency), that was absent in sleep spindles. This is accounted for the spike sequences in SWD I which manifest themselves in the power spectrum as harmonic frequency components.

ANOVA was used to analyze distribution of EEG power density (spectral power) in sleep spindles and SWD (factor 'spindles/SWD') over the selected frequency bands 'band' (Fig. 4.4).

Anterior spindles and SWD I showed a significantly different distribution of spectral density over frequency bands in the frontal EEG (F=38.9; d.f.=1.107; p<0.0001), but not in the occipital EEG, Fig 4.4A). Post-hoc test revealed that, in the frontal EEG, SWD I had significantly higher power in alpha, beta and gamma1 bands (e.g., in frequencies from 14 Hz to 59.5 Hz), as compared to anterior spindles. In the occipital EEG, the factors 'band' and interaction between 'spindles/SWD'*'band' were significant: SWD I had a significantly lower power in the delta band as compared to anterior spindles (post-hoc test, p<0.05).

Posterior sleep spindles and SWD II were characterized by significantly different distribution of spectral power over frequency bands in the occipital cortex (F=86.8; d.f.=1.107; p<0.0001, Fig. 4.4B), but not in the frontal cortex (Fig. 4.4B). In the occipital cortex, SWD II were distinguished from posterior spindles by higher power in theta and low power in alpha bands (*post-hoc* tests, p's<0.05).

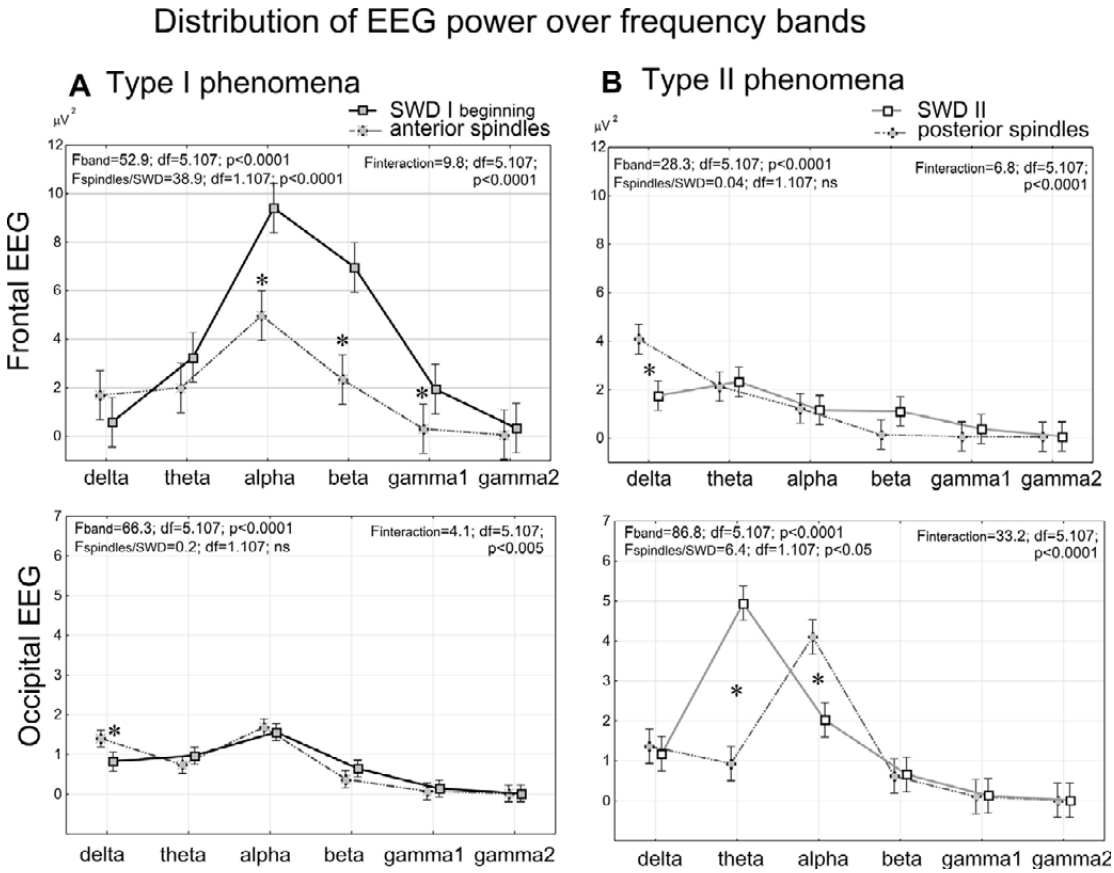

Figure 4.4. ANOVA power spectrum EEG analysis in the following frequency bands: 1-4.5 Hz (delta), 5-8.5 Hz (theta), 9-13.5 Hz (alpha), 14-31.5 Hz (beta), 32-59.5 Hz (gamma1) and 60-100 Hz (gamma2) (n=9 rats).
* - significant differences according to post-hoc Fisher test.

Type I phenomena

Figure 4.5 (dotted lines) illustrates the power spectrum of various subtypes of SWD I which were distinguished by EEG precursor activity (SWDn, SWDα, SWDθ, SWDΔ, see **Chapter 3.3**). Peak frequency of each subtype of SWD I was measured immediately after the seizure onset and it was ~ 10 Hz, e.g., similar to what was found in anterior sleep spindles (Fig. 4.5). Already 0.5 sec after the onset, the mean frequency of SWD I decreased to ~ 9 Hz (Figs 4.3 and 4.4) and the ~ 1 Hz frequency gap between SWD I and anterior spindles appeared to be significant (Table 4.1).

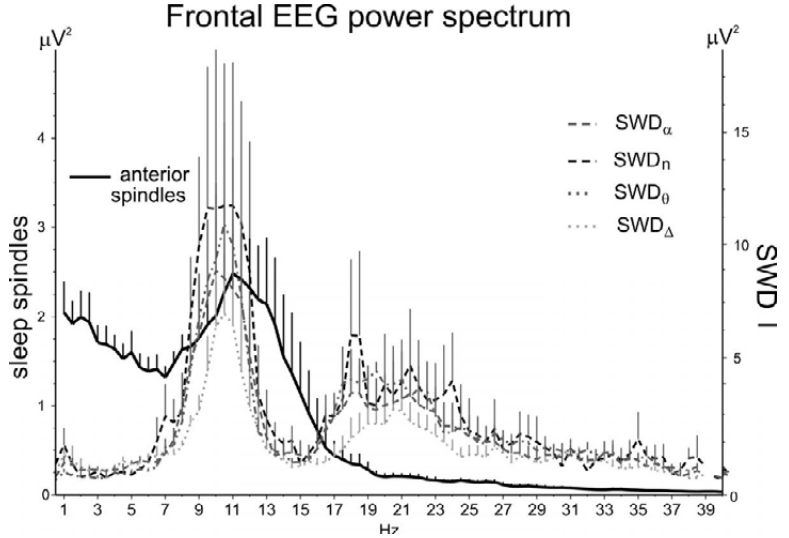

Figure 4.5. Anterior sleep spindles and spike-wave discharges (SWD I) showed different power spectra in the frontal cortex. SWD I were divided into four subtypes depending on the frequency profile of seizure precursor activity (**Chapter 3.2**): SWDn developed form desynchronized EEG, preSWDn (4.8 %), SWDθ were preceded by high theta (preSWDθ, 38.2%), SWDα - by high alpha (preSWDα, 33%) and SWDΔ – by high delta (preSWDΔ, 22%). Note scale difference in ordinate axis SWD versus spindles.

All subtypes of SWD I revealed a similar distribution of EEG power over the frequencies, including delta, theta and beta (Fig. 4.5, dotted lines). As compared to SWD I, sleep spindles demonstrated a relatively low power in beta frequencies and high delta and theta frequencies. This means that SWD I and anterior sleep spindles are distinguished by having different subdominant frequencies and different EEG waveforms. Fundamental frequencies of anterior spindles and SWD I appear in the same alpha band, despite that, the morphology of these events was remarkably different. Differences in EEG morphology between SWD I and anterior sleep spindles were examined with the continuous wavelet transform and reported in the following **Chapter 4.2**.

The collage in Figure 4.6 illustrates remarkable dissimilarities between power spectra of sleep spindles, seizure precursor activity (preSWDn, preSWDα, preSWDθ, preSWDΔ, see **Chapter 3.3**) and successive SWD. All types of preSWD, as expressed in the frontal EEG, differed from sleep spindles. PreSWDα, which comprised enlarged alpha component (Fig. 4.6e; see Fig. 3.12A) and were expected to most closely resemble sleep spindles, were still distinguished from them by having higher power in delta and theta frequencies (Fig. 4.6a). Even more sharp distinctions were pronounced in other precursor subtypes (preSWDn, preSWDθ, preSWDΔ Fig. 4.6 b-d). Noteworthy is that anterior sleep spindles comprised frequency components that were also present in preSWD (relatively high delta) and in SWD I (relatively high alpha).

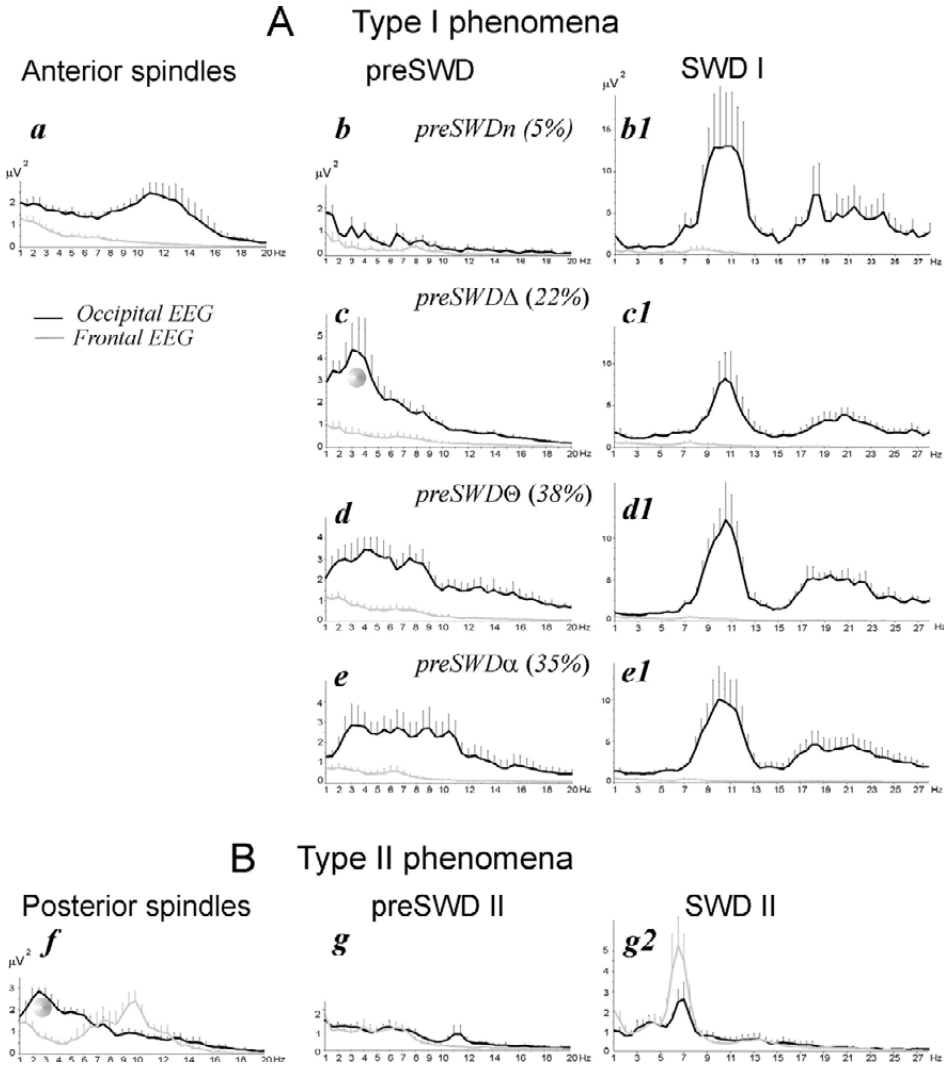

Figure 4.6. Average power spectra of type I and type II EEG phenomena as measured at the frontal and occipital cortical areas (all epochs length are equal to 1 sec). In both SWD types, immediate precursor activity (preSWD) showed variable power spectrum that was distinguished from the successive SWD and from sleep spindles.

Type II phenomena

Precursors of SWD II (Fig. 4.6g) showed a flat power spectrum in both frontal and occipital areas, suggesting that no oscillatory patterns in the cortex preceded the occurrence of SWD II. Posterior sleep spindles were characterized by a remarkable discrepancy between power spectra obtained in the frontal and occipital EEG channels (Fig. 4.6f); enhancement of alpha power in the occipital EEG (peak in ~10 Hz) coincided with the

elevation of delta in the frontal EEG (peak in ~3 Hz). SWD II showed more consistency between power spectra obtained in frontal and occipital EEG (Fig. 4.6f2); both cortical EEG channels revealed spectral peaks in ~ 6 Hz.

To sum up, substantial differences in EEG power spectrum of SWD, sleep spindles and SWD-precursor activity disagree with our hypothesis that there is a direct relationship between these EEG phenomena. The fundamental frequency of SWD I immediately after the onset was similar to that in anterior spindles and rapidly decreased ~ 1 Hz within half a second. Sleep spindles were significantly shorter than SWD I. We cannot exclude that anterior sleep spindles might be transformed into SWD I, but this transformation requires a serious dysfunction that leads to the introduction of sustained and regular spikes in the frontal EEG. This mechanism is not relevant to a putative transformation from posterior sleep spindles to SWD II.

Frequency profile of SWD I: its dynamics and resemblance to SWD II

In the present section we test hypothesis that SWD II appear as a result of dynamic transformation of SWD I. It was found that *in the frontal EEG*, the power spectrum of SWD I underwent dynamic transformation and at the end the spectrum of SWD I became resemble to that in SWD II (upper graph in Fig. 4.7A). SWD I showed a characteristic frequency drift toward lower frequency and showed peaks at 6.5 and 8 Hz. Interestingly is that 6.5 Hz peak was present at the end of SWD I and in SWD II.

Analysis of distribution of EEG power over selected frequency bands revealed significant differences between SWD I and SWD II (bottom graph in Fig. 4.7A; 'band' effect was $F(5.161)=47.6$, $p<0.0001$; 'SWD type' effect was $F(2.161)=47.3$, $p<0.0001$; the interaction was $F(10.161)=18.9$, $p<0.0001$). At the beginning, SWD I showed higher EEG power in *alpha*, *beta* and *gamma1* bands as compared to SWD II (all p's<0.05), but at the end of SWD I, these differences were no longer present (in *alpha* and *gamma1* bands) or became less significant (in *beta* band).

In the occipital cortex, SWD I and SWD II displayed different distribution of EEG power over frequency bands (bottom graph in Fig. 4.7B; the effect of 'band' was $F(5.161)=80.5$, $p<0.0001$; 'SWD type' - $F(2.161)=22.4$, $p<0.0001$; the interaction $F(10.161)=9.9$, $p<0.0001$). The most remarkable difference was found in *theta* frequency band. Theta for SWD II was higher than for SWD I (both for beginning and end, p's<0.05). The frequency profile of SWD I just slightly changed as seizure progress (upper graph in Fig. 4.7B). Significant differences were found in the delta band only: at the end of SWD I delta was higher as compared to the beginning of SWD I and to SWD II (bottom graph in Fig. 4.7B; *post-hoc* test, $p<0.05$). Enlargement of delta activity in occipital cortex may correspond to the elevation of the wave component during SWD I: the wave is known to be maximally expressed at the occipital cortex at the end of a SWD I [Midzianovskaia et al., 2001].

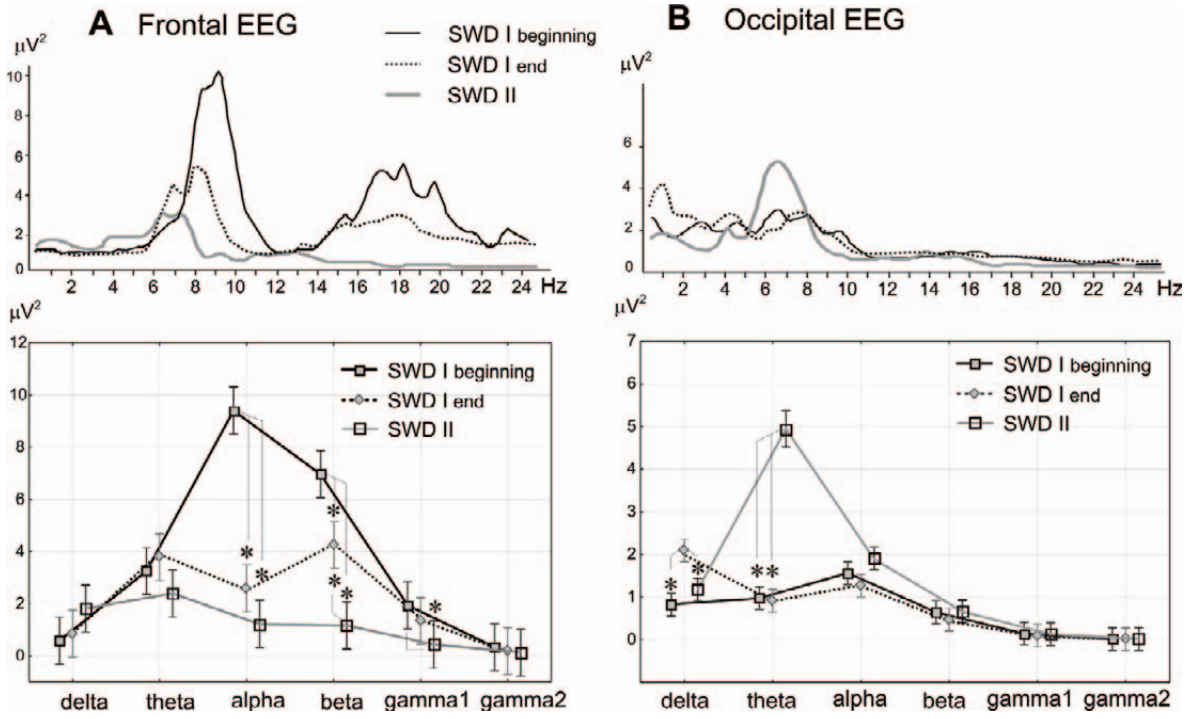

Figure 4.7. EEG power spectrum of two types of SWD (average over 9 rats). In the frontal EEG, the waveform of power spectrum at the end of SWD I mimicked that of SWD II and distribution of EEG power over frequency bands have changed correspondingly. In the occipital EEG, power spectrum of SWD I was nearly unchanged from the beginning to the end (except delta which was enlarged at seizure end). Significant differences: * - 0.05 > p > 0.01; ** - 0.01 > p > 0.001; *** - p < 0.001 (the paired t-test).

In all, the frequency profile of SWD I in the frontal EEG underwent dynamic changes, so that, at the end, SWD I bore a striking similarity with SWD II. However, in the occipital EEG, SWD II and SWD I were remarkably dissimilar. This implies that, despite the partial resemblance observed between SWD I end ('residual' seizures) and SWD II in the frontal cortex, the local occipital SWD II displayed a different frequency profile as compared to occipital SWD I. This indicates that SWD I and SWD II are indeed independent phenomena, yet the neuronal mechanisms in the frontal cortex might provide a probable (functional) link between them.

Thalamic and cortical activity during anterior sleep spindles and SWD I

Fourier analysis (frequency domain)

In order to directly compare frequency profiles of spindles and SWD as recorded in the frontal cortex and in the thalamus, we eliminated amplitude differences by normalizing the EEG power spectra (Fig. 4.8). Next, the frequency composure of pre-spindle epochs, anterior spindles and SWD I were compared.

During pre-spindle epochs (upper graph in Fig. 4.8), cortical and thalamic channels demonstrated closely similar frequency profiles, more specifically, all power spectra showed a maximum around 1 Hz and gradual decrease in power towards higher frequencies.

The most pronounced differences, characterizing changes from pre-spindle to anterior spindle activity, were found in the frontal EEG (i.e., an increase in power in alpha frequencies with a peak at 11 Hz and a decrease in delta frequencies), whereas changes in the thalamus were moderate and changes in the occipital channel were virtually absent.

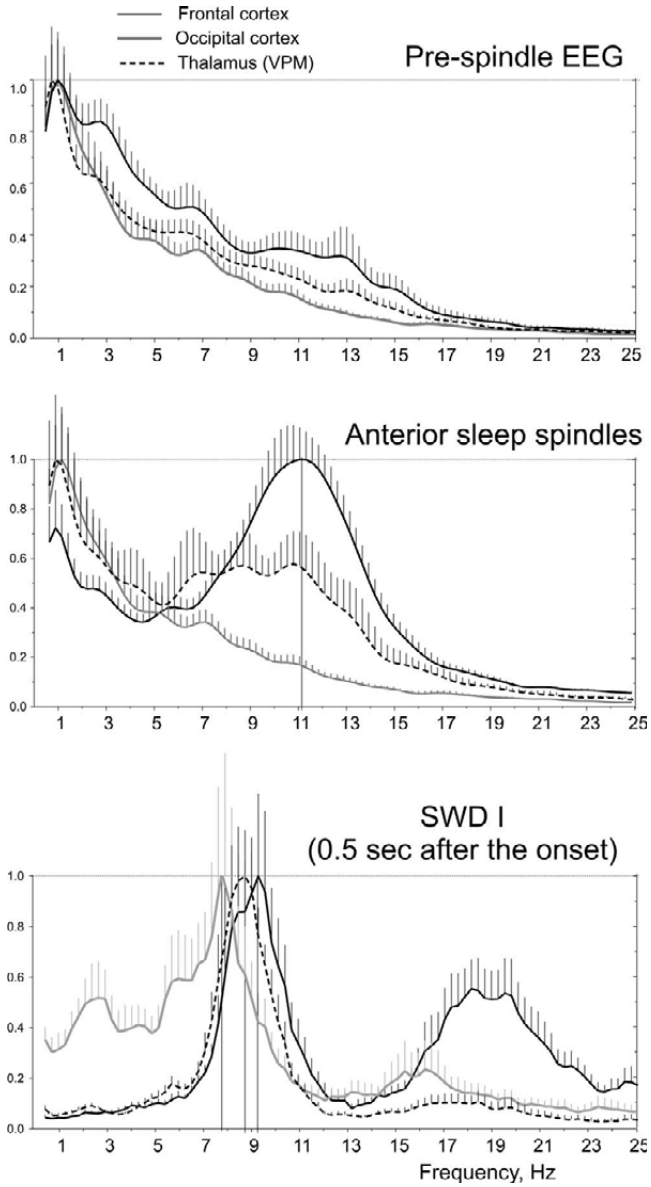

Figure 4.8. Normalized power spectra characterizing frequency profiles of electrical brain activity as recorded simultaneously in the cortex (solid lines) and in the thalamus (VPM – ventroposteromedial nucleus, dotted line) during anterior spindles, pre-spindle activity (immediately before spindles) and SWD I. Epoch length is 1 sec. Mean ± S.E.

SWD I (0.5-1.5 sec from the onset, bottom graph in Fig. 4.8) were characterized by a narrow spectral peak in 8-9 Hz in the cortex and the thalamus (ventroposteromedial nucleus, VPN), suggesting that both structures sustain stable and regular 8-9 Hz activity. However, the EEG power spectra in these loci were not completely congruent:

(1) discrepancies were found in the mean peak frequency of SWD I that were different in different locations: the peak was 7.75 Hz in the occipital EEG, 8.75 Hz in the thalamus, and 9.25 Hz in frontal cortex;
(2) both occipital and thalamic power spectra differed from the frontal spectrum by a relatively low power in beta frequencies;
(3) the occipital power spectra differed from the frontal and thalamic spectra by having high power in the low frequencies. This could be associated with local occipital delta activity corresponding to the wave component of seizure activity in the occipital cortex [van Luijtelaar and Coenen, 1986; Midzianovskaia et al., 2001; Sitnikova and van Luijtelaar, 2007].

Altogether, pre-spindle epochs and subsequent sleep spindles have similar low-frequency components in the cortex and in the thalamus, indicating that (1) the cortex and the thalamus sustain simultaneous delta activity; (2) this delta seems unchanged in transitioning from pre-spindle activity towards sleep spindles. During sleep spindles, besides high delta and theta, the thalamus sustains surprisingly low alpha activity as compared to relatively high alpha in the frontal cortex. Frequency profiles of SWD I (0.5-1.5 sec from the onset) in the frontal cortex and the thalamus were similar: frontal and thalamic spectra were congruent across delta-theta-alpha frequencies, suggesting that the frontal cortex and the thalamus operate at the same frequency mode; a narrow spectral peak in 8-9 Hz implies the presence of clearly dominating rhythm in the cortex and thalamus.

Analysis of cross-correlations (time domain)

The cross correlation function was used to characterize first-order (linear) dependency between cortical and thalamic signals in the time domain. This function estimates a time-varying correlation value between two signals (i.e., positive or negative correlation for every time lag). Fig. 4.9 shows average cross correlation function, $C_{xy}(\tau)$, during anterior sleep spindles, SWD I and wake EEG (passive wakefulness). In order to interpret cross-correlation functions more explicitly, we mention several *a posteriori* refinements, under assumption of linear relationship between these signals [Pereda et al., 2005]:

(1) Absolute value of $C_{xy}(\tau)$ depends on signal amplitude (it is higher in equipotential signals).
(2) The value of τ at maximum $C_{xy}(\tau)$ is the time delay measure between two phase-shifted signals.
(3) Negative value of $C_{xy}(\tau)$ implies an inverse correlation. $C_{xy}(\tau) = -1$ means that the two EEG signals of the same amplitude have an opposite direction. Positive $C_{xy}(\tau)$ implies direct correlation (the same direction).
(4) High correlation coefficients $C_{xy}(\tau)$ and symmetric cross-correlation function along the time (τ) axis imply that that the phases of the signals are synchronized; low correlation coefficients $C_{xy}(\tau)$ and asymmetric cross correlation functions characterise signals with arbitrarily changing phases.
(5) Asymmetric cross-correlation function along τ-axis may imply either that only one channel sustains oscillatory activity, but the other channel is not; or that associations between EEG channels are non-linear (a linear cross correlation is then inappropriate).

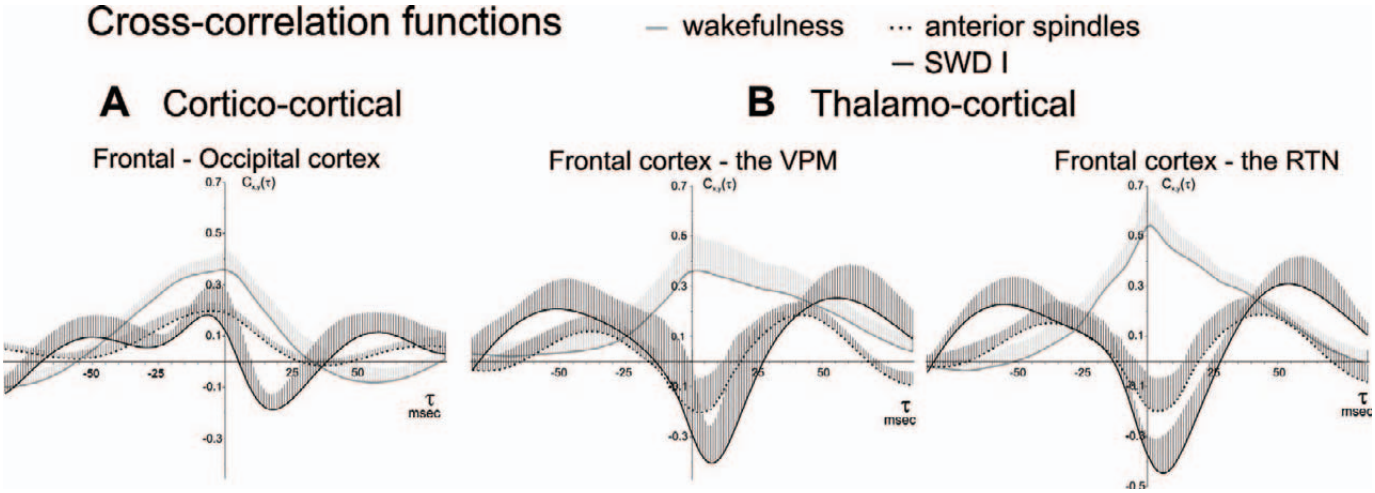

Figure 4.9. Averaged cross correlation functions in the cortico-cortical (**A**) and thalamo-cortical (**B**) EEG pairs during SWD type I, anterior sleep spindles and the waking EEG (n=5 rats). Mean ± S.E.

Waking EEG

Intracortical (fronto-occipital) cross-correlation function (Fig. 4.9A, grey line) had a sine wave profile (140-160 msec full cycle) with relatively high positive peak $C_{xy}(\tau) \sim 0.37$ (at $\tau \sim 0$) and a low negative peak $C_{xy}(\tau) \sim 0.1$ (at $\tau \sim$ +/- 40-50 msec). Cross-correlation function tend to have positive values [$C_{xy}(\tau)>0$]; this mean that the frontal channel has constantly higher amplitude as compared to the occipital channel.

Thalamo-cortical cross-correlation function 'frontal cortex – VPM' was positive [$C_{xy}(\tau) = 0.38$] with time lag largely fluctuating across zero (τ varied from -2 to +2 msec), suggesting an equal probability that frontal cortex lead the VPM or *vice versa*. The positive peak correlation 'frontal cortex – RTN' [$C_{xy}(\tau) = 0.54$] was higher than in 'frontal cortex – VPM' and displayed a more stable lag, $\tau \sim +2$ msec. Therefore, (i) the frontal cortex showed a direct (in-phase) synchronization with the VPM and RTN, (ii) there was more synchrony in a pair 'frontal cortex – RTN' than in 'frontal cortex – VPM' and (iii) the frontal cortex lead the RTN with one synapse delay (2 msec), but it associate with the VPM in bidirectional manner.

Anterior sleep spindles

Intracortical cross-correlation function (Fig. 4.6A, dotted line) was also sinusoidal (similar to that in waking EEG), but all its values were positive (maximum $C_{xy}(\tau) = 0.15$ at $\tau \sim$ - 5 msec and two minima $C_{xy}(\tau) \sim 0$ at $\tau \sim$ +/- 25-40 msec). This suggests that there was in-phase synchronization between the frontal and occipital channels. Positive orientation of cross-correlation function [$C_{xy}(\tau)>0$] suggests that the amplitude of the frontal EEG was much higher than that in occipital EEG. This fully agrees with the principle of spindle selection: anterior spindles were present locally in the frontal cortex and were virtually absent in the occipital cortex (see **Chapter 2.1**, Figs 2.1 and 2.8).

Thalamo-cortical cross-correlation function (Fig. 4.9B, dotted lines) differed from that observed in waking EEG (Fig. 4.9B, grey lines): they showed sinusoidal waveform and were almost symmetric along the τ-axis (full cycle lasted ~ 80 msec). 'Frontal cortex – VPM' correlations revealed negative peak [$C_{xy}(\tau) \sim -0.2$] (see also Fig. 2.8 for details). Time lag was $\tau \sim$ - 3 msec, suggesting that during spindles frontal cortex led the thalamus with 3 msec time delay.

SWD I

Intracortical cross-correlation function was asymmetric over the time (τ) scale (Fig. 4.9A, black line), that distinguished from symmetric function found in anterior spindles and waking EEG. This asymmetry implies that signals in the frontal and occipital channels have different waveforms. The same were present in anterior spindles and waking EEG, but they were less pronounced. In SWD I, the shape of cross-correlation function could be well explained by the presence of different Weir's components in the occipital and frontal channels (**Chapter 3.1**). In particular, the positive peak value $C_{xy}(\tau) = 0.14$ at $\tau = +4$ msec corresponds to the occurrence of the early occipital 'spike 1' and the following frontal 'spike 2' (time delay is 5-6 msec, Figs. 3.3 and 3.4). Similarly, the negative peak value $C_{xy}(\tau) = - 0.21$ at $\tau = +12$ msec corresponds to the presence of the late 'positive transient' in occipital EEG and 'spike 2' in the frontal EEG.

Thalamo-cortical correlations during SWD I (Fig. 4.9B, black lines) differed from that in waking EEG (Fig. 4.9B, grey lines). Cross-correlations function was almost symmetric along the τ-axis and had a sinusoidal waveform (full cycle was ~ 110 msec). 'Frontal cortex – VPM' correlations demonstrate a negative peak [$C_{xy}(\tau) \sim -0.42$] that was two times higher than found in sleep spindles. Time delay between the frontal cortex and the VPM was 5 msec. In terms of distribution of Weir's components in *SWD I*, this negative peak of cross-correlations implies a correspondence between the frontal 'spike 2' and thalamic 'positive transient' that appeared with 7-9 msec time delay (**Chapter 3.1**, Figs. 3.3 and 3.4).

Intracortical 'fronto-occipital' cross-correlations during anterior sleep spindles and during wakefulness did not differ much, but they were remarkably different from that in SWD I. In anterior sleep spindles and SWD I out-of-phase synchronization in both thalamo-cortical pairs were negative and opposite to that during wakefulness, suggesting a polarity inversion. The overall pattern of thalamo-cortical correlations in anterior spindles and in SWD I was the same and remarkably distinguished from what was found in waking EEG. This suggests the existence of at least two different modes of thalamo-cortical activity: one characterizes the state of wakefulness and another one - spindles and SWD. However, the absolute values of thalamo-cortical correlations during SWD I were higher than that in anterior spindles, suggesting that thalamo-cortical coupling during seizures were stronger that during spindles.

DISCUSSION

This Chapter describes similarities and distinctions between two types of sleep spindles and SWD: type I phenomena which are predominant in the frontal EEG, and type II phenomena which show occipital predominance. Earlier, a reciprocal relationship was found between the number of sleep spindles and the number of SWD [van Luijtelaar, 1997]. Results of our time-frequency EEG analysis make doubt about relationship between sleep spindles and SWD.

Type I phenomena are distinguished by amplitude and duration (as compared to anterior sleep spindles, SWD I have higher amplitude and last ten times longer), but type II phenomena (SWD II versus posterior sleep spindles) are distinguished by frequency, yet reveal very little difference in amplitude. This agrees with other studies demonstrating that SWD have higher power and they are longer (mean length 5 s, range 1–30 s), while sleep spindles are short lasting oscillations (0.5–2 s) [Buzsaki et al., 1988; Terrier and Gottesmann, 1978; van Luijtelaar, 1997; Shaw, 2004].

Frequency profile of sleep spindles and SWD

Fourier analysis of sleep spindles and SWD provide information about signal periodicity and other features of the investigated phenomena in EEG. Both *spindle types* show a smooth spectral peak in 10-11 Hz (in fact, it is a plateau extending from 9 to 11 Hz), suggesting a considerable variability of intra-spindle frequencies. Unfortunately it is not possible to detect any dynamic changes in intra-spindle frequencies with the current Fourier method. Time-frequency EEG analyses (e.g. wavelet transform, multitaper or others that provide good resolution in time domain) will be particularly helpful in investigating intrinsic frequency dynamics in sleep spindles and SWD.

As known, the power spectrum of a periodic sine wave signal has only the fundamental (the central) and sub-harmonics (reciprocal periods with the lower frequencies) peaks. Power spectrum of sleep spindles are characterized by fundamental and sub-harmonic peaks, therefore they might roughly correspond to a periodic signal. SWD I in the frontal EEG are characterized by several distinct signatures: (1) a sharp ~ 9-10 Hz peak that corresponds to mean frequency of seizure rhythm, (2) a harmonic component in beta band and (3) a very powerful gamma frequency band. These features are considered as hallmarks of high-amplitude spikes in seizure sequences.

Power spectrum of quasi-periodic EEG signal with repetitive spikes is known to show a narrow fundamental peak and additional peaks in multiple (harmonic) frequencies [Bullock et al., 2003]. Based on the structure of their spectrograms, we consider SWD I and II as quasi-periodic 'spiky' EEG phenomena, but sleep spindles as periodic ones. Fairly sharp spectral peaks in SWD I and SWD II suggest that both SWD types are periodic 'good' rhythms in terms of Bullock et al. (2003), who found that "good" rhythms have narrow peaks in power spectra (with frequency modulation of less than 5%).

None of the EEG phenomena contain a single rhythm, but all of them are rather complex signals consisting of multiple oscillations at various frequencies; the peaks in the spectrograms correspond to the most strong and periodic oscillations.

Sleep spindles (anterior and posterior) are distinguished from SWD I by (1) the presence of smooth ~ 9-11 Hz peak, suggesting a larger variability in intra-spindle frequencies as compared to relatively stable seizure rhythm, (2) high power in delta band and low power in beta and gamma bands. Therefore, we have found a considerable contribution of sub-harmonic frequencies (delta band) in both spindle types, rather than SWD I, which are mostly composed of harmonic frequencies (in double frequencies, i.e. beta) and high-frequency components (gamma).

We have found almost a two-fold difference in total EEG power between SWD I and anterior sleep spindles, this is in agreement with Mackenzie et al. (2004), who also has found that pathological oscillations (absence seizures or 'absence spindles') demonstrate a higher EEG power than physiological oscillations (sleep spindles). These authors suggest that this is because more cells are participating in the epileptic activity as compared to normal spindling. Another interesting finding that agrees with Mackenzie et al. (2004) observation is that EEG power of sleep spindles in the thalamus is not congruent to that in the neocortex. Indeed, *"for a structure to generate a rhythm it need not conceptually follow that it contains high levels of power at the rhythm frequency"* [p. 103, Mackenzie et al., 2004].

Our data suggest that pre-spindle epochs and subsequent sleep spindles contain relatively high delta frequency component in cortex and thalamus, indicating that (1) the cortex and thalamus exhibit delta activity simultaneously; (2) this delta does not change in transitions from pre-spindle activity towards sleep spindles. During sleep spindles, besides high delta and theta, the thalamus sustain surprisingly low alpha activity as compared to relatively high alpha in the frontal cortex. Frequency profiles of SWD I (0.5-1.5 sec from the onset) in the frontal cortex and the thalamus are similar: frontal and thalamic spectra are very congruent across delta-theta-alpha frequencies, suggesting that the frontal cortex and the thalamus operate at the same frequency mode. A narrow spectral peak in 8-9 Hz implies the presence of a clear dominating rhythm in the cortex and thalamus.

The power of the low frequency components (1-4.5 Hz) in sleep spindles is nearly as high as the power of the fundamental rhythm 9-13.5 Hz (Fig. 4.5). Also in preSWD, delta component was relatively high, but delta was low in subsequent SWD I. This may imply a role of slow activity in shaping sleep spindles, but not in SWD. Anterior sleep spindles combine some EEG features characteristic either for precursors of SWD (relatively high power in delta frequencies) and for SWD (powerful alpha band). In agreement with others [Pinault et al., 2001; Pinault, 2003], our data suggest that sleep spindles themselves could not trigger SWD (also, EEG features of sleep spindles are distinguished from that in the 'real triggers', i.e., seizure precursors). On the other hand, sleep spindles and SWD show somewhat similar thalamo-cortical cross-correlation functions, suggesting that both spindles and SWD can appear in EEG as a manifestation of synchronization processes taking place in the thalamo-cortical circuit during low vigilance state. We cannot affirm a direct correspondence between spindles and SWD, but it seems likely that spindles are interconnected with SWD on the level of thalamo-cortical network synchronization processes. Physiological oscillations (sleep spindles) appear when network synchrony is normal and pathological oscillations (SWD) may appear as a result of too strong synchrony in neuronal networks (hypersynchronization).

Frequency profiles of SWD I and SWD II – new insights

We found that the frequency content of SWD I has changed at seizure end, so that SWD I bear a striking similarity with SWD II. Based on that, we conclude that the frontal cortex (or other structures associated with the frontal cortex) may be endowed with the same unknown neuronal mechanisms providing a functional link between the two types of SWD. On the other hand, in the occipital EEG, SWD I do not resemble SWD II (neither at the beginning nor at the end). This confirms our observations made in Chapters 3.1 and 3.2 that SWD I and SWD II are independent phenomena. This is in agreement with the outcomes of genetic studies in WAG/Rij rats, since different chromosomal locations were found for SWD I and SWD II [Gauthier et al., 2005], of enrichment studies: SWD II were more sensitive for housing conditions than SWD I [Schridde and van Luijtelaar, 2004; 2005] and of pharmacological studies in which SWD I and SWD II showed different sensitivity to dopamine antagonists and agonists [Midzianovskaia et al., 2001].

Enlargement of delta activity in the occipital cortex may correspond to the elevation of the wave component during SWD I: the wave is known to have a maximum at the end of SWD I [Midzianovskaia et al., 2001]. We indicate here that the frequency content of the frontal and occipital EEG undergoes different modifications as seizure progresses. In particular, the frontal cortex shows a decrease in power in alpha and beta frequencies from the beginning to the end of SWD I, at the same time, occipital cortex shows an increase of delta (alpha and beta components do not change). This contradicts to Midzianovskaia et al. (2001) who found that dynamic changes in amplitude-frequency pattern of SWD I are the same in all cortical areas: in all cortical sites, amplitude of the wave-component is increased as seizure progress, also the spike-component is decreased all over the cortex. We tend to disagree with these data by showing that frontal and occipital areas specific in EEG properties from the beginning of a seizure to its end. In contrary to what was found in the frontal cortex, occipital cortex does not demonstrate dynamic changes in alpha band (10 Hz spikes provide the largest contribution in power content of this band) and in beta band (this band contains a harmonic of spike-component). Probably, changes in occipital EEG channel are too delicate and power spectrum analysis is not sufficient (sensitive) to investigate these changes.

We and others have found that the last epoch of SWD I are characterized by a low frequency and a prevalence of the wave component (Chapter 3.1, see also Drinkenburg et al., 1993; Midzianovskaia et al., 2001). As compared to fronto-parital cortical areas, electrical seizure activity in occipital cortex is mild: it shows less total power and a less regular EEG pattern. It seems that the occipital cortex plays a passive role at the initial state of SWD I: seizure activity may passively spread to occipital cortex from the primary epileptic source (the parietal area). We assume that reinforcement of occipital delta at the seizure end might govern the cession of SWD I, yet by some unknown mechanism. A role of EEG delta activity in finishing spike-wave seizures is indirectly conformed in humans EEG studies. The pure regular 3 Hz SWD are present during somnolence and during stage 1 of non-REM sleep, but EEG seizure waveform changes as sleep deepens. SWD become shorter and irregular in stage 2 and only fragments of SWD are present during stages 3 and 4 (sometimes seizures are interrupted by short periods of background activity) [Ross et al., 1966; Sato et al., 1973].

Here we propose a neurobiological correlates of 9-10 Hz SWD I expressed in the fronto-parietal cortex and 6-7 Hz SWD II localized in the occipital cortex. As known, rats exhibit two main types of rhythmical electrical activities under physiological circumstances [Semba and Komisaruk, 1984]: alpha waves (about 9 Hz) originating from the thalamo-cortical system [Nicolelis et al., 1995; Nicolelis and Fanselow, 2002] and theta waves (about 7 Hz) originating from septo-hippocampal system [Semba, 1980; Semba and Komisaruk, 1984]. These rhythms are closely linked with two different movements of vibrissae [Semba, 1980]: alpha waves trigger small amplitude movements (a fine tremor) and theta waves are responsible for large amplitude movements which are used in exploratory sniffing behavior. Perhaps, SWD I represent a modified (hypersynchronous) thalamocortical alpha (9 Hz) rhythmic activity and SWD II is modified septohippocampal theta rhythm (7 Hz).

For SWD I, this hypothesis has been confirmed by a group of Nicolelis. They showed that 'whisking twitching' in rats is accompanied by robust, coherent oscillations with a frequency of 7–12 Hz or 'somatosensory rhythm' that takes place in the vibrissal areas of the brainstem, thalamus and SmI [Nicolelis et al., 1995; Nicolelis and Fanselow, 2002]. Furthermore, Wiest and Nicolelis (2003) hypothesized that in rodent strains with a genetic predisposition to absence epilepsy, 7–12 Hz rhythmic activity might undergo some transformation and give rise to SWD, irrespective of whether it occurs during drowsiness, attentive wakefulness or during light non-REM sleep. This, once again, makes it doubtful that sleep spindles give rise to SWD I. We found that thalamo-cortical mechanisms do not play a role in SWD II, yet no evidence has been found on the putative role of septo-hippocampal neuronal networks in developing of SWD II.

Altogether our results show that the power-frequency content of SWD I at the end has been changed so that it became similar to that in SWD II, however, SWD II do not seem to be a 'residual' spike-wave seizure activity that is localized in the occipital cortex. SWD I invade fronto-parieto-thalamic(VPM-RTN) areas with limited propagation to the occipital cortex, whereas epileptogenic processes in the occipital cortex (or functionally related structures, other than cortico-thalamic circuit, e.g., septo-hippocampal structures) might underlie the occurrence of SWD II. Unfortunately, we have too little data to answer this question. In order to disclose the nature of SWD II, one needs to explore the strength and (in)dependency of the epileptogenic processes underlying spike-wave seizures in the frontal and occipital cortical areas.

4.2. Simulation of sleep spindles and spike and wave discharges using a novel method for the calculation of field potentials in rats [*]

ABSTRACT

We suggest a new method for calculation of extracellular field potentials generated by a large population of pyramidal cells (PCs), using a single PC compartmental model. This model assumes time difference between firing activity of cortical PC with regard to the degree of neuronal synchronization. The temporal variability in cell firing is described by a Gaussian distribution, the width of which defines the degree of synchronization/desynchronization. In addition, the suggested method allows for certain spatial spread of PCs in the population along longitudinal axis of the PCs.

The method is applied for simulating cortical local field potentials characteristic for sleep spindle oscillations and for epileptic spike-wave discharges (SWD). The current model is used to disclose synaptic processes that underlay occurrence of epileptic discharges. When synchronization between PCs is weak, rhythmic stimulation of the thalamus evoke fluctuations of cortical field potentials with spindle-like shape. When synchronization between PCs is strong, cortical field potentials take a shape of SWD, with clearly expressed spikes and waves components.

This suggests that changes of synchronization of cell firing in large population of pyramidal cells influence the shape of field potential. An increase of synchronization between PCs may underlay occurrence of SWD. The following synaptic processes underlay epileptiform elements in SWD (type I): the *spike* component ('Spike 2') is excitatory response of PCs to via AMPA-ergic input from the thalamus. The *positive transient* is a manifestation of AMPA-ergic mutual excitation of pyramidal cells. The *wave* component reflects the strength of GABA-ergic synaptic interactions between pyramidal cells and interneurons (feed-forward inhibition).

INTRODUCTION

In order to better understand neuronal mechanisms underlying occurrence of sleep spindles and SWD, we constricted a computational model that simulates local field potentials during these two EEG events [Sargsyan et al., 2007]. Local field potentials (that corresponds to our EEG) are generated by electrical currents flowing through neuronal membranes and they may cause distributed current 'sources' and 'sinks' [Lopes da Silva, 1996]. There are several techniques for computing of the extracellular field potentials and among them is a compartment-volume-conduction model that considers a population of neurons in which each neuron generates intracellular currents which are similar to other cells. If neurons in a population act simultaneously, field potential can be calculated based on distribution of the intracellular current produced by one model cell. The assumption about strict simultaneity of firing activity in neuronal population is often not eligible; therefore a degree of synchronization of neurons should be taken into account. In the current neuronal model we substantially modified the compartment-volume-conduction approach by adding an option to change degree of synchronization in a population of pyramidal neurons. The new algorithm takes into account also a disperse spatial organization of neocortical neurons and timing of pyramidal cells' firing.

We constructed then a simple model of cortical pyramidal cells (PC) population that is based on experimentally observed single unit activity recordings in WAG/Rij rats (Fig. 1.2 from Kandel and Buzsaki [1997]). As known, SWD are associated with synchronization in time firing of cortical neurons: a robust firing activity is recorded during the spike component and silence during the wave component, while the sleep spindles are associated with much less synchrony [Inoue et al., 1993; Kandel and Buzsaki, 1997; Sargsyan et al., 2007].

METHODS

The modeling was done under fundamental assumption that SWD are transformed sleep spindles (a cortico-reticular theory, see **Chapters 1.2** and **1.4**). The neuronal model (Fig. 4.10A) consists of cortical pyramidal cells and two types of cortical interneurons involved in feed-forward and recurrent inhibition. Afferents from thalamocortical cells (thalamic inputs) make excitatory synaptic contacts of AMPA and NMDA types on apical dendrites of pyramidal cells and of AMPA type on interneurons involved in feed-forward inhibition loop. These interneurons, in turn, make inhibitory synaptic contacts of GABAa and GABAb types on apical dendrites of

[*] Published in:
Sargsyan A, Sitnikova E, Melkonyan A, Mkrtchian H, van Luijtelaar G. Simulation of sleep spindles and spike and wave discharges using a novel method for the calculation of field potentials in rats. J Neurosci Methods, 2007; 164(1): 161-178

pyramidal cells, more proximally relative to the thalamic inputs. The axons of pyramidal cells make lateral excitatory contacts of AMPA and NMDA types with other pyramidal cells (on basal dendrites) and of AMPA type with interneurons involved in recurrent inhibition loops. These interneurons make inhibitory contacts of GABAa type on somata of pyramidal cells to perform recurrent inhibition. Details of the pyramidal cells and interneuron parameters (including their geometry, electrotonic parameters, parameters of synaptic conductances and parameters and equations for active ionic conductances) used for current simulations can be found in Sargsyan et al. (2001).

The number of pyramidal cells is much higher as compared to interneurons; also the location and orientation of the interneurons within the layers is much less regular. Therefore pyramidal cells have greater propensities to contribute to the large field potentials recorded from the surface of the cortex, while the direct contribution of interneuronal currents to the model field potential may be neglected. Field potentials are calculated assuming that a large number of identical and similarly oriented pyramidal cells uniformly occupy a cylindrical slab of given radius (Fig. 4.10B).

It is important that one of the main factors that strongly affects the shape of transmembrane currents, and hence the shape of the field potential, is the distribution of active ionic conductances along the dendritic compartments. For this simulation, only two types of intrinsic ionic currents are included into pyramidal cell model: fast sodium current, I_{Na}, and potassium delayed rectifier, $I_{K(DR)}$. Equations and parameters used for these currents are the same as previously used [Traub et al., 1991], but the distribution of densities of ionic conductances among compartments is assumed to have a normal (Gaussian) shape, with maximum in soma and zero values in distal compartments. The degree of synchronization/desynchronization is defined by the width of Gauss function i.e., by the parameter σ: The larger the σ, the smaller the degree of synchronization, and vise versa.

In all model experiments the thalamic inputs to pyramidal cells are stimulated with the same constant frequency of 10 Hz. This frequency is chosen because sleep spindles in rats have a frequency of 9–11 Hz. The strength of stimulation, which is regulated by the synaptic weight of the thalamic synaptic input to pyramidal cells, is chosen as such that a single stimulus applied to the thalamic input evokes an action potential in the pyramidal cell. This is done to activate the mechanisms of recurrent inhibition through a recurrent inhibition interneuron and mutual excitation of pyramidal cells in the model. The same thalamic stimuli evoke also action potentials in the feed-forward inhibition interneuron, which further inhibits the dendrites of pyramidal cells. The strength of excitatory connections between pyramidal cells is chosen strong enough so that the currents of these synapses have notable influence on the field potentials, but not as strong to produce action potentials in pyramidal cells. This is done to avoid permanent recurrent spike generation in the pyramidal cells.

The simulations were performed using the GENESIS simulator.

RESULTS AND DISCUSSION

The main series of model experiments were aimed to reveal how the shape of population field potentials depends on the degree of synchronization of the PC activity in the population. The modeled field potentials are calculated for σ values linearly changing from 0.003 to 0.029 s (Fig. 4.10C). The field potentials are calculated at: 250 μm depth (that corresponds to the middle of the apical dendrite of pyramidal cell). For small values of $\sigma f(\tau,\sigma)$ is narrow, which means that the activity of pyramidal cells in the population is highly synchronized. In this case the field potentials have a clearly expressed large sharp component and are similar in shape with intracortically recorded SWD. With increase of σ, i.e., with decrease of degree of synchronization of pyramidal cells in the population, the sharp peaks in the field potential gradually smooth, the components, which are clearly distinguishable at low σ, merge, and the field potential shows a sine wave a typical waveform of sleep spindles.

The field potential reveals a characteristic spindle waveform for $\sigma = 0.02$ s, suggesting that the model acts in 'spindle mode' and for $\sigma = 0.007$ s field potential has the spike-wave waveform ('SWD mode'). In the further investigations of the strengths synaptic connections we used fixed values for weak ($\sigma = 0.02$ s 'spindle' mode) and strong ($\sigma = 0.007$ s 'SWD mode') synchronization (Fig. 4.11). In order to identify which synaptic currents are responsible for which components of the field potential in the model, we varied the strengths of synaptic connections.

In SWD mode (Fig. 4.11A, left traces, dashed line), the reduction of AMPA weight of thalamic inputs to pyramidal cells results in a decrease of the amplitude of sharp negative deflection (the *spike* component) and increase of the amplitude of subsequent positive deflection of the field potential. In spindle mode (Fig. 4.11A, right traces, dashed line), a decrease in AMPA weight results in a slight positive shift of the entire field potential. In both cases, 1.3 times increase in AMPA weight does not result in significant changes in the shapes of field potentials (greater increase in AMPA weight is impossible since it would change the firing properties of pyramidal cells from single spike mode to bursting mode).

In SWD mode (Fig. 4.11B, left traces, dashed line), changes in feed-forward inhibition interneurons to pyramidal cells GABA synaptic weight has little effect on the amplitude of the *spike* component, but a pronounced

influence on the *wave* component: reduction of GABA weight results in negative shift in the *wave* component, while an increase has an opposite effect (dotted line). In spindle mode, (Fig. 4.11B, right traces), reduction of GABA weight results in a decrease of the amplitude of positive deflections of field potential and overall negative shift of the field potential (dashed line), and vice versa (dotted line).

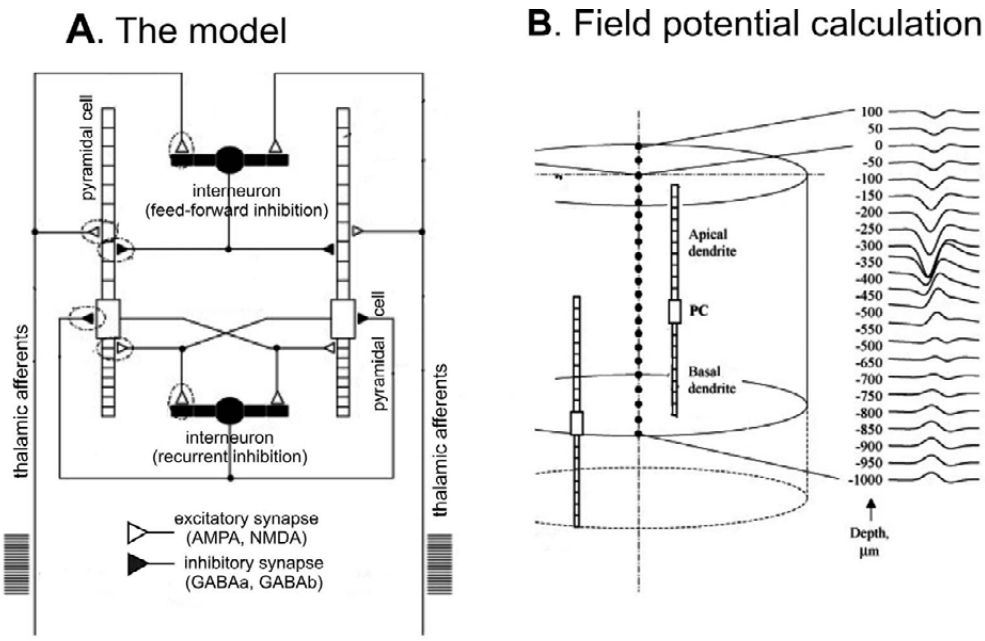

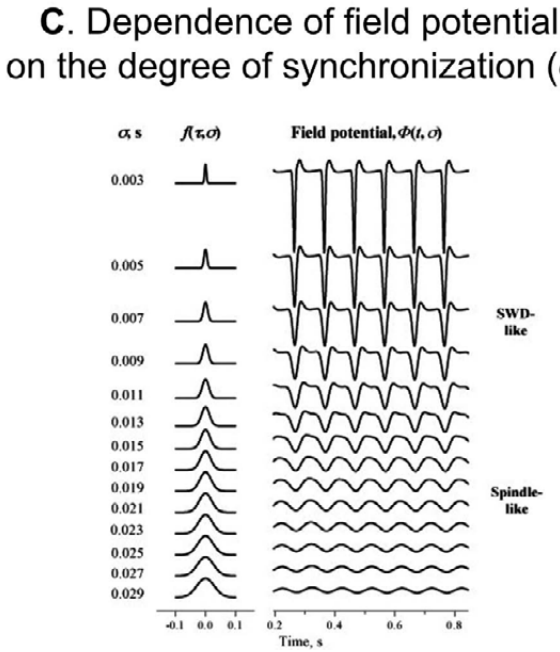

Figure 4.10. Illustration of neuronal model of cortical field potentials during sleep spindles and SWD. **A**. The model includes two types of pyramidal cell (PC, shown with its 19 compartments) and two types of interneurons: feed-forward inhibition interneuron (FFI) and recurrent inhibition interneuron (RI). Model inputs are the impulses applied to thalamic inputs. **B**. Activated pyramidal cells (PC) are assumed to occupy a cylindrical slab of radius R, such that the long axis of each pyramidal cell is parallel to the vertical (Z) axis of the cylinder. Each compartment of PC occupies a fixed depth in the cylinder. Field responses are calculated for a track along the Z-axis (in the points indicated by filled circles) from trans-membrane currents of modeled PCs. **C**. Dependence of field potential in response to rhythmic ~ 10 Hz thalamic input on the value of parameter σ (degree of synchronization). The left column shows the values of σ, the Gauss functions for corresponding σ values are shown in the middle column. The right column shows corresponding field potentials calculated at −250 μm depth (middle of the apical dendrite) relative to the upper surface of the cylinder. Note that the time scale for $f(\tau,\sigma)$ and for $\Phi(t,\sigma)$ is the same.

In SWD mode (Fig. 4.11C, left traces, dashed line), decreasing the strength of AMPA-ergic synaptic contacts between pyramidal cells results in an increase of the amplitude of the negative *spike* component and in a decrease of the amplitude of subsequent positive deflection, while increasing the weight of this synapse has opposite effects (dotted line). In spindle mode (Fig. 4.11C, right traces, dashed line), a reduction of the strength AMPA-ergic synaptic contacts between pyramidal cells increases the negative wave of the field potential, while an

increase diminishes the negative wave, augments the positive wave, and causes a phase shift of the field potential to the left (dotted line).

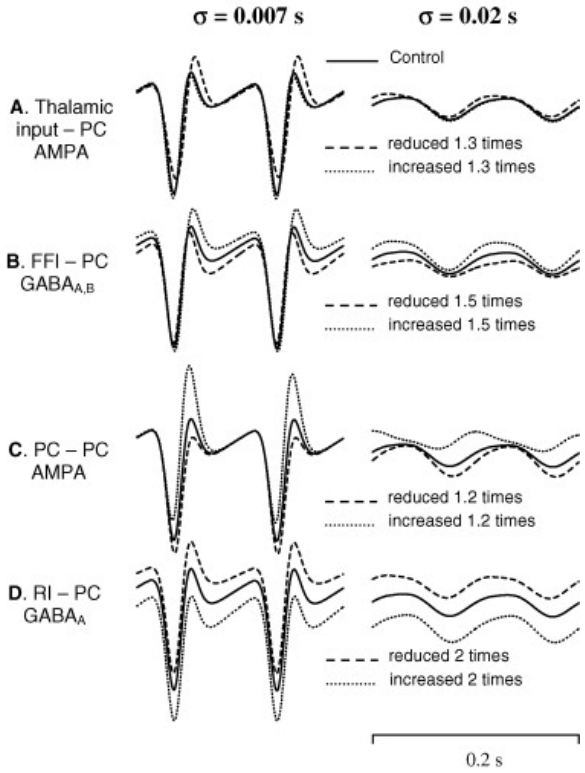

Figure 4.11 Influence of variations in weights of synapses located on the pyramidal cells (PC) on the shape of field potential at two σ values. The weights of AMPA-type synapses made on a PC by thalamic input (A) and by another PC (C), and of GABA-type synapses from interneurons involved in feed-forward inhibition (FFI) (B) and recurrent inhibition, RI (D) separately were reduced (dashed lines) and increased (dotted lines) with respect to their basic values ("control", straight lines). In most cases, the change in the strength of a single synapse influences all components of the field potential (positivity upward).

The effect of AMPA-ergic input from the thalamus to pyramidal cell (Fig. 4.11A) were distinguished from AMPA-ergic synaptic contacts between pyramidal cells (Fig. 4.11C). In particular, the component generated by thalamic input to pyramidal cell via AMPA synapses is negative and it is the main contributor to the *spike* component; while the component generated by AMPA-ergic contacts between pyramidal cells is positive and it contributes mostly to the *positive transient* which was followed by the *spike*.

Table 4.2 Changes in AMPA and GABA synaptic inputs influence the waveform of sleep spindles and SWD.

Synaptic input			**Changes in EEG waveform**	
			SWD mode	**Spindle mode**
AMPA (Fig. 4.7A)	thalamus → pyramidal cells	reduction	the *spike* is decreased the *positive transient* is increased	very little increase of the positive deflection
		increase	no significant changes	no significant changes
AMPA (Fig. 4.7C)	pyramidal cell ↔ pyramidal cell	reduction	the *spike* is slightly increased the *positive transient* is profoundly increased	negative deflection is increased (amplitude of field potential is increased)
		increase	the *wave* is increased (negative shift of field potential)	the negative deflection is disappeared; the positive deflection is increased (a phase shift of field potential)
GABAa,b (Fig 4.7B)	feed-forward inhibition interneurons → pyramidal cells	reduction	the *wave* is increased (the *spike* did not change)	the positive deflection is decreased (amplitude of field potential is decreased)
		increase	the *wave* is decreased; the *positive transient* is increased (the *spike* did not change)	the positive deflection is increased (the amplitude of field potential is increased)
GABAa (Fig 4.7D)	recurrent inhibition interneurons →	reduction	positive shift of the entire field potential	positive shift of the entire field potential

pyramidal cells	increase	negative shift of the entire field potential	negative shift of the entire field potential

In both SWD and spindle modes, decreasing and increasing the synaptic strength of $GABA_A$-ergic contacts between recurrent-inhibition interneurons and pyramidal cells (Fig. 4.11C) resulted, correspondingly, in positive and negative shift of the entire field potential, but the overall waveform of field potential did not change.

It is important that when synchronization parameter of the model (σ) is fixed and the model stays either in spindle or SWD mode, no changes in synaptic input strength can elicit a transformation from spindle to SWD and *vice versa*: the waveform of field potentials does not change in general, but it is underwent by moderate modifications. The model helps to assess the role of AMPA and GABA in shaping of sleep spindles and SWD (Table 4.2). Changes in the strength of AMPA-ergic synaptic contacts between pyramidal cells caused the most profound changes in the waveform of SWD and sleep spindles, whereas AMPA-ergic inputs from thalamus (to pyramidal cells) showed very little effect on the waveform of both SWD and sleep spindles. GABAa,b-ergic synaptic inputs from feed-forward inhibition interneurons to pyramidal cells predetermined the amplitude of both SWD and sleep spindles (the larger the inhibition, the larger the amplitude), but GABAa-ergic inputs from recurrent-inhibition interneurons to pyramidal cells do not influence the waveform of both SWD and sleep spindles (they only cause uniform positive/negative shift of field potential against baseline).

In all, we have shown that the shape of field potential substantially depends on how well the discharges of pyramidal cells in the population are synchronized in time, even when the trans-membrane currents in pyramidal cells are the same. When considering sleep spindles and SWD, the assumption about the invariability of trans-membrane currents in these two cases is a significant simplification. Whatever the mechanisms leading to the increase or decrease of synchrony in the population are, they, in one way or another, should affect the shape and amplitude of certain components of membrane currents of individual neurons. The differences in the EEG waveform of the oscillations (SWD and sleep spindle) may either be determined by differences in the composition of trans-membrane currents in the two different states of network activity, or result from the effects of spatiotemporal summation of trans-membrane currents under the conditions of high (as in SWD state) and low (as in sleep spindle state) degrees of synchronization of cortical neuronal activity.

CONCLUSIONS

The current neuronal model simulates local field potentials during sleep spindle and SWD. In this model, based on synaptic interactions between different types of cortical neurons we extended a compartment-volume-conduction approach of neuronal modeling by adding a new option to change a degree of synchronization in a population of pyramidal neurons.

The following synaptic processes that are responsible for the occurrence of epileptiform elements in SWD are disclosed with the current model:

(1) The main contributor of the negative spike component (‘Spike 2’ in terms of Weir) is generated by thalamic input to pyramidal cell via AMPA synapses.
(2) AMPA-ergic contacts between pyramidal cells generate positive fluctuation of field potential corresponding to the positive transient.
(3) GABA-ergic synaptic input to pyramidal cells, e.g., feed-forward inhibition from interneurons, plays the major role in shaping of the wave component.

4.3. Sleep spindles and spike-wave discharges in EEG: their generic features and distinctions disclosed with continuous wavelet transform *

ABSTRACT

Epileptic spike-wave discharges (SWD) appear in the electroencephalogram (EEG) during absence seizures. A relationship between SWD and normal sleep spindles is still not yet confirmed. This study compares time-frequency parameters of SWD and sleep spindles in WAG/Rij rat model of absence epilepsy using Fourier and continuous wavelet transformation. Wavelet analysis was performed in non-segmented full-length EEG. Specific wavelet-based algorithm is developed for the automatic identification of spindle events and SWD in EEG that required careful selection of (1) the optimal wavelet template and (2) adjustment of the optimal amplitude and frequency parameters.

None of standard wavelet templates provided precise identification of all sleep spindles and SWD in one dataset and different wavelet templates were necessary in order to accomplish this task. SWD are identified in EEG with high probability using standard Morlet-wavelet, but sleep spindles can be identified using two types of customized adoptive 'spindle wavelets'. Wavelet analysis revealed that (1) SWD belong to one family, but spindles comprise two families. (2) Almost 100% of SWD (but only 50-60% of spindles) were extracted using Morlet-based wavelet transform. (3) 82-91 % of sleep spindles were selected using adoptive 'spindle wavelet 1' (template's peak frequency ~12.2 Hz). The remaining spindles – with 'spindle wavelet 2' (peak frequency ~ 20-25 Hz). (4) Sleep spindles and SWD are detected by elevation of wavelet energy in different frequencies: SWD – in 30-50 Hz band, sleep spindles – in 7-14 Hz. It is concluded that the EEG patterns of sleep spindles and SWD are not comparable.

INTRODUCTION

Sleep spindles are abundantly preset in the electroencephalogram (EEG) during drowsiness and non-REM sleep in all mammalian species and in humans [reviewed in Jankel and Niedermeyer, 1985; De Gennaro and Ferrara, 2003; De Gennaro et al., 2005]. The name 'spindle' refers to a characteristic EEG waveform: sleep spindles are defined as "*a group of rhythmic waves characterized by progressively increasing then decreasing amplitude*" (IFSECN, 1974). Occurrence of sleep spindles in EEG is associated with loss of perceptual awareness and it is remarkable that this 'low vigilance' state is also favorable for the occurrence of absence epilepsy (e.g., a non-convulsive generalized epilepsy of unknown etiology). Typical absence seizures are characterized by bilaterally symmetric 3-5 Hz spike-waves complexes in EEG [Panayiotopoulos, 1997]. Some inbred rat strains, such as Genetic Absence Epilepsy Rats from Strasbourg (GAERS, Vergnes, 1987) and Wistar Albino Glaxo from Rijswijk (WAG/Rij, [van Luijtelaar and Coenen, 1986]), have a genetic predisposition to absence epilepsy and exhibit spike-wave seizure activity in their EEG [Coenen and van Luijtelaar, 2003]. Spike-wave discharges (SWD) in rat models and spike-and-wave complexes in humans are similar in respect to their waveform, duration (1 to 30 sec, mean 5 sec) and frequency dynamics [Midzianovskaia et al., 2001; Bosnyakova et al., 2007; Sitnikova and van Luijtelaar, 2007].

A generic relationship between sleep spindles and SWD has long been proposed and confirmed in feline penicillin model [Gloor, 1968; Kostopoulos, 2000]. In this model spike-wave seizures were induced pharmacologically by injections of penicillin. Previously, the EEG structure of sleep spindles and SWD in rats was investigated with the aid of traditional spectral analysis (fast Fourier transform) and this method yielded rather ambiguous results. As compared to sleep spindles, SWD displayed a higher total power and more beta activity (due to the presence of a strong harmonic component). In spite of that, both SWD and spindles were regarded as rather similar EEG phenomena considering the same peak frequency [Drinkenburg et al., 1993; Mackenzie et al., 2004][†]. In addition to that, EEG of WAG/Rij rats showed 'spiky' intermediate transients that were identified as not fully formed SWD [Drinkenburg et al., 1993]. Recent studies of spontaneous spike-wave seizures in genetic

---

[*] submitted to the Journal of Neuroscience Methods, 2008
Sitnikova E, Hramov AE, Koronovsky AA, van Luijtelaar G. Sleep spindles and spike-wave discharges in EEG: their generic features, similarities and distinctions disclosed with Fourier transform and continuous wavelet analysis

[†] Interestingly, different authors gave different names to 'spike-wave' discharges. Mackenzie et al. (2004) used the term 'absence *spindles*', Kandel and Buzsáki (1997) called them HVS, 'high voltage spike-wave *spindles*', thus emphasizing close relationship between SWD and spindles. The name 'spindles' does not seem appropriate for absence-related EEG phenomena, because absence epileptic discharges are asymmetric, have a clear large amplitude spike and a slow wave components, moreover, they do not have the for spindles characteristic waxing-waning morphology.

animal model (GEARS) entertained serious doubts about the pro-epileptogenic nature of spindle oscillations [Pinault et al., 2001; Pinault, 2006]. Our investigation WAG/Rij rats suggest that sleep spindles and SWD are rather independent physiological phenomena [van Luijtelaar and Sitnikova, 2006]. In order to better understand a putative functional relationship between these two kinds of rhythmic oscillations, in the current study we compare electroencephalographic features of SWD and sleep spindles.

Sleep spindles are abundant during non-REM sleep, also SWD preferably appear during passive awaking state and during transition between wakefulness and sleep [in WAG/Rij rats: van Luijtelaar and Coenen, 1988; Drinkenburg et al., 1991; in humans: Halasz, 1991; Halász et al., 2002]. SWD and sleep spindles show amplitude maximum in the frontal cortex [van Luijtelaar, Coenen, 1986; Midzianovskaia et al., 2001; Terrier and Gottesmann, 1978] and both of them are dynamic oscillations. This means that their frequency changes over time and restricts applicability of traditional frequency-domain measures (such as Fast Fourier Transform), in which time-domain information is lost. In wavelet decomposition, EEG signal can be represented in two-dimensional time–frequency domain, in which signal power changes as a function of time and frequency simultaneously [Daubechies, 1992; Kaiser, 1994; Torresani, 1995; Koronovskii and Hramov, 2003]. Wavelet transform employs wave-like scalable function (wavelet basis) that is well localized in both time and frequency. By selecting an optimal wavelet basis, we intended to retrieve earmarks of sleep spindles and SWD that have not been previously detected.

We chose continuous wavelet transform (CWT) as an appropriate method for time-frequency analysis of EEG signal. A lack of the requirement of stationarity is an advantage of using the CWT for the characterization of short non-stationary events in EEG, such as episodes of spindle and spike-wave activity, in which the signal-to-noise ratio is low [Jobert et al., 1994; van Vugt et al., 2007]. The present study also address the problem of individual variability and irregularity of EEG pattern of SWD and sleep spindle events that would be solved by selecting an optimal template wavelet functions. For the technical point of view, our study provides a clue for the selective identification, classification and statistical description of several phenomena in raw EEG.

METHODS

Animals, EEG data acquisition and description of EEG patterns

EEG activity was recorded in nine adult WAG/Rij male rats (11-12 months old, 310-345 g body weight). A recording electrode was implanted epidurally at the surface of the frontal cortex (amplitude maximum of the investigated events; coordinates: AP +2 mm and L 2.5 mm relatively to the bregma). Ground and reference electrodes were placed over the two symmetrical sides of the cerebellum. EEG recordings were made in free behavior during dark period of the light-dark cycle continuously for 5-7 hours. EEG signals were fed into a multi-channel differential amplifier via a swivel contact, band-pass filtered between 0.5-100 Hz, digitized with 1024 samples/second/per channel (CODAS software).

Sleep spindles were first selected visually in accordance to guidelines for clinical electroencephalography [Rechtschaffen and Kales, 1968; IFSECN, 1974] by taking into account specificity of sleep spindle activity in rats [Terrier and Gottesmann, 1978; Steriade et al. 1993; van Luijtelaar, 1997]. Sleep spindles in EEG were recognized as a sequence of 8-14 Hz waves with minimal duration of 0.4 sec (e.g., at least four wave cycles in a sequence). Sleep spindles had waxing-waning morphology and were characterized by twofold increase in amplitude as compared to EEG background. In order to facilitate expert's estimations, EEG records were additionally band-pass filtered 5-15 Hz. Visual spindle detections were double checked and verified by another expert.

SWD appeared in the EEG as a sequence of repetitive high-voltage negative spikes and negative waves that lasted longer than 1 sec [van Luijtelaar and Coenen, 1986; Midzianovskaia et al., 2001]. SWD were first detected automatically with EEG slope method (Dr. PLC van den Broek, NICI-Biological Psychology, Radboud University Nijmegen, the Netherlands) which provided about 90% of correct detections and than verified by two experts.

Power spectrum analysis

Power spectrum EEG analysis was performed in all nine rats. Hanning windowed Fast Fourier transform (FFT) was applied to compare frequency-domain features of sleep spindles and SWD (with 0.5 Hz resolution). Statistical analysis was performed in 1 sec epochs (30-40 SWD per subject and in 50 sleep spindles per subject) selected in EEG during light non-REM sleep. If spindle duration was shorter than 1 sec, the starting point of time-window was put so that the entire spindle was in the middle of the epoch. Power spectra were averaged per event type and per animal. The following quantitative parameters were computed and statistically compared: (i) duration (ii) frequency, (iii) EEG power over the characteristic frequency bands: 1-4.5 Hz (delta), 5-8.5 Hz (theta), 9-13.5 Hz (alpha), 14-31.5 Hz (beta), 32-59.5 Hz (gamma1) and 60-100 Hz (gamma2).

Continuous wavelet transform. General aspects of automatic detection of SWD and sleep spindles in EEG [*]

Step 1. Continuous wavelet analysis was carried out in five out of nine rats, in these subjects all episodes of SWD and all episodes of sleep spindles were marked in the full-length EEG (5-7 hours).

The continuous wavelet transform, the CWT, $W(s,\tau)$, was computed as a result of convolving of EEG signal, $x(t)$, with wavelet basis function, $\phi_{s,\tau}$ (Eq. 1, '*' denotes the complex conjugation).

$$W(s,\tau) = \int_{-\infty}^{+\infty} x(t)\varphi^*_{s,\tau}(t)dt \qquad (1)$$

$$\varphi_{s,\tau}(t) = \frac{1}{\sqrt{s}}\varphi_0\left(\frac{t-\tau}{s}\right) \qquad (2)$$

where s is the time scale and τ is the time shift of wavelet transform. Frequently, the parameter s in this formula is substituted by a reciprocal parameter f_s so that $f_s = 1/s$

Wavelet basis function, $\phi_{s,\tau}$ in Eq. 2, belongs to a family of prototype 'mother' wavelet, ϕ_0. The 'mother' wavelet can be either real or complex and should satisfy several conditions, such as continuity, zero mean amplitude, and finite or near finite duration [Chui, 1992; Koronovskii and Hramov, 2003].

Time (t) and time scales (s) (or corresponding frequencies, f_s) in wavelet basis function are related through the uncertainty principle, which states that it is impossible to extract the exact frequency at the exact time when this frequency occurs in a signal. This implies that the finer the time resolution in the CWT, the more coarse the frequency resolution, and vice-versa. In the CWT, time-frequency resolution can be adjusted by changing inner parameters of scalable wavelet basis function (e.g., parameter ω_0 in the complex Morlet wavelet), therefore, we first select a wavelet basis which would provide an optimal (for our purposes) time-frequency resolution of EEG signal and, allow to localize precisely sleep spindles and SWD in raw EEG.

Step 2. The choice wavelet basis function. It is known that wavelet coefficients in the CWT represent the degree of correlation of a mother (basis) wavelet function with the EEG signal $x(t)$. Therefore, the choice of the wavelet basis is crucial for the accurate representation of the EEG signal in wavelet space. Beforehand, we tested several basis functions in the CWT of EEG signal, e.g., real and complex Morlet wavelets, Mexican hat and Paul wavelet, and obtained the best time-frequency resolution with the *complex Morlet wavelet*

$$\psi_0(\eta) = \frac{1}{\sqrt[4]{\pi}} e^{j\omega_0\eta} e^{\frac{-\eta^2}{2}} \qquad (4)$$

The *complex Morlet wavelet* [Kaiser, 1994] is a complex exponential modulated Gaussian function, $\exp(j\omega_0\eta)$, where ω_0 is a specific parameter that defined the frequency of the complex exponential (Fig. 4.12). A Gaussian smoothing function, $\exp(-\eta^2/2)$, enables high resolution in both time and frequency domains.

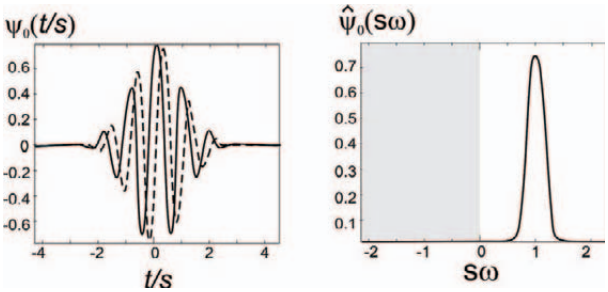

Figure 4.12. The complex wavelet Morlet (parameter $\omega_0=2\pi$) in time domain $\psi_0(t/s)$, and in the frequency domain, $\hat{\Psi}_0(s\omega)$. Solid line shows the real part and dotted line - the imaginary part.

In the *complex Morlet wavelet* family (Eq. 4), parameter ω_0 determines the shape and the width of the wavelet function, therefore, this parameter influences time and frequency resolution in the resultant CWT. When $\omega_0 < \pi$, the temporal resolution was high, but frequency resolution was too low so that the frequency information of analyzed EEG events was lost) and vice versa, when $\omega_0 > 4\pi$, the frequency resolution was high, but the time resolution was low. Value $\omega_0 = 2\pi$ provided an optimal time-frequency resolution of EEG signal that was sufficient

[*] Principles of the wavelet transform are given by Daubechies (1992); Chui (1992); Kaiser (1994); Koronovskii and Hramov (2003). Practical issue on the application of wavelet transform in EEG can be found in Jobert et al. (1994); Durka (1996); Le Van Quyen (2001).

for both investigated EEG phenomena. Another important feature of the *complex Morlet* wavelet is that in Fourier space ($\hat{\Psi}_s(s\omega)$ in Fig. 4.12), it shows only positive frequencies. The luck of negative Fourier frequencies in wavelet basis is profitable for time-frequency representation of EEG signal in wavelet space; the presence of negative frequencies in some wavelet basis functions (e.g., in Paul wavelet) might embarrass extracting frequency information from the analyzed signal and, thus, worsen time-scale resolution of the method.

In the *complex Morlet* wavelet family, the correspondence between time scales (*s*, in wavelet space) and frequencies (*f*, in Fourier space) can be computed by the formula Eq. 5 [Koronovskii and Hramov, 2003].

$$f = \frac{\omega_0 + \sqrt{2+\omega_0^2}}{4\pi s} \quad (5)$$

where ω_0 denotes the basis frequency of the Morlet mother wavelet. Noteworthy, for $\omega_0 = 2\pi$ the correspondence between *s* and *f* is simple, $s \approx 1/f$, but for the other ω_0, it is more complex.

Step 3. Qualitative analysis of wavelet power. The squared modulus of the CWT, $E(t,f_S)$, was used to measure instantaneous frequency energy at time τ (Eq. 6). The integral of $E(t,f_S)$ was averaged over time to obtain wavelet power spectrum (or scalogram), $\langle E(f_S)\rangle$, (Eq. 7).

$$E(t,f_S) = |W(t,f_S)|^2 \quad (6)$$

$$\langle E(f_S)\rangle = \frac{1}{T}\int_0^T |W(t,f_S)|^2\, dt \quad (7)$$

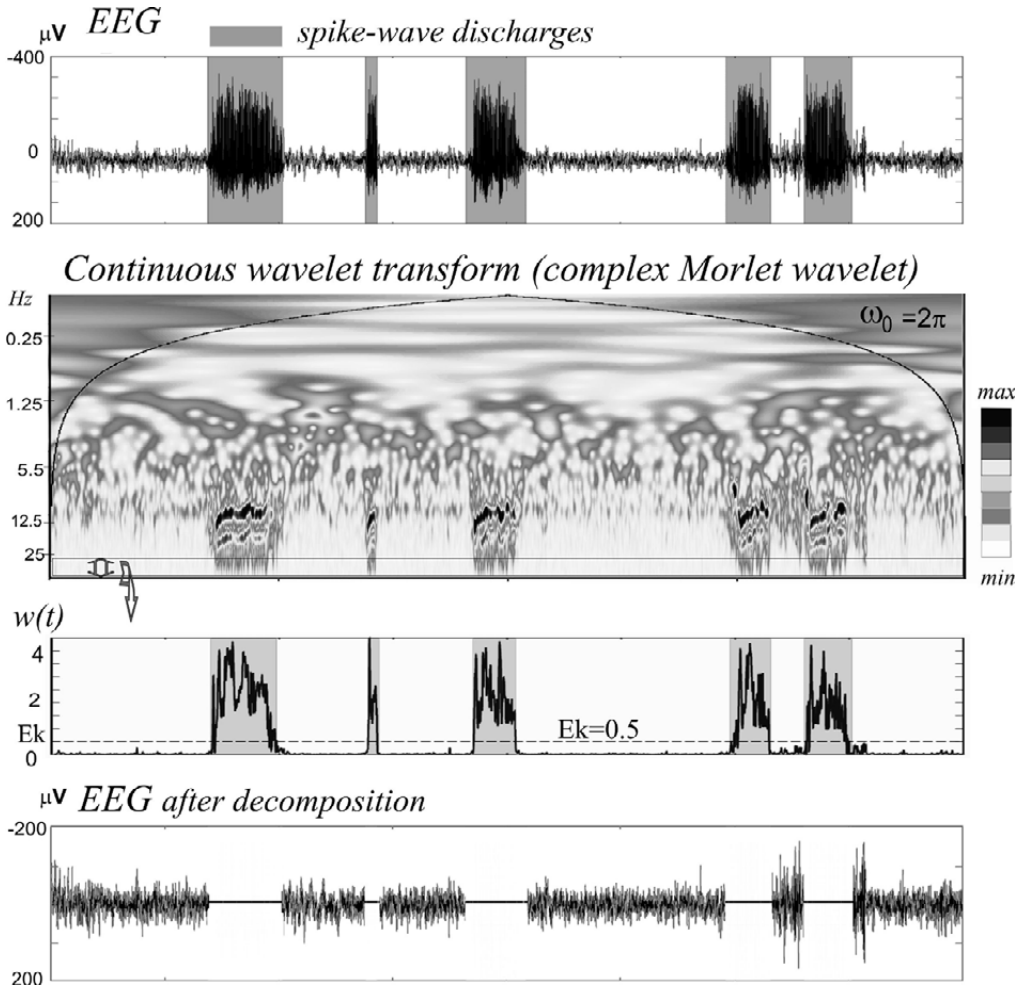

Figure 4.13. Amplitude-frequency parameters of spike-wave discharges (SWD, highlighted in grey) accessed with continuous wavelet transform (complex Morlet wavelet $\omega_0=2\pi$). In the wavelet spectrum, SWD were distinguished by a sudden increase in frequencies >10 Hz. Note that the dominant frequency of SWD at the beginning was higher (12-14 Hz) than that at the end (7-9 Hz). Domelike curve in the wavelet spectrum is a confidence curve that outlines an untrusty (upper) area in which 'boundary effects' are significant. Two bottom plates show principles of automatic detection of SWD. SWD were recognized automatically based on the value of wavelet energy $w(t)$ in the characteristic frequency band $F_{SWD} \in$ (30 to 50) Hz when $w(t) > E_k$, where E_k is threshold level (indicated by dashed line). Further, in order to avoid misapprehending of SWD as sleep spindles, EEG episodes with SWD were set to zero higher.

Distribution of wavelet energy over the frequency scale was visually inspected in order to access frequency characteristic band, $F_S \in (f_1,f_2)$, in which SWD (and sleep spindles) showed the most clear differences from background EEG (Fig. 4.13). Then instantaneous wavelet power, $w(t)$, was computed in the frequency band F_S (Eq. 8).

$$w(t) = \int_{F_S} E(t, f_S) df_S \qquad (8)$$

Step 4. Automatic detection of SWD and sleep spindles with the aid of the CWT (complex Morlet wavelet $\omega_0=2\pi$). SWD were recognized automatically when the wavelet energy, $w(t)$, in the characteristic frequency band $F_{SWD} \in$ 30 - 50 Hz exceeded the threshold $E_k = 0.5$ for a duration of 1 sec and longer (Fig. 4.13; Table 4.3A). Sleep spindles were first selected in the same EEG by higher wavelet power in $F_{sp} \in$ 8 - 14 Hz, but they were often mixed up with SWD. In order to prevent these error detections, segments of previously selected SWD were set to zero (bottom plate in Fig. 4.13). Even though, only 40% of sleep spindles were detection automatically (see below). The quality of automatic detections of sleep spindles was slightly improved when parameters F_{sp} and E_k were chosen individually, but percentage of true detections was still low (~60 %, Table 4.3B). The best performance of wavelet-based automatic identification of sleep spindles in EEG was achieved with the aid of specifically designed adaptive wavelet basis ('spindle wavelets', see below).

Construction of adaptive wavelet basis ('spindle wavelet') for the automatic recognition of sleep spindles

An adaptive wavelet basis function (spindle wavelet) was built up using sleep spindle prototype extracted from the native EEG (Fig. 4.14). The EEG signal was represented by the function $g(t)$ and transformed into a complex form, $\hat{g}(\eta)$. Time shift between the real and imaginary parts was $T_0/4$, where T_0 denotes the typical period of a sleep spindle oscillations.

$$\hat{g}(\eta) = g(\eta) + jg(\eta + T_0/4), \qquad \text{where } j = \sqrt{-1} \qquad (10)$$

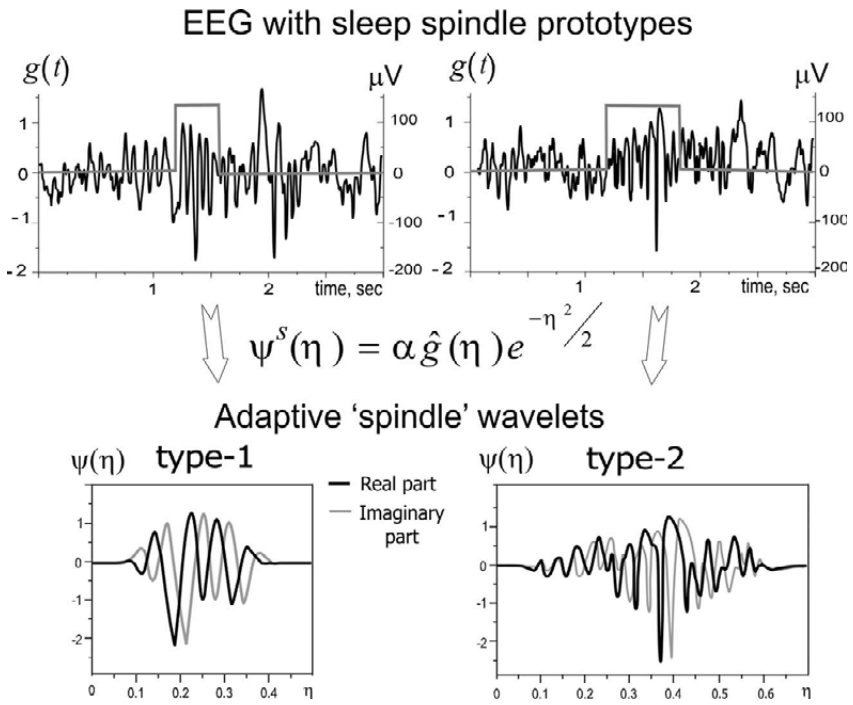

Figure 4.14. The schema illustrating the procedure of building up adoptive 'spindle wavelets'. Sleep spindle prototypes are selected in native EEG $g(t)$, converted into the complex form and normalized with Gaussian function (see text for details).

In order to construct a complex wavelet basis, $\psi^s(\eta)$, $\hat{g}(\eta)$ was normalized with Gaussian function (11):

$$\psi^S(\eta) = \alpha\hat{g}\exp(-\eta^2/2), \qquad (11)$$

In this formula α denotes the normalization factor, which was determined using the normalization condition

$$\int_{-\infty}^{+\infty}\left(\psi^S(\eta)\right)^2 d\eta = \alpha^2\int_{-\infty}^{+\infty}\hat{g}(\eta)^2\exp(-\eta^2)d\eta = 1. \qquad (12)$$

In order to select an optimal spindle template, eighty candidate spindle templates were selected in five rats (15-22 spindles per rat). Each spindle template was employed in the automatic detection system and tested as a wavelet basis. Wavelet energy, $w(t)$, was computed in the frequency band F_{sp}*(type 1)* ∈ 7 - 14 Hz and selections were made if $w(t) > E_k$ for a minimal duration of 0.35 sec. Finally, we chose a wavelet basis that provided maximum number of positive spindle detections. This 'spindle wavelet' (type 1) yielded the best performance in all animals (87.4 % of correct detections in average, Table 4.4A). Both 'spindle wavelets' fulfilled the requirements for wavelet bases (e.g. continuity, zero mean amplitude, and finite or near finite duration). Let us note that the same computational procedure can be applied to the harmonic, e.g., $sin(\omega_0 t)$ function, in order to construct the complex Morlet wavelet [Kaiser, 1994; Koronovskii and Hramov, 2003].

Combined application of 'spindle wavelets' type 1 and type 2 highly improved the quality of automatic detection of sleep spindles in EEG. Automatic selections of sleep spindles perfectly matched selections made by experts (Fig. 4.15). From the technical point of view, 'spindle wavelets' encouraged automatic recognition of sleep spindles and provided better results as compared to what has been obtained using the standard complex Morlet wavelet ($\omega_0 = 2\pi$).

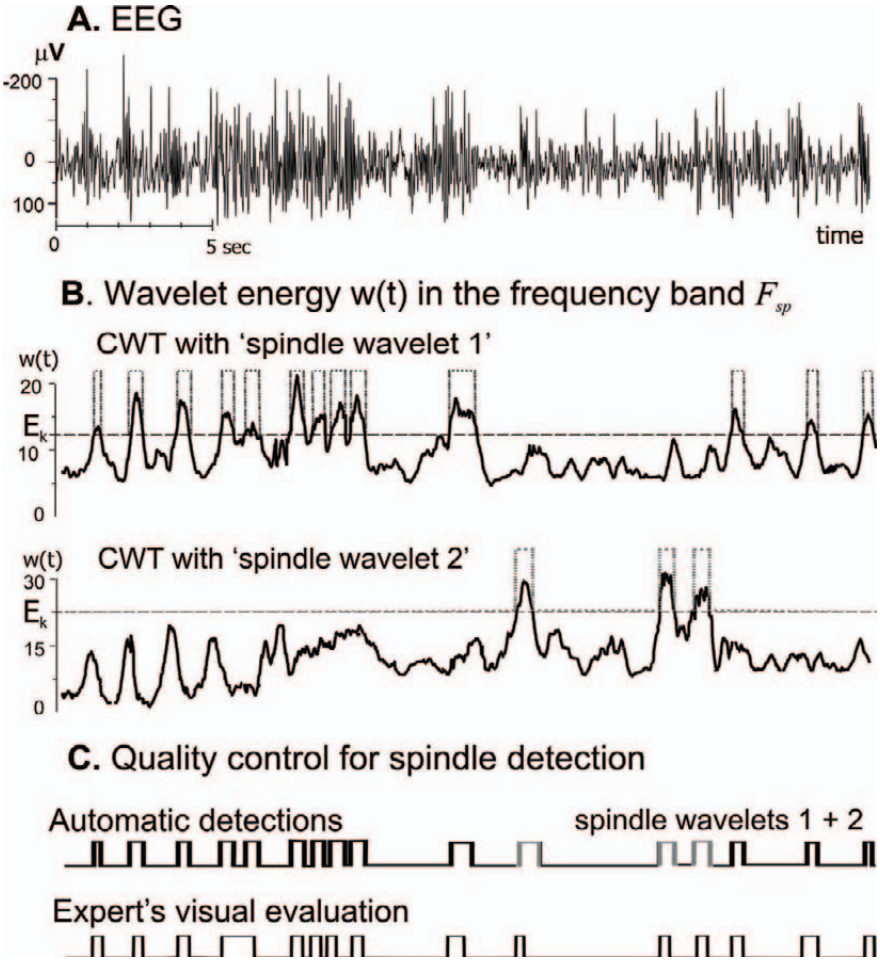

Figure 4.15. Automatic recognition of sleep spindles with the aid of two 'spindle wavelets'. (A) EEG record with sleep spindle oscillations. (B) Distribution of wavelet energy *w(t)* as obtained with type 1 and type 2 'spindle wavelets' in the characteristic bands (F_{sp}). Type 1 'spindle wavelet' sleep spindles in F_{sp}('type-1') = 7–14 Hz with threshold E_k =12.4; F_{sp}('type-2') = 20–25 Hz, threshold E_k = 21. (C) Automatic spindle detections coincided with experts' selections.

The software for the wavelet analysis is specifically designed at the Faculty of Nonlinear processes, Saratov State University (Russia). Power spectrum analysis was performed using Brain Vision Analyser software (© BrainProducts GmbH) and Spectranes software (Dr. PLC van den Broek and Dr. J van Egmond, © UMC, Sint Radboudsoftware). ANOVA (Fisher test for post-hoc analysis) and t-test for related samples were used for the statistical analysis.

Statistical analysis of automatically recognized SWD and sleep spindles

The performance of wavelet-based detection method was evaluated by measuring the percentage of true positive/negative detections, false positive/negative and by computing sensitivity and specificity.

True positive (TP) was computed as percentage of correct detections of SWD (or sleep spindles). True negative (TN) is the percentage of correct rejections of SWD (or sleep spindles). False positive (FP) represented a percentage of incorrect automatic detections of SWD (or sleep spindles). False negative (FN) - percentage of events missed by the automatic wavelet-based method.

The accuracy of automatic recognition was computed as $\rho = (TP/N_e)\times 100\%$ (where TP was the number of true positive detections and N_e - the number of expert selections). ρ^{SWD} denotes accuracy of SWD detection and ρ^{SS} - accuracy of spindle detection.

Sensitivity = TP/(TP+FN) ×100%.

Specificity = TN/(TN+FP)×100%.

Table 4.3. Results of automatic identification of SWD and sleep spindles using the CWT with the *complex Morlet* wavelet ($\omega_0=2\pi$).

4.3.A SWD *

Rat ID	The number of visual detections, N_e	The number of automatic detections			Performance of automatic recognition		
		TP	FP	FN	Accuracy ρ^S, %	Sensitivity %	Specificity %
1	105	105	0	0	100.0	100.0	100.0
2	81	79	2	1	97.5	98.8	97.5
3	249	247	1	2	99.2	99.2	99.6
4	120	117	1	3	97.5	97.5	99.2
5	66	65	2	1	98.5	98.5	97.0
Mean (± S.D.)	124 ± 73	123 ± 73	1.2 ± 0.8	1.4 ± 1.4	98.5 ± 1.1	98.8 ± 0.9	98.7 ± 1.3

* SWD were detected automatically when wavelet energy in frequencies $F_{SWD} \in (30, 50)$ Hz exceeded the threshold level, $E_k = 0.5$ (the same parameters F_{SWD} and E_k were used for all animals).

4.3.B Sleep spindles #

Rat ID	The number of visual detections, N_e	The number of automatic detections			Parameters of automatic recognition			Performance of automatic recognition		
		TP	FP	FN	E_k	f_1, Hz	f_2, Hz	Accuracy ρ^S, %	Sensitivity %	Specificity %
1	2341	1358	894	1359	1.5	6.25	12.5	58.0	47.7	60.3
2	1381	856	599	855	1.4	8.3	16.6	62.0	54.1	58.8
3	1491	999	772	1002	1.8	5.5	12.5	67.0	57.9	56.4
4	1305	718	505	720	2.2	6.25	16.6	55.0	48.6	58.7
5	1598	1007	866	1015	1.9	6.25	12.5	63.0	57.1	53.8
Mean (± S.D.)	1623 ± 416	987 ± 239	727 ± 169	990 ± 239	1.7 ± 0.3	6.5 ± 1.1	14.1 ± 2.3	61.2 ± 4.7	53.2 ± 4.8	57.7 ± 2.5

Sleep spindles were detected using individual parameters F_{SWD} and E_k.

TP – true positive detections: the percentage of correct automatic detections from the total amount of visually detected events.

FP – false positives: the percentage of incorrectly identified events from the true positive detections.

FN – false negatives: the percentage of missed events from the true negative detections.

Accuracy $\rho = (TP/N_e)\times 100\%$ Sensitivity = TP / (TP+FN) ×100% Specificity = TN / (FP + TN) ×100%

Table 4.4. Results of automatic identification of sleep spindles with the aid of adaptive wavelet templates

4.4.A. Type 1 'spindle wavelet' [#]

Rat ID	The number of visual detections, N_e	The number of automatic detections			Parameter	Performance of automatic recognition		
		TP	FP	FN	E_k	Accuracy ρ^S, %	Sensitivity %	Specificity %
1	2341	2130	23	281	12.4	91.1	88.4	98.9
2	1381	1132	28	110	14.2	82.2	91.2	97.6
3	1491	1312	30	149	14.9	87.8	89.8	97.8
4	1305	1096	39	104	13.6	83.9	91.3	96.6
5	1598	1422	16	144	16.4	88.9	90.8	98.9
Mean (± S.D.)	1623 ± 416	1418 ± 419	27 ± 9	157 ± 72	14.3 ± 1.5	86.8 ± 3.7	90.3 ± 1.2	97.9 ± 1.0

[#] Basis function 'spindle wavelet 1' was the same in all animals. Detections of 'type 1 spindles' were made if the wavelet power, *w(t)*, in frequency band F_{sp}(type 1) $\in (f_1, f_2)$ = (7, 14) Hz exceeded the threshold E_k.

4.4.B. Type 2 'spindle wavelet' [*]

Rat ID	Spindles missed by 'type 1' wavelet	The number of automatic detections				Parameters		Performance of automatic recognition		
		TP	TN	FP	FN	Mean freq. [†]	E_k	Accuracy ρ^S, %	Sensitivity %	Specificity %
1	211	140	2154	70	22	23±3	21.0	66.3	96.9	86.4
2	249	110	1215	69	21	24±4	23.5	44.2	94.6	84.0
3	179	164	1327	30	15	19±2	18.8	91.6	97.8	91.6
4	209	117	1175	26	18	17±2	18.5	56.0	97.8	86.7
5	176	112	1454	48	14	22±2	18.5	63.6	96.8	88.9
Mean (± S.D.)	27 ± 9	205 ± 30	1465 ± 400	48.6 ± 20.8	18 ± 6	21±3	20.1 ± 2.1	64.3 ± 17.5	96.8 ± 1.3	87.5 ± 2.9

* Basis function 'spindle wavelet 2' was chosen for each animal individually. 'Type 2 spindles' were detected when wavelet power, *w(t)*, in frequencies F_{sp}(type 2) $\in (f_1, f_2)$ = (20 - 25 Hz) exceeded the threshold E_k.

[†] Averaged peak frequency of 'spindle wavelet 2' basis (± S.D.).

RESULTS

Various oscillatory patterns were encountered in EEG of our subjects, WAG/Rij rats, during drowsiness and non-REM sleep; here we statistically analyzed spike-wave discharges (SWD) and spindle oscillations (Fig. 5), but disregarded intermediate oscillatory waveforms or so-called 'spiky oscillations'[*] (Fig. 4.15). As compared to sleep spindles, SWD lasted ten times longer, their amplitude was twice as lower and mean frequency was significantly lower (see **Chapter 4.1** and Table 4.1).

Sleep spindles and SWD in Fourier space

Fast Fourier transform (FFT, frequency domain measure), which is traditionally used for time-frequency analysis of EEG, showed serious disadvantages that limit its application for analysis of SWD and spindle events. An obstacle we faced in Fourier analysis was a necessity of fixing the time window length. Duration of the investigated events varied from half a second (mean duration of sleep spindles) to tens seconds (SWD) (Table 4.1). For example, Figure 3 shows that time window 7 sec was too narrow for SWD, but it is definitely too broad for sleep spindles and for spiky oscillations (the latter patterns were not included in the further analysis).

[*] 'spiky oscillations' were first described in EEG of WAG/Rij rats by Drinkenburg et al. (1991)

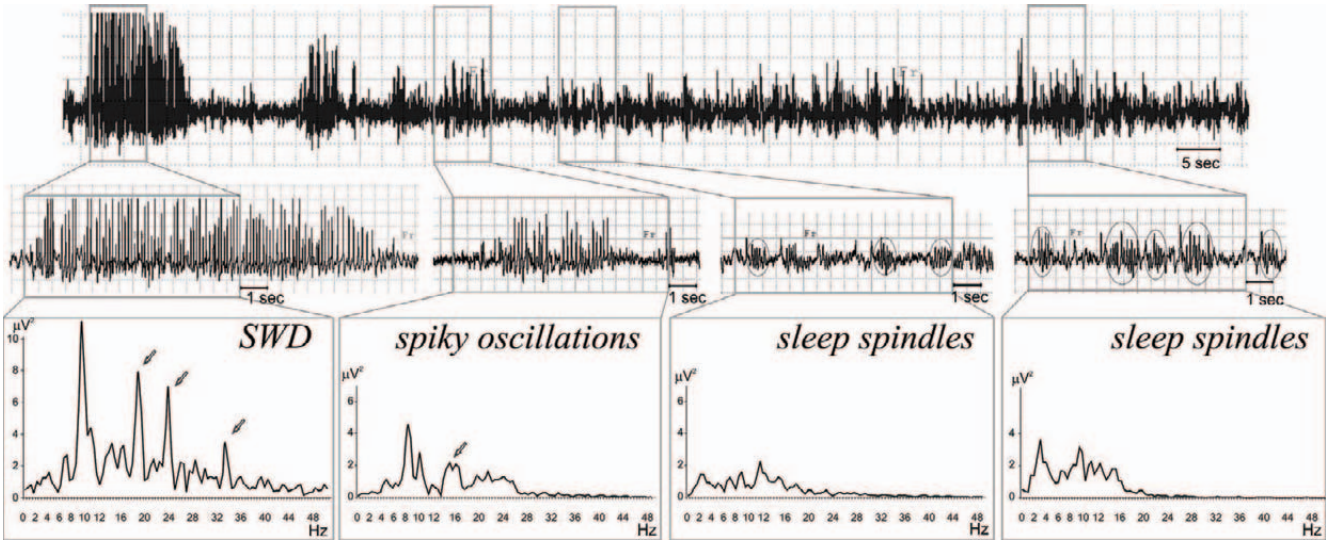

Figure 4.15. Various oscillatory EEG patterns that are encountered at the beginning of slow-wave sleep in WAG/Rij rat (in the time and in the frequency domain).

In FFT, time-domain information is missed and short-lasting changes are disregarded in Fourier space. This seriously limits applicability of this method for EEG analysis (sleep spindles were too short for being well explored by means of FFT) and this enforces us to use the CWT in the current study.

Power spectrum of SWD displayed harmonic component in 20 Hz (shown by arrows in Fig. 4.15) that replicates its mean frequency (10 Hz). 20 Hz harmonic component is likely to be elicited by the regular ~10 Hz spikes. The other spectral components (peaks in 24 Hz and in 35 Hz) do not fit to the expected 30 Hz and 40 Hz harmonics, suggesting that epileptic discharges do not represent a single rhythm. In EEG, SWD display regularly modulated rhythmic activity and characterized by complex frequency dynamics. Noteworthy is that ~8 Hz frequency component and it's harmonic (16 Hz) were also found in Fourier spectrum of 'spiky oscillations'.

Sleep spindles and SWD in the wavelet space

Preliminary time-frequency analysis of sleep spindles was performed using the CWT with the complex Morlet wavelet ($\omega_0=2\pi$). Based on the distribution of wavelet energy over the frequency scale, we specified frequency bands (F_{SWD} and F_{sp}), in which spindles and SWD could be best discriminated from background EEG. Selection criteria for the automatic recognition of SWD and sleep spindles was obtained by measuring wavelet energy, $w(t)$, in F_{SWD} (and F_{sp}), so that $w(t) > E_k$ (see 'Methods'). In total, analysis was performed in full-length EEG (5-7 hours) in five rats (66-249 samples of SWD per subject and 1305-2341 samples of sleep spindles, Table 4.3).

Epileptic discharges, SWD

In the wavelet spectrum (the CWT with the *complex Morlet* $\omega_0=2\pi$), SWD showed a vast increase of energy in frequencies above 10 Hz (Fig. 4.13). SWD were perfectly identified in wavelet space by elevation of wavelet power in high frequencies. Repetitive spikes in EEG seizure corresponded to the isolated bursts in the high-frequency part of its wavelet spectrum. In addition, the wavelet spectrum revealed a characteristic frequency dynamics of the fundamental frequency during SWD (Fig 4.13). At the beginning, maximum wavelet energy of SWD was at ~ 13 Hz and this maximum was gradually shifted to 7 Hz at the end of SWD. The same frequency dynamics in SWD was demonstrated in WAG/Rij rats and in human patients [Bosnyakova et al., 2005, 2007].

In wavelet-based automatic recognition system, it appeared that almost all SWD in all animals were identified correctly by having high wavelet power in frequency band $F_{SWD} \in$ 30 - 50 Hz and with a energy threshold set at E_k = 0.5 (Fig. 4.13). Table 4.3A shows that the accuracy of detections (ρ^{SWD}), selectivity and specificity were very high and almost reached 100 %. Incorrect detections (false positive, FP or error type I) were very rare (0-1.8 %). All this suggests that SWD can faithfully be distinguished from non-epileptic background EEG by having sustained increase in power in gamma frequency band.

Sleep spindles

As compared to SWD, sleep spindles showed a greater variability in shape and their electroencephalographic pattern was less stereotypic. This embarrassed the automatic detection of sleep spindles. The CWT with complex Morlet wavelet $\omega_0=2\pi$ (Fig. 4.16A) was used for time-frequency representation of sleep spindles. It appeared that distribution of wavelet energy over the frequency scale varied from spindle to spindle, indicating wade variability

of frequency content of EEG spindle events. Despite that, sleep spindles characterized by the presence of strong frequency components in 8-14 Hz (Fig. 4.16A) that met the definition of sleep spindles as short-lasting sinusoidal 8-14 Hz oscillations.

An increase of the wavelet energy in 8-14 Hz was necessary, but it was not sufficient requirement for detecting sleep spindles with the aid of Morlet-based CWT. Maximum 38-45% of true detections of sleep spindles (TP, data not shown) was obtained when a fixed threshold of wavelet energy in 8-14 Hz (E_k = 0.025) was applied to Morlet-based wavelet spectrum. Automatic detection was improved when parameters, such as the frequency band (f_1, f_2) and threshold value (E_k), were chosen in each rat individually. Even though, only 55-67 % of sleep spindles were identified correctly (Table 4.3B) by having higher wavelet power in frequencies from 6.5 to 14.1 Hz (mean values of f_1 and f_2). Most likely, sleep spindles bears similarities with other alpha oscillations in EEG and, therefore, they could not be easily distinguished from non-spindle oscillatory activity with the aid of the standard wavelet basis function. In order to extract generic properties of sleep spindles, we designed adoptive 'spindle wavelet' basis functions (see Methods).

Identification of two spindle types with the aid of two adoptive 'spindle wavelets'

Although the variability in the waveform of sleep spindles was rather high, spindle sequences were characterized by some shared elements (Fig. 4.17A). Sleep spindles showed different degrees of conformity to two types of spindle wavelets, e.g., 'spindle wavelets' type 1 and type 2 (see 'Methods'). When 'spindle wavelet 1' was used for the automatic recognition of spindle events, about 87.4 % of sleep spindles (so called type 1 sleep spindles) were identified correctly in the frequency band $F_{sp}(type\ 1) \in (f_1, f_2)$ = (7, 14) Hz (Table 4.4A). The remainder sleep spindles, which failed to be captured with 'spindle wavelet 1', were selected using the 'spindle wavelet 2' in $F_{sp}(type\ 2) \in (f_1, f_2)$ = (20 - 25 Hz). It was found that type 2 sleep spindles comprised 7.9 % from the total number of sleep spindles (Table 4.4B).

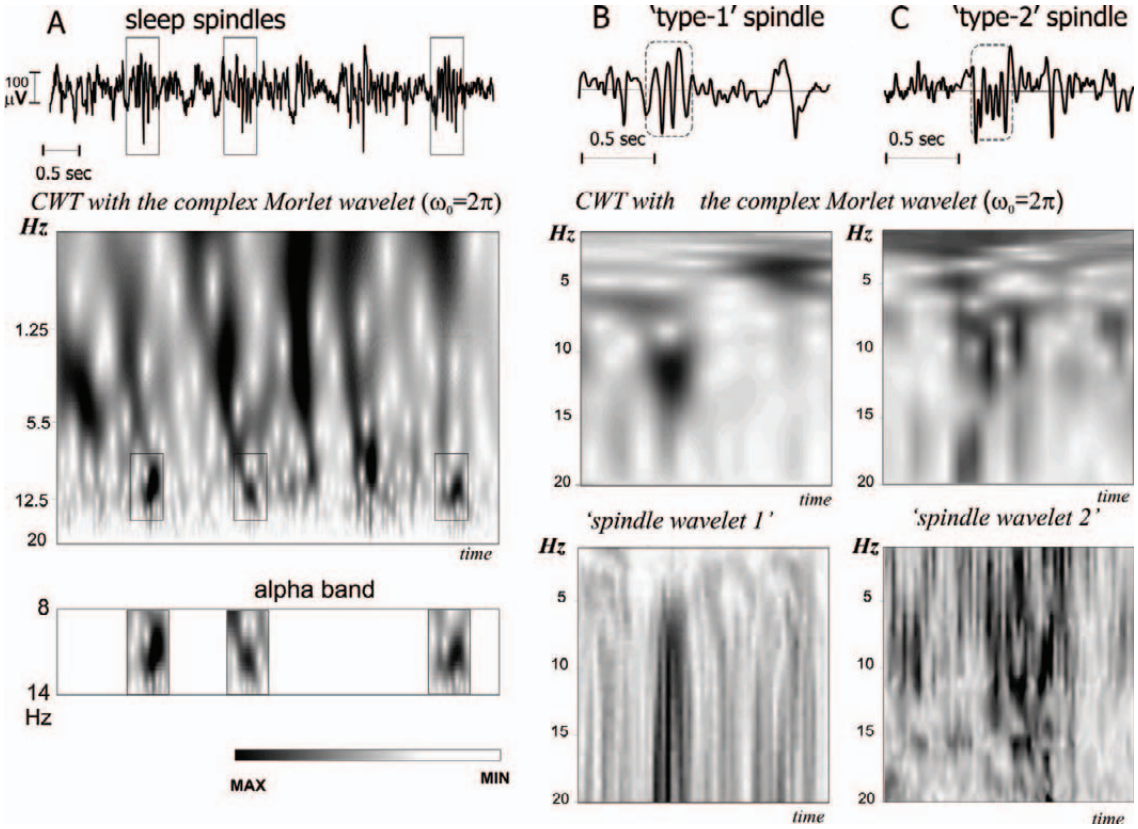

Figure 4.16. Continuous wavelet transform (CWT) of sleep spindles (shown by squares in EEG) with the complex Morlet wavelet (**A**) and two adaptive 'spindle wavelets' (**B-C**). **A.** The complex Morlet perfectly represents time-frequency characteristics of sleep spindles. In wavelet spectrum, a hallmark of spindles events was an increased energy in alpha band (8-14 Hz). **B-C**. A difference between 'type 1' and 'type 2' sleep spindles in Morlet-based wavelet spectrum (top plates) localized in frequencies above 16 Hz (a 'type 2' spindle demonstrate high energy in these frequencies, but 'type 1' spindle - not). The CWT with two adaptive 'spindle wavelets' (bottom plates) poorly represents time-frequency structure of EEG signal. 'Spindle wavelets' were specifically designed for extracting relevant spindle patterns in EEG and showed good performance in localizing sleep spindles, but they were not capable for extracting frequency band information.

Two types of sleep spindles and their relevance to SWD

There was a clear inconsistency in a population of sleep spindles sleep spindles: those that matched ‘spindle wavelet 1’ failed to be captured by ‘spindle wavelet 2’. In order to better understand a physiological meaning of this divergence sleep oscillations, we performed a power spectrum analysis of two spindle prototypes. ‘Spindle wavelet 1’ had a fundamental frequency 12.2 Hz that precisely corresponds to the mean frequency of sleep spindles in rats [Terrier and Gottesmann, 1978], in addition to that, it showed a peak in 7 Hz and elevations around 2 and 26 Hz.

In contrast to the spectrum of ‘spindle wavelet 2’, the spectrum of ‘spindle wavelet 1’ was more complex and also the majority of the peaks were more or less symmetrical in respect to their negative-positive values (Fig. 4.17B). `‘Spindle wavelet 2’ had to be selected individually and it’s fundamental frequency was 21±3 Hz. Typically, ‘spindle wavelet 2’ showed several sharp peaks in 1, 3, 16.7 and 21.3 Hz and moderate elevations in 8.5, 11, 24.5 and 27 Hz. It can be concluded that an atypical ‘type 2’ sleep spindles were distinguished from a common ‘type 1’ sleep spindles by having a larger individual variation; a powerful beta-component can be considered as a hallmark of ‘type 2’ spindles.

Occurrence of ‘type 2’ sleep spindles with the strong 16-25 Hz component might be accounted by processes of epileptogenesis taking place in our subjects. Previously, by means of EEG coherence method, we showed [Sitnikova and van Luijtelaar, 2006] that, besides fundamental and harmonic frequencies (10-12 and 20-24 Hz), the onset of SWD characterized by an increased synchronization in 15-16 Hz between bilaterally symmetric cortical areas. In the present study, the peaks with the same frequency (16.7 and 21.3 Hz) were detected in ‘type 2’ sleep spindles. It is therefore likely that neuronal synchrony in 16.7 and 21.3 Hz is common for SWD and for ‘type 2’ sleep spindles. ‘Type 2’ sleep spindles might be considered as a transitory oscillatory waveform between spindle and SWD.

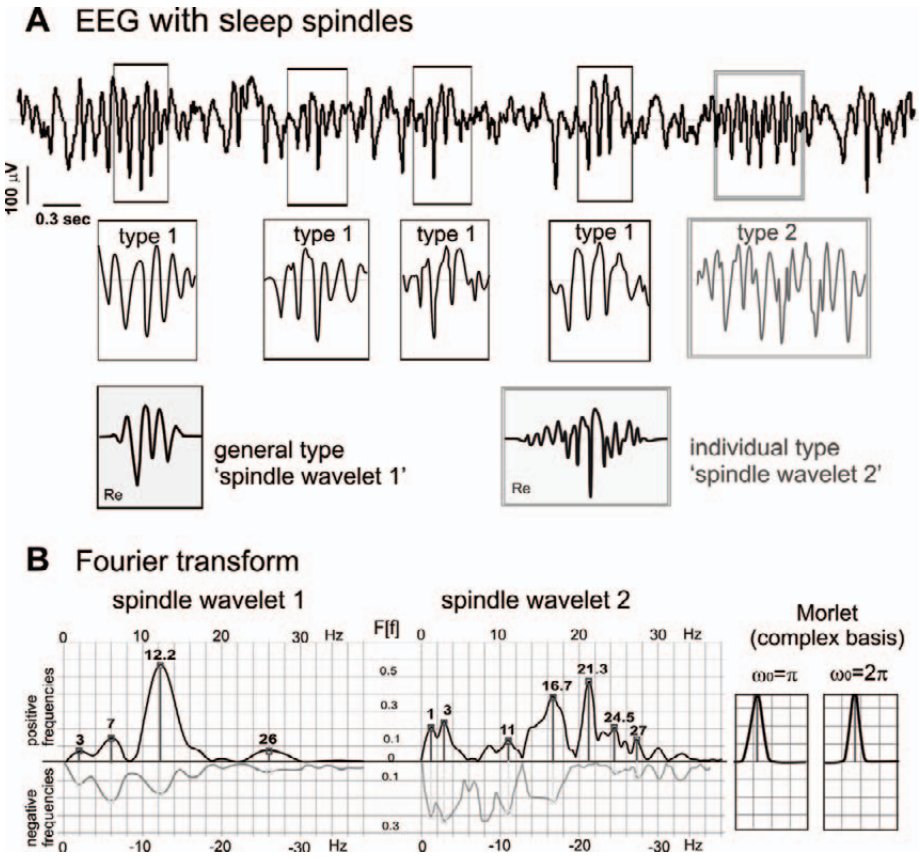

Figure 4.17. Variability EEG waveform of sleep spindles in WAG/Rij rats. **(A)** The majority of sleep spindles comprised characteristic repetitive elements from which a prototype for the adaptive ‘spindle wavelet 1’ has been derived. ‘Type 1’ sleep spindles were recognized equally well in all animals with common ‘spindle wavelet 1’. Some spindles, which cannot be recognized with ‘spindle wavelet 1’, match ‘spindle wavelet 2’ that was chosen individually. ‘Spindle wavelet 2’ displays a high inter-subject variability and a rather complicated structure. (B) Frequency profiles of ‘spindle wavelets’ type 1 and 2 and standard wavelet basis functions. ‘Type 1’ spindle wavelet shows an abundant increase in spindle frequencies 8-14 Hz in contrast to ‘type 2’ wavelet, which frequency profile is more complex and shows prominent peaks in non-spindle frequencies.

Sleep spindles and SWD were considered as alpha-band oscillations: they both demonstrate an elevation of power in 8-14 Hz in Fourier and wavelet space; SWD were mistakenly recognized as sleep spindles in EEG before

decomposition (bottom graph in Fig. 4.13 and 'step 4' in 'Methods'). For the other hand, they were best localized in wavelet spectrum in non-overlapping frequency bands (F_{Sp} and F_{SWD}). Besides that, different wavelet templates were necessary to extract EEG patterns of sleep spindles and SWD. The complex Morlet wavelet displayed a good affinity to SWD (it was successfully used for extracting almost 100% of SWD), but low affinity to sleep spindles (it yielded 50-60% of true spindle detections). Altogether point towards a fundamental difference between these EEG events.

DISCUSSION

The present Chapter examines two types of self-sustained thalamo-cortical oscillations: sleep spindles during drowsiness and sleep and pathological SWD, also preferentially occurring in the same vigilance states. We have applied Fourier transform and continuous wavelet transform in order to characterize amplitude-frequency parameters of spontaneous SWD and sleep spindles in the WAG/Rij rat model of absence epilepsy. We report on differences between SWD and sleep spindles in respect to their EEG power and degree of conformity with wavelet basis functions.

Application of wavelet transform for the identification of oscillatory patterns in EEG

In the field of EEG research, the CWT is basically used for two purposes: first, time-frequency analysis, in particularly, time-frequency analysis of spike-wave seizures in patients with absence epilepsy and in WAG/Rij rats [Bosnyakova et al., 2007] and, second, for extracting of EEG features and automatic recognition of patterns such as epileptiform discharges in human EEG [Senhadji and Wendling, 2002; Khan and Gotman, 2003] and sleep spindles [Jobert et al., 1994; Schonwald et al., 2003; Latka et al., 2005]. Here we develop a wavelet-based algorithm for the automatic identification of spindle events and SWD in EEG in non-segmented full-length EEG data. In order to optimally localize the investigated EEG patterns in time domain, we used the complex Morlet wavelet and specific spindle wavelet functions. Our strategy (we call it '*adaptive wavelet matching'*) is comparable with matching pursuit technique [Durka, 1996; 2003; Durka et al., 2005; Zygierewicz et al., 1999] in a sense that offers to choose a template function from stochastic dictionaries that constitute a set of Gabor, Dirac and Fourier basis waveforms in order to find the optimal approximation of the EEG event that should be detected. In the present study, 'spindle wavelet' basis functions are adopted directly from the EEG signal.

In our case, the best performance of automatic recognition of SWD and sleep spindles is achieved after selecting of the optimal wavelet template and adjustment of the optimal amplitude (E_k) and frequency (F_S) parameters. It appeared that variability of EEG structure of sleep spindles was high, therefore, a probability of correct detection with the aid of standard wavelet functions was low. Almost all sleep spindles (95.5%) were extracted with joint application of two different types of adaptive 'spindle wavelets'. Type 1 sleep spindles (85-90%) were recognized with the aid of one common template ('spindle wavelet 1') by having high power in 6.25-16.6 Hz. In opposite to type 1 spindles, type 2 sleep spindles (10-15%) revealed high individual variability ('spindle wavelet 2' had to be chosen individually) and showed high power in frequencies 20-25 Hz.

The 'spindle wavelet' functions displayed a complex profile in the Fourier space as compared to standard wavelet functions (Fig. 4.17B). The 'spindle wavelets' showed negative Fourier frequencies (negative frequencies were absent in complex wavelets, but present in real wavelets). Positive and negative Fourier frequencies did not mirror each other in the 'spindle wavelets', as they did in real standard wavelets. This suggests a complex correlation between the real and imaginary parts in the 'spindle wavelets'. Therefore, the CWT with the 'spindle wavelets' combined features of the complex transform (that was required for the adequate time-frequency representation of sleep spindles) and some features of the real transform (that was necessary for waveform extraction). As a result, 'spindle wavelets' were particularly good in extracting characteristic EEG features of each spindle type, but they were not suitable for time-frequency analysis. It is concluded that a combination of standard and adaptive wavelet transforms is favorable for discrimination and description of sleep spindles and epileptic EEG events.

Epileptic activity (SWD)

We found that a robust increase of high frequencies was typical for SWD, moreover, it was a distinguishing signature of seizure activity. An increase in wavelet energy in 30-50 Hz was a reliable criterion by which we identified almost 100 % of seizures without false alarms. A similar method has been proposed for detecting epileptic episodes in the EEG [Khan and Gotman, 2003]. They used a discrete wavelet transform and relied upon energy estimation in seizure-specific frequency scales (6–12 Hz and 12–25 Hz), resulting to 86 % sensitivity and 14 % of false alarms. We could detect SWD accurately based on energy in the gamma frequency band (30-50 Hz) and this was several times higher than the energy in the mean interspike frequency of SWD (8-12 Hz). Our result is in full agreement with other indications that fundamental frequencies ànd harmonic spectral components were elevated during absence seizures [Van Hese et al., 2003; Drinkenburg et al., 1993]. All this suggests that SWD

(and probably also other kinds of epileptic discharges with monotonous spikes) can be clearly identified by a robust increase in wavelet energy in frequencies several times higher than the mean frequency of discharges, i.e. harmonic frequencies.

Normal sleep spindle oscillations

In healthy humans, sleep spindles are recognized as "*bursts at 11-15 Hz, but mostly at 12-14 Hz*" (IFSECN, 1974, p. 547), however, sleep spindles are usually identified in wider frequencies, from 11 to 16 Hz (Schimicek et al., 1980; Zygierewicz et al., 1999; Huupponen et al., 2007). We had to expand an initially predetermined spindle frequency band 8-12 Hz to broader frequencies from 5.5 to 16.6 Hz (Morlet-based wavelet detections). This is in agreement with the literature: in mammalian species, including rats, sleep spindles appear in frequencies from 8 to 15 Hz [Gandolfo et al., 1990; Drinkenburg et al., 1993; Kandel and Buzsaki, 1997; Mackenzie et al., 2004].

The quality of automatic recognition of sleep spindle with the aid of the complex Morlet wavelet ($\omega_0=2\pi$) was low (only a half of sleep spindles was detected correctly and 39 % of the spindles were missed). The quality of detection cannot be improved by changing the frequency band (F_{sp}) or by adjusting the recognition threshold (E_k). The low affinity of the complex Morlet wavelet to sleep spindles disagrees with results from others [Latka et al., 2005]. These authors successfully applied the Morlet wavelet successfully for the identification of sleep spindles. *"It is apparent that the complex Morlet wavelet mimics wave-packet behavior of sleep spindle and provides a mathematical equivalent of the phenomenological description"* (p. 16, Latka et al., 2005). The disagreement with our results may lie in a different design of the experiments and in a species difference. We included in our analysis of SWD and sleep spindles periods of sleep and wakefulness (hundreds of sleep-wake cycles), while EEG sleep studies in humans are restricted to sleep periods and exclude waking EEG. Sleep spindles in rats tend to occur as sleep deepens, but spindle-like events in the alpha frequency range are also present during passive wakefulness [Fanselow et al., 2001].

Distinctions between SWD and sleep spindles

The present results cast some doubts about similarity between sleep spindles and SWD.

First, their basic parameters are distinguished: SWD last ten times longer than anterior spindles, their amplitude is nearly two times higher and their mean frequency is about 2 Hz lower (as measured in a period 0.5-1.5 sec after the seizure onset).

Second, power spectrum analysis demonstrates that SWD is characterized by higher power in 9 - 100 Hz and low power in delta as compared to sleep spindles. This difference in frequency composure correlates with the difference in their EEG waveforms that has been demonstrated with continuous wavelet transform. It is shown that the EEG pattern of SWD is not comparable with that in sleep spindles: (i) different wavelets are necessary for the identification of SWD and spindles; (ii) SWD are identified in EEG with the aid of the standard Morlet wavelet, but sleep spindles can be identified by means of two types of customized adoptive 'spindle wavelets'; (iii) spindle and SWD are detected with different frequencies F_{SWD} and F_{sp} SWD have high power between 30 and 50 Hz, sleep spindles – between 6-14 Hz. Besides that it is found that SWD represent one family, but sleep spindles - two families.

Previously, Drinkenburg et al. (1993) performed spectral analysis of sleep spindles, SWD and intermediate 'spiky' activity and found a striking resemblance between all these EEG events in respect to their frequency content and peak frequencies. Also Mackenzie et al. (2004) indicated that SWD have more power in their frequency spectrum than normal spindle oscillations. We found that sleep spindles and SWD are best extracted when different wavelet basis functions are applied in the CWT, suggesting that sleep spindles and SWD are independent phenomena. In addition, sleep spindles possess high inter- and intra-subject variability and their time-frequency characteristics were more heterogeneous than that of SWD; the EEG pattern of sleep spindles was less stereotyped and less uniform compared to SWD. It can be concluded that SWD represent a single family, but sleep spindles can be subdivided into two families: general and individual types (type 1 and 2 correspondingly).

The above mentioned dissimilarities between sleep spindles and SWD support the notion that the neurophysiological substrate of spindle oscillations and SWD is not the same. As compared to SWD, spindle oscillations are less generalized (they are rather local oscillations [Terrier and Gottesmann, 1978; Jankel and Niedermeyer, 1985; De Gennaro and Ferrara, 2003]), their EEG waveform is less regular (the own data). Previously we showed [van Luijtelaar and Bikbaev, 2007] that that sleep spindles and SWD are controlled by different age-related mechanisms. Density of sleep spindles in WAG/Rij rats is the same with that in control rats, despite the large strain difference in number of SWD (the incidence of SWD in WAG/Rij rats highly increased with age, yet control rats exhibit just sporadic SWD). Comprehensive *in vivo* and *in vitro* neurophysiological examinations in GAERS demonstrate that SWD do not originate sleep spindles, but have a plausible source of SWD, e.g. 5–9 Hz oscillations [Pinault, 2001; Pinault et al., 2006].

It is noteworthy that rat models of absence epilepsy (i.e., GAERS and WAG/Rij) are distinguished from the feline generalized penicillin epilepsy [Gloor 1969; Kostopoulos, 2000] in a sense that absence seizures in our subjects are spontaneous, but not induced by penicillin. Sleep spindle oscillations in rodents might just indirectly correlate with absence epilepsy. At least in type 2 sleep spindles, strong beta component in SWD-harmonic frequency (~21 Hz) and in the middle frequency (~16 Hz) might sign indicating pro-epileptic nature of these oscillations, therefore, type 2 sleep spindles could be considered as a deviant spindle form. It is assumed that 'type 1' spindles are normal oscillatory phenomena (with no aberrant features), while 'type 2' is an aberrant spindle type that appears in epileptic animals due to an impairment of thalamo-cortical network mechanisms. This agrees with results of neuronal modeling, indicating that sleep spindles and SWD can be simulated in a common cortical neuronal model [Sargsyan et al., 2007]; therefore, both spindles and SWD can appear in EEG as a manifestation of synchronization processes taking place in the same thalamo-cortical circuit during low vigilance state. It seems that, besides SWD, EEG of epileptic rats might exhibit various intermediate electroencephalographic patterns, such as type 2 sleep spindles and spiky EEG events (mentioned by Drinkenburg et al., 1991).

Chapter 5
Thalamo-cortical network mechanisms of SWD type I

CONTENTS

Episodes of typical absence epilepsy start unpredictably. Absence epilepsy has no clinical signs which can anticipate seizure onset, likewise, for example, a specific aura in temporal lobe epilepsy. Although some changes in breathing, cardiac activity and sedation might precede absence seizures [Mirksy and Van Buren, 1965], these changes are not specific and may appear in non-epileptic states as well, and, therefore, they can not be used as predictors of an absence seizure.

EEG monitoring and subsequent analysis of EEG data have provided more promising results in respect to early predictors of a seizure, however, findings are not always straightforward. Anticipatory changes in EEG amplitude and frequency can be observed several seconds before the onset of spike-wave discharges [Inoue et al., 1990]. This specific electroencephalographic pattern of seizure-precursor activity is called '*poorly developed epileptiform discharges*'. Also Genetic Absence Epilepsy Rats from Strasbourg (GAERS), reveal a characteristic pro-epileptic pattern, namely, medium-voltage 5–9 Hz oscillations, which precede the onset of spike-wave discharges (SWD) [Pinault et al., 2001]. However, it is unfortunate that 5–9 Hz oscillations in GAERS are not always followed by SWD; moreover, the same oscillatory pattern is encountered in non-epileptic rat strains, suggesting that 5–9 Hz oscillations have a physiologic nature and cannot be regarded as unique predictors of SWD.

Serious advances in disclosing early predictors of absence seizures are achieved with computational techniques applied to multi-channel EEG data. In patients with a mixed form of absence epilepsy (close to *petit mal* status), Niedermeyer et al (1979) has first found that the pre-ictal period is characterized by an increased rhythmical activity and stronger synchronization between bilaterally symmetric (homotopic) cortical areas. In patients with absence epilepsy, Garcia Dominguez et al (2005) and Aarabi et al (2007) have indicated significant changes in intracortical synchrony several seconds before the onset of SWD. According to Aarabi et al (2007), 48% of pre-ictal periods reveal a significant drop in synchronization with respect to the baseline level, 46% show a significant increase in the synchronization and 6% no changes in synchronization. It has been stressed that "*the spatiotemporal cortical synchronization is different from patient to patient but reproducible in each patient*" (p.216). Individual variations of intracortical synchrony have led to a failure in detecting a common synchronization pattern during seizure-precursor activity in human patients.

In the WAG/Rij rat model of absence epilepsy, spatiotemporal synchronization during pre-ictal periods does not reveal large individual variations [Meeren et al., 2002]. In all subjects, non-linear associations (intracortical and thalamo-cortical) appear to be reinforced before the onset of SWD. The small between-subject differences are likely to correlate with genetic homogeneity in a population of this inbred rat strain that cannot be assumed for the human population. However, in **Chapter 3.3** a common prototype of SWD-precursor (preSWD) for all subjects could not be identified. With EEG power spectrum and coherence analysis substantial differences in amplitude-frequency parameters of pre-SWD have been found. Among the four types of pre-SWD, each pre-SWD type could be distinguished from others by the spectral characteristics of the EEG power and by EEG coherence patterns in cortex and thalamus. Altogether, the nature of pre-epileptic processes underlying highly stereotypic SWD is intricate and poorly understood. We have investigated this question in the present **Chapter 5** and have focused on pre-epileptic cortico-thalamo-cortical network mechanisms of absence seizures. In **Chapter 5.1** we have used EEG coherence in order to examine changes in spatiotemporal synchronization over the thalamo-cortical system during transition from pre-SWD to the fully grown seizures. Finally, In **Chapter 5.2** we have used linear Granger causality in order to investigate cortico-thalamic bidirectional relationship before, during, and after SWD.

5.1 Changes of EEG coherence at the onset of SWD *

ABSTRACT

The study examines cortico-cortical and cortico-thalamic network synchronization at the onset of spike-wave discharges† (SWD) in a genetic model of absence epilepsy, WAG/Rij rats. Coherence was measured between multiple cortical areas (intracortical), reticular and rely thalamic nuclei (intrathalamic) and between the cortex and the thalamus. SWD-related increase of coherence (5 - 60 Hz) was found in all investigated pairs.

The highest increase of coherence was around the mean frequency of SWD (8-11.5 Hz) and in the harmonic band 16-21.5 Hz with two central maxima around 10 and 20 Hz. The frequency profile of coherence was different in different intracortical networks, therefore latter were divided into local, global and transhemispheric networks. The presumable source of SWD in the somatosensory cortex and its closest surroundings formed a minimal (local) circuit, in which occurrence of SWD was facilitated by a consistent shift of network synchrony from delta to alpha/beta frequencies. Transhemispheric coherence revealed the largest increase with an additional 16 Hz peak, suggesting a crucial involvement of the corpus callosum in the pathophysiology of absence seizures. The increase in interhemispheric coherence was largest between relatively remote somatosensory or frontal areas, supporting the assumption that SWD originate from the lateral fronto-parietal cortical area.

INTRODUCTION

Absence epilepsy is common among idiopathic primary generalized epilepsies [Commission, 1989]. Typical absence seizures appear without warning as a sudden interruption of consciousness and are accompanied by a characteristic electroencephalographic (EEG) signature: symmetric bilateral, widespread ~ 3 Hz spike-and-wave complexes. Simultaneous occurrence of clinical and EEG signs are necessary for accurate diagnosis of absence seizures. However, it is obscure why clinical manifestation of absence epilepsy associates with EEG spike-wave complexes, ultimately, the putative neurophysiological mechanisms of this disorder are still unknown. The benign nature of absence epilepsy precludes invasive investigation in humans, but at the same time, studies in different kinds of animal models (acute, chronic, pharmacological, genetic etc.) have largely contributed to our understanding of pathogenesis of absence epilepsy. In particular, aberrant transformations of thalamocortical rhythms are usually recognized as primary cause of absence seizures [Steriade, 2001]. In the present study we investigate thalamocortical dysfunction in a genetic model the of absence epilepsy, WAG/Rij rats (Wistar Albino Glaxo from Rijswijk [Coenen and van Luijtelaar 2003]). All individuals of this strain develop spontaneous spike-wave discharges (SWD) in the EEG [van Luijtelaar and Coenen, 1986]). SWD in WAG/Rij rats are accompanied by behavioral arrest and immobility, minimal facial myoclonic jerks, twitching of eyes and vibrissae altogether mimicking clinical manifestation of absence epilepsy in humans (face validity of WAG/Rij model). Also the pharmacological profile of seizures in WAG/Rij rats and in humans is similar: this enables predictions from the model to the patient (predictive validity of WAG/Rij model). Finally, absence seizures in WAG/Rij rats and in humans are based on the same theoretical grounds (construct validity). Therefore, our subjects fulfill all the necessary criteria for a valid and reliable animal model of absence epilepsy [Coenen and van Luijtelaar, 2003].

Field mapping of spike-wave activity in humans showed the earliest EEG changes in the posterior area, than the seizure moved anteriorly and had amplitude maximum in the frontal regions [Rodin and Ancheta, 1987; Rodin, 1999]. In WAG/Rij rats, EEG pattern of SWD gradually also changed from the onset to the end of a seizure [Midzianovskaia et al., 2001]. In GAERS (genetic absence epilepsy rats from Strasbourg [Pinault et al., 2001]) as well as in human patients (Inouye et al., 1990), SWD emerge suddenly from a normal background EEG and do not seem to be anticipated by any peculiar EEG changes. This gives an impression that spike-wave seizures are "suddenly generalized". Forerunners of spike-wave seizures are almost invisible on macroscopic EEG level, whereas, neuronal activity has definitely been changed before the seizure onset: *"…although the common definition of SW seizures, regarded as suddenly generalized and bilaterally synchronous activities, may be valid at the macroscopic EEG level, cortical neurons display time lags between their rhythmic spike trains, progressively increased synchrony*" [Steriade and Amzica, 1994, p. 2051]. These neuronal processes may case subtle EEG changes that cannot be easily seen in EEG, but can be detected with mathematical analysis of EEG signal. Unfortunately, only a few studies reported on EEG changes during transitional state between background activity and spike-wave seizures. As found, multiple causal relations of EEGs among different cortical loci start changing

* Published paper. Sitnikova E, van Luijtelaar G. Cortical and thalamic coherence during spike–wave seizures in WAG/Rij rats. Epilepsy Research, 2006; 71: 159–180.

† generalized SWD type I

more than ten seconds before spike-wave complexes could be visualized in EEG [Inouye et al., 1995]. In the present study we utilize EEG coherence as a powerful tool to measure synchronization throughout the cortex and the thalamus at transitions from normal to paroxysmal EEG pattern. By measuring network synchrony between different loci, we aim to identify probable network dysfunction that may prerequisite epileptic discharges.

Evidences are accumulating that the neocortex comprises a minimal substrate to produce spike-and-wave paroxysms [Steriade and Contreras, 1998; Steriade, 2005]. Clinical EEG data convincingly showed that spike-and-wave activity could originate from the frontal cortex [Pavone and Niedermeyer, 2000; Holmes et al., 2004]. The outcomes of the nonlinear association analysis of SWD in WAG/Rij rats showed a consistent cortical "focus" within the region of perioral projections of vibrissae and lips in the somatosensory cortex (SmI) [Meeren et al., 2002]. In WAG/Rij rats, this epileptic zone revealed a cytoachitectonical disorder [Karpova et al., 2005]. Local reduction of the excitability in the cortical epileptic focus with lidocaine in WAG/Rij rats [Sitnikova and van Luijtelaar, 2004] and with ethosuximide in GAERS [Manning et al., 2004] decreased SWD. The abovementioned studies supported the new "cortical focus" theory of generalized absence seizures [Meeren et al., 2005]. The further elaboration of this concept requires better understanding the local and global mechanisms of absence epilepsy. To approach this issue, we hypothesize that the epileptic focus in the SmI interacts with functionally and anatomically related regions, i.e. adjacent parietal and frontal (sensory and motor) areas, thus creating an oscillatory loop that generates SWD. If this is indeed the case, than the onset of SWD would relate to abundantly increase in fronto-parietal coherence and less significant changes of coherence between distant and functionally divergent areas (fronto-occipital and parieto-occipital coherence). Here we check this assumption.

Spike-wave seizures show strong bilateral synchronization in patients with absence epilepsy [Panayiotopoulos, 1997; Avoli et. al., 2001] and in GAERS and WAG/Rij rats]Danober et al., 1998; van Luijtelaar and Coenen, 1986]. Because intrahemispheric propagation of a seizure takes fairly short time (6 ms in average), it is proposed that the thalamus is not relevant for the bilateral spreading of seizure activity [Steriade and Contreras, 1998]. As known, the corpus callosum has a major role in bilateral synchronization of SWD, since after callosectomy the vast majority of SWD were no longer bilateral symmetrical, although occasionally bilateral synchronous SWD were seen after callosal transection [Vergnes et al., 1989]. Therefore, in addition to callosal pathways, there might be other pathways for trans-hemispheric spreading of SWD. Here we measure SWD-associated changes of trans-hemispheric interconnections between different cortical loci. According to the literature, spike-wave seizures reach the highest amplitude at the frontal cortex in patients [Holmes et al., 2004] and in rat models [Midzianovskaia et al., 2001; Mackenzie et al., 2004]. This led to the hypothesis that SWD-related bilateral associations in the frontal cortex would be stronger than in parietal and occipital areas.

Likewise the neocortex, the thalamus is actively participates in spike-wave activity [e.g. Seidenbecher et al., 1998; Avanzini and Franceschetti, 2003; Steriade 2003]. At least two thalamic structures are essentially involved in the genesis of discharges: reticular thalamic nucleus (RTN) and the thalamic relay nuclei [Inoue et al. 1993; Seidenbecher, 1998; Pinault et al., 2001]. The RTN consists of GABA-ergic neurons which have intrinsic membrane mechanism and generate rhythmic activity [e.g., Crunelli and Leresche, 2002; Avanzini and Franceschetti, 2003]. Those cells intimately associate with neurons in the dorsal thalamus, but do not project to the neocortex [Ohara and Lieberman, 1985]. A massive intra-thalamic synchronization may underlie the development of SWD, suggesting an increase of coherence between the RTN and specific thalamic nuclei, ventroposteromedial complex, VPM. This issue is also addressed in the present study.

Functionally interconnected cortical and thalamic sites appear to influence each other. During the first 500 milliseconds, one of the two bilateral neocortical foci consistently leads its thalamic counterpart (the VPM and the RTN) and after that the cortex and thalamus alternately lead and lag each other in an unpredictable way [Meeren et al., 2002]. Meeren and her co-authors (2005) supposed that (1) cortex and thalamus form a unified oscillatory network in which both cortex and thalamus drive each other and (2) "the role of the thalamus probably lies in providing a resonant circuitry to amplify and sustain the discharges" [Meeren et al., 2005, p.375]. Here we are challenged to find particular associations which may characterize thalamic network as a "resonant circuitry". For that purpose, we measure and compare coherence between the cortex (frontal and occipital) and thalamus (RTN and VPM). The primary sensory areas of neocortex receive only ipsilateral thalamic afferents [Jones, 1985], therefore we consider here only unilateral cortico-thalamic associations.

Coherence in the human EEG is usually measured in pre-determined frequency bands such as delta, theta, alpha, beta and gamma. We also used these "classical" frequency bands to evaluate statistically changes of EEG coherence leading to SWD. The frequency of SWD is known to fluctuate between 7-10 Hz: it is higher in the beginning and decreases towards the end [Midzianovskaia et al., 2001]. It is assumed that the coherence around 10 Hz would largely contribute to the expected increase of total coherence while the contribution of other frequencies may be less significant. This analysis of coherence in the frequency domain provides additional information on carrier frequencies of network associations and characterized frequency-specific pattern of network associations.

In all, we investigate cortico-thalamic network mechanisms which underlie transitions from normal oscillatory activity towards pathological spike-wave rhythm.

METHODS

Subjects and surgery

Fourteen male WAG/Rij rats (eleven-twelve months old, body weight ~ 310-390 g) were used. Experiments were carried out in accordance with the international principles of animal care and approved by the Ethical Committee on Animal Experimentation of the Radboud University Nijmegen. Chronic stainless still electrodes (electrode diameter = 0.2 mm) were implanted in small separate circular openings of the skull (diameter ~ 1 mm) during stereotactic surgery under isoflurane anesthesia. The first experimental group of rats (n = 8 rats) received epidural electrodes over both sides of cerebral cortex. Electrodes were placed over the frontal [AP +2, L 2], parietal (somatosensory representation area of paws, hindpaw [AP -1; L 2.5] and forepaw [AP 0, L 4], and vibrissal projections [AP –2, L +6]) and occipital [AP –6; L 5] areas. The second group (n = 6 rats) was implanted with four recording electrodes in the right hemisphere; among them one depth electrode was immersed into the ventroposteromedial thalamic nucleus, VPM [AP –3.5; L 2.5; H 7.2] and the other - into the rostral part of the reticular thalamic nucleus, RTN [AP –1.5; L 2.2; H 7.2]; two other electrodes were put epidurally over the frontal [AP +2, L 2] and occipital [AP –6; L 5] cortical areas. In both groups, ground and reference electrodes were located symmetrically in both sides of the cerebellum.

After the EEG part of the study, animals were deeply anesthetized with pentobarbital and direct current was passed through each thalamic electrode for iron repositioning. Brains were fixed and serial coronal sections were stained with Nissl. Positioning of thalamic electrodes was verified referring to the atlas of the rat brain [Paxinos and Watson, 1986]. EEG data from only those rats, which had both electrodes successfully implanted in the VPM and the RTN, was used for the statistical analysis.

EEG recording and analysis

Electrical activity was recorded during 5-7 hours in free behavior during dark period of dark-light cycle. SWD were identified using criteria described elsewhere [van Luijtelaar & Coenen, 1986; Midzianovskaia et al., 2001]. Briefly, SWD were easily distinguished from background EEG as high-voltage surface negative deflections consisting of 7-10 Hz spikes and slow waves (amplitude of SWD was several times higher than background activity). SWD lasted more than 1 sec with voltage maximum in the frontal area. In the frontal EEG, the first spike in the sequence of spikes and waves was used as a marker for SWD-onset (Fig. 5.1).

Signal analysis was performed using Brain Vision Analyser (© BrainProducts GmbH). We used coherence to assess changes of synchrony within thalamo-cortical circuit in the transitioning from the early stage to seizure onset. Coherence estimates phase consistency of the two EEG signals as a function of frequency independently from signal amplitude [Challis and Kitney, 1991]. Here we analyzed two subsequent (non-overlapping) 1 sec epochs - one before and one after the marked SWD-onset ($Coh_{beforeSWD}(\omega)$ and $Coh_{SWD}(\omega)$ correspondingly) using the following formula:

$Coh_{1,2}(\omega) = |G_{1,2}(\omega)|^2 / |G_{1,1}(\omega) x G_{2,2}(\omega)|$;where $Coh_{1,2}(\omega)$ - coherence between selected channels (1 and 2); ω - discrete frequencies; $G_{1,2},(\omega)$ - cross-power spectrum between channel 1 and channel 2; $G_{1,1}(\omega)$ and $G_{2,2}(\omega)$ – power spectra (autospectra) of ch 1 and 2.

First, coherence spectra of cortico-cortical, thalamo-cortical and thalamo-thalamic signals were computed within the frequency range 1-60 Hz with frequency resolution 0.5 Hz. Cortico-cortical coherence was examined in all possible combinations of the frontal, parietal (SmI, projection areas of vibrissae and paws) and occipital EEGs; thalamo-cortical coherence was established between two cortical EEGs (frontal and occipital) and two thalamic EEGs (from VPM and RTN); the thalamo-thalamic coherence was established between VPM and RTN (Fig. 5.1).

Next, changes of coherence, that accompanied SWD-onset, were established by computing differential coherence, $\Delta Coh(\omega) = Coh_{preSWD}(\omega) - Coh_{SWD}(\omega)$. Spectrum of $\Delta Coh(\omega)$ was averaged per channel pair and per animal. The $\Delta Coh(\omega)$ spectra were inspected for the maxima. In the majority of cases, $\Delta Coh(\omega)$ spectra showed independent maxima around 10 Hz and 20Hz (that is the mean frequency of SWD and harmonic); these extreme values were measured. To characterize resonance frequencies of network interactions, we performed two kinds of statistical analysis. First, we defined peaks on the averaged spectra of $\Delta Coh(\omega)$ and used frequencies of these peaks (resonance frequencies) as a constraint among all animals. Further statistical analysis determined the strength of network associations in pre-defined resonance frequencies. Second, we denominated peaks on individual spectra of ΔCoh, than frequency and amplitude of these peaks were measured and statistically compared. Analyses performed separately for intra-hemispheric, trans-hemispheric cortical and cortico-thalamic associated pairs. Factorial

ANOVA (followed by the post-hoc LSD test) was used to determine whether there was a significant difference between peak frequency and peak amplitude of ΔCoh(ω) among investigated pairs.

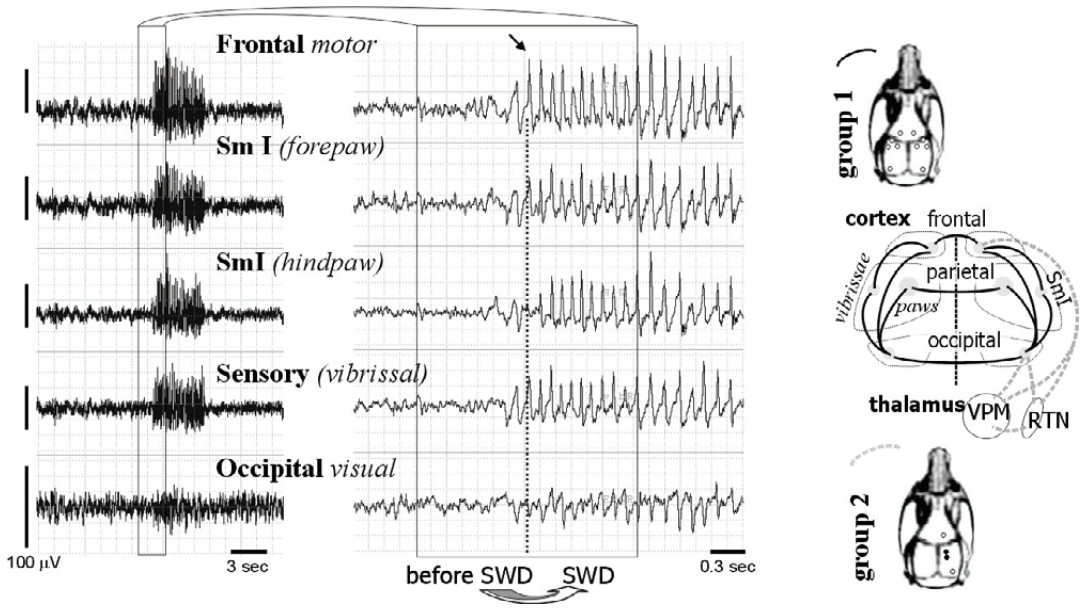

Figure 5.1. Spike-wave activity in WAG/Rij rat. EEG record containing SWD is shown on the left. Small black arrow pin-points the first spike (the formal marker of SWD-onset) on the frontal EEG tracing. Coherence was computed in two sequential intervals: 1 sec before and 1 sec after SWD-onset and statistically compared. Right side illustrates the location of the electrodes. Rats in Group 1 (n=9, black connecting lines in the schema of a brain) were equipped with epidural electrodes over the frontal, parietal and occipital cortical areas to measure coherence within one hemisphere (intra-hemispheric) and between the two hemispheres (trans-hemispheric or bilateral coherence). Group 2 (n=6 rats, gray dotted connecting lines) was implanted with two depth thalamic electrodes (in the ventroposteromedial thalamic nucleus, VPM, and in the reticular thalamic nucleus, RTN) and with two epidural electrodes in the frontal and occipital areas. All electrodes were located in the right hemisphere, therefore thalamo-cortical and intrathalamic coherence was established in unilateral (intra-hemispheric) pairs.

In order to quantify changes of network associations, differential coherence was determined for certain frequency bands [ΔCoh(Δω)], where Δω = 1-4.5; 5-7.5; 8-11.5; 12-15.5; 16-21.5; 22-27.5; 28-35.5; 36-47.5 and 48-60 Hz. We conducted a two-way ANOVA of the differential coherence [ΔCoh(Δω)] with factors 'band' (nine frequency bands) and electrode 'pair' separately for intra-hemispheric, trans-hemispheric cortical and cortico-thalamic associated pairs. Fisher LSD test was used to test for significant differences of ΔCoh(Δω) between the investigated pairs.

In order to evaluate statistically differences of ΔCoh(Δω) across frequency domain in a single population design, we averaged coefficients of ΔCoh with bin = 0.5 Hz in the following bands of interest: (1) mean frequency of SWD 8-11.5 Hz (ΔCoh8-11.5) and (2) the first harmonic, 16-21.5 Hz ($\Delta Coh_{16\text{-}21.5}$). Statistical analysis of $\Delta Coh_{8\text{-}11.5}$ and $\Delta Coh_{16\text{-}21.5}$ was carried out with ANOVA with consequent post-hoc LSD test. STATISTICA 6 software (StatSoft, Inc) was used for statistical evaluation of the data.

RESULTS

All fourteen experimental animals expressed a high amount of spontaneous SWD (10-45 seizures per hour). The EEG profile of SWD was typical and consistent among all animals. Pre-seizure EEG did not differ from the normal background activity, until the normal EEG continuum was suddenly interrupted by the first EEG aberrant sign (Fig. 5.1). The initial spike was followed by a long-lasting train of successive spikes and waves. Maximum amplitude of spikes was found in the frontal channel. The first eminent negative spike was easily recognized in all experimental animals and used to mark the formal onset of a SWD (Fig. 5.1).

Intra-hemispheric cortico-cortical coherence

Analysis of differential coherence (ΔCoh) revealed an increase of intra-hemispheric coherence associated with the onset of SWD (ΔCoh > 0). The average ΔCoh in all unilateral cortical pairs significantly exceeded zero $\Delta Coh_{avg}(ALL) = 0.08 \pm 0.09$ (± SD, $p<10\text{-}5$, t-test). Factorial ANOVA test showed that the increase of coherence was band-specific ($F=23.6$; $df=3,40$; $p<10\text{-}7$). Post-hoc LSD test indicated a significant increase of coherence in all

investigated pairs (p>0.05), except the *SmI(vib) - frontal* pair (Fig. 5.2A). The increase of coherence between *SmI(paws)* and the frontal cortex was significantly higher than in other investigated pairs (all p's<10-5), suggesting that occurrence of SWD may specifically overexcite *SmI(paws) - frontal* pathway. Besides that, *SmI(vib)* showed significantly stronger associations with an adjacent area, i.e. projection area of paws (ΔCoh_{avg}[SmI(vib)-SmI(paws)]=0.09 ± 0.08, Fig. 5.2A) comparing to associations with remote areas such as frontal cortex (ΔCoh_{avg}[SmI(vib)-frontal]= 0.06 ± 0.11) and occipital cortex (ΔCoh_{avg}[SmI(vib)-occipital]=0.05 ± 0.05, LSD test, all p's<0.05).

Occurrence of SWD caused frequency-specific changes of intra-hemispheric coherence (F[band]=30.5 df=8,40; $p<10^{-8}$). The increase of coherence was significant in frequencies $\Delta\omega_{sgf}$ = 5 to 36 Hz (ΔCoh ($\Delta\omega_{sgf}$), one-sample t-test, Table 5.1, Fig. 5.2A). The highest magnitude of ΔCoh was found in *SmI(paws)-frontal* EEG pair, where the increase of coherence was found in the whole 5 to 60 Hz range (Table 5.1). Noteworthy was that *SmI(paws) - frontal* EEG pair was the only cortico-cortical couple in which we found an increased functional coupling in gamma frequencies. Increase of coherence in *SmI(vib)-frontal* and *SmI(vib)-SmI(paws)* EEG pairs was slightly lower than that in *SmI(paws)-frontal* pair. In addition to that, low-frequency coherence (1-4.5 Hz) decreased in *SmI(vib)-frontal* and *SmI(vib)-SmI(paws)* pairs (Table 5.1).

As expected, the least intensive, albeit significant, was the increase of coherence between the most distant electrodes: in the *fronto-occipital* and *SmI(vib)-occipital* pairs (Table 5.1, Fig. 5.2A).

Table 5.1. Changes of coherence per frequency band (ΔCoh(Δω) ± SD) in transition period around the onset of SWD (ΔCoh(ω) = Coh[SWD] – Coh[beforeSWD]).

	ΔCoh(Δω) > 0				**ΔCoh(Δω) < 0**	
	$\Delta\omega_{sgf}$, Hz	**$\Delta Coh(\Delta\omega_{sgf})$**	**$\Delta Coh_{8\text{-}11.5}$**	**$\Delta Coh_{16\text{-}21.5}$**	**$\Delta\omega_{sgf}$,** Hz	**$\Delta Coh(\Delta\omega_{sgf})$**
INTRACORTICAL intra-hemispheric						
SmI(vib)–frontal	8–35.5	0.14±0.07	0.12±0.10	0.24±0.06 [B]	1–7.5	-0.08±0.07
SmI(vib)–SmI(paws)	5–35.5	0.12±0.08	0.14±0.04	0.17±0.07	1–5.5	-0.11±0.07
SmI(vib)–occipital	8–11.5/16–35.5	0.06±0.03	0.09±0.12	0.13±0.09		
SmI(paws)–frontal	5–59.5[G]	0.21±0.10	0.22±0.09	0.33±0.07 [B]		
SmI(paws)–occipital	8–11.5/16–35.5	0.11±0.07	0.12±0.15	0.17±0.12		
Frontal-occipital	8 – 35.5	0.06±0.03	0.13±0.13	0.15±0.09		
TOTAL		0.12±0.07	0.13±0.09	0.20±0.10 [B]		
INTRACORTICAL trans-hemispheric						
Frontal	5–27.5	0.15±0.10	0.33±0.11	0.28±0.19		
SmI(vib)	5–27.5	0.16±0.10	0.43±0.12	0.38±0.13	1–4.5	-0.12±0.12
SmI(paw)	5–11.5/16–21.5	0.18±0.07	0.35±0.09	0.16±0.13 [B]	1–4.5	-0.14±0.09
Occipital	8–35.5	0.12±0.08	0.14±0.18	0.19±0.17		
TOTAL		0.12±0.07	0.31±0.16	0.25±0.18		
CORTICO –THALAMIC						
Frontal–VPM	5–47.5[G]	0.19±0.08	0.37±0.13	0.26±0.07 [B]		
Frontal–RTN	8–47.5[G]	0.19±0.09	0.38±0.11	0.22±0.08 [B]		
Occipital–VPM	8–11.5/16–21.5	0.08±0.09	0.09±0.12	0.07±0.07		
Occipital–RTN	5–11.5/16–21.5	0.09±0.06	0.11±0.14	0.08±0.04		
TOTAL			0.24±0.18	0.16±0.10		
INTRATHALAMIC						
VPM–RTN	8–11.5	0.21±0.18	0.21±0.18	0.05±0.06 [B]	1–7.5/36–60	-0.08±0.09

The table presents only significant values of differential coherence (ΔCoh) per frequency band (Δω).
$\Delta\omega_{sgf}$ are those frequency bands in which increase of coherence, $\Delta Coh(\Delta\omega_{sgf})$ was significant (one-sample t-test).
$\Delta Coh_{8\text{-}11.5}$ and $\Delta Coh_{16\text{-}21.5}$ are averaged values of ΔCoh in 8 -11.5 Hz and 16-21.5 Hz bands correspondingly.
[B] - $\Delta Coh_{8\text{-}11.5}$ significantly different from $\Delta Coh_{16\text{-}21.5}$ (two-tailed t-test);
[G] – ΔCoh in gamma frequencies (above 35.5 Hz) was significantly higher than zero;
ns – ΔCoh was not significantly different from zero.

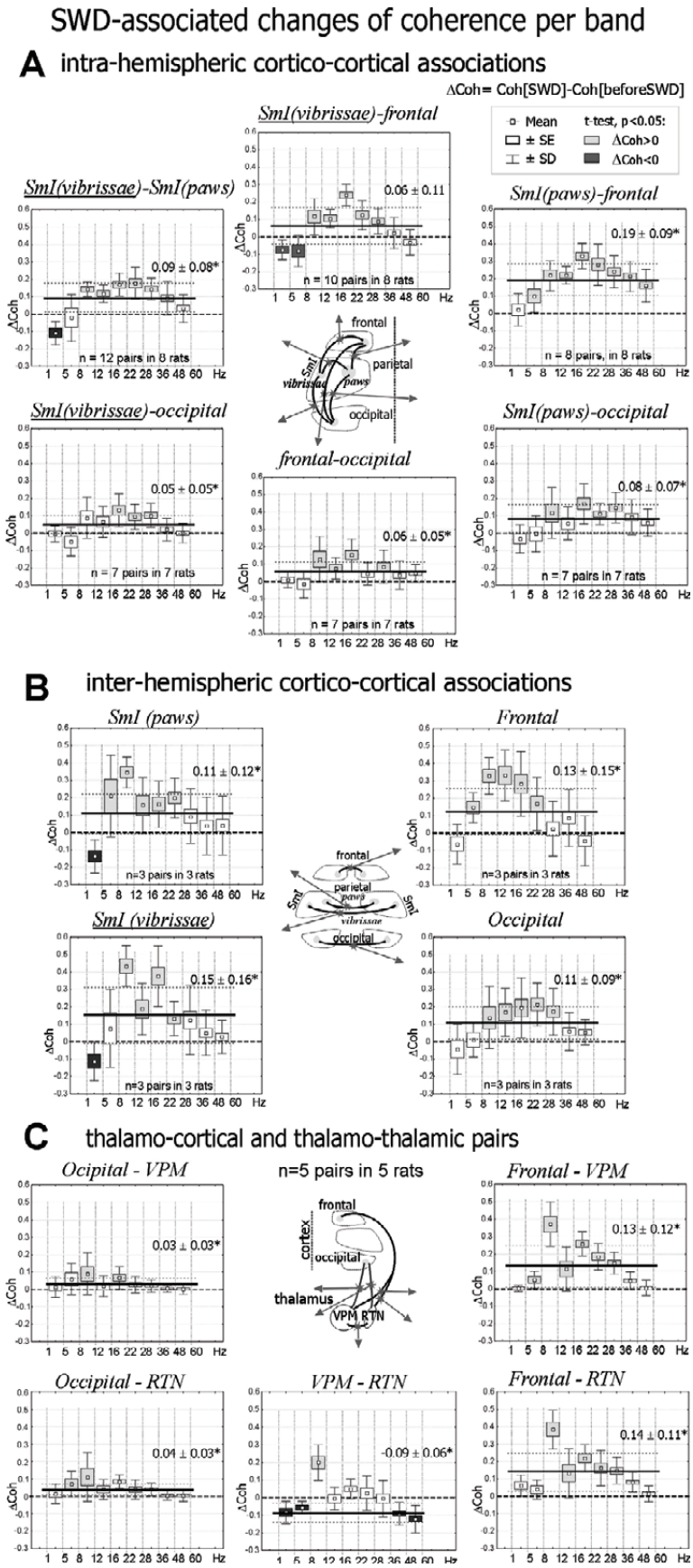

Figure 5.2. Changes of coherence that occurred with the onset of SWD. Axis of ordinates shows the differential coherence, $\Delta Coh=Coh[SWD]-Coh[beforeSWD]$, averaged per frequency band ($\Delta\omega$, abscissas) ± SD. Those bands in which increase of coherence was significant, $\Delta Coh(\Delta\omega)>0$, are colored in light gray; those bands in which coherence decreased, $\Delta Coh(\Delta\omega)<0$, are filled in black ($p<0.05$, one-sample t-test). Mean levels of ΔCoh (the average over bands from 1 Hz ending 60 Hz, ΔCoh_{avg}) are outlined with thick black line; numbers above the lines show ΔCoh_{avg} ± SD and asterisks indicate those values of ΔCoh_{avg} which were significantly above zero (one-sample t-test, $p<0.05$).

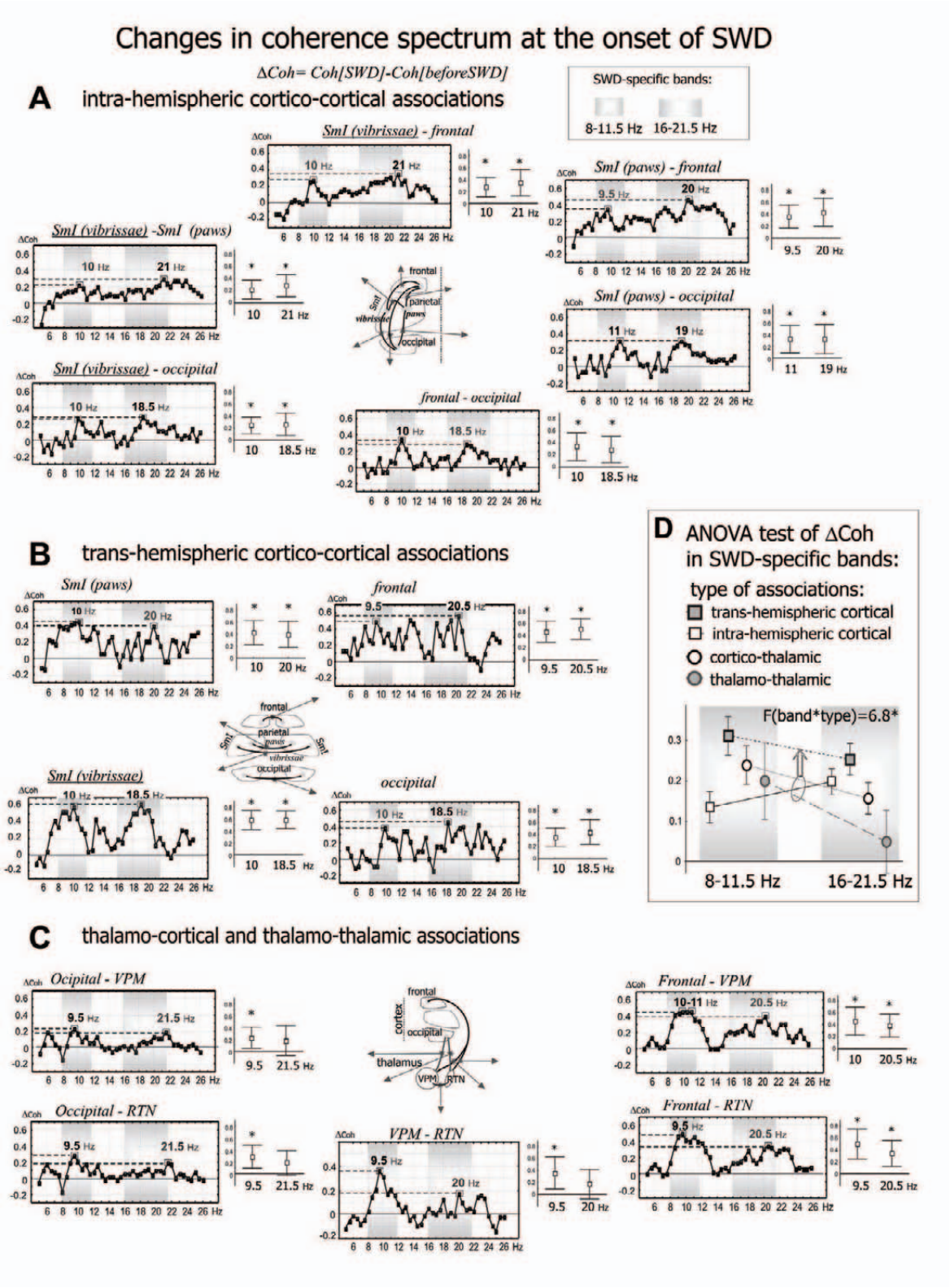

Figure 5.3. The averaged spectra of differential coherence ΔCoh(ω) for ω = 5 - 25 Hz. Two characteristic SWD-specific bands ($\Delta\omega_{SP}$) are indicated with gray transparent rectangles. These bands involve the mean frequency of SWD (~10 Hz, band 8-11.5 Hz) and the first harmonic (~ 20 Hz, band 16-21.5 Hz). **A-C**. Peak spectral values (encompassed with squares) characterize resonance frequencies of network associations: the dominant and subdominant frequencies (the highest and second high peaks correspondingly). Statistical data characterizing peak values (resonance frequencies) of ΔCoh are shown in box-whisker charts on the right. Those peaks which significantly exceeded zero (one-sample t-test) are asterisked. **D**. ΔCoh in SWD-specific frequency bands, $\Delta Coh_{8\text{-}11.5}$ and $\Delta Coh_{16\text{-}21.5}$ correspondingly (factor 'band') in different association pairs (factor 'type'). There was a significant effect of the 'band' and 'type' factors, also the interaction between them, 'band*type', was significant (all p's<0.01, two-way ANOVA). Note that associations in trans-hemispheric pairs were significantly higher than in other types (Fisher LSD test, thick upward arrow).

Fig. 5.3A presents the averaged spectrum of ΔCoh with two major spectral peaks: the first, low-frequency peak occurred around mean frequency of SWD, 9.5-11 Hz, and the second, high-frequency peak was in the harmonic range, 18.5-21 Hz. Amplitude of both peaks was significantly higher than zero (ΔCoh>0, one-sample t-test, p's<0.05, Fig. 5.3A). Low-frequency and high-frequency peaks were of the same magnitude and did not differ in different investigated pairs (two-way ANOVA, p's>0.05).

The increase of intra-hemispheric cortical coherence in SWD-specific frequencies was evaluated separately for 8-11.5 Hz and harmonic 16-21.5 Hz band. In total, the averaged ΔCoh in 8 -11.5 Hz band was significantly lower than ΔCoh in 16-21.5 Hz ($\Delta Coh_{8\text{-}11.5} > \Delta Coh_{16\text{-}21.5}$, F=6.8, df=5,108, p<0.01, Table 1, Fig. 5.4Aa). Further ANOVA analysis of differences among the six intra-cortical pairs showed that $\Delta Coh_{8\text{-}11.5}$ differed in different pairs (F=4.9, df=3.16, p<0.01). According to LSD test, $\Delta Coh_{8\text{-}11.5}$ in *SmI(paw)-frontal* cortex was significantly higher than in the other pairs (p<0.05, Fig. 5.4A). The same results were obtained in 16-21.5 Hz band, where the effect of 'pair' was significant (F= 21.1, df=5.25, p<0.01) and LSD test showed that $\Delta Coh_{16\text{-}21.5}$ was significantly higher in *SmI(paw)-frontal* and in *SmI(vib)-frontal* pairs (p<0.05, Fig. 5.4A).

As can be seen in averaged spectra in Fig. 5.3A, both low-frequency and high-frequency peaks were relatively flat. The sharpness of peaks was reduced with averaging across subjects because of slight fluctuations in frequencies of peaks in different individuals. Peaks on coherence spectra (coherence maxima) characterize the network resonance (carrier) frequencies.

Table 5.2. SWD-associated changes of coherence in frequency bands of interest, ΔCoh(Δω) and pooled ΔCoh_{full} (± SD, bin = 0.5 Hz).

	Pooled ΔCoh_{full} [1 - 60] Hz	**SWD-specific** (1) $\Delta Coh(\Delta\omega_{SP})$ [8-11.5]+[16-21.5] Hz	**SWD-nonspecific** (2) $\Delta Coh(\Delta\omega_{noSP})$ [12-15.5]+[22-35.5] Hz	**Low freq.** (3) $\Delta Coh(\Delta\omega_{LOW})$, [1 - 7.5] Hz	**High freq.** (4) $\Delta Coh(\Delta\omega_{HIGH})$ [36 – 60] Hz
INTRACORTICAL intra-hemispheric					
SmI(vib)–frontal	0.05±0.12	**0.19 ± 0.10** ^{H}	**0.11±0.07** ^{H}	**-0.08±0.07** ^{L}	**-0.01±0.09** ^{L}
SmI(vib)–SmI(paws)	0.06±0.09	**0.16 ± 0.06** ^{H}	**0.15±0.07** ^{H}	**-0.03±0.14** ^{L}	0.06±0.09
SmI(vib)–occipital	0.05±0.09	**0.11 ± 0.10** ^{H}	0.08±0.07	**-0.02±0.07** ^{L}	**0.01±0.06** ^{L}
SmI(paws)–frontal	0.20±0.12	**0.28 ± 0.09** ^{H}	**0.25±0.10** ^{H}	**0.05±0.09** ^{L}	0.18±0.10
SmI(paws)–occipital	0.09±0.11	**0.15 ± 0.13** ^{H}	0.11±0.09	**-0.04±0.09** ^{L}	0.07±0.09
Frontal-occipital	0.06±0.09	**0.14 ± 0.11** ^{H}	0.07±0.08	**0.01±0.06** ^{L}	**0.01±0.06** ^{L}
INTRACORTICAL trans-hemispheric					
Frontal	0.09±0.21	**0.30 ± 0.16** ^{H}	0.14±0.19	0.03±0.15	**-0.01±0.18** ^{L}
SmI(vib)	0.12±0.19	**0.40 ± 0.15** ^{H}	0.14±0.16	**-0.01±0.18** ^{L}	**0.04±0.11** ^{L}
SmI(paw)	0.10±0.18	**0.24 ± 0.15** ^{H}	0.14±0.15	**-0.02±0.12** ^{L}	0.04±0.16
Occipital	0.11±0.14	0.17 ± 0.17	**0.18±0.13** ^{H}	**-0.02±0.13** ^{L}	**0.06±0.09** ^{L}
CORTICO –THALAMIC					
Frontal–VPM	0.11±0.13	**0.30±0.11** ^{H}	0.15±0.09	**0.02±0.04** ^{L}	**0.02±0.05** ^{L}
Frontal–RTN	0.12±0.12	**0.38±0.12** ^{H}	0.15±0.10	**0.05±0.06** ^{L}	**0.05±0.06** ^{L}
Occipital–VPM	0.02±0.06	**0.09±0.09** ^{H}	0.02±0.04	**0.03±0.07** ^{L}	**0.01±0.03** ^{L}
Occipital–RTN	0.03±0.06	**0.11±0.09** ^{H}	0.04±0.05	**0.04±0.07** ^{L}	**0.01±0.03** ^{L}
INTRATHALAMIC					
VPM–RTN	-0.03±0.11	**0.20 ± 0.11** ^{H}	0.01±0.09	**-0.07±0.05** ^{L}	**-0.10±0.07** ^{L}

The table shows mean value of the pooled differential coherence (ΔCoh_{full}, the average across 1-60 Hz) with the averaged values of ΔCoh in the following bands of interest: (1) - ΔωSP, specific SWD frequencies that includes mean frequency of SWD (8-11.5 Hz) and first harmonic (16-21.5 Hz); (2) ΔωnonSP, SWD-non-specific frequencies, 12-15.5 and 22-35.5 Hz Hz; (3) low frequencies $\Delta\omega_{LOW}$ 1-7.5 Hz and (4) high frequencies, $\Delta\omega_{HIGH}$, 36-60 Hz.

Mean values of differential coherence in bands which significantly differed from pooled differential coherence (ΔCohΔω versus ΔCoh_{full}, two-tailed t-test), are typed in bold.

^{H} – differential coherence in a band, ΔCohΔω, was significantly higher than ΔCoh_{full} ($\Delta Coh\Delta\omega > \Delta Coh_{full}$);

^{L} – $\Delta Coh\Delta\omega < \Delta Coh_{full}$, p<0.05.

We enhanced accuracy of coherence analysis and isolated the carrier frequencies of intra-hemispheric associations by measuring peaks in individual spectra of ΔCoh. Usually, it was possible to distinguish two (or three) maxima in ΔCoh(ω) which were considered as resonance frequencies of network associations. The first peak, P_{low}, was found around 10.2±1.3 Hz (± SD) and it's amplitude was 0.44±0.12 ANOVA analysis did not show any significant differences of P_{low} across all investigated pairs. The second peak (P_{high}) occurred in 20.6±1.8 Hz with amplitude 0.48±0.18 (Fig. 5.5A). Mean frequency of P_{high} in posterior pairs (that included occipital cortex: *SmI-occipital* and *fronto- occipital*) was 19.3 ± 1.3 Hz that is significantly lower than frequency of P_{high} in the

anterior pairs, *SmI(vib)-frontal* and *SmI(raws)-frontal* pairs 21.1 ± 1.7 Hz (F=11.9, df=5.64, p<0.01, LSD test p<0.05). *SmI-frontal* and *SmI(raws)-SmI(vib)* were distinctive from others by the presence of the third additional peak around 15.9±1.3 Hz (P_{middle}) which was of high amplitude 0.54±0.20 (Fig. 5.5A)

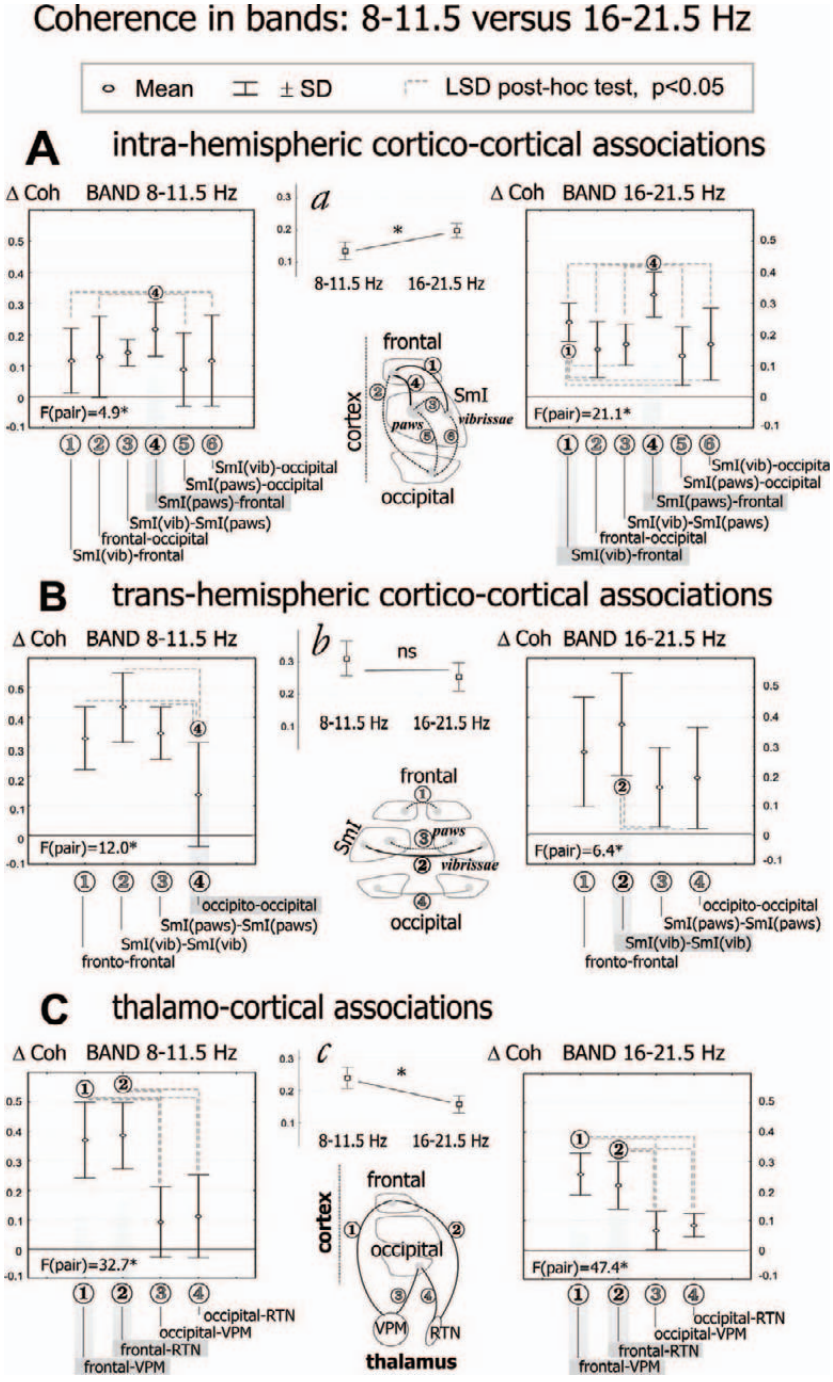

Figure 5.4. Changes of coherence in two characteristic frequency bands: 8-11 Hz (around mean frequency of SWD, $\Delta Coh_{8-11.5}$) and in 16-21.5 Hz (harmonic range, $\Delta Coh_{16-21.5}$). **A-C**. ANOVA of differences between coefficients of ΔCoh among investigated EEG pairs; asterisks denote F-values significance at p<0.05. Dotted lines are drawn between those pairs in which differences of ΔCoh were significant (post-hoc analysis with Fisher's LSD test). In-between frames **Aa**, **Bb** and **Cc** show statistical data on $\Delta Coh_{8-11.5}$ versus $\Delta Coh_{16-21.5}$ (averaged in all EEG pairs; ANOVA, factor 'band': *ns* – difference was not significant and * - significant differences at p<0.05).

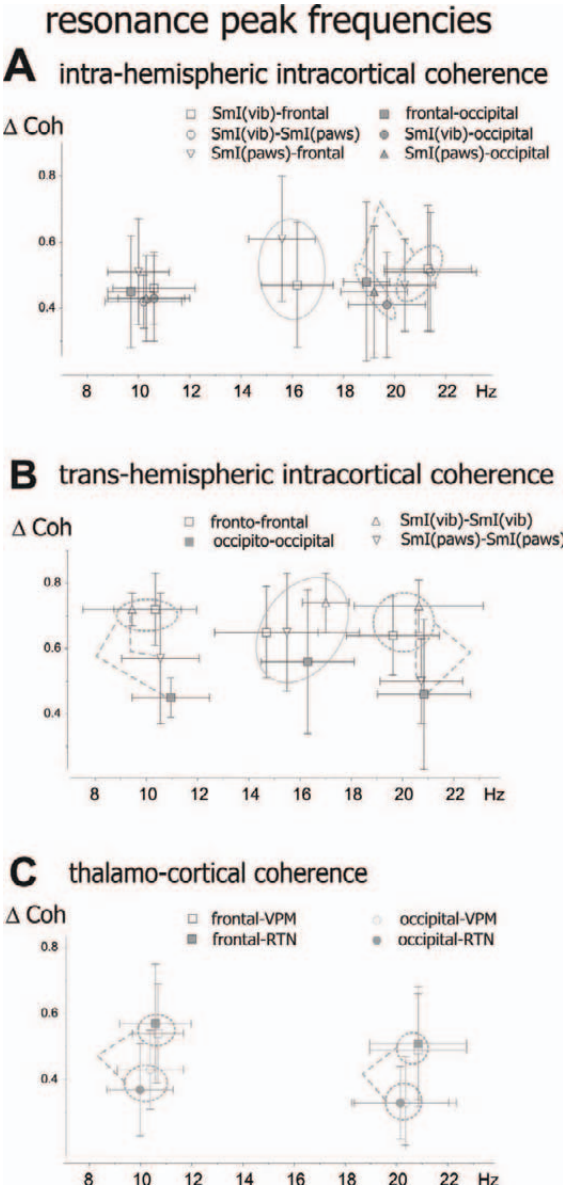

Figure 5.5. Statistical data of individual peaks of ΔCoh (mean amplitude and mean frequency ± SD) representing carrier frequencies of cortico-cortical and thalamo-cortical network associations. All investigated pairs showed two main peaks: low-frequency peak, P_{low} ~ 10 Hz and high-frequency peak, P_{high} ~20 Hz. An additional ~ 16 Hz peak was typical for bilateral associative pairs and was seldom in other EEG pairs. Encircled are EEG pairs in which peak measures (amplitude and frequency) were similar. Thick gray dotted lines show EEG pairs in which peak amplitude was significantly different (factorial ANOVA, $p<0.05$).

Trans-hemispheric cortico-cortical coherence

Two-way ANOVA test demonstrated that the onset of SWD caused significantly more intensive increase of coherence in trans-hemispheric pairs as compared to intra-hemispheric pairs ($F=6.3$, $df=1.72$, $p<0.01$); this effect was frequency-specific ($F=3.43$, $df=8.72$, $p<0.01$). The results are graphically displayed in Fig 5.2B, 5.3B and 4B. The increase of the averaged ΔCoh per band (ΔCoh_{avg}) was also significant: the overall average of trans-hemispheric coherence was ΔCoh_{avg} (ALL)=0.12 ± 0.13 (± SD), $p<10\text{-}6$, t-test. In all bilateral frontal, parietal and occipital areas increase of averaged coherence (ΔCoh_{avg}) was the same (ANOVA test, factor 'pair', $p<0.05$). However, there was a significant different distribution of ΔCoh over frequency bands (ANOVA test, factor 'band', $F=11.3$ $df=8.24$; $p<10\text{-}6$). No significant interaction was found between bands and pairs, demonstrating that changes of trans-hemispheric coherence were not the same for all bands. The most intensive increase of coherence was found in frequencies 5 - 27.7 Hz (one-sample t-test, Table 5.1).

Two homologous sites in the *SmI* (paws and vibrissal regions) showed a significant ($p<0.05$) decease of low frequency (1-4.5 Hz) synchronization. This decrease was absent in the *frontal* and *occipital* areas (Fig. 5.2B).

The averaged spectra of trans-hemispheric ΔCoh showed two central spectral peaks (Fig. 5.3B): one with low-frequency (9.5-10 Hz) and anther – with high-frequency (18.5-20.5 Hz); those peaks were equal to each other

and showed the same magnitude in different investigated pairs (two-way ANOVA, $p>0.05$). However, both peaks significantly exceeded zero ($\Delta Coh>0$, one-sample t-test, p's<0.05, Fig. 5.3B).

Changes of trans-hemispheric ΔCoh in 8-11.5 Hz ($\Delta Coh_{8\text{-}11.5}$) and harmonic 16-21.5 Hz ($\Delta Coh_{16\text{-}21.5}$) frequencies were compared with two-way ANOVA (Fig. 5.4B, 5.4Bb). The total value of $\Delta Coh_{8\text{-}11.5}$ was equal to $\Delta Coh_{16\text{-}21.5}$ (Fig. 5.4b). Independent analysis of ΔCoh in these bands revealed that the increase of coherence significantly differed in different pairs ($F(\Delta Coh_{8\text{-}11.5})$ =12.0, df=3.16, $p<0.01$ and $F(\Delta Coh_{16\text{-}21.5})$ =6.4, df=3.24, $p<0.01$). In 8-11.5 Hz band, occipital pair had a significantly lower $\Delta Coh_{8\text{-}11.5}$ compared to that in other pairs (LSD test, $p<0.05$, Fig. 5.4B). In 16-21.5 Hz band, two symmetrical loci in the *SmI(vib)* were coupled significantly higher than bilateral *occipital* and *SmI(paws)* loci (LSD test, $p<0.05$, Fig. 5.4B). Trans-hemispheric $\Delta Coh_{16\text{-}21.5}$ in *SmI(vib)* was equal to that in the frontal cortex. This suggests that anterior cortical territories more easily communicate in 16-21.5 Hz than in 8-11.5 Hz. Furthermore, in 16-21.5 Hz bilateral coherence in the *SmI(vib)* was significantly higher than in other EEG pairs, because the *SmI(vib)* tie in with the focal epileptic zone (Meeren et al., 2002), a particularly bilateral synchrony in 16-21.5 Hz may be primarily responsible for the genesis of SWD.

It is important that the trans-hemispheric coherence did not correlate with inter-electrode distance. Distances between symmetrical left/right electrodes in *SmI(vib)* were 12 mm > *occipital* 10 mm > *SmI(paws)* ~ 6mm > *frontal* 4 mm (see Fig. 5.1 for the schematic electrode location), but mean values of bilateral ΔCoh_{full} did fall in this sequence: ΔCoh[SmI] > ΔCoh[frontal] > ΔCoh[occipital] (Table 5.1). Although the distance between left/right electrodes in SmI(vib) was roughly comparable to that of the occipital pair (12 and 10 mm), coherence in SWD-specific bands showed a three-hold difference: $\Delta Coh_{8\text{-}11.5}$ SmI(vib)/occipital=0.43/0.14 and $\Delta Coh_{16\text{-}21.5}$ SmI(vib)/occipital=0.38/0.19 (Table 5.1, Fig. 5.4C).

The individual spectra of ΔCoh were also inspected for the presence of spectral peaks. Tree peaks were detected in all trans-hemispheric pairs (Fig. 5.5B): Plow (mean frequency of 10.3 ± 1.6 Hz and $\Delta Coh(P_{low})=0.62 \pm 0.16$ (± SD)), P_{middle} (15.8 ± 1.8 Hz and $\Delta Coh(P_{middle}) = 0.65 \pm 0.14$) and P_{high} (20.3 ± 1.9 Hz and $\Delta Coh(P_{high}) = 0.61 \pm 0.15$). According to the outcomes of the ANOVA, the frequencies of P_{low}, P_{middle} and P_{high} were the same in all investigated pairs ($p>0.05$); however, the magnitude of these peaks was significantly different in different investigated pairs ($F=7.6$, df=3.36, $p<10\text{-}4$, $p>0.05$). LSD test showed that the amplitude of P_{low} and P_{high} was significantly higher in the frontal and *SmI(vib)* pairs than in *SmI(paws)* and occipital pairs ($p<0.05$, Fig. 5.5B). Pmiddle had equal amplitude in all trans-hemispheric pairs.

Because this additional peak of coherence ~ 16 Hz was found in all *trans-hemispheric* pairs, we assume that bilateral spreading of SWD is governed by supplementary mechanism of global synchronization. Frequency of P_{middle} (~16 Hz) fell almost halfway between fundamental (10 Hz) and harmonic (20 Hz) frequencies of SWD. This particularity of trans-hemispheric synchronization might be accounted for the *corpus callosum*.

To summarize, occurrence of SWD requires stronger cross-hemispheric communications (between functionally analogues areas) as compared to unilateral associations (functionally heterogeneous areas), this may promote bilateral propagation of SWD and further generalization of seizure activity. In total, there were no differences in *trans-hemispheric* coherence among investigated pairs. Anterior bilateral pairs (*frontal* and *SmI*) revealed more intense associations in SWD-specific frequency bands (including mean frequency of SWD and it's harmonic), while occipital coherence was centered around SWD-nonspecific frequencies. *Trans-hemispheric* pairs in the *vibrissal* area of the *SmI* and, to a lesser extent, in the *frontal* cortex showed particularly high coherence in the harmonic frequencies of SWD. Coherence in low frequencies (1-5 Hz) is diminished, especially in the *SmI* (in vibrissal and paws regions). Coherence in frequencies above 30 Hz was also relatively low.

Cortico-thalamic and thalamo-thalamic coherence

The results are graphically displayed in Fig 5.2C. The onset of SWD caused a significant aggravation of coherence between the frontal cortex and both thalamic nuclei: the ventroposteromedial thalamic nucleus, VPM (fronto-VPM pair, $\Delta Coh_{avg} = 0.13 \pm 0.12$ (± SD), $p<10^{-7}$) and the reticular thalamic nucleus, RTN (fronto-RTN pair, $\Delta Coh_{avg} = 0.14 \pm 0.12$ (± SD), $p<10^{-6}$). The increase of occipito-thalamic coherence was also significant but small (in occipital-VPM pair $\Delta Coh_{avg} = 0.03 \pm 0.03$ (± SD), $p<10^{-5}$) and occipital-RTN pair, $\Delta Coh_{avg} = 0.04 \pm 0.04$ (± SD), $p<10^{-5}$).

The interaction between the VPM and the RTN also changed with the onset of SWD but these changes were remarkably different from that in *cortico-thalamic* pairs. First, ΔCoh averaged per band from 1 to 60 Hz appeared significantly below zero ($\Delta Coh_{avg} = -0.09\pm0.06$ (± SD), $p>0.05$ t-test, Fig. 5.2C). Averaging of ΔCoh with 0.5 Hz bin in the same frequency range (1-60 Hz) gave also a negative value ($\Delta Coh_{full} = -0.03 \pm 0.11$) but it was indistinguishable from zero (ΔCoh_{full} in Table 5.2). This discrepancy was caused by differences in frequency resolution which emerged with the averaging of nonuniform spectrum of ΔCoh: the strong increase of ΔCoh was limited to a narrow SWD-specific band (8-11.5 Hz), however, the decrease of ΔCoh spread over the low and high-

frequency bands (Table 5.1, Fig. 5.2C). We used full-range ΔCoh, which was computed with high frequency resolution (ΔCoh_{full}) in order to contrast changes of coherence in different frequency bands. Table 2 shows that ΔCoh in low and high frequencies ($\Delta\omega_{LOW}$ and $\Delta\omega_{HIGH}$) was lower than ΔCoh_{full}, while in SWD-specific frequencies ($\Delta\omega_{SP}$) it exceeded ΔCoh_{full} and in SWD-nonspecific frequencies ($\Delta\omega_{nonSP}$) it was equal to ΔCoh_{full}.

VPM-RTN was the only pair in which ΔCoh in 16-21.5 Hz band was not significantly different from zero and $\Delta Coh_{16\text{-}21.5}$ was lower than $\Delta Coh_{8\text{-}11.5}$ ($\Delta Coh_{8\text{-}11.5} > \Delta Coh_{16\text{-}21.5}$, $p<0.05$, Table 5.1). This pair also differed from others by a significant decrease of coherence in gamma range 36-60 Hz (Fig. 5.2C, Table 5.1).

The averaged *thalamo-thalamic* spectrum of ΔCoh (Fig. 5.3C) had only a 9.5 Hz peak with amplitude significantly different from zero (one-sample t-test, $p<0.05$), while the ~ 20 Hz peak was indistinguishable from zero ($p>0.05$).

The onset of SWD affected *cortico-thalamic* coherence in a frequency-specific manner ($F[band]=12.6$ $df=8,32$; $p<10^{-9}$). The strongest increase of coherence was observed in 8-11.5 Hz (LSD test, $p<0.001$). In total, $\Delta Coh_{8\text{-}11.5}$ was significantly higher that $\Delta Coh_{16\text{-}21.5}$ (Fig. 5.4C). Post-hoc analysis demonstrated that this effect was significant only in *fronto-thalamic* pairs, but not in *occipito-thalamic* pairs. Fig. 5.3C illustrates that the averaged spectrum of ΔCoh of *fronto-thalamic* associations had two peaks and both of them significantly exceeded zero, but in *occipito-thalamic* pairs only the 9.5 Hz peak appeared to be significantly above zero. Individual analysis of these peaks showed that frequency of P_{low} was around 10.3 ± 1.2 Hz (± SD, Fig. 5.5C) and amplitude was 0.48 ± 0.15. P_{high} occurred in 20.5 ± 1.9 Hz and it's amplitude was 0.42 ± 0.15 (Fig. 5.5C).

DISCUSSION

It is found here that the onset of SWD was associated with higher functional coupling throughout cortico-*cortical*, *thalamo-thalamic* and *thalamo-cortical* associative pairs. This increase of oscillatory synchrony has been topographically and frequency specific, suggesting that functional relationship explicitly distinguishes between different oscillatory circuits. This may imply non-homogeneous spreading of SWD over *thalamo-cortical* system and contradicts the former viewpoint that spike-wave seizures occur without localizing features (Panayiotopoulos, 1997). We found persistent transitive changes of EEG coherence at the onset of a seizure, that lead to uncertainty regarding the belief that absence seizures are suddenly (primary) generalized. A transitional period (for at least one second) is needed for seizure to become generalized, during this period all parts of *thalamo-cortical* loop develop more coherence in 10 Hz and some parts of the loop exhibit more synchrony in supplementary frequencies such as harmonic frequency ~ 20 Hz and intermediate ~ 16 Hz. In the following section we put our findings in parallel with other related EEG studies of absence epilepsy and discuss how network dysfunction can lead to epileptic activity.

Technical considerations: EEG coherence as a measure of thalamo-cortical network synchrony

A crucial question in epileptology concerns possibilities of extracting information from the EEG to describe the dynamics of epileptic seizures. Because seizures are manifestation of excessive neuronal synchronization ('hypersynchronization'), one can use coherence to measure synchronization and highlight transformation from normal to pathological EEG pattern [e.g. Jerger et al., 2001, Worrell et al., 2004]. Coherence estimates a consistency in the phase between two EEG signals independently from signal amplitude [Challis and Kitney, 1991; Nunez et al., 1997] and it is a measure of functional interactions (functional coupling) between two regions. Recently this technique became a main focus of scientific interest in neuropsychiatric diseases, it is also widely used in psychophysiology and in clinical EEG studies [Schnitzler and Gross, 2005]. Besides its effective usage in humans [Nunez et al., 1997], EEG coherence is extremely rarely applied to animal EEG data. Virtually no attempts were made to use coherence EEG analysis to describe dynamic features of absence epilepsy in animal models.

Besides advantages of using rats as experimental subjects, some peculiarities in EEG recording design in animals differ from the standard EEG techniques used in humans. The first distinction concerns electrode location and skull conductance. In our experiments, recording electrodes were surgically implanted onto the brain either on the cortical surface (epidurally) or in-depth of the brain to reach thalamic structures. In both cases EEG was recorded directly from neural sources (in fact, it was recording of epidural field potentials). Human EEG is typically recorded from 16 – 128 (256) scalp locations with EEG sensors located about 1 cm from the nearest neural sources. This method allows measurements of scalp potentials, which comprise low-pass filtered version of epidural EEG [Nunez, 2000]. The advantage of our EEG montage is that EEG data was not contaminated by conducting skull, however, we were not able to place more than ten EEG electrodes.

A second difference of our EEG method from human EEG lies in the size and construction of EEG sensors. Apparently, the information content of EEG can be affected by physical properties of EEG sensors (i.e. the electrode size and contact impedance etc). The standard EEG sensors used in human electroencephalography are

much larger than electrodes used in the present study (tip diameter 0.2 mm). For instance, the diameter of cup EEG electrodes is 6 mm (pediatric) or 10 mm (adult). Considering this difference in electrode size, EEG signal recorded with our fine electrodes has thirty to fifty times higher temporal resolution as compared with standard EEG sensors. Taking for granted that electrical processes during absence seizures are comparable in humans and in rat model, one should consider anatomical differences and differences in size (human brain is approximately 450 times larger than rat brain) and probable specificity of spatial organization of electrical fields in our subjects and in human patients. In spite of all these details, it was possible to identify the EEG signatures of absence epilepsy, spike-wave discharges in the WAG/Rij model. The schema of EEG recording that was used in the present study and coherence analysis provided statistically significant results, suggesting that with the analysis of EEG coherence one can appropriately study EEG correlates of absence epilepsy.

Strictly speaking, coherence measures linear interdependence between two stationary signals. Since many features of EEG signals cannot be generated by linear models, it is generally argued that non-linear measures may give more information than the one obtained with conventional linear approaches [Quian Quiroga et al., 2002; Thakor and Tong, 2004]. Quian Quiroga and his colleagues (2002) performed a case study rat EEG to compare various synchronization measures such as linear (cross-correlation and coherence) and non-linear (non-linear interdependences, phase-synchronizations and mutual information). It was shown that all kinds of measurements, including coherence, gave qualitatively the same results. This approves sufficient validity of the chosen method of EEG analysis. The results of the present analysis of coherence convincingly shows that forthcoming absence seizures has been associated with complex changes of EEG coherence within intracortical, thalamo-cortical and intrathalamic circuitry, moreover, these changes had topographical and frequency dependency.

EEG coherence and neuronal network mechanisms at the earliest stages of spike-wave seizures

In the present study we characterize changes of EEG coherence in transition state from SWD-precursor activity to SWD. In our subjects, we were able to mark the onset of SWD with relatively high degree of precision (using the first high-voltage spike in spike-wave sequence as a starting point) and the period one second before SWD (preSWD). This disagrees with studies that have found a gradual transitioning from the background activity to the spike-wave complexes [Inouye et al., 1990; Inouye et al., 1995]. Unlike that in WAG/Rij rats, in GAERS SWD were gradually transformed from normal delta/5–9 Hz oscillations: *"…the onset of the SWD was difficult to detect because there was no apparent discontinuity between the delta/5–9 Hz oscillations and the SWD, the amplitude of the spike in the SW tending to increase progressively with occasional irregularities"* [Pinault et al., 2000]. We need to admit that abrupt onset of SWD in our subjects has been observed in the frontal and parietal EEGs, but this cannot be seen at the occipital area EEG and in the thalamus.

Even though the onset of SWD in our subjects was clearly distinguished from the background EEG, it does not mean that SWD are *"suddenly generalized"* EEG paroxysms. Our data support the general theoretical idea of Prof. Steriade and his group that spike-wave seizures are not *"suddenly generalized"* [Steriade and Amzica, 1994]. One should add that visually abrupt onset of SWD in the frontal and parietal EEGs has been anticipated by continuous changes of coherence between key elements in the thalamus and neocortex. Our work describe macroscopic EEG changes at the early stages of SWD and may be linked with the cellular, neuronal and network mechanisms of epileptogenesis that was perfectly described in a number of papers of Steriade's group [i.e. Steriade, 2001; Steriade, 2003]. Changes of membrane properties and neuronal activity before the onset of spike-wave seizures [Steriade and Amzica, 1994; Steriade, 2003] on the macro EEG level may be caused by the dynamic interaction of the neuronal circuitry. Just before seizure start, more and more neuronal territories are getting involved (recruited) in seizure activity. Synchrony between neuronal networks gradually increases resulting in excessive hypersynchronous activity with characteristic EEG pattern. We found that abnormal functional cortical and thalamic interactions can attribute seizure initiation.

In the present study, we found that changes of coherence between different parts of *thalamo-cortical* loop involved different frequencies. This can manifest specific synchronization processes in local and distant neuronal networks. A general increase of coherence around mean frequency of SWD may characterize the recruitment of neuronal activities arising in local and distant sites and the progressive increase of synaptic excitability preceding the onset of seizures.

Recent study of Pinault (2003) indicated that abovementioned 5–9 Hz precursors of SWD in GAERS were associated with rhythmic neuronal bursts in the somatosensory-related areas in the cortex and in the thalamus [Pinault, 2003]. The author suggested that strengthening of synaptic interactions between cortical and thalamic neurons may underlie transformation of 5-9 Hz oscillations into SWD, therefore, one can expect an increased that EEG synchrony in 5-9 Hz. This was not observed in the present study, because data in GAERS was obtained in anesthetized rats, in which frequency of the SWD was lower than in awake animals (6-8 Hz versus 9 Hz

respectively) that is nearly the same with the frequency of 5-9 Hz precursor oscillations. Our animals, WAG/Rij rats, were drug-free and had slightly faster SWD (9-11 Hz) compared to that in GAERS. This difference in frequency might be a reason why we did not observe SWD-associated increase of coherence in 5-9 Hz in WAG/Rij rats. Instead, we found profound increase of synchrony in higher frequency, including alpha, beta in partly gamma bands. Some (global) changes of coherence were found in all parts *thalamo-cortical* system (increase of synchrony in 8-11.5 Hz and coherence peak 9.5-10.5 Hz), other changes of coherence appeared in local EEG pairs. It can be concluded that combination of local and global network synchrony can underlie genesis of SWD in the *thalamo-cortical* circuitry. Our experimental data fit well to the local/global dynamic theory of Nunez (2000). In Figure 5.6 we try to generalize our data and account for *thalamo-cortcal* mechanisms of SWD in the framework of Nunez's theory.

According to "the cortical focus theory" [Meeren et al., 2002; Meeren et al., 2005], the cortical focus in the somatosensory cortex lead the thalamus during the first five hundred milliseconds, and after this initial period, the cortex and the thalamus led and lagged each other unpredictably until seizure end. It is important to note that transitioning from locally driven (by cortical focus) to more generalized (driven by cortico-thalamic network) SWD takes about half a second after the first spike of SWD, this corresponds to the second half of the investigated interval (SWD). Here we discriminate synchronization in the *cortico-thalamic* resonant circuitry at the onset of SWD and identify "resonance frequencies" within *thalamo-cortical* network. We found that local circuit involving the epileptic zone in the somatosensory cortex showed specific changes of EEG coherence. In all, we tend to consider our study as a contribution to the 'cortical focus' theory.

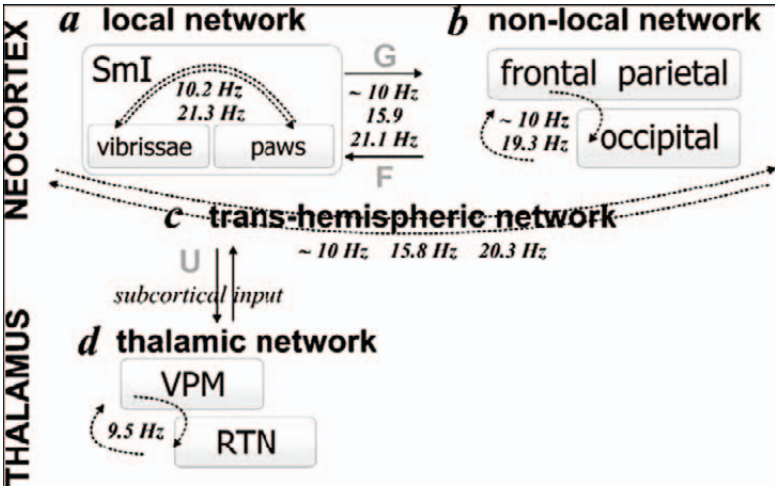

Figure 5.6. The schema characterizes dynamic interactions between local networks and the global network mechanisms involved in the genesis of SWD in WAG/Rij rats. It is based on local/global field theory by Nunez (2000) and indicates resonant frequency in the four different oscillatory networks (a-d). Terms "*local*" and "*non-local*" networks were borrowed from Nunez's theory. We adopted the definition of the "*local network*" with slight modifications: it is short-range intracoritcal network comprising functionally and anatomically related areas including both positive and negative feedback. *"Non-local network*" employs sufficiently distant areas, which are functionally heterogeneous and anatomically unrelated.
Putative intracortical pacemaker of SWD is located in the somatosensory cortex (*SmI*) [Meeren et al., 2002]. By means of short- and long-range interactions it communicates with multiple intracortical networks, thus forming local (a) and *non-local* (b) oscillatory networks. Development of SWD needs high bilateral synchrony (c - trans-hemispheric network). Thalamic network (d) shows resonance in 9.5 Hz and seems to be relatively autonomous from neocortical networks.

Physiological implications of EEG coherence study.

Intracotical network mechanisms by which vibrissal area of the SmI may initiate SWD. Here we were particularly motivated to examine short- and long-range functional interactions which were established by the perioral region of the SmI with the rest cortical circuit. As known, perioral area of the *SmI* contains a *"cortical focus"* of generalized absence epilepsy [Meeren et al., 2002]. We found evidences supporting our hypothesis that epileptic focus in vibrissal area of *SmI* cooperates with parietal and frontal (sensory and motor) areas in a specific way. First, occurrence of SWD in the local cortical network *SmI(paw)-SmI(vib)-frontal* cortex was associated with double-faced changes of coherence: reduction of coherence in low frequency band (1-5 Hz) and increase of coherence in 8 - 35.5 Hz. Second, the resonance frequency of network associations between *SmI(vib)-frontal* cortex and *SmI(vib)-SmI(paws)* areas was significantly higher than in other investigated pairs (21 Hz versus 18.5-20 Hz). The epileptic focus in the *SmI(vib)* and it's closest neighborhood creates a minimal neuronal circuit that may initiate SWD. A consistent shift of coherence from delta to alpha/beta frequencies may facilitate network synchronization within local network *SmI(vib)-SmI(paws)-frontal* cortex ("*local*" network in Fig. 5.6a), so that this

minimal circuit may drive the remote *cortico-cortical* network ("*non-local*" and trans-hemispheric networks in Fig. 5.6b-c) to turn on fundamental frequency of SWD (~ 10 Hz) and ~ 20 Hz harmonic. Interestingly, the minimal circuit did not include a neighboring SmI(paws)-frontal pair. The pattern of EEG coherence in this pair was somewhat peculiar: very intensive and widespread (5-60 Hz) increase of coherence occurred without any sign of reduction of coherence. This might imply that somatosensory cortex is involved in functionally heterogeneous neuronal networks. The one, including Meeren's focal epileptic zone *SmI(vib)-SmI(paws)-frontal* cortex, may be crucial for the initiation of SWD. Another one, including *SmI(paws)* and *frontal* cortex, may be involved in augmentation and provide anterior propitiation of SWD.

Role of short- and long-range SWD intracortical associations in maintenance of SWD

The chosen cortical areas are specialized for different functions, but they are coupled to each other and intimately involved in absence epilepsy. Our choice of cortical recording sites is based on the following rationales. (1) Investigated region in the *frontal cortex* is the motor representation of limbs [Neafsey et al., 1986]; it has dense mutual interconnections with the dorsal thalamus, including the ventrobasal complex [Aldes, 1988]. Comparing to other cortical regions, this area manifests SWD with the highest amplitude [Meeren et al., 2002; Midzianovskaia et al., 2001]. (2) In the *parietal* cortex, we record from the two different areas of the primary somatosensory cortex (SmI), projective zone of *vibrissae* and *paws*. The first, vibrissal area triggers SWD in our subjects [Meeren et al., 2002]; amplitude of SWD in this area is lower than that in the adjacent representative area of paws [Midzianovskaia et al., 2001; Meeren et al., 2002; Mackenzie et al., 2004]; both investigated loci in the SmI send projections to the RTN, to the VPM and VPL [Price and Webster, 1972]. (3) In the *occipital* cortex, we recorded activity from the secondary visual area (Oc2L), which relates to the lateral posterior thalamic nucleus and has mutual interactions with numerous cortical sites [Kolb, 1990]; among other cortical sites, occipital SWD are of the lowest amplitude and less stereotyped [Meeren et al., 2002; Midzianovskaia et al., 2001].

Based on the aforementioned pattern of anatomic and functional relations between investigated sites, we suggest that being initiated in the projective area of *vibrissae*, epileptic spike-wave activity may be augmented in the *paw* area of SmI and reach maximum in the *frontal* region. Therefore, we expect that parieto-parietal (between vibrissal and paw regions of SmI) and parieto-frontal coherence would be especially strengthened with the occurrence of SWD, as well as parieto-thalamic and fronto-thalamic coherence. Investigated occipital region does not seem to be primarily involved into thalamo-cortical oscillatory integrity, therefore, we do not expect to find large SWD-associated changes of coherence in fronto-occipital, parieto-occipital and occipito-thalamic pairs.

Resonance frequencies in the thalamo-cortical system underling spike-wave seizures

We describe frequency-specific changes of EEG coherence, which may underlie development of SWD in the neocortex (Fig. 5.6): (1) in all cortico-cortical pairs, strong reinforcement of coherence was centered around "resonance frequencies" ~10 Hz and ~20 Hz; (2) in intra-hemispheric pairs, strengthening of beta coherence (16-21.5 Hz) and in trans-hemispheric pairs, additional resonance peak in ~16 Hz (Fig. 5.6c). Apparently, development of SWD in cortico-cortical networks needs more synchrony in the fundamental (10 Hz) and harmonic (20 Hz) frequencies of SWD. Probably, minimal oscillatory cortical circuit (Fig. 5.6a) use a frequency of 10 Hz to communicate with remote areas in the cortex and the thalamus, therefore, coherence in 10 Hz throughout thalamo-cortical network is especially high.

In addition to fundamental and harmonic frequencies of SWD, all trans-hemispheric pairs showed a peculiar maximum coherence around 16 Hz. Taken alone, this peculiar maximum may reflect a specificity of bilateral network associations. The anatomical substrate for trans-hemispheric cortico-cortical synchronization is the *corpus callosum*. The midline thalamus played a minor role in bilateral transfer of SWDs in GAERS. Specific transection of this area did not affect SWDs, however, when the transection of the corpus callosum was associated with a midline cut through the thalamus, the bilateral desynchronization was almost complete [Danober et al., 1998]. There are some other subcortical trans-hemispheric pathways (such the hippocampal commissure, anterior commissure, massa intermedia, habenular commissure, posterior commissure, supramamillary commissure, collicular commissure), which are not likely involved in the bilateral synchronization of SWD [Vergnes et al., 1989]. Hence, trans-hemispheric intracortical synchronization during development of SWD can be accounted for solely *callosal* pathway. It seems important that *callosal* projections are responsible for bilateral generalization of SWD, but they have no role in the initiation of SWD. As known, total amount of seizures measured on both hemispheres after callosectomy was comparable to the values found in intact GAERS [Vergnes et al., 1989]. Nevertheless, trans-hemispheric associations appeared to be even stronger than intra-hemispheric associations, suggesting that trans-hemispheric cortical interactions play a crucial role in SWD.

We tend to believe that bilateral synchronization via *callosal* fibers result in emergence of additional 16 Hz peak of coherence. The frequency of this peak fell apparently halfway between two major peaks in 10 Hz and 20 Hz, therefore, bilateral synchronization of SWD may be controlled by an auxiliary mechanism which interferes with a common strategy of cortico-cortical (and thalamo-cortical) network to exhibit more coherency in 10 Hz and 20 Hz. Coherence maximum in 16 Hz was also found in two intra-hemispheric pairs, both involved *SmI* to the *frontal* cortex, suggesting that these areas may be reciprocally driven by symmetrical areas in the opposite hemisphere. Therefore, functional coupling between *SmI* and *frontal* cortex might be additionally reinforced by the callosal-dependent interhemispheric synchrony. This may cause hyper-synchronization in the local parieto-fronal cortical circuit and consequent onset of SWD with the anterior maximum.

Development of SWD needs more coherency in high frequencies

Coherence in beta frequencies. It was found that the majority of cortico-cortcal pairs show an increase of coherence in frequencies between 5 Hz and 36 Hz. The increase of high beta coherence (16-36 Hz) seemed to be equally (or even more) important for the cortical development of SWD as the enlargement of coherence in fundamental frequency of SWD. The harmonic peak of coherence was found between 18 and 21 Hz that is beta frequency domain. As known, EEG spectrum of SWD in the frontal and parietal cortex revealed a large peak in the harmonic frequency 18-24 Hz [Drinkenburg et al., 1993]. This harmonic peak in EEG spectrum is accounts for the presence of sharp EEG elements (sharp waves and spikes), this may also account for a harmonic peak in the coherence spectrum. It is possible that strengthening beta coherence was caused by the presence of the spike component of SWD. Making further assumptions, high coherence in 16-21.5Hz in cortico-cortical intra-hemisheric pairs (Fig. 5.3D) might be related to the genesis of the spike in SWD, but thalamo-thalamic coherence in 16-21.5Hz was low, therefore, the local thalamic networks might be less capable to sustain the spike.

Coherence in gamma frequencies. In our subjects, SWD onset was accompanied by moderate and local increase of gamma coherence in the cortex, while in thalamo-thalamic associations gamma coherence decreased. Mechanisms of thalamo-thalamic coherence are poorly explored. As to cortico-cortical coherence, it is known that fast oscillations (20-100 Hz) play an important role in synchronizing oscillatory activity between remote neocortical areas [Buzsaki and Draguhn, 2004]. In focal neocortical seizures, epileptic brain expresses pathological fast rhythms just before epileptic attacks; these fast rhythms reflect primordial neuronal synchronization [Steriade et al., 1996].

As known, gamma synchrony becomes extremely high in case of the sharp epileptiformic EEG phenomena, such as kainite-induced spikes, sharp waves and spike component of SWD [Medvedev, 2001]. Therefore, increase of gamma coherence in SmI(paws)-frontal pair may relate to the genesis of a spike. Quite intriguing шы the fact that gamma coherence increased only in SmI(paws)-frontal pair, while high-frequency coherence (35.5-100 Hz) was unchanged in the majority of intra-cortical electrode pairs. The consistent findings in patients with neocortical epilepsy showed that high-frequency (60-100 Hz) epileptiform activity, which was concentrated in the region of seizure focus, has been anticipated by an increase of high-frequency activity 20 min prior to seizure onset [Worrell et al., 2004]. In our case, absence epileptic discharges were also accompanied by local enhancement of high-frequency associations. Although, high gamma synchrony was developed in the local cortical anterior network and epileptic focus in the *SmI(vib)* was not directly involved in this network.

Role of thalamo-thalamic associations in the development of SWD

Involvement of the thalamus in the pathogenesis of absence epilepsy in humans is hardly explored. The problem is that direct measures of thalamic activity with depth electrodes have low clinical profit and they are highly invasive. As a consequence, the role of the thalamus in absence epilepsy seems to be underestimated. “With combined depth and scalp recordings in patients with absences, the results of early workers in the field were somewhat inconclusive but never pointing in the direction of primarily thalamic discharges” [Pavone and Niedermeyer, 2000]. Experiments in WAG/Rij model allowed us to record directly from the two thalamic loci, which are essentially involved into SWD (specific ventroposteromedial thalamic nucleus, VPM, and reticular thalamic nucleus, RTN), and to examine EEG coherence between these structures. We found SWD-associated increase of coherence between these two thalamic structures as well as enhancement of thalamo-cortical coherence. This suggests that the key thalamic structures are involved in sustaining SWD. However, EEG pattern of coherence between VPM and RTN was somewhat peculiar: there was a remarkable antagonism between low- and high-frequency coherence, in which gamma desynchronization was coincided with more synchrony in 8-11.5 Hz.

Role of thalamo-cortical associations in the development of SWD

A fMRI study of spontaneous SWD in WAG/Rij rats showed BOLD activation in the parietal (including SmI) and temporal cortical areas as well as in specific thalamic relay nuclei (VPM/VPL) and in the RTN. This underscores importance these structures in the pathophysiology of absence seizure disorder [Tenney at al., 2004]. As known, the SmI can control neuronal activity in the somatosensory-related thalamic nuclei (such as VPM) and the RTN via descending fibers [Kolb, 1990; Jones, 1985]. In WAG/Rij rats, the epileptic focus in the SmI set into motion a cascade of neuronal processes resulting to synchronous activity in the thalamocortical system which is recorded as SWD. The cortical focus drives the thalamus during the first few cycles and, consequently, the whole thalamo-cortical become entrained into the oscillation, providing a resonant circuitry [Meeren et al., 2002]. Also in GAERS, the SmI was found to play a major role in spike-wave rhythm. During development of SWD in GAERS, somatosensory neurons in layer VI massively synchronize cortical neurons of middle layers and neurons in relay and reticular thalamic nuclei [Pinault, 2003]. To sum up, SWD develops in the somatosensory-related parts of thalamo-cortical network as a resonance phenomenon, which is initiated and driven by neurons in the somatosensory cortex.

Functional connectivity between different parts thalamo-cortical network has been profoundly changed with the occurrence of SWD. The strengthening of network associations showed some frequency constraints: the "carrier" frequencies of coherence in different parts of oscillatory loop were significantly different, suggesting that each part of thalamo-cortical circuit may have its own strategy to sustain seizure activity. Strengthening of cortico-cortical coherence in the beta range may be associated with the genesis of 'spike' component in SWD. As known, spike component has its maximal expression in the frontal cortex and it is poorly developed in the thalamus and in the occipital cortex [Meeren et al., 2002]. Fronto-thalamic coherence in the beta range was not high, comparing to that in cortico-cortical pairs. The increase of beta coherency was not found in occipito-thalamic and thalamo-thalamic pairs.

We found that the development of a seizure in the thalamo-cortical network was associated with extensive increase of coherence in the physiological specific frequency of SWD (9.5–10.5 Hz). In addition to that, cortico-cortical coherence was highly aggravated in a broad frequency range, including the mean frequency of SWD and it's first harmonic. Possibly, there are multiple oscillators in the cortex which are entrained during SWD. Those individual oscillators develop synchronous high-frequency activity and they are also coupled to a low-frequency ~10 Hz driving force.

CONCLUSIONS

The onset of SWD was associated with strengthening of both unilateral and bilateral *thalamo-cortical* interactions. A significant increase of *cortico-cortical*, *cortico-thalamic* and *thalamo-thalamic* coherence was detected in frequencies from 5 to 60 Hz. In all investigated pairs, coherence showed two central maxima in 10 and 20 Hz. The highest increase of coherence was obtained in two frequency bands: around mean frequency of SWD (8-11.5 Hz) and in harmonic band 16-21.5 Hz.

Unilateral cortico-cortical coherence decayed with electrode distance: the highest coherence was found between the closest sites, i.e. in *SmI(vib)-SmI(par)* and *SmI-frontal* pairs, and the lowest coherence – between more distant sites, i.e. SmI-occipital and fronto-occipital. In contrast, bilateral coherence was not reduced with interelectrode distance: the highest values of bilateral coherence were found between the most distant sites in SmI(vib) and frontal pairs. It was concluded first, that the SWD-induced increase of coherence showed a clear dependence on topographical factors only in unilateral pairs, but this was not evident in bilateral pairs. Second, anterior areas had an intrinsic propensity to hyper-synchronization that may facilitate uni- and bilateral propagation of SWD over anterior cortical areas.

Trans-hemispheric cortical coherence was significantly higher than intra-hemispheric cortico-cortical and cortico-thalamic and thalamo-thalamic coherence (Fig.5.3D). Moreover, all investigated trans-hemispheric pairs showed an additional peak of ΔCoh around 16 Hz, which was absent in thalamo-cortical and thalamo-thalamic pairs (Fig. 5.4A-C). The most extensive increase of bilateral synchronization and the peculiar profile of trans-hemispheric coherence may imply the crucial involvement of the corpus callosum in the pathophysiology of absence seizures.

In all investigated pairs, the increase of coherence in 8-11.5 Hz was significant. In addition to that, unilateral cortico-cortical coherence (especially between *SmI* and *frontal* cortex) was particularly strengthened in 16-21.5 Hz ($\Delta Coh_{8\text{-}11.5} < \Delta Coh_{16\text{-}21.5}$), whereas *bilateral cortico-cortical* coherence in 16-21.5 Hz and in 8-11.5 Hz was equal ($\Delta Coh_{8\text{-}11.5} = \Delta Coh_{16\text{-}21.5}$), yet *occipito–thalamic* and *thalamo-thalamic* coherence in 16-21.5 Hz was relatively weak ($\Delta Coh_{8\text{-}11.5} > \Delta Coh_{16\text{-}21.5}$). It seems that each part of *thalamo-cortical* circuitry established specific relationships with other parts of the network during transition towards the onset of SWD. However, there might be a general principle that governs network synchronization: to achieve oscillatory unity, the entire network should

interact in 8-11.5 Hz resonant mode. Besides that, *unilateral intracortical* circuits need more synchrony in 16-21.5 Hz.

To generalize, absence seizures on the EEG are complex resonant phenomena, in which carrier frequencies have fallen in ranges of 8-11.5 Hz and the first harmonic, this may reflect hyper-synchrony of network rhythmic activity ~ 10 Hz. Additional 16 Hz peak of coherence, which was typical for all *interhemispheric* pairs, may imply specific involvement of the *callosal* pathway in network cooperation that favors bilateral propagation of SWD.

SWD-related decrease of coherence was found in narrow low-frequency band (up to 5 Hz) and it was limited to *cortico-cortical* couples formed by *SmI* and to the *thalamo-thalamic* pair. Reciprocal relationship between delta and alpha coherence (reduction of 1-5 Hz coherence and enhancement of 8-11.5 Hz coherence) characterized cortical and subcortical (thalamic) local oscillatory networks, suggesting that a common neurophysiologic mechanism may underlie *intrathalamic* and *intracortical* synchrony.

Occurrence of SWD required large-scale increment of functional interaction between frontal cortex and thalamus. The most intensive increase of coherence was obtained in the mean frequency of SWD (9.5-10 Hz) and coherence in higher frequencies (up till gamma) was also strengthened. The frequency profile of SWD-induced changes of *thalamo-thalamic* coherence was different from that obtained in any other investigated pairs: this was the only pair in which high-frequency associations were decreased.

5.2 Changes of Granger causality at the onset of SWD ‡

ABSTRACT

Linear Granger causality was used to identify the coupling strength and directionality of information transport between frontal cortex and thalamus during spontaneous absence seizures in a genetic model, the WAG/Rij rats. Electroencephalograms were recorded at the cortical surface and from the specific thalamus. Granger coupling strength was measured before, during and after the occurrence of spike-wave discharges (SWD).

Before the onset of SWD, coupling strength was low, but associations from thalamus-to-cortex were stronger than vice versa. The onset of SWD was associated with a rapid and significant increase of coupling strength in both directions. There were no changes in Granger causalities before the onset of SWD. The strength of thalamus-to-cortex coupling remained constantly high during the seizures. The strength of cortex-to-thalamus coupling gradually diminished shortly after the onset of SWD and returned to the pre-SWD level when SWD stopped. In contrast, the strength of thalamus-to-cortex coupling remained elevated even after cessation of SWD.

The strong and sustained influence of thalamus-to-cortex may facilitate propagation and maintenance of seizure activity, while rapid reduction of cortex-to-thalamus coupling strength may prompt the cessation of SWD. However, the linear estimation of Granger coupling strength does not seem to be sufficient for predicting episodes with absence epilepsy.

INTRODUCTION

Over the years electroencephalography is widely used in clinical practice for the investigation, classification and diagnosis of epileptic disorders. The electroencephalogram (EEG) provides valuable information in patients with typical and atypical epileptic syndromes and offers also important prognostic information.

Absence epilepsy, previously known as petit mal, is classically considered as non-convulsive generalized epilepsy (classification of the International League Against Epilepsy, ILAE) of unknown etiology [refs. in Panayiotopoulos, 1997[. Clinically, absence seizures occur abrupt, last several seconds up to a minute and are accompanied by a brief decrease of consciousness that interrupts normal behavior. Absences may either have or have no facial automatisms, e.g. minimal jerks and twitches of facial muscles, and eye blinks. In humans, EEGs during typical absence seizures are characterized by the occurrence of generalized 3–5 Hz spike-wave complexes which have an abrupt on-and offset [Bosnyakova et al., 2007; Panayiotopoulos, 1997]. Similar EEG paroxysms, spike-and-wave discharges (SWD) appear in rat strains with a genetic predisposition to absence epilepsy, such as GAERS [Vergnes, 1987] and WAG/Rij [Coenen and van Luijtelaar, 2003]. The EEG waveform and duration (1–30 s, mean 5 s) of SWD in rats and in humans are comparable, but the frequency of SWD in rats is higher, 8–11 Hz [Midzianovskaia et al., 2001; Sitnikova and van Luijtelaar, 2007; van Luijtelaar and Coenen, 1986].

Several modern computational techniques and advanced methods of EEG analysis have been developed to extract "hidden" information from the EEG in order to localize the region of onset and to anticipate the onset of 'absences' as early as possible (in rats [Meeren et al., 2002] and in humans Refs. in [Mormann et al., 2007]). Our experiments are carried out in WAG/Rij rats [van Luijtelaar and Coenen, 1986]. Every subject of this strain has typical absence seizures that are accompanied with spontaneous SWD in the EEG. Previously we used EEG coherence to measure neuronal synchrony between populations of thalamic and cortical neurons [Sitnikova and van Luijtelaar, 2006]. We found that the onset of SWD was characterized by area-specific increase of coherence and supports the idea that the cortico-thalamo-cortical circuitry is primarily involved in the initiation and propagation of SWD [Meeren et al., 2005; Steriade, 2005]. Coherence is a traditional measure of linear correlations between two EEG channels in the frequency domain, but it does not assume directionality of inter-channel interactions and does not provide temporal (time-domain) information of the EEG signals [Challis and Kitney, 1991]. Granger causality compensates for these limitations [Ancona et al., 2004; Feldmann and Bhattacharya, 2004; Granger, 1969; Hlavackova-Schindler et al., 2007; Pereda et al., 2005]. Granger causality concept can be used to determine directional coupling characteristics between recording sites in intracranial EEG and to reveal active abnormal causal relationships in epileptogenic networks [Chavez et al., 2003; Kaminski et al., 2001]. Usually, Granger causality estimations are performed in long time intervals that include a dozen or even more, basic periods. The pairwise analysis is based on the construction of vector autoregressive (AR) models from bivariate data that estimates how well the current measure of one process can improve the prediction of the future

‡ Published in:
Sitnikova E, Dikanev T, Smirnov D, Bezruchko BP, van Luijtelaar G. Granger causality: Cortico-thalamic interdependencies during absence seizures in WAG/Rij rats. Journal of Neuroscience Methods, 2008; 170(2): 245-254.

of another process [Granger, 1969]. Here we apply Granger causality to measure the strength of bidirectional functional interactions between neuronal assembles in thalamus and frontal cortex.

The present work aims to measure bidirectional (feedforward and feedback) network interdependences between local field potentials recorded simultaneously from the specific thalamus and the frontal cortex. Granger causality concept will be used to characterize the strength of functional connectivity between the cortical and thalamic EEGs for both directions before, during, and after SWD in rats.

METHODS

Animals, EEG data acquisition and description of EEG patterns

Experiments were performed in five male 11–12-month old WAG/Rij rats. The recordings were done at the Department of Biological Psychology, Radboud University Nijmegen in accordance with the European Communities Council Directive (86/609/EEC). Experiments were approved by the Ethical Committee on Animal Experimentation of Radboud University Nijmegen. Distress and suffering of animals were minimal.

EEGs were recorded from brain areas in which seizure activity is known to be the most robust: in the frontal cortex and in the ventroposteromedial thalamic nucleus, VPM [Vergnes et al., 1987]. Stainless steel EEG electrodes were implanted during stereotactic surgery under isofluorane anesthesia. One electrode was placed epidurally over the frontal cortex [AP 2; L 2.5] and the other depth electrode was implanted into the ventroposteromedial thalamic nucleus [VPM, AP .3.5; L 2.5; H 7.2]. Two additional electrodes, ground and reference, were placed symmetrically over the two hemispheres of the cerebellum. All electrodes were identical (diameter 0.25 mm) and had non-insulated tips. The coordinates are given in mm relative to bregma according to the rat brain atlas of Paxinos and Watson (1986).

After the surgery, animals were allowed to recover during at least 10 days. During this recovery period, animals received post-surgery care and their weight was monitored. Upon completion of the EEG recording sessions, rats were deeply anesthetized with overdose of sodium pentobarbital (200 mg/kg i.p.) and their brains were stained with Nissl. Electrode positioning was verified using the atlas of the rat brain [Paxinos and Watson, 1986].

EEG recordings were made in freely moving rats in a Faraday cage. Each recording session lasted from 5 to 7 h during the dark period of the day–night cycle. EEG signals were fed into a multi-channel differential amplifier, filtered between 1 and 200 Hz, digitized with 1024 samples/second per channel (CODAS software) and stored on hard disk.

SWD appeared in EEG as a train of stereotypic repetitive 7–10 Hz spikes-and-waves with high amplitude (that exceeded the background more than three times); SWD lasted longer than 1s [Midzianovskaia et al., 2001; van Luijtelaar and Coenen, 1986]. SWD were detected automatically in the frontal EEG records using the algorithm and original software developed by Dr. Ir. P.L.C. van den Broek (NICI, Radboud University Nijmegen, the Netherlands). This method is based on the detection of steep changes in the EEG.

Granger causality

Let $\{x_n\}$ and $\{y_n\}$ be the two EEG signals (time series) recorded simultaneously in different brain loci. x_n and y_n are EEG values measured at the *n*-th time point. In order to study causal relations between x_n and y_n, we use Granger's approach and analyze prediction improvement. First, we fit a univariate autoregressive (AR) model to the EEG data. The model takes the form

$$x_{n+1} = f(x_n, x_{n-1}, \ldots, x_{n-d+1}), \qquad (1)$$

It relates current EEG value to the *d* previous values, *f* is some function, e.g., algebraic polynomial whose order and coefficients are to be estimated from the observed data. Eq. (2) shows a widely used linear AR model

$$x_{n+1} = \alpha_0 + \sum_{i=1}^{d} \alpha_i x_{n+i-1}. \qquad (2)$$

The coefficients α_i are selected in order to minimize the mean squared error

$$\varepsilon_x^2 = \sum_n \left(x_{n+1} - \left(\alpha_0 + \sum_{i=1}^{d} \alpha_i x_{n+i-1} \right) \right)^2. \qquad (3)$$

where N is the number of predicted samples in a time series. If the number of model parameters is much less than the number of data points used for the estimation, a minimal value ε_x^2 can characterize the accuracy of the model: the less the error, the better the model (self-predictability of the model).

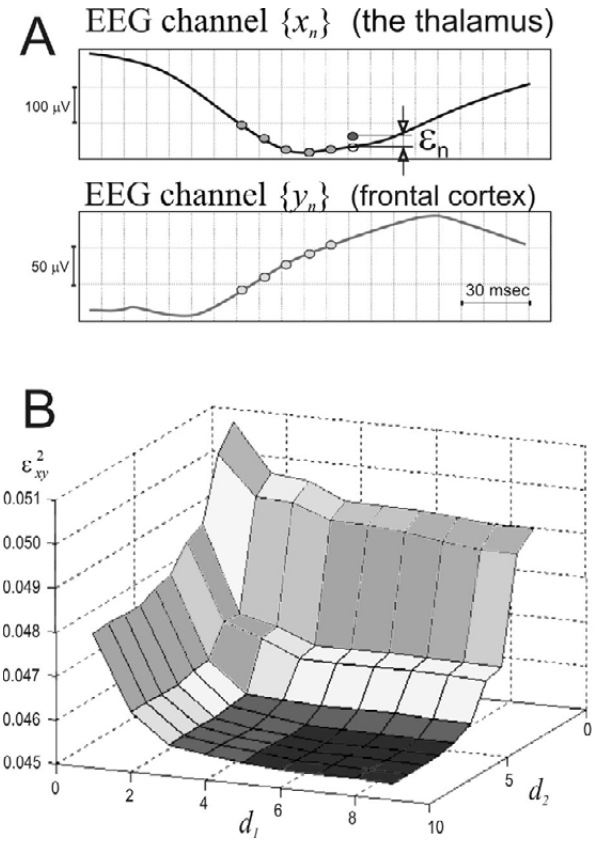

Figure 5.7. Estimation of Granger causality between EEG signals as recorded at thalamus and frontal cortex. The autoregressive model (AR) is used to characterize amplitude changes in two EEG signals, *{x_n}* and *{y_n}* over time.
(**A**) In the joint AR model, the information about the past of EEG signal *{y_n}* improves the prediction of EEG signal *{x_n}* (see Eq. (4)) with a reduction of the instantaneous prediction error, ε_n. The squared errors, ε^2_{xy}, characterize the quality of prediction of the chosen AR model. The value of ε^2_{xy} depends on the number of samples in signals *{x_n}* and *{y_n}* used in the AR model, so-called model dimensions, *d*.
(**B**) Dependencies between the prediction errors, ε^2_{xy}, and the model dimensions in our linear AR that predicted the future of the signal *{y_n}* (d_1 and d_2 is the number of samples in the signal *{x_n}* and signal *{y_n}* correspondingly).
An increase of dimensions d_1 and d_2 resulted in a decrease of the least mean square*d* error and the quality of predictions was improved until $d_1 = d_2 = 5$. Further increase of dimensions did not improve the accuracy of prediction, therefore in our computations we used $d_1 = d_2 = 5$.

Causal relations between process y and process x are present when prediction of signal $\{x_n\}$ can be improved by incorporation into the model the past of signal $\{y_n\}$ (illustrated in Fig. 5.7A). As a result, we construct a 'joint' AR model Eq. (4)

$$x_{n+1} = f(x_n, \ldots, x_{n-d1+1}) + g(y_n, \ldots, y_{n-d2+1}). \qquad (4)$$

where *f* and *g* are polynomials that we determine from the current data. Function *f* is the same as in the individual model Eq. (1) while function g describes the influence of process *y* on process *x*. Number d_1 is the same as the dimension *d* of the individual model Eq. (1). The number d_2 describes 'inertial' properties of the influence. If $d_2 = 1$, then the influence is instantaneous, otherwise it is non-local in time. Different values of d_1 and $d_2 \in (1; 25)$ are tested in order to select those values that provide the most faithful results. In the present study we used linear AR models Eq. (5):

$$x_{n+1} = \alpha_0 + \sum_{i=1}^{d_1} \alpha_i x_{n+1-i} + \sum_{i=1}^{d_2} \beta_i y_{n+1-i}. \qquad (5)$$

In Eq. (5) coefficients α_i are chosen using the least-squares estimations method. This method examines mean squared prediction error, ε^2_{xy} and when this error appears to be less then the ε^2_x it is assumed that process *y* influences process *x* (Fig. 5.7A). In order to measure coupling between channels, we use the relative prediction improvement, the so-called Granger-Sargent statistic [Hlavackova-Schindler et al., 2007]:

$$s_{xy}^2 = \frac{\varepsilon_x^2 - \varepsilon_{xy}^2}{\varepsilon_{xy}^2}. \quad (6)$$

Thus, the influence of channel $\{y_n\}$ on the channel $\{x_n\}$ is characterized by the value of the normalized prediction improvement, s_{xy}^2, and the reverse influence of $\{x_n\}$ on $\{y_n\}$, s_{yx}^2 is described by an equation similar to Eq.(6) in which *x* and *y* should be interchanged.

Application of Granger causality to EEG data

Nonlinear dynamics techniques consider EEG signals as nonlinear process and try to extract some nonlinear features from it. Typically, they require long epochs of stationary data [e.g., Arnhold et al., 1999; Le Van Quyen et al., 1999; Schiff et al., 1996]. Estimations of Granger causality, either linear or nonlinear, are performed under the same conditions. Linear estimates are usually less sensitive to the epoch length, because they are based on relatively simple models (with fewer free parameters). However, the EEG is known to be highly non-stationary [Kaplan, 1998]. This should be taken into account in order to specify the proper time window length for the estimation of autoregressive models when estimating Granger causality.

The choice of length of moving window

In fact, non-stationary is an intrinsic feature of the EEG signal that accounts for complex dynamics of electrical brain activity [Dikanev et al., 2005]. However, the classical estimation of Granger causality requires stationary data. Therefore we segmented the EEG into relatively short epochs in which the EEG signal reveals quasi-stationary behavior.

In order to get a correct approximation to the non-stationary EEG data with the AR model, it is important to define the optimal size of the moving time-window. By shortening the time-window, it is possible to improve the time resolution, but this reduces the reliability of the AR models. In non-stationary EEG data, the time-window should include several repetitive elements. In our case, the time-window lasts 0.5 s; this corresponds to four spike-wave cycles. This size of the time-window was found to be optimal. If the estimation window was shorter than 0.5 s, Granger causality estimations were unstable and longer time window (up to 1 s) did not improve the stability of coupling estimates.

Selection of the polynomial order (linearity–nonlinearity in EEG signals)

Originally, Granger causality principles were formulated without any assumption about the linearity or nonlinearity of the systems. Traditional Granger causality measures were based on linear models [Granger, 1969; Granger and Newbold, 1977]. In order to make a choice between linear and nonlinear AR models, we compared prediction accuracy of these two models. It was found that the introduction of nonlinearity (such as polynomials of the second and third order) had no significant influence on the prediction quality of the AR model. It was additionally found that a linear AR model was sufficient to describe the dynamic behavior of the baseline EEG. It suggests a predominance of the linear causal relations in non-seizure EEG. In contrast, seizure activity (SWD) contained a nonlinear component, which was not yet modeled. However, the construction of a specific nonlinear AR model that describes seizure-related processes in the EEG is beyond the scope of the present paper.

Adjusting parameters of AR model (the choice of 'dimensions')

The linear AR models Eqs. (2) and (5) are used to calculate the coupling characteristics s_{xy}^2 and s_{yx}^2. Fig. 5.7B shows the typical dependence of prediction error ε_{xy}^2 on the dimensions d_1 and d_2 of the AR model for a 0.5 s time-interval of SWD. By increasing the dimensions d_1 and d_2 from 1 to 5, the error of prediction decreases and a minimal error was obtained when both d-values were equal to 5. Further increase of d_1 and d_2 did not improve the accuracy of predictions, therefore, $d_1 = d_2 = 5$ were selected as optimal dimensions for the chosen model. Such a dependence is typical for the prediction error ε^2 as well.

All this suggests that also in our linear AR model the past of one signal improves the prediction of the other signal. This model provided significant and stable predictions with the chosen parameters (dimensions and time-window size), therefore, it was an appropriate model for the analysis of pairwise causal relations in the chosen EEG pairs.

Statistical evaluation of causal interactions

Coefficients of Granger causality (prediction improvements) were computed using EEG data from the cortical surface (frontal cortex) and from the specific part of the thalamus (ventral basal complex). The first and the last spike in spike-wave sequences were used to mark the onset and the offset of seizure activity.

Statistical analysis of the thalamus-to-cortex, s^2_{xy}, and cortex-to-thalamus, s^2_{yx} causalities was performed in two 10-s EEG epochs (Fig. 5.8A). The first epoch included two 5 s successive intervals, one before seizure onset (pre-SWD), the second was the first 5 s of a seizure (SWD-start). The second 10-s epoch included the last 5 s of a SWD (SWD-end) and the first 5 s after a seizure (post-SWD). Coefficients of Granger causality were computed with bin = 0.0049 (5 samples/1024) and averaged per 0.2 s and per rat. Factorial ANOVA (repeated measures) and post hoc tests (LSD and t-tests for paired observations) were used for the statistical analysis.

Evaluation of statistical significance with surrogate test estimation

There are some undesirable factors (EEG noise, nonlinearities, etc.) that can influence Granger causality measures and might mislead analysis. In order to control for these unwanted factors and evaluate the statistical significance of the Granger causality parameters, we performed surrogate data tests. Surrogate signals were constructed by taking two apparently uncoupled EEG signals recorded in the cortex and thalamus. For that purpose, two randomly chosen SWD were selected in the cortex and thalamus. Either the onset or the end of SWD were matched. Surrogate tests were performed using EEG data from all animals. In total, 1000 random pairs of SWD were made to construct an ensemble of surrogate time series which modeled uncoupled process in the thalamo-cortical system. Granger causalities in surrogate and in original data were computed using the same algorithm. The surrogate Granger measures in the uncoupled pairs were analyzed statistically by computing 95%-percentiles of their distributions, $s^2_{xy,0.95}$, and $s^2_{yx,0.95}$ respectively. The results of surrogate tests, $s^2_{xy,0.95}$, and $s^2_{yx,0.95}$ were plotted in Fig. 5.8B-C against the true data values, $s^2_{xy,0.95}$, and $s^2_{yx,0.95}$. Interdependence in EEG pair can be regarded as significant (at the significance level $p = 0.05$) whenever the true values $s^2_{xy,0.95}$, and $s^2_{yx,0.95}$ appeared above 95%-percentiles of the corresponding surrogate values $s^2_{xy,0.95}$, and $s^2_{yx,0.95}$. This surrogate test confirmed that interdependencies between EEG signals were significant in both directions.

RESULTS

All SWD were detected automatically in the full length EEG recordings (6–7 h). In total, 53, 111, 34, 33 and 63 epileptic discharges in five rats were detected and analyzed.

Dynamics of cortico-thalamo-cortical casual interactions at the on- and offset of epileptic discharges

Fig. 5.8B shows the dynamics of Granger causality during absence seizures. Before the onset of SWD, the Granger causality was weak and remained constant until SWD began. The first SWD-related disturbances of Granger's casual relationships were observed about half a second before SWD-onset. This effect was provoked by the seizure itself because the 0.5 s time window started to include or capture seizure activity. No changes in Granger causalities were found earlier than 0.5 s before SWD onset, suggesting that a linear approximation does not seem to be suitable for prediction of absence seizures. It can be concluded that the linear cortico-thalamo-cortical associations are reinforced during SWD.

It is important that in all rats surrogate values $s^2_{xy,0.95}$, and $s^2_{yx,0.95}$ were almost constant in time, equal in both directions and were much smaller (around 0.02–0.04) than the true data estimates, s^2_{xy} and s^2_{yx} (Fig. 5.8B-C). The difference between the true (s^2_{xy} and s^2_{yx}) and surrogate ($s^2_{xy,0.95}$ and $s^2_{yx,0.95}$) values strengthened our outcomes and confirmed that mutual interdependencies between cortex and thalamus during SWD was statistically significant.

The immediate onset of SWD was associated with a rapid growth of causal relations s^2_{xy} and s^2_{yx} Fig. 5.8B-C and Fig. 5.9A).

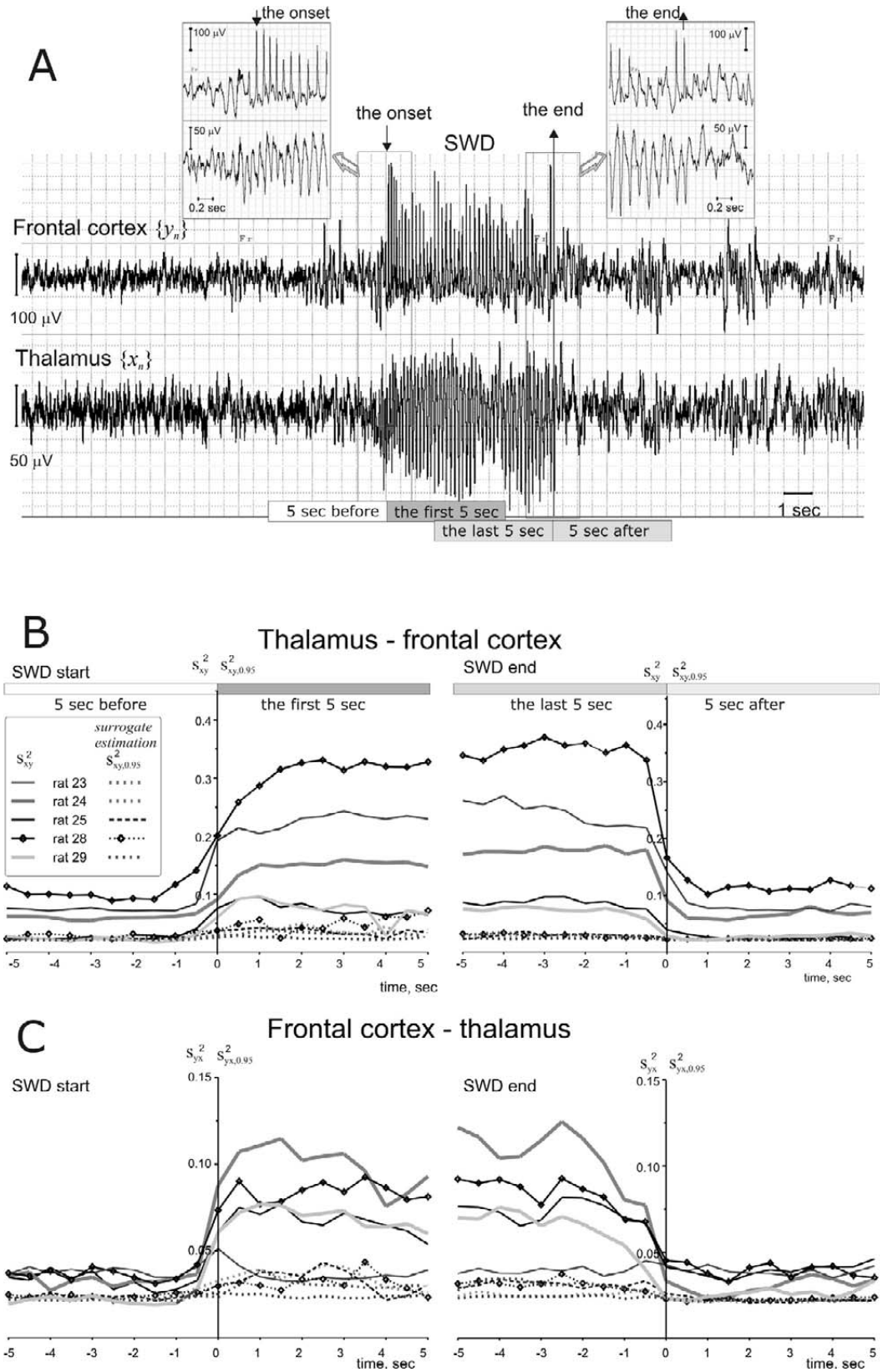

Figure. 5.8. Application of Granger causality in WAG/Rij rat model of absence epilepsy. (A) Electroencephalographic records of spike-wave discharges (SWD) in the frontal cortex and in the specific ventroposteromedial thalamic nucleus. Coefficients of Granger causality were computed in two 10-s epochs of continuous data (5 + 5 s) including pre-SWD/SWD and SWD/post-SWD (indicated by horizontal arrows). (B, C) The presence of SWD was associated with significant (and reversible) changes in Granger causality in both directions. Surrogate data tests (dotted lines) were performed in each animal in order to validate the results of Granger causality estimations. Surrogate values were very small and did not reveal any dynamic changes, suggesting that seizures affected the coupling strength in both directions. Note the large individual variations and two-hold difference in absolute values of cortex-to-thalamus and thalamus-to-cortex causalities

Granger causality reached its maximum within half a second after seizure onset (at that moment the time-window completely shifted from pre-SWD to SWD) and remained high during the first 5 s of a seizure.

Quantitative data in Table 1 shows that the onset of SWD was characterized by a significant increase of causalities in both directions as compared to pre-SWD ($F = 20.53$, d.f. = 1.4, $p < 0.02$) and that the ascending influence thalamus-to-cortex tended to be stronger than the descending influence cortex-to-thalamus ($F = 4.75$, d.f. = 1.4, $p < 0.1$) (Fig. 5.9B; Table 5.3). Interestingly, the occurrence of SWD was associated with a tendency for a larger increase of the thalamus-to-cortex as compared to the cortex-to-thalamus coupling. i.e., Δs^2_{xy} (SWD-start) = 0.117 versus Δs^2_{yx} (SWD-start) = 0.037, F (time) = 2.43, d.f. = 1.4, $p < 0.1$. All this suggests that a reinforcement of pre-SWD existing predominant thalamus-to-cortex coupling accompanied the occurrence of SWD.

Gross changes of Granger causality in the cortico-thalamo-cortical system before, during and after absence seizures

In spite of large between-subject variability in the values of Granger causality causalities (individual data are shown in Fig. 5.8B-C), a similar trend of SWD-related changes in Granger causality was observed in all subjects. Group statistics in Fig. 5.9 illustrate that the mutual relationships between the specific ventroposteromedial nucleus of the thalamus and the frontal cortex became stronger after the onset of SWD. The offset of SWD was characterized by a slight and gradual decrease of Granger causalities in both directions. A two-factor ANOVA was used to compare the average values of coupling strength on different stages of SWD. Factor 'time' had four levels: pre-SWD, SWD-start, SWD-end, post-SWD and factor 'direction' had two levels: cortex-to-thalamus and thalamus-to-cortex. Both factors were significant: F (time) = 58.4, d.f. = 3.992, $p < 0.0001$ and F (direction) = 319.6, d.f. = 1.992, $p < 0.0001$, as well as the interaction F (time×direction) = 17.9, d.f. = 3.992, $p < 0.0001$. Post hoc LSD tests revealed significant difference of causalities in both directions at pre-SWD and during SWD (Fig. 5.9B). The strength of cortex-to-thalamus coupling before (pre-SWD) and after (post-SWD) did not differ significantly (Fig. 5.9B).

In contrast, the thalamus-to-cortex coupling did not return to the pre-seizure level immediately after the cessation of the epileptic electroencephalographic activity, as did the cortex-to-thalamus coupling. Altogether, the analysis of Granger causality provided new information about neuronal network connectivity during absence seizures. We consider this method as a good alternative to the traditional measurements of functional interactions in the brain.

Table 5.3. Mean values of Granger causality as measured in 5 sec intervals immediately before and after the onset of SWD.

rat ID	Before SWD	SWD-start (the first 5 sec)	ΔS^2 (SWD-start)	SWD-end (the last 5 sec)	post-SWD	ΔS^2 (SWD-end)
S_{xy}^2			**THALAMO-CORTICAL COUPLING**			
23	0.074 ±0.039	0.177 ±0.093	0.103	0.097 ±0.062	0.045 ±0.028	-0.052
24	0.094 ±0.060	0.258 ±0.086	0.164	0.273 ±0.081	0.221 ±0.095	-0.052
25	0.034 ±0.021	0.080 ±0.044	0.046	0.043 ±0.028	0.037 ±0.024	-0.006
28	0.109 ±0.060	0.326 ±0.114	0.217	0.341 ±0.117	0.204 ±0.132	-0.137
29	0.027 ±0.021	0.080 ±0.044	0.053	0.081 ±0.048	0.079 ±0.041	-0.002
Total	0.066 ±0.053	0.183 ±0.125	0.117 ±0.073*	0.167 ±0.113	0.117 ±0.114	-0.049 ±0.075
S_{yx}^2			**CORTICO-THALAMIC COUPLING**			
23	0.060 ±0.033	0.103 ±0.041	0.043	0.064 ±0.036	0.027 ±0.020	-0.037
24	0.046 ±0.031	0.054 ±0.032	0.008	0.049 ±0.025	0.058 ±0.035	0.009
25	0.038 ±0.021	0.076 ±0.032	0.038	0.051 ±0.030	0.045 ±0.028	-0.006
28	0.042 ±0.030	0.099 ±0.037	0.075	0.091 ±0.033	0.059 ±0.037	-0.032
29	0.022 ±0.018	0.064 ±0.027	0.042	0.054±0.026	0.062 ±0.028	0.008
Total	0.042 ±0.030	0.079 ±0.039	0.037 ±0.020	0.062 ±0.035	0.047±0.032	-0.012 ±0.024

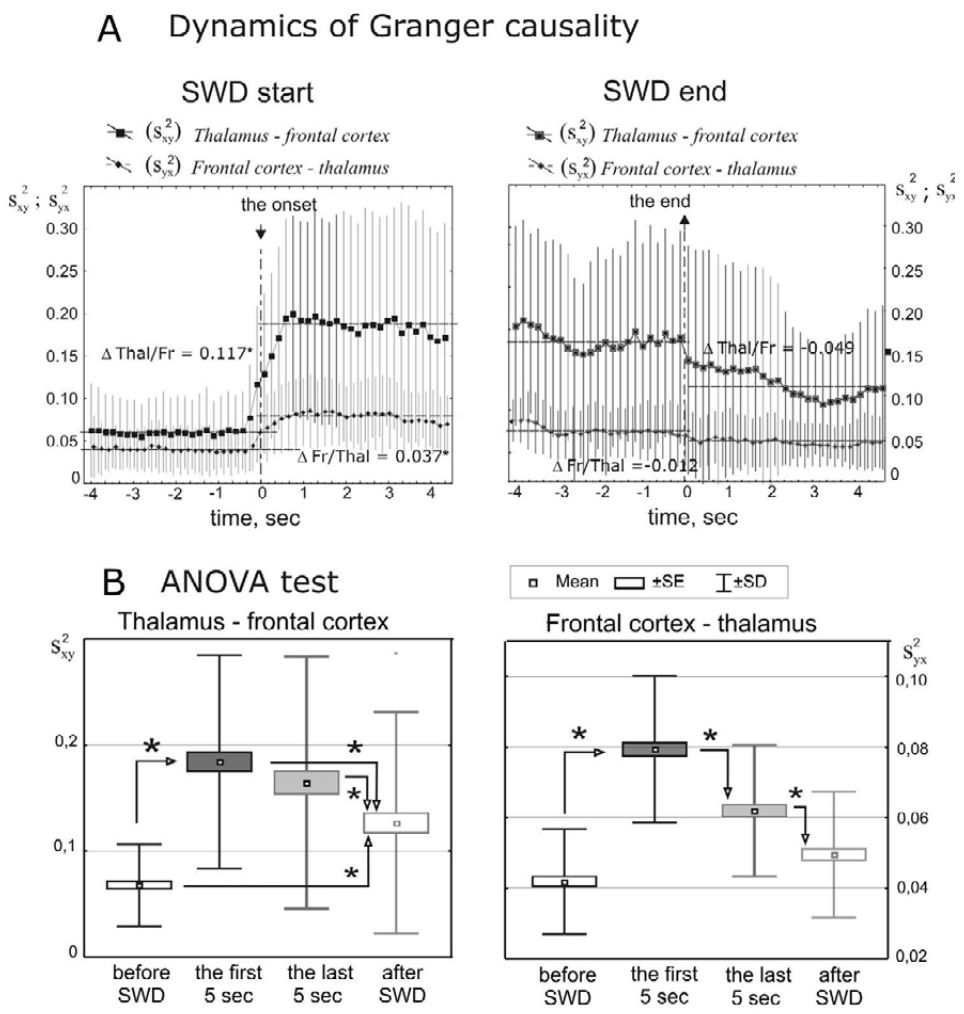

Figure 5.9. Statistical assessment of changes in Granger causalities associated with the onset and end of spike-wave discharges (SWD). (**A**) Bidirectional causal relationship between the frontal cortex and the thalamus at the onset and the end of SWD. Coefficients of Granger causality were averaged per 0.2 s intervals and per rat (mean±S.D.). The increase in Granger causalities at the onset of SWD was abrupt and significant (ANOVA, $p < .001$ post hoc LCD-test), but seizure offset was characterized by smooth and prolonged changes in Granger causalities. (**B**) Group statistics of Granger causality coefficients averaged in 5 s intervals (five rats, 30 SWD per rat). Asterisks show significant differences (the post hoc LSD test).

DISCUSSION

This study tackles a challenging problem of predictability of absence seizures in EEG. Using the concept of Granger causality, we measured bidirectional (straightforward and backward) linear interdependences between the thalamus and the cortex during absence seizures and obtained new yet comprehensive information about functional thalamo-cortical interactions during absence epilepsy. Traditional methods, such as crosscorrelation analysis of unit activity in a model of generalized epilepsy in cats [e.g. Steriade and Amzica, 1994) and coherence analysis in a genetic absence model (Sitnikova and van Luijtelaar, 2006] demonstrated that the genesis of generalized spike-and-wave discharges required mutual interrelationship between thalamus and cortex. The current study aims to evaluate a novel method for assessing directionality in thalamo-cortical network associations during absence epilepsy and this led to principally new conclusions:

(1) Information transfer in the direction 'thalamus→frontal cortex' was more intensive than in the backward direction. This is the first indication of anisotropy in thalamo-cortical interactions.
(2) Coupling strength 'frontal cortex→thalamus' slightly (but significantly) increased at the onset of SWD and rapidly restored to the initial level before cessation of a seizure. A strong and sustained increase in 'thalamus→frontal cortex' interactions was found not only during SWD, but also after the end of the seizure.

Implications of the linear Granger causality in EEG analysis of absence epilepsy

In patients with absence epilepsy, as well as in WAG/Rij rats, spike-wave seizures appear unpredictably from a normal EEG background and associated with sudden behavioral arrest, e.g. 'absences' [Panayiotopoulos, 1997; van Luijtelaar and Coenen, 1986]. As known, SWD are produced in the cortico-thalamocortical oscillatory

network [Avanzini and Franceschetti, 2003; Blumenfeld, 2002; Meeren et al., 2002, 2005; van Luijtelaar and Sitnikova, 2006]. Traditionally, coherence analysis is used to estimate functional associations between different brain areas [Challis and Kitney, 1991; Pereda et al., 2005]. Previously, we have used coherence to measure linear thalamocortical network associations in the frequency domain [Sitnikova and van Luijtelaar, 2006]. Granger causality is a time domain measure of functional interactions, assuming directionality and information transfer. Directionality of thalamo-cortical interactions during SWD in WAG/Rij rats has already been explored by means of nonlinear association EEG analysis [Meeren et al., 2002]. It was found that directionally of thalamo-cortical coupling varied throughout the seizure and it was the most constant during the first half a second, when the cortical epileptic focus consistently led the thalamus.

Hereby, by measuring Granger causality we also planned to identify early changes in thalamo-cortical relationships that may anticipate the onset of absence seizures. We adjusted a linear autoregressive model of Granger causality in order to describe causal relations between cortical and thalamic electrical activity during absence seizures in WAG/Rij rats. Surrogate data test confirmed the statistical significance of the observed interdependence.

We first found that the linear estimation of Granger causality provided a good approximation to baseline EEG (pre-SWD), e.g. linear autoregressive model was sufficient to obtain stable results of non-seizure activity. However, with linear estimations of Granger causality we failed to identify early changes of causal relationships that may anticipate the onset of absence seizures. It is however possible that early changes of interdependencies can be described with additional nonlinear autoregressive models or with phase-synchronization methods [Le Van Quyen and Bragin, 2007]. On the one hand, introduction of nonlinearity into the model may be necessary to get comprehensive information about network associations that prerequisite seizure activity or/and take place during a seizure. On the other hand, application of nonlinear AR model requires more careful selection of model parameters (such as dimensions and nonlinear model functions). This piece of work will be done in the future.

Several conclusions can be drawn from the present results. First, ‘thalamus→frontal cortex’ coupling characteristic, numerically, was greater than that in the opposite direction. This was found before, during and after SWD. The onset of SWD was associated with an amplification of pre-SWD existing tendencies. However, it is difficult to compare couplings in both directions to each other since thalamus and cortex signals are essentially different from each other even in respect of their waveforms [Sitnikova and van Luijtelaar, 2007]. More meaningful is to trace changes in coupling characteristics over time.

Second, ‘thalamus→frontal cortex’ coupling remained constantly high during a seizure and did not return to pre-SWD level even after cessation of SWD. It seems intriguing that although SWD were stopped, the thalamo-cortical network did not rapidly return to the non-epileptic state and causal relationships remained abnormal. Clinically, both start and end of SWD are regarded as abrupt and unpredictable, but we observe that changes in Granger causalities at the onset of SWD were more sharp and fast as compared with that at the end of SWD (post-SWD periods were characterized by smooth and prolonged changes in Granger causalities).

Third, Granger coupling strength increased with seizure onset, although differentially in two directions: reinforcement of ‘thalamus→frontal cortex’ coupling was greater than that in backward direction. However, this latter comparison should be interpreted with care, as mentioned above.

Granger causality and functional interactions in epileptic networks

In the present study we elaborate interactions between the frontal cortex and the thalamus during absence seizures. In our rats, EEG was recorded from the areas in which seizure activity is known to be the most robust, e.g. in the frontal cortex and in the VPM (specific thalamus) [Vergnes et al., 1987]. There are no direct anatomic connections between these sites, yet the VPM has bidirectional connections with the somatosensory cortex [Jones, 1985]. This midpoint, the peri-oral region of the somatosensory cortex in WAG/Rij rats, is known as ‘epileptic focus’ which initiate SWD [Meeren et al., 2002]. In our animals, the frontal EEG electrode was relatively far away from the ‘epileptic focus’ and we did not measure electrical activity in focal epileptic zone. Interestingly, a French group has recently confirmed and extended the Meeren et al. (2002) data in GAERS [Polack et al., 2007]. They showed that neurons in deep layers of the somatosenory cortex started firing much earlier than the first changes of local field potential could be visualized at the onset of SWD. This exaggerated neuronal firing at the early stages of SWD was only found in neurons localized in the epileptic cortical area, but it neither was detected in other areas in epileptic rats, nor in the similar areas in non-epileptic rats. Equally important is that our previous studies in WAG/Rij rats and others clearly demonstrated that neuronal activity in cortical regions outside the peri-oral area of the somatosensory cortex did not lead thalamic activity during SWD [Inoue et al., 1993; Seidenbecher et al., 1998].

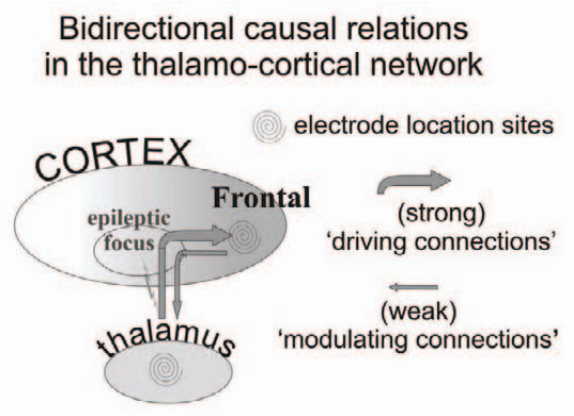

Figure 5.10. Physiological implication of Granger causality estimations. Ascending and descending anatomical connections from the thalamus to the frontal cortex go through the somatosensory cortex [Jones, 1985]. Somatosensory cortex in WAG/Rij rats contains the 'epileptic focus' that triggers epileptic activity [Meeren et al., 2002]. As known, SWD easily spread from the epileptic somatosensory area to the frontal cortex (EEG coherence study, [Sitnikova and van Luijtelaar, 2006]). Also anatomic connections 'somatosensory cortex (epileptic focus)→frontal cortex' are stronger than the backward 'frontal cortex→somatosensory cortex' [Kolb, 1990], this may prompt anterior propagation of SWD from the epileptic cortical zone to the frontal cortex. The 'epileptic focus' has strong connections ('driving connections' in terms of Crick and Koch, 1998) with the frontal cortex ('somatosensory cortex (epileptic focus)→frontal cortex'), but less strong 'modulating connections' with the thalamus ('somatosensory cortex (epileptic focus)→thalamus').

We study interdependencies between two indirectly connected structures that communicate via the 'epileptic focus': 'thalamus↔somatosensory cortex (epileptic focus)↔frontal cortex' (Fig. 5.10). In order to interpret our results, we put together several theoretical considerations: the 'cortical focus' theory [Meeren et al., 2002, 2005], our concept on global and local synchronization in oscillatory networks [Sitnikova and van Luijtelaar, 2006; van Luijtelaar and Sitnikova, 2006] and ideas of 'driving' and 'modulating' connections in neuronal networks [Crick and Koch, 1998]. We propose that the 'epileptic focus' not merely triggers, but also acts as a distributor of epileptic activity. In particular, seizure may easily propagate to those areas which have dense connections with the 'epileptic focus' [Sitnikova and van Luijtelaar, 2006]. In order to explain the quantitative differences between coupling strength between the thalamus and frontal cortex, we use a concept of two different kinds of network associations, e.g. 'driving' and 'modulating' connections [Crick and Koch, 1998] (Fig. 5.10). We hypothesize that the strong ascending coupling 'thalamus→frontal cortex' may prompt propagation and maintenance of SWD. These are 'driving connections' which are strong and induce an increase of firing activity in corresponding neurons. Less strong 'frontal cortex→thalamus' coupling may correspond to relatively weak 'modulating' connections which prevent spreading of SWD and are, therefore, involved in stopping SWD. In our case, the thalamus may excite the pathway from somatosensory to frontal cortex and this excitation may be a 'driving' force of seizure activity (Fig. 5.10). This schema agrees with outcomes of our coherence analysis where we found an enhancement of linear associations between somatosensory and frontal cortical areas at the onset of SWD [Sitnikova and van Luijtelaar, 2006].

EEG studies in animals: what can we gain from them?

Animals EEG research in epilepsy and other neurological diseases have some advantages. It was advantageous to use the WAG/Rij rat strain in the context of the present study. First, large amount of EEG epochs with seizure activity were required for the statistical analysis. These long time recordings with many SWD are not readily available in humans. Second, our aim was to clarify the role of the thalamus in absence epilepsy (this problem is still far from being solved, e.g. [Avanzini and Franceschetti, 2003; Blumenfeld, 2002; Huguenard and McCormick, 2007; Meeren et al., 2005; Steriade, 2005]). For this purpose our animals were implanted with depth thalamic electrodes, yet depth EEG recordings are nearly impossible in patients with absence epilepsy in which invasive depth EEG examination is exceptional. Third, human scalp EEG is affected by volume conduction (the outer tissues of the scalp act as a low pass filter). EEG electrodes in our animals were placed epidurally on the cortical surface. It is crucial that both cortical and thalamic electrodes recorded signals originating directly from the neuronal sources and the influence of volume conduction was excluded.

Chapter 6
Cortical mechanisms of SWD I *

CONTENTS

In 1931, Hans Berger observed characteristic changes in electroencephalogram (EEG) in humans during epileptic attacks; besides that, he was the first who noted spike-and-wave activity in epileptic patients (Fig. 1.1, cited by Goldensohn et al., 1997). Spike-wave discharges (SWD, type I) are regarded as EEG hallmark of absence epilepsy [Gibbs et al., 1935; Gibbs and Gibbs, 1950; INSECN, 1974; Panayiotopoulos, 2005]. Several theories have been proposed concerning neuronal substrate of SWD, among them are the 'centrencephalic' concept [Penfield and Jasper, 1954], 'cortico-reticular' theory [Gloor, 1968; 1969], 'cortical' theory [Bancaud et al., 1972; Niedermeyer, 1996], 'cortical focus' theory [Meeren et al., 2002; 2005] and other theories. The latter theory is grounded onto a nonlinear association analysis of multichannel EEG in WAG/Rij rats and it states that the perioral area of the somatosensory cortex contains a focus of epileptic activity [Meeren et al., 2002]. From this focus, seizure activity rapidly spreads throughout the cortex and the thalamus. The 'cortical focus' theory for generalized absence epilepsy [Meeren et al., 2002, 2005] bridges the earlier theories, i.e., the 'cortico-reticular' theory of Gloor (1969, 1978), the 'cortical' theory [Bancaud, 1969; Niedermeyer, 1972; Lüders et al., 1984] and the 'thalamic' theory [Buzsáki, 1991]. This **Chapter** presents some data in favor of the 'cortical focus' theory and early theories (these theories are briefly overviewed below).

---

* Chapter introduction is adopted from:
1) van Luijtelaar G, Sitnikova EY, Midzyanovskaya IS. Cortical control of absence seizures: focal initiation, spreading and modulation. In: Generalized seizures: from clinical phenomenology to underlying systems and networks. Eds: E. Hirsch, F. Andermann, P. Chauvel, J. Engel, F. Lopes da Silva, H. Luders. Libbey, 2006, pp. 93-117.
2) van Luijtelaar G, Sitnikova E. Global and focal aspects of absence epilepsy: the contribution of genetic models. Neurosci Biobehav Rev. 2006; 30(7): 983-1003.

SWD appear synchronously in the two hemispheres; this strong bilateral symmetry of SWD has long been thought to reflect paroxysmal activity of subcortical (central) structure which has diffuse ascending projections and distributes paroxysmal activity bilaterally to the cortex. The existence of a subcortical pacemaker of SWD was proposed by Jasper and Kershman (1941) and, a few years later, Penfield and Jasper (1954) introduced the 'centrencephalic' concept. These authors assumed that a 'centrencephalic integrating system' is localized in the brainstem and in the diencephalon and it is responsible for the bilateral onset of the SWD and for the decrease of consciousness. Later, it was found that SWD begin in the thalamus and spread to the cortex with 1–2 sec delay were obtained in patients with absence epilepsy by means of simultaneous thalamic and cortical recording of local field potentials [Williams, 1953] and 'centrencephalic' concept give rise to a 'thalamic' theory.

Another successor of the 'centrencephalic' concept, the 'cortico-reticular' theory, assumed that a common subcortical pacemaker is responsible for physiological sleep spindles and SWD [Gloor, 1969]. The 'cortico-reticular' theory was developed in the feline generalized penicillin absence epilepsy model [Gloor, 1968; 1969; 1979; Gloor et al. 1990; Kostopoulos, 2000]. In this model, systemic injections of penicillin (a weak $GABA_A$ receptor antagonist) caused a gradual dose-dependent transformation of spindles into SWD. The same results were obtained by local application of penicillin into the cortex, but not in the thalamus [Gloor et al., 1979; Gloor and Fariello, 1988]. In 1977, Gloor and co-workers stressed the role of the cortex in absence epilepsy: "*diffuse cortical epileptogenic state, with subcortical structures involved in spindle generation and recruiting responses, (particularly the "thalamic reticular system") acting as the most potent triggers of generalized bilaterally synchronous spike and wave discharge. Thus both cortical and subcortical mechanisms are important for the elaboration of generalized bilaterally synchronous spike and wave discharge*".

The 'cortico-reticular' theory assumes that the cortex in epileptic subjects is more excitable than in nonepileptic ones. Surprisingly few studies have directly tested whether cortical hyperexcitability underlies absence epilepsy. Excitability of the sensorimotor cortex for various types of afterdischarges and seizure types in WAG/Rij rat strain with absence epilepsy did not differ from that in non-epileptic control rats (ACI rat strain) [Tolmacheva et al., 2004]. In vitro, electrophysiological properties of cortical cells in epileptic rats (WAG/Rij and GAERS) non-epileptic control rats show just slight differences in respect to the waveform of evoked local field potentials, the percentage of different types of neurons (intrinsically bursting versus regular spiking cells) and intrinsic membrane properties, whereas passive neuronal responses remain the same [Luhmann et al., 1995; Avanzini et al., 1996; D'Antuono et al., 2006]. Altogether, it does not seem likely that, in general, the neocortex in WAG/Rij rats is more excitable than the neocortex in nonepileptic control rats. The present **Chapter** reconsiders a global role of the neocortex in absence epilepsy and focuses in focal aspects of this disease.

A global role of the cortex has been confirmed by studies in GAERS and WAG/Rij rats: cortical deactivation by the spreading depression technique (unilateral diffusion of KCl) resulted in immediate abolishment of SWD in the injected cortex and in the ipsilateral thalamus [Vergnes and Marescaux, 1992; Meeren, 2002]. The same effect was found in cats with penicillin-induced SWD during cortical spreading depression [Avoli and Gloor, 1981; Gloor et al., 1990]. Besides higher excitability of cortical neurons, some local abnormalities in the cortex might lead to absence epilepsy. According to the 'cortical' theory [Niedermeyer, 1996], generalized SWD are generated in the mesiofrontal cortex, from where they rapidly spread to other cortical areas. This theory is based on EEG data in epileptic patients. First, bilateral synchrony during typical SWD is not as perfect as previously believed [Lüders et al., 1980], suggesting that some cortical regions might be prone to absence epilepsy and others are more resistant. Second, depth recordings in epileptic patients revealed that the spontaneous discharges occurring during spontaneous 'petit mal' or 'grand mal' seizures may initially be localized to the cerebral cortex, in the vicinity of an identified lesion, particularly in the frontal lobe [Bancaud, 1969; 1972]. The thalamus certainly participates, but it only 'plays second fiddle' in carrying out normal physiological thalamo-cortical interactions [Niedermeyer, 1996].

The 'cortical focus' theory implies that a focus in the somatosensory cortex is primarily involved in the epileptic activity and initiates a cascade of events that ultimately leads to the occurrence of the bilateral and generalized SWD [Meeren et al., 2002]. **Chapter 6.1** shows that local transient events (ripples and double spiking) are present in fronto-parietal EEG during the early stages of SWD. These transient events may attribute the process of initiation and further propagation of seizure activity. The neocortical neurons are able to control thalamic activity throughout cortico-thalamic projections, which are especially dense (descending projections 'neocortex → specific thalamus' are several times more dense than ascending 'specific thalamus → neocortex' [Deschênes et al., 1998; Rouiller and Welker, 2000]). **Chapter 6.2** shows local cortical deactivation of a small part of the somatosensory cortex with microinjection of low doses of lidocaine temporally abolished SWD in WAG/Rij rats.

6.1 The fast components in SWD (type I) as recorded in the cortex †

INTRODUCTION

The EEG hallmark of absence seizures are symmetric, bilateral, widespread spike-and-wave discharges (SWD) of 3 Hz which typically occur without lateralizing or localizing features [Panayiotopoulos, 2005]. However, examination of EEG patterns of SWD revealed that bursts of generalized SWD usually predominate in frontal and central areas and occur much less in parietal, occipital and temporal regions [Rodin and Ancheta, 1987; Holmes et al., 2004; Craiu et al., 2006]. In patients with idiopathic generalized epilepsy, the onset of SWD was found in discrete focal regions of the frontal lobe (most often, in the orbitofrontal cortex), affecting either one side or the other. The frontal distribution of SWD has been studied with a dense-array recording technique and further examined electrical with the aid of distributed (LORETA) and point dipole (BESA) analyses [Holmes et al., 2004]. Results confirmed the importance of a frontopolar source to the spike-transition events that appeared interposed with the anterior negative slow wave.

The 'cortical focus' theory of absence epilepsy that was first introduced in WAG/Rij rat model of absence epilepsy [Meeren et al., 2002; 2005], suggests that a focal area in the somatosensory cortex (SmI, in the projection area of the snout, vibrissae and upper lip) is able to initiate SWD and to drive the rest of the corticothalamic circuitry. The 'cortical focus' theory is supported by clinical observations that spike-and-wave seizures have a focal onset [Holmes et al., 2004; Craiu et al., 2006].

The hypothesis that SWD are initiated in the SmI was also proposed by Seidenbecher et al. (1998), based on work in GAERS. It was found that SWD were accompanied by a spike concurrent, rhythmic burst-like activity in (mono-) synaptically connected regions of specific (somatosensory) thalamic areas, the SmI (layers IV/V), and the RTN. SWD-correlated activity in the SmI layers IV/V started significantly earlier than correlated burst firing in reticular and in ventrobasal thalamic neurons [Seidenbecher et al., 1998]. This implies that focal epileptic area in the somatosensory cortex (the area of facial projections) might that exhibit some pro-epileptic transient events, similar to what have been described in epileptic foci in human and animal in some neocortical seizures, namely, ripples (>60 Hz) or high-frequency oscillations [Worrell et al., 2004; Grenier et al., 2003]. We hypothesized that EEG in the focal epileptic zone in SmI might be endowed by aberrant transient phenomena (ripples) which are associated with the onset of SWD. The putative transient EEG phenomena may correspond to the primary epileptogenic processes in the epileptic areas in SmI, e.g., increased neuronal excitability, higher synchronization in neuronal networks, changes in firing activity.

In the present **Chapter** we examine SWD in the primary epileptic zone in order to disclose those transient components or local events, such as polyspiking or ripples, which could correspond to the process of initiating and spreading of seizure activity.

METHODS

Experiments were performed in nine male WAG/Rij rats (11-12 month old, body weight 370-410 g). Rats were equipped with 10 active epidural electrodes that were put bilaterally over the frontal cortex [AP +2, L ±2.5], parietal cortex, including projections of hind limbs [AP -1; L ±2.5], fore limbs [AP 0, L ±4] and vibrissae [AP –2, L ±5.5], and occipital cortex [AP –6; L ±5]. Some animals were implanted two additional electrodes in the occipital cortex [occipital 2, AP –5; L ±4]. In addition, one electrode was implanted into the right side of the dorsal hippocampus CA1 region [AP –3, L +3; H 3]. Electrodes were made of stainless steel wires of 0.20 mm diameter and had non-insulated tips. The ground and the reference electrodes were placed at two symmetrical sides over the cerebellum. EEGs were recorded in freely moving rats during the dark period of the day-night. Recordings were performed in a noise-isolated experimental chamber continuously during 5-7 hours. EEG signals were fed into a multi-channel differential amplifier via a swivel contact, filtered between 1 and 500 Hz, digitized with 1024 samples/second/per channel (CODAS software) and stored on hard disk.

SWD (type I) were detected using criteria described in van Luijtelaar and Coenen (1986) and Midzianovskaia et al. (2001). SWD were recognized in the frontal EEG as a train of surface negative 7-10 Hz spikes with amplitude at least three times higher than the background. Duration of SWD I was more than 1 sec. Here we employed an automatic system for detecting SWD I that relied upon the threshold value of the EEG slope in the frontal channel. Fine details of seizure morphology (e.g., transient elements, ripples and aberrations in EEG) were examined in the multichannel EEG as recorded at various cortical and hippocampal regions. In order to

† A part of the paper is published. Sitnikova E, van Luijtelaar G. Electroencephalographic characterization of Spike-Wave Discharges in cortex and thalamus in WAG/Rij rats. Epilepsia, 2007; 48 (12): 2296–2311.

access area-specific elements in SWD, episodes with SWD were visually inspected for the presence of a consistent trend in the spatiotemporal distribution of electrical seizure activity.

RESULTS

It was found that SWD in multiple cortical areas encompassed fast transient events, such as small spikes (arrows in Fig. 6.1), ripples (arrows in Fig. 6.2). These fast transient events were inconstant throughout the seizure and were asynchronous. They were encountered in epileptic discharges, but not in non-epileptic sleep oscillations (spindles and K-complexes).

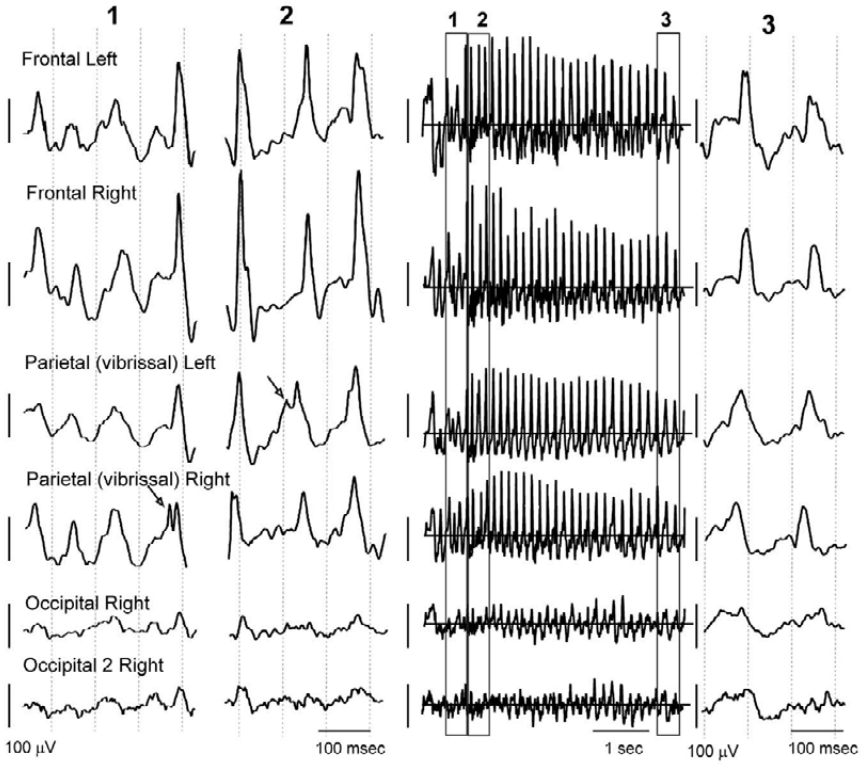

Figure 6.1. Spatial distribution of generalized SWD I across the cortex. The whole seizure is presented in time-compressed scale. The initial and final episodes are extracted in time-stretched windows. In two subsequent episodes, 1-2, in a few initial cycles of a seizure, occasional small spikes (each of them is indicated by an arrow) appeared on the descending slope of EEG curve just prior the generalized large Spike 2, so the pattern looks like "double spiking" phenomena. In some SWD I, the small transient spikes resembled Spike 1, but the small transients were often unilateral and asymmetrical, and occasionally formed double-spike complexes together with Spike 2.

One example in Fig. 6.1 illustrates that an additional spike (pointed by an arrow in epoch 1) was followed by the first gross spike (Weir's 'Spike 2', see also **Chapter 3.1**) in SWD (type I). This 'double-spiking' complex was found in the parietal right EEG, but not in other loci. In the subsequent epoch 2, a similar 'double-spiking' complex was present in the symmetrical area on the left side of the parietal cortex (arrow in epoch 2). Noteworthy is that double-spiking phenomena appeared in the area of vibrissae in the somatosensory cortex that corresponds to the focal epileptic zone (Meeren et al., 2002). Small spikes in SWD I coincided with minor fast irregular components that resembled EEG ripples (arrows in Fig. 6.2). 'Double-spiking' complexes and ripples were found during SWD I in the frontal EEG channel (arrows in Fig. 6.2). Ripples were sometimes present in the occipital areas (encircled in Fig. 6.2). We conclude that, besides gross Weir's components, SWD in the fronto-parietal cortex comprise minor irregular fast components.

Similar results were reported by Kandel and Busáki (1997) who found fast ripples (200–800 Hz) associated with the Spike components in EEG seizures in several rat strains with absence epilepsy. These findings are also is in line with the previous observations that the onset of generalized neocortical seizures and, probably, other forms of epilepsy [Worrell et al., 2004; Jirsch et al., 2006] associates with fast (60-100 Hz, [Worrell et al., 2004]) and very fast activity (200 Hz and higher [Grenier, 2003]). In our model, fast seizure components in the cortex are likely to result from intracortical epileptogenic processes and may underlay focal cortical initiation and further intracortical horizontal propagation of seizure activity.

In the framework of the current research we have to stress an importance of filtering of EEG data. The quality of low-pass <70 or 100 Hz filtered EEG is usually good enough for clinical purposes, but it may hamper

high frequencies which are expected to be involved in the process of epileptogenesis. The problem is that the fast transient elements can be attenuated if low-pass filters are too low (> 30 Hz). To address this problem we used several low-pass EEG filters with different cut-off frequencies: 25, 40, 85 and 150 Hz (Fig. 6.2). It was shown that the small transient spikes did not pass the 40 Hz filter barrier and were not visible in the filtered EEG. 40 Hz low-pass filtering resulted in a smooth EEG, in which repetitive 8-10 Hz spikes in SWD I were less sharp as compared to sharp spikes in unfiltered SWD I. A low pass filter of 85 or 150 Hz did not cut the fast transient events in the EEG.

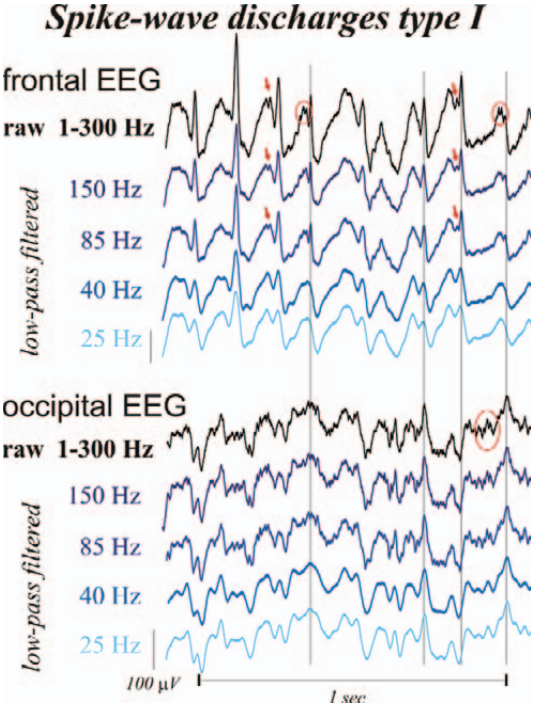

Figure 6.2. The influence of low-pass filtering on the visual appearance of SWD I in EEG. The choice of cut-off frequencies below 85 Hz results in a dissipation of the fast and sharp spikes (black arrows). The small spikes are present in 200 and 85 Hz low-pass filtered EEG, but absent in 40 Hz filtered data (grey arrows).

DISCUSSION

In the present study, we used low pass filtering > 85 Hz (preferably 200 Hz) in order to define fast transient phenomena. The small spikes in SWD are occasionally seen in the frontal and parietal cortex and, together with the 'Spike 2', formed 'double-spiking' complexes during initial period of SWD. Therefore, the EEG profile of absence seizures in WAG/Rij rats fits well to the definition given by IFSECN to spike-and-slow-wave complex and multiple spike-and-slow-wave complex (= polyspike-and-slow-wave complex: *'a sequence of two or more spikes associated with one or more slow waves*'). We propose that EEG transient events at initial period of SWD may result from an aberration of neuronal mechanisms, possibly, synaptic modification and progressive reinforcement of local epileptogenic circuits. It is also possible that cytoarchetectonic disorder in fronto-parietal cortex may conbtribute to the occurrence of ripples and multiple mini-spikes in SWD [Karpova et al., 2005].

A plausible morphological substrate of fast transient phenomena during initial period of SWD

It is a common belief that typical absence epilepsy is a purely 'functional' disease since no structural lesion of any kind has ever been identified [Berkovic et al., 1987; Niedermeyer, 1996]. However, the cellular structure of cortical tissue is poorly explored. There was an indication of microdysgenesis in childhood absence epilepsy with an increased number of dystrophic neurons in neocortex and the subcortical white matter of the frontal lobe [Meencke, 1989].

Recently, in WAG/Rij animal model of absence epilepsy, Karpova and co-workers (2005) examined the cytoarchitecture of the frontal cortex (motor area) and parietal cortex (somatosensory area, including the area of perioral projections, e.g., the plausible trigger site of SWD). Typical for both frontal and parietal areas in WAG/Rij rats was a disorder in the distribution of pyramidal cells in the superficial cortical layers (I–III). Apical dendrites of superficial pyramidal cells were often split in two branches, declined and went in non-perpendicular directions. Quantitative morphometric measurements of dendrites such as the total length of dendrites, mean length of dendritic segments and the size of the dendritic arbor, were increased as compared to non-epileptic rats. Disturbances in dendritic trees (a receptive part of neurons) may cause impairment in communication between

individual neurons. Altogether, fronto-parietal area of neocortex in WAG/Rij rats may express abnormal associations with other cortical areas that may facilitate synchronization and propagation of SWD.

Intracortical epileptogenic mechanism of the initiation-propagation-augmentation of SWD

There are two kinds of transient events in EEG that have been found during the initial period of SWD:
(1) the small transient spikes were clearly pronounced during SWD in the frontal and parietal areas (Fig. 6.1).
(2) low-amplitude ripples appeared irregularly in the investigated cortical areas (Fig. 6.2).

These transient events are considered as an integrated part of the EEG absence seizures. The functional significance of fast EEG events in epileptogenesis is not very clear. High-frequency oscillations may be unfairly treated in human EEG due to low-pass filtering at 70 or 100 Hz. from layer V. Recordings of neuronal field potentials in different rats strains with absence epilepsy (WAG/Rij, Brown Norway, Fischer) unambiguously showed that the fast ripples (400–600 Hz) are associated with spike component in EEG epileptic discharges and correspond to the increased neuronal synchrony [Kandel and Busáki, 1997]: '*ripples represent a fast transient event by which action potentials of different neurons can be synchronized with a high temporal precision*' (p.6791). Fast ripple oscillations (80–200 Hz) are known to be present during the early stages of neocortical seizures in epileptic patients [Worrell et al., 2004] and they are found in the feline penicillin model [Grenier et al, 2003]. In both cases, the fast oscillations may be caused by fast neuronal processes that are responsible for the initiation of neocortical seizures. We assume that the newly observed fast transient events (ripples and double spiking events in the parietal cortex) at the beginning of SWD have also pro-epileptic nature. Polyspiking in a spike-and-wave complex (polyspike-wave complexes) is likely to result from impairment of intrinsic cortical mechanisms [Timofeev et al., 1998]. In addition to that, in human patients, the presence of more than 3 spikes per wave may indicate a bad prognosis [Panayiotopoulos, 2005].

Previously we have found that the onset of SWD corresponded to a broadband increase of intracortical coherence and strengthening of the anterior-parietal associations in gamma frequencies up to 60 Hz [Sitnikova and van Luijtelaar, 2006]. It is likely that, in our subjects, the increase of intracortical fast oscillatory synchrony (in the fronto-parietal area) results in fast transient events in the EEG and may contribute to a further increase in synchrony. The presence of an additional spike (as in double spiking complexes that were found at the onset of SWD I in the parietal cortex) may suggest that neurons in this area have an intrinsic ability to oscillate and to produce hypersynchronous bursts. This hypersynchronous activity can be expressed in the EEG as double spiking, it further spread to the thalamus and, finally, reinforces the reproduction of 7-11 Hz rhythm within the cortico-thalamo-cortical circuit.

Altogether, transient events in EEG recorded in the parietal cortex and neighboring area support the 'cortical focus' theory of absence epilepsy [Meeren et al., 2002; Meeren et al., 2005]. The present results and our previous data [Sitnikova and van Luijtelaar, 2006; Sitnikova et al., 2008] altogether suggest that SWD are initiated in a small region of the parietal cortex, and that global cortico-thalamic mechanisms are important for the further generalization of seizure activity [Meeren et al., 2005].

CONCLUSIONS

Fast cortical components, e.g. EEG ripples and double spiking in the anterior-middle part of the cortex are integrated in generalized SWD (type I). This suggests fast cortical processes may be implicated in the initiation and in further horizontal propagation of seizure activity.
We found that, in our genetic rat model, relatively high (> 85 Hz) cut-off frequencies are required to notify the fast transient events.

6.2 Cortical control of SWD (type I): effect of lidocaine applied to the somatosensory cortex ‡

ABSTRACT

The role of the somatosensory cortex (SmI) in the incidence of spike–wave discharges (SWD) was studied in a genetic model of absence epilepsy, WAG/Rij rats. SWD were recently shown to initiate at the perioral area of the SmI and spread over the cortex and thalamus within a few milliseconds [Meeren et al., 2002]. It was hypothesized that functional deactivation of the SmI might reduce the appearance of SWD.

This was tested using unilateral microinjections (1 μl) of 2% lidocaine into the SmI in 13 WAG/Rij rats. Electrocorticogram (EEG) was recorded in free moving animals from four cortical sites after lidocaine and control (saline) injections. Lidocaine effectively diminished the total power of the EEG mostly in the area surrounding the injection site. Deactivation of the perioral region of the SmI reduced the incidence of SWD at the entire cortex in both hemispheres. The number of SWD gradually returned to a control level at the end of the second hour after lidocaine injections. These data show that proper functioning of SmI is important for the occurrence of SWD, supporting the idea that absence seizures might have a focal cortical origin.

INTRODUCTION

Clinical manifestation of typical absence epilepsy is a sudden, brief interruption of consciousness. This corresponds to generalized, synchronous, stereotyped 2.5–4 Hz spike–wave discharges (SWD) in the electroencephalogram EEG [e.g., Gibbs et al., 1935; Panayiotopoulos, 1999 and 2005]. In feline generalized penicillin epilepsy, systematic or intracortical injections of penicillin resulted in a stepwise transformation of 6–12 Hz sleep spindles into 3 Hz SWD. Therefore, it was assumed that bilaterally synchronous SWD derive from natural sleep oscillations due to the gradual increase of cortical excitability [Gloor, 1968; 1969; 1979; Gloor et al. 1990; Kostopoulos, 2000]. With *in vivo, in vitro* studies and neuronal model computations it was proved that both sleep spindles and SWD require the same thalamocortical interplay between specific and reticular thalamic nuclei [Vergnes et al., 1987; Steriade and Llinas, 1988; Avanzini et al., 1992; Destexhe and Sejnowski, 2001; McCormick, 2002]. More specifically, it was shown that SWD and sleep spindles invade the ventrobasal complex of thalamus and reticular thalamic nuclei (RTN) [Inoue et al., 1993; Seidenbecher, 1998; Slaght et al., 2002]; the RTN was proposed to be the pacemaker for both SWD and sleep spindles [Avanzini et al., 1992; 1993; 2000; Avanzini and Franceschetti, 2003; Avoli and Gloor, 1982; Buzsáki et al., 1988].

According to recent investigations in rat models of absence epilepsy, e.g., WAG/Rij [Meeren at al, 2002; 2005] and GAERS [Manning, et al., 2003] the thalamus plays a secondary role in SWD: (1) it was found that the somatosensory cortex (SmI, region of perioral projections) triggers SWD and seizures quickly spreads from this epileptic focus over the cortex and to the ventrobasal thalamus, e.g. ‘cortical focus’ theory [Meeren at al, 2002]. (2) Studies in GAERS with microinfusion of ethosuximide in the cortex and in the thalamus have confirmed a ‘cortical focus’ theory. A substantial decrease in the number of SWD was found after microinfusion of ethosuximide (anti-absence drug) into the SmI; whereas, were no or less effect was observed when ethosuximide was injected into the other cortical regions (forelimb projection area of SmI, motor cortex, ventrobasal complex of the thalamus and RTN) [Manning, et al., 2003; 2004; Richards et al., 2003].

The perioral region of SmI in rodents produces regular neuronal oscillations [Silva et al., 1991; Nicolelis et al., 1995] which could be recorded in EEG as 7–12 Hz somatosensory rhythm [Ahissar et al., 1997, Nicolelis et al., 1995]. It is striking that this perioral region is known to be a primary source of SWD, suggesting that normal neuronal circuits which are responsible for 7–12 Hz somatosensory rhythm in non-epileptic rats, may initiate hypersynchronous discharges (SWD) in epileptic rat strains. This suggestion was tested with microinjections of 2% lidocaine for local temporarily deactivation [Malpeli and Schiller, 1979; Tehovnik and Sommer, 1997; Martin and Ghez, 1999] of the activity in the perioral region of SmI. The present section describes the effect of local deactivation of SmI on the incidence of SWD and in EEG power spectrum of ictal and interictal EEG.

‡ Published in:
Sitnikova E, van Luijtelaar G. Cortical control of generalized absence seizures: effect of lidocaine applied to the somatosensory cortex in WAG/Rij rats. Brain Res., 2004; 1012(1-2): 127-137.

METHODS

Animals and surgery procedure

13 male WAG/Rij rats (6 - 9 months old, body weight320–470 g) were used. Animals were born and raised in the laboratory of the Department of Biological Psychology at University of Nijmegen. Before surgery, rats were kept in standard cages in small groups with free access to food and water and 12–12 h light–dark cycle (white lights on at 20.00); after surgery, animals were housed individually. The Ethical Committee on Animal Experimentation of the University of Nijmegen approved the experiments.

Each rat was equipped with two tripolar stainless steel electrode sets (Plastic One, Roanoke, VI, USA: MS 333/2), four out of six electrodes were used for local monopolar recordings, two others were used as ground and reference. A stainless steel guided cannula (Plastic One: C131G; tubing inner diameter—0.4 mm, outer diameter—0.7 mm) was implanted over the right SmI [AP -2; L + 7], above the perioral region [Chapin and Lin, 1984]. Two out of four active electrodes were placed on the frontal cortex (AP + 2, L±3 mm, distance between the tip of the cannula, and right ipsilateral electrode was 4.8±0.5 mm and was 9.8±0.2 mm for the left-side electrode), the third recording electrode was over the SmI, in the immediate proximity to the cannula (1.5±0.7 mm in the rostro–medial direction, AP -1; L + 6) and the fourth electrode—over the occipital right cortex (AP -6, L + 4, distance to the cannula was 5.4±0.4 mm). Ground and reference electrodes were implanted symmetrically over both sides of cerebellum. All coordinates are given relative to bregma; positioning of electrodes and cannula was verified by post mortem measurements.

Stereotactic surgery was performed under isofluorane anesthesia (Forene®, Abbott Lab., Queenborough, Kent, UK) after premedication with 0.2 ml atropine sulfate s.c. (Centrofarm©, Etten Leur, the Netherlands). For local analgesia, 2% lidocaine HCl was used. Body heat of animals was maintained at 37jC with a heating pad. Electrode sets and cannula were fixed to the skull surface with two stainless steel screws and dental cement. Cannula was attached to the sloping side of the skull; muscular tissues were carefully displaced avoiding any incisions and bleeding. The plastic part of cannula was covered by dental cement and strongly stuck to the bone. Rats received a 0.1–0.2 mg/kg i.m. injection of 0.324 mg/ml buprenorfinehydrochloride (Temgesic®, Reckitt and Colman Products, Kingston-Upon-Hull, UK) for postsurgery analgesia immediately after completion of surgery. Daily cleaning of wounds with iodine solution prevented inflammation. Body weights were daily monitored, recording sessions began after the recovery period of 10–18 days when body weighs were restored.

Experimental design

Two successive unilateral injections were made into the SmI: 1 μl of 2% lidocaine HCl and 1 μl of 0.9% NaCl. A Hamilton syringe (2 μl capacity) was used for injecting, the syringe itself was fixed into a mechanic holder so as its piston was set into motion by turning the holder-screw. One full turn of the screw displaced the piston in such a way that 0.025 Al was released, so liquids were injected steadily with a very slow speed (0.5–0.7 μl/min). The injection needle (outer diameter: 0.4 mm) fitted well to the guide cannula and was connected with the Hamilton syringe via a flexible plastic tube. The needle went 1.5 mm out the inner tip of the cannula at the time of injections. The tip of the guide cannula was placed just above the dura mater and did not penetrate the cortex. Chosen volume of injections (1 μl) and low speed were small enough to keep cortical tissue out of any mechanical damage due to volume displacement [Demer and Robinson, 1982]. At the same time, 1 μl of 2% lidocaine was sufficient for local deactivation of neuronal activity. Being injected in this volume, 2% lidocaine is known to produce a reversible reduction of synaptic activity during 40–60 min [Burton and Robinson, 1987; Martin and Ghez, 1999].

The period between two successive injections was 7–10 days. In 7 out of 13 rats, lidocaine was injected first; in other six animals, saline was injected prior to lidocaine. The order of injections (saline/lidocaine or lidocaine/saline) was taken into account as a factor in the ANOVA.

EEG was recorded in free moving rats in a noise-isolated Faraday cage. Subjects were placed into Plexiglas recording cages (25 X 30 cm width, 35 cm high) at least half an hour before onset of EEG recordings. A few days before experiments, baseline EEG was recorded for 2 hours in all subjects. At the time of experiments, the EEG was recorded 1 h before and 2 h after injection. The experiments were performed during the middle and later hours of the dark period, when incidence of SWD is known to higher [van Luijtelaar and Coenen, 1988].

EEG recording and analysis

The EEG signals were fed into a multichannel differential amplifier via a swivel contact, band-pass filtered between 1–500 Hz, digitized with 256 samples per second and stored onto hard disk (Data Acquisition Hardware and Software, DATAQ Instruments, Akron, OH). SWD were visually detected in the frontal EEG from the intact

(left) hemisphere. SWD were defined as a characteristic train of sharp asymmetric large-amplitude spikes and slow waves; the first and last spikes in a train were used as start and end points of SWD (Fig. 6.3B). SWD (type I) were detected using criteria described in the earlier reports [van Luijtelaar and Coenen 1986; Midzianovskaia et al., 2001]. Number of SWD was first scored on the frontal intact cortex of the full-length EEG records, i.e., during 2 h after the injection. Duration of SWD was determined also in the frontal intact EEG within the first hour after injections (5–12 SWD per animal).

The number of SWD was corrected in respect to the amount of sleep, because it is known that SWD mainly occur during drowsiness and light sleep [Drinkenburg et al., 1991; Coenen et al., 1992]. Duration of non-sleep EEG was measured per 5 min intervals and used for computing the 'coefficients of vigilance'. Uncorrected and corrected data were analyzed independently. The number of SWD were summarized per 30 min periods after injections and statistically analyzed using an ANOVA for repeated measures (with 'Time' and 'Drug' as within-subject factors and the 'Order' of injection as a between-subjects factor). Neither the effect of the factor 'Order' was significant, nor the interactions, therefore, the factor 'Order' was removed from the ANOVA. The changes over the 30 min blocks (lidocaine is expected to act temporarily) were analyzed with orthogonal trend analyses (one-tailed).

In order to study whether lidocaine equally affected spike–wave activity in all four channels, SWDs were also automatically detected in each recording channel based on the threshold value of slopes of spike of the SWD. This method gave us 97% of hits (software was developed by P.L.C. van den Broek, NICI, Nijmegen University, the Netherlands). The identification of SWDs in all four channels was performed in a period of 30 min, from 30 to 60 min after injection of 2% lidocaine, when the decrease in number of SWD was most pronounced. EEG epochs of equal length and time after injection of saline served as a control.

Results were analyzed with an ANOVA for repeated measures; again, 'drug' and 'location' were used as within subject factors, 'Order' of injection as a between-subjects factor.

A Hanning windowed Fast Fourier Transformation (FFT) was performed in order to study the changes in power and spectral characteristics in EEG after lidocaine and saline injections in all four EEG channels during the first hour after both injections. Computations of EEG power spectrum included periods of passive wakefulness (4 s epochs, n = 13 rats, 10–15 per animal) and SWD (2 s epochs, n = 10 rats, 5–15 per animal). Total power of EEG and power in the specific frequency bands (i.e., 0.5–4, 4–8, 8–12, 12–30 and 30–100 Hz) was statistically analyzed. In these frequency bands, 0.5–4 Hz characterized slow–wave activity (characteristic for sleep), 4–8 Hz is theta activity (characteristic of active wakefulness), 8–12 Hz band included main frequency of SWD (that is about 8–10 Hz, Fig), 12–30 Hz beta waking EEG (in the case of SWD it contains the first and second harmonics (16–20 and 24–30 Hz respectively). EEG power was statistically analyzed using two-tailed Wilcoxon paired test for repeated measures ($p < 0.05$). A decrease in EEG power after lidocaine injections was used to estimate the effectiveness of cortical deactivation.

RESULTS

All subjects showed numerous spontaneous SWD. SWD appeared as generalized 7 - 10 Hz discharges (Fig. 6.3). Wave component was predominant at the occipital cortex and spike – in the frontal cortex.

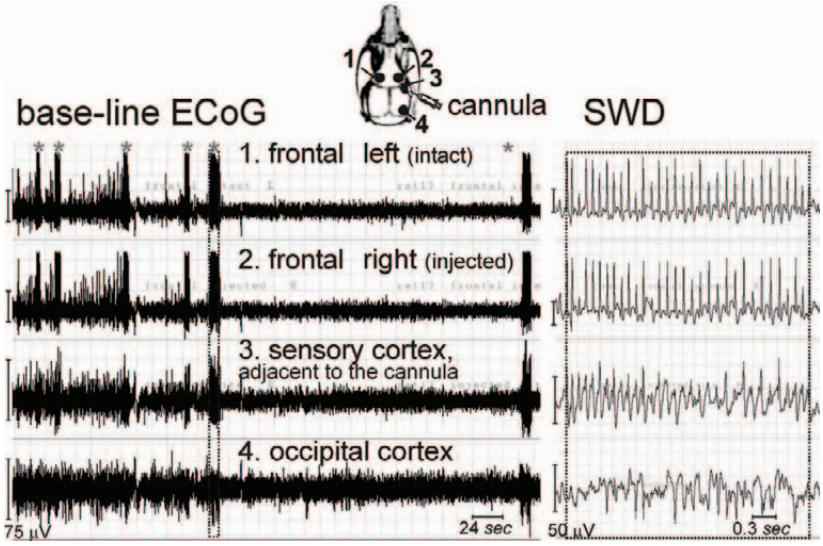

Figure 6.3. Multichannel EEG record in baseline (spontaneous SWD are asterisked). Note amplitude differences between channels.

General changes in EEG after microinjections of 2% lidocaine

EEG pattern of SWD was disturbed shortly after administration of 2% lidocaine comparing to what was seen after saline injections. Fig. 6.4 illustrates the EEG recorded immediately after saline and 2% lidocaine injections After control injection, SWD occur with a normal periodicity and their EEG pattern was not distinguished from SWD in control. After injection of 2% lidocaine, SWDs were eliminated and substituted by irregular oscillations which appeared asynchronously in different EEG channels. These irregular oscillations no longer meet the criteria for SWD and were no longer recognized with the automatic routine.

Effect of lidocaine in power spectrum of EEG during passive wakefulness and SWD

FFT-transformation of the EEG was used to access changes in the cortex induced by the local administration of lidocaine. Averaged spectra from the four cortical sites were obtained during the state of passive wakefulness and during SWD. In 10 out of 13 (77%) rats, injection of lidocaine resulted in significant decrease in total EEG power as compared to saline. In these animals, deactivation of was considered to be significant and their EEG data were used for statistical analysis.

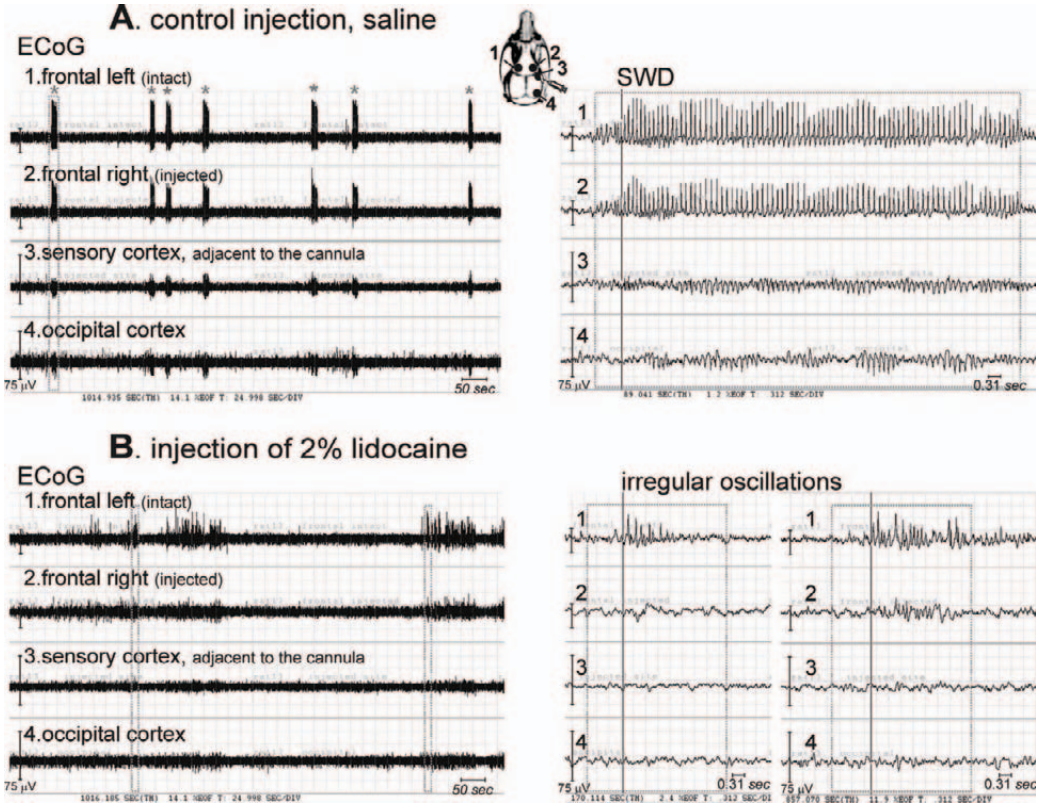

Figure 6.4. EEG recorded immediately after injections of saline (A) and 2% lidocaine (B) in the same animal. Outlined are the first SWD after the injection of saline (A) and the first and latter irregular oscillations (B); these phenomena are shown on the right with a higher time resolution. Note amplitude differences between EEG channels.

Averaged EEG power spectra of multichannel EEG data are presented in Fig. 6.5 (passive wakefulness) and in Fig. 6.6 (SWD). The most significant decrease of EEG power was obtained in the SmI, near the injection site. This area showed the most pronounced (1) dissimilarities in frequency distribution of spectral power (graphs 3 in Figs. 6.5 and 6.6) and (2) reduction of total EEG power ($p < 0.05$ during passive wakefulness, $p < 0.005$ during SWD, paired Wilcoxon test). The decrease in EEG power involved 8–30 Hz frequencies (in SWD and in passive wakefulness). In the occipital cortex, during passive wakefulness (graph 4, Fig. 6.5), the reduction of the EEG amplitude after lidocaine injection in 8-12 Hz was significant and during SWD - in 0.5–4 and 12–30 Hz (graph 4, Fig. 6.6).

Table 6.1. The effect of intracortical microinjection of 2% lidocaine in the number of SWD (mean±S.E.M.)

		Number of SWDs (uncorrected)		Number of SWD (corrected for the state of vigilance)	
		Saline (control)	2% lidocaine	Saline (control)	2% lidocaine
Hour after injection	1-st	23.7 ± 7.0	10.4 ± 3.3	10.8 ± 3.2	5.2 ± 1.5
	2-nd	24.3 ± 5.7	11.1 ± 2.8	7.5 ± 1.6	5.7 ±1 .3
Sum for 2 h		47.5 ± 12.1	21.8 ± 6.7	18.2 ± 4.7	10.8 ± 2.9

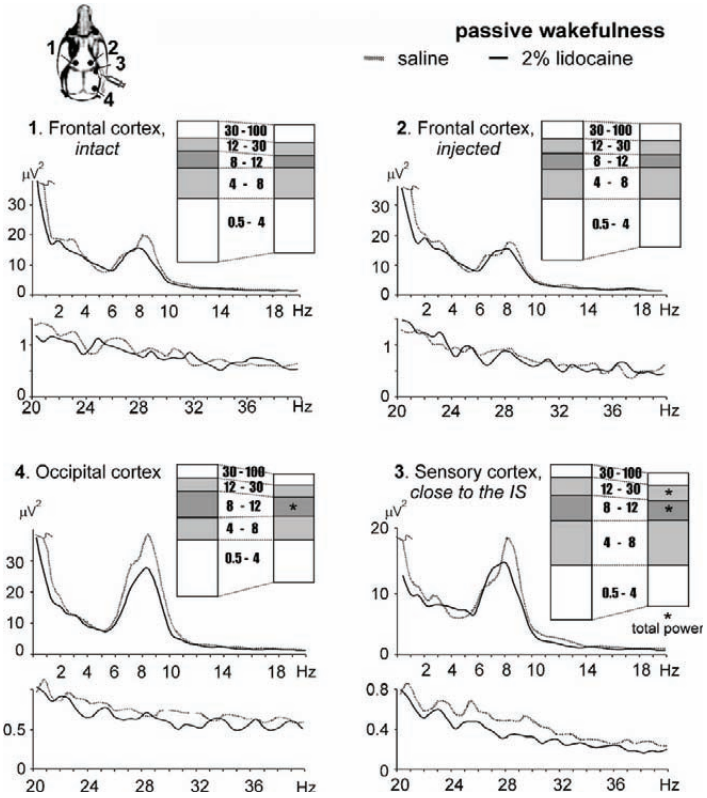

Figure 6.5. Power spectra of EEG during passive wakefulness after local application of 2% lidocaine and saline (average of 10 rats). Stacked columns show distribution of power over frequency bands (saline injection are on the left and lidocaine - on the right, asterisked are significant differences; Wilcoxon test for the repeated measures, $p < 0.05$). In the area surrounding the injection site (graph 3), lidocaine injections resulted in significant decrease in power of 8–12 and 12– 30 Hz bands and in total power. In occipital EEG (graph 4), power is decreased after lidocaine only in 8– 12 Hz.

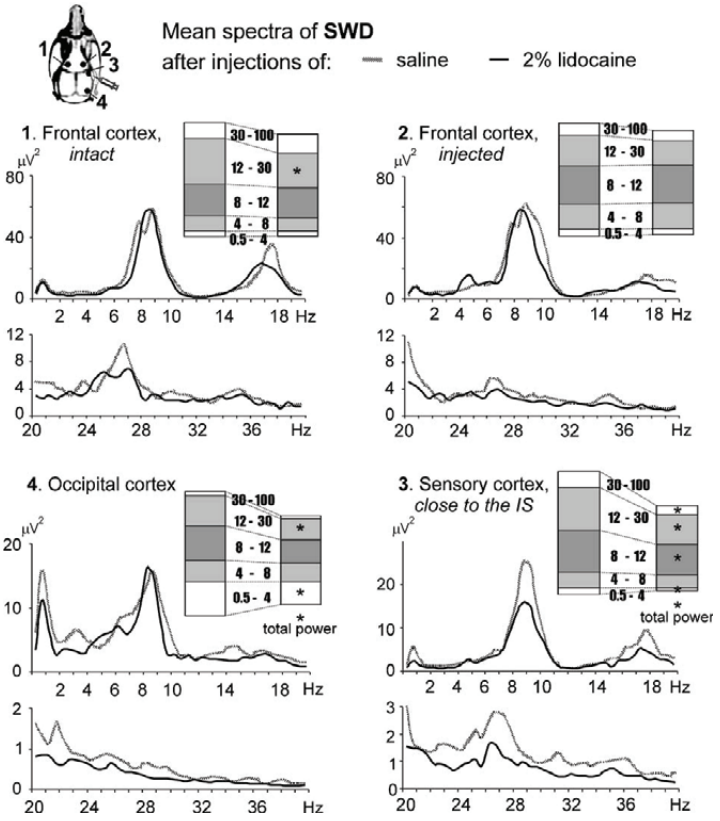

Figure 6.6. Power spectra of SWD as measured during the first hour after administration of saline and 2% lidocaine (n=8 rats). After application of lidocaine, the total EEG power reduced in the SmI surrounding the injection site (graph 3) and in the occipital cortex (graph 4). In the SmI (graph 3), lidocaine injection caused reduction of spectral peak in ~9 Hz (corresponding to fundamental frequency of SWD), in ~18 Hz (first harmonic) diminished, and in ~ 27 Hz (second harmonic). In other EEG channels the changes in EEG power are less pronounced.

Total power of SWD, as measured in left and right frontal EEG, after lidocaine and saline injections was the same. Yet, SWD in the left intact hemisphere showed a less power in 12–30 Hz as compared to saline (this corresponds to diminution of the first and second harmonics of SWD, e.g. ~18 and ~27 Hz, graph 1, Fig. 6.6). SWD are known to differ from spiky oscillations or sharp sleep spindles by the presence of higher harmonics in their EEG spectrum [Drinkenburg et al., 1991], suggesting that lidocaine caused greater impairment of pattern of SWD at the intact hemisphere as compared to that in the injected side.

In all, power spectrum analysis showed that microinjections of 2% lidocaine in the SmI caused a local reduction of EEG power in the area surrounding the injection site and partly in the occipital cortex. An effect in the frontal EEG was very little. Cortical inactivation of the SmI with 2% lidocaine was successful and local.

Effect of lidocaine on the incidence of SWD

The mean duration of SWD in baseline was 5.8±2.1 sec (mean±SD). It neither significantly change after of 2% lidocaine injections (5.1±2.2 sec) nor and after saline injections (4.4±1.5 sec).

The incidence of SWD significantly reduced after lidocaine injections as compared to the effect of saline (Table 1). The ANOVA of the number of SWD per hour revealed that lidocaine significantly reduced SWD for both uncorrected ($F(1,12) = 10.60$, $p<0.001$) and for vigilance-corrected data ($F(1,12) = 3.34$, $p<0.05$). Effect of the order of injections was not significant as well as the interactions 'drug' * 'order', suggesting that sequence of injections did not influence the effect of lidocaine. The number of SWD was summed in four 30-min time blocks in both uncorrected and corrected for vigilance datasets. In vigilance corrected data, orthogonal trend analyses showed that the two groups differed in the linear trend component ($F_{lin}(1,12) = 4.23$, $p<0.05$). This demonstrates that the changes over time were different for the two groups. From Fig. 6.7 (right panel) and the outcomes of the statistical analyses, it became clear that the initial difference between lidocaine and saline is getting smaller over time and tends to diminish.

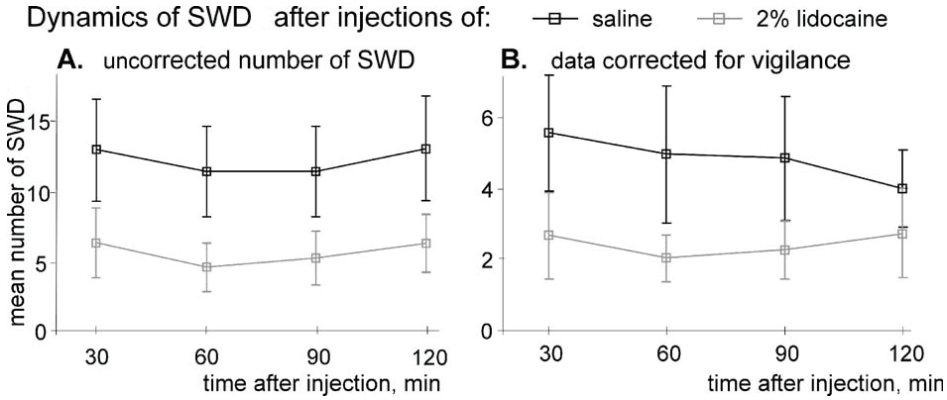

Figure 6.7. Time course of SWDs after injections of saline and lidocaine. The number of SWD is summed up in four successive 30 min intervals (in total, 2 h after injectionsб n = 12 rats, mean±S.E.M.). In vigilance-corrected data, (B) dynamics of SWD differs from that in control. Reduction of SWD is temporal; number of SWD gradually restore to the control level at the end of the second hour after lidocaine injection.

The decrease in the number of SWD after lidocaine injection was temporal and lasted approximately one hour as could be seen in the vigilance-corrected data (Fig. 6.7B). The number of SWD at the end of the second hour after lidocaine injections did not differ from control.

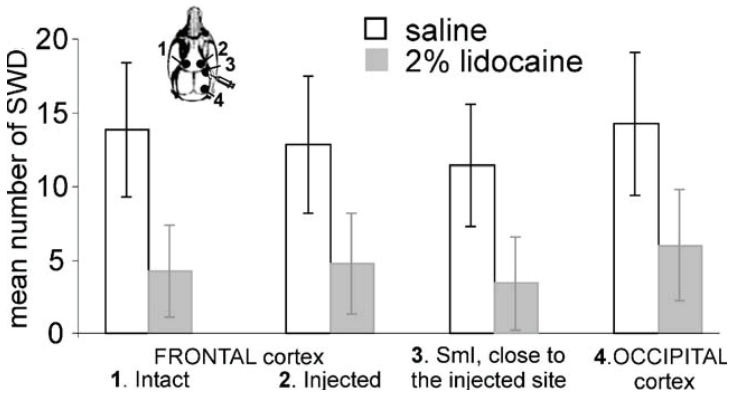

Figure 6.7. The number of SWD 30-60 min after lidocaine and control injections into the SmI (n = 12 rats, mean±S.E.M.). SWD were scored automatically in each EEG channel independently.

Although unilateral injection of 2% had a local effect in the SmI (reduction of EEG power was found in the close vicinity to the injected site, but not in the remote areas) and affected generalized seizure activity, it might have a different effect on SWD at different locations. To examine whether the reduction of SWD was local or generalized, the number of SWD scored automatically and independently in four EEG channels. Analysis was done in time interval 30–60 min after injection, when effect of lidocaine was the largest (Fig. 6.8). An ANOVA showed that the factor 'Order' of injections (saline/lidocaine or lidocaine/saline) did not significantly affect the number of SWD. 'Location' and 'Drug' were used as within-subject factors. Compared to saline, injections of 2% lidocaine caused a significant decrease in number of SWD ($F(1,11) = 4.2$, $p<0.05$). Neither the factor 'Location', nor interaction 'Location'*'Drug' were significant.

Altogether, these data suggests that local deactivation of the SmI with 2% lidocaine affected generalized seizure activity, reducing the number of SWD in all recording sites.

DISCUSSION

We have found here that unilateral local deactivation of the SmI in WAG/Rij rats caused a temporal reduction of the number of generalized SWD in both hemispheres. Amount of SWD gradually restored at the end of the second hour. In the majority of subjects (77%), unilateral injection of lidocaine effectively diminished total EEG power (it mainly suppressed of higher frequencies) in the area surrounding the injection site (SmI). Spectral features of SWD after lidocaine injections were essentially changed in the SmI and in occipital cortex, while, changes in the frontal cortex were absent or minor.

Dynamics of SWD after control injection was significantly different from that obtained after application of lidocaine. In the vigilance-corrected data, it was proven that reduction of SWD after lidocaine was temporal. After saline injections, we saw slow decrease of SWD over time that corresponds to the circadian changes in the appearance of SWD [van Luijtelaar et al., 1988; van Luijtelaar et al., 2001]. Experiments and EEG recordings started during the middle and later hours of the dark period and in this circadian phase the number of SWD is known to be maximal and decreases in the subsequent hours. Therefore, it seems that the dynamics of SWD in case of the control injection just reflects the normal circadian distribution of SWD.

As known, local application of lidocaine reduced neuronal activity for 40-60 minutes [Burton and Robinson, 1987; Martin and Ghez, 1999]. This fits very well to the decrease in the incidence of SWD that we observed during 1 hour after local deactivation of SmI with 2% lidocaine.

Interpretation of EEG power spectrum analysis of SWD

EEG power spectrum of SWD after injections of lidocaine have changed in the SmI and in occipital cortex; in the frontal cortex changes were minimal. This could be explained by the differences in distribution of spike and wave components in SWD over the cortex. As known, amplitude of the waves is high in posterior areas (occipital cortex), whereas the spikes are maximum in the anterior areas (frontal cortex) [Midzianovskaia et al., 2001; Sitnikova and van Luijtelaar, 2007]. Probably, a reduced power in 0.5–4 Hz in the SmI and occipital cortex (graphs 3-4, Fig. 6.6) corresponds to the reduction f the wave component in SWD.

In the frontal EEG, lidocaine caused a decrease in harmonic frequencies in SWD (only in the intact hemisphere). It is known that the high-amplitude regular spike component in SWD yields several peaks in power spectra: one peak is in fundamental frequency (~9 Hz) and another peak in double frequency (the first harmonic, ~18 Hz) [Drinkenburg at al., 1991]. In addition to that, we have found the second harmonic (~27 Hz) in power spectrum of SWD. Therefore, the reduction of the higher harmonics after administration of 2% lidocaine may be interpreted as a slight modification of the spike component in SWD as recorded in the frontal cortex and in the SmI. This effect was found in the intact hemisphere, but it was nearly absent in the injected hemisphere.

In the close vicinity to the injected site (in the SmI), EEG power spectrum of SWD displayed a decrease in power of fundamental frequency (~9 Hz) and in beta frequencies (12–30 Hz, which includes the first and the second harmonics, ~18 Hz and ~27 Hz) whereas power in 0.5–4 Hz did not change. This suggests that lidocaine injections influenced the spike component in SWD, but the wave component was not affected. Altogether, changes in power spectrum of SWD may reflect the impairment of the EEG pattern of SWD, in particular, the spike component is modified in the frontal cortex and SmI and the wave component is reduced in the occipital cortex.

The role of the cortex in SWD

Deactivation of local cortical area in the SmI with unilateral administration of 2% lidocaine reduced the amount of SWD at all recording sites, suggesting that this effect was generalized (i.e., global effect of the local treatment). This is in line with analogous studies in GAERS (a rat model of absence epilepsy similar to WAG/Rij) microinfusion of ethosuximide into the SmI of GAERS substantially decreased the number of SWD [Manning et al., 2003; 2004], but injections in other cortical regions, in the ventrobasal thalamus and in the RTN resulted in

less marked changes in number of SWD [Richards et al., 2003]. Another finding in GAERS disagrees with our results [Brailowsky et al., 1999]: GABA, which was unilaterally infused into the fronto–parietal area of SmI, blocked SWD for 24 hours only at the injected hemisphere, but at the contralateral (intact) side SWD were present. Perhaps, Brailowsky et al., (1999) found this unilateral effect, because they injected of GABA relatively far from epileptic zone (in the medial part of SmI). Here we observe full bilateral effect, because w injected lidocaine directly to the focal epileptic zone in the perioral area of SmI [Meeren et al., 2002]. It could also be that lidocaine had a stronger effect in neuronal activity as compared to GABA: as known, lidocaine completely blocks sodium channels and prevent neurons from generating epileptic bursts [Tehovnik and Sommer, 1997; Burton and Robinson, 1987]. In order to disclose a particular role of the SmI in SWD, it is worth to inactivate different cortical sites and record electrical activity simultaneously in the cortex and thalamus.

Our study confirms that the SmI plays a crucial role in initiating of SWD. This is in agreement with neurophysiological, pharmacological and fMRI studies in rat model of absence epilepsy and in human patients. In GAERS, SWD are receded by specific rhythmic EEG activity (‘embryonic SWDs’) which can be found in the sensory cortex a few cycles before the manifestation of fully generalized seizures [Seidenbecher et al., 1998]. In fMRI studies in rats, SWD were induced by gamma-butylolactone. It was found that all cortical areas expressed negative BOLD response during SWD, but only the SmI showed a simultaneous positive BOLD response, suggesting that this area exhibits a specific activity before and during spike–wave seizures [Tenney et al., 2003]. In some patients with absence epilepsy, generalized SWD were shown to begin in the frontal neocortical area [Ferri et al., 1995; Niedermeyer, 1996, Rodin et al., 1994]. Depth recordings showed that 3 Hz SWD were initially located in the mesiofrontal cortex and rapidly propagated to the rest of the cerebral regions [Bancaud, 1969; Holmes et al., 2004]. Taken together, these data strongly suggest that SWD in rats have a primary neocortical source at the somatosensory cortex (in humans this source is likely to be located at the frontal cortex) that lead the thalamus and result in generation of rhythmic discharges in the cortico–thalamo-cortical loop; some clinical data are in agreement with this idea.

Rhythmic activity in the SmI (somatosensory rhythm) as probable substrate of SWD

The perioral region of the SmI seems to be endowed by is specific neuronal mechanism that could be responsible for generation of SWD in rodent models of absence epilepsy. SmI produces physiological oscillations in the frequency domain of SWDs (7–12 Hz) [Ritz and Sejnowski 1997; Ahissar et al., 1997], so called somatosensory rhythm [Nicolelis et al., 1995; Nicolelis and Fanselow 2002]. This rhythm appears as result of synchronous firing activity of the ‘intrinsically bursting’ (pyramidal) cells and inhibitory interneurons [Silva et al., 1991]. Somatosensory rhythm in rodents originates from the cortex: local injection of muscimol (GABAa-agonist) into the vibrissal region of the SmI abolishes 7–12 Hz oscillations and bursting activity in the cortex and in the ventroposteromedial thalamic nucleus (VPM) [Nicolelis and Fanselow 2002]. In rodents, somatosensory oscillations launch rhythmical movements of tactile organs, vibrissae, and trigger ‘whisking’ activity [Ahissar et al., 1997; Semba and Komisaruk, 1984; Nicolelis et al., 1995; Nicolelis and Fanselow 2002].

There are a number of similarities between somatosensory rhythm and SWD:

(1) the same frequencies 7–12 Hz;
(2) the same trigger site in the area of perioral projections in the SmI [Meeren, 2002; Nicolelis et al., 1995];
(3) the same temporal dynamics: they begun into the sensory cortex and within a few milliseconds spread over the cortex, the thalamus and other corresponding subcortical structures [Meeren, 2002; Nicolelis et al., 1995].
(4) both of them are developed in the thalamo-cortical system and involve somatosensory thalamus, in particular, the ventroposterior complex of the thalamus [Inoue et al., 1993; Nicolelis et al., 1995; Vergnes et al., 1987; Seidenbecher et al., 1998];

We share the ideas of Wiest and Nicolelis (2003) that transformation of the 7–12 Hz rhythmic activity to SWD may emerge only in rodents with predisposition to absence epilepsy. In WAG/Rij rats, serious genetically predetermined changes in neuro–molecular mechanisms: protein and enzyme synthesis, properties of ion channels and membrane, neurotransmission and neuromodulation etc. [reviewed by Coenen and van Luijtelaar (2003)] may underlay an increased cortical excitability, deficit of inhibition and, finally, they may be responsible for a transformation of 7–12 Hz somatosensory oscillations into hypersynchronous generalized SWD.

Our data fit to the ‘cortical focus’ theory of generalized absence seizures [Meeren et al., 2002; 2005]. We add that oscillatory activity in the perioral area in the SmI plays an important role in pathophysiology of absence seizures. Normal oscillatory pattern in this area represents somatosensory rhythm in nonepileptic rodents and it can be modified in epileptic rat strains and give rise to spontaneous SWD. Generally speaking, the role of the neocortex in generalized absence epilepsy seems to be more important than previously assumed.

Chapter 7
General discussion

CONTENTS

The current thesis examines two forms of thalamo-cortical oscillations: naturally occurring sleep spindles and paroxysmal spike-wave discharges (SWD, absence seizures). These oscillations are generated in a neuronal circuit formed by the neocortex, the specific thalamic and the reticular thalamic nuclei [Steriade and Deschenes 1984; Steriade et al., 1993; Steriade, 2003; Avanzini et al., 1996; Kostopoulos, 2000; Destexhe and Sejnowski, 2001]. The minimal substrate accounting for spindle oscillations is specific neuronal interaction between thalamic reticular and relay cells; sleep spindles can still be generated even if these neurons are disconnected from the cortex and from the remaining thalamus [Steriade and Deschenes 1984; Destexhe and Sejnowski 2001; Steriade, 2005]. Sleep spindles are characteristic EEG hallmarks of sleep stages I-II. Similar to sleep spindles, SWD preferentially occur during drowsiness and light slow-wave sleep [van Luijtelaar and Coenen, 1986; Drinkenburg et al., 1991] but, in contrast to sleep spindles, SWD have a cortical origin [Niedermeyer, 1996; Meeren et al., 2002; 2005; Polack, 2007]. SWD are generated in local cortical foci and they rapidly became generalized, spreading over the cortex and other structures throughout intracortical (ipsilateral and callosal) pathways and descending projections [Steriade and Amzica, 1984; Lemieux and Blume, 1986; Sitnikova and van Luijtelaar, 2006]. On the other hand, thalamic neurons are implicated in generating of SWD [e.g., Avanzini et al., 1992; 2000; Blumenfeld, 2002; Buzsáki et al., 1988; Buzsáki, 1991]. Cortex and thalamus certainly play an important role in both sleep spindles and SWD, but functional aspects of cortico-thalamic interactions are still not fully understood. This thesis (1) elaborates cortico-thalamic network mechanisms of sleep spindles (including anterior and posterior spindle types) and SWD (including initiation, propagation and cessation of seizures); (2) critically evaluates the *cortico-reticular* theory of absence epilepsy in respect to the relationship between sleep spindles and SWD [Gloor, 1968; 1969]; (3) examines basic EEG parameters of SWD and SWD-precursor activity in the cortex and in the thalamus and (4) provides evidence in favor to a 'cortical focus' theory of absence epilepsy, which states that the somatosensory cortex (SmI) initiates SWD [Meeren et al., 2002].

SLEEP SPINDLES in WAG/Rij rats

Issue 1. EEG analysis of sleep spindles: similarities and distinctions between anterior and posterior sleep spindles

Chapter 2 focuses on sleep spindles occurring in the EEG during natural sleep in WAG/Rij rats. The general outcome is that sleep spindles appear in frontal and occipital EEG channels independently, suggesting that our rats exhibit two 'area-specific' types of sleep spindles that is similar to humans.

In humans, sleep spindles are topographically distinctive. 12 Hz sleep spindles appear in the frontal cortex and 14 Hz spindles - in the central and parietal areas [Jankel and Niedermeyer, 1985; Jobert et al., 1992; Werth et al., 1997; Zygierewicz et al., 1999; Anderer et al., 2001]. Basic mechanisms of sleep spindles in humans and in animals are principally the same, but a topographical distribution of sleep spindles in animals is less well or even poorly explored. To our knowledge, the only systematic study of spindle topography has been performed in Wistar rats ин Terrier and Gottesmann (1978) and Gandolfo et al. (1985). In these two papers, the authors distinguish between anterior and posterior sleep spindles, which is later confirmed in WAG/Rij rats [van Luijtelaar, 1997].

- Anterior sleep spindles (~10.6 Hz) have maximum in the frontal region and they are less intensive (or absent) in the posterior area. They appear immediately after the onset of sleep, and their number, duration and amplitude increase as sleep deepens. Anterior spindles are fully developed during the intermediate state, where they are associated with *theta* rhythm in the hippocampus and in the occipital cortex.

- Posterior spindles (~12.4 Hz) are predominant in the occipital region, they are less pronounced in parietal area and not present in the frontal cortex. Posterior spindles are unique for the slow-wave sleep. As compared to anterior spindles, they are less frequent, have significantly lower amplitude, higher frequency and shorter duration.

The aforementioned is in agreement to what we find in our subjects, the WAG/Rij rats (**Chapter 2.1**): anterior and posterior spindles are local phenomena. Anterior spindles are more numerous than posterior spindles; the former have a higher frequency (~11 Hz versus ~ 10 Hz) and a longer duration (Table 2.1). The discrepancy concerns the frequency of posterior spindles ~ 10 Hz that is lower than that described in Wistar rats ~ 12.4 Hz [Terrier and Gottesmann, 1978]. It is possible that this lower spindle frequency is related to the fact that WAG/Rij rats are suffering from absence epilepsy. Epileptogenic processes may influence oscillatory patterns of electrical brain activity and, consequently, the EEG properties of sleep spindles in WAG/Rij rats are slightly changed.

The significant differences between two topographically distinctive spindle types (anterior and posterior spindles) contradict to the results obtained *in vivo* in cats [Destexhe et al, 1999; Destexhe and Sejnowski, 2001]. The spatial consistency in cortical sleep spindles in cats is found to be very high, e.g., sleep spindles appear

simultaneously over large neocortical territories. However in rats, there are regional differences in the distribution of EEG power sleep spindles over the cortex during natural sleep [Mackenzie et al., 2004]. In the fronto-parietal areas, sleep spindles have a maximal power, whereas power in the occipital cortex and in subcortical structures is moderate or low. In fact, spindle activity in the fronto-parietal area may correspond to our anterior spindle type. All authors, however, did not distinguish posterior spindles as independent phenomena, probably because posterior spindles occur less frequently and have less power as compared to anterior sleep spindles.

The total power of anterior sleep spindles as measured in the frontal cortex is higher than the total power of posterior sleep spindles in the occipital cortex. Amplitude differences between occipital and frontal EEG are also found in the pre-spindle epochs. The amplitude of the frontal EEG signal is 2.5-3 times higher than the amplitude of the occipital signal. This difference may be accounted for the neuronal composure of these two areas in the neocortex. The frontal (motor) area is distinguished from other areas by the presence of large pyramidal cells in layer V (e.g., Betz cells in M1). These neurons have large electric dipole moments, and they are capable to generate high-amplitude fluctuations of field potentials. The occipital (visual) cortex contains regular-sized pyramidal cells, in which dipole moments are smaller, therefore, field potentials in this area have a lower amplitude [Lopes da Silva and van Rotterdam, 1982].

From pre-spindle activity to sleep spindles

No significant differences between periods immediately prior to anterior and posterior spindles (pre-spindle activity) are detected in (**Chapter 2.1**), neither in EEG waveform nor in EEG power spectra. However, the transition from pre-spindle EEG to anterior and to posterior spindle types is associated with different frequency modulation.

Analysis of power density in the selected frequency bands reveals the following differences between sleep spindles and pre-spindle epochs (Fig. 2.6):

- Both types of sleep spindles have higher power in *alpha* band, as compared to pre-spindle epochs.
- Anterior spindles are accompanied by a broader increase in power densities in the frontal cortex ($alpha_{low}$+$alpha_{high}$, e.g., 9-12 Hz), in the VPM (*delta*+*theta*+$alpha_{low}$) and in the RTN (*delta*).
- Posterior spindles are characterized by an increase in $alpha_{low}$ (9-10.5 Hz) and by a decrease in *delta* in the occipital cortex, whereas no significant changes are found in the thalamus.

Alpha band is divided in two sub-bands: $alpha_{high}$ that comprise the mean frequency of anterior spindles (~11 Hz) and $alpha_{low}$ that comprise the mean frequency of posterior spindles (~10 Hz). In anterior spindles, an increase in $alpha_{high}$ is locally found in the frontal cortex, whereas an enhancement of $alpha_{low}$ is detected in the frontal cortex and in the VPM. It seems that the VPM readily sustains $alpha_{low}$, but not $alpha_{high}$, suggesting that fundamental EEG frequency of anterior spindles (in the range of $alpha_{high}$) might be reinforced in local neuronal circuits in the frontal cortex. Similarly, posterior spindles are only accompanied by an increase in $alpha_{low}$ (9-10.5 Hz) in the occipital cortex, but not in the frontal cortex or thalamus. This suggests that posterior spindle activity (~10 Hz) is maintained by local neuronal circuits in the occipital cortex and that these circuits hardly interact with the investigated parts of the thalamus (VPM and RTN).

Only anterior spindles, but not posterior spindles, are accompanied by an elevation of *delta(theta)* activity in the thalamus. It seems that, during anterior spindles, thalamic and cortical neurons stay in different oscillatory modes. Thalamic neurons generate field potentials with more powerful *delta(theta)* frequency components (see below), but cortical neurons (in the frontal cortex) are prone to sustain oscillations in *alpha* band. It is known that the cellular mechanisms of spindle generation are different in the thalamus and the cortex (e.g., intrinsic currents, membrane properties, propensity of neurons for burst firing, neuronal network processes), resulting in differences between frequency composition of thalamic and cortical counterparts of spindle types.

The role of delta activity in two spindle types

In the cortex, the power spectra of both spindle types show, besides ~10 and ~11 Hz peaks (Fig. 2.2A, B), protruding and additional peaks in the *delta* range. The power spectrum of anterior spindles reveals two prominent peaks in 1 Hz and in 11 Hz and their relative amplitude is 0.7 : 1. In posterior spindles, the peaks are centered in 1 and 10 Hz with nearly equal amplitude, i.e., 1 : 0.95.

In the thalamus, both spindle types display a relatively large *delta* component (Fig. 2.2C), although power in *delta* band in anterior sleep spindles is higher than in posterior spindles (Fig. 2.5B). The neuronal mechanism of the *delta*-component in thalamic spindles is obscure. It is well known that thalamo-cortical neurons can produce sustained oscillations (either delta or spindle waves) due to the interplay of two hyperpolarization-activated currents, I_h and I_t [Steriade, 2001; 2003; 2005; Destexhe and Sejnowski 2001]. The degree of hyperpolarization of these neurons is determined by GABA-ergic inhibitory inputs from the RTN. Thalamo-cortical neurons generate

clock-like *delta* if they are hyperpolarized below -70 mV and generate sleep spindles at membrane potentials between -55 and -65 mV [Nunez et al., 1992; Steriade, 2005]. This scheme implies that sleep spindles (i.e., oscillations with *alpha* frequency) and *delta* activity are mutually exclusive. However, we found that *delta* in the thalamus coexists with spindle (*alpha*) activity in the cortex. Unfortunately, this could not be interpreted using the above mentioned scheme.

Probably, some thalamic neurons may be hyperpolarized enough to produce local thalamic *delta* oscillations, while other cells are involved in thalamo-cortical neuronal networks producing *sleep spindles.* Therefore sleep spindles are present in the cortex simultaneous with delta in the thalamus. Alternatively, thalamic *delta* during cortical sleep spindles can be brought up by yet unknown neuronal mechanisms, which differ from that underlying clock-like thalamic 1-4 Hz delta.

Cortical spindle oscillations are not merely a fingerprint of the electrical activity in the thalamus (results of power spectrum analysis)

The current thesis is focused on two thalamic nuclei, the ventroposteromedial and reticular thalamic nuclei (VPM and RTN). These nuclei are known to be intimately involved in the generation of sleep spindles [Spencer and Brookhart, 1961; Morin and Steriade, 1981; Steriade, 1993, 2003, 2005; Steriade and Llinas, 1988]. As far as the electrical activity in the thalamus during sleep spindles is concerned, data in animals are scare and are almost completely absent in humans, because intracranial recordings are not easily available as they are highly invasive.

In **Chapter 2** we measured and analyzed sleep spindles in the VPM and RTN. It is surprising that spindle activity is poorly visible in the VPM and RTN, whereas simultaneous spindle oscillations are pronounced in the cortex. We use the principle of Lopes da Silva and van Rotterdam (1982 and 1987; Lopes da Silva, 2002) to explain why local sleep spindles cannot be easily recorded in the thalamus (discussed on page 28). But, we still conclude that the thalamus (VPM and RTN) are involved in anterior sleep spindles, because in the cross-spectrum 'thalamus-frontal cortex' during sleep spindles we see synchronization in alpha band. Differences in total power between anterior and posterior sleep spindles are found in the cortex, but they are not present in the thalamus. Unfortunately, this analysis is not sufficient to define principal differences between two spindle types with respect to the electrical activity in the VPM and RTN.

During spindle types, both thalamic nuclei (VPM and RTN) sustain substantial power in *delta* and *theta* bands (Fig. 2.2A, B), while cortical spindles display a clear peak in ~ 10-11 Hz (Fig. 2.3). Similar results were obtained by Mackenzie et al. (2004) in epileptic as well as in non-epileptic rats. These authors demonstrate that thalamic structures express a relatively low power during sleep spindles as compared to fronto-parietal areas of the neocortex, in the latter area sleep spindles have the largest power. This, by no means, discourages the role of the thalamus in the genesis of spindle oscillations, but '*for a structure to generate a rhythm it need not conceptually follow that it contain high levels of power at the rhythm frequency'* [p.103, Mackenzie et al., 2004]. Altogether, cortical spindle oscillations are not just a fingerprint of the electrical activity in the thalamus.

Issue 2. Thalamo-cortical network mechanisms of anterior and posterior sleep spindles

In **Chapter 2.2**, we have measured associations throughout thalamo-cortical circuit in the frequency domain (using cross-spectrum analysis) and in time domain (using cross-correlation analysis). A combination of EEG frequency domain and time domain analyses have helped us to find mechanisms of functional integration and segregation by which the thalamo-cortical system is able to maintain two separate types of sleep spindles. It is found that anterior and posterior sleep spindles differ in respect to thalamo-cortical interactions: two spindle types are generated in different oscillatory networks and distributed over different cortical areas.

Two types of sleep spindles are produced in different thalamo-cortical networks

A frequency-domain analysis of thalamo-cortical associations during anterior sleep spindles reveals a strong coupling in the network [RTN] - [VPM] - [frontal cortex], with peak frequencies in 2-3 Hz, 8-10 Hz and 11-12 Hz. The presence of 11-12 Hz peaks in cross-spectra 'VPM-RTN' suggests that the generation of spindle rhythm requires a strong coupling between these structures. It is intriguing that anterior spindles show additional peak associations in the thalamus in the 2-3 Hz band.

Posterior sleep spindles are characterized by weak associations between [RTN] – [VPM] – [occipital cortex]. It is notable that associations in 'occipital cortex – RTN' pair are centered in non-spindle frequencies (7.5-8 Hz), suggesting that the RTN is not directly involved in the sustaining and propagating of posterior sleep spindles. In posterior sleep spindles, a functional coupling between the occipital cortex and the thalamus (VPM and RTN) is relatively weak, suggesting that the RTN plays an inconspicuous role in posterior sleep spindles.

A time-domain (cross-correlation) analysis of anterior sleep spindles demonstrates correlations in the network [RTN] – [vVPM+dmVPM] – [frontal cortex]; in posterior spindles correlations are detected [RTN] – [dmVPM] – [occipital+frontal cortices].

It seems that a broad area in the VPM (vVPM+dmVPM) associates with a narrow area in the frontal cortex in anterior sleep spindles and a narrow area in the VPM (dmVPM) associates with a broad area in the frontal+occipital cortex in posterior spindles. The latter suggests that the dmVPM, rater than the vVPM, sustains posterior sleep spindles.

The above mentioned analyses of effective connectivity **(**cross-correlation and cross-spectrum**)** parameters of thalamo-cortical network functional associations do not imply that there are straightforward anatomic connections between the investigated structures. The anterior sleep spindles are examined in the primary motor area (Fr1) in the frontal cortex. In this area, anterior sleep spindles show an amplitude maximum [Terrier and Gottesmann, 1978], yet, there are no direct anatomic connections between this frontal cortical area and the VPM. The Fr1 is innervated by the ventrolateral thalamus (VL, input from the cerebellum, mainly from the dentate nucleus), ventromedial thalamus (VM, thalamic relay nucleus for pain and temperature pathways), posterior thalamus (PO, higher order somatosensory relay nucleus), intralaminar nuclei including the centrolateral (CL) and centromedial (CM) [Jones, 1985]. The VPM is a principle relay thalamic nucleus (as a relay nucleus, it consists of thalamo-cortical neurons which are known to trigger sleep spindle sequences and send them to the corresponding cortical areas). The VPM is a relay nucleus, it receives trigeminothalamic terminals and projects to the prime somatosensory cortex (SmI). Noteworthy, both the frontal cortex and the VPM have dense bidirectional connections with the SmI [Welker et al., 1984; Neafsey, 1990]. Considering the anatomic aspects of the investigated thalamo-cortical system, the SmI links the VPM and the frontal cortex, thus providing functional connectivity in this oscillatory neuronal network.

The posterior spindles are most intensive in the secondary visual area in the occipital cortex (Krieg's area 18A or Oc2L). This area has reciprocal interconnections with the visual thalamus, mainly with the high-order lateral posterior (LP) thalamic nucleus [Jones, 1985 and 2006]. It is also densely innervated by various cortical areas, including the SmI [Kolb and Walkey 1987; Kolb, 1990]. Throughout the SmI, occipital zone Oc2L may co-operate with the dmVPM, yet, with two synaptic delays.

In both spindle types, the RTN strongly associates with the VPM. It is now well accepted that neurons in the RTN are able to initiate sleep spindle activity [e.g., Steriade and Deschenes 1984; Destexhe and Sejnowski 2001; Steriade, 2005]. Our study adds that the RTN may be differently involved in distributing two spindle types over the cortex. It is yet not possible to identify anatomic pathways that distribute anterior and posterior sleep spindles throughout the brain.

The cortical areas, in which we analyzed local spindle activity, receive multiple thalamic inputs (it is discussed above) and therefore, sleep spindles might be delivered to the cortex from several different sources. In addition to that, sleep spindle oscillations might spread over the cortex via dense intracortical afferents. It seems that the distribution of sleep spindles is governed by high order functional interactions in thalamo-cortical and cortico-cortical neuronal networks. For example, the frontal cortex (the area of anterior spindles) receives direct input from the motor (ventrolateral) thalamus and indirect input from the VPM via somatosensory cortex (SmI). Occipital cortex (the area of posterior spindles) receives afferents from the visual part of specific thalamus and from other cortical areas, including the SmI, therefore, it indirectly cooperates with specific thalamic nuclei (e.g., dmVPM).

A notable difference between the dmVPM and vVPM in respect to their anatomic connections and physiological functions may underlie the existence of different oscillatory neuronal networks, and correspondingly, different types of local spindle activity (it is discussed below).

Two poles of the VPM (dorsomedial and ventral) sustain different spindle types

Anterior and posterior sleep spindles are not equally propagated over the VPM. The dorsomedial part of the VPM (dmVPM) exhibits more theta, especially during anterior sleep spindles, while the ventral part (vVPM) has more alpha, especially during the presence of posterior sleep spindles. In anterior spindles, analysis of cross-correlations showed significant associations between the VPM (both dm- and vVPM) and the frontal cortex, but in posterior spindles, only between the dmVPM and the occipital cortex. This suggests that the vVPM is preferably involved in anterior sleep spindles and the dmVPM in both type sleep spindles.

As known, the VPM is a somatosensory nucleus of the specific part of the thalamus that receives projections from head and vibrissae [Jones, 1985 and 2006; Sherman and Guillery, 2006]. In rodents, this nucleus is organized in a somatotopic manner and it is divided in two parts corresponding to different sensory pathways [Yu et al., 2006; Pierret et al., 2002]: (1) lemniscal pathway, ascending through the dorsomedial sector (dmVPM) and (2) a recently discovered extralemniscal pathway that ascends through the ventrolateral sector of the VPM

(vVPM). Both dmVPM and vVPM project to the SmI. The vVPM (the extralemniscal pathway) conveys to the cortex signals of contact 'touch' (these signals are used for localizing an object, e.g., 'where'-information).

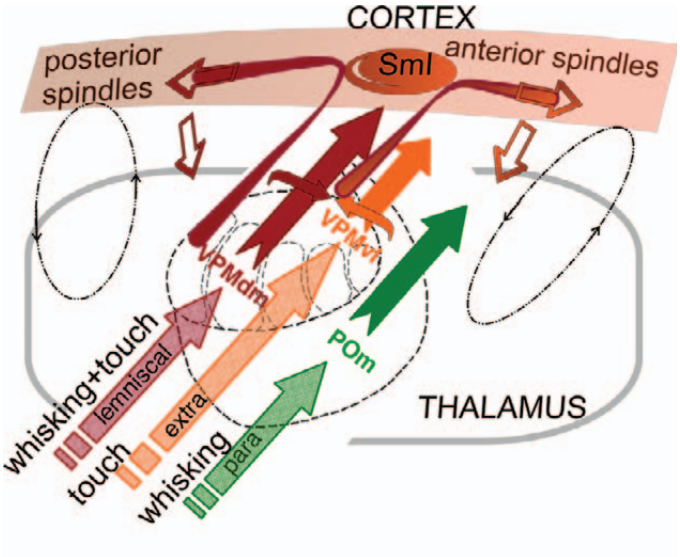

Figure 7.1. Anterior and posterior sleep spindles invade different poles of the VPM (dmVPM and vVPM). The dmVPM and vVPM belong to a system of trigeminal projections, e.g., lemniscal and extralemniscal pathways correspondingly. Lemniscal and extralemniscal afferents convey different information and ascend to the somatosensory cortex (SmI). During sleep, lemniscal and extralemniscal pathways may be involved in distributing sleep spindles originating from the VPM to the cortex. Anterior sleep spindles are delivered to the cortex (SmI) by lemniscal and extralemniscal afferents and are further distributed intracortically in frontal direction; posterior spindles are delivered by lemniscal afferents and spread occipitally (the figure modified from Yu et al., 2006: DOI: 10.1371/journal.pbio.0040124.g005. Authors' abbreviations: extra - extralemniscal pathway; para - paralemniscal pathway; VPMvl – ventrolateral pole of the VPM (= vVPM); VPMdm – dorsomedial pole of the VPM (=dmVPM); POm – posterior nucleus of the thalamus, medial part).

The dmVPM (the lemniscal pathway) conveys complex signals combined 'whisking+touch' (these signals are involved in identification of objects and carry on 'what'-information). Extralemniscal and lemniscal pathways appear to be trigeminal analogs of the neospinothalamic and dorsal column–lemniscal pathways respectively. These pathways have targets in different layers in the SmI and in other cortical areas thus comprising different sensory-motor loops at different levels of brain hierarchy [Kleinfeld et al., 1999; Yu et al., 2006]. This functional segregation of dorsomedial and ventral compartments in the VPM (corresponding to extralemniscal and lemniscal systems) raises the possibility that, during sleep, dmVPM and vVPM also keep this functional independency and may be involved in different spindle-producing loops, thus producing slightly different spindles (Fig.7.1). According to our analysis, anterior sleep spindles invade both dmVPM and vVPM, therefore, they may be delivered to the cortex by lemniscal and extralemniscal afferents and further distributed over the cortex in the frontal direction. Posterior spindles, which mostly involve the dmVPM, may be delivered to the cortex through lemniscal pathway and spread occipitally.

The present thesis is focused on the role of the VPM in two spindle types, but, eventually, there are other relay nuclei in the thalamus that may be involved in the production of sleep spindles and distributing them to the corresponding cortical areas (dotted circles in Fig. 7.2). In particular, there are 'first order' and 'high order' thalamic relay nuclei [Sherman and Guillery, 2006], which can be distinguished in respect to its role in spindle activity. 'First order' thalamic relay nuclei (i.e., *the ventral posterior nucleus*, including the VPM, for the somatosensory system and *the lateral geniculate nucleus* for the visual system) consist of classical thalamo-cortical cells that reciprocally interconnect with the primary cortical areas. 'First order' thalamic relay neurons are involved in the initiation and propagation of sleep spindles. It is likely that *the lateral geniculate nucleus*, which innervates the primary visual zone in the occipital cortex (Oc1) [Kolb and Walkey 1987; Kolb, 1990], plays a principle role in posterior spindles. Involvement of 'high order' thalamic relay nuclei in sleep spindles is not easily perceived. These nuclei (i.e., *the posterior nucleus* (PO) for the somatosensory system [Yu et al., 2006] and *the pulvinar* for the visual system [Jones, 2006]) have diffuse projections to the primary and other cortical areas [Sherman and Guillery, 2006]. All thalamic relays receive feedback from layer VI of the cortex, but the 'higher order' relays receive an additional input from layer V of cortex. Generally speaking, the 'higher order' thalamic relays represent a key link in cortico-thalamo-cortical network associations [Sherman and Guillery, 2006] and, therefore, these nuclei may be in greater extent involved in synchronization and generalization of thalamo-cortical oscillations (sleep spindles and SWD).

We hypothesize that both first and high order relay thalamic nuclei are involved in the propagation of sleep spindle oscillations. Other structures, which are known to be involved in synchronization and maintenance of neuronal oscillations, e.g., *intralaminar* thalamic nuclei and the brain stem reticular formation [Glenn and Steriade, 1982; Seidenbecher and Pape, 2001], may also play a role in spindle activity. The future analysis, such as investigation of spatial distribution of spindle activity with the aid of cortical and subcortical maps of sleep spindles that can be plotted using electrophysiological optical imaging techniques, functional imaging studies (PET, fMRI), electrocortical stimulation etc, should provide convenient information about network mechanisms underlying topographically distinctive sleep spindles.

SWD in WAG/Rij rats (average EEG waveform analysis)

Chapter 3 elucidates two types of spike-wave paroxysms, e.g., generalized SWD I (the true absence epileptic discharges) and local occipital SWD II (which have no clinical correlate) [van Luijtelaar and Coenen, 1986]. Grand average EEG waveforms of SWD I and SWD II are examined in **Chapter 3.1**. In this Chapter, we report on a statistical analysis and comparison of electroencephalographic features of SWD I and SWD II in spatially and functionally segregated parts of the cortico-thalamic system. The major achievements are the following:

- Archetypal patterns of SWD I and SWD II are rendered by computing grand average EEG waveforms in cortex and thalamus (Fig. 3.4).
- Electroencephalographic pattern of SWD in WAG/Rij rats resembles spike-wave activity in humans. SWD I and SWD II in our subjects comprise a sequence of elements, similar to elements in spike-wave complexes as has been described in patients with absence seizures [Weir, 1960].
- SWD I comprise different set of epileptiform elements in the frontal and occipital cortex and in the thalamus, suggesting that SWD I has an area-specific EEG pattern.
- SWD II are localized in the occipital cortex and hardly involve the frontal cortex and the investigated nuclei in the thalamus.
- In SWD I, the waveform and amplitude is changed from the beginning to the middle stage of seizure train. These dynamic changes are area-specific. In the frontal cortex and in the thalamus, SWD I show moderate changes in amplitude, but virtually no changes in the waveform. In the occipital cortex, the waveform of SWD I is completely changed.

SPIKE-WAVE DISCHARGES in WAG/Rij rats

Issue 3. Electroencephalographic features of SWD

Issue 3(1). EEG profiles of SWD type I and type II in WAG/Rij rats

Chapter 3.1 demonstrates that SWD I are generalized, e.g. they are well pronounced in the frontal cortex and in the thalamus, in contrast to the local SWD II, which is merely expressed in the occipital cortex and hardly seen in the fronto-parietal cortical areas and in the thalamus (Fig. 3.1) [Sitnikova and van Luijtelaar, 2007]. Electroencephalographically, SWD I and SWD II represent multi-phasic negative-positive-negative potentials composed by epileptiform elements analogous to the components of spike-wave complex identified in human EEG [Weir, 1965], such as Spike 1 (Sp1), Spike 2 (Sp2), positive transient (PT) and Wave.

SWD I: characterization of cortical field potential

In **Chapter 3.1** it is found that SWD I appear in the fronto-parietal cortex as three-phasic potentials consisting of the early positive transient (PT_{early}), the high-voltage negative Spike 2 and the late positive component PT_{late}. The shape and magnitude PT_{early} varies across seizures, across channels and across animals, is an inconsistent element. So, frontal SWD I represent a sequence of (PT_{early}) – Sp2 – PT_{late}. Possible neuronal correlates of epileptiform components of SWD are discussed below.

1) Neuronal processes

Several electrophysiological studies aim to explore neuronal correlates of spike-and-wave seizures. First, Pollen (1964) using intracellular recordings demonstrates that the ‘spike’-component is associated with neuronal firing, whereas the ‘wave’ is associated with a hyperpolarization of neurons, suggesting an active role of inhibition. A large body of experimental studies yield the same results confirming that cortical and thalamic

neurons produce prolonged firing bursts during the 'spike'-component in EEG (local field potential) and are silent during the 'wave' [e.g., Steriade, 1974; Avoli et al., 1983; Buzsaki et al., 1988; Inoue et al., 1993; Seidenbecher et al., 1998].

Here we intend to disclose the neuronal mechanisms of a sequence of epileptiform elements in the frontal SWD I (PT_{early}– Sp2 – PT_{late}) with regard to a comprehensive study of Kandel and Buzsaki (1997), in which they combined recordings of single unit activity and electrical field potentials during high-voltage spike-wave discharges [1]. Their study suggests that the abovementioned epileptiform elements can be a manifestation of excitation-inhibition processes taking place at different cortical layers. Furthermore, the authors distinguished three putative neuronal sources or dipoles (Fig. 7.2).

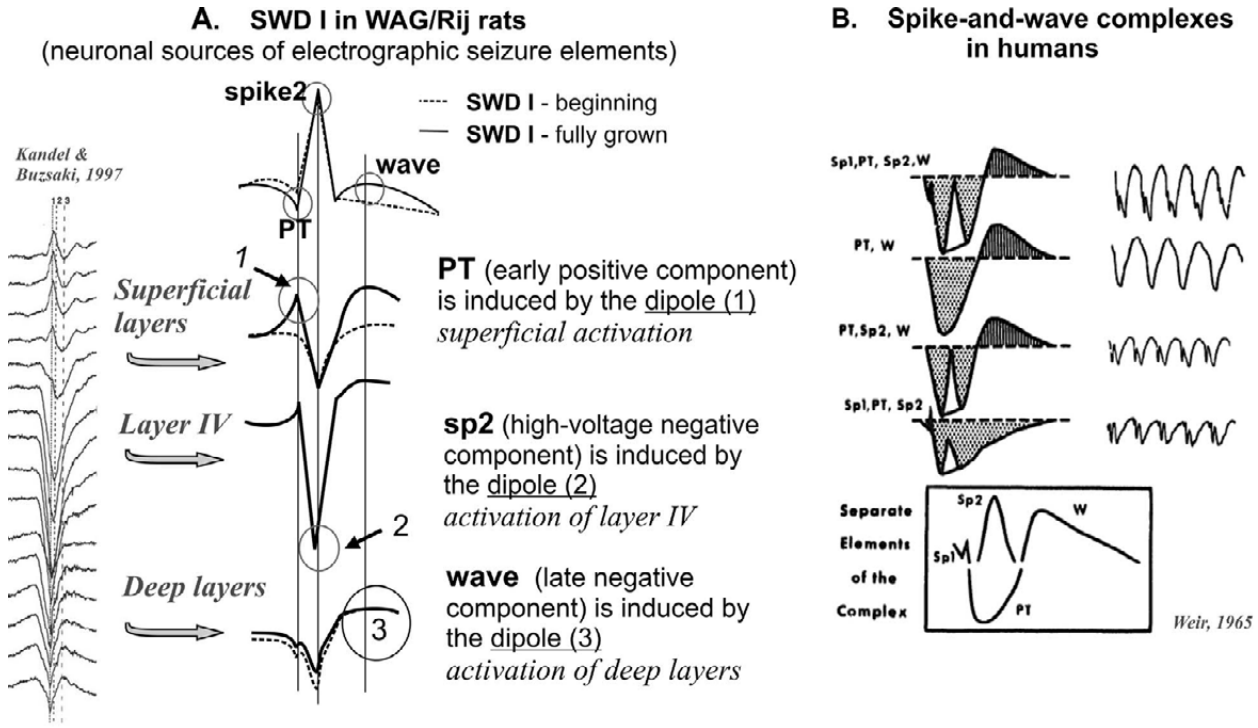

Figure 7.2. Details of electrical field potentials recorded during spike-wave seizures in the awake rat (**A**) and in human patients (**B**, adopted from Weir, 1965). **A**. Correspondence between local field potential at the different cortical layers of the somatosensory cortex (adopted from Kandel and Buzsaki, 1997) and archetypal SWD I obtained at the fontal cortex (own data, epidural recordings). Kandel and Buzsaki (1997) distinguished three putative dipoles contributing to local field potentials in SWD I (this generalized seizure type referred by the authors to as 'high-voltage spindles', HVS): dipole 1 is early surface-positive component may render PT_{early}; dipole 2 is a maximum negative potential in layer IV that may result in Spike 2; and dipole 3 is a delayed surface-negative component may yield the Wave. **B.** High variability of epileptiform elements in spike-wave complexes in humans complexity of underlying cortical neuronal dipoles. For example, dipole 2 that brings along the Spike 2 may be more or less pronounced and, in some EEG channels, even absent.

It seems that each dipole corresponds to individual epileptiform (Weir's) elements in SWD I (in **Chapter 3.1** and in [Sitnikova and van Luijtelaar, 2007]). In particular,

- Dipole 1 represents simultaneous excitation of neurons in superficial cortical layers and gives rise to an early surface-positive component, e.g. the PT_{early} as recorded at the cortical surface.
- Dipole 2 derives from layer IV and corresponds to a sharp high-amplitude surface-negative component (Spike 2).
- Dipole 3 is a delayed surface-negative component elicited by co-activation of neurons in deep cortical layers that might correspond to the Wave component.

2) Synaptic processes

In **Chapter 4.2**, we present a cortical neuronal model that simulates local field potentials during SWD I (when it stays in SWD-mode, Fig. 4.10). The model contains a neuronal network with both feedforward and feedback loops, GABA interneurons and pyramidal cells with AMPA-ergic excitatory and inputs from the thalamus [Sargsyan et al., 2007]. The results of various simulations have helped us to disclose synaptic processes

[1] experiments were performed in WAG/Rij rats (66 rats), in the F1 cross of Fischer 344 and Brown Norway rat strains (8 rats).

underlying occurrence of epileptiform elements in SWD I (Table 7.1). In particular (Fig. 4.11), the model demonstrates that the negative *spike* component ('Spike 2' in terms of Weir) reflects excitatory response of pyramidal cells elicited by AMPA-ergic the thalamic input. The *positive transient* is a manifestation of AMPA-ergic contacts between pyramidal cells (mutual intracortical excitation). Amplitude and the waveform of the *wave* component is largely depends on GABA-ergic synaptic input to pyramidal cells, e.g. feed-forward inhibition from the interneurons.

Table 7.1. Neuronal sources of epileptiform components in SWD.

Epileptiform components		**Neuronal sources of epileptiform components**	
Spike-wave complexes (discharges) in humans [1]	SWD type I in WAG/Rij rats [2]	Analysis of neuronal sources and sinks of spike-wave seizures in WAG/Rij rats [3]	Neuronal model of field potential during SWD I in WAG/Rij rats [4]
Positive transient (PT)	PT_{early}	Dipole 1: simultaneous excitation of neurons in superficial cortical layers	AMPA-ergic contacts between neighboring pyramidal cells
Spike 2 (sp2)	Sp2	Dipole 2: excitation of layer IV	Thalamic input to pyramidal cell via AMPA synapses
Wave	(late) Wave	Dipole 3: co-activation of neurons in deep cortical layers	GABA-ergic feed-forward inhibitory input from interneurons to pyramidal cells

[1] [Weir, 1965] [2] [Sitnikova and van Luijtelaar, 2007], [3] [Kandel and Buzsaki, 1997] [4] [Sargsyan et al., 2007], **Chapter 4.2**

3) The role of occipital cortex in SWD I

The occipital cortex does not seem to be actively involved in SWD I. The waveforms of SWD I in the occipital cortex and in the thalamus are congruent (Figs. 3.3 and 3.4), suggesting that the occipital cortex simply mirrors thalamic seizures and might play a role in propagation of spike-wave activity. Another characteristic feature of occipital SWD I is the occurrence of atypical elements during the initial seizure cycle. These atypical elements disappear in mature SWD I. Probably, at the beginning of SWD I, the occipital cortex is not perfectly integrated in the thalamo-cortical oscillatory loop. In that sense, SWD I is not completely generalized at the initial seizure stage. Perhaps, after several cycles SWD I become fully generalized, seizures invade the remote cortical areas (such as the occipital one) and acquire a mature waveform. The spike-wave rhythm exhibits a high degree of stability and constancy of pattern in the frontal cortex and thalamus since there are only minor dynamic modification in the waveform of SWD I.

SWD I: cortical versus thalamic field potentials

Chapter 3.1 demonstrates that SWD I appear in the thalamus as bi-phasic potentials consisting of positive sharp waves ('PT') and slow dome-shaped negative waves ('Wave'). The positive polarity of thalamic SWD I is opposite to that observed in the fronto-parietal cortex (Fig. 3.2B). In the grand average waveform, a peculiar element, 'Spike 1', is seen in the VPM, but it not in the frontal cortex and RTN (Fig. 3.4). In spite of its small amplitude, 'Spike 1' is not eliminated by the averaging process, suggesting that this element is constantly present across seizures and across animals. This finding is in agreement with Meeren's et al's (2002) observation that a sharp negative spike (e.g., 'Spike 1') is present during SWD (type I) in the VPM, but absent in the RTN. Besides that, elements of SWD I appear in two thalamic nuclei (the RTN and the VPM) without a time delay, suggesting that epileptogenic processes in these two nuclei are closely interconnected.

It is difficult to assess the nature of low-amplitude early 'Spike 1'. We found that 'Spike 1' in the VPM lead the frontal 'Spike 2' with 12 msec time delay and appears simultaneously (without time delay) with the frontal PT_{early} (PT_{early} substantially varied across seizures and across rats, therefore, it is not possible to obtain statistical characteristics of this element). As it is said above, PT_{early} may manifest simultaneous excitation of superficial cortical layers, therefore 'Spike 1' in the thalamus may reflect back-propagation of cortical excitation. Further electrophysiological experiments are needed in order to clarify neuronal processes behind the 'Spike 1'.

In the frontal cortex, SWD I shows a disproportionately large 'Spike 2', therefore, in this location, EEG pattern of SWD I is strongly asymmetric. Asymmetry in frontal SWD I increases as seizure progresses (Fig. 3.4). In the thalamus, EEG pattern of SWD I is more symmetrical, as compared to their cortical counterparts. Seizure polarity changes in the cortex and the thalamus from initial to the middle part of a seizure. Temporal evolution of

SWD I in the thalamus is associated with an increase of the positive phase (amplitude of the PT is increased), but in the cortex, vice versa, the negative phase appears to be increased.

The waveform of SWD I in the thalamus differ from that in the frontal cortex:

- SWD I in the anterior-middle cortex and in the thalamus have an opposite polarity. This polarity reversal is likely to reflect an opposite orientation of electrical currents formed by the superficial and deep neural mass [Lopes da Silva and van Rotterdam, 1982].
- The sharp positive transient (PT) in thalamic SWD I appears in both thalamic loci 7-9 msec after the frontal 'Spike 2'. It is likely that the PT appears in the thalamus due to a back-propagation of cortical 'Spike 2'.

To date, cortical and thalamic seizures consist of different components which follow each other with a consistent time shift. The lack of congruency between cortical and thalamic counterparts of SWD I suggests that the propagation of seizure throughout thalamo-cortical circuit is not merely a transduction of electrical activity, but that each part of the circuit is actively involved in maintaining SWD I.

SWD II: characterization of field potentials, their relationship with SWD I and probable origin

In **Chapter 3.1** it is found that SWD II are expressed in the occipital channel, but they are hardly visible in the fronto-parietal cortical area, dorsal hippocampus and thalamus (Fig. 3.1). The local occipital SWD II are two-phasic negative-positive deflections comprising the high amplitude sharp PT and the dome-shaped negative wave (Fig. 3.2). In the occipital cortex, SWD I and SWD II consist of the same components (PT and Wave), although SWD I display 'Spike 1', but SWD II not (Fig. 3.3A vs 3.3B). Two types of SWD are clearly different at the level of the thalamus. Only rudimentary SWD II are present in the thalamus, in contrast, SWD I are well pronounced in the thalamus.

Chapter 4.1 demonstrates that the frequency profile of SWD I in the frontal EEG undergoes dynamic changes, so that, at the end, SWD I bear a striking similarity with SWD II. On the other hand, in the occipital EEG, SWD I do not resemble SWD II (neither at the beginning nor at the end). This confirms our observations made in **Chapters 3.1** and **3.2** that SWD I and SWD II are independent phenomena. In **Chapter 4.1** we assume that epileptogenic processes in the occipital cortex (or functionally related structures, other than cortico-thalamic circuit, e.g., septo-hippocampal structures) might underlie the occurrence of SWD II. It is hypothesized that SWD I and SWD II derive from physiological rhythmical electrical activities described by Semba and Komisaruk (1980, 1984), e.g., alpha (9 Hz) and theta (7 Hz) rhythms. In particular, SWD I might represent a hypersynchronous thalamo-cortical alpha rhythmic activity and SWD II could be a modification of septo-hippocampal theta rhythm. The role of the hippocampus in SWD II is not obvious and needs to be explored in the future.

Issue 3(2). Correspondence between SWD in WAG/Rij rats and spike-and-wave complexes in humans

Almost all literature about generalized spike-wave discharges in rodent models refer to generalized spike-wave discharges, e.g., SWD (type I). This type of paroxysmal activity in genetic animal models of absence epilepsy closely resembles absence seizures occurring in humans [Danober et al., 1998; Coenen and van Luijtelaar, 2003; Depaulis and van Luijtelaar, 2006]. In humans, typical absence seizures usually begin (in children) between 5 and 8 years old and clinical seizures are accompanied by generalized 3–4 Hz spike-wave discharges 'invading the whole brain' [Panayiotopoulos, 1999; 2005]. WAG/Rij rats fulfill all requirements to be considered as a valid model of absence epilepsy[1] and predictive validity (they should be standardized, enabling predictions from the model to the patient), although absence seizures in our rats are not completely the same to that in epileptic patients. It is essential that the frequency of SWD in rats (in all strains, such as WAG/Rij, GAERS, Fischer 344, Wistar and others) is three times higher than in humans (7-11 Hz versus 3 Hz). This difference is brought about by physiological and anatomical differences between the brains of rodents and humans. In contrast to humans, rats do not have inhibitory interneurons in the relay thalamic nuclei except in *the lateral geniculate nucleus* [Ohara et al., 1983; Jones, 1985]. In rats, the majority of thalamic neurons receive solely external inhibitory input from the RTN. The lack of internal inhibition in the rodents' thalamus may influence the intrinsic properties of thalamo-cortical neuronal oscillations, resulting in a three-fold increase in the frequency of spike-wave activity.

Despite the differences in frequency, SWD I in WAG/Rij rats are analogous to generalized spike-wave seizures (absence epilepsy) in humans [van Luijtelaar and Coenen, 1986; Coenen and van Luijtelaar, 2003]. SWD II has no clinical manifestations, they are not present in all adult WAG/Rij rats and they are also found in non-

[1] A valid animal model should fulfil several requirements such as face validity (seizures in animal model and in humans should have the same clinical, pharmacological, and aetiological characteristics), construct validity (they should based on the same theoretical grounds) [Coenen and van Luijtelaar, 2003].

epileptic ACI rats[1] [Schridde and van Luijtelaar, 2005], suggesting that SWD II are non-epileptic in nature. It is unknown whether SWD II correspond to any kind of epilepsy in humans. However, there are some indications[2] that SWD II in WAG/Rij rats may correspond to 'a benign epilepsy with occipital spike-waves' [Gastaut, 1982] or to 'Panayiotopoulos type of occipital lobe epilepsy' [Panayiotopoulos, 2000]. Both epilepsies are characterized by high-amplitude spikes or/and spike-wave discharges (frequency 1 – 4 Hz) over the occipital and adjacent regions [Gastaut, 1982]. Moreover, Kuznetsova (personal communication) has found occipital SWD in adult patients. Further examination of epileptogenic processes in the occipital cortex and related areas are necessary to disclose the nature of SWD II.

Based on principles of clinical electroencephalography and on the classification of Weir, we found that the EEG profile of spike-wave seizures in our rats is similar to that in patients with absence epilepsy (**Chapter 3.1**). In humans, topography of spike-wave discharges complexes is difficult to explore, because of great individual variability of seizure waveforms. The EEG profile of spike-wave complexes (discharges) can vary from patient to patient, moreover, morphology of different spike-wave discharges in the same patient may also vary [Rodin and Cornellier, 1989; Rodin and Ancheta, 1987; Rodin, 1999]. It is striking that WAG/Rij rats showed relatively small individual variations in the topographic distribution of SWD I and II across the neocortex [Midzianovskaia et al, 2001]. In **Chapter 3.1** we describe a similar assemble of epileptiform elements in SWD in all individuals. Figure 7.2B illustrates some morphological differences in SWD in humans, for example, spike 2 (sp2) may be more or less pronounced or even absent. This substantial variability in the waveform of locally recorded spike-wave discharges in humans is distinguished from the constant waveform of local SWD in rats. This may be accounted for that (1) cortical neuronal dipoles, underlying epileptiform components in humans,, may have more complex and may be dynamically organized as compared to simple dipoles in rats (e.g., neuronal dipoles in Fig.7.2); (2) cortico-thalamic interrelations in humans are much more intricate and compound compared to that in rats. Therefore the distribution of field potentials during spike-wave seizures might be more complex in humans than in rats.

The field maxima in patients are usually found in the frontal lobe (at Fz extending laterally to F3 and F4 and posteriorly to Cz) [Rodin and Cornellier, 1989; Rodin and Ancheta, 1987; Rodin, 1999]. The 'classical' negative spike (Weir's spike 2) is known to show amplitude maximum in frontal areas [Weir, 1965], and this is similar to what we found in WAG/Rij rats (**Chapter 3.1**, [Sitnikova and van Luijtelaar, 2007]).

In human patients, spike-wave seizures are characterized by complicated dynamics, which is not yet explored in details. Seizures often begin with the positive component (the wave) that rises up in the posterior head regions (at O1, Oz, O2 or Pz) [Rodin and Ancheta, 1987]. This can be distinguished from the dynamics of SWD I in WAG/Rij rats:

- SWD I in the frontal area are well formed at the beginning (Figs. 3.1 and 3.3) and their waveform just slightly changes as seizure progress (the asymmetry of SWD I is progressively increased).
- The initial cycle of SWD I in the occipital cortex comprises atypical elements, which disappear in mature seizures. Several cycles should pass until SWD I become fully developed and the spike-wave pattern in the remote cortical areas (such as occipital one) acquire a mature waveform.

It seems that dynamic changes of seizure morphology of local field potentials during spike-wave seizures (dynamics), dynamics of special distribution in humans is much more sophisticated than in rats, and it could not be explained by the abovementioned logic.

Issue 4. Noradrenergic control of SWD I and SWD II

Chapter 3.2 stresses the importance of noradrenergic modulation of thalamo-cortical network activity. It is found that depletion of noradrenergic innervations (with systemic injections of alpha-2 agonist clonidine) increases the number of SWD I and affects the EEG power spectrum of SWD I, SWD II and sleep EEG.

Clonidine alters the EEG power in cortex and thalamus:

- In sleep EEG, a decrease in delta band is found in cortex and thalamus.
- In SWD II, a decrease in theta band is found in all locations.
- In SWD I, a decrease in alpha band is found only in the frontal cortex, an increase in alpha band in the RTN.

These findings suggest that clonidine affected power around the main frequency of oscillations (delta – during sleep, alpha – during SWD I and theta – during SWD II).

[1] Agouti Copenhagen Irish rats, commonly used as a control strain since these rats showed no or at least very few SWD in a comparative strain study [Inoue et al., 1990].
[2] Prof. G.D. Kuznetzova, personal communication.

The incidence of SWD I is highly aggravated after injections of clonidine, in agreement with earlier reports [Buzsaki et al., 1991; van Luijtelaar, 1997]. The aggravation is also in line with McCormick's (1989) suggestion that weakening of noradrenergic neuromodulatory system promotes thalamo-cortical oscillations. The number of SWD II does not change after clonidine injections. Different sensitivity of SWD I and SWD II to adrenergic neuromodulatory supply suggests that these phenomena are produced by different neuronal networks.

Pharmacological reduction of noradrenergic neurotransmission with low-dose of alpha-2 agonist clonidine has the following effects:

- more time was spent by the animals in the waking state;
- a higher incidence and increased duration of SWD I;
- a reduced fronto-occipital coherence during SWD I (for one hour);
- a decrease of EEG power during sleep, SWD I and SWD II;
- Two-way changes of electrical activity in the RTN: an increase of total EEG power and alpha activity during SWD I, and a decrease of theta activity during SWD II.

In all, clonidine injections cause a decrease of EEG power over the cortex and the thalamus mainly in 9-14 Hz, except the RTN, where an increase in power is found only during SWD I and mainly in 9-14 Hz. This could mean that reinforcement of electrical activity in the RTN, rather than in the VPM, may encourage the propagation or generation of SWD I by putative modulatory alpha2-adrenergic mechanisms.

In contrast, clonidine treatment diminishes activity in RTN during SWD II: the power in 5-9 Hz band is lower than in control. In comparison to the rest of the thalamus, the RTN receives a more dense noradrenergic innervation [Swanson and Hartman, 1978]; therefore, the RTN could be more sensitive to noradrenergic modulation than other thalamic nuclei.

Frequency profile of SWD I and SWD II is changed after clonidine injections. As compared to controls SWD I in clonidine conditions show opposite changes in alpha band as measured in the frontal cortex (a decrease) and in the RTN (increase). An increase of alpha activity in the RTN suggests a reinforcement of oscillatory activity in the frequency of SWD I. This results in more numerous and long-lasting SWD I; a decrease in alpha in the frontal cortex might encourage this effect (via complex, yet unknown, feedback cortico-thalamus processes operating at synaptic level). Elevation of absence seizures in clonidine conditions seems to be accounted for the intricate co-resonance between the cortex and the thalamus. Altogether, our data imply that the noradrenergic neuromodulatory system affects frequency profile of both SWD I and SWD II; it also directly controls the incidence of SWD I most likely via the reinforcement of oscillatory activity in the RTN, but it does not affect the incidence of SWD II.

Issue 5. The role of the thalamus in SWD type I and type II

SWD type I

A few depth EEG recordings that have been done in humans in the past cast some doubt on the role of the thalamus in absence seizures. For instance, it has been found that subcortical SWD are less regular and they are usually less pronounced as compared to SWD recorded simultaneously in the cortex [Angeleri et al., 1964]. Recently, application of magnetic resonance imaging techniques (MRI) and magnetic resonance spectroscopy (MRS)[1] in humans provided new evidences for a crucial involvement of the thalamus in absence epilepsy. In particular, MRS studies have demonstrated a significantly lower thalamic NAA/Cr ratio in patients with typical absence epilepsy when compared to the healthy controls [Fojtiková et al., 2006]. This clearly indicates neuronal dysfunction in the thalamus of patients with typical absence epilepsy and confirms the role of the thalamus as an important structure in the pathogenesis of typical absence epilepsy. Also simultaneous EEG-fMRI in drug-naive children with newly diagnosed absence epilepsy, BOLD signal changes associated with 3 Hz spike-wave discharge, which were associated with a bilateral increase in the BOLD signal in the medial thalamus [Moeller et al., 2008a]. Taking into account the normal delay in the hemodynamic response, the authors suggest that the onset of BOLD signal changes coincided with the onset of spike-wave seizures. Furthermore, the same technique (combined EEG-fMRI) applied in children with idiopathic generalized epilepsy, revealed an increase in BOLD signal in the medial thalamus approximately 6 sec before SWD can be visualized in EEG, whereas a decrease in cortical BOLD signal were mainly found in fronto-parietal areas starting 6 to 3 sec before the onset of SWD. The

[1] MRS is a non-invasive imaging technique providing metabolic information from different body tissues, including the brain. This technique is able to detect metabolic abnormalities, which might be missed by conventional magnetic resonance imaging techniques (MRI). In MRS spectra, there are three major peaks characterizing long-echo time 1H: N-acetylaspartate (NAA) – the marker of neuronal and axonal viability and density; creatine (Cr) – used as internal reference, since it is the most stable cerebral metabolite; choline – reflecting cellular proliferation.

authors conclude that the thalamus shows an increase in neuronal activity along with regional decreases in cortical activity [Moeller et al., 2008b]. In Chapter 3.1 we describe well pronounced SWD I in the thalamus and conclude that thalamic structures are capable to reproduce stereotypic epileptic activity on the level of local field potentials.

In animals, *in vivo* and *in vitro* examinations indicate that SWD (type I) are initiated in the RTN [Seidenbecher et al., 1998; Avanzini and Franceschetti, 2003]. SWD in GAERS are suppressed after large electrolytic lesions of the lateral thalamus [Vergnes and Marescaux, 1992] and also after more restricted chemical lesions of the RTN [Avanzini et al., 1992, 1993]. The same observations are made in WAG/Rij rats: SWD are completely abolished after ibotenic lesions of large parts of the thalamus including the RTN [Meeren, 2002]. The primarily role of the RTN in pathogenesis of absence epilepsy has been established by *in vitro* neurophysiological studies in which a pacemaker of spike-wave seizures has been identified as a pool of GABA-ergic neurons with an intrinsic propensity to generate rhythmic bursts [e.g., Crunelli and Leresche, 2002; Avanzini and Franceschetti, 2003]. The RTN does not project to the neocortex, yet innervates the dorsal thalamus [Ohara and Lieberman, 1985] (in rats, the RTN provides the solely inhibitory input to the major part of dorsal thalamus). We assume that an increased synchrony between the RTN and specific thalamic nuclei, ventroposteromedial complex, VPM may accompany the onset of SWD.

In **Chapter 5.1**, it is shown that the initiation of SWD I is accompanied by a narrow-band increase of RTN-VPM coherence in 8-11.5 Hz. RTN-VPM is the only pair in which gamma-band associations are decreased. There may be a functional correlation between stronger synchronization in alpha frequencies and desynchronization (decrease of coherence) in the gamma band, for example, a reduction of high frequencies may encourage the functional coupling in the frequencies of SWD (8-11.5 Hz). Noteworthy is that the RTN may play a specific role in an increase of SWD I after blocking the release of noradrenaline (clonidine injections, **Chapter 3.2)**. This pro-epileptic effect is accompanied by the local narrow-band (9-12 Hz) increase of electrical activity in the RTN, therefore, the normally occurring SWD I are accompanied by an increased 8-11.5 Hz synchronization between RTN and VPM (as reported in **Chapter 5.1**) and this might be initially driven by the RTN.

In general, our data are in agreement with other studies [Meeren et al., 2002; Meeren, 2002; Richards et al., 2003; Steriade 2003, 2005; Pinault, 2003; Pinault et al., 2006] showing that the RTN has a supplementary role in SWD I. In particular,

- Examination of the microstructure (light and electronic microscopy) in animal models of absence epilepsy shows no signs of pathology in the RTN. In WAG/Rij rats, the synaptic organization of the RTN is similar to that in non-epileptic ACI rats [van de Bovenkamp-Janssen et al., 2004]; in GAERS, the RTN shows neither significant changes in structure, nor neuronal loss [Sabers et al., 1996].
- Electrophysiological *in vivo* studies and computational modeling both demonstrate that spike-wave seizures are progressively built up in intracortical synaptic networks with subsequent excitation of the RTN, leading to inhibition of the dorsal thalamus [Meeren, 2002; Destexhe and Sejnowski, 2001; Steriade, 2003; 2005].

Our study of EEG coherence (**Chapter 5.1**) indicates that occurrence of SWD I requires a large-scale increment of functional interaction between the frontal cortex and the thalamus. As known, a cortical focus in the peri-oral region of the somatosensory cortex drives the thalamus during the first few cycles until the whole thalamo-cortical system becomes entrained into the seizure activity [Meeren et al., 2002]. SWD I may appear in the cortico-thalamo-cortical network as a complex resonance phenomenon initiated and driven by neurons in the somatosensory cortex. Changes in local thalamic and cortical-thalamic network interactions reinforce the propagation of absence seizures. This is in agreement with Meeren's et al. (2005) statement that the thalamus interacts with the cortex, providing a resonant circuitry to amplify and sustain the generalized spike-wave discharges.

SWD type II

The thalamus does not seem to play a role in SWD II. In **Chapter 3.1** (Fig. 3.2c): a grand EEG average of SWD II in both thalamic nuclei is negligibly small (in contrast to SWD I, which well-shaped grand average in the thalamus). During SWD I, sharp and well-formed field potentials are recorded in the thalamus, in opposite to sleep spindles, in which thalamic field potentials were not shaped in spindle-like waveform (the principle of Lopes da Silva and van Rotterdam (1982 and 1987), see Issue 2 on page 146). It is likely that SWD I are much more synchronized and generalized than sleep spindles, therefore, SWD I are easily projected subcortically and elicit strong fluctuations of field potentials in the thalamus. Sleep spindles are too mild and less synchronized oscillations and their thalamic counterpart is relatively weak. Also SWD II, might be less synchronous and less generalized, as compared to SWD I, therefore, they cannot be projected in the thalamus and form large field potentials there (in this respect SWD II are similar to sleep spindles).

Based on time-frequency analysis in **Chapter 4.1**, we conclude that thalamo-cortical mechanisms do not play a role in SWD II. This statement is confirmed in **Chapter 3.2**. Depletion of noradrenergic innervation with systemic clonidine injections causes a tendency to decrease the number of SWD II, and the total power as well as theta activity during SWD II decreases significantly (Fig. 3.9C). This effect is observed in the occipital cortex and in the thalamus. It is hypothesized that there is a functional connection between neuronal source of theta activity and a putative source of SWD II. Clonidine suppresses 'SWD II'-related theta activity, therefore, the theta component in SWD II is suppressed and the total amount of SWD is reduced.

Issue 6. Precursors of SWD I

Investigations in GAERS clearly demonstrate that spike-wave seizures[1] are preceded by medium-voltage 5–9 Hz oscillations [Pinault et al., 2001]. The presence of 5–9 Hz precursors of absence seizures in other animal models of absence epilepsy and in humans has never been confirmed. Considering the close resemblance between GAERS and WAG/Rij rat strains [Danober et al., 1998; Depaulis and van Luijtelaar, 2006], we expect that spike-wave seizures in WAG/Rij rat can also be preceded by the same 5–9 Hz oscillations. In **Chapter 3.3** we examine time-frequency EEG parameters of 1 sec episodes immediately before the onset of SWD I (so-called precursor epochs of SWD I, preSWD epochs) in WAG/Rij rats. Our data suggest that there is a remarkable diversity in the waveform and frequency profile of preSWD epochs. This somehow disagrees with Pinault and co-worker's (2001) findings in GAERS that medium-voltage 5–9 Hz rhythm constantly precedes the onset of SWD. We propose an empirical classification of preSWD based on significant difference of EEG power as measured in traditional frequency bands, namely, preSWDΔ, preSWDθ, preSWDα and preSWDn. These classes are significantly different in respect to EEG power in characteristic *delta-theta-alpha* bands as measured in the frontal EEG (Fig. 3.11 and 3.12A). More precise, preSWDΔ epochs are characterized by the highest power *delta* band, preSWDθ - the highest power in *theta* band, preSWDα - the highest power in *alpha* band and preSWDn showed the least power in all investigated frequency bands.

In contrast to GAERS, the precursor activity of SWD in WAG/Rij rats does not represent a well-formed 5–9 Hz rhythm. Instead, around 73% of SWD exhibit a well pronounced *theta*-component just prior to SWD in WAG/Rij rats (preSWDθ+preSWDα), suggesting that the majority of SWD in WAG/Rij is preceded by substantial 5-9 Hz (*theta*) activity. This is in agreement with the results obtained in GAERS [Pinault et al., 2001, 2006; Pinault, 2003]; however, *delta* precursor activity characterizing the onset of SWD in WAG/Rij rats (95% of all SWD), was not in GAERS (this will be discussed in the next paragraph).

As it is found in **Chapter 3.3**, the shape of the power spectra of preSWD in the frontal cortex is clearly distinguished from that obtained in both RTN and VPN (Fig. 3.13). It is remarkable that, in the thalamus, all classes of preSWD epochs have the same power in *delta* and *theta* bands, but not in the frontal cortex (it is discussed above). There are no indications that oscillations of any kind precede absence seizures in human patients. Recent investigations of spike-wave discharges in human EEG [Aarabi et al. 2007] yield contradictory results demonstrating that 71% of seizure-precursors characterized by the disappearance of *theta* and *alpha* components in background EEG.

In **Chapter 4.1** it is found that some properties of SWD (e.g., the length) are predetermined by the properties of seizure precursors: preSWDα and preSWDθ are followed by longer SWD I, but preSWDn and preSWDΔ - by shorter seizures. An important finding in **Chapter 3.3** is that a correspondence between EEG power content of preSWD and subsequent SWD I is rather simple. In the frontal and occipital EEG recordings, no relationship is found between a distribution of EEG power over *delta-theta-alpha* bands in SWD and the type of SWD-precursor activity. In the thalamus, there is some relationship between EEG properties of preSWD epoch and subsequent SWD: (1) a desynchronized precursor activity (preSWDn epochs) is followed by SWD (5% of total seizures) that displayed an enlarged *delta* (in the thalamus, but not in the cortex); (2) seizures, whose precursor epochs had exaggerated *alpha* activity in the frontal EEG (preSWDα) displayed high *alpha* activity in the thalamus (but no longer in the cortex).

Issue 6(1). Electrographic features and power spectrum analysis of SWD I precursor activity

A distinctive feature of preSWD epochs is the presence of a *delta*-component. Power spectra of 95% of all seizure-precursor epochs (except preSWDn), in addition to peaks in preSWD-specific frequencies, display peaks in *delta* as measured in the frontal cortex (around 3-4 Hz, Fig. 13.11) and in the thalamus (1-2 Hz, Table 3.4). We assume that *delta* components in preSWD may be produced by two relatively independent sources – in the cortex

[1] the same to SWD type I in WAG/Rij rats

and in the thalamus. This is in agreement with *in vitro* investigations demonstrating an independency between intrinsically generated thalamic *delta* rhythm and cortical *delta* waves [Steriade, 2002][1].

The presence of delta-component in the frontal EEG in almost all preSWD epochs (95%) implies an essential (and probably, primary) role of *delta* activity in initiation of SWD in WAG/Rij rats. In addition to *delta*, 73% of preSWD epochs expressed large 5-9 Hz (*theta*) component. Therefore, a coalescence of *delta* and *theta* activities may be favorable for the occurrence of SWD I. Altogether, we stress that the co-existence of cortical and thalamic *delta* activity may play an important role in the initiation and further development of SWD I.

Issue 6(2). Thalamo-cortical network associations in shaping of SWD I precursors and subsequent seizure activity

Chapters 3.3 and **5.1** describe network associations and synchronization in thalamo-cortical circuit during pre-ictal and early ictal stage of absence seizures with the aid of ordinary coherence (Figs. 3.15 and 5.2). Frequency profile of EEG coherence slightly differs in different classes of preSWD, yet no features of EEG coherence can be considered as unique for any class of preSWD epochs. In general, preSWD epochs are characterized by high coherence between RTN and VPM, suggesting that these nuclei are highly coupled even before the onset of SWD I. 'Fronto-thalamic' coherence is lower as compared to coherence in 'RTN-VPM' pair and the least coherence is found in 'fronto-occipital' pair.

Our findings suggest that amplitude-frequency properties of preSWD **(Chapters 3.2**) and subsequent SWD (**Chapters 5.1**) depend upon coordination and consolidation between thalamic and cortical counterparts within the entire network. In general, the transition preSWD→SWD is associated with an increase of 'fronto-occipital' and 'fronto-thalamic' coherence in 9.5-14 Hz and in double frequencies (*beta* band). The most widespread and strong increase is observed in preSWDΔ→SWDΔ and in preSWDθ→SWDθ, moderate increase - in preSWDα→SWDα, and the least increase - in preSWDn→SWDn. In all it suggest that the occurrence of SWD is accompanied with changes in network interactions in very specific frequency bands.

SLEEP SPINDLES and SWD

Chapter 4 examines similarities and distinctions between sleep spindles and SWD. **Chapter 4.1** tests the hypothesis that anterior sleep spindles are functionally linked to SWD I and posterior spindles – to SWD II. **Chapter 4.2** examines a fundamental assumption that SWD (type I) are derived from (anterior) sleep spindles using cortical neuronal model. **Chapter 4.3** extracts and compares key elements in EEG characterizing SWD I and anterior spindles.

Issue 7. Distinctions between SWD and sleep spindles disclosed with time-frequency EEG analysis

In Chapter 4 we report on differences between SWD and sleep spindles in spectral content and other characteristics. Results of our time-frequency EEG analysis cast some doubts about similarity between sleep spindles and SWD.

Anterior sleep spindles and SWD I

The following differences between anterior sleep spindles and SWD I are found:

- SWD I last ten times longer than anterior spindles, their amplitude is nearly two times higher and their mean frequency is about 2 Hz lower (as measured in a period 0.5-1.5 sec after the onset) (**Chapter 4.1**).
- Power spectrum analysis (frontal EEG) demonstrates that SWD I express higher power in beta frequencies and lower power in delta and theta bands as compared to anterior spindles. This difference in frequency composition (in frequency-domain) between SWD I and anterior spindles (**Chapter 4.1**) correlates with the difference in their EEG waveforms (in time-domain, as found by means of EEG grand average analysis of SWD I in **Chapter 3.1** and wavelet analysis in **Chapter 4.3**)
- Continuous wavelet analysis shows that the EEG pattern of SWD I is not comparable with that in anterior sleep spindles (**Chapter 4.2)**: different wavelets are necessary for the identification of SWD and spindles. SWD I are identified in EEG with high probability using standard Morlet-wavelet, but sleep spindles can be identified

[1] the neuronal mechanisms of the thalamic and cortical *delta* have been discussed on pages 63 and 146)

using two types of customized adoptive 'spindle wavelets'. Besides that, it is found that SWD I represent one family, but anterior spindles - two different families.

- Cross-correlations analysis shows that 'fronto-occipital' associations in anterior sleep spindles are similar to that in the waking EEG (both cross-correlation functions are symmetric over the time scale), but differ from that in SWD I. In SWD I, cross-correlation function is asymmetric (Fig. 4.9A). This asymmetry implies differences in signal waveforms at the frontal and occipital channels (**Chapter 4.1**) and can be well explained by the presence of different Weir's components in the frontal and occipital SWD I (**Chapter 3.1**).
- The above mentioned dissimilarities between sleep spindles and SWD support the notion that the neurophysiological substrate of spindle oscillations and SWD is not the same. As compared to SWD, spindle oscillations are less generalized (they are more local, **Chapter 2.1** and **3.1**), their EEG waveform is less regular (**Chapter 4.2**). Density of anterior sleep spindles in genetic epileptic WAG/Rij rats is the same with that in control rats, despite the large strain difference in the number of SWD I. The incidence of SWD I in WAG/Rij rats highly increases with age, yet control rats exhibit just sporadic SWD I. Altogether suggests that sleep spindles and SWD are controlled by different age-related mechanisms [van Luijtelaar and Bikbaev, 2007]. Pharmaco-EEG study reveals a reciprocal relationship between the number of anterior sleep spindles and the number SWD I: phenobarbital and flunitrazepam suppress the incidence of SWD I, but enhance anterior sleep spindles in opposite, while clonidine promotes SWD I and reduces anterior sleep spindles [van Luijtelaar, 1997]. Comprehensive *in vivo* and *in vitro* neurophysiological examinations in GAERS demonstrate that SWD do not originate from sleep spindles, but a plausible source of SWD is 5–9 Hz oscillations [Pinault, 2001; Pinault et al., 2003; Pinault et al., 2006]. The authors show that dissimilarities between sleep spindle and SWD already appear on the level of intracellular events in cortical and thalamic neurons, e.g., different modulation of membrane potential resulting to more or less synchronized firing activity of corresponding neurons.

It is noteworthy that rat models of absence epilepsy (i.e., GAERS and WAG/Rij) can be distinguished from the feline generalized penicillin epilepsy [Gloor 1969, Kostopoulos, 2000], in a sense that spindle oscillations in rodents, unlike cats, do not seem to correlate with absence epilepsy. This difference between can be accounted for, first, by interspecies variations: in rodents, unlike higher mammal species (ferrets and cats), interneurons are missed in the majority of relay thalamic nuclei [Jones, 1985]. Second, by cellular and network properties of somatosensory system in rodents: spindle oscillations are pronounced in slices of the visual thalamus in ferrets [von Krosigk et al. 1993], but they are not studied in the somatosensory thalamus in ferrets and they are known to be absent in the somatosensory thalamic slices in rats [Jacobsen et al. 2001].

Posterior sleep spindles and SWD II

Differences between posterior sleep spindles and SWD II are as follows (**Chapter 4.1**):

- Mean frequency of SWD II is lower as compared to posterior sleep spindles (difference was ~3.5 Hz).
- Power spectrum analysis (occipital EEG) demonstrates that SWD II can be distinguished from posterior spindles by having higher power in theta frequencies and low power in alpha band.
- SWD II shows compatible power spectra in the frontal and in the occipital EEG, in contrast to posterior spindles, which reveal a remarkable discrepancy between power spectra obtained in the frontal and occipital EEG (enhancement of occipital alpha coincides with the elevation of frontal delta).

Here we demonstrate that posterior sleep spindles (**Chapter 2**) and SWD II (**Chapter 4.1**) have a very limited propagation throughout the thalamo-cortical circuitry (in contrast to anterior sleep spindles and SWD I, which are referred to as purely thalamo-cortical oscillations). Other studies assume that posterior sleep spindles might originate from the thalamus or from limbic system [Gandolfo et al., 1985, van Luijtelaar, 1997, Meeren et al., 2002, Sitnikova and van Luijtelaar, 2004].

Based on these data we tend to consider posterior sleep spindles and SWD II as clearly dissimilar and independent EEG phenomena. On the other hand, the number of posterior sleep spindles in old WAG/Rij rats is known to have a positive age-related correlation with the number of SWD II, suggesting that a common age-related factor plays a role in these oscillations [van Luijtelaar and Bikbaev, 2007].

Issue 8. Neuronal network mechanisms of sleep spindles and SWD

The analysis which is performed in **Chapters 3.3, 4.1, 4.3** reveals only weak, if any, straightforward correspondences between SWD and sleep spindles. Outcomes of **Chapter 3.3** reveal a similarity between precursors of SWD I in WAG/Rij rats and 5-9 Hz rhythmic activity preceding SWD in GAERS [Pinault, 2001; Pinault et al., 2003; Pinault et al., 2006]. In particular, preSWD in WAG/Rij rats comprise in about 75% of the SWD a strong theta component in the frontal EEG. Altogether, this suggests that preSWD in rodent models is profoundly distinctive from sleep spindles, thus pointing out a crucial difference between genetic rodent models

and outcomes of the feline penicillin model (in the latter model sleep spindles are well-defined forerunners of spike-wave discharges [Gloor 1969, Kostopoulos, 2000]). In **Chapter 4.1** we have carried out a power spectrum analysis of sleep spindles, preSWD and SWD I and have found that preSWD might have a dual nature. In fact, preSWD contain frequency components that are characteristic for anterior sleep spindles (relatively high delta) and for SWD I (relatively high alpha). On the other hand, sleep spindles and SWD demonstrate a similar thalamo-cortical cross-correlation functions (**Chapter 4.1**) and they are modeled by a common neuronal model (**Chapter 4.2**), suggesting that both spindles and SWD can appear in EEG as a manifestation of synchronization processes taking place in the same thalamo-cortical circuit during low vigilance states.

Intracortical neuronal processes underlying occurrence of sleep spindles and SWD (network modeling)

In **Chapter 4.2** we go deep into neuronal mechanisms of sleep spindles and SWD using a cortical neuronal model that can act in two states, producing SWD or sleep spindles (SWD-mode and spindle-mode). This model considers a population of cortical cells, in which each neuron (pyramidal cell) produces electrical currents. Cellular currents are summed up in respect to their spatial-temporal distribution, direction and amplitude, resulting in neuronal local field potentials. It is found that the shape of field potential generated in SWD-mode and spindle-mode is different and this difference can be accounted for by a degree of synchrony between neurons. The following factors influence the waveform of field potential: (1) the difference in transmembrane currents; (2) the effects of spatiotemporal summation of transmembrane currents when synchronization of pyramidal cells is high (in SWD-mode) or low (in sleep spindle mode). The latter observation indicates that local field potentials in the cortex approximate SWD shapes when synchronization between pyramidal cells exceeds certain limits.

Neuronal organization of the neocortex is very complex and the model in **Chapter 4.2** simplifies the representation of cortical cells, e.g., it disregards the size of neurons and laminar distribution of different types of neurons. This is partly compensated by introducing a vertical spread of pyramidal cells in the population model. Out model does not aim to reproduce fine details of field potentials as recorded *in vivo* at different cortical layers, but it gives a sufficiently well approximation of the waveform of superficially recorded field potentials during SWD and sleep spindles. According to the outcomes of **Chapter 4.2**, large pyramidal cells in layer V provide the major source of cortical field potentials during wide-spread synchronous oscillatory activity.

Achievements made by other computational models of generalized spike-and-wave seizures [1]

Computational models have been used for decades to investigate mechanisms of epileptogenesis. The cortical neuronal model in **Chapter 4.2** simulates local field potentials [Sargsyan et al., 2007], yet it does not investigate mechanisms by which a thalamo-cortical network can switch from the spindle-mode to the SWD-mode. The latter problem has been investigated with several computational models, which show that networks of excitatory and inhibitory neurons can generate seizure activity.

Destexhe et al. (2001) show in a model of cortical seizures that seizure activity arises from inhibition-rebound interactions between cortical cells. Another model of cortical seizures [Timofeev et al., 2002] includes excitatory connections of pyramidal neurons in addition to inhibitory inputs from interneurons. Although, cortical circuits can generate some form of spike-and-wave activity in both models, this activity differs from the typical absence seizures (frequency of spike-and-wave oscillation are low. 1-2 Hz; the 'spike' component is usually less pronounced as compared to the typical absence patterns) [Destexhe et al., 2001].

Computational models give better approximation to real spike-wave seizures when the thalamus is included in the model [Destexhe, 1998, 1999]. This thalamo-cortical model (Fig. 7.4) contains two thalamic cell types: thalamocortical (TC) and thalamic reticular (RE) cells, and two types of cortical neurons: pyramidal (PY) cells and interneurons (IN). This model shows that synchronous oscillations (sleep spindles and SWD) can be simulated by changing membrane currents activated by $GABA_B$ receptor-mediated responses (Fig. 7.4C). In the regime of sleep spindle generation (Fig. 7.4A), when the cortex is under strict control of fast $GABA_A$ receptor-mediated inhibition, cortical pyramidal cells and interneurons periodically discharge with single spikes, which is insufficient to activate the $GABA_B$ currents. A strong corticothalamic feedback can 'switch' thalamic circuits into a slow oscillatory mode around 3 Hz. This strong feedback is caused by an increased cortical excitability, and such a system can generate spike-and-wave oscillations (Fig. 7.4B), and a progressive transformation from spindle to SWD as cortical excitability is increased (Fig. 7.4D). Spike-wave activity of higher frequency (~ 10 Hz characteristic for rodent models) can also be simulated by the same model, based on a different balance between $GABA_A$ and $GABA_B$ receptors [Destexhe, 1999].

[1] Materials from Alain Destexhe (2007). Spike-and-wave oscillations. Scholarpedia, 2(2):1402 http://www.scholarpedia.org/article/Spike-and-wave_oscillations

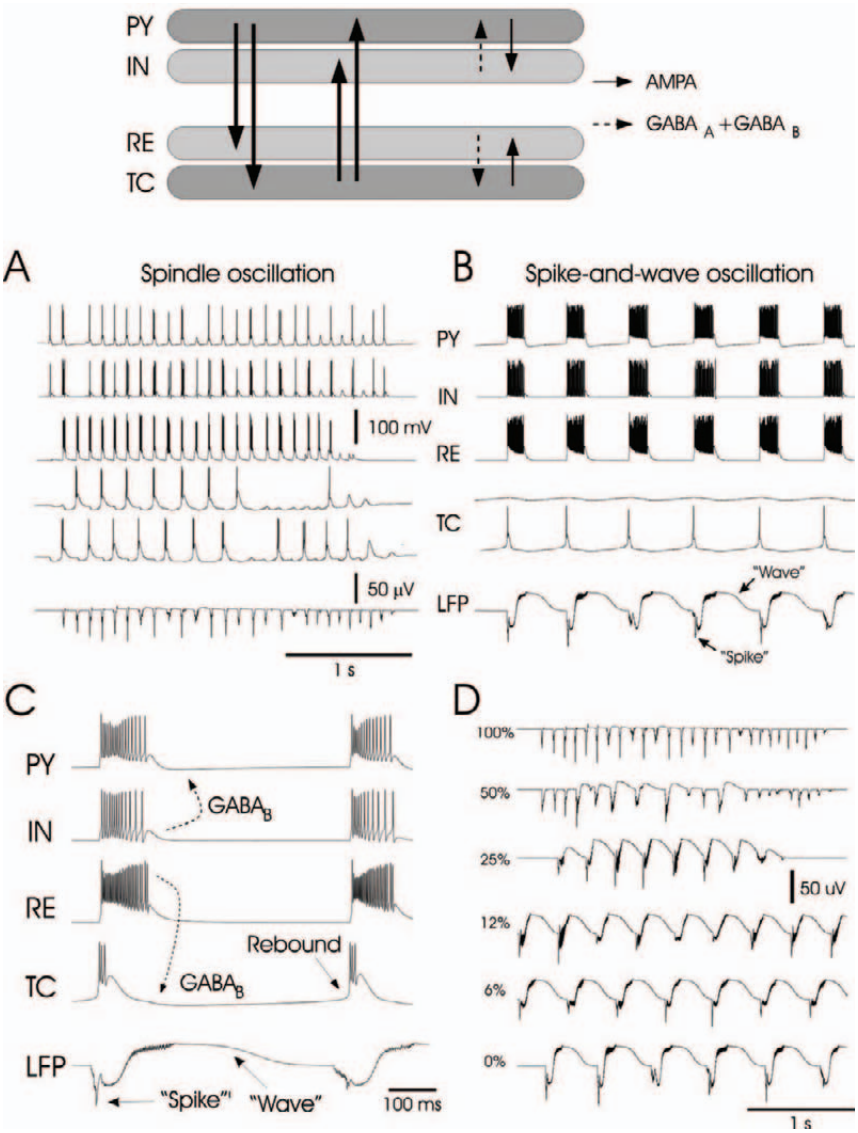

Figure 7.3[1]: The thalamocortical model of spike-wave seizures and sleep spindle oscillations [Destexhe, 1999] contains two types of thalamic cell: thalamocortical (TC) and thalamic reticular (RE) neurons and two types of cortical neurons: pyramidal (PY) cells and interneurons (IN). **(A)** Spindle oscillations around 10 Hz simulates local field potentials (LFP) displaying negative deflections. **(B)** After suppressing $GABA_A$-mediated inhibition selectively in cortex, the model exhibits slow (2-3 Hz) oscillations, which are more synchronized. These oscillations generate LFPs with spike-and-wave patterns. (**C**) Detail of a cycle of the oscillation showing the role of $GABA_B$-mediated inhibition and thalamic rebound. (**D**). Progressive transformation from spindle oscillations to spike-and-wave patterns for different percentages of cortical fast inhibition (100% = control as in A, 0% = total suppression of $GABA_A$ inhibition as in B; (modified from Destexhe, 1998).

In general terms, the thalamo-cortical model of Destexhe and cortical neuronal model presented in **Chapter 4.2** both disclose neuronal and membrane mechanisms, which underlie progressively increased synchronization of firing activity between various neurons and, finally, govern mechanisms by which the thalamo-cortical network stays in 'spindle mode' or in 'SWD mode'.

The above mentioned computational neuronal models simulate local field potentials and describe the phenomenology of SWD and sleep spindles. Spindles and SWD are manifestations of synchronization processes taking place in the thalamo-cortical circuit during low vigilance states. Unfortunately, this model is not capable to predict under what physiological conditions *in vivo* sleep spindles will be transformed into SWD.

Issue 9. Relationship between SWD I and anterior sleep spindles: their EEG structure disclosed with continuous wavelet transform and further implication

Essential differences between anterior sleep spindles and SWD I have been acknowledged in **Chapter 4.1 (Issue 7)** and are studied in more detail in **Chapter 4.3** by means of continuous wavelet transform. In **Chapter**

[1] © Alain Destexhe (2007), Scholarpedia, 2(2):1402. http://www.scholarpedia.org/article/Image:Cx-Th_SW_model2.jpg

4.3, statistical identities of anterior sleep spindles and SWD I are obtained with the aid of wavelet analysis in non-segmented full-length EEG data (hereafter we refer to anterior spindles and SWD I simply as 'spindles' and 'SWD'). We have first developed a wavelet-based algorithm for the automatic identification of spindle events and SWD in EEG. The best performance of automatic recognition system is achieved after selection of the optimal wavelet template and adjustment of the optimal amplitude (E_k) and frequency (F_S) parameters.

None of standard wavelet templates is able to provide a precise identification of all sleep spindles and SWD in one dataset and, in order to accomplish this task, we have applied different wavelet templates. It is found that different wavelets are necessary for the identification of SWD and spindles, from which we conclude that the EEG patterns of sleep spindles and SWD are not comparable. Wavelet analysis has revealed the following distinctions between sleep spindles and SWD:

- SWD I represent one family, but spindles comprise two families.
- Almost 100% of SWD I (but only 50-60% of spindles) are extracted using Morlet-based wavelet transform.
- Sleep spindles and SWD are detected by high wavelet energy in different frequencies F_{SWD} and F_{sp} SWD have between 30 and 50 Hz, sleep spindles – between 7-14 Hz.
- SWD I are identified in EEG with high probability using standard Morlet-wavelet, but sleep spindles can be identified using two types of customized adoptive 'spindle wavelets'.

Variability of sleep spindle waveforms

Sleep spindles represent a very heterogeneous group of oscillations and this causes difficulties with extraction and recognition of spindle events in the EEG. In all our rats, almost all sleep spindles (95.5%) are extracted with joint application of two different types of adaptive 'spindle wavelets'. 'Spindle wavelets' are built up using spindle prototypes in which the most typical (generic) features of sleep spindles are preserved (Fig. 4.17A). A frequency profile of these two spindle prototypes is crucially different (see Fourier spectrum of 'spindle wavelets' type 1 and type 2 in Fig. 4.17B).

- A majority of sleep spindles (85-90%) is selected after the CWT with 'spindle wavelet' type 1have a higher power in frequencies 6.25-16.6 Hz. These typical sleep spindles are referred to as 'type 1' and, based on their EEG features, are considered as normal spindle oscillations.
- A minority of sleep spindles (10-15%), which are missed by 'spindle wavelet' type 1, are captured with 'spindle wavelet 2' by having high power in frequencies 20-25 Hz. These 'type 2' sleep spindles show a deviant spindle-waveform and are considered as pro-epileptic events (somewhat transitory form between spindles and SWD).

'Type 1' sleep spindles in all experimental animals are selected using one common 'type 1' spindle wavelet, but 'type 2' sleep spindles are selected with individually chosen 'type 2' spindle wavelet. In all animals, 'type 2' spindle wavelet is characterized by a strong harmonic component (20-25 Hz). The same harmonic component is present in SWD and it is likely to be elicited by spikes; spikes could be also present in 'type 2' spindle sequence.

There is a parallel between the outcomes of power spectrum analysis of sleep spindles presented in **Chapter 3.1** and wavelet analysis in **Chapter 4.2,** although different EEG datasets are used for the analyses. Wavelet analysis **Chapter 4.2** is restricted to the frontal EEG, but it includes all automatically identified sleep spindles occurring at any stage of sleep, whereas in **Chapter 3.1** sleep spindles are manually selected during non-REM sleep. The average power spectrum of sleep spindles as measured in the frontal EEG (Fig. 2.2A, **Chapter 3.1)** fits well with the Fourier spectrum of 'type 1' spindle wavelet and it is completely different from the Fourier spectrum of 'type 2' spindle wavelet (Fig. 4.17B, **Chapter 4.2**). Anterior sleep spindles in **Chapter 3.1** display a peak in 11.4 Hz, have a short duration and a regular waveform. All this suggests that these sleep spindles are part of the large population of 'type 1' sleep spindles (peak ~12.2 Hz) characterized in **Chapter 4.2**.

It is striking that anterior sleep spindles (**Chapter 3.1**) show a remarkable delta component (~ 1 Hz), but a low delta component is found in 'type 1' spindle prototype ('type 1' spindle wavelet, **Chapter 4.2)**. It seems that delta is not typical for the common 'type 1' sleep spindles (**Chapter 4.2**), but local anterior sleep spindles, which were selected for the analysis in **Chapter 3.1**, may easily coincide with delta-wave activity. During deep slow-wave sleep, sleep spindles are often preceded by slow waves or overlap with delta[1] (Fig. 7.2A).

[1] Also in human sleep EEG, the slow waves associate frequently with sleep spindle rhythms (a combination of K-complex and sleep spindle) [Amzica and Steriade, 1999; 2002].

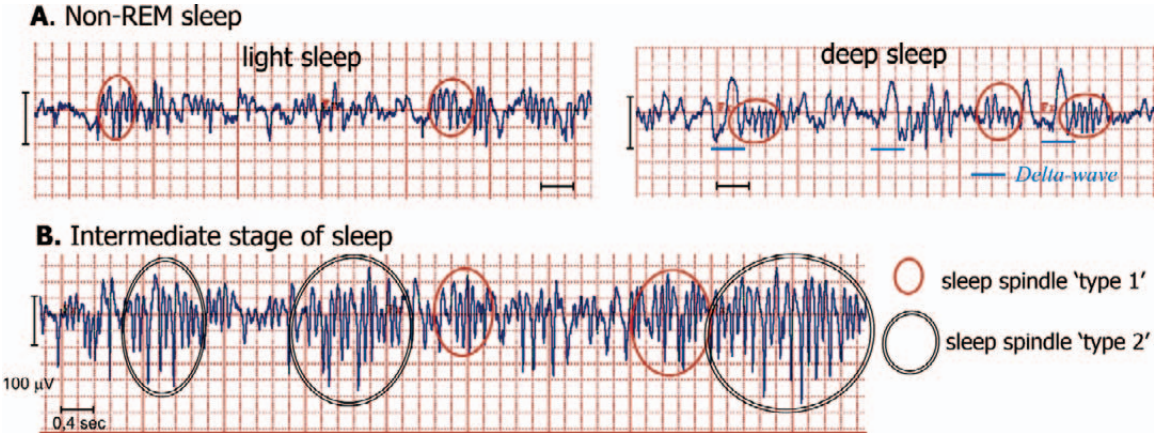

Figure 7.2. Sleep spindle activity (anterior spindles) as recorded in different stages of sleep at the frontal EEG (adult male WAG/Rij rat). In deep non-REM sleep, delta waves are often followed by sleep spindles. Non-REM sleep (**A**) is characterized by 'type 1' sleep spindles (**Chapter 4.3**). Intermediate stage of sleep (**B**) is distinguished by the presence of long high-voltage spindles with pro-epileptic properties ('type 2' spindles).

A pro-epileptic form of sleep spindle

Chapters 3.1 and **4.1** are focused on sleep spindles occurring during non-REM sleep. It is remarkable that the frequency of these spindles in our WAG/Rij rats (**Chapter 2**) is almost identical to that found in Wistar rats [Terrier and Gottesmann, 1978; Gandolfo et al., 1985] (Table 7.2). This may imply that the mechanisms of rhythmogenesis of sleep spindles is not impaired in genetic epileptic rats and, in this sense, sleep spindles are pretty normal[1].

It is well known that the amplitude of anterior spindles in rats gradually increases at the end of slow-wave sleep and reaches a maximum at the intermediate sleep stage [Terrier and Gottesmann, 1978; Gandolfo et al., 1985; Gandolfo et al., 1989; Gottesmann, 1996]. This is a short-lasting phase of sleep (~1% of the circadian cycle) that appear in transition from slow-wave to paradoxical sleep [Gottesmann, 1996] and is characterized by high-voltage spindle oscillations, co-existing with hippocampal theta rhythm. In non-epileptic Wistar rats, sleep spindles during intermediate sleep stage are of lower frequency and of higher duration in comparison to sleep spindles during slow-wave sleep (Table 7.2). In WAG/Rij rats, sleep spindles during intermediate sleep stage are three times longer than in Wistar rats (Table 7.2).

Table 7.2. Basic parameters of anterior sleep spindles as measured in different sleep stages in WAG/Rij and Wistar rats (mean ± SD)

	Rat strain	**State of vigilance**	**Frequency**, Hz	**Duration**, sec
This thesis				
Anterior spindles (Chapter 2)	WAG/Rij	Slow-wave non-REM sleep	11.1 ± 1.0	0.7 ± 0.1
SWD type I (Chapter 4.1)	- // -	low vigilance state	9.1 ± 0.5 [1]	**6.7 ± 0.6**
Anterior spindles in the literature				
Terrier and Gottesmann, 1978	Wistar	Slow-wave non-REM sleep	11.2 ± 0.4 [2]	1.5 ± 0.3 [2]
Gandolfo et al., 1985	- // -	Slow-wave non-REM sleep	11.2 ± 2.7	1.5 ± 0.2
Terrier and Gottesmann, 1978	- // -	Intermediate stage of sleep	9.7 ± 0.4 [2]	2.6 ± 0.3 [2]
Gandolfo et al., 1985	- // -	Intermediate stage of sleep	9.8 ± 2.5	2.6 ± 0.3
Gandolfo et al., 1989	- // -	Intermediate stage of sleep	9.7 ± 1.1	2.9 ± 1.0
Gandolfo et al., 1989	WAG/Rij	Intermediate stage of sleep	9.9 ± 0.8	**8.7 ± 3.0**

[1] – as measured in a period from 0.5 to 1.5 sec after the onset (average over SWDn, SWDα, SWDθ, SWDΔ.)
[2] ± SE

[1] The duration of sleep spindles in our subjects is twice shorter than in Wistar rats (0.7 sec vs 1.5 sec). This is likely to be accounted for by different criteria used for selecting borders between spindles. Sleep spindle are often in sequences, and two neighbouring spindles are defined as separate events unless period between them is 0.3 sec (roughly a half of spindle length)

It is sticking that, in WAG/Rij rats (in contrast to Wistar), the frequency and duration of intermediate stage sleep spindles [Gandolfo et al., 1989] is almost the same to what is found in SWD I (**Chapter 4.1)** (shaded rows in Table 7.2). It seems that, in addition to normal 'type 1' sleep spindles (those match 'spindle wavelet' type 1 in **Chapters 4.3**), WAG/Rij rats express a peculiar form of spindle activity, e.g., long sequences of high-amplitude sharp waves (sometimes with spiking), which might correspond to a pro-epileptic spindle 'type 2'. This peculiar spindle type can be encountered during intermediate as exaggerated and prolonged 'type 1' spindle oscillations resembling to SWD I (double circles in Fig. 7.2B).

SWD and sleep spindle oscillations are controlled by global mechanism of sleep-wakefulness cycle

In **Chapter 4.1** and **4.2** it is found that anterior sleep spindles and SWD I share the same thalamocortical circuitry, but that they essentially differ in respect to the intracortical and thalamocortical network associations. According to our analysis, there is no straightforward relationship between sleep spindles and SWD. The genetic WAG/Rij rat model does not demonstrate a direct transition 'sleep spindles → SWD' (**Chapter 3.3**, precursors of SWD I), in contrast to what have been convincingly demonstrated in the pharmacological feline penicillin model [i.e., Gloor, 1968; 1969; 1978; Kostopoulos, 2000]). However, it is well known that sleep spindles and spontaneous SWD (but not pharmacologically induced seizures) are intimately interconnected with manifestations of sleep: sleep spindles and SWD have similar distributions along different states of vigilance, e.g., both of them are promoted by transitory decreases of vigilance [e.g., van Luijtelaar and Coenen, 1988; Halász et al., 2002; Steriade, 2003; van Luijtelaar and Bikbaev, 2007].

We have failed to grasp a generic relationship between sleep spindles and SWD on the level of EEG, yet our data have convinced us that there is no 'mechanic' transformation of EEG patterns 'spindle wave' → 'spike-wave complex'. Our alternative hypothesis suggests that there is a functional relationship between SWD and sleep spindle oscillations on the level of mechanism controlling the vigilance state. In particular, besides abnormal neuronal functioning, absence epilepsy is characterized by an impairment of processes that govern transitional states between wakefulness and NREM sleep. These two factors, acting together, promote absence seizures in low vigilance states, but they do not prevent occurrence of normal spindle events.

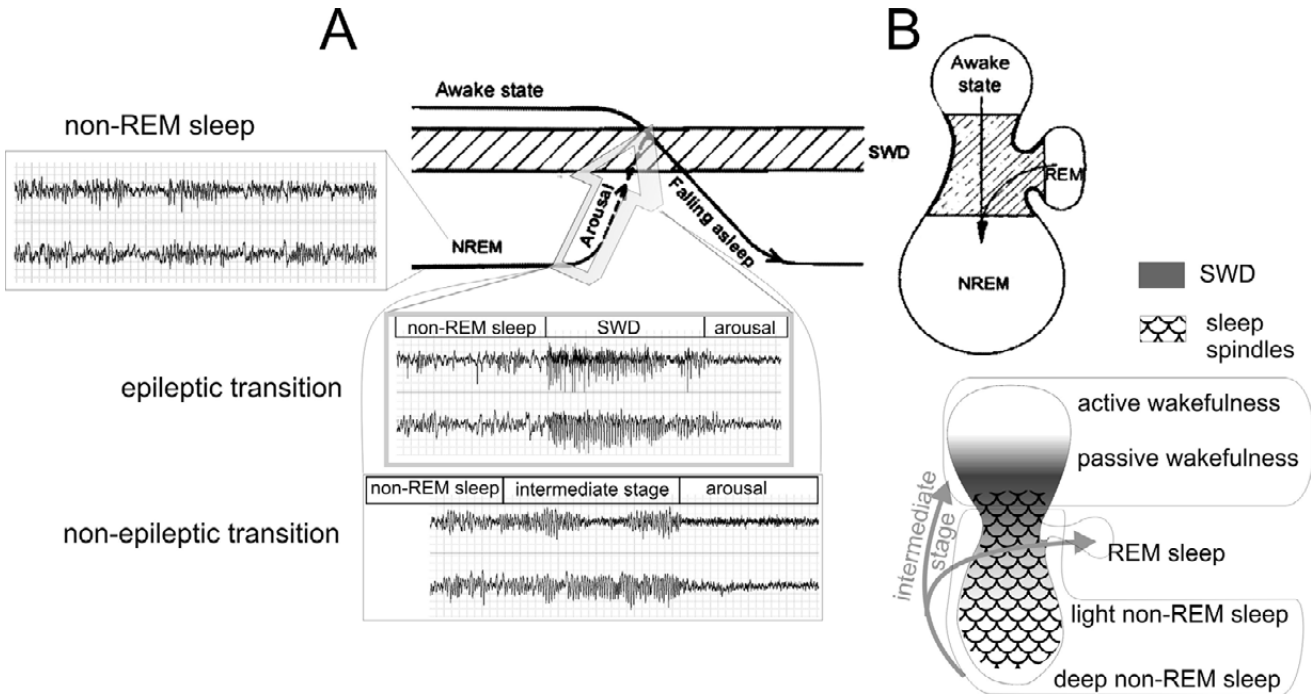

Figure 7.3. Schematic representation of changes in vigilance levels (adopted from Halász et al., 2002) indicating favorable states for the occurrence of SWD (darken and hatched areas) and sleep spindles (ribbed area). SWD are most numerous (hatched area) in transition period between wakefulness and sleep and especially on the intermediate stage of sleep. **A.** Intermediate stage of sleep in rats could be a 'critical zone of vigilance' when synchronizing thalamo-cortical system is unstable and a too strong synchronization at this stage could result in SWD (epileptic transition). **B**. Favorable states for the occurrence of SWD and sleep spindles. Distribution of SWD across vigilance state in WAG/Rij rats corresponds to human data (Halász et al., 2002); sleep spindles in our subjects are abundant during sleep, but SWD are concentrated during transient vigilance states between sleep and wakefulness.

The latter hypothesis is closely related to the concept of Halász (1991; 2002), suggesting that there is a 'critical zone of vigilance' (between non-REM sleep wakefulness and REM sleep) where SWD are more likely to occur (Fig. 7.3). Intermediate stage of sleep in rats could be a 'critical zone of vigilance', when the synchronizing thalamo-cortical system is unstable, therefore it is potentially 'dangerous' for the occurrence of absence seizures. This stage in WAG/Rij rats is known to last longer than in non-epileptic Wistar rats. In WAG/Rij rats, by the presence of SWD, intermediate sleep stage is less frequently be followed by paradoxical sleep and more frequently by slow-wave sleep and especially by arousals [Gandolfo et al., 1990]. In relation to that, other aspects of the architecture of sleep in epileptic rats is impaired: duration of sleep cycle and duration of REM sleep in WAG/Rij rats are substantially shortened as compared to non-epileptic ACI rats [van Luijtelaar and Bikbaev, 2007] while the amounts of total sleep and REM sleep are not different from other inbred rats [van Luijtelaar et al., 1988]. It seems that non-REM sleep in epileptic rats terminates often abruptly with SWD [Drinkenburg et al., 1991] and it is followed by arousal (Fig. 7.3A), therefore, epileptic rats show a deficiency of REM-sleep rats as compared to control subjects. In non-epileptic rats, termination of 'non-REM sleep' is smoother and it is followed by a short period of intermediate sleep and REM sleep (arousals are less frequent).

Altogether, neuronal mechanisms controlling micro-dynamics of sleep in WAG/Rij rats are impaired. This can disrupt coordination within oscillatory neuronal assembles, resulting in disturbances of rhythmic activity and occurrence of abnormal EEG patterns, e.g., hypersynchronous oscillations such as pro-epileptic spindle oscillations ('type 2' spindles) and SWD.

NETWORK MECHANISMS OF SPIKE-WAVE DISCHARGES in WAG/Rij rats

Issue 10. Cortico-cortical and cortico-thalamic network synchronization at the onset of SWD (analysis of EEG coherence)

Chapter 3.3 (time-frequency analysis of SWD-precursors) demonstrates that SWD in WAG/Rij rats are preceded by an increase of theta activity in the frontal EEG; this is similar what happens in GAERS, yet in GAERS the theta component is shaped into 5–9 Hz rhythmic oscillations [Pinault et al., 2001]. Apparently, 5–9 Hz rhythm can also be encountered in non-epileptic rats strains [Pinault, 2001]. Broadly speaking, 5–9 Hz oscillations in rodents are physiological and they are 'normal' in the sense that they are not related to epilepsy. A precondition (for example, a hyperexcitable cortex and an increased synchrony in the thalamo-cortical network) must be present in an epileptic brain for the 5–9 Hz oscillations to be followed by SWD.

In order to address this problem (**Chapter 5.1),** we have elucidated epileptic synchronization processes in cortico-thalamo-cortical network during early stage of absence seizures. For that purpose, linear associations are measured between cortical regions (intracortical coherence), reticular and relay thalamic nuclei (intrathalamic coherence) and between the cortex and the thalamus (thalamo-cortical coherence) at the onset of SWD type I. The major results are as following:

- In all investigated EEG pairs, the onset of SWD is associated with an increased coherence in frequencies 5 - 60 Hz with two maxima around 10 and 20 Hz, corresponding to the mean frequency of SWD (8-11.5 Hz) and harmonic frequency 16-21.5 Hz.
- The frequency profile of coherence is different in different intracortical networks; based on the further analysis, we have divided them into local, global and transhemispheric networks.
- The presumable source of SWD in the somatosensory cortex and its closest surroundings form a minimal local circuit. This circuit displays a consistent shift of network synchrony from delta to alpha/beta frequencies, which are considered as primary network processes that govern the initiation of SWD.
- Transhemispheric pairs are characterized by a large increase of coherence and an additional peak in ~16 Hz. This additional 16 Hz peak of coherence (in the middle between two main frequencies, 10 Hz and 20 Hz) may be brought about by bilateral projections via *callosal* fibers (transhemispheric synchronization). This indicates a crucial involvement of the *corpus callosum* in the pathophysiology of absence seizures.
- Intrathalamic coherence shows peculiar changes with the onset of SWD, e.g., a remarkable antagonism between low- and high-frequency coherence, in which desynchronization in gamma frequencies associates with increased synchrony in 8-11.5 Hz.

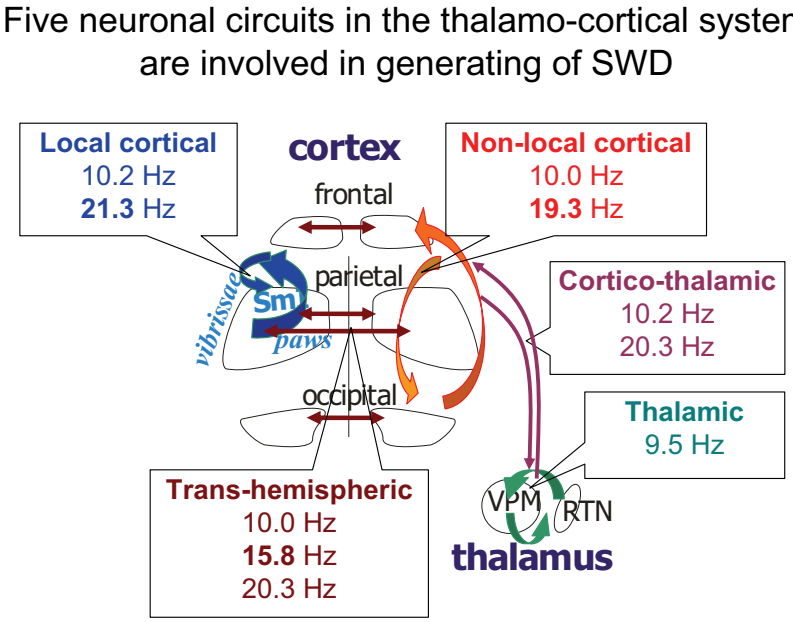

Figure 7.4. Schematic interpretation of EEG coherence analysis (based on the results of **Chapter 5.1**).

Absence seizures result from a very complex synchronization between different parts of thalamo-cortical network. Thalamo-cortical system comprises five interacting networks (resonant circuits). Each circuit is characterized by peculiar pattern of network synchronization (Fig. 7.3). Cortico-cortical networks are responsible for the initiation (local cortical networks with the highest coherence, maximum in 21.3 Hz), unilateral propagation (non-local cortical networks, in which coherence is medium, maximum in 19.3 Hz), bilateral spreading (trans-hemispheric networks, in which is high with an additional maximum in 15.8 Hz). Thalamus sustains the seizure rhythm 9.5 Hz and the cortical part of the oscillatory network keeps resonance with the thalamic part throughout cortico-thalamic pathways.

Issue 11. The local and global role of the neocortex in the development of SWD I

A global role of the cortex in absence epilepsy, as suggested by the 'cortico-reticular' theory [Gloor, 1969; Kostopoulos, 2000], has been confirmed in the feline penicillin model [Avoli and Gloor, 1981; Gloor et al., 1990] and in genetic rodent models, GAERS and WAG/Rij rats [Vergnes and Marescaux, 1992; Meeren, 2002]). **Chapter 6** reconsiders a global role of the neocortex in absence epilepsy and focuses in focal aspects of this disease. Some of our findings are consistent with the 'cortical' theory and confirms a secondary role of the thalamus in absence seizures [Niedermeyer, 1996].

In **Chapter 6.1**, it is shown that the fast transient events (e.g., EEG ripples and double spiking) are localized in the somatosensory cortex and its closest neighborhood at the onset of SWD I. These fast EEG transients are considered as manifestations of epileptogenic processes in this anterior cortical region [Sitnikova and van Luijtelaar, 2007]. Several neuronal mechanisms underlie the impairment of functions of cortical neurons and are considered as a physiological trigger of SWD I in WAG/Rij rats. Among them is a deficit of the somato-dendritic hyperpolarization-activated cation current (I_h). It is known that deficits of I_h-mediated functions in cortical cells contribute to the onset and development of SWD I [Straus et al., 2004]. An impaired function of dendritic I_h-channels (HCN1) in layer 5 pyramidal neurons in WAG/Rij rats is suggested to provide a somato-dendritic mechanism for increasing the synchronization of cortical output, and therefore play an important role in the generation of SWD I [Kole et al., 2007]. In WAG/Rij rats, neurons in the neocortical deep layers are known to have an increased synaptic excitability (as compared to control rats) mediated by NMDA receptors [D'Antuono et al., 2006]. It is likely that I_h currents might be involved in the physiological trigger mechanisms of SWD. I_h currents might be responsible for the elevation of *delta* (1-4 Hz) activity that prerequisite the onset of SWD (**Chapter 3.3**). In fact, 95% preSWD express high power in delta band, but elevation of theta (5-9 Hz) is detected in a lower percentage of preSWD epochs, i.e., in 73% of cases.

In **Chapter 6.2**, it is demonstrated that local inactivation of the primary epileptic focus area (perioral area of somatosensory cortex) with microinjections of lidocaine prevents the occurrence of SWD I [Sitnikova and van Luijtelaar, 2001]. It is believed that the 'epileptic' cortical zone is capable of initiating SWD I because of genetically predetermined impairment of membrane properties of neurons [D'Antuono et al., 2006] or because of

impairment of fine structure of neuronal cells [Karpova et al., 2005]. Macro- and microscopic investigations of morphological changes in absence epilepsy are scare. It is believed that typical absence epilepsy is a purely *functional* disorder that has no structural lesion of any kind [Berkovic et al., 1987; Niedermeyer, 1996]. As far as the role of the neocortex in absence epilepsy is concerned, it must be stressed that rats with absence epilepsy (WAG/Rij) display serious modification of cellular microstructure in the focal cortical region [Karpova et al., 2005]. Absence epilepsy is not merely *functional*, but also a micro-*anatomical* cortical disorder.

Morphological correlates of cortical absence epilepsy: cytoarchitectural disorder in the somatosensory cortex and its closest neighborhood

In animal models of absence epilepsy, the cellular structure of cortical tissue is almost entirely escaped to consideration. In a pioneering study, Karpova and co-workers (2005) have compared the cytoarchitecture of pyramidal cells in superficial cortical layers (I–III) in the somatosensory and motor areas in WAG/Rij and ACI rats. The authors examined two zones: (1) an 'epileptic zone' including peri-oral and vibrissal projections in the SmI and (2) in a 'non-epileptic zone' - the area of hind limb projections in the SmI and the motor area in the frontal cortex.

In both rat strains, neurons in the 'epileptic zone' are characterized by an increased branching (as revealed by the three parameters: the number of free terminals, the number of branching points and the number of dendritic segments). This differences in branching parameters can be accounted for the regional differences (and functional) differences between the investigated zones without regard to epileptic processes.

It is important that atypical oriented pyramidal neurons are present in the 'epileptic zone' in WAG/Rij rats. Apical dendrites of these cells are obliquely oriented, often split in two branches; cellular bodies are localized outside the layer boundaries. Unfortunately, the authors do not explain this phenomenon; yet disorientation and atypical morphology of pyramidal cells may correlate with the epileptic activity and can be accounted for at least two factors:

- *An early disorder of migration*. In the rat's cortex atypically oriented pyramidal neurons appear in all cortical layers during the last prenatal week (gestational days 15-21) [Miller, 1998]. Orientation of cell bodies and apical dendrites do not change after the end of migration. As known, migration and orientation of pyramidal cells are guided by glial cells and impairment of neuro-glial interactions (probably, genetically determined) may result to the disorientation in a population of pyramidal cells.
- *A disorder of maturation*. Apical dendrites of pyramidal neurons ascend to the plexiform layer, where they are densely innervated by afferents of neuromodulatory systems (noradrenaline, serotonine etc). These contacts with neuromodulatory afferents are necessary for the normal maturation of neuronal cells [Raevsky, 1995] and presumable impairment of intracortical neuromodulatory mechanisms in WAG/Rij rats may encourage changes in the configuration of apical dendrites in superficial pyramids. Atypical cellular forms may either result from an impairment of axo-dendritic interactions in the plexiform layer or by deficit of neuromodulatory afferents in the plexiform layer.

Another important finding is that pyramid cells in the 'epileptic zone' in WAG/Rij rats differ from analogous cells in ACI: they have longer dendritic segments and a larger radius of dendritic area. We have interpreted these findings in relation to the fact that these animals have epilepsy that is triggered in this zone. Longer dendritic segments and larger radius of dendritic area may increase the area of synaptic contacts, increase excitability and facilitate spreading of seizure across this 'epileptic zone'.

Altogether, an impairment of structure of pyramidal neurons in superficial layers in WAG/Rij rats may be caused by a deficiency of neuromodulatory afferents in the plexiform layer and by disorders during early development. This alters a normal growth of dendrites and branching of dendritic trees, and causes a misdirection of apical dendrites in pyramidal neurons. The age-dependent increase in number of affected animals, and in number and duration of SWD is in favor of a developmental disturbance [Coenen and van Luijtelaar, 1987].

Dysfunction of somatosensory cortex: epileptogenic processes in the close neighborhood of the somatosensory cortex (as manifested by fast EEG components during initial state of spike-wave seizures)

The crucial role of the cortex in absence epilepsy is emphasized by a 'cortico-reticular' theory [Gloor, 1969; Kostopoulos, 2000] and by a 'cortical focus' theory [Meeren et al., 2002; Meeren et al., 2005]. Gloor's theory, which is grounded on experimental model of generalized seizures induced by penicillin injections, postulates that the transformation of thalamic spindle activity into SWD takes place in the cortex due to a diffuse increase of neuronal excitability. Meeren's theory, which is developed in genetic rats with spontaneous seizures, suggests that a local area in the somatosensory cortex triggers SWD. Our experimental data in **Chapter 3.3** (precursor activity of SWD), **4.1** and **4.3** (time-frequency EEG analysis of SWD and sleep spindles) contradict to Gloor's theory by

showing that spindle activity does not constitute a source of SWD. In contrast, findings in **Chapter 6** support Meeren's theory. In particular, **Chapter 6.2** shows that deactivation of the somatosensory cortex reduces the incidence of SWD I.

Chapter 5.1 demonstrates complex changes of intracortical, thalamo-cortical and intrathalamic associations in the thalamo-cortical network at the onset of absence seizures. Investigation of local field potentials during SWD I indicates that the fast cortical components (e.g. EEG ripples and double spiking) appear in the frontal and parietal (SmI) cortex at the initial stage of SWD I. A combination of the above mentioned facts suggests that the newly observed pro-epileptic fast transients are essential elements of SWD. It is striking that frontal and parietal cortical areas display the most broad-band increase of coherence (5-60 Hz, including gamma frequencies) at the onset of absence seizures. Therefore, it seems likely that fast EEG transients are produced by the local cortical network (e.g., somatosensory and frontal areas). In all, this leads us to the following assumptions about the nature of the fast transients in EEG: (i) they represent an impaired functioning of local cortical networks (but the thalamus is scarcely involved); (ii) they are implicated in the initiation of seizure activity, yet the intact thalamus is necessary for the further progress of seizure activity.

Our principal conclusion is that SWD I are initiated in the somatosensory cortex [Meeren et al., 2002; Sitnikova and van Luijtelaar, 2001; 2007, **Chapter 6.1** and **6.2**] and they are strongly involve the somatosensory part of the thalamo-cortical system [Sitnikova and van Luijtelaar, 2006]. In epileptic rats, interactions within somatosensory thalamo-cortical system are impaired (**Chapter 5.1)** and this may imply that absence epilepsy correlates with an impairment of basic sensory mechanisms that control processing of somatosensory information. Indeed, it is found that sensory processing is altered during SWD in WAG/Rij rats [Meeren et al., 1998; Inoue et al., 1992]. Human patients become irresponsive to external stimuli during absence seizures. It has been assumed [Yamauchi, 1998] that in humans responsiveness is mostly altered when the wave-component in spike-wave discharge reaches its maximum (the wave in SWD represents neuronal inhibition), thus when a very large percentage of the cortex is in the inhibitory phase. In all, severe impairments of functional abilities of cortical cells during absence seizures likely results in disturbances of sensory perception, causing an abrupt impairment of consciousness which is associated with absence epilepsy.

Issue 12. Interactions between thalamus and cortex during SWD (type I) examined with traditional methods (cross-correlation, grand average EEG, coherence) and with a novel approach (Granger causality for causal relations)

Thalamo-cortical relationships has been examined during the initial stage and in fully grown SWD I using several traditional EEG measures.

- Cross-correlation analysis between cortex and thalamus [1] (**Chapter 4.1**, Fig.4.9) demonstrates negative (out-of-phase) correlations between the frontal cortex and the VPM with a time delay 5 msec (frontal cortex leads). The amplitude of the negative peak of the cross-correlation [$C_{xy}(\tau) \sim -0.42$] function during SWD is two times higher than during sleep spindles, suggesting that during SWD I thalamo-cortical coupling is twice as strong as during sleep spindles.
- Grand average EEG analyses demonstrates a specific temporal relationship between Weir's components in thalamic and cortical counterparts of SWD I (**Chapter 3.1**, see also 'issue 11' and Fig.7.2). In particular,
  (i) High-voltage positive transient (PT) in the thalamus lags behind the 'Spike 2' in the frontal cortex (7-9 msec), suggesting that PT appears in the thalamus as back-propagation of cortical 'Spike 2'.
  (ii) Low-voltage 'Spike 1' in the relay thalamic nucleus (VPM) seems to be locked in phase with PT_{early} in the frontal cortex.
- Fourier-based coherence analysis is focused on the changes in the strength and frequency profile of thalamo-cortical functional interactions at the onset of SWD (**Chapter 5.1**). It is found that functional interactions between the frontal cortex and the thalamus (both the VPM and the RTN) are profoundly increased and the strongest increase appeared in 8-11.5 Hz Occipito-thalamic interactions are also increased, yet this increase is not as high as obtained in fronto-thalamic pairs.

Chapter 5.2 introduces a new concept for the analysis of network associations. It describes thalamo-cortical *causal relations* in terms of Granger causality [Sitnikova et al., 2008]. Granger causality uses the knowledge about the immediate past of one signal in order to improve prediction of another signal. In our computations, we use linear model of Granger causality in order to establish bidirectional coupling strength between cortex and thalamus

[1] The cross-correlation function is a measure of the linear correlation between two functions regarding their time delay. This time delay may reflect a causal relationship between the signals [e.g., Quian Quiroga et al., 2000; Pereda et al., 2005].

and assess directionality of information flow for both directions. Unfortunately, the linear estimation of Granger coupling appeared insufficient for predicting absence epilepsy (non-linear model Granger causality is needed in order to detect early changes in causal network relationship and, therefore, to prerequisite the onset of SWD I), and the dynamics of thalamo-cortical network associations that govern transition 'normal state ↔ paroxysmal state ↔ normal state'. The following achievements are made:

- Linear Granger causalities do not change before the onset of SWD I: coupling strength is constant and very low, yet associations *thalamus→cortex* are stronger than vice versa.
- The onset of SWD I is characterized by a rapid increase of coupling strength in both directions.
- The strength of *thalamus→cortex* coupling remains continuously high during the seizures and does not return to the initial level even after cessation of SWD.
- The strength of *cortex→thalamus* coupling gradually diminishes shortly after the onset of SWD I and returns to the pre-SWD level when SWD I is stopped.

It is hypothesized that propagation and maintenance of seizure activity may be facilitated under the strong and sustained influence of *thalamus→cortex*, while rapid reduction of *cortex→thalamus* strength may promote the cessation of SWD I.

In general, Granger causality appears to be an effective way to gain more insight into the dynamics of the thalamo-cortical neuronal network mechanism underlying dynamical properties of SWD I. Results of this study may shed more light on predictability of SWD I and may explain the classic clinical observation that absence seizures in humans occur without warning. A computational model of thalamo-cortical neuronal network [Sejnowski et al., 2004] explains the unpredictability of SWD simply by the fact that fluctuations of control parameters (synaptic and cellular properties of thalamic and cortical cells) are unpredictable by definition. **Chapter 5.2** extends our knowledge on dynamic properties of SWD I by showing that there are certain dynamics and strong directionality of information transfer between thalamic and cortical neurons before, during and after SWD I. In particular, a strong feedforward (*thalamus→cortex*) transfer may be necessary for maintenance of SWD, in opposite, an increase of the feedback (*cortex→thalamus*) transfer may be responsible for seizure cessation. The linear estimation of Granger causality is suitable for studying thalamo-cortical mechanisms involved in maintenance and stopping of SWD, yet it is not sufficient for predicting episodes with absence epilepsy. Application of non-linear Granger estimations might help to solve this problem.

Issue 13. Methodological considerations and technical questions

In this thesis we have employed various techniques of time-frequency analysis in order to assess electrographic properties of normal (sleep spindles) and abnormal (SWD) EEG oscillations and local changes of electrical activity in thalamo-cortical circuit that may underlie transformation 'sleep spindles → SWD'. Time-frequency signal analysis is performed using traditional fast Fourier transform (frequency domain measure) and continuous wavelet analysis (time+frequency domain measure). The strength of associations between EEG signals is measured with the aid of Fourier coherence and cross-spectrum (in frequency domain). In addition to that, we employed linear Granger causality in order to assess bidirectional information transfer between frontal cortex and the thalamus before, during and after SWD I. Below we will describe advantages and limitation of the above mentioned methods.

Fourier analysis

In **Chapters 2.1**, **3.2**, **3.3** and **4.1** Fast Fourier transform (FFT) is applied in order to elucidate the spectral content of sleep spindles and SWD. The Fourier transform decomposes a signal into sine waves of different frequencies, which sum up to the original waveform. The amplitudes of sine functions of various frequencies throughout the entire duration of the signal provide spectral power of these identities. FFT has the following limitations:

- The FFT is only suitable for stationary processes (i.e. in which statistical properties remain constant). To a certain approximation, relatively long intervals (lasting from several seconds to several minutes) of uniform and stable EEG activity may represent stationary processes [Freeman, 1975]. SWD have relatively long duration (from one to tens of seconds) and stereotypic morphology, they can approximately considered as stationary (or quasi-stationary) processes, but short-lasting sleep spindles obviously represent non-stationary EEG processes.
- Frequency resolution of the FFT is limited by two factors:

  (i) The size of time window, which determines the slowest detectable wave; short epochs low frequencies);

  (ii) The sample rate: the highest frequency extracted with the FFT is twice lower than the sampling frequency. In addition to that, computation are faster if sample rate is n^2, where n is an integer number.

In the present thesis we use the same sample rate (usually, 1024 per second) and achieved the same frequency resolution of SWD and sleep spindles by selecting periods with the equal length, 1 sec (1 Hz is the lowest captured frequency).

- Time-domain information is lost after FFT, therefore, transient or location features of EEG are omitted.

Fourier analysis versus Wavelet transform

An obstacle in interpreting the outcomes Fourier analysis is that it works under assumption that a signal (EEG) has a sinusoidal waveform. This is true for some neural oscillations, such as sleep spindles, but for SWD I have clearly non-sinusoidal waveform. SWD I consist of several repetitive sharp elements (Weir's elements, **Chapter 3.1**) and, therefore, their power spectrum displays additional harmonic components (at double frequency) which are likely to be elicited by the presence of high-amplitude sharp repetitive spikes. Noteworthy, the same harmonic components are found in Fourier spectrum of 'spindle wavelet type 2' that characterized 10-15% of anterior sleep spindles [**Chapter 5.2**].

In spite of the limitations, Fourier analysis appears to be convenient for comparing frequency profile of spontaneous sleep spindles and SWD (**Chapter 2, 3.3, 4.1**). In addition to that, FFT power spectrum analysis and analysis of power content in frequency bands allows us to assess changes in EEG properties of epileptic activity after pharmacological treatments, such as systemic injections of clonidine [**Chapter 3.2**; Sitnikova and van Luijtelaar, 2005] and local microinjections of 2% lidocaine [**Chapter 6.2**; Sitnikova and van Luijtelaar, 2004].

SWD and sleep spindles are dynamic oscillations. This means that their frequency changes over time. FFT does not provide information regarding the dynamic changes of spectral components (it is a frequency-domain measure) and, therefore, it is not suitable for the analysis of the signal waveform (time-domain information is lost). With wavelet decomposition, EEG signal can be represented in two-dimensional time–frequency domain, therefore, signal power as a function of time and frequency simultaneously. Wavelet transform employs wave-like scalable function (wavelet basis), that is well localized in both time and frequency [Kaiser, 1994; Koronovskii and Hramov, 2003]. In **Chapter 4.3,** a complex Morlet wavelet is chosen amongst others wavelet basis as optimal function for obtaining desired frequency resolution. In a family of complex Morlet wavelets, the best time–frequency representation of EEG signal is achieved when function parameter (ω_0) is equal to 2π.

A problem of stationarity in the Fourier analysis

The term of stationarity can be applied to a random process whose statistical characteristics do not change with time. The lack of stationarity in EEG causes a major problem in the implementation of mathematical methods for the analysis of EEG data [Kaplan, 1998; Dikanev et al., 2005], for the interpretation of results and it also embarrasses automatic detection EEG events [Mäkinen et al., 2005]. There are some periods in EEG which can approximate to a stationary behavior. In appropriately short time intervals during SWD, statistical properties change slowly enough for the stationary pattern to be established. Sleep spindles are very non-stationary oscillations; their frequency and amplitude considerably vary over the time. As known, Fourier representation of stationary (neuronal) processes give more sharp and high amplitude spectral peaks as compared to non-stationary processes [Mäkinen et al., 2005]. There is more stationary in the EEG during SWD than during sleep spindles, therefore, SWD might reveal sharper and high amplitude spectral peak ~10 Hz.

A high level of stationary of SWD may be accounted for the presence of the regular spike component. However, the spike trains can represent the second-order stationary [Jarvis and Mitra, 2001]. The stationary pattern of spike-wave complexes in human patients has been associated with spatial consistency of activation among seizures [McKeown et al., 1999].

Estimation of coupling strength between two signals

Methods of quantification of functional coupling and synchronization EEG has long been used to assess functional interaction between brain regions. In the present thesis we have used convenient tools for measuring coupling strength between two EEG signals, the cross-correlation function (**Chapter 4.1**), the cross-spectrum (**Chapter 2**) and the Fourier coherence (**Chapters 3.3** and **5.1**).

Cross-spectrum and coherence estimations are linear techniques, which are easily applicable to EEG data and are easy to be interpreted in mathematical terms (and with a certain approximations, in physiological terms [Le Van Quyen and Bragin, 2007; Pereda et al., 2005]). However, they are appropriate only for the analysis of coupling between two signals, yet these pair wise estimations cannot distinguish between 'direct' and 'indirect' coupling. In the cross-correlation function, the time lag indicates directionality of coupling between two signals. Very promising results are obtained by Meeren et al. (2002), who used a nonlinear association coefficient (the simplest nonlinear statistical characteristics based on a generalization of cross-correlation function rather than on

dynamical systems theory) for investigating SWD in WAG/Rij rats. With that method they have revealed a cortical focus of these discharges that have never been detected with traditional methods.

A directionality of coupling between thalamic and cortical neurons is investigated in **Chapter 5.2**. In this Chapter we have estimated thalamo-cortical causal relations with the aid of Granger causality and have shown strong differences of information transfer in direction of '*thalamus→cortex*' as compared to '*cortex→thalamus*'. The first direction can facilitate propagation of SWD and the second is responsible for seizure cessation. Generally speaking, Granger causality seems to be an effective and promising tool for studying neuronal network structure and network dynamics. It can find many applications in neuroscience, for example, in psychophysiology for studying the architecture of directed couplings between brain areas during tasks, or in clinical EEG research for investigating the spreading of epileptic activity from a focal zone to other areas.

CONCLUSIONS

The current thesis presents results of electroencephalographic examination of physiologic sleep spindle oscillations and spike-wave discharges (SWD) as carried out at the cortical and thalamic levels in a genetic WAG/Rij rat model of absence epilepsy. SWD are well known obligatory electroencephalographic manifestations of absence epilepsy [Panayiotopoulos, 2001] and two types of spontaneous SWD are distinguished in WAG/Rij rats. The present thesis is focused onto electroencephalographic features of SWD and sleep spindles, thalamo-cortical network mechanisms and functional relationship between these phenomena. EEG data are obtained in freely moving rats, while multi-channel recordings are made throughout the cortex, from the ventroposteromedial thalamic nucleus (VPM, somatosensory part of the thalamus) as well as from the reticular thalamic nuclei (RTN).

Sleep spindles

Chapter 2 describes sleep spindles as recorded in EEG during natural sleep. The major conclusion is that sleep spindles independently appear in the frontal and occipital EEG channels, suggesting that WAG/Rij rats, similar to humans, exhibit two local 'area-specific' types of sleep spindles.

EEG features of anterior and posterior sleep spindles are compared in **Chapter 2.1**. It is shown that, compared to posterior spindles, anterior spindles appear more frequently, have a lower frequency (~10 Hz versus ~ 11 Hz) and a longer duration. EEG epochs immediately preceding anterior and posterior spindles (pre-spindle activity) do not reveal significant differences, neither in EEG waveform nor in EEG power spectra.

In **Chapter 4.3**, 85-90% of anterior sleep spindles are identified by means of common 'spindle wavelet 1' (so-called 'type 1' sleep spindles) and, based on their EEG features, 'type 1' sleep spindles are considered as normal physiological spindle oscillations. The rest (10-15%) of sleep spindles ('type 2') are captured by 'spindle wavelet 2' ('type 2' sleep spindles have a deviant spindle-form and are missed by 'spindle wavelet 1').

The role of the thalamus in anterior and posterior sleep spindles is elaborated in **Chapter 2.1.** Both spindle types are poorly pronounced in the VPM and the RTN. Differences in total power between anterior and posterior sleep spindles, which are determined in the cortex, are longer present in the thalamus. These data, however, do not exclude that the thalamus cooperates with the cortex during sleep spindles.

Chapter 2.1 describes dynamic changes in power spectrum as measured in the cortex and in the thalamus during transition from pre-spindle EEG to anterior and to posterior spindle types. In anterior spindles, an increase in $alpha_{high}$ (10.75-12 Hz) is found locally in the frontal cortex, whereas an enhancement of $alpha_{low}$ (9-10.5 Hz) is detected in the frontal cortex and in the VPM. Occurrence of anterior spindles is accompanied with elevation of *delta* in the RTN and $alpha_{low}$+*delta*+*theta* in the VPM. At the onset of posterior spindles, thalamic activity does not change. Altogether, occurrence of anterior and posterior spindles is associated with different frequency modulation of EEG, suggesting that thalamic and cortical neurons stay in different oscillatory modes.

The thalamo-cortical network mechanism of sleep spindles is studied in **Chapter 2.2** by means of cross-spectrum and cross-correlations analyses. It is found that anterior sleep spindles reveal strong a coupling in the network [frontal cortex] - [VPM] - [RTN], with peak frequencies in 2-3 Hz, 8-10 Hz and 11-12 Hz. The presence of 11-12 Hz associations 'VPM-RTN' suggests that the generation of spindle rhythm requires strong coupling between these structures. Posterior sleep spindles are characterized by weak associations between [occipital cortex] - [VPM] – [RTN], moreover, [RTN] - [occipital cortex] are centered in non-spindle frequencies (7.5-8 Hz), suggesting that the RTN is not directly involved in the sustaining and propagating of posterior sleep spindles.

The analysis of cross-correlations between the cortex and thalamus (two parts of the VPM: the ventral and dorsomedial poles, vVPM and dmVPM correspondingly) are differently involved in two spindle types. In anterior sleep spindles correlations are detected in the network [RTN] – [vVPM+dmVPM] – [frontal cortex]; in posterior spindles correlations - [RTN] – [dmVPM] – [occipital+frontal cortices].

A notable difference between the dmVPM and vVPM in respect to their anatomic connections and physiological functions may underlie the existence of different oscillatory neuronal networks that generate different types of local spindle activity. In general, cortical spindle oscillations are not merely a fingerprint of the electrical activity in the thalamus.

SWD

Two types of spike-wave paroxysms, e.g., the generalized SWD I (the true absence epileptic discharges) and the local occipital SWD II (which have no clinical correlate) are examined in **Chapter 3**.

Archetypal patterns of SWD I and SWD II in WAG/Rij rats are rendered by computing grand average EEG waveforms as recorded in the cortex and the thalamus (**Chapter 3.1**). It is demonstrated that SWD I and SWD II are multi-phasic negative-positive-negative potentials, comprising a set of epileptiform elements, analogous to the components of spike-wave complex identified in human EEG [Weir, 1965], such as Spike 1 (Sp1), Spike 2 (Sp2), positive transient (PT) and Wave. SWD I is expressed in the frontal EEG as a sequence of '(PT_{early}) – Sp2 – PT_{late}'; in the occipital EEG - '(Sp1) – PT – Wave'; in the VPM - 'Sp1 – PT – Wave' and in the RTN 'PT – Wave'. Altogether this suggests that EEG pattern of SWD I is area-specific. In the frontal cortex, SWD I show a disproportionately large 'Sp2' this makes the EEG pattern of frontal SWD I asymmetric. Asymmetry in frontal SWD I increase as seizure progresses. In the thalamus, EEG pattern of SWD I is more symmetrical, as compared to the cortical counterparts. A peculiar element of SWD I, 'Sp1', is detected in the VPM. 'Sp1'appeared simultaneously with the frontal 'PT_{early}' and it leads the frontal 'Sp2' with 12 msec time delay. Probably, 'Sp1' in the thalamus reflects back-propagation of cortical excitation.

In **Chapter 3.1**, it is found that the following synaptic processes may underlie epileptiform elements in SWD (type I): the *spike* component ('Spike 2') is the excitatory response of PCs via AMPA-ergic input from the thalamus. The *positive transient* is a manifestation of AMPA-ergic mutual excitation of pyramidal cells. The *wave* component reflects the strength of GABA-ergic synaptic interactions between pyramidal cells and interneurons (feed-forward inhibition).

The lack of congruency between cortical and thalamic counterparts of SWD I suggests that the propagation of seizure throughout the thalamo-cortical circuit is not merely a transduction of electrical activity, but that each part of the circuit is actively involved in maintaining SWD I.

SWD II is localized in the occipital cortex (it is composed of '(Sp1) – PT – Wave') and hardly involves the frontal cortex and the thalamus. Only rudimentary SWD II is present in the thalamus, in contrast, SWD I are well pronounced in the thalamus.

Noradrenergic control of SWD I and SWD II. **Chapter 3.2** examines the influence of depletion of noradrenergic neurotransmission with systemic injections of alpha-2 agonist of adrenoreceptors, clonidine, on the incidence and EEG properties of SWD I and SWD II. It is known that clonidine in low dose inhibits the release of noradrenaline and aggravates absence seizures. However, the mechanism of this pro-absence effect of clonidine is not known. It is found that the noradrenergic system modulates thalamo-cortical activity, thus promoting SWD I, but it does not affect mechanisms controlling SWD II and thus the number of SWD II remained unchanged.

In particular, it is found that clonidine injections increase the incidence of SWD I and affect its power spectrum: in the frontal cortex, total power is reduced (mainly in 1–9 and 30–100 Hz); in the VPM the power in 1–5 Hz is decreased and an opposite effect is found in the RTN - an increase in power in 9–14 Hz. An increase of alpha activity in the RTN suggests a reinforcement of oscillatory activity in the frequency of SWD I (~10 Hz); this results to more numerous and long-lasting SWD I; a decrease in alpha in the frontal cortex might encourage this effect.

Local occipital SWD type II have a tendency to be less numerous after clonidine injection. SWD II also have a lower power in the 5–9 Hz band in the occipital cortex, in the VPM and in the RTN.

Altogether, our data imply that the noradrenergic neuromodulatory system affects the frequency profile of both SWD I and SWD II; these data also imply that noradrenergic system can directly control the incidence of SWD I most likely via the reinforcement of oscillatory activity in the RTN, but it does not affect the incidence of SWD II.

The role of the thalamus in SWD I and SWD II. According the analysis of grand average EEG waveform (**Chapter 3.1**), SWD I are well pronounced in the VPM and RTN. This means that thalamic structures are capable to reproduce stereotypic epileptic activity on the level of local field potentials.

Chapter 5.1 shows that the initiation of SWD I is accompanied by an increase of RTN-VPM coherence in 8-11.5 Hz, whereas the gamma-band coherence in this pair is decreased. Probably, a desynchronization (decrease of coherence) in the gamma band may encourage the stronger synchronization in alpha frequencies, therefore, functional coupling in the frequencies of SWD (~10 Hz) is increased. A specific role of the RTN in SWD I is confirmed in **Chapter 3.2** (clonidine injections), when an increase of SWD I is observed after blocking the release of noradrenaline. EEG coherence study shows an elevation of local thalamic and cortical-thalamic at the onset of SWD I (**Chapter 5.1**). Although intracortical mechanisms are responsible for the initiation of SWD I (**Chapter 6**, Issue 11 in **Chapter 7**), the cortex should interact with the thalamus in order to provide a resonant circuitry which sustains and amplifies SWD I. In general, the data confirm that the RTN plays a supplementary role in SWD I and this is in agreement with Meeren et al. (2005) as well as with other studies.

Precursor activity of SWD I (preSWD epochs). We were incapable to establish a common EEG pattern that would be present in all seizure-precursor (likewise 5-9 Hz oscillations in GAERS), instead, preSWD epochs are classified in preSWDΔ, preSWDθ, preSWDα and preSWDn based on significant difference of EEG power in *delta-theta-alpha* as measured in the frontal EEG (**Chapter 3.3**). 73% of SWD (preSWDθ+preSWDα) exhibit a well pronounced *theta*-component (5-9 Hz), suggesting that the majority of SWD in WAG/Rij is preceded by substantial *theta*, yet this *theta* is not shaped into a single EEG rhythm (likewise in GAERS). Besides *theta*, almost all preSWD comprised a substantial delta component, suggesting that a coalescence of *delta* and *theta* activities in the cortex is favorable for the occurrence of SWD I.

Frequency profile of thalamo-cortical synchronization (EEG coherence) slightly differs in different classes of preSWD epochs, yet no features of EEG coherence can be considered as unique for any class of preSWD epoch. In general, preSWD epochs are characterized by a high coherence between RTN and VPM, suggesting that these nuclei are strongly coupled even before the onset of SWD I. 'Fronto-thalamic' coherence is lower as compared to coherence in 'RTN-VPM' pair and the least coherence is found in 'fronto-occipital' pair.

Thalamo-cortical network synchronization in transition 'preSWD→SWD I'. Our findings in **Chapters 3.2** indicate that amplitude-frequency properties of preSWD epochs and subsequent SWD depend upon coordination and consolidation between thalamic and cortical counterparts within the entire network. Analysis of synchronization in the intracortical, cortico-thalamic and intrathalamic neuronal networks during transition 'preSWD→SWD I' (**Chapter 5.1**) demonstrates that each part of thalamo-cortical circuit operates in a specific oscillatory mode, which is distinguished by frequency profiles. In particular, an increased coherence is found in frequencies 5 - 60 Hz with maxima around the mean frequency of SWD (8-11.5 Hz) and in the harmonic band 16-21.5 Hz. The epileptic focus in the SmI and its closest neighborhood creates a minimal neuronal circuit that may initiate SWD. This local cortical network includes area of limb and vibrissal projections in the SmI and the frontal cortex and it is characterized by specific changes of coherence during 'preSWD→SWD I', such as a reduction in the low frequency band (1-5 Hz), increase in 8 - 35.5 Hz and higher peak in harmonic frequency (21 Hz), as compared to the other pairs (18.5-20 Hz). Transhemispheric coherence showed the largest increase as compared to the other pairs and it is characterized by an additional peak in ~16 Hz. This additional 16 Hz peak is likely to reflect seizure propagation through bilateral *callosal* fibers (transhemispheric synchronization), suggesting a crucial involvement of the *corpus callosum* in the pathophysiology of absence seizures. Coherence in 'RTN-VPM' pair shows a remarkable antagonism between low- and high-frequency interactions, in which desynchronization in gamma frequencies associates with increased synchrony in 8-11.5 Hz.

Sleep spindles and SWD

In **Chapter 4**, we compare EEG features of sleep spindles and SWD and disclose some thalamo-cortical network mechanisms which are responsible for the occurrence of normal spindling and paroxysmal spike-wave activity.

Relationship between sleep spindles and SWD. In general terms, we find several counterarguments to the *cortico-reticular* theory, which states that SWD derive from spindle oscillations [Gloor, 1969; Kostopoulos, 2000]. In WAG/Rij rats, generalized SWD (type I) do not derive from anterior sleep spindles, but they emerge from a specific seizure-precursor activity (preSWD). EEG pattern of preSWD is clearly distinctive from that in spindle oscillations (**Chapter 4.1**). A relationship between posterior sleep spindles and SWD II is not confirmed: (1) the frequency profile of posterior spindles and SWD II is significantly different (**Chapter 4.1**); (2) the posterior sleep spindles involve thalamo-cortical network and are considered as thalamo-cortical oscillations), but thalamo-cortical systems play a secondary role in SWD II, if any (**Chapter 3.1**, **3.2** and **4.1**).

Some uncertainties are encountered in respect to a functional linkage between anterior sleep spindles and SWD I. On the one hand, these EEG phenomena revealed clearly dissimilar power spectra and display different patterns of 'fronto-occipital' network associations (cross-correlations), suggesting that neurophysiological substrate of anterior spindles and SWD I is not the same. Immediate precursors epochs of SWD I (preSWD epochs) in WAG/Rij rats differ from sleep spindles by having a different frequency profile. On the other hand, anterior spindles and SWD I cannot be considered as fully independent EEG phenomena. Analysis of cross-correlations reveals different patterns of thalamo-cortical interactions: one is characteristic for the waking state and another one ('oscillatory mode') is characteristic for anterior spindles and SWD I (**Chapter 4.1**). In the 'oscillatory mode', thalamus and cortex exhibit a stronger synchrony during SWD I than during anterior spindles. Sleep spindles and SWD are simulated by a common cortical neuronal model (**Chapter 4.2**), under assumption from an increase of synchronization in a population of pyramidal cells which underlie the occurrence of SWD I. Altogether this suggests that anterior spindles and SWD I are produced in the same thalamo-cortical circuit during appropriate

vigilance state, but they are underlain by different synchronization processes in the cortex (more strong synchronization is profitable for sleep spindles, but less strong synchronization – for sleep spindles).

We failed to grasp a generic relationship between sleep spindles and SWD on the level of EEG, apparently, there is no 'mechanic' transformation of EEG patterns 'spindle wave' → 'spike-wave complex'. Our alternative hypothesis suggests that there is a functional relationship between SWD and sleep spindle oscillations on the level of mechanism controlling the vigilance state. Two factors may promote absence seizures in low vigilance state: (1) abnormal functioning of cortical neurons and (2) impairment of processes that govern transitional states between wakefulness and NREM sleep, but these factors do not prevent occurrence of normal spindle events. As a result, sleep spindles and SWD I coincide in the thalamo-cortical circuit.

The local and global cortical mechanisms of SWD I

Cortical mechanisms are of highest importance in the pathogenesis of generalized SWD. Our findings stay in line with a *focal cortical* theory of absence epilepsy [Meeren at al., 2002], by showing that the somatosensory cortex (SmI) plays a crucial role in initiating SWD. It is found (**Chapter 6.2**) that deactivation of the SmI with local microinjections of lidocain, diminish SWD I. Although lidocaine has a local effect (it significantly diminished the total EEG power in the area surrounding the injection site in the SmI), the incidence of SWD I is reduced over the entire cortex in both hemispheres. The number of SWD gradually returned to a control level at the end of the second hour after lidocaine injections. These data show that proper functioning of SmI is important for the occurrence of generalized SWD. The perioral region of the SmI in rodents is endowed by specific neuronal mechanism to produce physiological oscillations in the frequency domain of SWD I (7–12 Hz), so called somatosensory rhythm [Nicolelis et al., 1995]. It is possible that somatosensory rhythm can be transformed in SWD in rodents with a predisposition to absence epilepsy [Wiest and Nicolelis, 2003], therefore, an intrinsic somatosensory rhythm produced by the SmI, but not sleep spindles, can be a source of SWD [van Luijtelaar and Sitnikova, 2006].

At the onset of SWD I, local field potential at the somatosensory cortex and its closest neighborhood is characterized by fast transient events (e.g., EEG ripples and double spiking, **Chapter 6.1**). These fast EEG transients are considered as a manifestation of epileptogenic processes, suggesting that epileptogenic processes in anterior and parietal cortical regions may be implicated in the initiation and in further propagation of seizure activity. In **Chapter 5.1,** it is found that the onset of SWD is associated with an increase of coherence in the anterior-parietal cortical pair, which is observed in gamma frequencies, up to 60 Hz. Probably, an increased gamma synchrony in the fronto-parietal area results in fast transient events in the EEG.

In **Chapter 5.2** we evaluate thalamo-cortical *causal relations* before, during and after SWD I, using a concept of Granger causality. In this concept, the knowledge about the immediate past of one signal can be used for the prediction of another signal. Linear estimation of Granger causality is used. It is found that *causal relations* does not change before the onset of SWD I, suggesting that the linear estimation of Granger is not sufficient for predicting absence epilepsy (non-linear model is needed in order to predict the onset SWD based on the early changes in causal network relationship). The onset of SWD I is characterized by a rapid increase of coupling strength in both directions. The strength of *thalamus→cortex* coupling remained constantly high until the end of SWD and it does not return to the initial level even after cessation of SWD. The strength of *cortex→thalamus* coupling is gradually diminished shortly after the onset of SWD I and returned to the pre-SWD level when SWD I is stopped. It is hypothesized that the strong and sustained influence *thalamus→cortex* is necessary for propagation and maintenance of seizure activity, while the influence *cortex→thalamus* promotes the cessation of SWD I.

SUMMARY

The current thesis presents an extensive electroencephalographic study of normal spindle events (anterior and posterior spindles), absence seizures (SWD I) and occipital paroxysm SWD II in genetic epileptic WAG/Rij rats. Cortical and thalamic activity is measured and analyzed with a high temporal and spatial resolution using traditional and new methods of time series analysis.

In general, it is concluded that SWD and sleep spindles in our rats are comparable to that in humans. Like in humans, WAG/Rij rats exhibit two kinds of sleep spindles in the frontal and occipital EEG channels, e.g., anterior (~11.4 Hz) and posterior spindles (~10.2 Hz) (**Chapter 2.1**). It is emphasized that local cortical sleep spindles are not just a fingerprint of the electrical activity in the thalamus, but that each type of spindle activity is generated in different thalamo-cortical oscillatory networks (**Chapter 2.2**). In anterior sleep spindles, the reticular thalamic nucleus (RTN) links with the specific thalamic nucleus (VPM) and the frontal cortex, while in posterior sleep spindles, occipital cortex cooperates with the VPM, but the RTN hardly plays a primary role.

Likewise humans, SWD in WAG/Rij rats are multi-phasic negative-positive-negative potentials (**Chapter 3.1**). SWD I and SWD II consist of epileptiform elements that are analogous to that identified in spike-wave complexes in human EEG, e.g., Spike 1, Spike 2, positive transient and Wave [Weir, 1965]. It is demonstrated that SWD I and SWD II clearly differ on the level of the thalamus: SWD I are well pronounced in the thalamus, but SWD II are present in rudimentary form (**Chapter 3.1**). Frequency profile of both SWD I and SWD II in the cortex and in the thalamus is found to be regulated by noradrenergic neuromodulatory systems. Reinforcement of electrical activity in the RTN, rather than in the VPM, encourages SWD I by putative modulatory alpha2-adrenergic mechanisms (**Chapter 3.2**).

Similar to that in GAERS [Pinault, 2001], preSWD epochs in WAG/Rij rats in the frontal cortex reveal a powerful 5-9 Hz rhythmic component (**Chapter 3.3**). Besides that, preSWD epochs in WAG/Rij rats show high *delta* component in the frontal cortex (3-4 Hz) and in the thalamus (1-2 Hz). We stress that the co-existence of cortical and thalamic *delta* activity may play an important role in the initiation and further development of SWD I.

As to the relationship between sleep spindles and SWD is concerned, our data contradict to a hypothesis about a relationship between posterior sleep spindles and SWD II (**Chapter 4.1**). Some uncertainties encountered in respect to a functional linkage between anterior sleep spindles and SWD I; these EEG phenomena reveal a clearly dissimilar power spectra and different profiles of 'fronto-occipital' network associations, suggesting that neurophysiological substrates of anterior spindles and SWD I are not the same. Immediate precursors of SWD I (preSWD) in WAG/Rij rats differ from sleep spindles by having different frequency profile (**Chapter 4.1**). Altogether this contradicts to a 'cortico-reticular' theory of absence epilepsy stating that spindles give rise to SWD [Gloor 1969, Kostopoulos, 2000]. Besides that, anterior spindles and SWD cannot be considered as fully independent EEG phenomena: they demonstrate a similar pattern of thalamo-cortical cross-correlation (**Chapter 4.1**) and they are simulated by a common cortical neuronal model (**Chapter 4.2**). This suggests that anterior spindles and SWD I are produced in the same thalamo-cortical circuit during appropriate vigilance state, but they are underlain by different synchronization processes in the cortex (more strong synchronization is profitable for SWD, but less strong synchronization – for sleep spindles).

We must emphasize the highest importance of the neocortex in initiation and maintenance of SWD I. Our study provides evidences in favor to a 'cortical focus' theory of absence epilepsy [Meeren at al., 2002], which states that the somatosensory cortex (SmI) plays a crucial role in initiating of generalized SWD. In particular, we demonstrate that deactivation of the SmI with local microinjections of lidocaine results in diminution of SWD I (**Chapter 6.2**). At the onset of SWD I, local field potentials in the frontal and parietal cortex are characterized by fast transient components (e.g., EEG ripples and double spiking), suggesting that neuronal epileptogenic processes in the fronto-parietal cortex may be implicated in the initiation and in further propagation of seizure activity (**Chapter 6.1**). Analysis of synchronization in the intracortical, cortico-thalamic and intrathalamic neuronal networks during transition 'preSWD→SWD I' (**Chapter 5.1**) demonstrates that each part of the thalamo-cortical circuit operates in a specific oscillatory mode, which is distinguished by frequency profiles. We also introduce a new concept for the analysis of *causal relations* within a network in terms of Granger causality (**Chapter 5.2**). Analysis of thalamo-cortical *causal relations* before, during and after SWD I brings us to an assumption that propagation and maintenance of seizure activity may be facilitated under the strong influence of *thalamus→cortex*, while a rapid reduction of the influence *cortex→thalamus* may promote the cessation of SWD I. Altogether this suggests that SWD are initiated in a small region of the parietal cortex, and that global cortico-thalamic mechanisms are important for the further generalization of seizure activity.

The general conclusion of this thesis is that the theory, which assumes an intimate relationship between sleep spindles and spike-wave discharges, as can be found in children with absence seizures and in genetic rodent models, is not in agreement with data as presented in this thesis and in the literature in general.

SUMMARY in Dutch

In dit proefschrift wordt een uitgebreide electroencefalografische studie van slaapspoelen (anterieure en posterieure), absence aanvallen (piek-golf ontladingen, spike-wave discharges type I [SWD I]) en spike-wave discharges type II [SWD type II]) gepresenteerd. Deze studie is uitgevoerd in genetisch epileptische ratten van de WAG/Rij stam. Corticale en thalamische activiteit is gemeten en geanalyseerd met een hoge temporele en spatiele resolutie, waarbij zowel traditionele als nieuwe tijdreeks-analyse methoden gebruikt zijn.

Een algemene conclusie is dat SWD en slaapspoelen in WAG/Rij ratten analoog zijn aan die van de mens. Ratten hebben, net als mensen, twee "gebieds-specifieke" type slaapspoelen in het frontale en het occipitale EEG, anterieure (~11.4 Hz) en posterieure spoelen (~10.2 Hz), die beide horen tot het domein van de slaapspoelen (**Hoofdstuk 2.1**). Benadrukt is dat de plaatselijke corticale slaapspoelen geen vingerafdruk zijn van de elektrische activiteit in de thalamus waar de spoelen opgewekt worden, maar dat ieder type spoelactiviteit opgewekt wordt in verschillende thalamo-corticale oscillerende netwerken (**Hoofdstuk 2.2**). De reticulaire thalamische kern (RTN), die nauw verbonden is met de frontale cortex en met de specifieke thalamus kern (VPM), is betrokken bij het opwekken van de anterieure spoelen, terwijl dezelfde RTN nauwelijks een rol speelt bij de posterieure slaapspoelen, waarbij de VPM met de occipitale cortex samenwerkt.

Piek-golf ontladingen zijn zowel bij de mens als bij de WAG/Rij rat multi-fasische negatief-positief-negatieve potentialen (**Hoofdstuk 3.1**). Zowel SWD I en SWD II bevatten epileptoforme elementen, analoog aan die welke bij de piek-golf ontladingen in het EEG van de mens beschreven zijn, o.a. "spike 1", "spike 2", "positive transient" en "wave", (Weir, 1965). SWD I en SWD II verschillen duidelijk van elkaar in de thalamus: Weir's elementen van SWD I komen in de thalamus goed tot uiting, daarentegen zijn SWD II slechts in rudimentaire vorm aanwezig (**Hoofdstuk 3.1**). Het frequentie-profiel van zowel SWD I als SWD II in de cortex en thalamus staat onder invloed van het noradrenerge neuromodulatoire systeem. Preferentiële bekrachtiging van de elektrische activiteit in de RTN boven die van de VPM, vergroot de kans op SWD I door mogelijke modulatoire alpha-2-adrenerge mechanismen (**Hoofdstuk 3.2**).

De EEG activiteit voorafgaand aan SWD vertoont in de frontale cortex van de WAG/Rij rat een krachtige 5 tot 9 Hz ritmische component, wat in overeenstemming is met gegevens van Pinault verkregen bij GAERS (2001) (**Hoofdstuk 3.3**). Daarnaast laat het EEG in de WAG/Rij rat voorafgaand aan de SWD een hoge delta component zien in de frontale cortex (3-4 Hz) alswel in de thalamus (1-2 Hz). Er is benadrukt dat de parallelle aanwezigheid van delta-activiteit in de cortex en thalamus een belangrijke rol speelt bij de genese en het handhaven van SWD I.

Met betrekking tot de veronderstelde relatie tussen slaapspoelen en SWD is gevonden dat de hypothese verworpen kan worden voor een specifieke relatie tussen de posterieure slaapspoelen en SWD II (**Hoofdstuk 4.1**). Ook zijn er enkele onzekerheden met betrekking tot de functionele relatie tussen anterieure slaapspoelen en SWD I opgelost: beide EEG verschijnselen laten duidelijke verschillende power-spectra en verschillende "fronto-occipitale" netwerk associaties zien. Dit suggereert dat het neurofysiologisch substraat van anterieure spoelen niet hetzelfde is als dat van SWD I. Ook is het frequentie-profiel van het EEG voorafgaand aan SWD en slaapspoelen verschillend (**Hoofdstuk 4.1**). Dit alles is in strijd met de cortico-reticulaire theorie van absence epilepsie, die stelt dat piek-golf ontladingen zich ontwikkelen uit slaapspoelen (Gloor 1969, Kostopoulos, 2000). Daar dient echter aan toegevoegd te worden dat anterieure spoelen en SWD een overeenkomstig kruis-correlatie profiel hebben en ze gesimuleerd kunnen worden door eenzelfde corticaal neuronaal model (**Hoofdstuk 4.1**; **Hoofdstuk 4.2**). Daarom kunnen ze niet als geheel onafhankelijk van elkaar gezien worden. Dit leidt tot de suggestie dat anterieure slaapspoelen en SWD I in hetzelfde thalamocorticale circuit gegenereerd worden tijdens een geschikte vigilantie toestand, maar dat ze van elkaar verschillen in de mate waarin synchronizatie in de cortex optreedt. Een sterkere synchronizatie is gunstig voor de aanwezigheid van SWD, en een minder sterke voor slaapspoelen.

De cortex is de belangrijkste structuur in het brein voor het opwekken en handhaven van SWD I. Ook de experimenten in deze studie ondersteunen de "focal cortical" theorie van absence epilepsie, zoals die door Meeren et al. (2002) geformuleerd is. Deze theorie veronderstelt dat de somatosensorische cortex (SmI) een cruciale rol speelt bij het opwekken van gegeneralizeerde SWD. In het bijzonder is aangetoond dat deactivatie van de somatosensorische cortex met locale unilaterale microinjecties met lidocaine, aanleiding geeft tot een vermindering van het aantal SWD I (**Hoofdstuk 6.2**).

Aan het begin van de genese van SWD I laten zogenaamde “local field potentials”, geregistreerd in de frontale en parietale cortex, de aanwezigheid zien van snelle transiente componenten, de zogenaamde EEG “ripples”, alswel van dubbele spikes. Dit suggereert dat neuronale epileptogene processen in de anteroparietale cortex betrokken zijn bij het ontstaan en de verspreiding van aanvals-activiteit (**Hoofdstuk 6.1**). Analyse van de synchronizatie in de intracorticale, corticothalamische en intrathalamische neuronale netwerken tijdens de overgang van preSWD naar SWD I (**Hoofdstuk 5.1**), laat zien dat ieder deel van het thalamocorticale circuit op eigen wijze opereert op een specifiek oscillerende wijze. Dit komt tot uiting in verschillen in frequentie-profielen van diverse structuren.

Een nieuw concept is geintroduceerd bij de analyse van causale relaties binnen een neuronaal netwerk: “Granger causality” (**Hoofdstuk 5.2**). De analyse van de thalamocorticale causale relaties vóór, tijdens en na SWD I, leidt tot de veronderstelling dat de verspreiding en duur van de aanvals-activiteit gefaciliteerd wordt door een sterke invloed van de thalamus op de frontale cortex, terwijl een snelle reductie van de invloed van de frontale cortex op de thalamus juist het afbreken van SWD I kan faciliteren. Dit houdt de verondersteling in dat SWD geïnitieerd worden in een klein deel van de parietale cortex en dat globale cortico-thalamische mechanismen belangrijk zijn voor de verdere verspreiding van de aanvals-activiteit.

De algehele conclusie van dit proefschrift is dat de theorie die verondersteld dat er een intieme relatie is tussen slaap spoelen en piek-golf ontladingen, zoals die bij kinderen met absence epilepsie en in genetische ratten modellen voorkomen, niet langer in overeenkomst is met de gegevens zoals die onder meer in dit proefschrift gepresenteerd worden.

SUMMARY in Russian (выводы и заключение)

В настоящей диссертационной работе представлены данные электроэнцефалографического (ЭЭГ) исследования нормальной ритмической активности головного мозга во время сна (сонных веретен) и пик-волновой активности, сопровождающей эпизоды абсанс-эпилепсии у крыс с генетической предрасположенностью к этой болезни (линия WAG/Rij). Был проведен анализ локальной электрической активности коры и таламуса с использованием традиционных (быстрое преобразование Фурье, спектральный и когерентный анализ, анализ кросс-спектров и кросс-корреляций) и новых методов (непрерывное вейвлетное преобразование, адаптивный вейвлетный анализ, казуальность Гранджера). Обнаружено, что общие характеристики сонных веретен и пик-волновых разрядов у крыс WAG/Rij аналогичны таковым у человека.

Сонные веретена

В **Главе 2.1** описаны свойства двух типов сонных веретен, представленных локально в передних областях коры (антериорные веретёна, средняя частота ~11.4 Гц) и в затылочной области (постериорные веретёна, средняя частота ~ 10.2 Гц). У сонных веретён обоих типов форма таламического потенциала отличалась от формы кортикального потенциала: в таламусе веретенообразные колебания были менее регулярными, а иногда даже отсутствовали. Сделано заключение, что свойства каждого типа веретен зависят от морфо-функциональных особенностей соответствующих областей коры и от взаимодействия этих областей со структурами таламуса.

Для исследования роли таламуса в формировании двух типов сонных веретен (**Глава 2.2**) был проведен анализ взаимодействий в таламо-кортикальной системе (методом кросс-спектров и кросс-корреляций). Показано, что антериорные сонные веретёна являлись результатом синхронной работы передних областей коры, ретикулярного таламического ядра (RTN) и вентропостеролтерального ядра (VPM). Постериорные веретёна в затылочной области коры формировались при участии VPM, при этом роль RTN оказалась спорной.

В **Главе 4.3** представлены данные частотно-временного анализа (непрерывное вейвлетное преобразование) сонных веретён, зарегистрированных на фронтальной ЭЭГ (антериорные веретёна). Для исследования степени взаимного подобия сонных веретен был использован адаптивный вейвлетный анализ. Показано, что 85-90% антериорных веретён имели высокую степень сродства к универсальному шаблону (вейвлетному базису «веретена 1-ого типа»). Остальные 10-15% веретен имели более сложную форму и ряд индивидуальных особенностей, поэтому для распознавания веретен 2-ого типа подбирался отдельно для каждого животного так, при этом средняя частота вейвлетного базиса («веретен 2-ого типа») колебалась от 17 до 23 Гц. Выделение веретён на ЭЭГ осуществляли автоматически после непрерывного вейвлетного преобразования, при котором материнской функцией служили вейвлетные базисы веретен 1-ого и 2-ого типа. Критерием для выделения веретён 1-ого было превышение порогового уровня энергии в

полосе частот 7-14 Гц; для веретён 2-ого типа - в полосе частот 20-25 Гц. Таким образом, была выявлена общая структурная единица, составляющая основу сонных веретен у крыс линии WAG/Rij («вейвлет веретена 1-ого типа»). Нетипичные формы веретен (соответствующие вейвлету «веретен 2-ого типа», но не имеющие сродства к «вейвлету веретена 1-ого типа») по-видимому, являются трансформацией нормального сонно-веретенного ритма вследствие нарушения возбудимости коры и других эпилептических процессов.

Пик-волновые разряды

В **Главе 3** описаны свойства пик-волновых разрядов 1-ого и 2-ого типов у крыс линии WAG/Rij. Пик-волновые разряды обоих типов были представлены в форме негативно-позитивно-негативных колебаний электрического потенциала. В составе пик-волновых разрядов были выделены эпилептиформные компоненты, которые являлись полными аналогами компонентов, входящих в состав пик-волновых комплексов на ЭЭГ человека [Weir, 1965]: «пик 1» (Sp1), «пик 2» (Sp2), позитивный компонент (PT) и негативная волна (Wave) (**Глава 3.1**, [Sitnikova и van Luijtelaar, 2007]). У крыс WAG/Rij пик-волновые разряды 1-ого типа во фронтальной коре были представлены в виде последовательности: 'PT_{early} – Sp2 – PT_{late}'; в затылочной коре - '(Sp1) – PT – Wave'; в таламусе (вентропостеромедиальное ядро) состояли из 'Sp1 – PT – Wave' и в ретикулярном ядре таламуса - 'PT – Wave'. Отличительным признаком пик-волновых разрядов 1-ого типа во фронтальной коре был «пик 2» (Sp2), который имел непропорционально высокую амплитуду. В состав пик-волнового комплекса в вентропостеромедиальном ядре таламуса входил пик 1 (Sp1, компонент, отсутствовавший в остальных исследованных структурах). Пик-волновые разряды 2-ого типа были локализованы в затылочной коре и состояли из последовательности '(Sp1) – PT – Wave'.

Глава 3.2 посвящена исследованию роли норадренергической системы в формировании пик-волновых разрядов 1-ого типа (характерного ЭЭГ коррелята абсанс-эпилепсии) и разрядов 2-ого типа (неясной этиологии) [Sitnikova и van Luijtelaar, 2005]. Кратковременную инактивацию норадренергической передачи осуществляли путём системного введения подпороговой дозы блокатора альфа-адренорецепторов – 2% раствора клонидина. Как следствие, судорожная активность значительно усиливалась по критерию увеличения количества и длительности пик-волновых разрядов 1-ого типа (количество и длительность разрядов 2-ого типа не изменялось). При этом увеличение амплитуды пик-волновых разрядов 1-ого типа было выявлено в узком диапазоне частот 9-14 Гц и только в ретикулярном ядре таламуса. Это свидетельствует, во-первых, о более интенсивной ритмической активности ретикулярного ядра таламуса в диапазоне частот, характерных для пик-волновых разрядов, и, во-вторых, об особой роли этой структуры в усилении судорожной активности. В остальных исследованных структурах таламо-кортикальной сети наблюдали противоположные изменения: во фронтальной коре амплитуда частотных составляющих 1-9 и 30-100 Гц была ниже, чем в контроле; в вентропостеромедиальном ядре таламуса снижение амплитуды наблюдали в диапазоне частот 1-5 Гц. Сделан вывод о том, что норадренергическая нейромедиаторная система (1) влияет на появление пик-волновых разрядов путём модуляции ритмогенеза в ретикулярном таламическом ядре, (2) влияет на структуру пик-волновых разрядов и их частотные характеристики посредством модуляции нейронной активности в коре и в таламусе.

Глава 3.3 посвящена исследованию особенностей ЭЭГ, предшествующей пик-волновым разрядам 1-ого типа. По нашим данным, наиболее характерным признаком «предвестников» эпилептических разрядов на фронтальной ЭЭГ являлся 5-9 Гц компонент. Это полностью соответствует данным, полученным на крысах линии GAERS [Pinault, 2001]. Отличительной особенностью «предвестников» пик-волновых разрядов (1-ого типа) у крыс WAG/Rij оказался высокоамплитудный компонент в диапазоне *дельта* частот, который был выявлен во фронтальной коре (3-4 Гц) и в таламусе (1-2 Гц). Наличие *дельта* активности в коре и таламусе может оказаться ключевым фактором инициации и дальнейшего развития эпизодов абсанс-эпилепсии.

Сравнительный анализ сонных веретен и пик-волновых разрядов

В **Главе 4** исследована функциональная взаимосвязь между сонными веретёнам и пик-волновыми разрядами. В **Главе 4.1** приведены результаты сравнительного анализа ЭЭГ характеристик антериорных сонных веретён и их гипотетических дериватов, пик-волновых разрядов 1-ого типа. Сонные веретена и пик-волновые разряды отличались по ряду признаков: (1) по форме ЭЭГ потенциала, (2) по частотным характеристикам, (3) по распределению спектральной мощности в основных полосах частот (Δ, ν, α, β и γ), (4) по характеру внутрикортикальных взаимодействий (между лобной и затылочной областями коры). Кроме того, сонные веретёна отличались от ритмической активности, непосредственно предшествующей пик-волновым разрядам 1-ого типа, по критерию формы ЭЭГ и по частотным характеристикам. Полученные результаты свидетельствуют о невысокой степени сродства сонными веретенами и пик-

волновыми разрядами и противоречат общепринятой кортико-ретикулярной теории, которая предполагает возможность трансформации сонных веретен в пик-волновые разряды [Gloor 1969, Kostopoulos, 2000].

Несмотря на принципиальные отличия в плане структурных и частотных характеристик, сонные веретена и пик-волновые разряды формируются в таламо-кортикальной сети и имеют ряд общих черт, относящихся к характеру взаимодействия между корой и таламусом (данные кросс-корреляционного анализа ЭЭГ, **Глава 4.1**).

В **Главе 4.2** был использован метод нейромоделирования для исследования возможного взаимного перехода между двумя типами ритмической активности: сонно-веретенной и пик-волновой. Этот подход позволил также раскрыть некоторые нейронные механизмы, лежащие в основе появления определенной формы ЭЭГ, характерной для сонных веретен и пик-волновых разрядов [Sargsyan и др., 2007]. Была создана нейронная модель, которая позволила реконструировать локальные потенциалы коры в ответ на ритмическую активность таламических афферентов. Был смоделирован нейронный модуль коры, состоящий из пирамидных нейронов с характерным послойным распределением и интернейронов двух типов, которые обеспечивали прямое и возвратное торможение (feed-forward и recurrent inhibition, соответственно). Вышеназванные клетки коры были связаны с глутамат-эргическими афферентами таламуса посредством AMPA- и NMDA-рецепторов (пирамидные нейроны) и AMPA-рецепторов (интернейроны прямого торможения).

Анализ работы модели показал, что компонент «пик», входивший в составе пик-волнового комплекса, формировался как реакция коры на возбудительный вход из таламуса, а высота пика модулировалась AMPA-рецепторами пирамидных клеток. Компонент «волна» возникал вследствие торможения активности коры; амплитуда волны зависела от силы прямого ГАМК-эргического торможения пирамидных нейронов (feed-forward inhibition). Принципиально важным был тот факт, что ритмическая стимуляция таламуса вызывала веретенообразные колебания в коре до тех пор, пока синхронизация между пирамидными нейронами оставалась слабой. При усилении степени синхронизации между пирамидными нейронами форма локального потенциала подвергалась трансформации, и появлялся характерный для абсанс-эпилепсии пик-волновый паттерн.

В **Главе 4.3** показано, что спектральные характеристики прототипа веретён 2-ого типа («вейвлета веретена 2-ого типа») по ряду параметров сходны с характеристиками эпилептических разрядов (пик-волновыми разрядами 1-ого типа). Это может свидетельствовать о том, что антериорные веретёна 2-ого типа являются промежуточной формой между нормальными осцилляциями на ЭЭГ (т.е., веретена 1-ого типа) и пароксизмальной пик-волновой активностью (разряды 1-ого типа).

Таламо-кортикальные механизмы инициации эпизодов абсанс-эпилепсии

Глава 5 посвящена анализу взаимодействий в таламо-кортикальной системе при переходе от нормальной (фоновой) к эпилептической активности (разряды пик-волна 1-ого типа). В **Главе 5.1** были выявлены особенности функциональных взаимосвязей между различными соседними и удаленными областями коры (локальные, не-локальные однополушарные и межполушарные взаимодействий), внутри таламуса (между специфическим вентропостеромедиальным ядром, VPM, и ретикулярным ядром, RTN), между корой и таламусом путём анализа спектров функции когерентности [Sitnikova и van Luijtelaar 2006; van Luijtelaar и др., 2006]. Показано, что процесс инициации эпилептических разрядов сопровождался усилением степени согласованности (по сравнению с нормальной) между всеми исследованными областями таламо-кортикальной системы, при этом частотные характеристики спектров когерентности между различными областями существенно отличались. Обнаружено существенное усиление взаимосвязей между различными областями коры (*внутрикортикальные* взаимодействия) в широком диапазоне частот (5-60 Гц) с максимальными значениями в диапазоне 8-11.5 Гц, соответствующем средней частоте пик-волновых разрядов, и диапазоне кратных частот 16-21.5 Гц (первая гармоника). Усиление функциональной связи между VPM и RTN (*внутриталамические* взаимодействия) было ограничено узким диапазоном частот, соответствующим средней частоте пик-волновых разрядов (8-11.5 Гц), тогда как степень синхронизация диапазоне гамма частот (36-60 Гц), напротив, снижалась.

Между симметричными областями коры был обнаружен дополнительный устойчивый максимум функции когерентности на частоте около 15.5 Гц. Этот пик занимал промежуточное положение между пиками, соответствующими средней частоте пик-волновых разрядов (около 9 Гц) и ее гармонической составляющей (около 18 Гц). Этот дополнительный пик межполушарных взаимодействий мог появиться в результате билатеральной синхронизации эпилептического ритма, осуществляемой посредством *corpus callosum*.

Таким образом, таламические структуры участвовали в поддержании основной ритмической компоненты эпилептического ритма (8-10 Гц). Кора, где было обнаружено усиление синхронизации в полосе частот (5-60Гц), по всей видимости, имеет дополнительные механизмы нейронной синхронизации,

благодаря которым возможно не только поддержание эпилептического ритма, но также его усиление и генерализацию. В целом, осцилляторная активность каждой части таламо-кортикальной системы в период инициации пик-волновых разрядов определятся внутренними особенностями отдельных частей и характером взаимодействий с остальными частями системы, в результате чего возможно поддержание, усиление и билатеральное распространение эпилептического ритма.

Глава 5.2 посвящена исследованию изменения функциональных связей между таламусом и фронтальной корой в течение пик-волновых разрядов 1-ого типа (включая периоды, предшествующие и следующие за разрядами) с учётом направленности этих связей [Sitnikova и др., 2008]. Анализ включал расчет функции Гранжера (Granger causality), которая позволяет предсказывать настоящее состояние сигнала ЭЭГ на основании его прошлого состояния. Использованная нами в расчетах линейная модели показала, что сила связи между корой и таламусом не изменялась вплоть до начала пик-волнового разряда. Таким образом, для предсказания эпизодов эпилепсии в расчетах функции Гранжера должна быть использована сложная нелинейная модель.

По нашим данным, момент появления пик-волновых разрядов на ЭЭГ сопровождался резким ростом двухсторонних таламо-кортикальных взаимосвязей, при этом связь в направлении «таламус – кора» оставалась высокой на протяжении всего разряда и не возвращалась к исходному уровню после прекращения пик-волновой активности. Обратная связь в направлении «кора - таламус», наоборот, во время разряда постепенно снижалась и возвращалась к исходному уровню к концу эпилептического разряда. Эти данные свидетельствует о том, что активность таламуса и его влияние на кору необходимо для поддержания эпилептической активности, тогда как обратное влияние коры на таламус оказывается критическим для прекращения пик-волновой активности.

Роль коры в формировании эпилептической активности (пик-волновых разрядов 1-ого типа)

В **Главе 6** систематизирован собственный экспериментальный материал, свидетельствующий о роли коры в патогенезе абсанс-эпилепсии, а также предложен новый взгляд на физиологические механизмы этой болезни [van Luijtelaar и Sitnikova, 2006]. В частности, рассмотрены причины, из-за которых у крыс с предрасположенностью к абсанс-эпилепсии область периоральных проекций в соматосенсорной коре может явиться источником пик-волновых разрядов [по Meeren at al., 2002]. В **Главе 6.2** [Sitnikova и van Luijtelaar, 2004] представлены результаты одной из первых экспериментальных работ, подтверждающих факт существования в коре источника пик-волновых разрядов. Локальная область соматосенсорной коры (зона проекций морды и вибрисс) была инактивирована путём микроинъекций 2% раствора лидокаина, что приводило к снижению количества эпилептических разрядов. Длительность эффекта составляла около 1,5-2 часов, что было сопоставимо с действием местного анестетика. Полученные данные свидетельствуют о ключевой роли соматосенсорной коры в развитии и патогенезе абсанс-эпилепсии у крыс линии WAG/Rij.

В **Главе 6.1** (Sitnikova и van Luijtelaar 2007) выявлен ряд особенностей ЭЭГ в соматосенсорной коре (кортикального источника пик-волновой активности по данным Meeren at al., 2002) и прилегающих областях. ЭЭГ в этих областях коры (фронто-париетальный отдел коры) характеризовалась наличием высокочастотных компонентов, которые появлялись в период инициации пик-волновых разрядов преимущественно. Эти локальные компоненты появлялись в виде вспышки высоко-амплитудной активности (ripples) и комплексы с двойными пиками (double spiking), не были регулярными и не входили в «канонический» комплекс ЭЭГ пик-волна. Появление данных компонентов (ripples double spiking) может оказаться свидетельством локальных внутрикортикальных эпилептических процессов, протекающих во фронто-париетальной коре в период инициации эпизодов абсанс-эпилепсии. Это предположение подтверждают данные когерентного анализа [**Глава 5.1,** Sitnikova и van Luijtelaar 2006; van Luijtelaar и др., 2006], где между фронтальной и париетальной областями коры было обнаружено мощное усиление когерентных взаимодействий в наиболее широкой полосе частот, включающей гамма диапазон (до 60 Гц). Таким образом, высокочастотные предвестники эпилептических разрядов могут иметь локальное внутрикортикальное происхождение, свидетельствовать о дисфункции соматосенсорной коры и прилегающих областей, то есть, о патологической активности кортикального источника пик-волновой активности.

References

Aarabi A, Wallois F, Grebe R, Does spatiotemporal synchronization of EEG change prior to absence seizures? *Brain Res.* 2007, doi:10.1016/j.brainres.2007.10.048

Ahissar E, Haidarliu S, Zacksenhouse M. Decoding temporally encoded sensory input by cortical oscillations and thalamic phase comparators, *Proc. Natl. Acad. Sci. USA,* 1997; 94: 11633– 11638.

Amzica F, Steriade M. The K-complex: its slow (<1-Hz) rhythmicity and relation to delta waves. *Neurology*. 1997; 49: 952-959.

Amzica F, Steriade M. The functional significance of K-complexes. *Sleep Medicine Rev*., 2002; 6: 139-149.

Ancona N, Marinazzo D, Stramaglia S. Radial basis function approach to nonlinear Granger causality of time series. *Phys. Rev. E*, 2004; 70:056221.

Anderer P, Klosch G, Gruber G, Trenker E, Pascual-Marqui RD, Zeitlhofer J, Barbanoj MJ, Rappelsberger P, Saletu B. Low-resolution brain electromagnetic tomography revealed simultaneously active frontal and parietal sleep spindle sources in the human cortex. *Neurosci*., 2001;103: 581-592.

Angeleri F, Ferro Milone G, Parigi S. Electrical activity and reactivity of the rhinencephalic, pararhinencephalic and thalamic structures: prolonged implantation of electrodes in man. *Electroencephalogr Clin Neurophysiol*., 1964; 16: 100-129.

Angeleri F, Nolfe G, Pucci E, Belardinelli N, Quattrini A, Signorino M. EEG spectral analysis in generalized absence epilepsies (awake, S2 sleep, spindles and K-complexes). In: Minciacchi D et al. (Eds.) Thalamic networks for relay and modulation. Pergamon Press, Oxford, New York, 1993: 409-424.

Arnhold J, Lehnertz K, Grassberger P, Elger CE. A robust method for detecting interdependences: application to intracranially recorded EEG. *Physica D*., 1999; 134: 419-30.

Aston-Jones G, Foote SL, Bloom FE. Anatomy and physiology of locus coeruleus neurons: functional implications. In: Ziegler M, Lake CR (Eds) Norepinephrine. Frontiers of clinical neuroscience. Vol. 2, Williams & Wilkins, Baltimore, 1984, pp. 92–116.

Avanzini G, de Curtis M, Marescaux C, Panzica F, Spreafico R, Vergnes M. Role of the thalamic reticular nucleus in the generation of rhythmic thalamo-cortical activities subserving spike and waves. *J. Neural Transm.,* 35 (Suppl.), 1992: 85–95.

Avanzini G, Vergnes M, Spreafico R, Marescaux C. Calcium-dependent regulation of genetically determined spike and waves by the RTN of rats. *Epilepsia*, 1993, 34, 1–7.

Avanzini G, de Curtis M, Franceschetti, S, Sancini, G, Spreafico, R. Cortical versus thalamic mechanisms underlying spike and wave discharges in GAERS. *Epilepsy Res*., 1996; 26: 37-44.

Avanzini G, Panzica F, de Curtis M. The role of the thalamus in vigilance and epileptogenic mechanisms. *Clin Neurophysiol.* 2000; Suppl 2: S19-26.

Avanzini G, Franceschetti S. Cellular biology of epileptogenesis. *Lancet Neurology* 2003, 2: 33-42.

Avoli M, Gloor P, Kostopoulos G, Gotman J. An analysis of penicillin-induced generalized spike and wave discharges using simultaneous recordings of cortical and thalamic single neurons. *J. Neurophysiol.*, 1983; 50: 819-837.

Avoli M, Gloor P. Role of the thalamus in generalized penicillin epilepsy: observations on decorticated cats. *Exp. Neurol.,* 1982, 77: 386–402.

Bazil CW. Epilepsy and sleep disturbance. *Epilepsy Behav*. 2003; 4(S2), S39-S45.

Bancaud J. Physiopathogenesis of generalized epilepsies of organic nature (Stereoencephalographic study), in: H. Gastaut, H.H. Jasper, J. Bancaud, A. Walteregny (Eds.), The Physiopathogenesis of the Epilepsies, Charles C. Thomas, Springfield, IL, 1969, pp. 158– 185.

Berger H. Über das Electrenkephalogramm des Menschen. *Arch Psychiatr* Neyenkr 1929; 87: 527-570.

Berthelsen S, Pettinger WA. A functional basis for classification of alpha-adrenergic receptors. *Life Sci.,* 1977, 21: 595-606.

Bischoff P, Mahlstedt D, Blanc I, Schulte am Esch J. Quantitative topographical electroencephalographic analysis after intravenous clonidine in healthy male volunteers. *Anesth. Analg*., 1998, 86: 202-207.

Blume WT, Lemieux JF. Morphology of spikes in spike-and-wave complexes. *Electroencephalogr Clin Neurophysiol.,* 1988; 69: 508-515.

Blume WT. Invited review: clinical and basic neurophysiology of generalised epilepsies. *Can J Neurol Sci*., 2002, 29:6-18.

Blumenfeld H. The thalamus and seizures. *Arch. Neurol*., 2002; 59:135-137.

Bosnyakova D, Gabova A, Kuznetsova G, Obukhov Y, Midzyanovskaya I, Salonin D, van Rijn C, Coenen A, Tuomisto L, van Luijtelaar G. Time-frequency analysis of spike-wave discharges using a modified wavelet transform. *J Neurosci Methods,* 2006; 154: 80-88.

Bosnyakova D, Gabova A, Zharikova A, Gnezditski V, Kuznetsova G, van Luijtelaar G. Some peculiarities of time-frequency dynamics of spike-wave discharges in humans and rats. *Clin Neurophysiol*., 2007; 118: 1736–1743.

Bouwman BM, van den Broek PL, van Luijtelaar G, van Rijn CM. The effects of vigabatrin on type II spike wave discharges in rats. *Neurosci Lett*., 2003; 338(3): 177-180.

Brailowsky S, Montiel T, Boehrer A, Marescaux C, Vergnes M. Susceptibility to focal and generalized seizures in Wistar rats with genetic absence-like epilepsy, *Neurosci.*, 1999; 93: 1173 - 1177.

Brecht M, Preilowski B, Merzenich MM. Functional architecture of the mystacial vibrissae. *Behav. Brain Res.*, 1997; 84: 81-97.

Bronzino JD. Quantitative analysis of the EEG: General concepts and animal studies. *IEEE Trans. Biomed. Eng*., 1984; 31: 850-856.

Bronzino JD. (Ed.) The Biomedical Engineering Handbook, Boca Raton, Fla.: CRC Press, 1995.

Broughton R, Healey T, Maru J, Green D, Pagurek B. A phase locked loop device for automatic detection of sleep spindles and stage 2. *Electroencephalogr. Clin. Neurophysiol*., 1978; 44: 677–680.

Bullock TH, McClune MC, Enright JT. Are the electroencephalograms mainly rhythmic? Assessment of periodicity in wide-band time series Neurosci., 2003, 121(1): 233-252

Burton H, Robinson CJ. Responses in the first or second somatosensory cortical area in cats during transient inactivation of the other ipsilateral area with lidocaine hydrochloride. *Somatosens. Res*., 1987, 4: 215–236.

Buzsáki G, Bickford RG, Ponomareff G, Thal LJ, Mandel R, and Gage FH. Nucleus basalis and thalamic control of neocortical activity in the freely moving rat. *J Neurosci.*, 1988; 8: 4007–4026.

Buzsáki G. The thalamic clock: emergent network properties. *Neurosci.*. 1991, 41: 351-364.

Buzsáki G. Memory consolidation during sleep: a neurophysiological perspective. *J. Sleep Res*. 1998; 7 (Suppl. 1): 17-23.

Buzsaki G, Laszlovszky I, Lajtha A, Vadasz C. Spike-and-wave neocortical patterns in rats: genetic and aminergic control. *Neurosci.*, 1990, 38: 323-333.

Buzsaki G., Kennedy B., Solt B.V., Ziegler M. Noradrenergic control of thalamic oscillation: the role of alpha-2 receptors. *Eur. J. Neurosci*. 1991, 3(3), 222–229.

Bylund DB, Eikenberg DC, Hieble JP, Langer SZ, Lefkowitz RJ, Minneman KP, Molinoff PB, Jr Ruffolo RR, Trendelenburg U. International union of pharmacology nomenclature of adrenoceptors. *Pharmacol. Rev*. 1994, 46: 121-136.

Carvell GE, Simons DJ. Biometric analyses of vibrissal tactile discrimination in the rat. *J Neurosci.*, 1990; 10: 2638-2648.

Campbel K, Kumar A, Hofman W. Human and automatic detection of a phase-locked loop spindle detection system. *Electroencephalogr Clin Neurophysiol*., 1980; 48: 602–605.

Cervo L, Samanin R. Clonidine causes antidepressant-like effects in rats by activating alpha 2-adrenoceptors outside the locus coeruleus. *Eur. J. Pharmacol*., 1991, 193: 309-313.

Castro MI, Eisenach JC Pharmacokinetics and dynamics of intravenous, intrathecal, and epidural clonidine in sheep. *Anesthesiology*. 1989, 71(3), 418-425

Challis RE, Kitney RI. Biomedical signal processing (in four parts). Part 2. The frequency transforms and their inter-relationships. *Med. Biol. Eng. Comput*., 1991; 2: 1-17.

Chapin JK, Lin CS. Mapping the body representation in the SI cortex of anesthetized and awake rats. *J. Comp. Neurol*., 1984, 229: 199–213.

Chapin JK, Woodward DJ. Distribution of somatic sensory and active-movement neuronal discharge properties in the MI-SI cortical border area in the rat. *Exp. Neurol*., 1986; 91: 502-523.

Chatrian GE (Chairman), Bergamini L, Dondey M, Klass DW, Lennox-Buchthal M, Petersen I. A glossary of terms most commonly used by clinical electroencephalographers. *Electroencephalogr Clin Neurophysiol.*, 1974, 37: 538-548.

Chávez M, Martinerie J, Le Van Quyen M. Statistical assessment of nonlinear causality: application to epileptic EEG signals. *J. Neurosci. Methods*, 2003; 124: 113-128

Chui CK. An Introduction to Wavelets. Academic Press Inc, San Diego, CA. 1993.

Civantos Calzada B, Aleixandre de Artinano A, Alpha-adrenoceptor subtypes. *Pharmacol. Res*., 2001, 44: 195-208.

Coenen AM, van Luijtelaar EL. Pharmacological dissociation of EEG and behavior: a basic problem in sleep-wake classification. *Sleep* 1991, 14: 464-465.

Coenen AML. Neuronal activities underlying the electroencephalogram and evoked potentials of sleeping and waking: implications for information processing. *Neurosci. Biobehav. Rev.*, 1995, 19, 447-463.

Coenen A, Zajachkivsky O, Bilski R. In the footsteps of Beck: the desynchronization of the electroencephalogram. *Clin. Electroencephalogr. Clin. Neurophys.* 1998, 106, 330-335.

Coenen AML, van Luijtelaar ELJM. Genetic animal models for absence epilepsy: a review of the WAG/Rij strain of Rats. *Behav. Genetics*, 2003, 33: 635-655. see also *http://www.socsci.ru.nl/wagrij/info.0.html*

Connors BW, Gutnick MJ. Intrinsic firing patterns of diverse neocortical neurons. *Trends Neurosci.* 1990, 13, 99–104.

Craiu D, Magureanu S, van Emde Boas W. Are absences truly generalized seizures or partial seizures originating from or predominantly involving the pre-motor areas? Some clinical and theoretical observations and their implications for seizure classification. *Epilepsy Res*., 2006, 70(Suppl 1): S141-155.

Crick F, Koch C. Constraints on cortical and thalamic projections: the no-strong loops hypothesis. *Nature* 1998; 391(6664): 245–250.

Danober L, Deransart C, Depaulis A, Vergnes M, and Marescaux C. Pathophysiological mechanisms of genetic absence epilepsy in the rat. Prog. Neurobiol., 1998, 55: 27–57

D'Antuono M, Inaba Y, Biagini G, D'Argancelo V, Avoli M. Synaptic hyperexcitability of deep layer neocortical cells in a genetic model of absence seizures. *Genes Brain Behav.,* 2006; 5: 73-84.

Daubechies I. Ten Lectures on Wavelets: Society for Industrial and Applied Mathematics, Philadelphia, PA. 1993.

De Gennaro L, Ferrara M. Sleep spindles: an overview. *Sleep Med. Rev*. 2003; 7: 423-440.

De Gennaro L, Ferrara M, Vecchio F, Curcio G, Bertini M. An electroencephalographic fingerprint of human sleep. *Neuroimage*. 2005; 26: 114–122.

Depaulis A, van Luijtelaar ELJM. Genetic models of absence epilepsy in the rat. In: Pitkänen A, Schwartzkroin PA, Moshé SL (Eds). Models of seizures and epilepsy. Elsevier Academic Press, Amsterdam, 2005, pp. 233-248

Deschênes M, Veinante P, Zhang ZW. The organization of corticothalamic projections: reciprocity versus parity. *Brain Res Brain Res Rev*. 1998, 28: 286-308.

Destexhe A, Sejnowski TJ. Thalamocortical assemblies. Oxford University Press, Oxford. 2001.

Destexhe A. Can $GABA_A$ conductances explain the fast oscillation frequency of absence seizures in rodents? *Eur. J. Neurosci*. 1999; 11: 2175-2181.

Destexhe A, Contreras D, Steriade M. Spatiotemporal analysis of local field potentials and unit discharges in cat cerebral cortex during natural wake and sleep states. 1999; *J. Neurosci.,* 19: 4595– 4608.

Demsey EW, Morison RS. The mechanism of thalamo-cortical augmentation and repetition. *Am J Physiol*, 1942, 138: 297–308.

Dikanev T, Smirnov D, Wennberg R, Perez Velazquez JL, Bezruchko B. EEG nonstationarity during intracranially recorded seizures: statistical and dynamical analysis. *Clin. Neurophysiol*., 2005; 116: 1796-1807.

Drake MEJr, Pakalnis A, Padamadan H, Weate SM, Cannon PA. Sleep spindles in epilepsy. *Clin. Electroencephalogr.*, 1991; 22: 144-149.

Drew GM, Gower AJ, Marriott AS. Alpha 2-adrenoceptors mediate clonidine-induced sedation in the rat, *Br. J. Pharmacol.*, 1979, 67: 133-141.

Drinkenburg WH, Coenen AM, Vossen JM, Van Luijtelaar EL. Spike-wave discharges and sleep-wake states in rats with absence epilepsy. *Epilepsy Res.*, 1991, 9: 218-24.

Drinkenburg WH, van Luijtelaar EL, van Schaijk WJ. Coenen AM Aberrant transients in the EEG of epileptic rats: a spectral analytical approach. *Physiol. Behav*. 1993; 54:779–783.

Durka PJ. Time-frequency analysis of EEG. PhD thesis. Warsaw University. 1996 (*http://brain.fuw.edu.pl/~durka/dissertation/)*

Durka PJ. From wavelets to adaptive approximations: time-frequency parametrization of EEG. *Biomed. Eng. Online*, 2003; 2:1 doi:10.1186/1475-925X-2-1.

Durka PJ, Malinowska U, Szelenberger W, Wakarow A, Blinowska KJ. High resolution parametric description of slow wave sleep. *J. Neurosci. Methods*, 2005; 147:15-21.

Emilien G, Effect of drugs acting on monoaminergic and cholinergic systems on the quantified EEG of rats. *Neuropsychobiol.*, 1989, 21: 205-215.

Fanselow EE, Sameshima K, Baccala LA, Nicolelis MA. Thalamic bursting in rats during different awake behavioral states. Proc. Natl. Acad. Sci. USA, 2001; 98:15330-15335.

Feldmann U, Bhattacharya J. Predictability improvement as an asymmetrical measure of interdependence in bivariate time series. *Int. J Bifurc. Chaos*, 2004; 14: 505-514.

Flint AC, Connors BW. Two types of network oscillations in neocortex mediated by distinct glutamate receptor subtypes and neuronal populations. *J. Neurophysiol*., 1996, 75, 951–957.

Frankhuyzen AL, Mulder AH. Pharmacological characterization of presynaptic alpha-adrenoceptors modulating [3H]noradrenaline and [3H]5-hydroxytryptamine release from slices of the hippocampus of the rat. *Eur. J. Pharmacol*., 1982, 81: 97-106.

Freeman WJ. Mass action in the nervous system. New York, Academic Press, 1975.

French N. Alpha 2-adrenoceptors and I2 sites in the mammalian central nervous system. *Pharmacol. Ther.,* 1995, 68: 175-208.

Ferri R, Iliceto G, Carlucci V. Topographic EEG mapping of 3/s spike-and-wave complexes during absence seizures, *Ital. J. Neurol. Sci*., 1995, 8: 541– 547.

Fojtiková D, Brázdil M, Horký J, Mikl M, Kuba R, Krupa P, Rektor I. Magnetic resonance spectroscopy of the thalamus in patients with typical absence epilepsy. *Seizure*, 2006; 15(7): 533 – 540

Fontana DJ, Schefke DM. Acute versus chronic clonidine treatment effects on conflict behavior in the rat. *Behav. Pharmacol.* 1989, 1: 201-208.

Gandolfo G, Glin L, Gottesmann C. Study of sleep spindles in the rat: a new improvement. Acta Neurobiol. Exp. (Wars), 1985; 45(5-6), 151-62.

Gandolfo G, Romettino S, Gottesmann C, van Luijtelaar G, Coenen A. Genetically epileptic rats show a pronounced intermediate stage of sleep. *Physiol Behav.,* 1990, 47: 213-215.

Gastaut H. A new type of epilepsy: benign partial epilepsy of childhood with occipital spike waves. *Clin. Electroencephalogr*., 1982; 13: 13–22.

Gauguier D, van Luijtelaar G, Bihoreau MT, Wilder SP, Godfrey RF, Vossen J, Coenen A, Cox RD. Chromosomal mapping of genetic loci controlling absence epilepsy phenotypes in the WAG/Rij rat. *Epilepsia,* 2004, 45: 908-915.

Genton P, Guerrini R, Perucca E. Tiagabine in clinical practice. *Epilepsia* 2001, 42 (S3): 42–45.

Gibbs FA, Davis H, Lennox WG. The electroencephalogram in epilepsy and in conditions of impaired consciousness. *Arc Neurol Psych* (Chicago) 1935, 34: 1133-1148

Gibbs FA, Gibbs EL. Atlas of electroencephalography. Addison Wesley Press, Cambridge, 1950 (second edition).

Giorgi F.S., Pizzanelli CF, Biagioni L., Murri Fornai F. The role of norepinephrine in epilepsy: from the bench to the bedside. *Neurosci. Biobehav. Rev.*, 2004, 28: 507-524.

Glenn LL, Steriade M. Discharge rate and excitability of cortically projecting intralaminar thalamic neurons during waking and sleep states. *J Neurosci*.; 1982; 2: 1387-1404.

Gloor P. Generalized cortico-reticular epilepsies: some consideraions on the pathophysiology of generalized bilaterally synchronous spike and wave discharge. *Epilepsia,* 1968; 9: 249-263.

Gloor P. Neurophysiological bases of generalized seizures termed centrencephalic. In: Gaustaut, H., Jasper, H.H., Bancaud, J., Waltregny, A. (Eds.), The Physiopathogenesis of the Epilepsies. Charles C. Thomas, Springfield, IL, 1969, pp. 209–236.

Gloor P. Generalized epilepsy with bilateral synchronous spike and wave discharge. New findings concerning its physiological mechanisms. *Electroenceph Clin Neurophysiol*., Suppl, 1978, 34, 245–249.

Gloor P, Pellegrini A, Kostopoulos GK. Effects of changes in cortical excitability upon the epileptic bursts in generalized penicillin epilepsy of the cat. *Electroencephalogr Clin Neurophysiol.* 1979; 46(3): 274-289.

Gloor P, Avoli M. and Kostopoulos G. Thalamocortical relationships in generalized epilepsy with bilaterally synchronous spike-and-wave discharge. In: Avoli, M., Gloor, P., Kostopoulos, G. and Naquet, R. (Eds) Generalized epilepsy: neurobiological approaches, Birkhauser, Boston, MA, 1990, pp. 190–212.

Gobert A, Rivet JM, Audinot V, Newman-Tancredi A, Cistarelli L, Millan MJ. Simultaneous quantification of serotonin, dopamine and noradrenaline levels in single frontal cortex dialysates of freely-moving rats reveals a complex pattern of reciprocal auto-and heteroreceptor-mediated control of release. *Neurosci*., 1998, 84: 413–429.

Gottesmann C. The transition from slow-wave sleep to paradoxical sleep: evolving facts and concepts of the neurophysiological processes underlying the intermediate stage of sleep. *Neurosci Biobehav Rev*. 1996; 20(3): 367-387.

Goldensohn ES, Porter RJ, Schwartzkroin PA. The American Epilepsy Society: an historic perspective on 50 years of advances in research. *Epilepsia*. 1997 38(1): 124-150.

Granger CWJ. Investigating causal relations by econometric models and cross-spectral methods. *Econometrica*, 1969; 37: 424-438.

Gray CM, McCormick DA. Chattering cells: superficial pyramidal neurons contributing to the generation of synchronous oscillations in the visual cortex. *Science,* 1996; 274: 109-113.

Grenier F, Timofeev I, Crochet S, Steriade M. Neocortical very fast oscillations (ripples, 80–200 Hz) during seizures: intracellular correlates. *J. Neurophysiol.,* 2003, 89: 841–852.

Grossman A, Morlet J. Decomposition of Hardy function into square integrable wavelets of constant shape. *SIAM J. Math. Anal*., 1984; 15: 723-736.

Guazzelli M, Feinberg I, Aminoff M, Fein G, Floyd TC, Maggini C. Sleep spindles in normal elderly: comparison with young adult patterns and relation to nocturnal awakening, cognitive function and brain atrophy. *Electroencephalogr. Clin. Neurophysiol*., 1986; 63: 526–539.

Guillery RW, Feig SL, Lozsadi DA. Paying attention to the thalamic reticular nucleus. *Trends Neurosci.,* 1998; 21: 28-32.

Happe HK, Coulter CL, Gerety ME, Sanders JD, O'Rourke M, Bylund DB, Murrin LC. Alpha-2 adrenergic receptor development in rat CNS: an autoradiographic study. *Neurosci.,* 2004 123: 167-178.

Haidarliu S, Ahissar E. Size gradients of barreloids in the rat thalamus. *J. Comp. Neurol*., 2001; 429: 372-387.

Halász P. Sleep, arousal and electroclinical manifestations of generalized epilepsy with spike wave pattern. *Epilepsy Res*., 1991; Suppl 2: 43-48.

Halász P, Terzano MG, Parrino L. Spike-wave discharge and the microstructure of sleep-wake continuum in idiopathic generalised epilepsy. *Neurophysiol. Clin.*, 2002; 32: 38-53.

Hayashi Y, Maze M. Alpha-2 adrenoceptor agonists and anaesthesia. *Br. J. Anaesth*., 1993, 71: 108-118.

Hayne RA, Belinson L, Gibbs FA Electrical activity of subcortical areas in epilepsy. *Electroencephalogr Clin Neurophysiol.,* 1949, 1: 437-445.

Himanen SL, Hasan J. Limitations of Rechtschaffen and Kales. *Sleep Med. Rev.* 2000; 4: 149-167.

Holmes MD, Brown M, Tucker DM. Are "Generalized" seizures truly generalized? Evidence of localized mesial frontal and frontopolar discharges in absence. *Epilepsia,* 2004, 45: 1568-1579.

Hlavackova-Schindler K, Palus M, Vejmelka M, Bhattacharya J. Causality detection based on information-theoretic approaches in time series analysis. *Physics Reports*, 2007; 441: 1-46.

Huguenard JR, McCormick DA. Thalamic synchrony and dynamic regulation of global forebrain oscillations. *Trends Neurosci.,* 2007; 30: 350-356.

Huupponen E, Gómez-Herrero G, Saastamoinen A, Värri A, Hasan J, Himanen SL. Development and comparison of four sleep spindle detection methods. *Artif. Intell. Med*., 2007; 40: 157-170.

Inoue M, van Luijtelaar ELJM, Vossen JMH, Coenen AML. Visual evoked potentials during spontaneously occurring spike-wave discharges in rats. *Electroencephalogr. Clin. Neurophysiol*., 1992; 84: 172–179.

Inoue M, Duysens J, Vossen JMH, Coenen AML. Thalamic multiple unit activity underlying spike-wave discharges in anesthetized rats. *Brain Res.,* 1993; 612: 35–40.

[IFSECN] International Federation of Societies for Electroencephalography and Clinical Neurophysiology. A glossary of terms most commonly used by clinical electroencephalographers. Electroencephalogr. *Clin. Neurophysiol*., 1974, 37: 538-553.

Ishii R, Dziewas R, Chau W, Soros P, Okamoto H, Gunji A, Pantev C. Current source density distribution of sleep spindles in humans as found by synthetic aperture magnetometry. *Neurosci. Lett.*, 2003, 340: 25-28.

Jacobsen RB, Ulrich D, Huguenard JR. $GABA_B$ and NMDA receptors contribute to spindle-like oscillations in rat thalamus in vitro. *J Neurophysiol*., 2001; 86: 1365–1375.

Jankel WR, Niedermeyer E. Sleep spindles. *J. Clin. Neurophysiol.,* 1985; 2: 1-35.

Janz D. Epilepsy and the sleeping-waking cycle. In Handbook of Clinical Neurology, Vol. 15, The Epilepsies. Ed. P.J Vincken and G.W Bruyn. North Holland, Amsterdam. 1974, pp. 457–490.

Jasper HH, Kershman J. Electroencephalographic classification of the epilepsies. *Arch Neurol Psychiatry.,* 1941; 45: 903-943.
Jasper HH, Drooglever-Fortuyn J. Experimental studies on the functional anatomy of petit mal epilepsy. *Res Publ Ass Res Nerv Ment Dis.* 1946, 26: 272–298.

Jirsch JD, Urrestarazu E, LeVan P, Olivier A, Dubeau F, Gotman J. High-frequency oscillations during human focal seizures. *Brain,* 2006, 129(Pt 6): 1593-608.

Jobert M, Tismer C, Poiseau E, Schulz H. Wavelets - a new tool in sleep biosignal analysis. *J. Sleep Res*., 1994; 3:223–232.

Jobert M, Poiseau E, Jahnig P, Schulz H, Kubicki S. Topographical analysis of sleep spindle activity. *Neuropsychobiol.*, 1992, 26: 210-217.

Jones EG. The Thalamus. Plenium Press, New York, 1985. 955pp.

Jones EG. The Thalamus Revisited. Cambridge University Press, Cambridge, U.K. 2006.

Jones LS, Gauger LL, Davis JN, Anatomy of brain alpha 1-adrenergic receptors: in vitro autoradiography with [125I]-heat. *J. Comp. Neurol.,* 1985. 231: 190-208.

Jones BE, Moore RY. Ascending projections of the locus coeruleus in the rat. II. Autoradiographic study, *Brain Res.,* 1977, 127: 25-53.

Kaminski M, Ding M, Truccolo WA, Bressler SL. Evaluating causal relations in neural systems: Granger causality, directed transfer function and statistical assessment of significance. *Biol. Cybern*., 2001; 85: 145–157.

Kaiser G. A Friendly Guide to Wavelets. Birkhäuser, Boston. 1994.

Kandel A, Buzsaki G. Cellular-synaptic generation of sleep spindles, spike-and-wave discharges, and evoked thalamocortical responses in the neocortex of the rat. *J Neurosci*., 1997, 17: 6783-6797.

Kaplan AYa. Nonstationarity of EEG: methodological and experimental analysis. *Uspekhi fiziol. Nauk*, 1998; 29(3): 35-55.

Karpova AV, Bikbaev AF, Coenen AM, van Luijtelaar G. Morphometric Golgi study of cortical locations in WAG/Rij rats: the cortical focus theory. *Neurosci Res.,* 2005, 51: 119-128.

Kellaway P. Sleep and epilepsy. *Epilepsia*, 1985; 26 Suppl. 1: S15-30.

Khan YU, Gotman J. Wavelet based automatic seizure detection in intracerebral electroencephalogram. *Clin. Neurophysiol*., 2003; 114: 898-908.

Kim D, Song U, Keum S, Lee T, Jeong M-J, Kim S-S, McEnery MW, Shin HS. Lack of the burst firing of thalamocortical relay neurons and resistance to absence seizures in mice lacking the alpha-1G T-type $Ca2^{+}$ channels. *Neuron*, 2001; 31: 35-45.

Kitchigina VF, Kutyreva EV, Brazhnik ES. Modulation of theta rhythmicity in the medial septal neurons and the hippocampal electroencephalogram in the awake rabbit via actions at noradrenergic alpha2-receptors. *Neurosci*., 2003, 120: 509-521.

Kleinlogel H. Spontaneous EEG paroxysms in the rat: effects of psychotropic and alpha-adrenergic agents. *Neuropsychobiol.*, 1985, 13: 206-213.

Kleinfeld D, Berg RW, O'Connor SM. Anatomical loops and their electrical dynamics in relation to whisking by rat. *Somatosens Mot Res*., 1999; 16: 69–88.

Klupp H, Knappen F, Otsuka Y, Streller I, Teichmann H. Effects of Clonidine on central sympathetic tone. *Eur. J. Pharmacol.,* 1970, 10(2): 225-229.

Kole MH, Bräuer AU, Stuart GJ. Inherited cortical HCN1 channel loss amplifies dendritic calcium electrogenesis and burst firing in a rat absence epilepsy model. *J Physiol*., 2007; 578: 507-525.

Kolb B, Organization of the neocortex in rat. In: Kolb B, Tees R. (eds). The cerebral cortex of the rat. The MIT Press, Cambridge, Massachusetts; London. 1990: 21-48.

Kolb B, Walkey J. Behavioural and anatomical studies of the posterior parietal cortex in the rat. *Behav. Brain Res*., 1987; 23: 127-145.

Koronovskii AA, Hramov AE. Continuous Wavelet Analysis and Its Applications. Fizmatlit, Moscow. 2003. [In Russian].

Kostopoulos GK. Spike-and-wave discharges of absence seizures as a transformation of sleep spindles: the continuing development of a hypothesis. *Clin Neurophysiol.* 2000, Suppl. 2: S27-38.

Langer SZ. Presynaptic regulation of catecholamine release. *Biochem. Pharmacol*. 1974, 23: 1793-1800.

Lannes B, Micheletti G, Vergnes M, Marescaux C, Depaulis A, Warter JM. Relationship between spike-wave discharges and vigilance levels in rats with spontaneous petit mal-like epilepsy. *Neurosci. Lett.*, 1988, 94: 187-191.

Landolt HP, Dijk DJ, Achermann P, Borbely AA. Effect of age on the sleep EEG: slow-wave activity and spindle frequency activity in young and middle-aged men. *Brain Res*., 1996; 738: 205-212.

Latka M, Was Z, Kozik A, West BJ. Wavelet analysis of epileptic spikes. *Phys. Rev. E*, 2003; 67: 052902-052906.

Latka M, Kozik A, Jernajczyk J, West BJ, Jernajczyk W. Wavelet mapping of sleep spindles in young patients with epilepsy. *J. Physiol. Pharmacol*., 2005; 56 Suppl 4: 15-20.

Le Van Quyen M, Martinerie J, Adam C, Varela F. Nonlinear analyses of interictal EEG map the brain interdependences in human focal epilepsy. *Physica D*, 1999; 127: 250-266.

Le Van Quyen M, Foucher J, Lachaux J, Rodriguez E, Lutz A, Martinerie J, Varela FJ. Comparison of Hilbert transform and wavelet methods for the analysis of neuronal synchrony. *J. Neurosci. Methods,* 2001; 111: 83-98.

Le Van Quyen M, Bragin A. Analysis of dynamic brain oscillations: methodological advances. *Trends Neurosc*i., 2007; 30: 365-.73.

Lemieux JF, Blume WT. Topographical evolution of spike-wave complexes. *Brain Res*., 1986, 373: 275-287.

Leutmezer F, Lurger S, Baumgartner C. Focal features in patients with idiopathic generalized epilepsy. *Epilepsy Res.* 2002, 50, 293–300

Lopes da Silva F, van Rotterdam A. Biophysical aspects of EEG and MEG generation. In: Niedermeyer E, Lopes da Silva F (Eds), Electroencephalography. Basic principles, clinical applications and related fields. Urban & Schwarzenberg, Baltimore, Munich, 1982: 5-26 (next edition 1987: 29-41).

Lopes da Silva FH, Givens AS, Remond A. (Eds.) Handbook of Electroencephalography and Clinical Neurophysiology. Elsevier Science Publisher B.V., Amsterdam, 1986.

Lopes da Silva FH, Electrical potentials. In: Ramachandran VS (Ed.), Encyclopedia of the human brain. Elsevier Science, 2002, pp. 147–167.

Luhmann HJ, Mittmann T, van Luijtelaar G, Heinemann U. Impairment of intracortical GABAergic inhibition in a rat model of absence epilepsy. *Epilepsy Res*., 1995, 22: 43-51.

Lüders H, Lesser RP, Dinner DS, Morris HH III. Generalized epilepsies: a review. Cleve Clin Q. 1984, 51: 205-226.

Mackenzie L, Pope KJ, Willoughby JO. Physiological and pathological spindling phenomena have similar regional EEG power distributions. *Brain Res*., 2004; 15: 92-106.

Malpeli JG, Schiller PH. A method of reversible inactivation of small regions of brain tissue. *J. Neurosci. Methods,* 1979, 1: 143– 151.

Manning JP, Richards DA, Bowery NG. Pharmacology of absence epilepsy. *Trends Pharmacol. Sci*., 2003; 24: 542– 549.

Manning JP, Richards DA, Leresche N, Crunelli V, Bowery NG. Cortical-area specific block of genetically determined absence seizures by ethosuximide. Neuroscience. 2004, 123(1): 5-9.

Marescaux C, Vergnes M, Depaulis A. Genetic absence epilepsy in rats from Strasbourg: a review. *J Neural Transm* [Suppl] 1992a, 35: 37– 69.

Marescaux C, Vergnes M, Depaulis A. Neurotransmission in rats' spontaneous generalized nonconvulsive epilepsy. *Epilepsy Res*. 1992b, Suppl. 8: 335-343.

Martin JH, Ghez C. Pharmacological inactivation in the analysis of the central control of movement, *J. Neurosci. Methods,* 1999, 86: 145– 159.

Maura G, Gemignani A, Raiteri M. Alpha 2-adrenoceptors in rat hypothalamus and cerebral cortex: functional evidence for pharmacologically distinct subpopulations. *Eur. J. Pharmacol*., 1985, 116: 335–339.

McCormick D.A. Cholinergic and noradrenergic modulation of thalamocortical processing. Trends Neurosci., 1989, 12(6): 215-221.

McCormick DA, Pape HC, Williamson A. Actions of norepinephrine in the cerebral cortex and thalamus: implications for function of the central noradrenergic system. *Prog. Brain Res*. 1991, 88: 293–305.

McCormick DA. Cortical and subcortical generators of normal and abnormal rhythmicity. *Int. Rev. Neurobiol*., 2002; 49: 99-114.

McCormick L, Nielsen T, Nicolas A, Ptito M, Montplaisir J. Topographical distribution of spindles and K-complexes in normal subjects. *Sleep*. 1997; 20(11): 939-941.

Medvedev AV. Epileptiform spikes desynchronize and diminish fast (gamma) activity of the brain: An “anti-binding” mechanism? *Brain Res. Bull*., 2002; 58: 115-128.

Meencke HJ, Janz D. Neuropathological findings in primary generalized epilepsy: a study of eight cases. *Epilepsia,* 1984, 25: 8-21.

Meeren HKM, van Luijtelaar ELJM, Coenen AML, Cortical and thalamic visual evoked potentials during sleep–wake states and spike-wave discharges in the rat. *Electroencephalogr. Clin. Neurophysiol*., 1998; 108: 306–319

Meeren HKM. Cortico-thalamic mechanisms underlying generalized spike-wave discharges of absence epilepsy. A lesional and signal analytical approach in the WAG/Rij rat. Nijmegen University, PhD thesis, 2002.

Meeren HK, Pijn JP, Van Luijtelaar EL, Coenen AM, Lopes da Silva FH. Cortical focus drives widespread corticothalamic networks during spontaneous absence seizures in rats. *J Neurosci*. 2002; 22: 1480-1495.

Meeren H, van Luijtelaar G, Lopes da Silva F, Coenen A. Evolving concepts on the pathophysiology of absence seizures: the cortical focus theory. *Arch Neurol.* 2005, 62: 371-376.

Merica H, Fortune RD. The neuronal transition probability model applied to the simulation of frequency continuity in NREM sleep. *Sleep Res. Online*, 1999; 2 (Suppl.1): 64.

Micheletti G., Warter J. M., Marescaux C., Depaulis A., Tranchant C., Rumbach L., Vergnes, M. Effects of drugs affecting noradrenergic neurotransmission in rats with spontaneous petit mal-like seizures. *Eur. J. Pharmacol*., 1987, 135: 397-402.

Midzianovskaia IS, Kuznetsova GD, Coenen AM, Spiridonov AM, van Luijtelaar EL. Electrophysiological and pharmacological characteristics of two types of spike-wave discharges in WAG/Rij rats. *Brain Res*., 2001, 911: 62-70.

Miller MW. Maturation of rat visual cortex: IV. The generation, migration, morphogenesis, and connectivity of atypically oriented pyramidal neurons. *J. Comp. Neurol*., 1988; 274: 387-405.

Moeller F, Siebner HR, Wolff S, Muhle H, Granert O, Jansen O, Stephani U, Siniatchkin M. Simultaneous EEG-fMRI in drug-naive children with newly diagnosed absence epilepsy. *Epilepsia*, 2008a. DOI 10.1111/j.1528-1167.2008.01626.x.

Moeller F, Siebner HR, Wolff S, Muhle H, Boor R, Granert O, Jansen O, Stephani U, Siniatchkin M. Changes in activity of striato-thalamo-cortical network precede generalized spike wave discharges. *Neuroimage*, 2008b; 39(4): 1839-1849.

Morin D, Steriade M. Development from primary to augmenting responses in the somatosensory system. Brain Res 1981, 205: 49–66.

Morison RS, Demsey EW. A study of thalamo-cortical relations. *Am J Physiol*, 1947; 135: 281–292.

Mormann F, Andrzejak RG, Elger CE, Lehnertz K. Seizure prediction: the long and winding road. *Brain*, 2007; 130 (Pt 2): 314-333.

Myatchin I, Lagae L. Sleep spindle abnormalities in children with generalized spike-wave discharges. *Pediatr. Neurol.,* 2007; 36: 106-111.

Nashmi R, Mendonca AJ, MacKay WA, EEG rhythms of the sensorimotor region during hand movements. Electroencephalogr. *Clin. Neurophysiol.,* 1994; 91: 456-467.

Neafsey EJ. The complete ratunculus: output organization of layer V of the cerebral cortex. In: Kolb, B. and Tees, R. (Eds) The cerebral cortex of the rat. Cambridge, MA: MIT Press, 1990: 197-210.

Nicolelis MA, Baccala LA, Lin RC, Chapin JK. Sensorimotor encoding by synchronous neural ensemble activity at multiple levels of the somatosensory system, *Science,* 1995, 268: 1353–1358.

Nicolelis MA, Fanselow EE. Thalamocortical optimization of tactile processing according to behavioral state. Nature *Neurosci*., 2002, 5: 517–523.

Niedermeyer E. The Generalized Epilepsies: A clinical electroencephalographical study. Springfield, Ill: Charles C Thomas Publisher; 1972.

Niedermeyer E. Primary (idiopathic) generalized epilepsy and underlying mechanisms. *Clin. Electroencephalogr.*, 1996, 27: 1–21.

Nuñez A, Curro Dossi R, Contreras D, Steriade M. Intracellular evidence for incompatibility between spindle and delta oscillations in thalamocortical neurons of cat. *Neurosci.*, 1992, 48: 75-85.

Ohara PT, Lieberman AR, Hunt SP, Wu JL. Neuronal elements containing GAD in the dorsal LGN of the rat: immunocytochemical studies by light and electron microscopy. *Neurosci.* 1983, 8: 189–211.

Osaka T, Matsumura H. Noradrenaline inhibits preoptic sleep-active neurons through alpha 2-receptors in the rat. *Neurosci. Res*., 1995, 21: 323-330.

Panayiotopoulos CP. Typical absence seizures and their treatment. *Arch. Dis. Child*., 1999, 81(4): 351-355

Panayiotopoulos CP. Benign childhood epileptic syndromes with occipital spikes: a new classification proposed by the International League Against Epilepsy. *J Child Neurol.,* 2000; 15: 548–552.

Panayiotopoulos CP. Idiopathic generalised epilepsies. In: Panayiotopoulos CP (Ed) The Epilepsies: Seizures, Syndromes and Management: Bladon Medical Publishing, Oxford, 2005, pp. 271-348.

Pastel RH, Fernstrom JD. The effects of clonidine on EEG wavebands associated with sleep in the rat. *Brain Res*. 1984, 300: 243-255.

Paxinos G, Watson C. The rat brain in stereotaxic coordinates. Academic Press, New York, 1986.

Pellegrini A, Musgrave J, Gloor P. Role of afferent input of subcortical origin in the genesis of bilaterally synchronous epileptic discharges of feline generalized epilepsy. *Exp. Neurol*., 1979; 64: 155- 173.

Pereda E, Quian Quiroga R, Bhattacharya J. Nonlinear multivariate analysis of neurophysiological signals. *Prog. Neurobiol.,* 2005; 77: 1-37.

Pickworth WB, Sharpe LG, Gupta VN. Morphine-like effects of clonidine on the EEG, slow wave sleep and behavior in the dog. *Eur. J. Pharmacol*., 1982, 81: 551-557.

Pierret T, Lavallee P, Deschenes M. Parallel streams for the relay of vibrissal information through thalamic barreloids. *J. Neurosci.,* 2000; 20: 7455-7462.

Pinault D, Vergnes M, Marescaux C. Medium-voltage 5-9-Hz oscillations give rise to spike-and-wave discharges in a genetic model of absence epilepsy: in vivo dual extracellular recording of thalamic relay and reticular neurons. *Neurosci*. 2001 105(1) 181-201.

Pinault D. Cellular interactions in the rat somatosensory thalamocortical system during normal and epileptic 5-9 Hz oscillations. *J Physiol*., 2003; 552(3): 881-905.

Pinault D, Slezia A, Acsady L. Corticothalamic 5-9 Hz oscillations are more pro-epileptogenic than sleep spindles in rats. *J Physiol.,* 2006; 574(Pt 1): 209-227.

Polack PO, Guillemain I, Hu E, Deransart C, Depaulis A, Charpier S. Deep layer somatosensory cortical neurons initiate spike-and-wave discharges in a genetic model of absence seizures. *J Neurosci*., 2007; 27: 6590–6599.

Pollen DA. Intracellular studies of cortical neurons during thalamic induced wave and spike. *Electroencephalogr. Clin. Neurophysiol,*, 1964; 17:398-404.

Quian Quiroga R, Arnhold J, Grassberger P. Learning driver-response relationships from synchronization patterns. *Phys. Rev. E*, 2000, 61: 5142–5148.

Quesney LF, Andermann F, Gloor P. Dopaminergic mechanism in generalized photosensitive epilepsy, *Neurology,* 1981; 31: 1542–1544.

Raevsky VV. Ontogenesis of Transmitter Systems. Nauka, Moscow. 1991. 144 p. [in Russian]

Rechtschaffen A, Kales AA. Manual of Standardized Terminology, Technique and scoring System for Sleep Stages of Human Subjects. Public Health Service, U.S. Government Printing Office, 1968.

Richards DA, Manning JP, Barnes D, Rombola L, Bowery NG, Caccia S, Leresche N, Crunelli V. Targeting thalamic nuclei is not sufficient for the full anti-absence action of ethosuximide in a rat model of absence epilepsy, Epilepsy Res. 2003, 54: 97–107.

Ritz R, Sejnowski TJ. Synchronous oscillatory activity in sensory systems: new vistas on mechanisms, *Curr. Opin. Neurobiol*., 1997, 7: 536– 546.

Rodin E., Ancheta O. Cerebral electrical fields during petit mal absences. *Electroencephalogr Clin Neurophysiol*., 1987, 66: 457-466.

Rodin E, Cornellier D. Source derivation recordings of generalized spike-wave complexes. *Electroencephalogr Clin Neurophysiol*., 1989, 73: 20-29.

Rodin E. Decomposition and mapping of generalized spike-wave complexes. *Clin Neurophysiol.,* 1999, 110: 1868-1875.

Rodin EA, Rodin MK, Thompson JA. Source analysis of generalized spike –wave complexes, *Brain Topogr*. 1994; 7: 113–119.

Ross J, Johnson LC, Walter RD. Spike and wave discharges during stages of sleep. *Arch Neurol*., 1966: 399–407.

Rouiller EM, Welker E. A comparative analysis of the morphology of corticothalamic projections in mammals. *Brain Res. Bull.*, 2000, 53: 727–741.

Ruffolo JrRR, Hieble JP. Alpha-adrenoceptors, *Pharmacol Ther.*, 1994, 61: 1-64.

Sabers A, Moller A, Scheel-Kruger J, Mouritzen Dam A. No loss in total neuron number in the thalamic reticular nucleus and neocortex in the genetic absence epilepsy rats from Strasbourg. *Epilepsy Res*., 1996; 26: 45–48.

Sargsyan A, Sitnikova E, Melkonyan A, Mkrtchian H, van Luijtelaar G. Simulation of sleep spindles and spike and wave discharges using a novel method for the calculation of field potentials in rats. *J Neurosci. Methods*. 2007; 164(1): 161-176.

Sato S, Dreifuss FE, Penry JK. The effect of sleep on spike-wave discharges in absence seizures. *Neurology*. 1973, 23: 1335–1345.

Schabus M, Modlmoser K, Gruber G, Sauter C, Anderer P, Klosch G, Parapatics S, Saletu B, Klimesch W, Zeitlhofer J. Sleep spindle-related activity in the human EEG and its relation to general cognitive and learning abilities. *Eur. J. Neurosci*. 2006; 23: 1738-1746.

Scheibner J, Trendelenburg AU, Hein L, Starke K. Alpha 2-Adrenoceptors modulating serotonin release: a study in alpha-2 adrenoceptor subtype-deficient mice. *Brit. J. Pharmacol*., 2001, 132: 925–933.

Schimicek P, Zeitlhofer J, Anderer, P. and Saletu, B. Automatic sleep-spindle detection procedure: aspects of reliability and validity. *Clin. Electroencephalogr*., 1994, 25: 26-29.

Schonwald SV, Gerhardt GJL, de Santa-Helena EL, Chaves MLF. Characteristics of human EEG sleep spindles assessed by Gabor transform. *Physica A* , 2003; 327: 180-184.

Schridde U, van Luijtelaar G. The role of the environment on the development of spike-wave discharges in two strains of rats. *Physiol Behav*., 2005, 84: 379-386.

Schiff SJ, So P, Chang T, Burke RE, Sauer T. Detecting dynamical interdependence and generalized synchrony through mutual prediction in a neural ensemble. *Phys. Rev. E*, 1996; 54: 6708-6724.

Schwarz SK, Puil E. Analgesic and sedative concentrations of lignocaine shunt tonic and burst firing in thalamocortical neurones. *Br. J. Pharmacol*., 1998, 124(8), 1633-1642.

Seidel WF, Maze M, Dement WC, Edgar DM. Alpha-2 adrenergic modulation of sleep: time-of-day-dependent pharmacodynamic profiles of dexmedetomidine and clonidine in the rat. *J. Pharmacol. Exp. Ther*., 1995, 275: 263-273.

Seidenbecher T, Pape HC. Contribution of intralaminar thalamic nuclei to spike-and-wave-discharges during spontaneous seizures in a genetic rat model of absence epilepsy. *Eur J Neurosci.,* 2001; 13: 1537–1546

Seidenbecher T, Staak R, Pape HC. Relations between cortical and thalamic cellular activities during absence seizures in rats. *Eur J Neurosci*., 1998; 10(3): 1103-1112

Semba K, Komisaruk BR. Neural substrates of two different rhythmical vibrissal movements in the rat, *Neurosci*., 1984, 12: 761– 774.

Senhadji L, Wendling F. Epileptic transient detection: wavelets and time-frequency approaches. *Neurophysiol. Clin*., 2002; 32: 175-192.

Sherman SM, Guillery RW. Exploring the thalamus and its role in cortical function. MIT Press, Cambridge. 2006.

Shih, J.J., Weisend, M.P., Davis, J.T. and Huang, M. Magnetoencephalographic characterization of sleep spindles in humans. J. Clin. Neurophysiol., 2000, 17: 224-231.

Silva LR, Amitai Y, Connors BW. Intrinsic oscillations of neocortex generated by layer 5 pyramidal neurons. *Science*, 1991; 251; 432–435

Sitnikova E, van Luijtelaar G. Cortical and thalamic coherence during spike-wave seizures in WAG/Rij rats. *Epilepsy Res.,* 2006, 71: 159-180.

Sitnikova E, van Luijtelaar G. Electroencephalographic characterization of Spike-Wave Discharges in cortex and thalamus in WAG/Rij rats. Epilepsia, 2007, 48 (12), 2296–2311

Slaght SJ, Leresche N, Deniau JM, Crunelli V, Charpier S. Activity of thalamic reticular neurons during spontaneous genetically determined spike and wave discharges. *J. Neurosci*., 2002; 22: 2323–2334.

Slobounov S, Ray W, Cao C, Chiang H. Modulation of cortical activity as a result of task-specific practice. *Neurosci. Lett*. 2007; 421: 126-131.

Steriade M. Interneuronal epileptic discharges related to spike-and-wave cortical seizures in behaving monkeys. *Electroencephalogr. Clin. Neurophysiol*., 1974; 37;247-263.

Steriade M, Deschenes M. The thalamus as a neuronal oscillator. *Brain Res. Rev.*, 1984, 8: 1-63.

Steriade M, Llinas RR. The functional states of the thalamus and the associated neuronal interplay. *Physiol. Rev.,* 1988; 68: 649–742.

Steriade M, McCormick DA, Sejnowski TJ. Thalamocortical oscillation in the sleeping and aroused brain. *Science* 1993; 262; 679–685.

Steriade M, Amzica F. Dynamic coupling among neocortical neurons during evoked and spontaneous spike-wave seizure activity. *J. Neurophy*siol., 1994; 72: 2051–2069.

Steriade M, Contreras D. Spike-wave complexes and fast components of cortically generated seizures. I. Role of neocortex and thalamus. *J. Neurophysiol*., 1998; 80: 1439-1455.

Steriade M. Cortical coupling in sleep and paroxysmal oscillations. *International Congress Series*, 2002; 1226: 71-85 (doi:10.1016/S0531-5131(01)00498-8)

Steriade M. Neuronal substrates of sleep and epilepsy. Cambridge University Press, Cambridge. 2003

Steriade M. Impact of network activities on neuronal properties in corticothalamic systems. *J. Neurophysiol.,* 2001; 86; 1–39.

Steriade M. Sleep, epilepsy and thalamic reticular inhibitory neurons. *Trends Neurosci*. 2005; 28(6): 317-324.

Steriade M. Grouping of brain rhythms in corticothalamic systems. *Neurosci*., 2006; 137: 1087-1106.

Strauss U, Kole MH, Bräuer AU, Pahnke J, Bajorat R, Rolfs A, Nitsch R, Deisz RA. An impaired neocortical Ih is associated with enhanced excitability and absence epilepsy. *Eur J Neurosci*., 2004; 19: 3048-3058.

Suffczynski P, Kalitzin S, Lopes Da Silva FH. Dynamics of non-convulsive epileptic phenomena modeled by a bistable neuronal network. *Neurosci.,* 2004; 126: 467-484.

Svensson TH, Bunney BS, Aghajanian GK. Inhibition of both noradrenergic and serotonergic neurons in brain by the alpha-adrenergic agonist clonidine. *Brain Res*, 1975, 92(2), 291-306.

Swanson LW, Hartman BK. The central adrenergic system. An immunofluorescence study of the location of cell bodies and their efferent connections in the rat utilizing dopamine-beta-hydroxylase as a marker. *J. Comp. Neurol*., 1975, 163: 467-505.

Szabo B. Imidazoline antihypertensive drugs: a critical review on their mechanism of action. *Pharmacol Ther*. 2002, 93(1): 1-35.

Szot P, Weinshenker D, White SS, Robbins CA, Rust NC, Schwartzkroin PA, Palmiter RD. Norepinephrine-deficient mice have increased susceptibility to seizure-inducing stimuli. *J. Neurosci*. 1999, 19: 10985–10992.

Tehovnik EJ, Sommer MA. Effective spread and time course of neural inactivation caused by lidocaine injection in monkey cerebral cortex. *J. Neurosci. Methods,* 1997, 74: 17– 26.

Temkin O. The Falling Sickness. A history of epilepsy from the Greeks to the beginnings of modern neurology, 2-nd Ed. Johns Hopkins Press, Baltimore. 1971.

Tenney JR, Duong TQ, King JA, Ludwig R, Ferris CF. Corticothalamic modulation during absence seizures in rats: a functional MRI assessment. *Epilepsia,* 2003; 44: 1133–1140.

Terrier G, Gottesmann CL. Study of cortical spindles during sleep in the rat. *Brain Res. Bull*., 1978, 3(6): 701-706.

Timofeev I, Grenier F, Steriade M. Spike-wave complexes and fast components of cortically generated seizures. IV. Paroxysmal fast runs in cortical and thalamic neurons. *J Neurophysiol.,* 1998, 80: 1495-1513.

Timofeev I, Bazhenov M, Sejnowski TJ, Steriade M. Cortical hyperpolarization-activated depolarizing current takes part in the generation of focal paroxysmal activities. *Proc. Natl. Acad. Sci. USA*, 2002; 99: 9533-9537.

Timofeev I, Steriade M. Neocortical seizures: initiation, development and cessation. Neurosci., 2004, 123: 299–336.

Tolmacheva EA, van Luijtelaar G, Chepurnov SA, Kaminskij Y, Mares P. Cortical and limbic excitability in rats with absence epilepsy. *Epilepsy Res*., 2004; 62: 189-198.

Uchida S, Maloney T, March JD, Azari R, Feinberg I. Sigma (12-15 Hz) and delta (0.3-3 Hz) EEG oscillate reciprocally within NREM sleep. *Brain Res. Bull.*, 1991, 27: 93-96.

Ueda K, Nittono H, Hayashi M, Hori T. Estimation of generator sources of human sleep spindles by dipole tracing method. Psychiatry *Clin. Neurosci*., 2000, 54: 270-271.

Uhlhaas PJ, Singer W. Neural synchrony in brain disorders: relevance for cognitive dysfunctions and pathophysiology. *Neuron*, 2006; 52(1): 155-168.

Vadász C, Carpi D, Jando´ G, Kandel A, Urioste R, Horvath Z, Pierre E, Vadi D, Fleischer A, Buzsáki G. Genetic threshold model of rodent spike-and-wave epilepsy. *Am J Med Genet.,* 1995; 60: 55–63.

van de Bovenkamp-Janssen MC, Korosi A, Veening JG, Scheenen WJJM, van Luijtelaar ELJM, Roubos EW. Neuronal parvalbumin and absence epilepsy in WAG/Rij rats. In: van Luijtelaar G, Kuznetsova GD, Coenen A, Chepurnov S (eds) *The WAG/Rij model of absence epilepsy: The Nijmegen-Russian Federation papers*. NICI, Nijmegen, 2004: 29-36.

van Hese P, Martens JP, Boon P, Dedeurwaerdere S, Lemahieu I, Van de Walle R. Detection of spike and wave discharges in the cortical EEG of genetic absence epilepsy rats from Strasbourg. *Phys Med Biol*., 2003; 48(12): 1685-1700.

van Luijtelaar ELJM, Coenen AML. Two types of electrocortical paroxysms in an inbred strain of rats. *Neurosci. Lett.* 1986, 70, 393-397.

van Luijtelaar EL, Coenen AM. Circadian rhythmicity in absence epilepsy in rats. *Epilepsy Res*. 1988; 2(5): 331-336

van Luijtelaar ELJM. Spike-wave discharges and sleep spindles in rats. *Acta Neurobiol Exp* (Warsz). 1997; 57(2): 113-121.

van Luijtelaar G, Budziszewska B, Jaworska-Feil L, Ellis J, Coenen A, Lason W. The ovarian hormones and absence epilepsy: a long-term EEG study and pharmacological effects in a genetic absence epilepsy model. *Epilepsy Res*., 2001, 46: 225 – 239.

van Luijtelaar G, Sitnikova E. Global and focal aspects of absence epilepsy: the contribution of genetic model. *Neurosci Biobehav Rev.,* 2006, 30: 983-1003.

van Luijtelaar G, Sitnikova, EY, Midzyanovskaya IS. Cortical control of absence seizures: focal initiation, spreading and modulation. In: Hirsch E, Andermann F, Chauvel P, Engel J, Lopes da Silva F, Luders H (Eds) Generalized seizures: from clinical phenomenology to underlying systems and networks. Montrouge, France: John Libbey Eurotext, 2006: 93–117.

van Luijtelaar G, Bikbaev A. Midfrequency cortico-thalamic oscillations and the sleep cycle: genetic, time of day and age effects. *Epilepsy Res*., 2007: 73: 259-265.

Vantini G, Perry BD, Guchhait RB, U'Prichard DC, Stolk JM. Brain epinephrine systems: detailed comparison of adrenergic and noradrenergic metabolism, receptor number and in vitro regulation, in two inbred rat strains, *Brain Res*. 1984, 296: 49-65.

van Vugt MK, Sederberg PB, Kahana MJ. Comparison of spectral analysis methods for characterizing brain oscillations. *J. Neurosci*. *Methods,* 2007; 162: 49-63.

Vergnes M, Marescaux C, Depaulis A, Micheletti G, Warter JM. Spontaneous spike and wave discharges in thalamus and cortex in a rat model of genetic petit mal-like seizures. *Exp Neurol.* 1987, 96: 127-136.

Vergnes M, Marescaux C. Cortical and thalamic lesions in rats with genetic absence epilepsy. *J Neural Transm*. (Suppl.), 1992; 35: 71–83.

von Krosigk M, Bal T, McCormick DA. Cellular mechanisms of a synchronized oscillation in the thalamus. *Science*, 1993; 261: 361–364.

Weinshenker D, Szot P. The role of catecholamines in seizure susceptibility: New results using genetically-engineered mice. *Pharmacol. Ther*., 2002, 94: 213–233.

Weir B. The morphology of the spike-wave complex. *Electroencephalogr Clin Neurophysiol*. 1965; 19: 284-290.

Welker W, Sanderson KJ, Shambes GM. Patterns of afferent projections to transitional zones in the somatic sensorimotor cerebral cortex of albino rats. *Brain Res*., 1984; 292: 261-267.

Werth E, Acherman P, Dijk DJ, Borberly AA. Spindle frequency activity in the sleep EEG: individual differences and topographic distribution. *Electroenceph. Clin .Neurophysiol*., 1997, 1103: 535-542.

Wiest MC, Nicolelis MA. Behavioral detection of tactile stimuli during 7–12Hz cortical oscillations in awake rats. *Nature Neurosci.*, 2003; 6: 913–914.

Williams D. A study of thalamic and cortical rhythms in petit mal. *Brain,* 1953, 76: 50-69

Willoughby JO, Mackenzie L. Nonconvulsive electrocorticographic paroxysms (Absence Epilepsy) in rat strains. *Lab. Anim. Sci.,* 1992, 42: 551-554.

Worrell GA, Parish L, Cranstoun SD, Jonas R, Baltuch G, Litt B. High-frequency oscillations and seizure generation in neocortical epilepsy. *Brain,* 2004, 127(Pt 7): 1496-506.

Yamauchi T. Impairment of consciousness during epileptic seizures with special reference to neuronal mechanisms. Epilepsia, 1998; 39(Suppl.5): 16-20.

Yu C, Derdikman D, Haidarliu S, Ahissar E Parallel thalamic pathways for whisking and touch signals in the rat. *PLoS Biol.,* 2006; 4(5): e124. DOI: 10.1371/journal.pbio.0040124.

Zygierewicz J, Blinowska KJ, Durka, PJ, Szelenberger W, NiemcewiczS, Androsiuk W. High resolution study of sleep spindles. *Electroencephalogr. Clin. Neurophysiol.,* 1999, 110: 2136-2147.

Curriculum vitae

Evgenia Sitnikova was born in July 27, 1974 in Volgograd (former Stalingrad-City), Russian Federation. She graduated in 1991 from secondary school with High Honors and entered Moscow Academy of Veterinary and Biotechnology (Department of Veterinary Medicine and Biology). She graduated in 1996 from the Academy with honors and obtained a Specialist Diploma in "Veterinary Medicine and Biophysics". Between 1994 and 1996 Evgenia did her students' study at the Department of Neuroontogenesis of the Institute of Higher Nervous Activity and Neurophysiology (IHNA) Russian Academy of Science. From 1996 she continued her studies as a young researcher at the same Department in IHNA RAS. In 1997-2001 she followed the post-graduate course at the IHNA (supervised by Prof. Dr. V.V. Raevsky).

In October 2001 Evgenia Sitnikova defended her PhD thesis at the IHNA and obtained a Doctoral degree in physiology of humans and animals. The topic of her PhD study was the influence of early sensory experience on the morphology and functional properties of neurons in the somatosensory cortex in rats.

Since December 2001 she was employed by the Department of Biological Psychology, Nijmegen Institute of Cognition and Information (NICI), Radboud University Nijmegen as an AIO (after 2002 she worked at NICI as a 'Junior onderzoeker'). The PhD project of Evgenia was supervised by Dr. Gilles van Luijtelaar. The study was focused on the role of the cortex and the reticular thalamic nuclei in absence epilepsy in WAG/Rij rats; the project was sponsored by the Dutch Epilepsy Foundation.

She finished her project at NICI-Biological Psychology in November 2005, and returned to Moscow, where she continued to work as a researcher at the Department of Neuroontogenesis (IHNA). Currently, she investigates mechanisms of functional and anatomical integration of somatosensory and motor neurons in rat's neocortex (the basic research theme of the Department of Neuroontogenesis, IHNA). She is actively engaged in multidisciplinary research, which examines electrical brain activity (EEG) in normal behavioral states (sleep-waking) and pathological conditions (epilepsy) with the aid of different techniques (e.g., methods of non-linear dynamics, mathematical and neuronal modeling). Recently, Evgenia Sitnikova is involved in a collaborative research with the group of Prof. Dr. G. D. Kuznetsova (IHNA, Moscow, Russia), of Dr. I. N. Pigarev (the Institute for Information Transmission Problems, Moscow, Russia), psychophysiologists from NICI-Biological Psychology (Nijmegen) and physics from the Department of Non-linear Processes of Saratov State University in Russia.

Acknowledgements

All this I took to heart, and my heart saw it all:
that the upright and the wise and their works are in the hand of God;
and men may not be certain if it will be love or hate;
all is to no purpose before them. **Ecclesiastes 9:1**

There is something extremely important behind science. Happily, I have room to express my sincere gratitude to my good colleagues and friends, who indeed have been helping me in my personal and professional development as a scientist. In the greatest degree of importance for me are the two formal leaders of the project, Ton Coenen and Gilles van Luijtelaar, who perfectly arranged all the formal sides of my scientific life in Nijmegen (e.g., investing their time, energy and money). Many thanks to Gilles for his patience to my 'chaotic behavior'[1], thanks for the never-ending master-classes on statistical analysis, for correcting my Russian English writings and, especially, for teaching me valuable skills (somewhat psychology, some Dutch way of thinking).

I express my kind gratitude to Prof. Galina Dmitrievna Kuznetsova, who recommended me as a PhD-candidate for this project. Her professional and personal care during the last six years was ultimately helpful and important for me. I am inspired by what Galina Dmitrievna is doing in order to extend collaborative research with the Dutch colleagues from NICI-Biological Psychology. I'm especially grateful to her for organizing our collaborative meeting in October, 2006 (first, in Moscow and later in Saratov).

It is a moment to express my appreciation to Jovita van Luijtelaar and, again, to Gilles, for their cordiality, empathy and for their valuable help in my everyday life. I remember my first day in Nijmegen (in Archipelhof), when the van Luijtelaar family presented me extremely useful gifts. For almost four years at the Muzenplaats, I enjoyed using household stuff that I found in large carton box.

Thanks to Tineke van Rijn, I have got an explicit knowledge about pharmacology and treatment of absence epilepsy. I was really impressed by Tineke's way of teaching – it is gentle, open-minded and the most humanistic teaching that I have ever seen. I am grateful to Tineke's help in grasping Dutch culture and for the in-depth experience in music and choir singing (the music and singing I listened at Tineke's concerts surpassed the pleasant and euphonic experience I have had before).

I deeply appreciate friendliness and encouragement of Saskia van Uum, who indeed made my life at the NICI a bit brighter. I thank everybody at the ERG department (head Jos Wittebrood) for their technical support; they perfectly solved all the technical issues concerning electronics, computing and EEG recording system. A lot of thanks goes to Gerard van Oijen for being in sympathy with me. I also very much appreciate Gerard's help in repairing broken things such as a bike and keyboard. The gentle heart care of Makiko Sadakata helped me to adapt to some of (difficult) Dutch cultural aspects. Makiko, I cherish in my heart the memory of cheerful days and evenings that we spent together with you and Pieter, Stephan Rossignol, Paul and Wen Yen. We took great enjoyment of spending hours together with my friendly neighbor in Muzenplaats, Svetlana Bialkova.

It was nice to share room B.02.24 in Spinoza B Gebouw with my two roommates: first with Pauline Dibbets and later with Inge Westmijse. Thanks also to Annika Smit, Anke Sambeth and the other PhD-students (Hester van Lier, Ulrich Schridde, Jeroen Knippenberg and Gitte Bouwman) for the friendly atmosphere I experienced at the Department.

I was able to accomplish computational tasks of EEG data analysis with the highly qualified help of Philip van den Broek. I very much appreciated Philip's help as a programmer (user-friendly software) and his technical advices concerning the methodology of EEG analysis were very useful. I am also grateful to Philip for inviting me to workshops on BrainVisionAnalizer. I appreciate the chances to learn some basic principles of EEG analysis and I enjoyed sharing some new ideas with Marijtje Jongsma. By good fortune, I met Armen Sargsyan and, after all, I

[1] in human biology, *chaotic behavior* was defined as *"an aperiodic, seemingly random behavior in a deterministic system that exhibit sensitive dependence on initial conditions"* (cited by: M. Jenicek, D. Hitchcock "Evidence-based Practice: Logic and Critical Thinking in Medicine", AMA Press, 2005)

was greatly encouraged by his neuronal models of oscillating cortical cells that he simulated in GENESIS program.

I was very happy to work together with Elly Willems-van Bree, who perfectly organized everything for a comprehensive procedure of histological control of brain tissue. Thanks to Hans Krijnen I went through a hard school of 'animal care', but I gained fairly good experience. Personal efforts of Saskia Hermeling and her best care provided my animals with long and joyful live. I loved to be engaged in Saskia's positive thinking and in positive emotions that she shared.

With genuine pleasure I express my deepest gratitude to my mother. Her veritable support and motherly love helped me a lot to overcome all troubles during all this time.

I am thankful to Vladimir Vjacheslavovich Raevsky, who accepted me back to the home Institute (IHNA) without any hesitations and let me continue my research. I indeed appreciate the personal help of Vladimir Vjacheslavovich in solving some problems with housing.

The kind care of Rustam Berdiev (Moscow State University) during my first visit to Nijmegen was indeed great. Thanks to Lena Tolmacheva for being open with me; I am glad that we share some feelings and experiences. I am pleased to say very warm words to Inna Midzyanovskaya. I experienced "homish feelings" during her visits to Nijmegen; it was great to listen to Inna's presentation at the Histamine Conference in Noordwijkerhout. Thanks to Inna, I got acquainted with the two groups of physics from Saratov State University so that we could start new fruitful joint research. Many thanks to Dmitry Smirnov and his team for their efforts in applying new methods (Granger causality) of EEG data analysis.

An extremely good fortune was to meet Alexei Koronovsky and Alexandr Hramov; these two young talented scientists became my fellows in arms and misery. My recent research is inspired by their enthusiasm. The goodwill of Alexei and Alexandr forces my personal development as a scientist; our collaboration with the team of Alexei and Alexandr is ultimately important, since it helps me to recover from a chronic disease called *'status promovendi'*.

I am very much in favor of the fascinating results obtained by Alexei's and Alexandr's group and by Dmitry's team. I am proud that these two groups are interested in extending collaborative research with my Institute and with NICI-Biological Psychology.

List of Publications

Full length papers (reviews)

1. Sitnikova E, Dikanev T, Smirnov D, Bezruchko BP, van Luijtelaar G. Granger causality: Cortico-thalamic interdependencies during absence seizures in WAG/Rij rats, J. Neurosci. Methods, 2008; 170(2): 245-254.
2. Sitnikova E, van Luijtelaar G. Electroencephalographic characterization of Spike-Wave Discharges in cortex and thalamus in WAG/Rij rats. Epilepsia, 2007; 48 (12), 2296–2311.
3. Sargsyan A, Sitnikova E, Melkonyan A, Mkrtchian H, van Luijtelaar G. Simulation of sleep spindles and spike and wave discharges using a novel method for the calculation of field potentials in rats. J. Neurosci. Methods, 2007; 164(1): 161-178.
4. Koronovskii AA, Minyukhin IM, Tyshchenko AA, Hramov AE, Midzyanovskaya IS, Sitnikova EYu, van Luijtelaar G, van Rijn CM. Application of continuous wavelet transform to analysis of intermittent behavior. Izvestia vuzov PND, 2007; 15(4): 34-54 (In Russian).
5. Koronovskii AA, Kuznetsova GD, Midzyanovskaya IS, Sitnikova EYu, Trubetskov DI, Hramov AE Regularities of Alternate Behavior in Spontaneous Nonconvulsive Seizure Activity in Rats. Doklady Biological Sciences. 2006, 409(1): 275-277.
6. Koronovskii AA, Kuznetsova GD, Midzyanovskaya IS, Sitnikova EYu, Trubetskov DI, Khramov AE. Regularities of Alternate Behavior in Spontaneous Nonconvulsive Seizure Activity in Rats. Doklady Academii Nauk, 2006; 409(2): 274-276 (In Russian).
7. Hramov A, Koronovskii AA, Midzyanovskaya IS, Sitnikova E, van Rijn CM. On-off intermittency in time series of spontaneous paroxysmal activity in rats with genetic absence epilepsy. Chaos. 2006; 16(4): 043111.
8. Sitnikova E, van Luijtelaar G. Cortical and thalamic coherence during spike-wave seizures in WAG/Rij rats. Epilepsy Res., 2006; 71(2-3): 159-180.
9. van Luijtelaar G, Sitnikova E. Global and focal aspects of absence epilepsy: the contribution of genetic models. Neurosci. Biobehav. Rev., 2006; 30(7): 983-1003 (Review).
10. Sitnikova E, van Luijtelaar G. Reduction of adrenergic neurotransmission with clonidine aggravates spike-wave seizures and alters activity in the cortex and the thalamus in WAG/Rij rats. Brain Res. Bull., 2005; 64(6): 533-540.
11. Sitnikova E, van Luijtelaar G. Cortical control of generalized absence seizures: effect of lidocaine applied to the somatosensory cortex in WAG/Rij rats. Brain Res., 2004; 1012(1-2): 127-137.
12. van Luijtulaar G. Sitnikova EY. From generalized to focal absence seizures. Epilepsi (Journal of the Turkish Epilepsy Society), 2004; 10(2): 112-128.

Book chapters or collection of articles

1. van Luijtelaar G, Sitnikova EY, Midzyanovskaya IS. Cortical control of absence seizures: focal initiation, spreading and modulation. In: Generalized seizures: from clinical phenomenology to underlying systems and networks. Eds: E. Hirsch, F. Andermann, P. Chauvel, J. Engel, F. Lopes da Silva, H. Luders. Libbey, 2006; pp. 93-117.
2. Sitnikova E, van Luijtelaar ELJM. Thalamic and cortical correlates of sleep spindles in rats. Sleep-wake research in the Netherlands, 2005; 16: 137-140.
3. Sitnikova E, van Luijtelaar ELJM. Evolution of anterior and posterior sleep spindles in rats. Sleep-wake research in the Netherlands, 2005; 16: 133-136.
4. Sitnikova E, van Luijtelaar G. Alpha-2 adrenergic mechanisms of spike-wave activity and sleep EEG in rats. Sleep-Wake in the Netherlands, 2004; 15: 67-70
5. Sitnikova E, van Luijtelaar ELJM. Cortical control of generalized absence seizures: effect of lidocaine applied to the somatosensory cortex in WAG/Rij rats. In: van Luijtelaar E.L.J.M., Kuznetsova, G.D., Chepurnov SA,

Coenen AML. (eds.) The WAG/Rij Model for Absence Epilepsy. The Nijmegen - Russian Federation Papers. Nijmegen University Press, Nijmegen, 2004: 37-54

6. Sitnikova E, van Luijtelaar G. Anterior and posterior sleep spindles in rats: a spectral analytical approach. Sleep-Wake in the Netherlands, 2003, 14: 76-79

Meeting materials (International Journals)

1. Sitnikova E, van Luijtulaar G. Microinjections of lidocaine into the somatosensory cortex have a dose-dependent effect on the paroxysmal activity in WAG/Rij rats. Methods and Findings in Exper. Clin. Pharmacol., 2004; 26, Suppl. 2: 117. P16.
2. Sitnikova E, van Luijtulaar G. Thalamo-cortical mechanisms of various types of sleep spindles in rats (abstracts of the 12-th Word Congress of Psychophysiology, Porto Carras, Greece, September 18-23, 2004). Int. J. Psychophysiol. 2004; 54(1-2). 169.
3. van Luijtulaar G, Sitnikova EY. EEG oscillations in the brain: selective and local effects of noradrenergic system (proceedings of the 13th biennial IPEG meeting, 10-12 September 2004, Antwerp, Belgium). Acta Neurobiol. Exp., 2004; 64: 532. O1.4.
4. van Luijtulaar G, Sitnikova EYu. The focal theory of absence epilepsy (Abstracts from the 25-th International Epilepsy Congress. Lisbon, Portugal October 2003). Epilepsia, 2003; 44, Suppl 8: 36. 009.
5. Sitnikova EYu, van Luijtulaar G. The relation between two types of spike-wave discharges and sleep spindles: a spectral analytical approach (Abstracts of the 25-th International Epilepsy Congress. Lisbon, Portugal October 2003). Epilepsia, 2003; 44, Suppl. 8: 72. P147.